UNIVERSITY OF SOUTHERN QUEENSLAND

Investigating the capability of pulsed ultrasound technology in improving the performance of surface water treatment systems

A thesis submitted in fulfilment of the requirements of the degree of
Doctorate of Philosophy

Raed Ahmed Mahmood Al-Juboori

Bsc. Chemical Engineering, University of Baghdad

MENR Environmental Engineering, University of Southern Queensland

2015

Dedication

To my late father who could not be here to witness this achievement and to my beloved mother who I hope to make proud in every way. I dedicate this thesis to them.

CERTIFICATION OF DISSERTATION

I certify that the ideas, experimental work, results, analyses, software and conclusions in this dissertation are entirely my own effort, except where otherwise acknowledged. I also certify that the work is original and has not been previously submitted for any award, except where otherwise acknowledged.
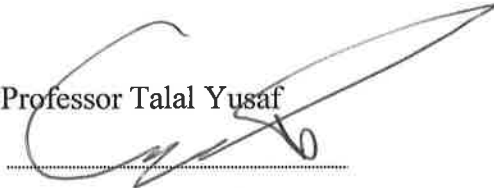
Raed Ahmed Al-juboori

....

Signature of Candidate

23 /10 / 2015

Date

ENDORSEMENT

Professor Talal Yusaf

....
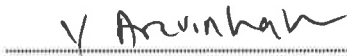
Signature of Principal Supervisor

23 / 10 / 2015

Date

Dr. Vasanthadevi Aravinthan

....
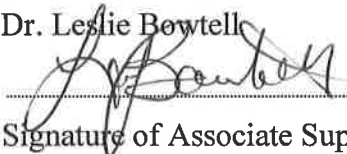
Signature of Associate Supervisor

23 /10 /2015

Date

Dr. Leslie Bowtell

....
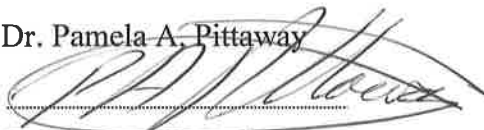
Signature of Associate Supervisor

23 /10 /2015

Date

Dr. Pamela A. Pittaway

....

Signature of Associate Supervisor

23/10/2015

Date

Table of Contents

Acknowledgements

Declaration

This thesis consists of my original work and does not contain any materials that previously published or written by another person, except where due reference has been made. I have clearly disclosed the contribution of others to jointly-authored work that I have included in my thesis.

I have clearly indicated the contribution of others to my thesis as a whole, including help with study design, data analysis and technical assistance required for the successful completion of my thesis. I declare that the content of my thesis is based on the results of experiments I have carried out since the commencement of my research higher degree candidature and does not contain a substantial part of work that has been submitted to qualify for the award on any other degree or diploma in any university. I have clearly stated wherever the substantial part has been used towards fulfilment of other degrees.

I acknowledge that an electronic copy of my thesis must be lodged with the University Library and subject to the General Award Rules of University of Southern Queensland, immediately made available for research and study in accordance with the *Copyright Act 1968.*

I acknowledge that copyright of all the materials contained in my thesis resides with the copyright holder(s) of that materials.

22/10/2015

Signature of Candidate   Date

Contributions by others to the thesis as a whole

No contribution by others.

Statement of parts of the thesis submitted to qualify for the award of another degree

None.

Statement of contributions to presented publications

The following tables detail the share of the co-authors in the presented publications in this thesis.

Al-Juboori, R. A., Yusaf, T., Bowtell, L. & Aravinthan, V., Energy characterisation of ultrasonic systems for industrial processes, Ultrasonics, (2014), 57, 18-30.- incorporated as *paper I*.

Contributor	Statement of contribution	Contribution significance
Al-Juboori, R. A. (candidate)	Al-Juboori, R. A. formulated the hypothesis, established the objectives of the research work, designed the experimental set-up, conducted the experimental work, wrote the initial draft and revised the final submission.	60%
Yusaf, T.	Yusaf, T. contributed to heat transfer calculations, layout of manuscript, technical discussion and development of methodology.	15%
Bowtell, L.	Bowtell, L. helped in designing the experimental set-up, electrical measurements and manuscript preparation.	15%
Aravinthan, V.	Aravinthan, V. reviewed the manuscript.	10%

Al-Juboori, R. A., Yusaf, T. & Bowtell, L., Energy Conversion Efficiency of Pulsed Ultrasound, Energy Procedia, (2015), 75, 1560-1568.-incorporated as *paper II*.

Contributor	Statement of contribution	Contribution significance
Al-Juboori, R. A. (candidate)	Al-Juboori, R. A. established the objectives of the research work, conducted the experimental work, performed chemical analysis wrote the initial draft and revised the final submission.	70%
Yusaf, T.	Yusaf, T. contributed to setting up the layout of manuscript, technical discussion and development of methodology.	15%
Bowtell, L.	Bowtell, L. helped in electrical measurements and manuscript preparation.	15%

Al-Juboori, R. A., Yusaf, T., Aravinthan, V., Pittaway, P. A. & Bowtell, L., Investigating the feasibility and the optimal location of pulsed ultrasound in surface water treatment schemes, Desalination and Water Treatment, (2015), 1-19.- incorporated as *paper III*.

Contributor	Statement of contribution	Contribution significance
Al-Juboori, R. A. (candidate)	Al-Juboori, R. A. established the objectives of the research work, collected water samples, designed the experimental set-up, conducted the experimental work, wrote the initial draft and revised the final submission.	60%
Yusaf, T.	Yusaf, T. helped in methodology development and setting up the layout of manuscript.	10%
Aravinthan, V.	Aravinthan, V. reviewed the manuscript.	10%
Pittaway, P. A.	Pittaway, P. A. reviewed the manuscript and helped in water samples collection.	10%
Bowtell, L.	Bowtell, L. reviewed the manuscript.	10%

Al-Juboori, R. A., Yusaf, T., Aravinthan, V., Pittaway, P. A. & Bowtell, L., Effect of ultrasound treatment on characteristics of terrestrial aquatic carbon: comparison between continuous and pulsed treatments, Applied Water Science, (2015), under review. -incorporated as *paper IV*.

Contributor	Statement of contribution	Contribution significance
Al-Juboori, R. A. (candidate)	Al-Juboori, R. A. established the objectives of the research work, collected water samples, designed the experimental set-up, conducted the experimental work, wrote the initial draft and revised the final submission.	60%
Yusaf, T.	Yusaf, T. helped in methodology development and setting up the layout of manuscript.	10%
Aravinthan, V.	Aravinthan, V. reviewed the manuscript.	10%
Pittaway, P. A.	Pittaway, P. A. reviewed the manuscript and helped in water samples collection.	10%

Bowtell, L.	Bowtell, L. reviewed the manuscript.	10%

Al-Juboori, R. A., Aravinthan, V. & Yusaf, T., Impact of pulsed ultrasound on bacteria reduction of natural waters, Ultrasonics Sonochemistry, (2015), 27, 137-147. -incorporated as *paper V*.

Contributor	Statement of contribution	Contribution significance
Al-Juboori, R. A. (candidate)	Al-Juboori, R. A. established the objectives of the research work, conducted the experimental work, collected data, performed statistical analysis wrote the initial draft and revised the final submission.	70%
Aravinthan, V.	Aravinthan, V. participated in statistical analysis and reviewed the manuscript.	15%
Yusaf, T.	Yusaf, T. contributed to manuscript preparation and helped in improving methodology and discussion parts.	15%

Al-Juboori, R. A., Yusaf, T., Aravinthan, V. & Bowtell, L., Investigating natural organic carbon removal and structural alteration induced by pulsed ultrasound, Science of the Total Environment, (2015), 541, 1019-1030.-incorporated as *paper VI*.

Contributor	Statement of contribution	Contribution significance
Al-Juboori, R. A. (candidate)	Al-Juboori, R. A. built and tested fractionation procedure, conducted the experimental work, collected data, performed statistical analysis wrote the initial draft and revised the final submission.	65%
Yusaf, T.	Yusaf, T. helped in methodology development and setting up the layout of manuscript.	10%
Aravinthan, V.	Aravinthan, V. helped in statistical analysis and reviewed the manuscript.	15%
Bowtell, L.	Bowtell, L. reviewed the manuscript.	10%

Al-Juboori, R. A., Yusaf, T., Aravinthan, V. & Bowtell, L., Tracking ultrasonically structural changes of natural organic carbon: chemical fractionation and spectroscopic approaches, Chemosphere, (2015), 145, 231-248.-incorporated as *paper VII*.

Contributor	Statement of contribution	Contribution significance
Al-Juboori, R. A. (candidate)	Al-Juboori, R. A. built and tested fractionation procedure, conducted the experimental work, collected data, performed statistical analysis, initiated the investigation of correlations between DOC fraction and UV-vis indices, wrote the initial draft and revised the final submission.	70%
Yusaf, T.	Yusaf, T. helped in methodology development and setting up the layout of manuscript.	10%
Aravinthan, V.	Aravinthan, V. helped in statistical analysis and reviewed the manuscript.	10%
Bowtell, L.	Bowtell, L. reviewed the manuscript.	10%

Al-Juboori, R. A., Yusaf, T. & Pittaway, P. A., Exploring the correlations between common UV measurements and chemical fractionation for natural waters, Desalination and Water Treatment, (2015), 1-12.-incorporated as *paper VIII*.

Contributor	Statement of contribution	Contribution significance
Al-Juboori, R. A. (candidate)	Al-Juboori, R. A. collected samples from different water bodies, conducted the experimental work, collected data, performed statistical analysis on the correlations between DOC fraction and UV-vis indices wrote the initial draft and revised the final submission.	75%
Yusaf, T.	Yusaf, T. helped in methodology development and setting up the layout of manuscript.	15%
Pittaway, P. A.	Pittaway, P. A. reviewed the manuscript and helped in water samples collection.	10%

Al-Juboori, R. A., Aravinthan, V., Yusaf, T. & Bowtell, L., Assessing the application and downstream effects of pulsed ultrasound as a pre-treatment for Alum coagulation, Ultrasonics Sonochemistry, (2015), 31, 7-19.-incorporated as *paper IX*.

Contributor	Statement of contribution	Contribution significance
Al-Juboori, R. A. (candidate)	Al-Juboori, R. A. planned the experimental work, collected data, performed statistical analysis, conducted confirmatory experiments, carried out downstream effects measurements wrote the initial draft and revised the final submission.	65%
Yusaf, T.	Yusaf, T. helped in methodology development and setting up the layout of manuscript.	10%
Aravinthan, V.	Aravinthan, V. helped in statistical analysis, developing the discussion and reviewed the manuscript.	15%
Bowtell, L.	Bowtell, L. reviewed the manuscript.	10%

Al-Juboori, R. A., Bowtell, L. A., Yusaf, T. & Aravinthan, V., Insights into the scalability of magnetostrictive ultrasound technology for water treatment applications, Ultrasonics Sonochemistry, (2016), 28, 357-366.-incorporated as *paper X*.

Contributor	Statement of contribution	Contribution significance
Al-Juboori, R. A. (candidate)	Al-Juboori, R. A. designed the large-scale system, planned evaluation criteria, collected data, performed data analysis, wrote the initial draft and revised the final submission.	55%
Bowtell, L.	Bowtell, L. helped in system design, conducted electrical measurements and analysis and reviewed the manuscript.	20%
Yusaf, T.	Yusaf, T. contributed to the development of large-scale design, layout of manuscript, technical discussion and development of methodology.	15%
Aravinthan, V.	Aravinthan, V. reviewed the manuscript.	10%

List of publications included in the thesis

- **Al-Juboori, R. A.**, Yusaf, T., Bowtell, L. & Aravinthan, V., Energy characterisation of ultrasonic systems for industrial processes, *Ultrasonics*, (2014), 57, 18-30.

- **Al-Juboori, R. A.**, Yusaf, T. & Bowtell, L., Energy Conversion Efficiency of Pulsed Ultrasound, *Energy Procedia*, (2015), 75, 1560-1568.

- **Al-Juboori, R. A.**, Yusaf, T., Aravinthan, V., Pittaway, P. A. & Bowtell, L., Investigating the feasibility and the optimal location of pulsed ultrasound in surface water treatment schemes, *Desalination and Water Treatment*, (2015), 1-19.

- **Al-Juboori, R. A.**, Yusaf, T., Aravinthan, V., Pittaway, P. A. & Bowtell, L., Effect of ultrasound treatment on characteristics of terrestrial aquatic carbon: comparison between continuous and pulsed treatments, *Applied Water Science*, (2015), under review.

- **Al-Juboori, R. A.**, Aravinthan, V. & Yusaf, T., Impact of pulsed ultrasound on bacteria reduction of natural waters, *Ultrasonics Sonochemistry*, (2015), 27, 137-147.

- **Al-Juboori, R. A.**, Yusaf, T., Aravinthan, V. & Bowtell, L., Investigating natural organic carbon removal and structural alteration induced by pulsed ultrasound, *Science of the Total Environment*, (2015), 541, 1019-1030.

- **Al-Juboori, R. A.**, Yusaf, T., Aravinthan, V. & Bowtell, L., Tracking ultrasonically structural changes of natural organic carbon: chemical fractionation and spectroscopic approaches, *Chemosphere*, (2015), 145, 231-248.

- **Al-Juboori, R. A.**, Yusaf, T. & Pittaway, P. A., Exploring the correlations between common UV measurements and chemical fractionation for natural waters, *Desalination and Water Treatment*, (2015), 1-12.

- **Al-Juboori, R. A.**, Aravinthan, V., Yusaf, T. & Bowtell, L., Assessing the application and downstream effects of pulsed ultrasound as a pre-treatment for Alum coagulation, *Ultrasonics Sonochemistry*, (2015), 31, 7-19.

- **Al-Juboori, R. A.**, Bowtell, L. A., Yusaf, T. & Aravinthan, V., Insights into the scalability of magnetostrictive ultrasound technology for water treatment applications, *Ultrasonics Sonochemistry*, (2016), 28, 357-366.

List of publications included in the appendices

- Yusaf, T. & **Al-Juboori, R. A.**, Alternative methods of microorganism disruption for agricultural applications, *Applied Energy*, (2014), 114, 909-923.

- **Al-Juboori, R. A.**, Yusaf, T. & Aravinthan, V., Evaluating the impact of operating parameters on biocidal effects of pulsed ultrasound in natural water disinfection, *Journal of Biotechnology*, (2015), 208, Supplement, S17-S18.

Abstract

Surface water is an important resource for drinking water production. Due to increasing contamination caused by floods and urbanisation, the quality of surface water continues to deteriorate. This problem is currently addressed by increasing the chemical additives used in water treatment processes. This practice introduces health-related problems such as the formation of disinfection by-products (DBPs) and the increase of Al residues. The application of physical rather than chemical treatments is a logical solution to the above problems. When evaluating various physical treatments, ultrasound appears a sensible choice for improving contaminants removal from surface water.

While numerous studies have addressed the application of ultrasound technologies in water treatment, most of these studies used single contaminant synthetic water samples which does not present a realistic assessment. The key focus of this study is using natural water samples with a representative mixture of contaminants.

The main challenge cited regarding ultrasound application is high energy consumption. To tackle this issue, the use of pulsed ultrasound has been proposed in this study. An improved calorimetric technique has been developed and tested to provide a fair evaluation of energy conversion in ultrasonic reactors. Sonochemical efficiency (SE) based on $^\bullet$OH and H_2O_2 measurements for the ultrasonic system along with the new calorimetric technique were employed.

The optimal location of pulsed ultrasound technology within the surface water treatment process was identified using natural water samples with different carbon origins. The optimal location was found to be prior to the coagulation stage. The operation of pulsed ultrasound in this location was optimized with regards to power, treatment time and pulse format. Total coliform, DOC and UV-vis measurements were applied along with chemical fractionation techniques to establish the optimal operating conditions. Overall, ultrasound treatments resulted in 10-70% of microbial removal and 7-15% of DOC removal with a decrease in the aromatic hydrophobic DOC and a marginal increase in the hydrophilic DOC. The effectiveness of these conditions in promoting further removal of contaminants with alum coagulation was also examined.

Turbidity, DOC removal and residual Al were measured for alum coagulation with and without pulsed ultrasound pre-treatment. Response optimization showed that pulsed ultrasound pre-treatment increased turbidity and DOC removal and reduced residual Al. Analysis of downstream effects revealed that pulsed ultrasound pre-treatment increased total coliform removal, decreased trihalomethane formation potential (THMFP) and improved the settling of coagulation sludge.

A large-scale laboratory magnetostrictive ultrasonic reactor operated on square-pulse waveform was designed and tested. It was observed that scaling up to 15 L improved sonochemical efficiency of ultrasonic reactor. Using a reactor tank with 45° inclined sides further improved sonochemical efficiency. The larger design was more energy efficient in removing water contaminants compared to the small scale. This study confirmed that pulsed ultrasound is an effective tool for improving surface water treatment system, however further investigations required using other coagulants and monitoring of subsequent effects on other DBPs. It is also important to evaluate the performance and economic viability of the large scale reactor in continuous systems.

Introduction

Background and thesis structure

1. Common problems in surface water treatment systems

Water is an essential element for living systems. It facilitates the transport of nutrients and waste products within the body of living creatures (Tansel, 2008). Surface water is a major resource for drinking water production (Fawell and Nieuwenhuijsen, 2003). Recently, surface water has been increasingly contaminated by microorganisms, organic matter, particles and solids due to the developing effects of human activities and climate change as is depicted in Figure 1 (Tetzlaff et al., 2013, Kicklighter et al., 2013, Delpla et al., 2009). This increase in the concentration of surface water contaminants has led to the increase in the cost associated with the treatment of water. The quality of the produced water has also deteriorated as a result of the increasing contamination. According to the World Health Organization (WHO) five million death cases per year worldwide are caused by poor quality drinking water (Blanco et al., 2009). These problems have made the enhancement of surface water treatment to cope with the increasing levels of contamination an ultimate goal for the current research activities.

Technically, the performance of surface water treatment systems depends on the efficiency of the individual treatment processes in removing contaminants. Conventional surface water treatment systems consist of main operational units; coagulation/flocculation, filtration and disinfection (Tansel, 2008). A number of operational and health problems arise in the surface water treatment process as a result of increasing contamination. The most common problems are the presence of dangerous residual levels of metal coagulants such as aluminum (Al) (Srinivasan et al., 1999), fouling of filtration media (Zularisam et al., 2006) and the formation of hazardous disinfection by-products (DBPs) (Kim et al., 2003).

The residual metals from coagulation such as Al can cause operational and health problems. Increasing the concentration of Al in water increases turbidity, causes filtration fouling and interferes with disinfectants (Driscoll and Letterman, 1988, Gabelich et al., 2002, Costello, 1984). In addition to the technical problems, the residual Al in the finished water can cause neuropathologic disorders, neurological diseases (e.g. Alzheimer and presenile dementia) and kidney diseases (Driscoll and Letterman, 1988, Wasana et al., 2015).
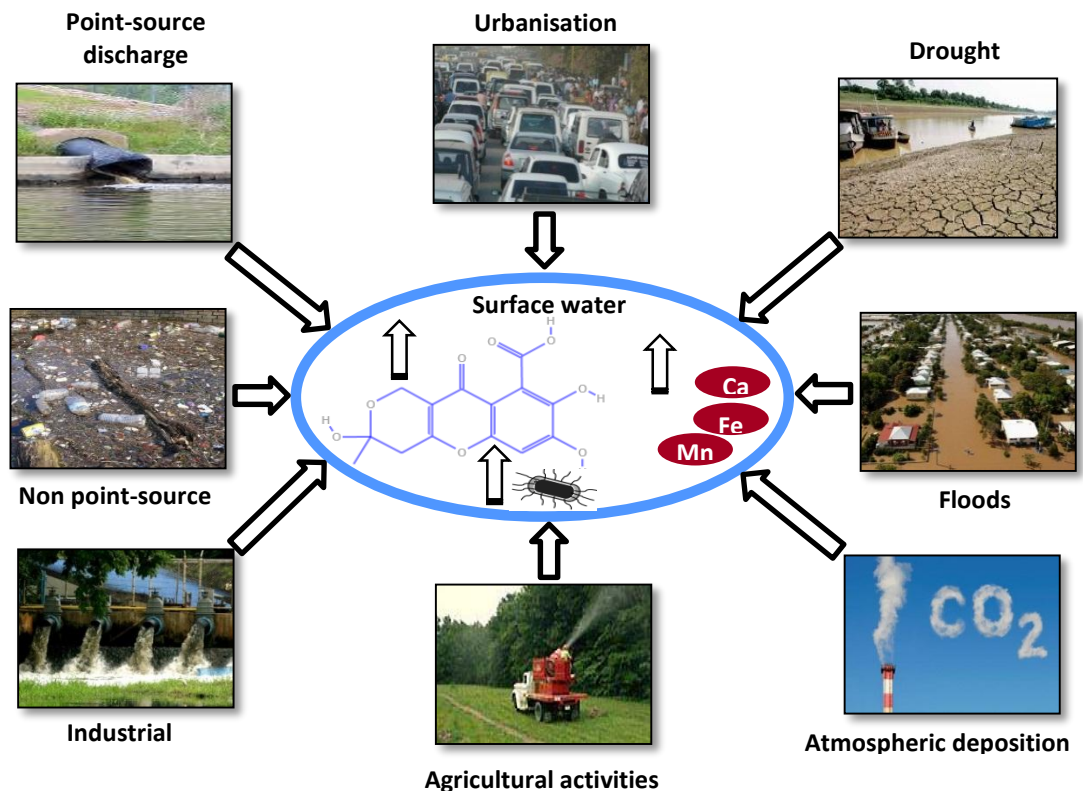
Figure 1: sources of surface water contamination

Fouling of filtration/adsorption media is another challenge that is commonly encountered by surface water treatment plant operators. Fouling can occur as a result of the deposition of various foulants such as solid particles, organic contaminants, inorganic contaminants and microorganisms onto various filter surfaces (Flemming, 1997). Fouling of filters inflicts extra cost and delay on the filtration process as well as reducing the quality of the water produced (Flemming, 2002, Abdul Azis et al., 2001). For instance, the deeply embedded microorganisms in the filtration media can not only act as a hidden source of pathogens but also release toxic metabolic products into water treatment systems (Wingender, 2011).

The formation of DBPs is a result of the reaction between chemical disinfectants (e.g. chlorine and ozone) with the organic matter (Richardson, 2003, Richardson et al., 2002, Kim and Yu, 2005, Matilainen et al., 2011). DBPs include a wide spectrum of carcinogenic and mutagenic chemical complexes that pose a threat to both humans and the environment. The two most prevalent classes of DBPs in drinking water are Trihalomethanes (THMs) and Haloacetic acids (HAAs) Farré et al. (2011). Total THMs (TTHMs) is the sum of four compounds; chloroform, bromodichloromethane, dibromochloromethane and bromoform (Clesceri et al., 2005). HAAs include nine compounds which encompass derivatives of the HAAs (i.e. mono, di and trihaloacetic acid), iodine containing HAAs and bromine containing HAAs (Farré et al., 2011). The most common HAAs are di and trihaloacetic acid. Epidemiological and toxicological studies indicated that the human exposure to chlorinated water that contains DBPs may lead to bladder cancer (Neale et al., 2012), deterioration in the functionalities of liver, kidney and nervous system (Sadiq and Rodriguez, 2004) and congenital diseases (Richardson, 2003). Therefore, a Maximum Contamination Level (MCL) of the DBPs has been established. In Australia, the MCL of THMs is 250 $\mu g L^{-1}$, while the MCL of

Monochloroacetic acid (MCAA), Dichloroacetic acid (DCAA) and Trichloroacetic acid (TCAA) are 150, 100 and 100 μgL^{-1}, respectively (Australian National Health and Medical Research Council, 2011, Sadiq and Rodriguez, 2004).

2. Physical treatment methods as effective solutions

Research efforts have been directed towards minimizing the challenges encountered in surface water treatment systems. It is obvious that the increasing levels of contamination and the conventional chemicals used for the purpose of treatment are the main reasons behind these challenges. Hence, the quantities of chemicals added to water should be minimized without compromising the quality of the treated water. In order to meet this aim, physical treatment methods for reducing the levels of water contaminants are recommended to be applied in surface water treatment schemes. It should be mentioned here that this study focuses on organic and microbial contamination, hence, the discussion in the following sections will be limited to aspects pertaining to the removal of these forms of contamination.

The common physical treatment methods include electrical techniques (e.g. pulsed electric field and plasma discharge) (Gusbeth et al., 2009, Stratton et al., 2015), magnetic field (Ambashta and Sillanpää, 2010), hydrodynamic cavitation (Sawant et al., 2008), Ultraviolet (UV) light (Armstrong et al., 2006) and ultrasound (Mason et al., 2003). The combinations of physical-physical treatments such as UV light and ultrasound and physical-chemical treatments such as ultrasound and chlorine dioxide, ultrasound and ozone and UV and ozone have also been recommended (Naddeo et al., 2009b, Ayyildiz et al., 2011, Al-Hashimi et al., 2015, Bustos-Terrones et al.).

2.1. Organic contamination

The organic contamination of natural surface water is represented by the existence of natural organic matter (NOM) in water resources. NOM can be categorized based on its size into particulate organic carbon (POC) and dissolved organic carbon (DOC). NOM that passes through 0.45 μm filter is termed as DOC, while the retained fraction of NOM is termed as POC. The latter only forms 10% of NOM and can easily be removed from water (Leenheer and Croué, 2003). Therefore, attention should be directed towards improving DOC removal from natural water.

2.1.1. DOC structure

DOC encompasses a vast array of organic materials that varies in their characteristics spatio-temporally (Sharp et al., 2006). DOC can be classified into groups based on origin and structure. Origin based classification of DOC categorizes it into three groups: allochthonous, autochthonous and anthropogenic (Knapik et al., 2015). Allochthonous is derived from the natural decomposition of soil and plants. The origin of autochthonous DOC in surface water is algal and microbial activities. The anthropogenic DOC is a resultant of human activities and the microbial products emanates from biological wastewater treatment processes (Knapik et al., 2015). The surface water resources that are normally utilized for drinking water production contain mainly allochthonous and autochthonous carbon (Park et al., 2009). The concentration of autochthonous DOC in surface water depends strongly on the

hydraulic residence time of water in reservoirs and this would naturally reduce its contribution to overall organic contamination. Hence, improving allochthonous DOC removal would be of more importance to drinking water treatment practices.

The structural classification mainly divides DOC into hydrophobic and hydrophilic fractions (Matilainen and Sillanpää, 2010). The proportion of these fractions in natural water catchments depends on the carbon source and other factors such as microbial activities and natural photo-degradation. The hydrophobic fraction is comprised mainly of humic acids, fulvic acids, phenolic DOC and double bond structures (Ghernaout, 2014). The hydrophilic fraction mainly contains aliphatic and nitrogenous compounds such as carbohydrates, sugars and amino acids (Matilainen and Sillanpää, 2010). Knowing the DOC structure is important from a water treatment perspective as these fractions are associated with certain health and operational problems (Xing et al., 2012). For instance, the hydrophobic DOC is known to have a tendency to react with chlorine forming DBPs (Soh et al., 2008). Fractionating DOC with regard to its affinity to water (hydrophobic/hydrophilic proportion) is normally performed using a series on anion exchange resins (Chow et al., 2004). The resin fractionation method is a valuable tool for studying DOC structural alteration with different treatment processes (Raspati et al., 2011), however it has a relatively long turnaround time (Chow et al., 2004). Thus, finding a rapid surrogate replacement for this technique is of great importance for the water treatment industry.

2.1.2. DOC removal mechanisms

There are three main mechanisms through which the physical treatments can remove DOC: i) chemical reactions (e.g. radicals attack), ii) physical effects (e.g. shear forces, pyrolysis) and iii) alteration of physical properties (absorptivity). A wide range of radicals are produced when exposing water to physical treatments such UV and ultrasound. The most important radical species is the hydroxyl ($^{\bullet}$OH) as it possesses a high oxidation potential (2.8 V) that exceeds the oxidation potentials of common oxidants such as atomic oxygen (2.42 V), ozone (2.07 V) and hydrogen peroxide (1.78 V) (Hartnett et al., 2007). The known reaction pathways of $^{\bullet}$OH with NOM are: 1) addition to double bonds, 2) hydrogen abstraction and 3) electron abstraction (Matilainen and Sillanpää, 2010). Some physical methods such as electrical and UV techniques utilize chemical mechanisms for removing DOC, while others such as ultrasound and hydrodynamic cavitation utilize both chemical and physical mechanisms for the same purpose (Lifka et al., 2003). Physical treatments that utilize magnetic fields are capable of altering physical properties of DOC, making it more susceptible to removal via adsorption (Ambashta and Sillanpää, 2010, Blanco et al., 2009). It is worth mentioning that the physical methods that produce $^{\bullet}$OH are also capable of altering the nature of remnant DOC (Chen et al., 2004, Buchanan et al., 2005).

2.1.3. DOC removal feasibility: comparison between physical methods

Generally, DOC removal levels are low with the physical treatments as stand-alone technologies, however combining these methods with chemicals addition can significantly boost DOC removal (Matilainen and Sillanpää, 2010). Chemical addition to some treatment methods such as UV and electrical methods can be problematic. For instance, the addition of TiO_2 in photo-catalysis (UV/semi-conductors) requires an

additional treatment to remove TiO_2 particles from the treated water, and this in turn introduces extra cost (Klavarioti et al., 2009). The addition of electrolytes such as NaCl (Matilainen and Sillanpää, 2010), or KCl (Motheo and Pinhedo, 2000) in electrochemical oxidation can also cause some technical problems. The addition of electrolytes into water can alter the ionic strength leading to conformational change of DOC (Ghosh and Schnitzer, 1980) that would eventually result in the formation of a compact fouling layer of DOC on the surfaces that come in contact with the treated water. Electrical current and UV sources in water are prone to fouling problems that would frequent maintenance (Zhe et al., 2008). Furthermore, the use of the UV method, particularly vacuum UV (VUV) was found to produce undesired nitrite by-products that could potentially increase the chances of nitroso-DBPs formation (Matilainen and Sillanpää, 2010). Similarly, the use of magnetic fields for removing NOM is associated with some additional health problems. It has been reported that the use of magnetically treated water negatively affects the functionality of rats' kidneys suggesting that magnetic treatment can cause unstable changes to bio-mechanisms of tissue fluid (Singh et al., 2004). The electrical, magnetic and UV treatments do not induce liquid movements and since the effect of these treatments is concentrated in the area close to the source of energy, extra mixing is required to ensure uniform effective treatments. By way of contrast, mixing is not required for dynamic treatments such as ultrasound and hydrodynamic cavitation. These treatments were also found to have benign environmental effects (Gogate and Kabadi, 2009). However, hydrodynamic cavitation has some disadvantages such as the unclear effect of operating parameters on cavitation events (Arrojo and Benito, 2008), the requirement of long treatment times to achieve perceptible change and mechanical erosion of equipment (Gogate and Kabadi, 2009). The main disadvantage of ultrasound is high operational energy demand (Hulsmans et al., 2010), nevertheless the installation and maintenance cost is low due to its simple configuration (Furuta et al., 2004). Recent studies have reported that ultrasound is more energy efficient compared to hydrodynamic cavitation and UV in removing organic materials (Stratton et al., 2015).

In spite of the attractive traits of ultrasound technology, little attention has been paid to the application of this technology in removing DOC (Klavarioti et al., 2009). The majority of the previous research work on the use of ultrasound for DOC removal were conducted using synthetic water samples consisting of a single pollutant. Such practice does not reflect the real case of industrial water treatment as synthetic DOC differs in its structure from natural DOC (Chen et al., 2004). Furthermore, natural water does not contain only a single contaminant, rather it contains a complex mixture of various DOC structures co-existing with other contaminants such as microbes. Hence, the use of natural water samples is required for an accurate unbiased assessment of ultrasound performance (Naddeo et al., 2007). In addition, the studies concerning DOC removal with ultrasound mostly focus on removal levels and little attention is given to structural alteration of the treated DOC (e.g. (Chemat et al., 2001)). The possible downstream effects of ultrasound application in water treatment (e.g. effects on DBPs formation) is still an area that needs to be explored thoroughly (Naddeo et al., 2009a).

2.2. Microbial contamination

Various species of microbes are present in surface water. However, microbial contamination of water is normally evaluated through indicators such as total coliform and *E. coli* (Wright et al., 2004). The mechanisms of microbial removal/inactivation using physical treatment methods are similar to those of NOM removal. Detailed discussion of microbial removal/deactivation with physical treatments other than magnetic methods is presented in ***paper XI***. It should be noted here that magnetic methods are mostly applied for removing inorganic and organic contamination, but rarely for microbial removal/inactivation.

The discussions presented in the above sections and ***paper XI*** clearly show that the application of physical methods in water treatment can reduce the usage of chemicals and improve the quality of water produced. It is also clear that amongst other physical treatment methods, the advantages of ultrasound outweigh the disadvantages. For this reason, ultrasound has been proposed in this study to reduce the challenges encountered in surface water treatment processes.

3. Ultrasound technology

3.1. Fundamentals of ultrasound

Ultrasound is a longitudinal wave with frequency ranges between 16 kHz and 500 MHz (Thompson and Doraiswamy, 1999). The propagation of the ultrasound waves through liquids (e.g. water) produces alternating cycles of positive and negative pressures. When the magnitude of the ultrasonic pressure exceeds the tensile strength of the liquid, cavitational bubbles are created. The formed cavitational bubbles and existing gas bubbles in the liquid grow to a size larger than their original size during the negative cycle of the ultrasonic pressure. Some bubbles grow to a very large size due to gas transfer across bubble skin (rectified diffusion) or coalescence with other bubbles, and eventually float to the surface of the liquid. The other bubbles collapse during the positive cycle of the ultrasonic wave. In terms of collapse intensity, there are two kinds of bubbles; bubbles with gentle collapse "stable bubbles" and bubbles with severe collapse "transit bubbles" (Young, 1999). There are two sources for bubbles generated in ultrasonically excited liquid medium: dissolved gas and gas entrapped in crevices of the solid surfaces. The formation of bubbles from dissolved gas is normally termed as homogeneous cavitation, while the formation of bubbles on the liquid-solid interface is termed as heterogeneous cavitation (Al-Juboori and Yusaf, 2012c).

The physics and chemistry of transit bubbles are of interest for research and industrial applications owing to the powerful effects produced from the collapse of such bubbles. These effects are represented by the generation of localized areas of high temperature and pressure of around 5000 K and 500 atm respectively, usually referred to as hot spots (Lifka et al., 2003). There is a variation in the temperature profile within the localized areas of hot spots which determines the nature of reactions occurring in each area. The three recognized zones of the hot spots are (Chen et al., 2011, Lifka et al., 2003):

1. ***Thermolytic centre***, which represents the centre of the cavitational bubble. During bubble collapse, the temperature and the pressure of this zone reach approximately

5000 K and 500 atm, respectively. The materials phase in this region is gaseous, so it can be inferred that the high temperatures in this region can lead to the thermolysis of the volatile DOC and water vapor exist in the region (pyrolysis reactions) (Flint and Suslick, 1991, Washington, 1995). The thermolysis of water vapor produces free radicals (ultrasonic chemical effects). The free radicals produced in the thermolytic centre can further decompose the volatile DOC.

2. *Interfacial zone* between bubble skin and the bulk solution. The thickness of this region is around 200 nm, and the life time of this region is about 2 µs (Chen et al., 2011). The temperature in this region reaches to approximately 2000 K at the final collapse of the bubble (Riesz et al., 1985). The material phase in this region is a supercritical fluid (Chen et al., 2011). The high temperature in the interfacial zone facilitates the thermolysis and the oxidation of the nonvolatile DOC by free radicals.

3. *Bulk solution region*, the pressure in this region is similar to the ambient pressure of ultrasonic systems, whereas the temperature is variable depending on the operating parameters of ultrasound being applied. The hydroxyl radicals recombine in the bulk solution region producing hydrogen peroxide which in turn can oxidize the nonvolatile DOC.

Bubbles oscillate and collapse generating acoustic streaming, micro-streaming, micro-jetting, turbulence, shock wave and shear stress (Gogate, 2007, Doosti et al., 2012). Acoustic streaming is defined as the convective liquid motion due to the passage of ultrasound waves. Micro-streaming is the liquid motion in the adjacent area to the oscillating bubble. Micro-jetting is the resulting liquid motion from bubble symmetrically collapse close to the solid/liquid interface (Birkin and Silva-Martinez, 1996). The physical and chemical effects of ultrasound can be harnessed to destroy the structure of organic and microbial contaminants in water.

3.2. Effects of acoustic cavitation events on water contaminants

Figure 2 provides an illustration of the ways through which the physical and chemical effects of acoustic cavitation destruct various water contaminants. The physical effects of acoustic cavitation represented by the powerful turbulences and shock waves are capable of disintegrating the organic and microbial structures. Such events have been confirmed by large number of studies (Price et al., 2002, Gogate, 2007, Hulsmans et al., 2010, Yusaf, 2011). The mechanisms of ultrasound effects in rupturing microorganisms were discussed in *paper XI*. Hence the discussion related to this subject will not be included herein.

Although inorganic contamination is outside of the scope of this study, it is worth mentioning that the chemical and physical effects of ultrasound are capable of removing inorganic contaminants through oxidation reactions. For example, Stępniak et al. (2008) found that ultrasound is capable of oxidizing Fe(II) to Fe(III), which facilitated the removal of iron from water. In a similar fashion, Nishida (2004) reported a promotion in the precipitation of calcium in the form of calcium carbonate with the aid of ultrasound. Some other studies reported the oxidation of manganese with sonication (Anderson et al., 1982). Micro-streaming and the liberation of oxidative agents from bubble collapse are believed to be the main trigger of inorganic reactions in ultrasound treatments (Nishida, 2004).

The chemical effects of ultrasound are evident through the liberation of highly reactive species that have the capacity to cleave chemical bonds. The reactive species are short lived intermediates (Kondo et al., 1988), therefore their effects are expected to appear in the collapsing bubble. As explained earlier in section 3.1, volatile

compounds are likely to decompose in the thermolytic centre due to the effects of free radicals.

Ultrasound waves

Ultrasound source

Acoustic streaming

Micro-streaming

Micro-jets

Shock waves

Physical effects

Macromolecules (i.e. NOM)

Micro-molecules

Cell fragments and intracellular materials

Chemical effects

Bubble collapse (hot spots)

Thermolytic centre, production of reactive species

Interfacial zone, decomposition of

Pyrolysis

$H_2O_{(v)} \longrightarrow H^{\bullet} + {}^{\bullet}OH$

$H^{\bullet} + O_{2(g)} \longrightarrow HO_2^{\bullet}$

Bulk solution region, recombination of hydroxyl radicals

${}^{\bullet}OH + {}^{\bullet}OH \longrightarrow H_2O_2$

${}^{\bullet}OH, H_2O_2, HO_2^{\bullet}$ & ${}^{\bullet}O$

-C-R-, R-X, R$=$O & microorganisms

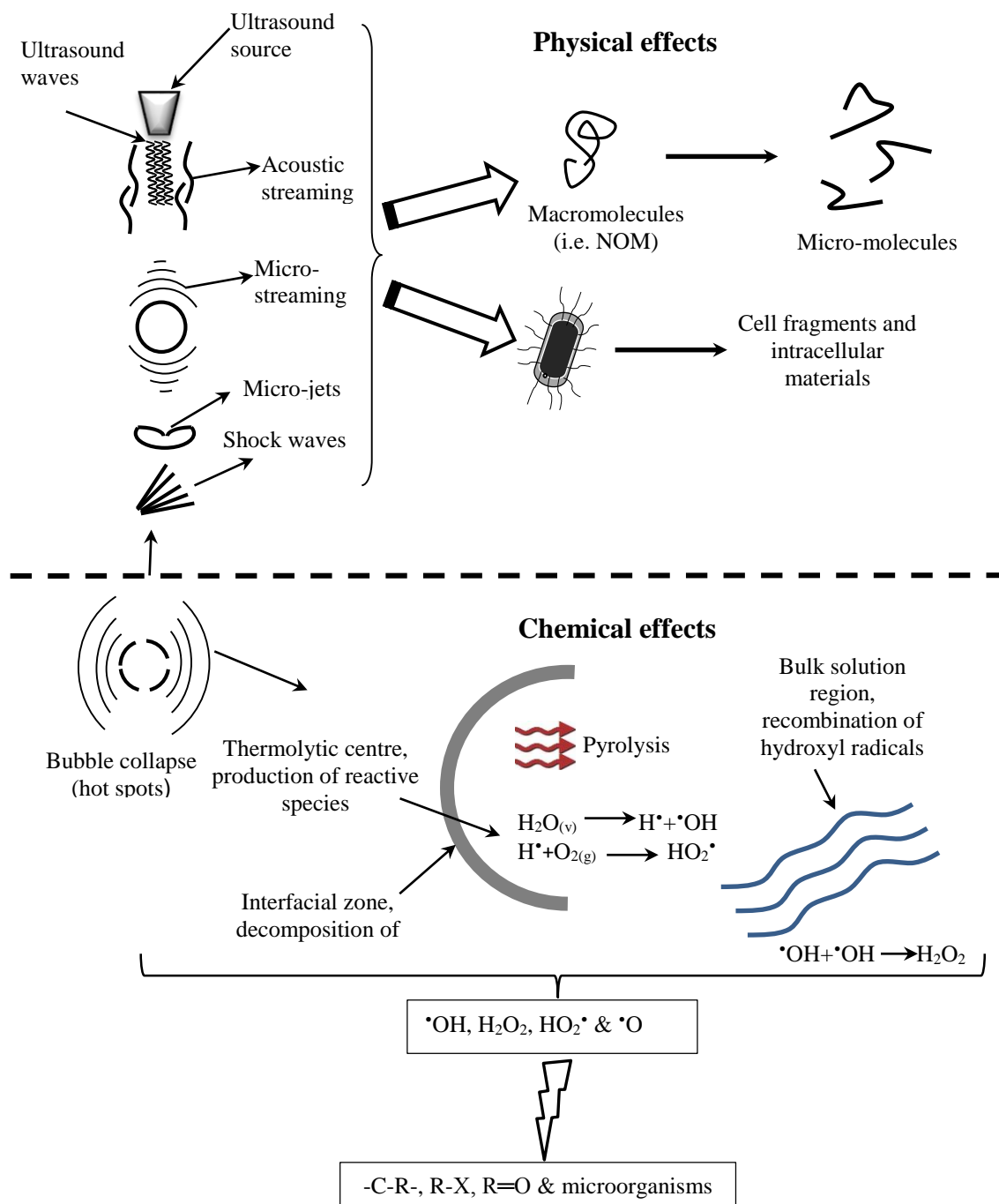**Figure 2:** Mechanisms of acoustic cavitation in degrading water pollutants.

As explained in section 2.2.1., the nonvolatile compounds in water are divided into two groups; hydrophobic and hydrophilic compounds. The repulsive nature of hydrophobic compounds to water forces these compounds to accumulate in the area adjacent to the collapsing bubbles, which in turn facilitates the ultrasonic-induced

chemical decomposition of these compounds by the free radicals as demonstrated in Figure 2.

The case is different for the nonvolatile hydrophilic compounds, as the concentration of such compounds in the sheath around the bubble is similar to that in the bulk solution region. So the hydrophilic compounds are either chemically disintegrated by reactive species and recombination oxidative agents or mechanically destructed via the mechanical shear and shock waves resulting from bubble oscillations and collapse (Henglein and Gutierrez, 1990). The shear stresses and shock waves degradation of organic materials is attributed to the slight phase difference especially for humic polymeric structures. Many researchers have pointed out the capacity of shear stresses and shockwaves on breaking the chain structure of polymeric organic materials or opening the ring structure of cyclic organic materials (Price et al., 2002, Chen et al., 2011). Additionally, the extreme conditions in the collapsing bubbles centre and the surrounding areas can lead to the formation of acids in these areas (Feng et al., 2002), which can reduce the solubility of humic acid and consequently increases its degradation by the physical effects.

3.3. Methods of producing ultrasound waves

Ultrasound waves are normally generated by converting electrical or mechanical power into vibrational power using transducers. Generally, there are three types of transducers that are used for producing ultrasound waves based on three different physical principles: liquid-driven (liquid whistle), magnetostrictive and piezoelectric transducers (Povey and Mason, 1998). A graphical representation for typical configurations of these transducers is shown in Figure 3.

In the liquid driven whistle, the vibration waves are generated due to the impact of the liquid jet on the thin metal blade as illustrated in Figure 3a. The leading end of the thin produces pressure waves as the liquid flows, while the trailing face generates cavitation (Povey and Mason, 1998). This type of transducers converts the mechanical energy into vibrational energy, while the case is different for the other two transducers where the electrical power is converted to vibrational power.

In the case of magnetostrictive transducers, the electrical current is passed through coils inducing a magnetic field that causes contraction and expansion of the ferromagnetic core (Terfenol-D of Nickel in most cases) as shown in Figure 3b. For piezoelectric transducers, the vibration is created via exciting the piezoelectric crystal with electrical current as demonstrated in Figure 3c. The last two types of transducers are the most commonly used transducers. Comprehensive comparison between the characteristics of magnetostrictive and piezoelectric transducers is provided in ***paper X***. Although the performance of magnetostrictive transducers outstrips that of piezoelectric transducers (Claeyssen et al., 1991, Claeyssen et al., 2003), there is hardly any studies concerning the use of these transducers for water treatment applications.
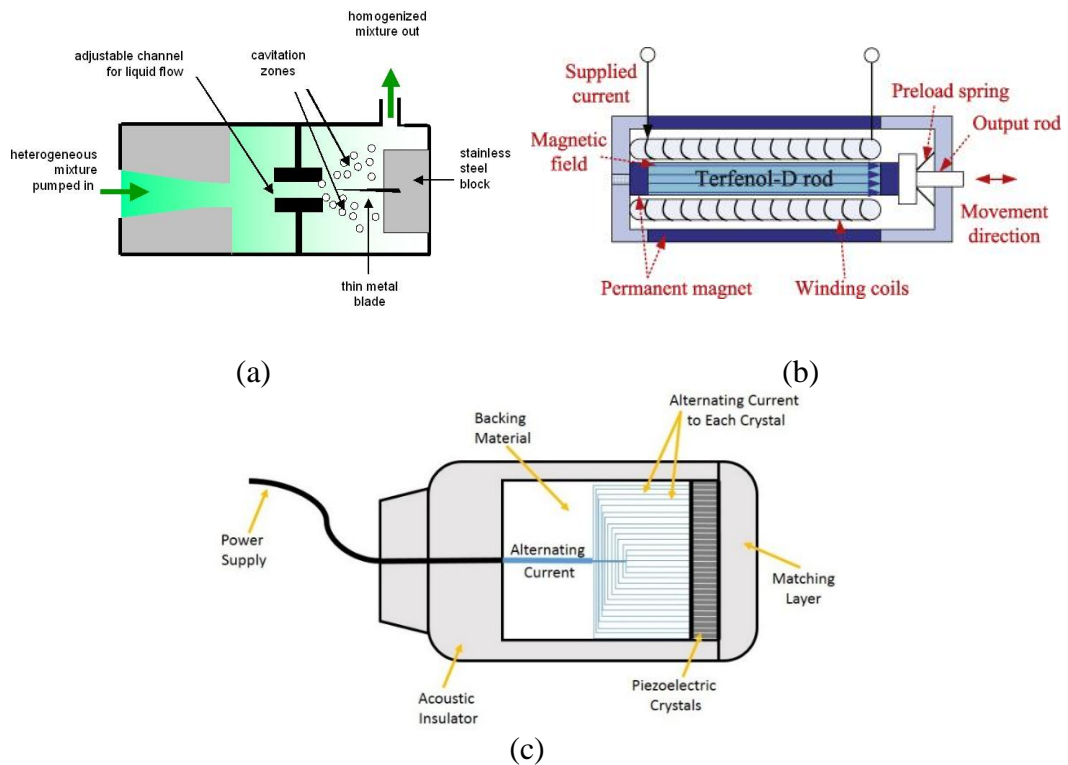
Figure 3: Typical configuration of (a) liquid whistle (The sonochemistry centre at Coventry University, 2014), (b) magnetostrictive transducer (Gu et al., 2013) and piezoelectric transducer (VAULT, 2012)

3.4. Modes of operation

Ultrasound equipment is typically operated in two modes: the standard most commonly used mode, continuous and the less popular mode, pulsed. In pulsed mode, the operation is interrupted for a pre-set amount of time. The period during which ultrasound operates is known as pulse, whereas the interruption time is normally called interval. The pulse and interval are denoted respectively as *On* and *Off* periods in this thesis. The *On:Off* ratio is commonly denoted as *R*. Operating ultrasound in a pulsed mode is more energy efficient as it minimizes the size of bubbles cloud that occurs near the irradiating surface especially at high power levels (reduction of shielding effects) (Chen et al., 2011). During the *Off* period, the ineffective cloud bubbles dissolve and/or float to the surface of the water leaving less number of ineffective bubbles close to the irradiating surface which means less energy absorbed/scattered by the bubbles (Roy, 1999) as illustrated in Figure 4. Other positive aspects of applying pulsed mode ultrasound include improvement of pollutants transport to the reaction sites of collapsing bubbles, spatial enlargement of the active zone and utilization of acoustic residual energy during the *Off* period. Detailed information regarding the performance of ultrasound system operated on pulsed mode are presented in *papers II* and *VI*. Operating ultrasound in pulsed mode also reduces temperature rise that can be undesirable for some water treatment applications such as filtration (Mason and Peters, 2002, Al-Juboori and Yusaf, 2012a). Therefore this operational mode was chosen in this study to improve the performance of surface water treatment systems.
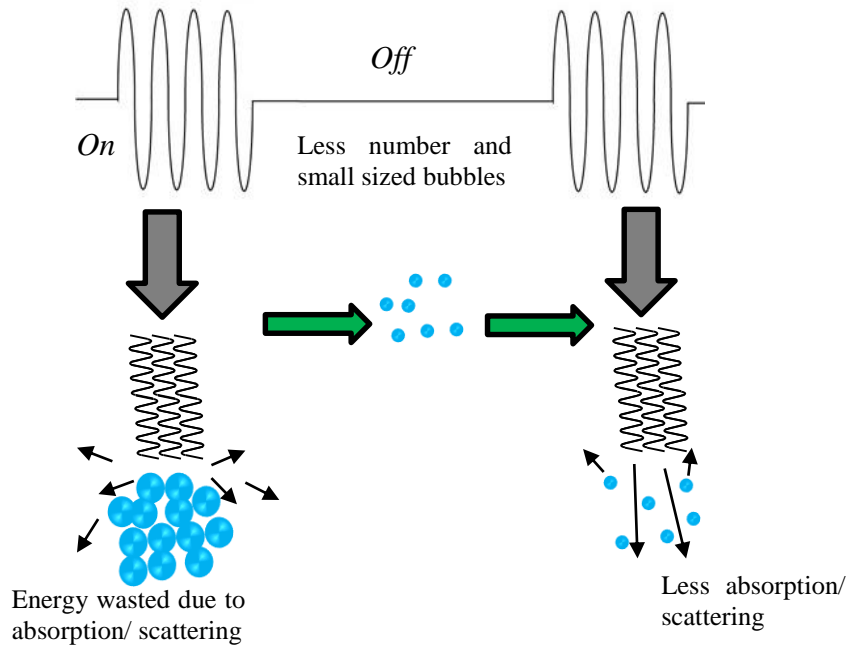
Figure 4: Illustration of pulsed mode alleviation of shielding effects

Operating ultrasound in pulsed mode does not always result in improved performance (Gutierrez and Henglein, 1990), it depends on applying a suitable power level for the chosen *R* ratio. Hence, optimizing pulse ratios and power levels are of utmost importance for pulsed ultrasound applications. Pulsed ultrasound applications for removing water contaminants was investigated by a limited number of studies such as the studies conducted by Casadonte et al. (2005) and Ashokkumar et al. (2003). These studies dealt only with synthetic water samples. So there is clearly a need for exploring the capability of pulsed ultrasound in removing natural water contaminants.

3.5. Influential parameters on ultrasound effectiveness

Like other treatment technologies the performance of ultrasound is influenced by several factors. These factors can be broken down into three groups: system operating conditions, medium characteristics and design-related aspects. The operating parameters of ultrasonic equipment include power, frequency, treatment time and shape of the exciting waves (i.e. sine, triangle etc.). The effects of these parameters on ultrasound performance in water treatment were addressed in *paper X*.

The characteristics of the medium that have an impact on ultrasound performance involve medium viscosity, pressure, temperature and contents of solid and gas impurities. The viscosity of the liquid medium has a negative effect on ultrasound performance. The propagation of sound waves through a viscous medium is hard and hence less effective acoustic events would be achieved (Leadley and Williams, 2006). However, for the case of surface water treatment few or very minor changes in the water viscosity are to be expected, so the effect of this factor is of a little concern.

The effect of the ambient pressure on ultrasound performance only becomes important when dealing with closed system treatment chambers. Increasing the ambient pressure has two conflicting effects on ultrasound performance. Increasing ambient pressure decreases the vapor content in the collapsing bubble leading to more

effective bubble collapse (Thompson and Doraiswamy, 1999). At the same time, such increases in the ambient pressure negatively affects bubble growth leading to less violent collapse (Al-Juboori and Yusaf, 2012b). Similarly, the ambient temperature has contradicting effects on ultrasound performance as increasing the temperature facilitates formation of cavitational bubbles, however the vapor content in the formed bubbles would be high (Al-Juboori and Yusaf, 2012b). It should be mentioned that increasing the ambient temperature can accelerate both microbial disruption and chemical reactions under the effect of ultrasound (Al-Juboori and Yusaf, 2012b, Thompson and Doraiswamy, 1999).

The impact of solid particles and dissolved gas bubbles on ultrasound performance depends on the nature of particles/dissolved gas and treatment purpose. Bubbles formed from gases with high specific heat ratio produce better cavitation effects than the ones generated from gases with low specific heat ratio (higher temperature and larger number of radicals) (Chen, 2011). The presence of solid particles in the water being treated by ultrasound can be beneficial if the treatment is targeting microbes' removal (Ince and Belen, 2001, Dadjour et al., 2005) or adverse if the treatment goal is DOC removal (Bossio et al., 2008). In the case of surface water treatment, the dissolved gas would mostly be air resulting in relatively high acoustic effects compared to other gases such as O_2 and Ar (Entezari et al., 1997). The presence of solids in surface water is inevitable and they would be a mixture of soil aggregates that release DOC upon ultrasound exposure (Bossio et al., 2008) and silica-like particles that promote heterogeneous cavitation (Dadjour et al., 2005).

The aspects of ultrasonic reactor design such as reactor shape and liquid height play crucial roles in the homogeneity of acoustic energy distribution and the uniformity of treatment across the treated volume. Generally, reactors with curvatures (e.g. conical or cylindrical) are more effective in utilizing ultrasound power compared to the standard rectangular shaped reactors (Capelo et al., 2005, Priego-López and Luque de Castro, 2003). The reason is the waves get reflected back from the curved walls to the water in different directions resulting in more acoustic effects. However, reactors with flat surfaces are easier to design and it less complicated to equip them with monitoring and measurements gear (Chen et al., 2011). As an example of such a design is the hexagonal reactor proposed by Gogate et al. (2003) where waves still can be reflected from the inclined walls. The liquid height has a negative effect on ultrasound performance, the further away the contaminants are from ultrasonic source the less effect the treatment has on them (Chen et al., 2011). Interestingly though, in a study conducted by Asakura et al. (2008) on the effect of liquid height on ultrasound chemical activity at different frequencies showed that at largest height investigated (500 mm), low frequency ultrasound resulted in the highest chemical throughput compared to other tested frequencies (>100 kHz). In the same manner, Sharma and Sanghi (2012) reported that low frequency results in better distribution of acoustic energy in large-scale volumes. This suggests that low frequency ultrasound operation has the potential to be successfully scaled up to industrial levels.

3.6. Ultrasound scalability in surface water treatment

The scalability of ultrasound in the field of drinking water production requires multi-disciplinary expertise such as chemistry, electrical engineering, environmental engineering, and material sciences etc. One essential step towards scalability is applying an accurate energy characterisation technique. The use of an inappropriate

characterisation method would produce discouraging energy figures that would be disincentive for industries interested in adopting ultrasound technology.

There are many techniques for determining the capacity of ultrasound equipment in converting electrical power to useful acoustic power. These techniques were reviewed in *paper I*. Among all the reported energy characterisation techniques, calorimetric technique is the most commonly used one owing to its simplicity and cost-effectiveness (Taurozzi et al., 2012). However, this technique must be carefully applied. The use of a single location for temperature measurements as being representative for the whole irradiated volume is not appropriate especially for the low power levels where standing wave effects are evident (Faïd et al., 1998). The other aspect that needs to be carefully considered is the heat loss via convection during the time of temperature recording. Convective heat loss would be more noticeable in the cases of high power application and pulsed operation. At high ultrasonic power, the temperature rise is rapid which would accelerate thermal energy dissipation through the walls of the containing vessel to the atmosphere. In the case of pulsed ultrasound, long irradiation time is required to obtain tangible temperature rise and this would allow enough time for the generated heat to escape to the atmosphere. This explains why some studies have reported efficiency as low as 30 % for ultrasonic horn (Virkutyte et al., 2010), while others reported efficiency as high as 60-70% (Löning et al., 2002) for the same reactor type as the latter used a sophisticated adiabatic reaction vessel that prevents convective heat loss. The development of an accurate energy characterisation technique is an essential pre-requisite for ultrasound use in any application.

Many attempts to scale up ultrasonic reactors were reported in the literature (Gallego-Juárez and Graff, 2014). The prominent approaches were: multistage reactors (Hulsmans et al., 2010), flow-cells (Sun, 2011), sonitube (Faïd et al., 1998), super-positioning multiple transducers of similar or different frequencies (Chen et al., 2011) and the use of reflectors (Seymour et al., 1997, Adewuyi and Oyenekan, 2007). The approach of combined multi-transducers and reflectors seems to be a promising strategy for ultrasonic reactor scale-up as the interaction of waves emitted from transducers and the reflected waves from reflectors would enlarge the active zone in the reactor. However, it is worth mentioning that most of these scale-up attempts utilized the commercially available piezoelectric transducers that operate largely on sine wave excitation. Recent studies have shown that some waveforms other than the sine wave can result in better excitation of transducers (Suomi et al., 2015). Thus, exploring the use of other transducers types and waveforms in large scale applications is imperative to provide broader options to industry and may be more efficient.

3.7. Ultrasound application in water treatment processes

3.7.1. Coagulation/flocculation

It appears from the literature that ultrasound has mainly been applied as a pre-treatment for coagulation to improve blue-green algae removal (Zhang et al., 2009). The presence of blue-green algae in the water treatment system has been associated with many problems such as clogging membrane pores, undesirable taste and odour, production of DBPs and the release of toxic compounds such as Microcystin (Lee et al., 2001). The mechanism of ultrasound used in removing algae lies in the capability of ultrasound in destroying the gas vacuoles that are responsible of algae buoyancy (Zhang et al., 2009). There is also a recent study that has utilized ultrasound as a means

of mixing for algae removal using chitosan (Fast and Gude, 2015). Removing algae requires applying low frequency, moderate input power and short treatment time (Jong Lee et al., 2000).

The application of low power ultrasound for a short treatment time in algae removal applications can solve the seasonal problem of algal bloom, but it does not tackle the problems of other forms of contamination that occur all year around. For better implementation of ultrasound in water treatment, the use of moderate to high ultrasonic power and long treatment times for solving the common problems of water treatment needs to be investigated. There is a very limited work conducted on the use of high power ultrasound in combination with coagulation such as the work performed by Ziylan and Ince (2013). However, this work only focused on DOC removal levels while DOC structural change and downstream effects of the treatment were not investigated. For proper evaluation of ultrasound treatment, the effect of the treatment on the characteristics of unremoved DOC and its downstream effects on the subsequent treatment processes should also be considered.

3.7.2. Filtration

Ultrasound technology has been harnessed by many studies for alleviating fouling problems in membrane filtration. Ultrasound-assisted membrane technology can be applied in two ways; as either a cleaning technique or pre-treatment technique. Ultrasonic cleaning of membrane filtration can be performed directly or indirectly. In direct ultrasonic-membrane cleaning, there is no barrier that isolates the membrane from ultrasound irradiation (Chen et al., 2006b, 2006c). In an indirect ultrasonic-membrane cleaning, the membrane is isolated from ultrasonic irradiation by the membrane cell body (Muthukumaran et al., 2005). Most of the reports regarding ultrasound-cleaning membranes dealt with flat sheet membranes, however, in a few cases ultrasound was also used for cleaning hollow fiber membrane modules (Li et al., 2011) and capillary membrane fibers (Naddeo et al., 2014).

Although ultrasonic cleaning has been recognized by many studies as an effective alternative to chemical cleaning (Bhatnagar and Cheung, 1994, Li et al., 2011, Krinks et al., 2015), there are still some shortcomings that limit its application in membrane fouling control. Shortcomings include the dependence of cleaning effectiveness on the distance between that effective cavitational region and membrane and the detrimental effect of ultrasound on membrane construction materials as shown in Figure 5 (Chen et al., 2006a, Chen et al., 2006c, Li et al., 2011). Deteriorating the structure of the membrane filter could potentially lead to a failure in filtration. Thus, the direct interaction between ultrasonic irradiation and membrane should be avoided in ultrasound-assisted membrane applications.

As a pre-filtration process, it was found that ultrasound is capable of reducing bio-fouling formation in membrane systems (Al-Juboori et al., 2012). Ultrasound can also remove other contaminants as indicated in Figure 2. In spite of the advantages of ultrasound as a filtration pre-treatment, there are some concerns related to the disintegration of the contaminants into smaller sizes, which may then lead to a pore-plugging type of fouling (Lim and Bai, 2003). For this reason, distancing ultrasound from the filtration process is recommended.
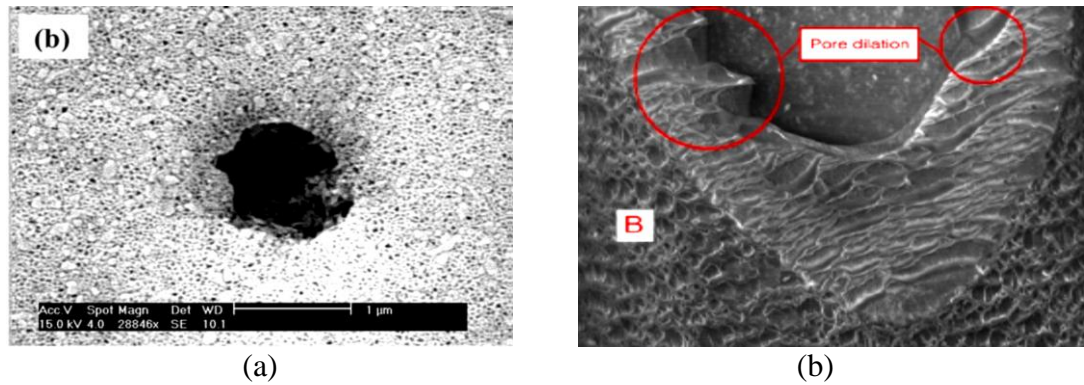
Figure 5: Ultrasound damage of (a) flat sheet membrane (Chen et al., 2006a) and (b) hollow fibre membrane (Li et al., 2011).

3.7.3. Disinfection

Ultrasound is recognized as an effective disinfection technique (Hua and Thompson, 2000, Piyasena et al., 2003, Koda et al., 2009, Gogate and Kabadi, 2009, Hulsmans et al., 2010, Al-Juboori and Yusaf, 2012b). Disinfection is typically applied after filtration at the end of the surface water treatment process. The purpose of disinfection is to disinfect water on-site and prevent microbial growth in the water while moving within the distribution network. However, as ultrasound has no residual effect as described in *paper XI*, it would be more beneficial to apply ultrasound in the earlier stages of surface water treatment.

4. Research gaps

This study was designed to investigate for the first time the use of pulsed ultrasound for treating natural water samples. From the above discussions, the research gaps in the application of ultrasound in general and the pulsed mode in particular for surface water treatment can be identified as:
1. Current ultrasonic energy characterisation methods do not account for convective heat loss that may lead to production of misleading energy figures.
2. The optimum operating conditions and location of pulsed ultrasound within the existing surface water treatment schemes have not been conclusively identified in the literature.
3. Most of the studies on ultrasound in water treatment used synthetic waters where the focus of the study centred on the effect of ultrasound on decomposition/removal of a single or known matrix of a few contaminants.
4. The research work on ultrasound application in water treatment lacks information on ultrasound effects on DOC structure.
5. Evaluation of ultrasound potential to form DBPs has not been investigated in previous studies.
6. Scaling up of ultrasound has been mostly confined to the use of commercially available transducers while there are other options that can be more efficient.

5. Research Questions

The main research questions that were addressed through the course of this study are:
- Can the convective heat loss be determined during the characterisation of ultrasonic energy?
- Where should pulsed ultrasound be applied in surface water treatment process?
- What are the effects of pulsed ultrasound on naturally occurring microbes and DOC concentration and structure in its suggested location?
- What are the downstream effects of pulsed ultrasound treatment?
- Compared to the current ultrasonic designs, is it more efficient to design large-scale ultrasonic reactors using magnetostrictive transducers?

6. Objectives of the study

The objectives of this work are:
1. Developing an energy characterisation method that can accurately evaluate the energy conversion efficiency of ultrasound transducers.
2. Identifying the optimal location and operating conditions of pulsed ultrasound for surface water treatment applications.
3. Inspecting the effect of ultrasound treatment on the concentration and structure of contaminants in the treated water.
4. Evaluating the downstream effects of pulsed ultrasound application in its suggested location within the surface water treatment scheme.
5. Investigating the possibility of scaling up ultrasound technology utilizing magnetostrictive technology with different excitation waveforms.

7. Addressing thesis objectives through publications

The first objective was successfully accomplished and the outcomes were presented in *papers I* and *II*. The convective heat loss through the reactor walls was determined using accurate temperature sensors and empirical heat transfer correlations. The efficiency of the generator, transducer and horn were evaluated by applying systematic electrical measurements. The chemical yield of ultrasonic system at various operating conditions was determined using common dosimeters such as potassium iodide (KI), Fricke solution and 4-nitrophenol. The optimum power and pulse ratio settings were identified based on sonochemical efficiency (SE) of these settings (see *paper I* for SE definition).

The second objective was addressed in *papers III* and *IV*. The optimal location of pulsed ultrasound in surface water treatment scheme was identified based on the effect of ultrasound on the concentration and nature of water contaminants (*papers III* and *IV*). In view of the importance of allochthonous DOC in surface water treatment, two surface water bodies mainly contaminated with such DOC originated from different sources such as vegetative (Pittaway pond) and terrestrial (Logan water) were used in the location optimization step. Surrogate measurements were applied to gauge whether the changes induced by ultrasound were positive or negative.

The effect of optimum power and pulse settings (***papers I*** and ***II***) on total coliform removal, DOC removal and DOC structure of natural water with DOC originating from a mixture of vegetative and terrestrial sources (Narda lagoon) was examined in ***papers V-VII*** (objective 3). Microbial and DOC removal percentages were normalized by the consumed calorimetric energy to find the most energy efficient treatment scenario. The effect of the treatment on DOC structure was regarded positive if there is a maximum decrease in hydrophobic DOC and minimum increase in hydrophilic fraction. Taking leads from the fact that the fractionation technique is a lengthy process, the correlations between DOC fractions and UV-vis indices were explored for treated Narda water in ***paper VII***. Afterward, the correlations between DOC fractions and UV-vis measurements for number of natural water bodies from the same geographical area of Narda water (Southeast Queensland) were also examined in ***paper VIII*** to confirm the validity of the obtained correlations.

The most energy efficient treatment scenario obtained from the outcomes of ***papers V-VII*** was applied as a pre-treatment for alum coagulation in ***paper IX*** (objective 4). The effect of the pre-treatment on turbidity removal, DOC removal and residual dissolved aluminum was subsequently evaluated. The trihalomethane formation potential (THMFP) and total coliform levels of treated water with coagulation only and pulsed ultrasound and coagulation were measured as indicators for the downstream effects of pulsed ultrasound applications in surface water treatment.

After confirming that ultrasound applications can significantly improve the performance of the conventional surface water treatment methods, a large-scale reactor with a maximum capacity of 17 L was designed from magnetostrictive transducers (***paper X***) (objective 5). The effects of different waveforms viz. sine, triangle and square on the performance of the large-scale system were investigated by measuring the efficiency of the system in driving chemical dosimetry reactions and removing natural water contaminants.

8. Thesis structure

Introduction
- Provide Background for research
- Identify research Gaps
- Formulate research objectives

Papers I & II

Objective 1:
- Accurate techniques for energy characterisation of a continuous ultrasound system were developed and tested.

- Ultrasonic energy conversion to physical and chemical effects in pulsed ultrasound system scrutinized.

Summary outcomes:
The most effective parameters for treatment time and amplitude including dwell time were found. Ultrasonic energy conversion of 60-70% was determined.

Papers III & IV

Objective 2:
- The Effect of ultrasound treatments on concentration and structure of allochthonous DOC of vegetative and terrestrial origins was explored using surrogate measurements.

Summary Outcomes:
- Based on surrogate measurements analyses, the optimal location of ultrasound in drinking water treatment scheme was found to be prior to coagulation/flocculation.

Papers V, V1 & VII

Objective 3:
These papers looked at Ultrasound treatment effects on:
- Microbial removal (Total coliform)
- DOC removal
- DOC structure (fractionation spectroscopic analyses)

Summary Outcomes:
- Most energy efficient parameters of ultrasound treatment times, applied power and pulse setting were determined.

Papers VIII, IX & X

Objectives 4 & 5 :
- Confirm the strong correlation between spectroscopic and fractionation measurements. Apply these observed correlations to the large scale system.

- Evaluate downstream effects of ultrasound as a pretreatment for coagulation.

- Develop a Large scale magnetostrictive ultrasonic reactor for application in industrial scale water treatment systems.

Summary Outcomes:
- improved contaminants removal, reduction of DBPs and enhanced settling of coagulation sludge

- Significant efficiency improvements in removal of natural water contaminants compared to lab scale piezoelectric ultrasonic reactors used in previous work.

Conclusions
- Summary of key outcomes from all publications.
- Recommendations for future work detailed.

9. References

Abdul Azis, P. K., Al-Tisan, I. & Sasikumar, N., "Biofouling potential and environmental factors of seawater at a desalination plant intake", Desalination, (2001), 135, 69-82.

Adewuyi, Y. G. & Oyenekan, B. A., "Optimization of a sonochemical process using a novel reactor and Taguchi statistical experimental design methodology", Industrial & engineering chemistry research, (2007), 46, 411-420.

Al-Hashimi, A. M., Mason, T. J. & Joyce, E. M., "Combined Effect of Ultrasound and Ozone on Bacteria in Water", Environmental Science & Technology, (2015), 49, 11697-11702.

Al-Juboori, R. A. & Yusaf, T., "Biofouling in RO system: Mechanisms, monitoring and controlling", Desalination, (2012a), 302, 1-23.

Al-Juboori, R. A. & Yusaf, T., "Identifying the Optimum Process Parameters for Ultrasonic Cellular Disruption of E. Coli", International Journal of Chemical Reactor Engineering, (2012b), 10, 1-32.

Al-Juboori, R. A., Yusaf, T. & Aravinthan, V., "Investigating the efficiency of thermosonication for controlling biofouling in batch membrane systems", Desalination, (2012), 286, 349-357.

Al-Juboori, R. A. & Yusaf, T. F., "Improving the performance of ultrasonic horn reactor for deactivating microorganisms in water", IOP Conference Series: Materials Science and Engineering, (2012c), 36, 1-13.

Ambashta, R. D. & Sillanpää, M., "Water purification using magnetic assistance: A review", Journal of Hazardous Materials, (2010), 180, 38-49.

Anderson, A., Reimers, R. & DeKernion, P., "A Brief Review of the Current Status of Alternatives of Chlorine Disinfection of Water", American Journal of Public Health, (1982), 72, 1290-1293.

Armstrong, G. N., Watson, I. A. & Stewart-Tull, D. E., "Inactivation of B. cereus spores on agar, stainless steel or in water with a combination of Nd:YAG laser and UV irradiation", Innovative Food Science & Emerging Technologies, (2006), 7, 94-99.

Arrojo, S. & Benito, Y., "A theoretical study of hydrodynamic cavitation", Ultrasonics Sonochemistry, (2008), 15, 203-211.

Asakura, Y., Nishida, T., Matsuoka, T. & Koda, S., "Effects of ultrasonic frequency and liquid height on sonochemical efficiency of large-scale sonochemical reactors", Ultrasonics Sonochemistry, (2008), 15, 244-250.

Ashokkumar, M., Vu, T., Grieser, F., Weerawardena, A., Anderson, N., Pilkington, N. & Dixon, D. R., "Ultrasonic treatment of Cryptosporidium oocysts", Health-related Water Microbiology, (2003), 47, 173-177.

Australian National Health and Medical Research Council 2011. Australian drinking water guidelines 6.

Ayyildiz, O., Sanik, S. & Ileri, B., "Effect of ultrasonic pretreatment on chlorine dioxide disinfection efficiency", Ultrasonics Sonochemistry, (2011), 18, 683-688.

Bhatnagar, A. & Cheung, H. M., "Sonochemical Destruction of Chlorinated C1 and C2 Volatile Organic Compounds in Dilute Aqueous Solution", Environmental Science & Technology, (1994), 28, 1481-1486.

Birkin, P. R. & Silva-Martinez, S., "A study of the effect of ultrasound on mass transport to a microelectrode", Journal of Electroanalytical Chemistry, (1996), 416, 127-138.

Blanco, J., Malato, S., Fernández-Ibañez, P., Alarcón, D., Gernjak, W. & Maldonado, M. I., "Review of feasible solar energy applications to water processes", Renewable and Sustainable Energy Reviews, (2009), 13, 1437-1445.

Bossio, J. P., Harry, J. & Kinney, C. A., "Application of ultrasonic assisted extraction of chemically diverse organic compounds from soils and sediments", Chemosphere, (2008), 70, 858-864.

Buchanan, W., Roddick, F., Porter, N. & Drikas, M., "Fractionation of UV and VUV pretreated natural organic matter from drinking water", Environmental science & technology, (2005), 39, 4647-4654.

Bustos-Terrones, Y., Rangel-Peraza, J. G., Sanhouse, A., Bandala, E. R. & Torres, L. G., "Degradation of organic matter from wastewater using advanced primary treatment by O3 and O3/UV in a pilot plant", Physics and Chemistry of the Earth, Parts A/B/C.

Capelo, J. L., Galesio, M. M., Felisberto, G. M., Vaz, C. & Pessoa, J. C., "Micro-focused ultrasonic solid–liquid extraction (μFUSLE) combined with HPLC and fluorescence detection for PAHs determination in sediments: optimization and linking with the analytical minimalism concept", Talanta, (2005), 66, 1272-1280.

Casadonte, D. J., Flores, M. & Petrier, C., "The Use of Pulsed Ultrasound Technology to Improve Environmental Remediation: A Comparative Study", Environmental Technology, (2005), 26, 1411-1418.

Chemat, F., Teunissen, P., Chemat, S. & Bartels, P., "Sono-oxidation treatment of humic substances in drinking water", Ultrasonics Sonochemistry, (2001), 8, 247-250.

Chen, D., He, Z., Weavers, L. K., Chin, Y.-P., Walker, H. W. & Hatcher, P. G., "Sonochemical reactions of dissolved organic matter", Research on Chemical Intermediates, (2004), 30, 735-753.

Chen, D., Sharma, S. K. & Mudhoo, A. (eds.) 2011. *Handbook on Applications of Ultrasound: Sonochemistry for Sustainability*: CRC Press.

Chen, D., Weavers, L. K. & Walker, H. W., "Ultrasonic control of ceramic membrane fouling by particles: Effect of ultrasonic factors", Ultrasonics Sonochemistry, (2006a), 13, 379-387.

Chen, D., Weavers, L. K. & Walker, H. W., "Ultrasonic control of ceramic membrane fouling: Effect of particle characteristics", Water Research, (2006b), 40, 840-850.

Chen, D., Weavers, L. K., Walker, H. W. & Lenhart, J. J., "Ultrasonic control of ceramic membrane fouling caused by natural organic matter and silica particles", Journal of Membrane Science, (2006c), 276, 135-144.

Chen, X., "Nanoplatform-Based Molecular Imaging", (2011), Wiley, New Jersey.

Chow, C., Fabris, R. & Drikas, M., "A rapid fractionation technique to characterise natural organic matter for the optimisation of water treatment processes", Aqua, (2004), 53, 85-92.

Claeyssen, F., Colombani, D., Tessereau, A. & Ducros, B., "Giant dynamic magnetostrain in rare earth-iron magnetostrictive materials", Magnetics, IEEE Transactions on, (1991), 27, 5343-5345.

Claeyssen, F., Lhermet, N. & Maillard, T.,"Magnetostrictive actuators compared to piezoelectric actuators". *In:* European Workshop on Smart Structures in Engineering and Technology, 2003 Giens, France. SPIE, (2003), 194-200.

Clesceri, L. S., Rice, E. W., Greenberg, A. E. & Eaton, A. D. (eds.) 2005. *Standard methods for examination of water and wastewater : centennial edition,* Washington, D.C.: American Public Health Association.

Costello, J. J., "Post precipitation in distribution systems", Journal of American Water Works Association (1984), 76**,** 46-49.

Dadjour, M. F., Ogino, C., Matsumura, S. & Shimizu, N., "Kinetics of disinfection of Escherichia coli by catalytic ultrasonic irradiation with TiO2", Biochemical Engineering Journal, (2005), 25**,** 243-248.

Delpla, I., Jung, A. V., Baures, E., Clement, M. & Thomas, O., "Impacts of climate change on surface water quality in relation to drinking water production", Environment International, (2009), 35**,** 1225-1233.

Doosti, M., Kargar, R. & Sayadi, M., "Water treatment using ultrasonic assistance: A review", Proceedings of the International Academy of Ecology and Environmental Sciences, (2012), 2**,** 96-110.

Driscoll, C. & Letterman, R., "Chemistry and Fate of Al(III) in Treated Drinking Water", Journal of Environmental Engineering, (1988), 114**,** 21-37.

Entezari, M. H., Kruus, P. & Otson, R., "The effect of frequency on sonochemical reactions III: dissociation of carbon disulfide", Ultrasonics sonochemistry, (1997), 4**,** 49-54.

Faïd, F., Contamine, F., Wilhelm, A. M. & Delmas, H., "Comparison of ultrasound effects in different reactors at 20 kHz", Ultrasonics Sonochemistry, (1998), 5**,** 119-124.

Farré, M. J., King, H., Keller, J., Gernjak, W., Knight, N., Watson, K., Shaw, G., Luesch, F., Sadler, R., Bartkow, M. & Burrell, P. 2011. Disinfection By-Products in South East Queensland: Assessing Potential Effects of Transforming Disinfectants in the SEQ Water Grid. *In:* Begbie, D. K. & Wakem, S. L. (eds.) *Urban Water Security Research Alliance Science Forum and Stakeholder Engagement, Biulding Linkages, Collaboration and Science Quality.* Brisbane, Australia: CSIRO Publishing.

Fast, S. A. & Gude, V. G., "Ultrasound-chitosan enhanced flocculation of low algal turbid waters", Journal of Industrial and Engineering Chemistry, (2015), 24**,** 153-160.

Fawell, J. & Nieuwenhuijsen, M. J., "Contaminants in drinking water: Environmental pollution and health", British Medical Bulletin, (2003), 68**,** 199-208.

Feng, R., Zhao, Y., Zhu, C. & Mason, T. J., "Enhancement of ultrasonic cavitation yield by multi-frequency sonication", Ultrasonics Sonochemistry, (2002), 9**,** 231-236.

Flemming, H.-C., "Reverse osmosis membrane biofouling", Experimental Thermal and Fluid Science, (1997), 14**,** 382-391.

Flemming, H. C., "Biofouling in water systems – cases, causes and countermeasures", Applied Microbiology and Biotechnology (2002), 59**,** 629-640.

Flint, E. B. & Suslick, K. S., "The Temperature of Cavitation", Science, (1991), 253**,** 1397-1399.

Furuta, M., Yamaguchi, M., Tsukamoto, T., Yim, B., Stavarache, C. E., Hasiba, K. & Maeda, Y., "Inactivation of Escherichia coli by ultrasonic irradiation", Ultrasonics Sonochemistry, (2004), 11**,** 57-60.

Gabelich, C. J., Yun, T. I., Coffey, B. M. & Suffet, I. H. M., "Effects of aluminum sulfate and ferric chloride coagulant residuals on polyamide membrane performance", Desalination, (2002), 150, 15-30.

Gallego-Juárez, J. A. & Graff, K. F., "Power Ultrasonics: Applications of High-Intensity Ultrasound", (2014), Elsevier Science.

Ghernaout, D., "The hydrophilic/hydrophobic ratio vs. dissolved organics removal by coagulation – A review", Journal of King Saud University - Science, (2014), 26, 169-180.

Ghosh, k. & Schnitzer, m., "Macromolecular Structures of Humic Substances", Soil Science, (1980), 129, 266-276.

Gogate, P. R., "Application of cavitational reactors for water disinfection: Current status and path forward", Journal of Environmental Management, (2007), 85, 801-815.

Gogate, P. R. & Kabadi, A. M., "A review of applications of cavitation in biochemical engineering/biotechnology", Biochemical Engineering Journal, (2009), 44, 60-72.

Gogate, P. R., Mujumdar, S. & Pandit, A. B., "Large-scale sonochemical reactors for process intensification: design and experimental validation", Journal of Chemical Technology & Biotechnology, (2003), 78, 685-693.

Gu, G.-Y., Li, Z., Zhu, L.-M. & Su, C.-Y., "A comprehensive dynamic modeling approach for giant magnetostrictive material actuators", Smart Materials and Structures, (2013), 22, 125005.

Gusbeth, C., Frey, W., Volkmann, H., Schwartz, T. & Bluhm, H., "Pulsed electric field treatment for bacteria reduction and its impact on hospital wastewater", Chemosphere, (2009), 75, 228-233.

Gutierrez, M. & Henglein, A., "Chemical action of pulsed ultrasound: observation of an unprecedented intensity effect", The Journal of Physical Chemistry, (1990), 94, 3625-3628.

Hartnett, J. P., Fridman, A., Cho, Y. I., Greene, G. A. & Bar-Cohen, A. (eds.) 2007. *Transport Phenomena in Plasma,* London, UK: Elsevier Science.

Henglein, A. & Gutierrez, M., "Chemical effects of continuous and pulsed ultrasound: a comparative study of polymer degradation and iodide oxidation", Journal of Physical Chemistry, (1990), 94, 5169-5172.

Hua, I. & Thompson, J. E., "Inactivation of Escherichia coli by sonication at discrete ultrasonic frequencies", Water Research, (2000), 34, 3888-3893.

Hulsmans, A., Joris, K., Lambert, N., Rediers, H., Declerck, P., Delaedt, Y., Ollevier, F. & Liers, S., "Evaluation of process parameters of ultrasonic treatment of bacterial suspensions in a pilot scale water disinfection system", Ultrasonics Sonochemistry, (2010), 17, 1004-1009.

Ince, N. H. & Belen, R., "Aqueous Phase Disinfection with Power Ultrasound: Process Kinetics and Effect of Solid Catalysts", Environmental Science & Technology, (2001), 35, 1885-1888.

Jong Lee, T., Nakano, K. & Matsumura, M., "A new method for the rapid evaluation of gas vacuoles regeneration and viability of cyanobacteria by flow cytometry", Biotechnology Letters, (2000), 22, 1833-1838.

Kicklighter, D. W., Hayes, D. J., McClelland, J., Peterson, B. J., McGuire, A. D. & Melillo, J. M., "Insights and issues with simulating terrestrial DOC loading of arctic river networks", Ecological Applications, (2013), 23, 1817–1836.

Kim, H.-C. & Yu, M.-J., "Characterization of natural organic matter in conventional water treatment processes for selection of treatment processes focused on DBPs control", Water Research, (2005), 39, 4779-4789.

Kim, J., Chung, Y., Shin, D., Kim, M., Lee, Y., Lim, Y. & Lee, D., "Chlorination by-products in surface water treatment process", Desalination, (2003), 151, 1-9.

Klavarioti, M., Mantzavinos, D. & Kassinos, D., "Removal of residual pharmaceuticals from aqueous systems by advanced oxidation processes", Environment International, (2009), 35, 402-417.

Knapik, H., Fernandes, C. S., de Azevedo, J., dos Santos, M., Dall'Agnol, P. & Fontane, D., "Biodegradability of anthropogenic organic matter in polluted rivers using fluorescence, UV, and BDOC measurements", Environmental Monitoring and Assessment, (2015), 187, 1-15.

Koda, S., Miyamoto, M., Toma, M., Matsuoka, T. & Maebayashi, M., "Inactivation of Escherichia coli and Streptococcus mutans by ultrasound at 500 kHz", Ultrasonics Sonochemistry, (2009), 16, 655-659.

Kondo, T., Krishna, C. M. & Riesz, P., "Free Radical Generation by Ultrasound in Aqueous Solutions of Nucleic Acid Bases and Nucleosides: An ESR and Spin-trapping Study", International Journal of Radiation Biology, (1988), 53, 331-342.

Krinks, J. K., Qiu, M., Mergos, I. A., Weavers, L. K., Mouser, P. J. & Verweij, H., "Piezoceramic membrane with built-in ultrasonic defouling", Journal of Membrane Science, (2015), 494, 130-135.

Leadley, C. E. & Williams, A. 2006. Pulsed Electric Field Processing, Power Ultrasound and Other Emerging Technologies. *In:* Brennan, J. G. (ed.) *Food Processing: Handbook.* Weinheim, Germany: WILEY-VCH Verlag GmbH & Co. KGaA.

Lee, T. J., Nakano, K. & Matsumara, M., "Ultrasonic Irradiation for Blue-Green Algae Bloom Control", Environmental Technology, (2001), 22, 383-390.

Leenheer, J. A. & Croué, J.-P., "Peer Reviewed: Characterizing Aquatic Dissolved Organic Matter", Environmental Science & Technology, (2003), 37, 18A-26A.

Li, X., Yu, J. & Nnanna, A. G. A., "Fouling mitigation for hollow-fiber UF membrane by sonication", Desalination, (2011), 281, 23-29.

Lifka, J., Ondruschka, B. & Hofmann, J., "The Use of Ultrasound for the Degradation of Pollutants in Water: Aquasonolysis – A Review", Engineering in Life Sciences, (2003), 3, 253-262.

Lim, A. L. & Bai, R., "Membrane fouling and cleaning in microfiltration of activated sludge wastewater", Journal of Membrane Science, (2003), 216, 279-290.

Löning, J.-M., Horst, C. & Hoffmann, U., "Investigations on the energy conversion in sonochemical processes", Ultrasonics Sonochemistry, (2002), 9, 169-179.

Mason, T. J., Joyce, E., Phull, S. S. & Lorimer, J. P., "Potential uses of ultrasound in the biological decontamination of water", Ultrasonics Sonochemistry, (2003), 10, 319-323.

Mason, T. J. & Peters, D., "Practical sonochemistry: Power ultrasound uses and applications", (2002), Woodhead Publishing.

Matilainen, A., Gjessing, E. T., Lahtinen, T., Hed, L., Bhatnagar, A. & Sillanpää, M., "An overview of the methods used in the characterisation of natural organic matter (NOM) in relation to drinking water treatment", Chemosphere, (2011), 83, 1431-1442.

Matilainen, A. & Sillanpää, M., "Removal of natural organic matter from drinking water by advanced oxidation processes", Chemosphere, (2010), 80, 351-365.

Motheo, A. J. & Pinhedo, L., "Electrochemical degradation of humic acid", Science of The Total Environment, (2000), 256, 67-76.

Muthukumaran, S., Kentish, S., Lalchandani, S., Ashokkumar, M., Mawson, R., Stevens, G. W. & Grieser, F., "The optimisation of ultrasonic cleaning procedures for dairy fouled ultrafiltration membranes", Ultrasonics Sonochemistry, (2005), 12, 29-35.

Naddeo, V., Belgiorno, V., Borea, L., Secondes, M. F. N. & Ballesteros, F., "Control of fouling formation in membrane ultrafiltration by ultrasound irradiation", Environmental Technology, (2014), 36, 1299-1307.

Naddeo, V., Belgiorno, V., Landi, M., Zarra, T. & Napoli, R. M. A., "Effect of sonolysis on waste activated sludge solubilisation and anaerobic biodegradability", Desalination, (2009a), 249, 762-767.

Naddeo, V., Belgiorno, V. & Napoli, R., "Behaviour of natural organic mater during ultrasonic irradiation", Desalination, (2007), 210, 175-182.

Naddeo, V., Landi, M., Belgiorno, V. & Napoli, R., "Wastewater disinfection by combination of ultrasound and ultraviolet irradiation", Journal of hazardous materials, (2009b), 168, 925-929.

Neale, P. A., Antony, A., Bartkow, M. E., Farré, M. J., Heitz, A., Kristiana, I., Tang, J. Y. M. & Escher, B. I., "Bioanalytical Assessment of the Formation of Disinfection Byproducts in a Drinking Water Treatment Plant", Environmental Science & Technology, (2012), 46, 10317-10325.

Nishida, I., "Precipitation of calcium carbonate by ultrasonic irradiation", Ultrasonics Sonochemistry, (2004), 11, 423-428.

Park, H. K., Byeon, M. S., Shin, Y. N. & Jung, D. I., "Sources and spatial and temporal characteristics of organic carbon in two large reservoirs with contrasting hydrologic characteristics", Water resources research, (2009), 45.

Piyasena, P., Mohareb, E. & McKellar, R. C., "Inactivation of microbes using ultrasound: a review", International Journal of Food Microbiology, (2003), 87, 207-216.

Povey, J. W. & Mason, T. J., "Ultrasound in Food Processing", (1998), Springer.

Price, G. J., Lenz, E. J. & Ansell, C. W. G., "The effect of high-intensity ultrasound on the ring-opening polymerisation of cyclic lactones", European Polymer Journal, (2002), 38, 1753-1760.

Priego-López, E. & Luque de Castro, M. D., "Ultrasound-assisted extraction of nitropolycyclic aromatic hydrocarbons from soil prior to gas chromatography-mass detection", Journal of Chromatography A, (2003), 1018, 1-6.

Raspati, G. S., Høvik, H. N. & Leiknes, T., "Preferential fouling of natural organic matter (NOM) fractions in submerged low-pressure membrane filtration", Desalination and Water Treatment, (2011), 34, 416-422.

Richardson, S. D., "Disinfection by-products and other emerging contaminants in drinking water", TrAC Trends in Analytical Chemistry, (2003), 22, 666-684.

Richardson, S. D., Simmons, J. E. & Rice, G., "Peer Reviewed: Disinfection Byproducts: The Next Generation", Environmental Science & Technology, (2002), 36, 198A-205A.

Riesz, P., Berdahl, D. & Christman, C., "Free radical generation by ultrasound in aqueous and nonaqueous solutions", Environmental health perspectives, (1985), 64, 233.

Roy, R. A., "Cavitation sonophysics", Sonochemistry and Sonoluminescence, (1999), 524, 25-38

404.

Sadiq, R. & Rodriguez, M. J., "Fuzzy synthetic evaluation of disinfection by-products—a risk-based indexing system", Journal of Environmental Management, (2004), 73**,** 1-13.

Sawant, S. S., Anil, A. C., Krishnamurthy, V., Gaonkar, C., Kolwalkar, J., Khandeparker, L., Desai, D., Mahulkar, A. V., Ranade, V. V. & Pandit, A. B., "Effect of hydrodynamic cavitation on zooplankton: A tool for disinfection", Biochemical Engineering Journal, (2008), 42**,** 320-328.

Seymour, J. D., Wallace, H. C. & Gupta, R. B., "Sonochemical reactions at 640 kHz using an efficient reactor. Oxidation of potassium iodide", Ultrasonics sonochemistry, (1997), 4**,** 289-293.

Sharma, S. K. & Sanghi, R., "Advances in Water Treatment and Pollution Prevention", (2012)*,* Springer Netherlands.

Sharp, E. L., Parsons, S. A. & Jefferson, B., "Seasonal variations in natural organic matter and its impact on coagulation in water treatment", Science of The Total Environment, (2006), 363**,** 183-194.

Singh, M., Singh, U., Singh, K. & Mishra, A., "Effect of 50-Hz powerline exposed magnetized water on rat kidney", Electromagnetic Biology and Medicine, (2004), 23**,** 241-249.

Soh, Y. C., Roddick, F. & van Leeuwen, J., "The impact of alum coagulation on the character, biodegradability and disinfection by-product formation potential of reservoir natural organic matter (NOM) fractions", Water Science & Technology, (2008), 58 1173–1179

Srinivasan, P., Viraraghavan, T. & Subramanian, K., "Aluminium in drinking water: An overview", WATER SA, (1999), 25**,** 47-55.

Stęgpniak, L., Kęgpa, U. & Stańczyk-Mazanek, E., "The research on the possibility of ultrasound field application in iron removal of water", Desalination, (2008), 223**,** 180-186.

Stratton, G. R., Bellona, C. L., Dai, F., Holsen, T. M. & Thagard, S. M., "Plasma-based water treatment: Conception and application of a new general principle for reactor design", Chemical Engineering Journal, (2015), 273**,** 543-550.

Sun, D. W., "Handbook of Frozen Food Processing and Packaging, Second Edition", (2011)*,* Taylor & Francis, Boca Raton, FL.

Suomi, V., Cleveland, R. & Edwards, D.,"Measuring and modelling of harmonic acoustic radiation force induced deformations". *In:* 15th International Symposium on Therapeutic Ultrasound, 2015 Utrecht, Netherlands. International Society for Therapeutic Ultrasound (ISTU), (2015), 45.

Tansel, B., "New technologies for water and wastewater treatment: a survey of recent patents", Recent Patents on Chemical Engineering, (2008), 1**,** 17-26.

Taurozzi, J., Hackley, V. & Wiesner, M., "Preparation of nanoparticle dispersions from powdered material using ultrasonic disruption", NIST Special Publication, (2012), 1200**,** 2.

Tetzlaff, D., Carey, S. & Soulsby, C., "Catchments in the future North: interdisciplinary science for sustainable management in the 21st Century", Hydrological Processes, (2013), 27**,** 635-639.

The sonochemistry centre at Coventry University. 2014. *Introduction to Sonochemistry* [Online]. Available: http://www.sonochemistry.info/introdution.htm [Accessed 09/09/2015 2015].

Thompson, L. H. & Doraiswamy, L. K., "Sonochemistry: Science and Engineering", Industrial & Engineering Chemistry Research, (1999), 38**,** 1215-1249.

VAULT. 2012. *Transducers* [Online]. Available: http://www.vaultrasound.com/educational-resources/ultrasound-physics/transducers/ [Accessed 09/09/2015 2015].

Virkutyte, J., Varma, R. S. & Jegatheesan, V., "Treatment of Micropollutants in Water and Wastewater", (2010)*,* IWA Publishing, London.

Wasana, H. S., Perera, G. R. K., De Gunawardena, P. & Bandara, J., "The impact of aluminum, fluoride, and aluminum–fluoride complexes in drinking water on chronic kidney disease", Environmental Science and Pollution Research, (2015), 22**,** 11001-11009.

Washington, J. W., "Hydrolysis rates of dissolved volatile organic compounds: principles, temperature effects and literature review", Ground Water, (1995), 33**,** 415-424.

Wingender, J. 2011. Hygienically Relevant Microorganisms in Biofilms of Man-Made Water Systems

Biofilm Highlights. *In:* Flemming, H.-C., Wingender, J. & Szewzyk, U. (eds.). Springer Berlin Heidelberg.

Wright, J., Gundry, S. & Conroy, R., "Household drinking water in developing countries: a systematic review of microbiological contamination between source and point-of-use", Tropical Medicine & International Health, (2004), 9**,** 106-117.

Xing, L., Murshed, M. F., Lo, T., Fabris, R., Chow, C. W. K., van Leeuwen, J., Drikas, M. & Wang, D., "Characterization of organic matter in alum treated drinking water using high performance liquid chromatography and resin fractionation", Chemical Engineering Journal, (2012), 192**,** 186-191.

Young, F. R., "Cavitation", (1999)*,* Imperial College Press, London.

Yusaf, T. F.,"Mechanical treatment of microorganisms using ultrasound, shock and shear technology", PhD thesis, (2011), University of Southern Queensland.

Zhang, G., Zhang, P. & Fan, M., "Ultrasound-enhanced coagulation for Microcystis aeruginosa removal", Ultrasonics Sonochemistry, (2009), 16**,** 334-338.

Zhe, C., Hong-wu, W. & Lu-ming, M., "Research progress on electrochemical disinfection technology for water treatment ", *Industrial Water & Wastewater*, (2008), 39**,** 1-5.

Ziylan, A. & Ince, N. H., "Ozonation-based advanced oxidation for pre-treatment of water with residuals of anti-inflammatory medication", Chemical Engineering Journal, (2013), 220**,** 151-160.

Zularisam, A. W., Ismail, A. F. & Salim, R., "Behaviours of natural organic matter in membrane filtration for surface water treatment — a review", Desalination, (2006), 194**,** 211-231.

Paper I

Al-Juboori, R. A., Yusaf, T., Bowtell, L. & Aravinthan, V., Energy characterisation of ultrasonic systems for industrial processes, *Ultrasonics*, (2014), 57, 18-30.

Energy characterisation of ultrasonic systems for industrial processes

Raed A. Al-Juboori [a,*], Talal Yusaf [b], Leslie Bowtell [b], Vasantha Aravinthan [a]

[a] School of Civil Engineering and Surveying, Faculty of Health, Engineering and Sciences, University of Southern Queensland, Toowoomba, 4350 QLD, Australia
[b] School of Mechanical and Electrical Engineering, Faculty of Health, Engineering and Sciences, University of Southern Queensland, Toowoomba, 4350 QLD, Australia

A B S T R A C T

Obtaining accurate power characteristics of ultrasonic treatment systems is an important step towards their industrial scalability. Calorimetric measurements are most commonly used for quantifying the dissipated ultrasonic power. However, accuracy of these measurements is affected by various heat losses, especially when working at high power densities. In this work, electrical power measurements were conducted at all locations in the piezoelectric ultrasonic system equipped with ½″ and ¾″ probes. A set of heat transfer calculations were developed to estimate the convection heat losses from the reaction solution. Chemical dosimeters represented by the oxidation of potassium iodide, Fricke solution and 4-nitrophenol were used to chemically correlate the effect of various electrical amplitudes and treatment regimes. This allowed estimation of sonochemical-efficiency (SE) and energy conversion (X_{US}) of the ultrasonic system. Results of this study showed overall conversion efficiencies of 60–70%. This correlated well with the chemical dosimeter yield curves of both organic and inorganic aqueous solutions. All dosimeters showed bubble shielding and coalescence effects at higher ultrasonic power levels, less pronounced for the ½″ probe case. SE and X_{US} values in the range of 10^{-10} mol/J and 10^{-3} J/J respectively confirmed that conversion of ultrasonic power to chemical yield declined with amplitude.

© 2014 Elsevier B.V. All rights reserved.

1. Introduction

Despite the many and varied potential applications of high power ultrasound technologies for different treatment purposes, industrial scalability of ultrasonic treatment processes is still difficult to achieve. One of the crucial elements of ultrasound scalability is the quantification of energy losses involved in the conversion of the electrical energy into several forms of mechanical energy [1]. The ultrasonic energy distribution of acoustic cavitation effects within an ultrasonic reactor is also important for scalability as this aspect allows engineers to determine the optimum operating conditions for a particular application. Furthermore, scrutinizing energy conversion in ultrasonic reactors enables researchers to rigorously compare results of different experiments and report reproducible reaction conditions [2].

For typical ultrasonic treatment systems the mains frequency electrical power is transformed electronically from low frequency (50–60 Hz) into high frequency (20–40 kHz). The input and output power to the generator and transducer is normally measured by means of wattmeters and oscilloscopes. However, measuring these

forms of power is rarely conducted due to the general difficulty of access and electrical shock hazards involved.

The correlation between the electrical power supplied to the vibrating probe and the acoustic events can be established through localized and/or bulk average techniques [3–5], which include:

(1) Physical properties measurement methods.

The propagation of ultrasound waves causes pressure variation in the irradiated medium that results in changing some properties such as the optical index of refraction [4]. This change can be detected via measuring the diffraction in an optical beam [6], schlieren visualization [7] and interferometric technique [4]. These measurements are unsuitable for high power quantification and they require sophisticated setups.

(2) Acoustic cavitation based methods.

The acoustic cavitation effects that occur inside or in the vicinity of the collapsing bubbles can be evaluated through Sonoluminescence methods, sonochemical methods or erosive and dispersive effects measurements [3]. Sonoluminescence methods are used for acquiring spatial and temporal resolution of cavitation sites. These methods have some shortcomings such

as the requirement for specific experimental conditions (i.e. transparent media under blackout), unclear mechanisms of light emission and their restriction to the events occur at the gas phase of the collapsing bubbles [3,8].

Sonochemical techniques are normally applied to measure the chemical efficiency of ultrasonic reactors using chemical probes such as oxidation of potassium iodide (KI) and Fricke solution or decomposition of macromolecules [9]. Using sonochemical techniques alone may give an under-estimation of the overall ultrasonic energy dissipated as they are only concerned with the power involved in chemical reactions [10]. The recombination of the free radicals is another limitation of these techniques [11]. Hence, performing sonochemical measurements jointly with calorimetric measurements is encouraged in the literature [12,13].

Power measurements based on dispersive and erosive effects are only correlated to the strong mechanical effects of ultrasound propagation and their measurement accuracy is negatively affected by corrosive actions of free radicals. These downsides make their application unsuitable for ultrasonic power measurements [3].

(3) Energy or flow velocity method.

These methods involve radiation force, sound pressure measurements and calorimetric techniques. The mechanism of radiation force measurement is that when an object is exposed to ultrasonic energy, the object experiences a steady force (radiation pressure force) [14]. This force is directly proportional to the applied ultrasonic power. This technique can only be used for measuring ultrasonic power in medical imaging devices below the cavitation threshold [15,16].

Measuring sound pressure using hydrophones is conducted for identifying the spatial distribution of ultrasonic pressure intensity. The fragile nature of hydrophones and their sensitivity to the interfering pressure signals of the oscillating bubbles can limit their application high power measurements [17,18].

The calorimetric measurement of ultrasonic power is based on the notion that almost all the ultrasonic power is converted into heat [19,20]. The calorimetric techniques represent the most suitable methodology for measuring high ultrasonic power due to its simplicity and cost-effectiveness. However, calorimetric measurements for high power densities can be inaccurate due to convective heat losses [18]. Because of this limitation, heat transfer models have been proposed in this work to account for such losses during calorimetric measurements. Electrical power measurements were conducted at various locations within the system and the energy conversion efficiency of all system components was evaluated. The chemical efficiency at various amplitudes for 5, 10 and 15 min was investigated using the oxidation of potassium iodide, Fricke solution and 4-nitrophenol. The ultrasonic energy fractions consumed by the chemical reactions were determined using two approaches SE and X_{US}.

2. Materials and methods

2.1. Experimental setup

The experimental setup of this study is illustrated in Fig. 1. The setup consists of electrical power measurements gears, an ultrasound horn system, cavitation chamber, temperature sensors and data acquisition system. An ultrasonic reactor with maximum power of 400 W and frequency of 20 kHz was used in this study. Two different stainless steel tapped probes; one with a diameter of ½″ and the other with diameter of ¾″ were tested. In a typical run, the horn was immersed in a steel cavitation chamber that contains deionised water at a depth of 1.5 cm.
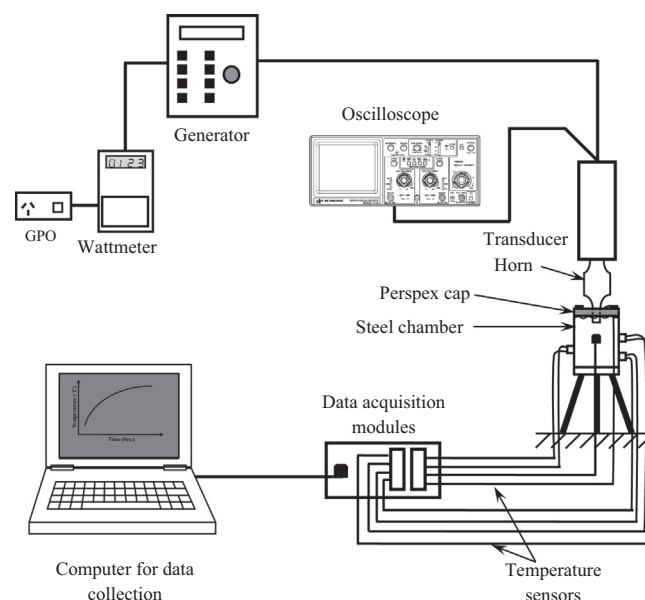

Fig. 1. Schematic of the experimental setup.

The cavitation chamber was fabricated at the workshop of the University of Southern Queensland with a capacity of 400 mL. The chamber is made of 316 stainless steel cylinder with 1 cm wall thickness. The cylinder is sealed from the bottom by a 1 cm thick 316 stainless steel disk with the use of screws and fitting O-ring. The top of the cylinder is sealed with a 2 cm thick Perspex disk. The probe is fitted through the Perspex disk with the aid of Viton O-rings. The cavitation chamber was fabricated from a thick wall steel body in order to examine the suitability of the intended calorimetric measurements in this study for the calibration of the industrial scale ultrasonic reactors where such reactors are anticipated to be made of thick metals.

Eight temperature sensors were set at various sites in and outside the chamber. Platinum thin film detectors (supplied by RS Australia) were used for measuring the temperature. These detectors are positive temperature coefficient sensors in which the resistance of the construction materials (platinum) increases linearly with temperature. These detectors have been chosen for this study due to their high stability (±0.05% as indicated by the manufacturer), ease of calibration and ability to outperform thermocouples in cavitation measurements. Thermocouples are susceptible to the corrosive action of cavitation due to their bi-metallic nature. This corrosive action causes a variable voltage to be produced which interferes with the temperature induced voltage generated by the thermocouples. Platinum films are inert to such an action, this removes one source of error when trying to estimate the actual ultrasonic energy produced. The temperature sensors were calibrated within the range of 5–100 °C using TH8000 precision immersion circulator (Ratek, Australia).

The distribution of the temperature sensors was as follows;

- Three temperature sensors were set axially underneath the irradiated surface of the vibrating probe at a distance of $\lambda/2$, $3\lambda/4$ and λ to capture the effect of the standing waves on temperature rise in the irradiated water.
- One temperature sensor was fixed close to the irradiating face of the horn where the effect of energy absorption by the bubbles is the least [21] and hence the highest temperature is expected.
- Four sensors where installed on the inner and outer surfaces of the steel cylinder and the Perspex disk.

The temperature sensors signals (resistance) were collected at a sample rate of 40 samples/s by data acquisition modules (National instrument, Australia) and recorded on a computer with the aid of Lab View software.

2.2. Power measurements

Different power measurements at various locations in the ultrasonic system were conducted in this study to identify the losses of each component in the system (see Fig. 1). The input electrical power into the generator was measured using a high precision wattmeter (EDMI MK7C Single Phase Smart Meter). The input power into the transducer was measured using a high accuracy oscilloscope (Tektronix, TDS5034B Digital Phosphor Oscilloscope) equipped with current probe (Tektronix, TCP 202) and high voltage differential probe (Tektronix, P5200). The consumed electrical power by the generator without load (when the transducer is not operating) was found to remain constant at 23.5 W. The input powers, output powers and efficiencies of the generator, transducer and the vibrating probes were determined as follows;

$$P_{G_{(in)}} = P_{W_{(L)}} - 23.5 \tag{1}$$

$$P_{G_{(out)}} = P_{OSC_{(L)}} \tag{2}$$

$$P_{T_{(in)}} = P_{OSC_{(L)}} \tag{3}$$

$$P_{T_{(out)}} = P_{OSC_{(L)}} - P_{OSC_{(0)}} \tag{4}$$

$$P_{p_{(in)}} = P_{OSC_{(L)}} - P_{OSC_{(0)}} \tag{5}$$

$$P_{p_{(out)}} = P_{cal} \tag{6}$$

$$\eta = \frac{P_{(out)}}{P_{(in)}} \tag{7}$$

where $P_{G_{(in)}}$ is the input power to the generator, $P_{W_{(L)}}$ is the reading of the wattmeter when there is a load (the case where there is a known volume of water, 400 mL is being irradiated by ultrasound), $P_{G(out)}$ is the output power of the generator, $P_{OSC_{(L)}}$ is the oscilloscope reading when there is a load, $P_{T_{(in)}}$ is the input power to the transducer, $P_{T_{(out)}}$ is the output power from the transducer, $P_{OSC_{(0)}}$ is the oscilloscope reading in the case of zero load (ultrasound irradiation in the air), and this reading represents the losses in the transducer, $P_{p_{(in)}}$ is the input power to the probe, $P_{p_{(out)}}$ is the output power from the probe and P_{cal} is the calorimetrically measured ultrasonic power which will be discussed in details in Section 3. η is the efficiency, and if it is calculated for a system component, it can be obtained by dividing the output power by the input power of the system component. If it is applied to determine the overall efficiency of the system, it can be obtained by dividing the output power to the input power of the whole system (i.e. $P_{cal}/P_{G_{(in)}}$).

3. Calorimetric energy analysis

Ultrasonic energy dissipated into the reaction solution can be measured appropriately using calorimetric measurements as most of the ultrasonic energy converts to several forms of mechanical energy that ultimately produces heat [20]. The dissipated ultrasonic power into the water (the reaction solution in this study) is converted into thermal energy that heats up the water and the components of the chamber as illustrated in Fig. 2. The dissipated ultrasonic power can be determined by performing energy balance for the water as a system as given below;

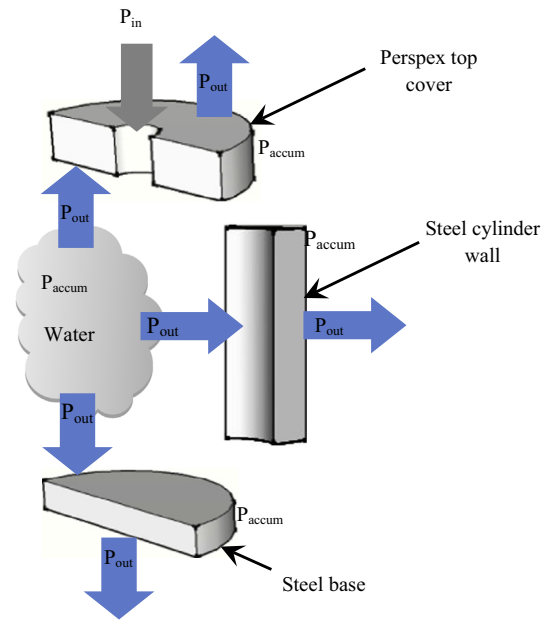$$P_{cal} = P_{out} + P_{accum} \tag{8}$$

Fig. 2. Illustration of heat transfer for the chamber.

where P_{cal} is the ultrasonic energy dissipated into water determined calorimetrically and P_{accum} is the accumulated thermal energy in water body during ultrasound treatments. The accumulated energy in water is calculated from Eq. (9)

$$P_{accum} = mC_p \, dT/dt \tag{9}$$

where m is the mass of the irradiated water (400 g), C_p is the heat capacity per unit mass of water (J/kg K) and dT/dt is the slope of the temperature rise versus time (K/s).

P_{out} is the thermal energy leaving the water to the chamber components, or in other words, it is the input energy to the chamber components. P_{out} can be determined by repeating Eq. (8) for each component. P_{accum} of each component (cylindrical steel wall and base and Perspex top cover) can be calculated using Eq. (9) by substituting the properties and the slope of the temperature versus time for each component. The mass of the steel wall and base is 3 kg and the heat capacity of the steel is 500 J/kg K [22]. The same calculation is applied to the heat accumulated in the Perspex top cover. Mass of the Perspex top cover is 203 g and the heat capacity of Perspex is 1450 J/kg K [23]. Due to the low thermal diffusivity of the Perspex (0.11×10^{-6} m²/s) and the large thickness (2 cm), the heat losses from the outer Perspex surface to the ambient via convection is very minor and can be neglected. The heat transferred from the steel surfaces to the ambient is determined using Eq. (10).

$$P_{out,steel} = \bar{h}_c A (T_w - T_\infty) \tag{10}$$

where $\bar{h}_c$ is the average convection heat transfer coefficient (W/m² K), A is the surface area of the steel cylinder and base (m²), T_w is the average temperature of the steel surface during ultrasound operation (K) and T_∞ is the ambient temperature (293 K). The average convection heat transfer coefficient for the cylindrical wall and the base can be approximated from the empirical correlations between the dimensionless numbers at film temperature equal to the average of the maximum wall temperature at a particular amplitude and the ambient temperature (293 K) as presented in Eqs. (11)–(14), respectively [24].

$$\overline{Nu_D} = 0.68 Pr^{1/2} \frac{Gr_D^{1/4}}{(0.952 + Pr)^{1/4}} \tag{11}$$

$$\overline{Nu_L} = \frac{\overline{h_c}D}{k} = 0.54Ra_L^{1/4} \tag{12}$$

$$Gr_D = \frac{g\beta(T_w - T_\infty)D^3}{v^2} \tag{13}$$

$$Ra = GrPr \tag{14}$$

where $Nu_{D,L}$ is the Nusselt number of the air film surrounding a cylinder with a diameter of D, or plate with surface area to perimeter ratio of L. Pr is the Prandtl number of the air film, which is constant at 0.71 for the temperature range recorded in this study. Gr_D is the Grashof number of the air film surrounding the chamber. Ra is the Rayleigh number. k is thermal conductivity of air film (W/m K), g is the gravitational acceleration (9.8 m/s^2), β is coefficient of thermal expansion of the air (1/K) and v is kinematic viscosity (m^2/s).

4. Validation of calorimetric analysis

In this section, the connective portion of the dissipated ultrasonic energy (P_{out} in Eq. (8)) will be calculated in some other ways depending upon the flow information inside the chamber to verify the suitability of the approach followed in the previous section. The results of this calculation will subsequently be compared to the obtained results from Eqs. (8)–(14). To determine the heat transferred from the water body to the internal cylinder wall via convection, the average heat transfer coefficient is required. The average convection heat transfer coefficient of a flow in circular geometry (the cylindrical chamber in the case of this study) for turbulent flow which is the case for most horn reactors with a small volume of the irradiated liquid can be calculated from the empirical relations between Nusselt number, Reynolds and Prandtl numbers as shown in Eq. (15).

$$\overline{Nu_D} = \frac{\overline{h_c}T}{k} = 0.023Re_D^{0.8}Pr^{0.3} \tag{15}$$

First, the type of the flow needs to be identified to confirm the suitability of applying Eq. (15), and this can be achieved from calculating Reynolds number for the flow at a certain water temperature. To calculate Reynolds number the average water circulation velocity is required, and this can be calculated from the equation below [25];

$$v_c = \frac{5 \times \text{Loop length}}{\theta_{mix}} \tag{16}$$

The loop length (henceforth denoted as L) of the ultrasonic flow in the chamber is calculated as follows;

$$L = T + 2Z \tag{17}$$

where T is the internal diameter of the chamber (m), Z is the height of the liquid (m) and θ_{mix} is the mixing time (s).

The mixing time of the circulation inside the chamber is given below [25];

$$\theta_{mix} = C_2 \left[\frac{Z^{3/2}T^3L^{-2}d_h^{-4}}{v_h^2 g^{1/2}\mu^{-2}\rho^2} \right] \tag{18}$$

C_2 is a function of the distance between the irradiating face of the horn and the base of the vessel. C_2 is expressed as;

$$C_2 = 7 \times 10^6 d^{-0.235} \tag{19}$$

where d is the distance between the horn tip and the base of the chamber (m), d_h is the diameter of the horn (m). μ and ρ are the dynamic viscosity (N s/m^2) and density (kg/m^3) of water. v_h is the mean velocity of the displaced fluid from the vibrating probe face in the case of planar wave, and it can be determined from the equation below:

$$v_h = a \times f \tag{20}$$

where f is the frequency (20 kHz) and a is amplitude of horn oscillation (m). The use of planar waves analysis in this study is justified, as spherical waves can only form when there is a large clearance between the horn and the surrounding walls of the reaction vessel [25].

The amplitude of planar waves is computed from the equation below:

$$a = \frac{1}{2\pi f}\sqrt{\frac{2I}{\rho C}} \tag{21}$$

I is the ultrasonic intensity (W/m^2) and C is the sound velocity (1500 m/s).

Reynolds number of the water circulation inside the chamber can be calculated from the circulation velocity as follows;

$$Re = \frac{\rho v_c T}{\mu} \tag{22}$$
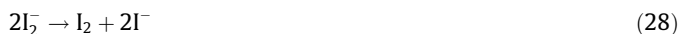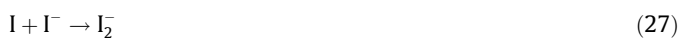
5. Chemical dosimetry

Chemical effects of ultrasound are largely related to the generation of the reactive free radicals that are produced from the thermal decomposition of water vapor and dissolved gasses during the adiabatic collapse of bubbles as shown in Eq. (23). Some of the generated radicals may react with each other or with other radicals or gases to form new radicals or oxidative agents (see Eqs. (23)–(25) [26,27]).

$$H_2O \rightarrow H^\cdot + {}^\cdot OH \tag{23}$$

$$H^\cdot + O_2 \rightarrow HOO^\cdot \tag{24}$$

$$2^\cdot OH \rightarrow H_2O_2 \tag{25}$$

The chemical effects of ultrasonic systems are normally measured via standard reaction models. The reaction models that are considered in this study are the oxidation of KI, Fricke solution and 4-nitrophenol. The energy conversion of ultrasound in oxidizing the chosen chemical probes has been investigated with ten various ultrasonic amplitudes for three treatment times; 5, 10 and 15 min. All the chemicals used in this study are analytical reagent grade (supplied by Sigma–Aldrich, Australia). The volume of reaction solution was 400 mL. Prior to ultrasound irradiation, the final KI and ferrous solutions were air-saturated by introducing filtered air bubbles into the solution for 30 min as instructed in [28,29]. For the sake of consistency, the 4-nitrophenol solution was also air saturated the same way. The presence of electron acceptor (i.e. oxygen) is important to lessen the recombination reactions between the radicals [30,31] and achieve good sonochemical yield. Besides, a study conducted by Chen and Ray [32] showed that the destruction of 4-nitrophenol with advanced oxidations reached 70% when the partial pressure of the oxygen in the solution was 0.2 atm. This signifies the suitability of using air as an economical alternative to pure oxygen in the process of oxidizing 4-nitrophenol by sonication. All of the ultrasonic treatment runs were performed under thermally controlled environment as the temperature was held at 20 ± 2°C by means of water bath to eliminate the effect of temperature on chemical yield of sonication. Ultrasound treatments at particular amplitude for a certain treatment time were conducted in triplicate. Solutions' preparation and the reaction pathways involved in the aforementioned reaction models will be explained in the following sections.

5.1. KI dosimetry

Ultrasonic irradiation of KI aqueous solution leads to the oxidation of iodine ions by the generated hydroxyl radials into iodine (reactions (26)–(28) [26]). Subsequently, iodine reacts with the excess of I^- ions producing triiodide ions as illustrated in reaction (29). The triiodide ions in the solution can be quantified spectrophotometrically at a wavelength of 355 nm with molar absorptivity (ε) = 26,303 L/mol cm [28].

$$\cdot OH + I^- \rightarrow I + OH^- \tag{26}$$

$$I + I^- \rightarrow I_2^- \tag{27}$$

$$2I_2^- \rightarrow I_2 + 2I^- \tag{28}$$

$$I^- + I_2 \rightarrow I_3^- \tag{29}$$

Potassium iodide solution was prepared by dissolving 0.1 mole of KI in 1 L deionised water. The spectrophotometric measurements in this study were performed by JENWAY UV/Vis spectrophotometer, model 6705 with a single cell holder. Quartz cuvette with path length of 1 cm was used for the spectrophotometric analysis. Deionised water was used as baseline.

5.2. Fricke dosimetry

Oxidation reaction of ferrous to ferric has been adapted in this study as an additional chemical probe besides KI oxidation owing to the importance of this reaction in industrial ultrasonic applications such as water treatment. The conversion of ferrous to ferric takes place via oxidation reactions with hydroxyl radicals as illustrated in the following reaction pathways [26,33];

$$\cdot OH + Fe^{2+} + H^+ \rightarrow Fe^{3+} + H_2O \tag{30}$$

$$HOO\cdot + Fe^{2+} + H^+ \rightarrow Fe^{3+} + H_2O_2 \tag{31}$$
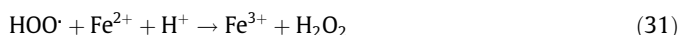
It is important to note here that the oxidation of ferrous to ferric is pH sensitive [34], and it may lead to ferric precipitation at neutral and alkaline pH. To avoid such phenomenon from happening, the oxidation of ferrous is performed in an acidic environment using the recipe of Fricke solution where ferrous ions are dissociated in diluted H_2SO_4. Fricke solution was prepared by dissolving 10^{-3} mole $Fe(NH_4)_2(SO_4)_2 \cdot 6H_2O$, 0.4 mole H_2SO_4 and 10^{-3} mole NaCl in 1 L of deionised water. The amount of the produced ferric ions was measured spectrophotometrically at wavelength 304 nm (ε = 2197 L/mol cm) [28]. However, in realty if ultrasound is used to treat natural water on a large scale, the addition of acid would be an undesirable option as it is costly, unsafe and may alter the chemistry of water in a way that disturbs the performance of other treatment processes. Therefore, to avoid the adverse effect of metals precipitation, it would be more beneficial if ultrasound treatment was applied before a settling step where the oxidized form of the metals can be safely screened.

5.3. 4-Nitrophenol dosimetry

It is important to obtain some knowledge about the chemical efficiency of ultrasound for oxidation of cyclic organic compounds such as nitrophenols, because such compounds have strong structure and they pose significant health risk in some applications (i.e. water treatment) [35]. In the present work, the oxidation of 4-nitrophenol with hydroxyl radicals induced by ultrasound to 4-nitrochatecol has been used as model reaction for cyclic organic oxidation by ultrasound (reaction (32) [36]). Reaction (32) is a

hydrogen abstraction reaction that involves the hydroxyl radial attack at the ortho position of the benzene ring.

$$\tag{32}$$
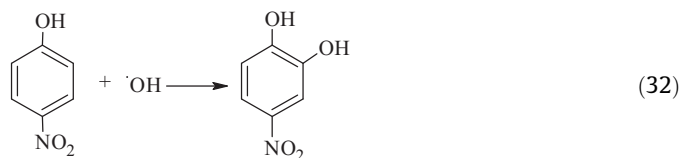
Tauber et al. [37] found that the reaction kinetics and products of 4-nitrophenol oxidation under the effect of ultrasound varies with pH of the reaction solution. It was found that 4-nitrophenol oxidized mainly by OH radicals in the aqueous phase (alkaline conditions), or pyrolytic mechanisms in gaseous phase (acidic conditions). This phenomenon provides a great opportunity to investigate the effect of various levels of ultrasonic power on the chemical activities of ultrasound in the gaseous and aqueous phases. The oxidation of 4-nitrophenol was investigated under two pH conditions; 4 and 10. 4-nitrophenol solution was prepared by dissolving 100 μmole of 4-nitrophenol in 1 L of deionised water. The production of 4-nitrocatechol was detected by the spectrophotometric measurements at wavelength 512 nm (ε = 12,500 L/mol cm) [38].

6. Results and discussions

6.1. Effect of standing waves

The effect of standing waves on temperature distribution in the reaction vessel was examined in this study as shown in Figs. 3 and 4. These figures show the temperature increment of the amplitude ranges of 10–40% for the ½″ probe and 10–30% for the ¾″ probe for a treatment time of 4 min. It appears that the standing waves effect was only detected in low amplitudes, and as the amplitude increased to higher ranges, such effect disappeared. Although standing waves effects are mostly evident in reactor configuration like cleaning bath or cup-horn [39], the temperature profiles in Figs. 3 and 4 show that such effects still occur in horn type reactor but only at the low range of ultrasonic power. The results obtained in this study are in agreement with a previous work conducted by Faïd et al. [40] as both studies showed that increasing ultrasonic power leads to the disappearance of standing waves. The standing wave effect persists up to 30% amplitudes in the case of the ½″ probe and up to 20% in the case of the ¾″ probe. It can be noticed from Figs. 3 and 4 that there is a noise in the recorded temperature signals for 10% amplitude. This noise is attributed to the irregular vibration of the irradiating face of the probe for the case of minor amplitudes [41].

The observation of standing wave effects in this study indicates that when conducting calorimetric measurements for ultrasonic power of horn reactor type, a special care needs to be paid not only to the non-uniformity of ultrasound wave emission but also to standing waves effect in low power levels. So, if the power characterisation for the full amplitude spectrum or for lower amplitudes is of interest, the use of at least three locations of temperature measurements as representative to the temperature of the irradiated liquid is important to achieve accurate measurements. Hence, for the sake of accuracy, the temperature of the irradiated water that is applied in the calorimetric measurements is taken as an average of the readings of four temperature sensors, the three axially set sensors and the sensor close to the vibrating probe (highest temperature).

6.2. Ultrasonic power quantification

Before discussing the obtained relationship between the calorimetrically measured ultrasonic power and the amplitude settings,
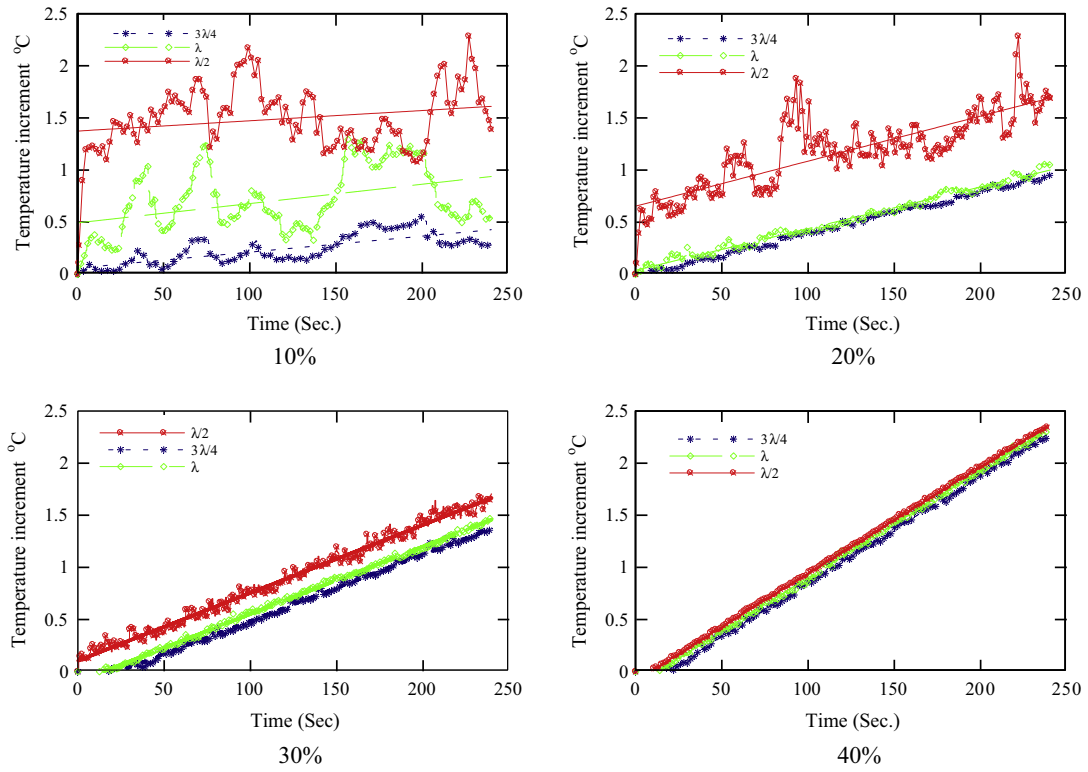
Fig. 3. Temperature variation with three different axial locations; $\lambda/2$ (○), λ (◇) and $3\lambda/4$ (✱) for the ½″ probe.
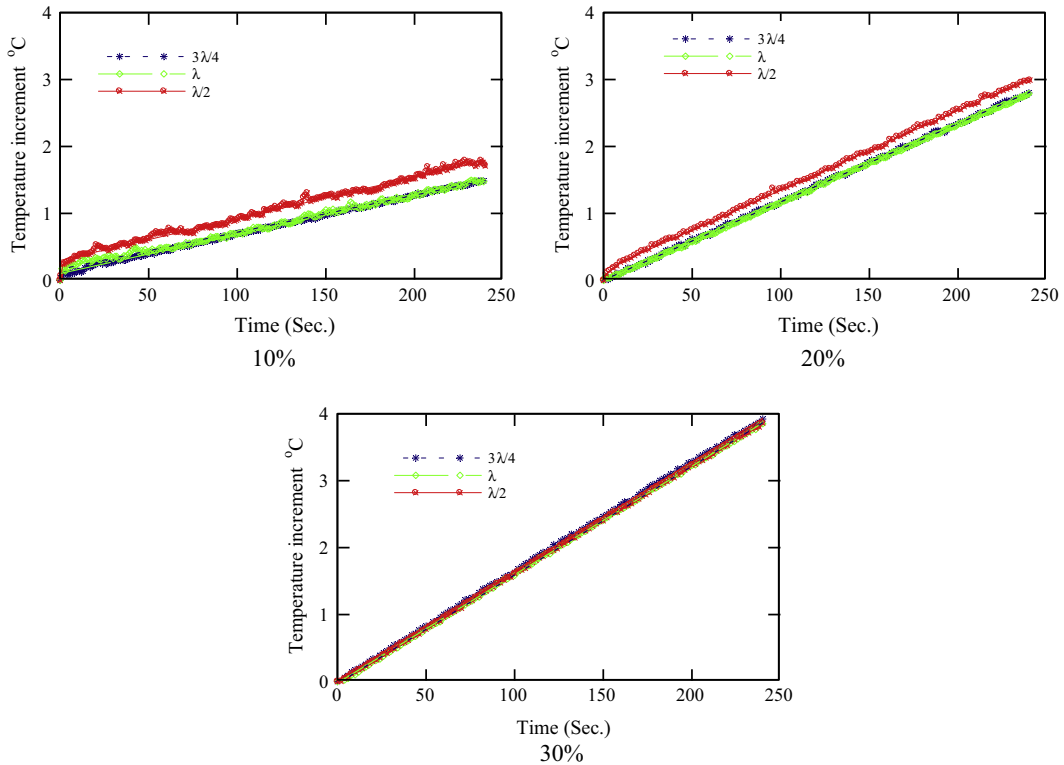

Fig. 4. Temperature variation with three different axial locations; $\lambda/2$ (○), λ (◇) and $3\lambda/4$ (✱) for the ¾″ probe.

it is important to present here the extent of the agreement between the approach followed in calculating the convection term of the heat losses (Eqs. (8)–(14)) and the validity approach (15)–(22). Table 1 shows the calculated convective heat losses from the

irradiated water during ultrasound treatment using the aforementioned approaches for the two used probes. The value of the Q_{conv} of the ½″ probe at 10% amplitude for the validity approach in Table 1 is null, and this is because the Reynolds number of this

Table 1
Convective heat losses of two vibrating probes.

Amplitude (%)	½″ probe		¾″ probe	
	Q_{conv} (W) Eqs. (8)–(14)	Q_{conv} (W) Eqs. (15)–(22)	Q_{conv} (W) Eqs. (8)–(14)	Q_{conv} (W) Eqs. (15)–(22)
10	2.8	–	6.3	6
20	5.3	6	11.6	11
30	7.8	7	16.4	16
40	9.8	10	21.1	21
50	12.6	13	25.7	25
60	17	16	32.1	32
70	19.8	20	36.4	36
80	22.5	22	43	43
90	26.2	27	45.9	46
100	30.4	30	54.3	54

amplitude falls in the intermediate region between laminar and turbulent flows and hence this approach is not valid. It is worth mentioning that the values of Q_{conv} calculated using Eqs. (15)–(22) were approximated from the figures of Q_{conv} versus time. Samples of these figures for both probes are shown below (see Fig. 5).

Table 1 confirms the validity of the applied approach in this study for estimating convective heat losses during calorimetric measurements represented by the good agreement between the values calculated using Eqs. (8)–(14) and those approximated from Fig. 5. It should be mentioned here that the calculated convective heat losses from the chamber to the air was found to be very little, about 5% of the total convective losses from water. Hence, to further simplify the approach, only applying Eq. (9) for the reaction vessel components may be sufficient for obtaining an estimation

of the convective heat losses of thick wall reaction vessels. This simple procedure and calculations can serve well the industrial need for practical ways of measuring ultrasonic power, especially at high ultrasonic powers.

So far the convective heat losses term has been quantified, this term is now added to the accumulated heat in water (Eq. (9)) to determine the converted ultrasonic power into heat (calorimetric power). Fig. 6 shows the relationship between the amplitude settings, the calorimetrically calculated ultrasonic power and the measured electrical input power to the system for the two probes used in this study.

Generally, the overall efficiency and the efficiency of the system components of the ¾″ probe are better than that of the ½″ probe. In the case of the ¾″, the overall efficiency of the ultrasonic system is about 70%, and the efficiency of the probe is fluctuating around 85%. The efficiency of the generator increases from 80% to 90% as the percentage amplitude increases from 10% to 100%. The case is exactly the opposite for the transducer as the efficiency of the transducer decreases from 98% to 90% with the increase of the percentage amplitude from 10% to 100%. In comparison, the overall efficiency of the system with the ½″ probe is around 60%. The efficiency of the horn and the generator increases from approximately 70% to 90% as the amplitude increases which coincides with a drop in the transducer efficiency from around 95% to 80%. The results presented in Fig. 7 are quite similar to the results reported by Löning et al. [2]. It is worth mentioning here that Löning et al. [2] used adiabatic reaction vessel in their work to avoid heat losses in the calorimetric measurements, and the resembling between their results and ours indicate that the heat transfer calculation applied in this study can be adapted as an alternative to the use of adiabatic vessel. Similarly, van Iersel et al. [42] reported an
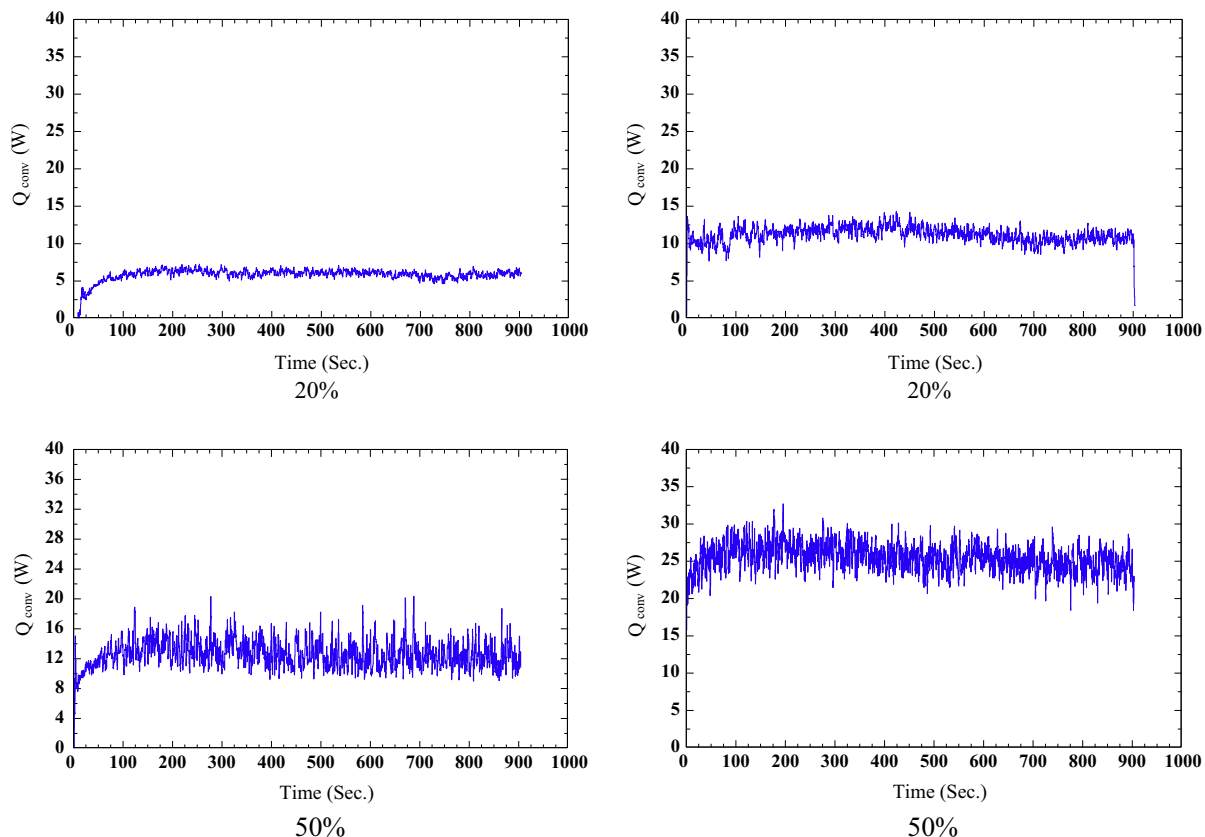

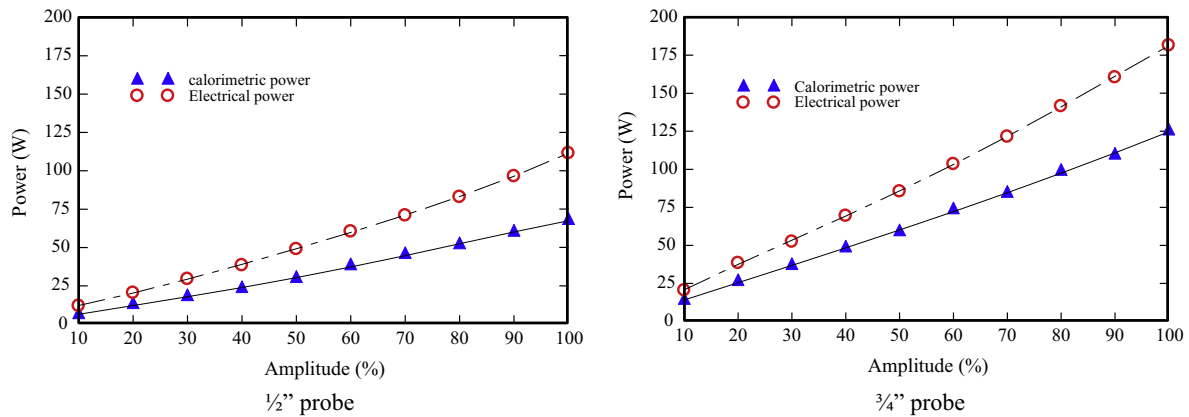**Fig. 5.** Q_{conv} versus time for the ½″ probe (left) and the ¾″ probe (right).

Fig. 6. Power measurements versus amplitude for the ½″ probe (left) and the ¾″ probe (right).

overall efficiency of ultrasonic horn system to be approximately 80% by applying calorimetric measurements using a high-pressure reaction calorimeter. The reaction calorimeter used in [42] counts for the heat losses to the reaction wall. However, the higher efficiency reported in [42] as compared to our study is attributed to the higher hydrostatic pressure applied, 5 bars as opposed to the atmospheric pressure (the case of our study). Higher hydrostatic pressure increases the cavitation threshold [43] and more ultrasonic energy is drawn from the system. The available studies on the accurate calorimetric measurements of ultrasound power uses sophisticated systems such as adiabatic vessels while the industrial needs especially high power ultrasound applications where heat losses of concern demand convenient methods of measurement that can be applied on a periodic base [44]. Thus, the calculation and the measurement procedures presented in this work are believed to be sufficient to satisfy such need with an acceptable level of accuracy.

6.3. KI dosimetry

The production of triiodide from sonication of aqueous KI solution for two probes; the ½″ and the ¾″ at different amplitudes and treatment times is depicted in Fig. 8. It can clearly be seen from Fig. 8 that the production of triodide for the two probes increases with increasing the percentage amplitude (input ultrasonic power). The triiodide yield with the ¾″ probe is at least twofold higher than that of the ½″ for the same treatment time. This is attributed to the higher ultrasonic energy dissipated into the reaction solution when ¾″ is used as compared to the ½″ probe.

The triiodide production exhibits an exponential increase where triodide concentration reaches a plateau at the end of the curve (the case of the ½″) or close to the curve end and then drops (the case of the ¾″). This observation can be explained by a number of phenomena namely decoupling, bubbles shielding and bubbles coalescence [1,45,46]. Bubbles shielding phenomenon is the occurrence of a dense cloud of bubbles close to the ultrasonic emitter that absorbs and scatters the waves. The decoupling effect becomes evident where there is large number of bubbles in the irradiated media that reduce the acoustic impedance of the medium and subsequently hinders the ultrasonic power conversion into chemical or mechanical effects [42,47]. The presence of a large number of bubbles could also lead to the coalescence of bubbles forming larger bubbles that implode less violently than the bubbles with a smaller initial size [48].

The overall efficiency of the ultrasonic system with the two probes used is constant and it did not drop at higher ultrasonic power (see Fig. 7). This means that the decoupling effect on the chemical yield of the ultrasonic system can be ruled out from the reasons given above for the chemical yield drop at higher ultrasonic power. Hence, the most likely scenarios for the chemical yield drop at high ultrasonic power are bubbles shielding and coalescence. The drop in the triiodide yield for the ¾″ probe as compared to the plateau for the ½″ is ascribed to the higher dissipated power of the ¾″ as compared to the ½″. The number of the cavitational bubbles generated is directly correlated to the dissipated ultrasonic power [10,45,49]. Such correlation has been examined in this study by determining the approximate number of bubbles in the reaction solution for the two probes. The number
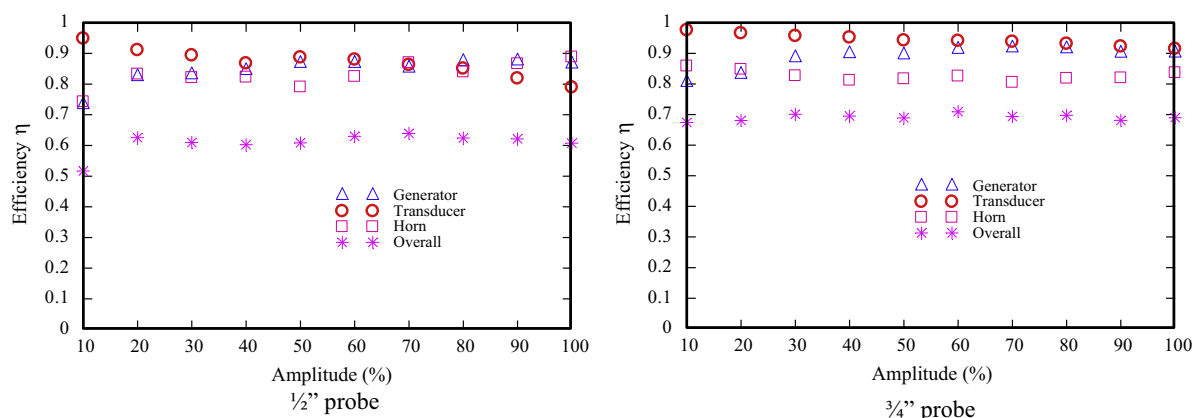

Fig. 7. Ultrasonic system components efficiencies versus amplitude for the ½″ probe (left) and the ¾″ probe (right).

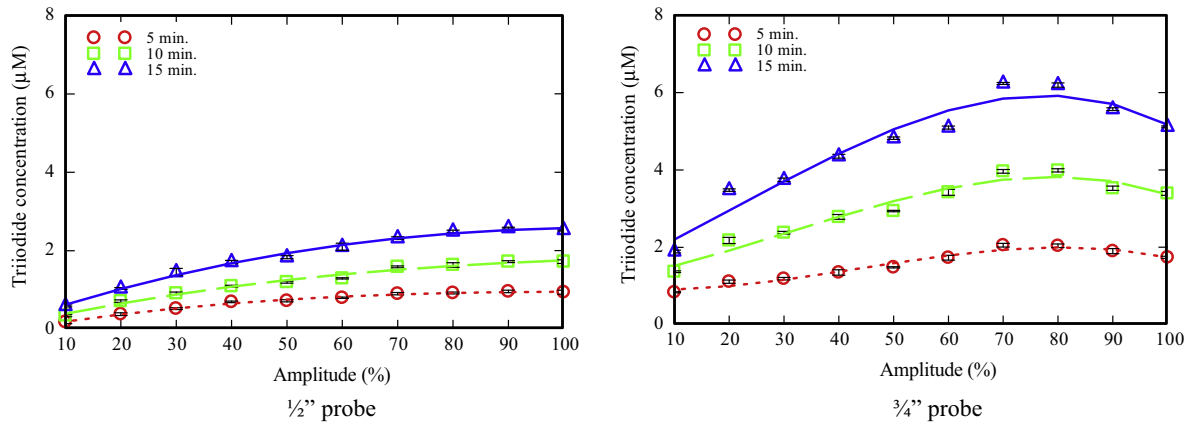**Fig. 8.** Production yield of triiodide versus percentage amplitude for the ½″ probe (left) and the ¾″ probe (right) for three treatment times; 5 min (○), 10 min (□) and 15 min (△).

of the bubbles can be estimated from the work required to expand a population of bubbles as given by Eq. (33) [50];

$$W_{cav} = 4/3\pi P(R_{max} - R_{\circ})^3 N \tag{33}$$

where W_{cav} is the work required to grow N number of bubbles, P is the sum of the acoustic and hydrostatic pressures, R_{max} is the maximum radius of the bubble before collapse and $R_{\circ}$ is the initial radius of the bubble.

The acoustic pressure can be calculated from the equation provided below;

$$P_A = \sqrt{2I\rho C} \tag{34}$$

where I is the ultrasonic power intensity (W/m^2), ρ is the density of the irradiated liquid ($\approx$1000 kg/m^3), and C is the sound speed in water ($\approx$1500 m/s).

$R_{\circ}$ is assumed to be 0.01 mm and R_{max} can be found from the following equation [51].

$$R_{max} = \frac{4}{3\omega_a}(P_A - P_h)\left[\frac{2}{\rho P_A}\right]^{0.5}\left[1 + \frac{2}{3P_h}(P_A - P_h)\right]^{0.33} \tag{35}$$

where ω_a is the angular frequency ($=2\pi f$), f is the applied acoustical frequency (Hz), P_h is the atmospheric pressure (Pa).

By assuming that all the calorimetric ultrasonic power is consumed for generating bubbles, now we can substitute the calorimetric power to replace W_{cav} in Eq. (33) to estimate the number of bubbles generated for the last four amplitude percentages of each probe (the range where shielding and coalescence observed). Fig. 9 shows the approximate number of bubbles generated for amplitude percentage range of 70–100%. It can be clearly seen that the number of bubbles generated by the ¾″ probe is higher than that of the ½″ and that explains the pronounced effects of shielding and coalescence phenomena on the ¾″ as opposed to the ½″ probe. It can also be noticed that the number of bubbles increases with increasing ultrasonic power which justifies the observation of shielding and coalescence effect at high ultrasonic power.

6.4. Fricke dosimetry

Fig. 10 shows ferric production for the ultrasonic system equipped with the ½″ and the ¾″ probes at ultrasonic amplitude percentages ranging from 10% to 100% for three treatment times of 5, 10 and 15 min. It can be noticed from Figs. 8 and 10 that the production of Fe^{3+} is higher than that of I$_3^-$ for the same operating conditions, and these results are in agreement with previous
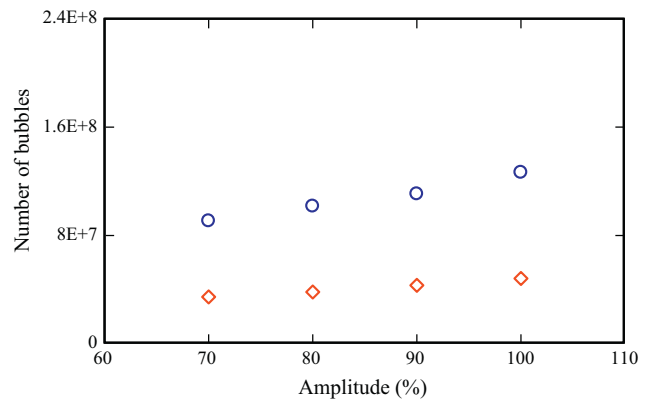

Fig. 9. Number of bubbles versus amplitude for the ½″ (◇) and the ¾″ (○) probes.

works [26,28]. This is attributed to the fact that I$_3^-$ production undergoes two stages; production of I$_2$ and then reaction with excess I$^-$, whereas Fe^{3+} production happens directly through the reaction of ferrous ions with the free radicals. It is also clear that the Fe^{3+} production is affected by the shielding and coalescence effects which were explained in the previous section.

As it was mentioned earlier that the oxidation of ferrous to ferric is an important model reaction in sonochemistry applications, it also has a special value in estimating the energy conversion of ultrasound power into chemical yield. In sonochemical studies, the term sonochemical efficiency (SE) is normally used to express the energy conversion of ultrasound into chemical effects [33]. SE is the ratio of the reacted moles toward certain ultrasonic energy (calorimetric determined energy) [28]. Kuijpers et al. [52] proposed the use of X_{US} for evaluating the efficiency of ultrasonic energy conversion into chemical effects. The unit of X_{US} is J/J, as it is a resultant of dividing the energy required to produce free radicals at a certain rate by the ultrasonic energy dissipated into the reaction solution. X_{US} can be calculated from the equation below;

$$X_{US} = \frac{1/2\Delta H dn_{rad}/dt}{P_{cal}} \tag{36}$$

where ΔH is the bond energy, dn_{rad}/dt is the radical formation rate.

The free radicals in an aqueous solution are generated from the dissociation of H–OH bond, which has bond energy of 4.99×10^5 J/mol [53]. The H–OH bond energy will be substituted in Eq. (36) to calculate X_{US}. The rate of radical formation can be estimated from
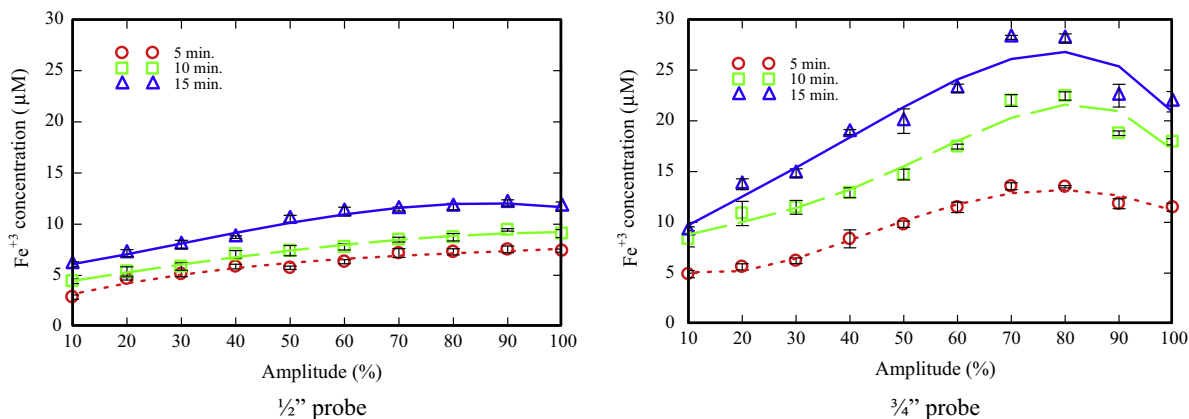
Fig. 10. Production yield of Fe^{3+} versus percentage amplitude for the ½″ probe (left) and the ¾″ probe (right) for three treatment times; 5 min (○), 10 min (□) and 15 min (△).

the production rate of Fe^{3+} for each ultrasonic power and treatment time. The radical formation rate of an irradiated aqueous solution by ultrasound under air is estimated to be half of the formation rate of Fe^{3+} [54]. The X_{US} values of various amplitude percentages for two probes; the ½″ and the ¾″ were calculated and the results are presented in Fig. 11. The data describe the relationship between the energy conversion term (X_{US}) and the percentage amplitude of the ½″ probe shows a strong agreement with the results obtained by Kuijpers et al. [52] who used a similar ultrasonic device (ultrasonic reactor with ½″ probe). It is obvious that as the amplitude increases, the energy conversion into chemical yield decreases. Fig. 11 also shows that the sharp deterioration in X_{US} as the amplitude increases is less pronounced for the ¾″ probe as compared to the ½″ probe. This indicates better chemical efficiency of ultrasound system with the ¾″ probe as opposed to the ½″ for all the range of applied amplitudes except the very low amplitude, 10%, and this trend agrees with results presented in Fig. 7.

It is important to investigate the correlation between the sosnochemical efficiency scales (i.e. SE and X_{US}) to find out whether they yield the same information. SE values of ferric formation at various amplitudes for the ½″ and the ¾″ probes have been plotted in Fig. 12. Fig. 12 shows that the SE value of Fe^{3+} is in the range of 10^{-10} mol/J, and this is in agreement with the results obtained in [28]. It can clearly be seen from Figs. 11 and 12 that SE and X_{US} show an almost identical trend of decline in the conversion efficiency of ultrasound power into chemical yield as the power increases. The high chemical efficiency of ultrasound at low

amplitudes can be explained by the enhancement of the standing wave to the chemical activity at low amplitudes (see Figs. 3 and 4) [55], which would also explain the higher SE and X_{US} for the ½″ probe as opposed to the ¾″ probe at 10% amplitude. The decrement trend in SE and X_{US} figures indicates that these two efficiency indices yield similar information and they can be used to estimate each another.

6.5. Organic dosimetry (4-nitrophenol)

The yield of 4-nitrocatchol from 4-nitrophenol under ultrasonic treatment at various amplitudes for three treatment times; 5, 10 and 15 min in alkaline and acidic environment for the ½″ and the ¾″ probes is illustrated in Fig. 13. The production of 4-nitrocatechol with various ultrasonic amplitudes in both acidic and alkaline environments seems to follow the same pattern as ferric and triiodide, as it increases with increasing the amplitude up to a limit after which the production decreases with an increase in the amplitude. The 4-nitrochatecol is produced by the hydroxyl oxidation in the aqueous phase (alkaline environment) or the pyrolytic oxidation in the gas phase (acidic environment) [37]. The variation in oxidation pathways of 4-nitrophenol can be adequately attributed to the change in ionization states and the tendency of interaction with water molecules as pH changes [31]. Lin et al. [56] provided an explanation for the difference in the sonochemical (ultrasound/H_2O_2) decomposition rates of 2-chlorophenol in acidic and alkaline environments. As pH exceeds the pKa value, the compound exists in an ionic form, but when the pH is less than the pKa
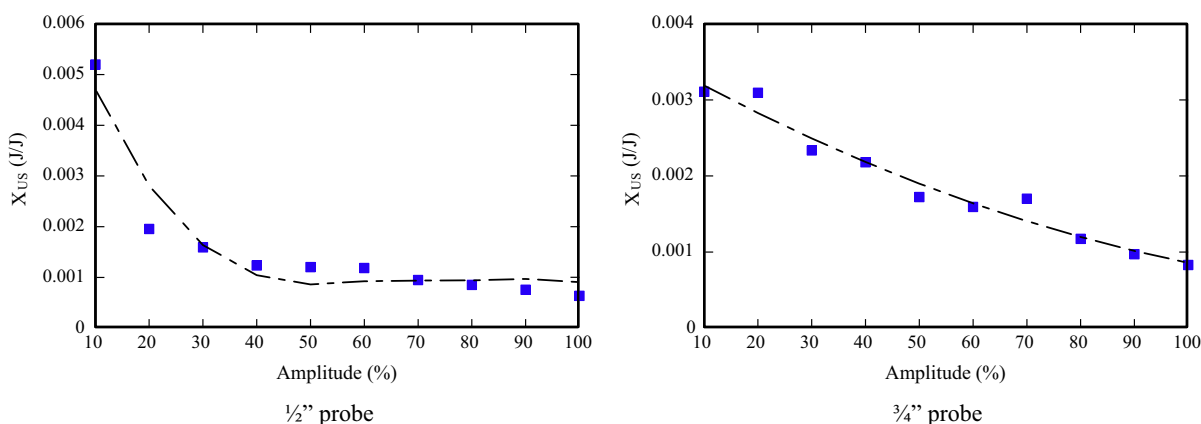

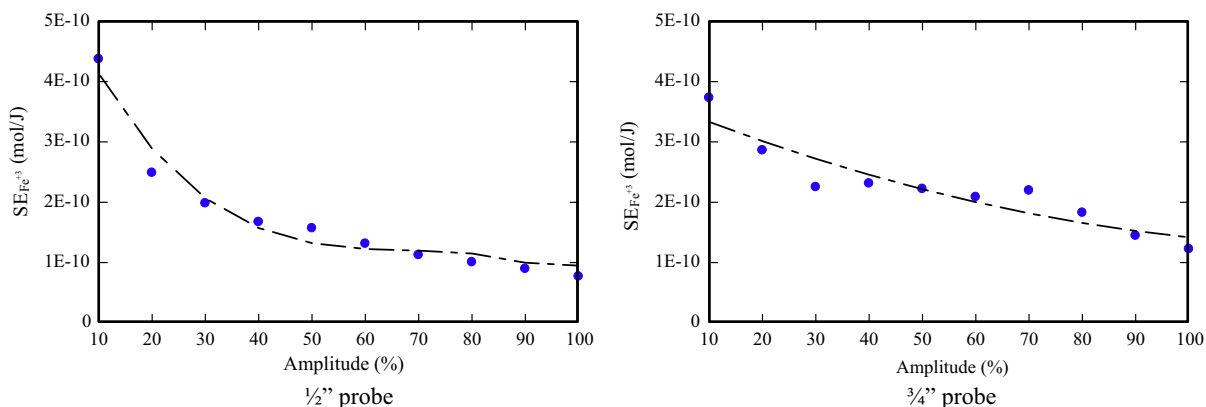**Fig. 11.** Energy conversion of ultrasound at various amplitude percentages for the ½″ probe (left) and the ¾″ probe (right).

Fig. 12. Sonochemical efficiency of ultrasound at various amplitude percentages for the ½″ probe (left) and the ¾″ probe (right).

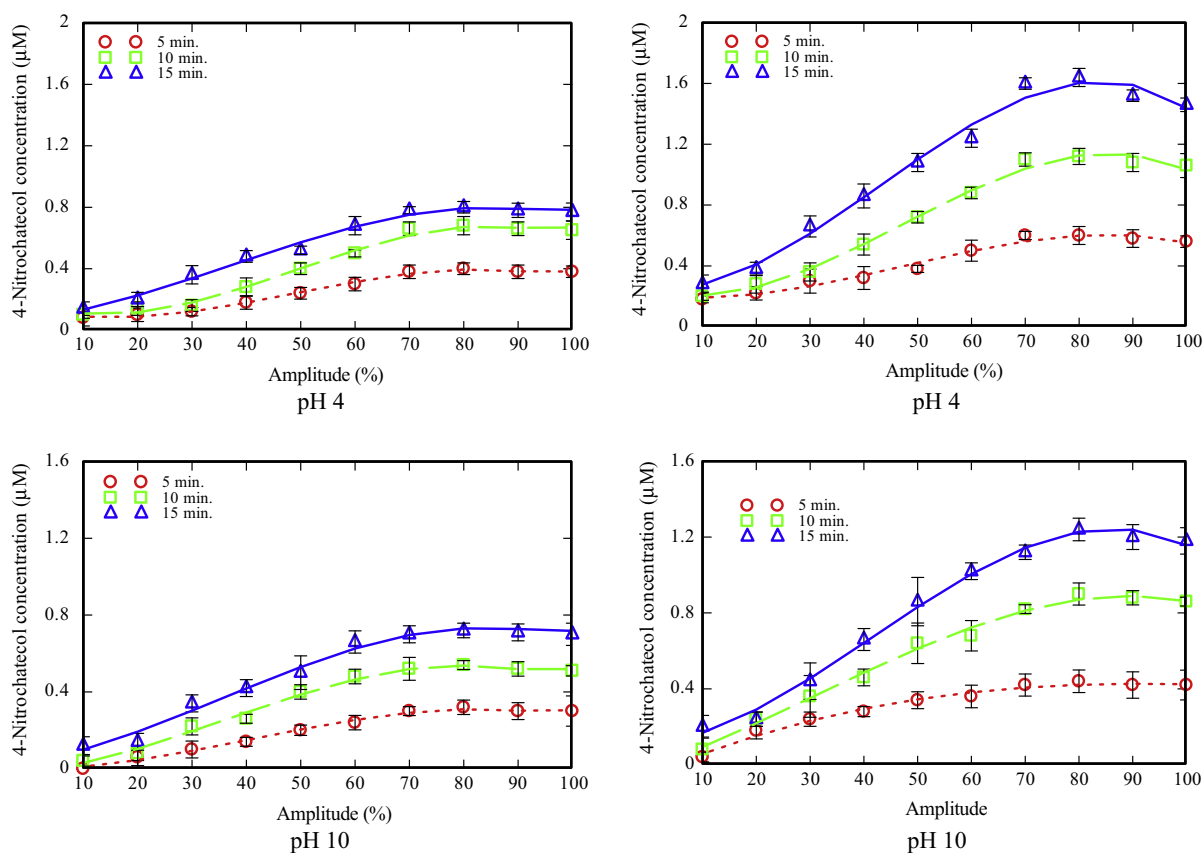**Fig. 13.** Production yield of 4-nitrochatecol versus percentage amplitude for the ½″ probe (left) and the ¾″ probe (right) for three treatment times; 5 min (○), 10 min (□) and 15 min (△) at two pH conditions; 4 and 10.

value, the compound exists in its molecular form. In the ionic form, the compound does not vaporize into the collapsing cavities and the oxidation reactions happen via hydroxyl attacks at the liquid sheath surrounding the bubble. By comparison, in the molecular form, the oxidation sites occur at both inside (pyrolysis) and outside the collapsing cavities (hydroxyl attacks). Tauber et al. [37] on the other hand attributed the pH related decomposition difference of 4-nitrophenol to the hydrophobicity enrichment of 4-nitrophenol when the pH falls below the pKa value (7.1).

Hydroxyl attack and pyrolysis represent the main decomposition mechanisms of cavitation [11]. The intensity of the hydroxyl attack is a function of the number of the hydroxyl species released into the reaction solution which is directly related to the power

dissipated into the solution. The intensity of the pyrolysis depends on the maximum temperature of the collapse which is also related to ultrasonic power as shown in Eqs. (37)–(39) [51].

$$T_{max} = T_\circ[P_m(\gamma - 1)/P] \tag{37}$$

where T_{max} is the maximum temperature obtained during bubble collapse, $T_\circ$ is the temperature of the bulk solution ($\approx$20 °C), P_m is the pressure in the liquid at the moment of collapse [57], which can be found from Eqs. (38 and 39), γ is the polytropic index of the saturating gas [11] ($\approx$1.4 for saturated solution with air) and P is the pressure in the bubble at its maximum size (usually assumed to be equal to the vapor pressure of the sonicated solution [57] which in this case is water, so $P \approx$ 2333.14 Pa [58]).

$$P_m = P_h + P_a \tag{38}$$

$$P_a = P_A \sin 2\pi ft \tag{39}$$

where t is time (s).

Hence, hydroxyl attack and pyrolysis mechanisms improve as the ultrasonic power increases, and such a trend is clearly shown in Fig. 13. However, as it was mentioned earlier that the shielding and bubbles coalescences limit the extent of the sonochemical reactions at high levels of ultrasonic power.

The results shown in Fig. 13 are in agreement with previous studies, for instance, Wu et al. [1] found that there is a similarity between the ultrasonic degradation pattern of cyclic organic compounds such as benzene and triiodide. Hua et al. [49] showed that increasing ultrasonic intensity up to a certain level increased the degradation rate of 4-nitrophenol. After this level the degradation rate decreased when the ultrasonic intensity increased. The decomposition of Rhodamine B, a wastewater organic contaminant under ultrasound irradiation was also found to have an optimum power level after which the decomposition decreases [59]. The findings of this study show that the relationship between sonochemical effects and the dissipated ultrasonic power is the same for aqueous organic and inorganic solutions. Hence, the use of simple chemical dosimetry such as the production of triiodide or ferric can be sufficient to predict the behavior of ultrasound with more complex chemical reactions such as the degradation of organic compounds, and it can also be used to identify the optimum ultrasonic power that can be applied to achieve the highest chemical throughput.

7. Feasibility of the test procedure for various ultrasonic devices

Although this study was conducted using a low frequency ultrasound device, the procedure and the theoretical calculations can readily be applied to higher frequency ultrasonic devices where the chemical yield of ultrasound is more favorable [31]. It would be beneficial to discuss here the expected outcome of the calorimetric and sonochemical measurements adopted in this study when applying them to higher frequencies ultrasonic devices. Many theoretical studies have shown that the pressure and the temperature of bubble collapse are inversely related to frequency [43,60]. This means compared to low frequency devices the calorimetric power of high frequency devices would be lower due to the lower temperature rise associated with less violent collapse, and such trends have been already observed by Asakura et al. [61]. However, as the number of collapsing bubbles of high frequency devices is expected to be greater than that of a similar powered low frequency devices, a larger number of free radicals will be produced [62]. Since SE and X_{US} of ultrasound devices is determined by dividing the number of moles produced for a certain ultrasonic power by the calorimetrically measured power, high frequency devices are expected to have higher values of SE and X_{US} than low frequency devices.

8. Conclusions

Electrical power measurements were conducted at different points in the ultrasonic system to measure the efficiency of each component of the system with two different probes; the ½″ and the ¾″. The energy dissipated into the reaction solution (deionised water) was measured calorimetrically, and the convection heat loss from the reaction solution was determined using heat transfer calculations based on the physical properties of the solution and the reaction chamber components. The results of these calculations were compared with the results obtained from another set of heat calculation based on the flow information inside the reaction chamber. The results of both calculations showed good agreement which reflects the suitability of using such calculations as a convenient alternative to the use of an adiabatic vessel in calorimetric measurements.

Chemical dosimeters using inorganic and organic solutions such as KI, Fricke and 4-nirophenol were performed for the ultrasound system at various amplitude percentages for three treatment times; 5, 10 and 15 min. The yield of triiodide, ferric and 4-nitro-catechol was shown to follow the same pattern with ultrasonic amplitude, which indicates the suitability of using the common chemical probes such as KI decomposition for predicating the ultrasonic oxidation behavior for complex organic solutions. The effect of bubbles shielding and coalescence on the chemical yield of ultrasound appeared clearly at high amplitude percentage ranges of 90% and 100% for the ½″ and the ¾″ probes. The experimental observation of bubbles shielding and coalescence was confirmed via theoretical estimation for the number of bubble generated at high amplitude percentages for the two probes used.

Sonochemical efficiency and energy conversion of the ultrasound system were determined based on the chemical yield of the dosimeters applied. Generally, both scales showed that the ultrasonic energy transformation into chemical yield decreases with an increase in the amplitude. Sonochemical efficiency and energy conversion of the used ultrasound system in this study were in the range of 10^{-10} mol/J and 10^{-3} J/J, respectively. The techniques used in this study can conveniently be applied for the calibration of various industrial scale ultrasonic reactors that operate with different parameters such as power and frequency.

Acknowledgements

References

[1] Z.L. Wu, J. Lifka, B. Ondruschka, Comparison of energy efficiency of various ultrasonic devices in aquasonochemical reactions, Chem. Eng. Technol. 29 (2006) 610–615.

[2] J.-M. Löning, C. Horst, U. Hoffmann, Investigations on the energy conversion in sonochemical processes, Ultrason. Sonochem. 9 (2002) 169–179.

[3] E.A. Neppiras, Measurement of acoustic cavitation, IEEE Trans. Sonics Ultrason. 15 (1968) 81–88.

[4] H. Stewart, Ultrasonic measurement techniques and equipment output levels, in: M. Repacholi, D. Benwell (Eds.), Essentials of Medical Ultrasound, Humana Press, 1982, pp. 77–116.

[5] V.S. Sutkar, P.R. Gogate, Design aspects of sonochemical reactors: techniques for understanding cavitational activity distribution and effect of operating parameters, Chem. Eng. J. 155 (2009) 26–36.

[6] A. Shaw, M. Hodnett, Calibration and measurement issues for therapeutic ultrasound, Ultrasonics 48 (2008) 234–252.

[7] T.L. Szabo, Diagnostic Ultrasound Imaging: Inside Out, Academic Press, New York, 2004.

[8] T.G. Leighton, A Strategy for the Development and Standardisation of Measurement Methods for High Power/Cavitating Ultrasonic Fields: Review of Cavitation Monitoring Techniques, ISVR, 1997.

[9] J. Rae, M. Ashokkumar, O. Eulaerts, C. von Sonntag, J. Reisse, F. Grieser, Estimation of ultrasound induced cavitation bubble temperatures in aqueous solutions, Ultrason. Sonochem. 12 (2005) 325–329.

[10] P.R. Gogate, I.Z. Shirgaonkar, M. Sivakumar, P. Senthilkumar, N.P. Vichare, A.B. Pandit, Cavitation reactors: efficiency assessment using a model reaction, AIChE J. 47 (2001) 2526–2538.

[11] J. González-García, V. Sáez, I. Tudela, M.I. Díez-Garcia, M. Deseada Esclapez, O. Louisnard, Sonochemical treatment of water polluted by chlorinated organocompounds. A review, Water 2 (2010) 28–74.

[12] S. de La Rochebrochard, J. Suptil, J.-F. Blais, E. Naffrechoux, Sonochemical efficiency dependence on liquid height and frequency in an improved sonochemical reactor, Ultrason. Sonochem. 19 (2012) 280–285.

[13] Y. Kojima, Y. Asakura, G. Sugiyama, S. Koda, The effects of acoustic flow and mechanical flow on the sonochemical efficiency in a rectangular sonochemical reactor, Ultrason. Sonochem. 17 (2010) 978–984.

[14] G.T. Silva, Dynamic radiation force of acoustic waves on absorbing spheres, Braz. J. Phys. 40 (2010) 184–187.

[15] K. Jaksukam, S. Umchid, A primary level ultrasonic power measurement system developed at national institute of metrology, Thailand, Int. J. Appl. Biomed. Eng. 4 (2011) 24–29.

[16] B. Karaböce, E. Sadikoğlu, E. Bilgiç, Ultrasound power measurements of HITU transducer with a more stable radiation force balance, in: Journal of Physics: Conference Series, IOP Publishing, 2011, pp. 012014.

[17] K.-S. Kim, Y. Mizuno, K. Nakamura, Fiber-optic ultrasonic hydrophone using short Fabry–Perot cavity with multilayer reflectors deposited on small stub, Ultrasonics 54 (2014) 1047–1051.

[18] R.K. Banerjee, S. Dasgupta, Characterization methods of high-intensity focused ultrasound-induced thermal field, Adv. Heat Transfer 42 (2010) 137.

[19] X. Zeng, R.J. McGough, Optimal simulations of ultrasonic fields produced by large thermal therapy arrays using the angular spectrum approach, J. Acoust. Soc. Am. 125 (2009) 2967–2977.

[20] M. Toma, S. Fukutomi, Y. Asakura, S. Koda, A calorimetric study of energy conversion efficiency of a sonochemical reactor at 500 kHz for organic solvents, Ultrason. Sonochem. 18 (2011) 197–208.

[21] M. Romdhane, A. Gadri, F. Contamine, C. Gourdon, G. Casamatta, Experimental study of the ultrasound attenuation in chemical reactors, Ultrason. Sonochem. 4 (1997) 235–243.

[22] J.R. Davis, Stainless Steels, ASM International, 1994.

[23] T.F. Yusaf, Mechanical Treatment of Microorganisms using Ultrasound, Shock and Shear Technology, University of Southern Queensland, Toowoomba, 2011.

[24] F. Kreith, Principles of Heat Transfer, seventh ed., SI ed., Cengage Learning, Stamford, CT, 2011.

[25] N.P. Vichare, P.R. Gogate, V.Y. Dindore, A.B. Pandit, Mixing time analysis of a sonochemical reactor, Ultrason. Sonochem. 8 (2001) 23–33.

[26] S. Merouani, O. Hamdaoui, F. Saoudi, M. Chiha, Influence of experimental parameters on sonochemistry dosimetries: KI oxidation, Fricke reaction and H_2O_2 production, J. Hazard. Mater. 178 (2010) 1007–1014.

[27] R. Torres, F. Abdelmalek, E. Combet, C. Pétrier, C. Pulgarin, A comparative study of ultrasonic cavitation and Fenton's reagent for bisphenol A degradation in deionised and natural waters, J. Hazard. Mater. 146 (2007) 546–551.

[28] S. Koda, T. Kimura, T. Kondo, H. Mitome, A standard method to calibrate sonochemical efficiency of an individual reaction system, Ultrason. Sonochem. 10 (2003) 149–156.

[29] K.i. Sugimoto, R. Tsujino, S. Musha, A continuous dosimeter by use of the Fricke dosimeter, Bull. Univ. Osaka Prefect. Ser. A, Eng. Nat. Sci. 11 (1963) 75–80.

[30] P.R. Gogate, A.B. Pandit, Sonophotocatalytic reactors for wastewater treatment: a critical review, AIChE J. 50 (2004) 1051–1079.

[31] Y.G. Adewuyi, Sonochemistry: environmental science and engineering applications, Ind. Eng. Chem. Res. 40 (2001) 4681–4715.

[32] D. Chen, A.K. Ray, Photodegradation kinetics of 4-nitrophenol in TiO_2 suspension, Water Res. 32 (1998) 3223–3234.

[33] G. Mark, A. Tauber, R. Laupert, H.-P. Schuchmann, D. Schulz, A. Mues, C. von Sonntag, OH-radical formation by ultrasound in aqueous solution–Part II: terephthalate and Fricke dosimetry and the influence of various conditions on the sonolytic yield, Ultrason. Sonochem. 5 (1998) 41–52.

[34] E.J. Roekens, R. Van Grieken, Kinetics of iron (II) oxidation in seawater of various pH, Mar. Chem. 13 (1983) 195–202.

[35] A.A. Pradhan, P.R. Gogate, Degradation of p-nitrophenol using acoustic cavitation and Fenton chemistry, J. Hazard. Mater. 173 (2010) 517–522.

[36] W. Zhang, X. Xiao, T. An, Z. Song, J. Fu, G. Sheng, M. Cui, Kinetics, degradation pathway and reaction mechanism of advanced oxidation of 4-nitrophenol in water by a UV/H_2O_2 process, J. Chem. Technol. Biotechnol. 78 (2003) 788–794.

[37] A. Tauber, H.-P. Schuchmann, C. von Sonntag, Sonolysis of aqueous 4-nitrophenol at low and high pH, Ultrason. Sonochem. 7 (2000) 45–52.

[38] A.O. Ifelebuegu, J. Onubogu, E. Joyce, T. Mason, Sonochemical degradation of endocrine disrupting chemicals 17β-estradiol and 17α-ethinylestradiol in water and wastewater, Int. J. Environ. Sci. Technol. 11 (2014) 1–8.

[39] R.F. Contamine, A.M. Wilhelm, J. Berlan, H. Delmas, Power measurement in sonochemistry, Ultrason. Sonochem. 2 (1995) S43–S47.

[40] F. Faïd, F. Contamine, A.M. Wilhelm, H. Delmas, Comparison of ultrasound effects in different reactors at 20 kHz, Ultrason. Sonochem. 5 (1998) 119–124.

[41] P. Boldo, V. Renaudin, N. Gondrexon, M. Chouvellon, Enhancement of the knowledge on the ultrasonic reactor behaviour by an interdisciplinary approach, Ultrason. Sonochem. 11 (2004) 27–32.

[42] M.M. van Iersel, N.E. Benes, J.T.F. Keurentjes, Importance of acoustic shielding in sonochemistry, Ultrason. Sonochem. 15 (2008) 294–300.

[43] R.A. Al-Juboori, T. Yusaf, Identifying the optimum process parameters for ultrasonic cellular disruption of *E. coli*, Int. J. Chem. Reactor Eng. 10 (2012) 1–32.

[44] T. Kimura, T. Sakamoto, J.-M. Leveque, H. Sohmiya, M. Fujita, S. Ikeda, T. Ando, Standardization of ultrasonic power for sonochemical reaction, Ultrason. Sonochem. 3 (1996) S157–S161.

[45] M. Sivakumar, A. Gedanken, Insights into the sonochemical decomposition of $Fe(CO)_5$: theoretical and experimental understanding of the role of molar concentration and power density on the reaction yield, Ultrason. Sonochem. 11 (2004) 373–378.

[46] S. Fındık, G. Gündüz, E. Gündüz, Direct sonication of acetic acid in aqueous solutions, Ultrason. Sonochem. 13 (2006) 203–207.

[47] B.P. Wilson, Ultrasound, Cavitation and Cleaning, Department of Materials Engineering, University of Wales, Swansea, 1997.

[48] R.A. Al-juboori, Ultrasound Technology as a Pre-treatment for Biofouling Control in Reverse Osmosis (RO) System, Engineering, University of Southern Queensland, Toowoomba, 2012.

[49] I. Hua, R.H. Hochemer, M.R. Hoffmann, Sonochemical degradation of p-nitrophenol in a parallel-plate near-field acoustical processor, Environ. Sci. Technol. 29 (1995) 2790–2796.

[50] V.A. Shutilov, Fundamental Physics of Ultrasound, CRC Press, 1988.

[51] Y.G. Adewuyi, Sonochemistry in environmental remediation. 1. Combinative and hybrid sonophotochemical oxidation processes for the treatment of pollutants in water, Environ. Sci. Technol. 39 (2005) 3409–3420.

[52] M. Kuijpers, M. Kemmere, J. Keurentjes, Calorimetric study of the energy efficiency for ultrasound-induced radical formation, Ultrasonics 40 (2002) 675–678.

[53] C. von Sonntag, Free-radical-induced DNA Damage and Its Repair: A Chemical Perspective, Springer, 2006.

[54] Y. Nagata, K. Hirai, H. Bandow, Y. Maeda, Decomposition of hydroxybenzoic and humic acids in water by ultrasonic irradiation, Environ. Sci. Technol. 30 (1996) 1133–1138.

[55] Y. Son, M. Lim, J. Khim, L.-H. Kim, M. Ashokkumar, Comparison of calorimetric energy and cavitation energy for the removal of bisphenol-A: the effects of frequency and liquid height, Chem. Eng. J. 183 (2012) 39–45.

[56] J.-G. Lin, C.-N. Chang, J.-R. Wu, Y.-S. Ma, Enhancement of decomposition of 2-chlorophenol with ultrasound/H_2O_2 process, Water Sci. Technol. 34 (1996) 41–48.

[57] T.J. Mason, J.P. Lorimer, Applied Sonochemistry: Uses of Power Ultrasound in Chemistry and Processing, Wiley-VCH Verlag GmbH & Co. KGaA, UK, 2003.

[58] J. Moore, C. Stanitski, P. Jurs, Chemistry: The Molecular Science, Cengage Learning, 2007.

[59] M. Sivakumar, A.B. Pandit, Ultrasound enhanced degradation of Rhodamine B: optimization with power density, Ultrason. Sonochem. 8 (2001) 233–240.

[60] C.K. Holland, R.E. Apfel, An improved theory for the prediction of microcavitation thresholds, IEEE Trans. Ultrason., Ferroelectr. Freq. Control 36 (1989) 204–208.

[61] Y. Asakura, T. Nishida, T. Matsuoka, S. Koda, Effects of ultrasonic frequency and liquid height on sonochemical efficiency of large-scale sonochemical reactors, Ultrason. Sonochem. 15 (2008) 244–250.

[62] L.A. Crum, Comments on the evolving field of sonochemistry by a cavitation physicist, Ultrason. Sonochem. 2 (1995) S147–S152.

Paper II

Al-Juboori, R. A., Yusaf, T. & Bowtell, L., Energy Conversion Efficiency of Pulsed Ultrasound, *Energy Procedia*, (2015), 75, 1560-1568.

The 7th International Conference on Applied Energy – ICAE2015

Energy Conversion Efficiency of Pulsed Ultrasound

Raed A. Al-Juboori [a]*, Talal Yusaf[b] and Leslie Bowtell[b]

a) *School of Civil Engineering and Surveying, Faculty of Health, Engineering and Sciences, University of Southern Queensland, Toowoomba, 4350 QLD Australia*

b) *School of Mechanical and Electrical Engineering, Faculty of Health, Engineering and Sciences, University of Southern Queensland, Toowoomba, 4350 QLD Australia*

Abstract

Energy characterization of a pulsed ultrasonic system was carried out using a modified calorimetric method. Sonochemical efficiency (SE) for the oxidation of Fe^{+2} and the formation of H_2O_2 was determined for selected *on:off* ratios (*R*) and different power levels. The measured efficiency of the pulsed ultrasonic system of 60-70% in converting electrical energy into calorimetric energy was found to be constant for all *R* ratios and equivalent to that for continuous operation. SE of Fe^{+2} and H_2O_2 for pulsed ultrasound was higher than that of continuous ultrasound. The ratio *R*=0.2:0.1 had the highest SE values overall, while for long off-time ratios, *R*=0.1:0.6 recorded the highest value of SE. These results were supported by the production rates results for Fe^{+2} and H_2O_2.

Keywords: Pulsed ultrasound;sonochemical effeciency; calorimetric energy; Fricke dosimeter; H_2O_2 dosimeter

1. Introduction

   Ultrasound technology refers to the use of sound energy in the frequency spectrum that exceeds the human hearing limit (> 20 kHz) [1]. Ultrasound is a chemical-free energy that can be harnessed in various applications such as water treatment [2], fuel preparation [3], food processing [4, 5] and chemical synthesis [6]. Ultrasound has the disadvantage of being high energy demand technology [4]. Therefore, the current research in ultrasound field focusses on finding ways to reduce energy requirement for this technology.

---

* Corresponding author. Tel.: +61413424126.
   E-mail address: RaedAhmed.mahmood@usq.edu.au, RaedAhmed.mahmood@gmail.com.

There are several ways suggested in the literature [4, 7] for reducing energy demand in ultrasound. One of these ways is operating ultrasound on pulsed mode (pulsed ultrasound).

Pulsed ultrasound is defined as the operation of ultrasound on a chosen *on:off* ratio *R*. The period during which ultrasound is turned on is known as pulse length whereas the off-time is known as interval length. Although pulsed ultrasound is mostly proposed as energy saving operational mode, it can be just as or even less effective than continuous ultrasound in some instances [8]. Such low efficiency of pulsed ultrasound is mostly related to the choice of operating parameters (e.g. *R* ratio, pulse length and interval length) and the way through which the energy characterisation is carried out. Hence, it is of utmost importance to scrutinize energy conversion in pulsed ultrasonic system and optimize it with regards to the aforementioned parameters. The objectives of this study are to improve on the current techniques for determining energy conversion in pulsed ultrasound and to investigate the effect of the operating conditions on the chemical yield of pulsed ultrasound. The second objective will help in identifying the optimum process parameters for pulsed ultrasound. The electrical energy conversion into vibrational energy for a low frequency high power ultrasonic horn reactor was characterized based on a modified calorimetric method reported in our previous study [9]. Sonochemical effects of ultrasound are normally determined via measuring the production of $HO^{\cdot}$ and H_2O_2 [7, 10, 11]. SE of $HO^{\cdot}$ and H_2O_2 for pulsed and continuous ultrasound were measured and the operating conditions with the highest SE were identified. The production rates of $HO^{\cdot}$ (measured from ferrous oxidation) and H_2O_2 were also determined to further understand the effect of the operating parameters on the chemical throughput of ultrasound in both modes pulsed and continuous.

Nomenclature

R	*on:off* ratio
P_{cal}	calorimetric power (W)
P_{out}	output power from the system (W)
P_{accum}	accumulated power in the system (W)
m	mass of the irradiated water (kg)
C_p	heat capacity per unit mass (J/kg.K)
dT/dt	slope of the temperature rise versus time (K/s)
$\bar{h}_c$	average convection heat transfer coefficient (W/m^2.K)
A	surface area of the cavitation chamber (m^2)
T_w	average temperature of the cavitation chamber surface (K)
T_∞	ambient temperature (K)
η	efficiency
P_{in}	input electrical power (W)
SE	sonochemical efficiency
C	concentration (mole/L)
V	volume of the treated water (L)
t	treatment time
t_p	treatment time for pulsed ultrasound
$t_\circ$	treatment time for continuous ultrasound

2. Materials and methods

2.1. Experimental setup

The system used in the experimental work is consisted of electrical power measurement equipment, ultrasonic horn reactor, temperature sensors and data acquisition system. The electrical power withdrawn

by the system components (i.e. generator, transducer and horn) was measured using a high precision wattmeter (EDMI MK7C Single Phase Smart Meter) and oscilloscope (Tektronix, TDS5034B Digital Phosphor Oscilloscope). Ultrasonic horn reactor (maximum power of 400 W, 20 kHz) equipped with 3/4″ titanium horn was used to perform the experiments. In-house fabricated stainless steel cavitation chamber was used to hold 400 mL of reaction solution. Eight calibrated platinum thin film detectors (supplied by RS Australia) were fixed in and outside the cavitation chamber to measure temperature rise of the irradiated solution and the walls of the chamber during ultrasound operation. Detailed description of the experimental setup is available in [9].

2.2. Power measurements

Electrical and calorimetric power measurements were performed on the system components to determine the energy conversion efficiency of the system as whole and its components for continuous and pulsed modes. Power measurements of the continuous mode were discussed in our previous work [9], and the results showed overall efficiency of the system between 60-70% and for system components ranged between 80-98%. To check whether efficiency figures of the continuous mode can be applied on the pulsed mode, the precision of the generator in controlling the output power needs to be tested. This was achieved by monitoring the output current wave of the generator using current probe (Tektronix, TCP 202) for two R ratios at the same power.

The temperature rise of the sonicated liquid (deionized water) and the walls of the cavitation chamber was collected to measure the calorimetric energy of ultrasound by applying energy balance on the irradiated water as follows:

$$P_{cal} = P_{out} + P_{accum} \qquad (1)$$
$$P_{accum} = m\overline{C_p}\ dT/dt \qquad (2)$$
$$P_{out} = \overline{h_c}\ A\ (T_w - T_\infty) \qquad (3)$$

The energy exiting the irradiated water is consumed in heading up the cavitation chamber. Hence, energy balance equations (1-3) can be applied on the chamber walls to calculate the convective energy lost to the atmosphere. More details on the calorimetric calculations can be found in [9]. The overall efficiency of the system is calculated from the equation bellow:

$$\eta = P_{cal}/P_{in} \qquad (4)$$

The input electrical power into the pulsed ultrasonic system was measured by averaging instantaneous power over treatment time. It is noteworthy that calorimetric measurements of long off-time ratios at low power requires long operating time to achieve tangible temperature rise in the liquid and the chamber
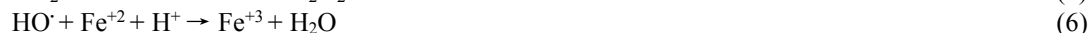
2.3. Experimental procedure

Ultrasound device was run on continuous and pulsed modes. The energy conversion efficiency of pulsed ultrasound was investigated for three groups of R ratios within 1 second time window. Long interval group include 0.1:0.8, 0.1:0.6, 0.1:0.4 and 0.1:0.2. Long pulse group include 0.8:0.1, 0.6:0.1, 0.4:0.1 and 0.2:0.1. The third group only contained one ratio of 0.1:0.1 (pulse=interval). Ultrasound was operated for 15 minutes for each R ratio and for the continuous mode at different power levels. Samples were withdrawn after each 5 minutes and the concentration of the targeted chemical species was quantified as explained in

the following section. The production rates of the chemical species were determined from the concentration vs. time curves.

2.4. Chemical dosimetry

Fricke and H_2O_2 dosimeters were applied in this study to evaluate ultrasonic energy conversion into chemical yield. Frick dosimeter is based on the oxidation of ferrous to ferric in an acidic environment under the effect of oxidants. Fricke dosimeter is used to measure the generation of $HO^{\cdot}$ and other radical species as illustrated in equations 5-7 [11]. H_2O_2 dosimeter is based on the conversion of iodine ion to triiodide ion under the oxidative effects of H_2O_2 (equations 8 and 9). Peroxide dosimeter is used to measure the recombination activity of $^{\cdot}OH$.

$$HO_2^{\cdot} + Fe^{+2} + H^+ \rightarrow Fe^{+3} + H_2O_2 \tag{5}$$
$$HO^{\cdot} + Fe^{+2} + H^+ \rightarrow Fe^{+3} + H_2O \tag{6}$$
$$H_2O_2 + Fe^{+2} + H^+ \rightarrow Fe^{+3} + H_2O + HO^{\cdot} \tag{7}$$
$$H_2O_2 + 2I^- + 2H^+ \rightarrow I_2 + 2H_2O \tag{8}$$
$$I_2 + I^- \leftrightarrow I_3^- \tag{9}$$

Fricke solution was prepared by dissolving 10^{-3} mole $Fe(NH_4)_2(SO_4)_2.6H_2O$, 0.4 mole H_2SO_4 and 10^{-3} mole NaCl in 1 L of deionised water. The amount of the produced ferric ions was measured spectrophotometrically at wavelength 304 nm ($\varepsilon = 2197$ L/mol.cm) [12]. Fricke solution was air saturated prior to ultrasound exposure by bubbling filtered air through it for 30 mins as suggested in [13].

H_2O_2 was produced by sonicating deionised water and its concentration was measured using iodometric method [14]. Aliquot sample of irradiated water was withdrawn from the reaction solution and added to the spectrophotometer cuvette that contained equal amount of solutions A and B. Solution A was prepared by dissolving 33 g of KI, 1 g of NaOH and 0.1 g of $(NH_4)6Mo_7O_{24}.4H_2O$ in 500 mL of deionised water. Solution B was prepared by dissolving 10 g of KHP in 500 mL deionized water. Solution A was always kept in the dark to avoid any inadvertent Photo-oxidation. The spectrophotometric measurements were performed using JENWAY UV/Vis spectrophotometer, model 6705 and 1 cm path length Quartz cuvette. The absorbance of Fricke solution and the mixture of A and B solutions was subtracted from the absorbance of the samples. Deionised water was used as baseline. The measurements were conducted in triplicate. All the chemicals used for the dosimetry measurements were AR grade supplied by Sigma-Aldrich and Chem-Supply, Australia.

SE of Fe^{+3} and H_2O_2 were calculated based on the yielded concentrations after 10 minutes of ultrasonic operation by applying the formula below:

$$SE = CV / P_{cal} t \tag{10}$$

3. Results and discussions

3.1. System efficiency based on calorimetric measurements

Figure 1 shows the sinusoidal current wave of pulsed ultrasound at 50% amplitude for two *R* ratios. It can be noticed from figure 1 that the generator produced precise *on:off* ratios for the supplied power. This confirms that the efficiency of the system components with continuous mode is the same as that of the pulsed mode which is supported by the overall efficiency results (Figure 2). The overall efficiency of pulsed ultrasound is slightly higher than that of continuous ultrasound due to the more sever collapse of the bubbles form at the start of each pulse as compared to collapse of the steady state bubbles (continuous ultrasound)

[15]. The results shown in figures 1 and 2 affirm that operating ultrasonic system on pulsed or continuous modes has no effect on the electrical power conversion into vibrational energy (calorimetric power). Hence, the efficiency figures of the continuous system components measured in our previous study [9] can perfectly represent the pulsed mode. The time required for pulsed ultrasound to produce the same level of energy as that of continuous ultrasound can be appropriately calculated using equation 11.

$$t_p = t \circ (1 + 1/R) \tag{11}$$

Monitoring the energy conversion in ultrasound system is an important practice for ultrasound technology especially when such technology is criticized as being high energy demand technology. This practice is mostly overlooked which leads to overestimation to the electrical power required for a particular ultrasonic application. It is also important to measure the efficiency of individual component in the ultrasonic system as this would enable manufacturers to identify the most power consuming components and improve on their performance.
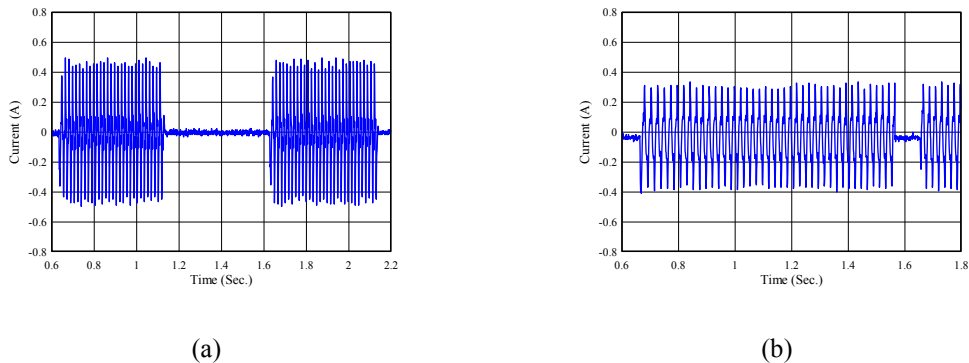

(a)   (b)

Figure 1: Sinusoidal current wave Vs. time of pulsed ultrasound for a) *R*=0.5:0.5 and b) *R*=0.9:0.1
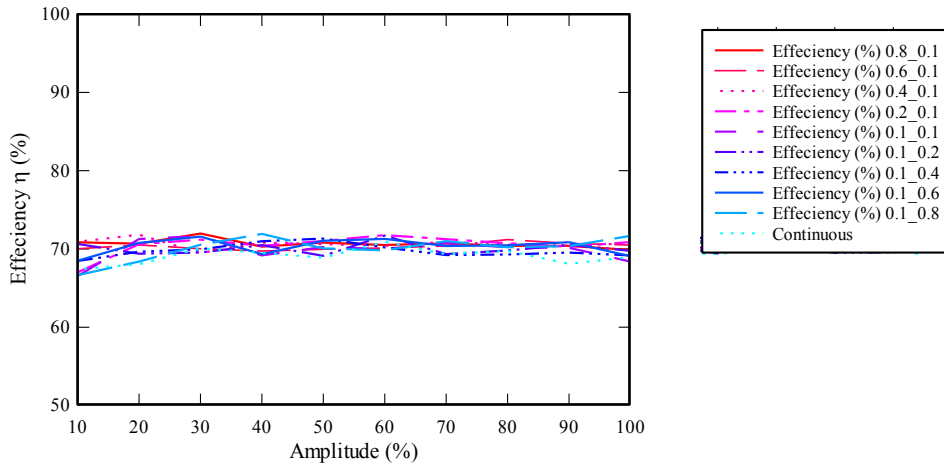

Figure 2: Overall efficiency of ultrasound with continuous and pulsed mode

3.2. Sonochemical efficiency

Sonochemical efficiency of ferric denoted as SE_{Fe+3} for continuous and pulsed ultrasound at various amplitude percentages are shown in Figure 3a. Generally, SE_{Fe+3} of pulsed ultrasound for all the examined R ratios showed a multiple fold increase as compared to continuous ultrasound over the amplitude range of 10-100%. The increase of Fe^{+3} yield in pulsed ultrasound reflects an increase in the production of free radicals and their recombination products (equations 5-9). This trend is supported by the results of the SE for H_2O_2 (SE_{H2O2}), Figure 3b.

The increment of SE_{H2O2} production of pulsed ultrasound as opposed to continuous ultrasound peaked at approximately 1.5 fold, while the maximum increment of SE_{Fe+3} was more than 8 fold. These results are in close agreement with the observation of Casadonte Jr, Flores and Petrier [8]. The large difference observed in sonochemical enhancement of SE_{Fe+3} compared to SE_{H2O2} suggests that the oxidation of ferrous happened mostly via free radicals and H_2O_2 might have evaporated into the collapsing bubbles providing a substrate for the formation of further hydroxyl radicals [16]. Interestingly, the maxima of SE for both Fe^{+3} and H_2O_2 shifted from 10% amplitude in continuous ultrasound to 30-40% amplitude for pulsed ultrasound. This shift in the maxima highlights the importance of these power levels (30-40% amplitude) in a pulsed mode ultrasonic system.
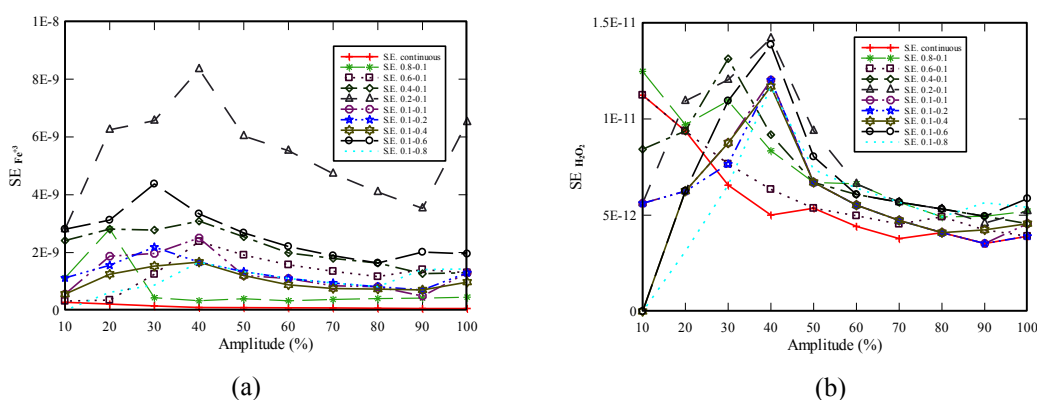

Figure 3: Sonochemical efficiency vs. amplitude percentage of pulsed and continuous ultrasound for (a) Fe^{+3} and (b) H_2O_2

The improvement in sonochemical activities of pulsed mode is attributed to different mechanisms. Yang, Rathman and Weavers [17] and Casadonte Jr, Flores and Petrier [8] suggest that the oxidation of chemical species with an ionic or polar nature such as Fe^{+3} under the effect of cavitation occur via a diffusion mechanism. The intervals between the subsequent pulses allow enough time for the chemicals of interest to diffuse into the seeding bubbles of the following pulse leading to better reactions. Dekerckheer, Bartik, Lecomte and Reisse [15] found that the residual acoustic pressure and active bubbles in the *off* period of pulsed ultrasound could be behind the difference in the levels of sonochemical activities for pulsed mode as compared to the continuous mode. Tuziuti, Yasui, Lee, Kozuka, Towata and Iida [18] have ascribed sonochemical enhancement of pulsed ultrasound to residual acoustic pressure and the spatial enlargement of the chemically active zone in the irradiated solution. However, they concluded that the residual pressure has a superior role in the chemical enhancement. Others [7] suggest that the enhancement in the chemical activities of pulsed ultrasound particularly at higher power levels (> 70% amplitude), is attributed to the lower shielding effects which allow better energy transmission through the irradiated liquid compared to continuous ultrasound. This trend was evident in this study, as it can be seen from figure 3 (a) and (b) that after the maxima, SE for most of R ratios decreased as the amplitude increased until 90 % amplitude after

which SE went up again. To further elaborate on this point, the production rates of Fe^{+3} and H_2O_2 were plotted against amplitude percentages as shown in figures 4 and 5 respectively. The data in these figures clearly shows an increase in the chemical yield of pulsed ultrasound at higher power level. It is worth mentioning that the production rates of Fe^{+3} and H_2O_2 exhibited zero-order kinetics with values close to those reported in the literature [19]. Using high power and low frequency ultrasonic energy results in a low number of powerful bubbles with each pulse [1]. Thus the residual number of bubbles would be very small and that would confine the enhancement mechanisms in this study to residual acoustic pressure, spatial enlargement and lowering of shielding effects. These analyses are reasonable as a high power wave can propagate through the liquid for longer distances ($P_A/P_{A°} = e^{-\alpha x}$ [15]) and its residual effect can last longer in liquid.

Regardless of the chemical enhancement mechanisms, pulsed ultrasound had higher chemical effects than continuous ultrasound for the same energy level. This confirms that pulsed mode can reduce the energy demand of ultrasound technology considerably. To make this mode more energy efficient, the suitable pulse and interval lengths need to be optimized for specific ultrasonic systems as they vary from case to case [7]. In this study, it was observed that $R=0.2:0.1$ resulted in the highest SE for all the tested groups of R ratios. While $R=0.1:0.6$ had the highest SE among the long time-off ratios.
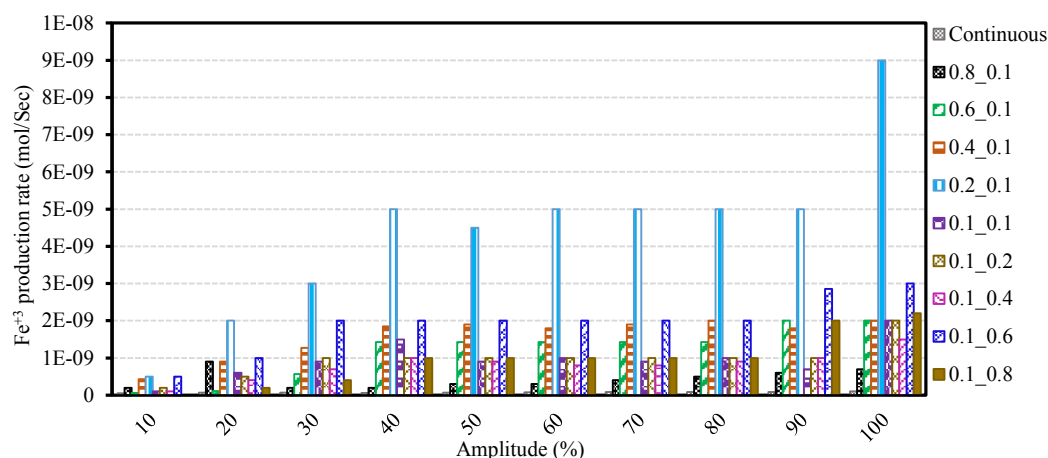

Figure 4: Fe^{+3} production rates vs. amplitude percentage of pulsed and continuous ultrasound
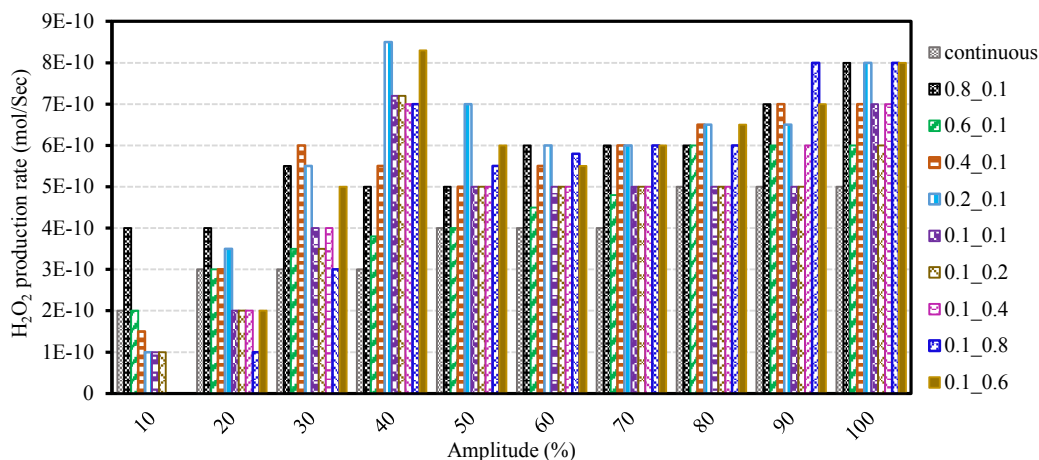
Figure 5: H_2O_2 production rates vs. amplitude percentage of pulsed and continuous ultrasound

4. Conclusion

Systematic investigation into the conversion of electrical energy into calorimetric energy and chemical yield was carried out for a low frequency high power ultrasonic horn reactor. It was found that operating the ultrasonic system in pulsed mode did not affect the performance of the system with regards to its efficiency in converting the electrical power to calorimetric power. However, the conversion of electrical power to chemical yield expressed as SE was more efficient for pulsed ultrasound compared to continuous ultrasound. SE_{Fe+3} and SE_{H2O2} of pulsed ultrasound was higher than that of continuous ultrasound by a small fraction to several fold depending on the applied *R* ratio. *R*=0.2:0.1 had the highest SE compared to other ratios, whilst *R*=0.1:0.6 resulted in the highest SE values among the long off-time ratios. The effectiveness of these two *R* ratios in ultrasonic applications needs to be examined in the future to confirm their potential in saving energy in ultrasonic systems.

References

[1] Al-Juboori, RA, T Yusaf. Identifying the Optimum Process Parameters for Ultrasonic Cellular Disruption of E. Coli. *International Journal of Chemical Reactor Engineering* 2012;**10**: 1-32.
[2] Al-Juboori, RA, T Yusaf, V Aravinthan. Investigating the efficiency of thermosonication for controlling biofouling in batch membrane systems. *Desalination* 2012;**286**: 349-57.
[3] Al-lwayzy, SH, T Yusaf, RA Al-Juboori. Biofuels from the Fresh Water Microalgae Chlorella vulgaris (FWM-CV) for Diesel Engines. *Energies* 2014;**7**: 1829-51.
[4] Yusaf, T, RA Al-Juboori. Alternative methods of microorganism disruption for agricultural applications. *Applied Energy* 2014;**114**: 909-23.
[5] Chemat, F, H Zill e, MK Khan. Applications of ultrasound in food technology: Processing, preservation and extraction. *Ultrasonics Sonochemistry* 2011;**18**: 813-35.
[6] Wongpisutpaisan, N, P Charoonsuk, N Vittayakorn, W Pecharapa. Sonochemical synthesis and characterization of copper oxide nanoparticles. *Energy Procedia* 2011;**9**: 404-9.
[7] Chen, D, SK Sharma, A Mudhoo, Handbook on Applications of Ultrasound: Sonochemistry for Sustainability, in, CRC Press, 2011.

[8] Casadonte Jr, DJ, M Flores, C Petrier. Enhancing sonochemical activity in aqueous media using power-modulated pulsed ultrasound: an initial study. *Ultrasonics Sonochemistry* 2005;**12**: 147-52.
[9] Al-Juboori, RA, T Yusaf, L Bowtell, V Aravinthan. Energy characterization of ultrasonic systems for industrial processes. *Ultrasonics* 2014, http://dx.doi.org/10.1016/j.ultras.2014.10.003.
[10] Nowak, FM. *Sonochemistry: Theory, Reactions, Syntheses, and Applications*. Nova Science Publishers, Incorporated; 2010.
[11] Virot, M, L Venault, P Moisy, SI Nikitenko. Sonochemical redox reactions of Pu(iii) and Pu(iv) in aqueous nitric solutions. *Dalton Transactions* 2015.
[12] Koda, S, T Kimura, T Kondo, H Mitome. A standard method to calibrate sonochemical efficiency of an individual reaction system. *Ultrasonics Sonochemistry* 2003;**10**: 149-56.
[13] Sugimoto, Ki, R Tsujino, S Musha. A Continuous Dosimeter by Use of the Fricke Dosimeter. *Bulletin of University of Osaka Prefecture. Series A, Engineering and natural sciences.* 1963;**11**: 75-80.
[14] Klassen, NV, D Marchington, HC McGowan. H2O2 determination by the I3-method and by KMnO4 titration. *Analytical Chemistry* 1994;**66**: 2921-5.
[15] Dekerckheer, C, K Bartik, J-P Lecomte, J Reisse. Pulsed Sonochemistry. *The Journal of Physical Chemistry A* 1998;**102**: 9177-82.
[16] Chakma, S, VS Moholkar. Investigations in Synergism of Hybrid Advanced Oxidation Processes with Combinations of Sonolysis + Fenton Process + UV for Degradation of Bisphenol A. *Industrial & Engineering Chemistry Research* 2014;**53**: 6855-65.
[17] Yang, L, JF Rathman, LK Weavers. Degradation of Alkylbenzene Sulfonate Surfactants by Pulsed Ultrasound. *The Journal of Physical Chemistry B* 2005;**109**: 16203-9.
[18] Tuziuti, T, K Yasui, J Lee, T Kozuka, A Towata, Y Iida. Mechanism of Enhancement of Sonochemical-Reaction Efficiency by Pulsed Ultrasound. *The Journal of Physical Chemistry A* 2008;**112**: 4875-8.
[19] Petrier, C, M-F Lamy, A Francony, A Benahcene, B David, V Renaudin, et al. Sonochemical Degradation of Phenol in Dilute Aqueous Solutions: Comparison of the Reaction Rates at 20 and 487 kHz. *The Journal of Physical Chemistry* 1994;**98**: 10514-20.

Biography

Raed A. Al-Juboori is a researcher with a background in Chemical and Environmental engineering. Read's research interests are advance oxidation techniques, membrane technology, disinfection techniques, water treatment and alternative energy solutions.

Summary-Objective 1

Objective 1 was fulfilled in *papers I* and *II*. The conversion of electrical power to acoustical effects was scrutinised in these papers. In *paper I*, the efficiency of continuous ultrasonic system was evaluated using physical and chemical measurements. An accurate calorimetric technique was developed and tested in this paper. The new calorimetric technique counts for the convective heat loss from the irradiated solution using a set of empirical heat transfer correlations. Organic and inorganic chemical dosimeters were applied in *paper I* to determine the efficiency of the system in producing hydroxyl radicals. Overall energy conversion efficiency of the system was 60-70%. All the chemical dosimeters showed the same pattern with the change in ultrasonic power. In general, the products of hydroxyl reactions declined after 70-80% amplitude indicating the occurrence of shielding effects. In *paper II*, the same energy measurement protocols developed in *paper I* was applied on pulsed ultrasound system. Hydroxyl radical and hydrogen peroxide produced from continuous and pulsed ultrasonic systems were measured in *paper II*. Sonochemical measurements showed that ultrasonic amplitude of 40% and *R* ratios of 0.2:0.1 and 0.1:0.6 s are the most energy efficient operating parameters. The outcomes of *paper I* and *II* suggest that ultrasonic amplitudes of 40% and 70% and *R* ratios of 0.2:0.1 and 0.1:0.6 s are important operating parameters for the ultrasonic system used in this work. Hence, the effect of these parameters on the removal of aquatic natural contaminants will be investigated in the following sections of this thesis.

Paper III

Al-Juboori, R. A., Yusaf, T., Aravinthan, V., Pittaway, P. A. & Bowtell, L., Investigating the feasibility and the optimal location of pulsed ultrasound in surface water treatment schemes, *Desalination and Water Treatment*, (2015), 1-19.

Desalination and Water Treatment

Investigating the feasibility and the optimal location of pulsed ultrasound in surface water treatment schemes

Raed A. Al-Juboori[a], Talal Yusaf[b], Vasantha Aravinthan[a], Pamela A. Pittaway[c] & Leslie Bowtell[b]

[a] Faculty of Health, Engineering and Sciences, School of Civil Engineering and Surveying, University of Southern Queensland, Toowoomba, 4350 QLD, Australia, Tel. +61 413424126, +61 7 4631 1366, Tel. +61 7 4631 2299

[b] Faculty of Health, Engineering and Sciences, School of Mechanical and Electrical Engineering, University of Southern Queensland, Toowoomba, 4350 QLD, Australia, Tel. +61 7 4631 2691, Tel. +61 7 4631 1383

[c] Cooperative Research Centre for Irrigation Futures, National Centre for Engineering in Agriculture, University of Southern Queensland, Toowoomba, 4350 QLD, Australia, Tel. +61 7 4631 2144
Published online: 02 Jan 2015.

PLEASE SCROLL DOWN FOR ARTICLE

Investigating the feasibility and the optimal location of pulsed ultrasound in surface water treatment schemes

Raed A. Al-Juboori[a,*], Talal Yusaf[b], Vasantha Aravinthan[a], Pamela A. Pittaway[c], Leslie Bowtell[b]

[a]Faculty of Health, Engineering and Sciences, School of Civil Engineering and Surveying, University of Southern Queensland, Toowoomba, 4350 QLD, Australia, Tel. +61 413424126, +61 7 4631 1366; emails: RaedAhmed.mahmood@gmail.com, RaedAhmed.Mahmood@usq.edu.au (R.A. Al-Juboori), Tel. +61 7 4631 2299; email: Vasanthadevi.Aravinthan@usq.edu.au (V. Aravinthan)
[b]Faculty of Health, Engineering and Sciences, School of Mechanical and Electrical Engineering, University of Southern Queensland, Toowoomba, 4350 QLD, Australia, Tel. +61 7 4631 2691; email: talal.yusaf@usq.edu.au (T. Yusaf), Tel. +61 7 4631 1383; email: bowtelll@usq.edu.au (L. Bowtel)
[c]Cooperative Research Centre for Irrigation Futures, National Centre for Engineering in Agriculture, University of Southern Queensland, Toowoomba, 4350 QLD, Australia, Tel. +61 7 4631 2144; email: pam.pittaway@usq.edu.au

ABSTRACT

The deterioration of surface water quality due to extreme weather events and increasing human activities has exacerbated the common problems in drinking water production such as filtration fouling and DPBs formation. This in turn has urged for exploring alternative methods for the traditional treatment methods that are able to improve the removal of contaminants with minimal impact on environment and human health. In this study, the application of pulsed and continuous ultrasound for improving the quality of natural water with fresh natural organic matter (NOM) mainly driven from vegetation has been evaluated. The evaluation was performed using cost-effective and quick measurements such as specific UV–vis absorbance, COD_{Mn}, alkalinity and conductivity. The changes in the characteristics of NOM induced by ultrasound were used to develop a framework for evaluating ultrasound performance in improving conventional surface water treatment processes and to identify the best fit of ultrasound within the treatment scheme. Results of this study showed that pulsed ultrasound was as effective as or in some cases better than continuous ultrasound in improving water quality. According to the adapted assessment criteria supported by an extensive literature survey, the most effective location of ultrasound treatment within surface water treatment scheme was found to be prior to coagulation/flocculation.

Keywords: Pulsed ultrasound; Continuous ultrasound; NOM; Filtration fouling; DBPs

*Corresponding author.

1. Introduction

Surface water is a major resource for drinking water production [1]. The contamination levels, particularly, of natural organic matter (NOM) in surface water resources have recently increased due to climate change and progressive human activities [2–4]. Increasing surface water contamination results in operating and health problems such as frequent filtration fouling [5,6] and formation of hazardous materials in finished water (e.g. disinfection by-products, DBPs). To find effective solution for the challenges of surface water treatment, the problems encountered in individual treatment processes within the treatment scheme need to be carefully identified.

Generally, surface water treatment systems consist of three main operational units; coagulation/flocculation, filtration and disinfection. Fig. 1 illustrates a schematic of surface water treatment scheme with emphasis on the problems associated with the main treatment processes. Coagulation/flocculation processes remove organic materials and pathogens via various mechanisms such as adsorption and charge neutralization. The common problem in coagulation/flocculation processes is the residual of coagulants. The residual coagulants (e.g. aluminium) are involved in technical and health problems, such as increasing turbidity, filtration fouling, interfering with disinfectants and causing neuropathologic disorders and neurological diseases [7–9]. Filtration removes metals and

other contaminants under the effect of physiochemical interaction and sieving capacity of filters. Fouling of filtration media is another challenge commonly encountered by the operators of surface water treatment systems. Fouling is the deposition of solids, organic/inorganic and micro-organisms onto the interactive surface of the filtration media [10]. The accumulation of organic and microbial foulants on the filtration media is of particular concern when membranes are used as filtration media [5]. The adhesion of organic and microbial foulants to filters inflicts extra cost and delay to filtration process as well as reduction in the quality of the product [11,12].

Disinfection is the last process in the surface water treatment scheme and it is applied to remove biological contamination and control the regrowth of micro-organisms in the distribution network. This process usually suffers from the formation of the hazardous DBPs [13]. DBPs are caused by the reaction between the chemical disinfectants (e.g. chlorine and ozone) with NOM [14–16]. DBPs include a wide spectrum of carcinogenic and mutagenic chemical complexes that pose a threat to human health and the environment. Epidemiological and toxicological studies indicate human exposure to chlorinated water-containing high concentrations of DBPs increases the risk of serious health problems such as bladder cancer [17] and congenital diseases [14].

It is clear that if the dosages of coagulants and disinfectants used in water treatment are not carefully
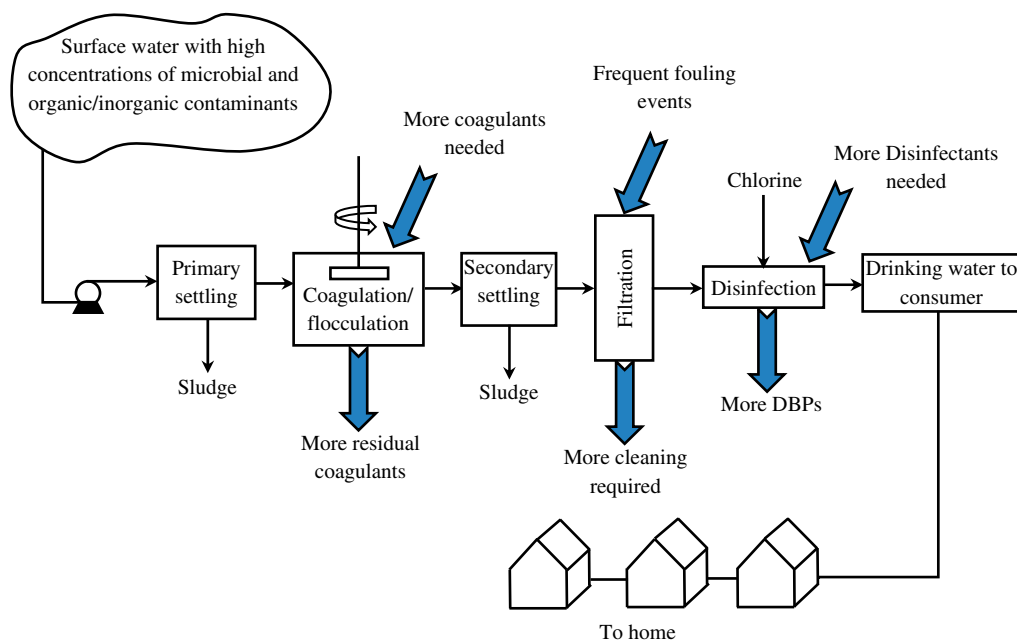

Fig. 1. Typical surface water treatment system.

manipulated, they can exacerbate the problems of surface water treatment systems. Hence, the key solution to reduce surface water treatment challenges is by reducing the amounts of chemicals added to water without compromising the quality of the finished water. This can be achieved by applying physical treatment methods capable of improving the quality of surface water. The use of ultrasound as a physical treatment method has been suggested in this study. Ultrasound has the ability to reduce the common problems of surface water treatment by destroying micro-organisms and oxidizing organic and inorganic contaminants [18–20]. Ultrasound has the advantage of having minimal impact on the environment and human health and is simple to implement in water treatment systems [21,22].

The high energy demand and rapid temperature rise associated with the use of continuous ultrasound in water treatment systems are of concern [5]. To overcome these problems, the use of pulsed ultrasound will be investigated in this study. In continued sonication, some bubbles grow to a bigger size through rectified diffusion mechanisms [20,23]. Large bubbles are not able to produce powerful shock waves and shear stress [20], and they absorb part of ultrasonic energy. Additionally, the existence of large bubbles in the liquid hinders the transfer of ultrasound waves through the liquid (shielding effect) [24]. In pulsed ultrasound treatment, the problem of stable bubbles is less as the size of such bubbles reduces during the interval period (Off period of pulsed ultrasound) due to the dissociation of the gases. This in turn decreases the shielding effect and reduces the energy that could have been absorbed by stable bubbles in the subsequent pulse train. The use of pulsed ultrasound for water treatment can also lessen the needs for extensive cooling process during the treatment, which may introduce additional cost.

Ultrasound has the potential to be effectively integrated into the existing surface water treatment schemes (Fig. 1), however, with which treatment process can ultrasound perform the best is a question that has not been addressed yet. In addition, Most of the studies on ultrasound implantation for water treatment used synthetic waters which focuses on particular contaminants and does not reflect the real case in water treatment plants. The practical evaluation to ultrasound application in water treatment requires the use of natural water samples [25]. It is also important to investigate the effect of ultrasound on DBPs formation [26,27].

It is known that ultrasound wave propagation causes an increase in bulk temperature of water due to friction produced from agitation and liquid circulation as well as cavitation. To separate the effect of

bulk temperature rise on water properties from that of the cavitational effects of ultrasound, thermal treatments that are identical to ultrasound treatments in their temperature profile will be performed using electrical heater operated with DC. Comparison between the performances of pulsed ultrasound at different pulse/interval ratios with that of continuous ultrasound will also be carried out using rapid evaluation techniques such as dissolved organic carbon (DOC), specific UV–vis absorbance (SUVA), COD_{Mn}, alkalinity and conductivity.

The criteria that will be used to assess the application of ultrasound in surface water treatment will consider the effect of ultrasound on the characteristics of the water that influence the proclivity of its NOM to (1) the removal by coagulation/flocculation, (2) filtration media fouling and (3) formation of DBPs. The outcome of this study will provide guidelines that help in choosing the most suitable location for ultrasound treatment within surface water treatment schemes.

2. Materials and methods

2.1. Water samples

Pittaway pond water located at the south-east Queensland was selected as a model for surface waters of Queensland,Australia in this study. Pittaway pond is an ephemeral, small pond containing highly coloured water with fresh NOM mainly produced by decomposition of tree leaves and bark litter.

Water samples were collected and stored frozen in polyethylene bottles at $-10°C$ until the experimental work commence. Table 1 shows the physiochemical properties of the collected water samples expressed in

Table 1
Characteristics of Pittaway pond water

Physiochemical properties		Measured values
pH, 25°C		8.2 ± 0.20
DOC (mg/L)		6.5 ± 0.15
Specific COD_{Mn} (mg O_2/mg DOC)		0.54 ± 0.06
SUVA (L/mg.cm)	254	0.038 ± 0.007
	260	0.036 ± 0.009
	280	0.029 ± 0.0010
	250/365	4.56 ± 0.12
	254/204	0.35 ± 0.050
	254/colour 436	15.45 ± 1.64
Alkalinity (meq/L)		2.99 ± 0.013
Conductivity (mS/cm), 25°C		0.16 ± 0.006
Iron (mg/L)		0.12 ± 0.0014
Nitrate (mg/L)		0.47 ± 0.02
Chloride (mg/L)		67.3 ± 3.9

mean value ± the standard of error of the mean of three measurements.

2.2. Analytical methods

2.2.1. DOC measurements

The DOC of untreated and treated water samples was measured using Total Carbon Analyser (TOC-V$_{CSH}$, SHIMADZU, Australia). The DOC of each sample was measured in duplicate. At least three injections of each measured sample were made, which resulted in coefficient of variance (CV) lower than 0.02. Water samples were filtered through 0.45 μm glass-fibre filters using syringe filter holder prior to DOC measurements.

2.2.2. UV–vis spectroscopy analysis

UV absorbance of the sample is directly related to the concentration of the absorber (i.e. DOC) [28].

Therefore, to better express the change in the nature of the NOM, the UV absorbance of a sample will be standardized by DOC of water sample (SUVA). JENWAY UV/Vis spectrophotometer, model 6705 with a single cell holder was used for measuring the absorbance of untreated and treated water samples at UV and visible ranges. Quartz cuvette with path length of 1 cm was used in the UV measurements. The water samples were filtered through 0.45 μm glass-fibre filter prior to UV analysis. The samples were scanned in a wavelength range of 200–500 nm to measure the absorbance at 204, 250, 254, 260, 280, 365 and 436 nm. Table 2 details the indicative characteristic of the NOM that corresponds to each measured wavelength. Distilled water was used as a baseline.

UV absorbance of water samples is sensitive to pH and the content of interfering species, such as iron, nitrate, nitrite, chloride and bromide [29,30]. Under acidic conditions (pH < 2), some of the NOM such as humic acids precipitate resulting in a bias judgement to the change of UV–vis absorbance [29]. To eliminate

Table 2
Measured UV–vis wavelengths with interpretation

Wavelength (nm)	Indicative characteristics of water
254	UV absorbance at 254 nm will be used as an indicator for humic fraction in aquatic DOC [32,33], as it reveals the electronic structure of DOM especially detecting the presence of conjugated structure [34] such as those in aromatic compounds. It inversely correlates to the aliphatic carbon content of DOM [35]
260	The absorbance at 260 nm will be used to detect the change in the hydrophobic fraction of NOM [31,36]. The use of SUVA$_{260}$ as indicator for the hydrophobicity will be strictly applied to estimate the effect of the treatments on the hydrophobicity of the aromatic compounds in the treated water samples as some of the hydrophobic acids moieties are aliphatic [37] which do not absorb the UV light [38]
280	SUVA$_{280}$ will be applied as an indicator for the bulk aromaticity of aquatic NOM [39]. The electron delocalization in the pi orbital of the conjugated structure of some of the aromatic compounds such as phenolic arenes, benzoic acids, aniline derivatives, polyenes and polycyclic aromatic hydrocarbons [40] occurs at UV range 270–280 nm is the basis behind the application of this wavelength as measure for aromaticity
254/204	The quotient SUVA$_{254}$/SUVA$_{204}$ will be adapted as a measure for the degree of functionality of the aromatic ring [41]. This ratio represents the proportional composite absorbance of the chromophores of NOM at electron transfer (ET) band to benzenoid (Bz) band [30], sometimes denoted as A$_{ET}$/A$_{Bz}$. This ratio can be used as an indicator to the prevalence of aromatic compounds substituted with oxygen-containing functional groups such as hydroxyl, carboxyl, ester and carbonyl which are mostly involved in adsorption and complexation processes [30,42]
250/365	This ratio is commonly known as E$_2$/E$_3$ ratio and it will be used as indicative for the proportion of low to high molecular size organic compounds in the treated water [40,43–45]. The use of E$_2$/E$_3$ will be applied in this study as alternative to the expensive and time-consuming laborious techniques such as high-pressure size exclusion chromatography, vapour pressure osmometry and ultracentrifugation [46,47]
254/436	The absorbance ratio 254/436 will be used to detect the change in the UV-absorbing groups to colour-forming groups of NOM in the treated water [42]. The absorption at 436 nm represents the functional groups that produce the yellow to brown colour in water samples [42,45,48]. Absorbance at 436 nm is a recommended spectrophotometric method for measuring water colour in the Australian Drinking Water Guidelines [49]

the effect of pH on UV absorbance, pH of water samples was adjusted to pH range of 6–7 using 0.1 N of HCl or NaOH as this range is suitable for the applied UV–vis measurements [29,31,32]. Titration workstation TitraLab, TIM 845 (Radiometer-Analytical, Australia) was used to measure pH of the samples during the adjustment.

The concentrations of nitrate, nitrite, chloride and bromide in water samples were measured using Ion Chromatography system ICS-2000 according to the standard method 4110 B detailed in Ref. [29]. The iron content of the water was quantified using Atomic Absorption Spectrophotometer (AAS) model AA-7000 (SHIMADZU, Australia) by following the standard method 3111 B, direct air–acetylene flame method explained in Ref. [29]. Anions such as chloride and nitrite are unlikely to interfere with UV measurements in this study. The minimum detection limit of chloride in UV measurements is 500 mg/L, which is higher than the concentration of chloride of the water sample (Table 1), and it only causes change in the absorbance peaks at $\lambda < 200$ nm, while nitrite is unstable and mostly oxidized to nitrate [50]. The concentration of bromide was not detectable in the applied measurement method, which indicates that the concentration of bromide is under the method detection level set by the standard methods [29] (i.e. 14 µg/L). So the effect of bromide on UV absorbance was neglected in this study. The concentrations of iron and nitrate in water samples were lower than the effective limit of these minerals which is between 0 and 0.5 mg/L for iron [32] and 5 mg/L for nitrate [50] as shown in Table 1. The UV absorbance measurements were performed in triplicate for each water sample.

2.2.3. COD$_{Mn}$, alkalinity and conductivity

The COD$_{Mn}$ of the water samples was measured following the standard procedure described in Ref. [51]. COD$_{Mn}$ can be expressed as the amount of permanganate oxidized per one litre of the water sample or the amount of oxygen consumed in the oxidation of one litre of water sample [52], and this measurement unit will be adapted in this study. This procedure is valid for water samples with chloride concentration of less than 300 mg/L as it is the case of Pittaway pond water (Table 1). The alkalinity of the untreated and treated samples was measured using autotitrator, workstation TitraLab, TIM 845 (Radiometer-Analytical, Australia).

Ion analyser, MeterLab model ION-450 supplied by Radiometer-Analytical, Australia was used for measuring the conductivity of water samples. COD$_{Mn}$, alkalinity and conductivity measurements for Pittaway water were performed in triplicate.

2.3. Ultrasound treatments

A commercial ultrasonic horn device (Branson Sonifier 450) with variable input power and fixed frequency of 20 kHz was used in this study. The probe tip is made of titanium with diameter (∅) of 19 mm.

Fig. 2 shows a schematic illustration of the laboratory set-up used in conducting the experimental work. Ultrasound and thermal treatments were performed in a batch mode. A 400 mL Pyrex beaker was used to contain water samples. The temperature rise caused by ultrasound treatments was measured using calibrated thermocouple type *K*. The signals from thermocouple were recorded at a rate of 40 samples/s using A/D card and Lab-View software.

Ultrasound treatment variables such as power, treatment time and depth of the probe in the treated water were set at 21.5 W/cm^2, 4 min and 1 cm, respectively. The effect of continuous and pulsed ultrasound at three pulse/interval ratios (denoted as *R*) of 0.5/0.5, 0.6/0.3 and 0.6/0.2 s correspond to *R*1:1, *R*2:1 and *R*3:1, respectively. In order to compare the effect of pulsed ultrasound to that of continuous ultrasound, the applied acoustic power has to be equal for both cases. This can be achieved by applying longer treatment time for pulsed ultrasound at certain value of *R* as shown in below equation [53].

$$t = t_0 \left(1 + \frac{1}{R} \right) \tag{1}$$

where t is the treatment time of pulsed treatments and t_o is the treatment time of continuous ultrasound. From Eq. (1), the treatment time of the pulsed treatments *R* 1:1, 2:1 and 3:1 was calculated to be 480, 360 and 320 s, respectively.

The frozen water samples were thawed and mixed well before ultrasound and thermal treatments. The beaker was filled with 200 mL of the sample and immersed in an ice bath to bring down the temperature of the sample to approximately 2℃ prior to the treatments. Ultrasound treatments were conducted in triplicates for each water sample.

2.4. Temperature mimicry (thermal treatments)

Ultrasound treatment of water especially for small to moderate volume samples (the most probable case in the laboratory investigations) usually induces a rapid heat rise in the samples. In the case of this study, the temperature rise was minimized by immersing the water sample in an ice bath to reduce the starting temperature to around 2℃. In spite of using the ice bath, water temperature increased to a
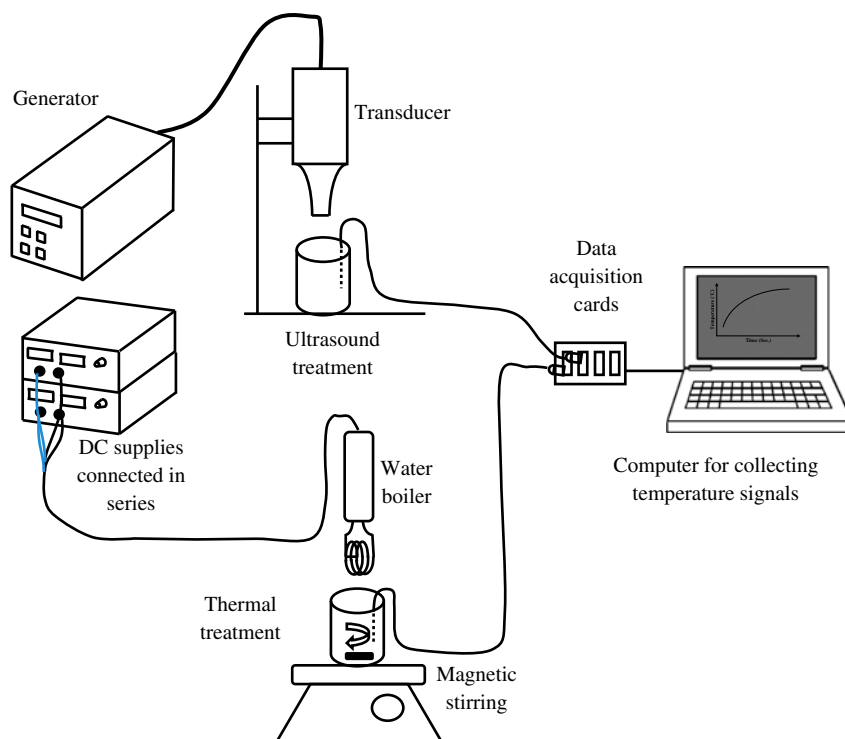
Fig. 2. Graphical representation of the experimental set-up.

maximum of 11℃ in the most heat-inducing ultrasound treatment (i.e. continuous). The increase in the bulk temperature of the samples within the range of 2–11℃ may affect the physiochemical properties of the NOM in water samples.

To investigate the thermal effect of ultrasound treatments on the properties of NOM, thermal treatments that simulate the range and pattern of temperature during ultrasound treatments were designed. A water boiler was used as a heat source in thermal treatments. Tap water was used as a medium in the temperature mimicry experiments. The heated water was continuously stirred to obtain homogeneous temperature rise. The temperature profile of tap water under ultrasound and thermal treatments was obtained with the aid of data acquisition system as shown in Fig. 2.

2.5. Statistical analyses

Analysis of variance (one way ANOVA) was performed to each set of experiments (ultrasound and heat experiments) separately to determine any significant change in the dependent variables (water characteristics) at $p < 0.05$. The experiments of heat and ultrasound treatments were conducted in four levels;

R 1:1, R 2:1, R 3:1 and continuous. Least significant difference (LSD) post-hoc test was applied to compare the differences between the treatment levels (pulsed and continuous treatments) when there is an overall significant change in the studied characteristic. Statistical analyses were carried out using SPSS 19 statistics.

3. Results and discussion

3.1. Mimicry of temperature rise and its effect on water samples characteristics

Fig. 3 shows the temperature rise of ultrasound treatments with their corresponding thermal treatments. The voltages that successfully resulted in temperature increase analogous to that of ultrasound treatments; R 1:1, 2:1, 3:1 and continuous were 75, 79, 82 and 90 V, respectively. The effect of ultrasound pulsation on temperature rise curve appears clear in the temperature curve fluctuation in Fig. 3. To match the temperature fluctuation of pulsed ultrasound, the corresponding temperature mimicry experiments were performed in pulsation with On/Off ratios same as R of pulsed ultrasound treatments. The obtained levels of voltage were applied in continuous and pulsing modes in the thermal treatments for surface waters.
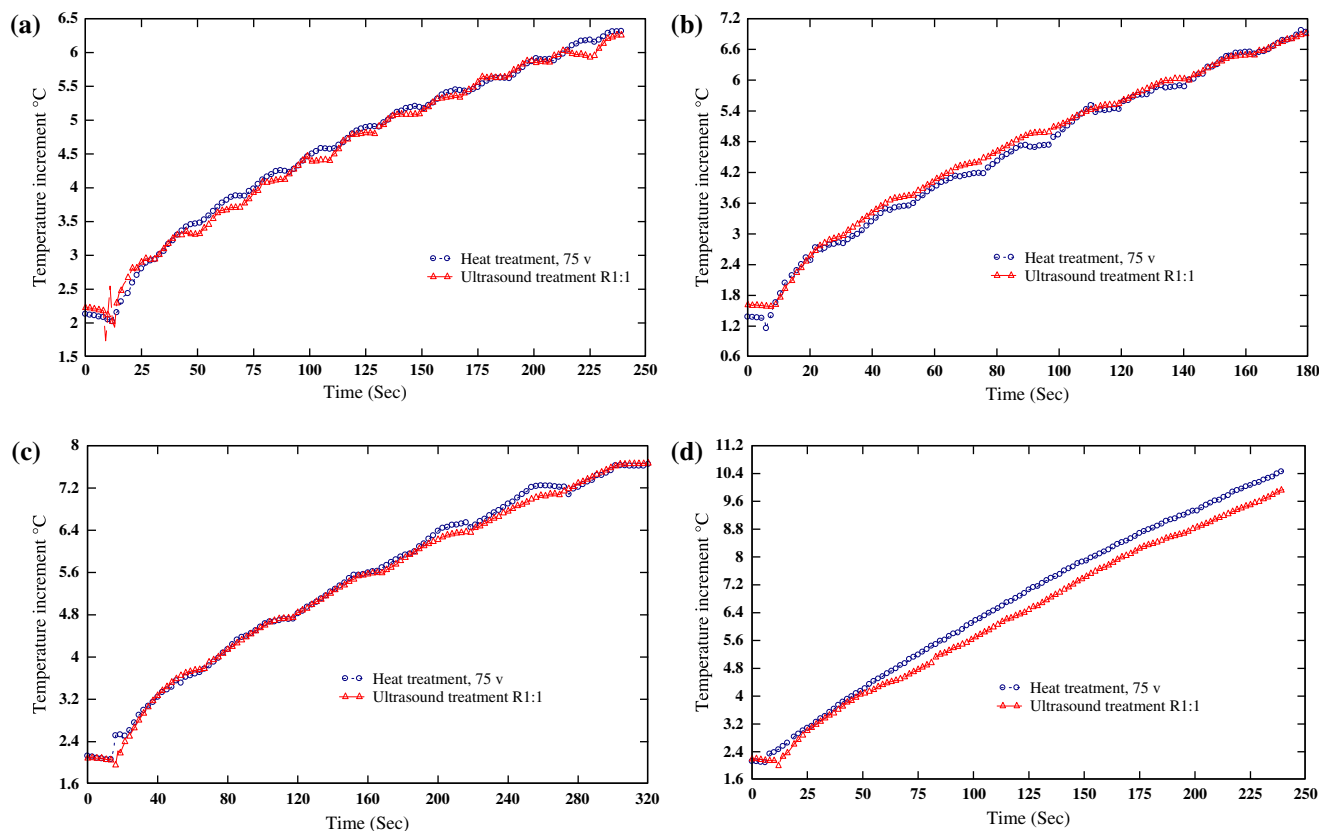
Fig. 3. Temperature rise vs. time for the treatments ultrasound (○) and thermal treatments (△); (a) ultrasound R 1:1 and heat at 75 v, (b) ultrasound R 2:1 and heat 79 v, (c) ultrasound R 3:1 and heat at 82 v and (d) continuous ultrasound and heat at 90 v.

The analysis of variance and the descriptive statistics for the overall effect of ultrasound and heat treatments on the characteristics of Pittaway pond water are presented in Tables 3 and 4, respectively. The mean values in Tables 3 and 4 represent the average of the measured characteristics of the treated samples normalized by that of the untreated samples. p-value lower than the considered significant level (0.05) indicates significant change. Table 3 illustrates that ultrasound treatment significantly altered six characteristics

Table 3
Descriptive statistics and summary of analysis of variance (ANOVA) for ultrasound treatment of Pittaway pond water

Normalized characteristics	Mean	SD	F-value	p-value
$SUVA_{254}$	0.8897	0.0420	3.223	0.082
$SUVA_{260}$	0.8834	0.0362	1.500	0.287
$SUVA_{280}$	0.8963	0.0371	4.921	0.032[*]
E_2/E_3	1.0861	0.0348	11.407	0.003[**]
$SUVA_{254}/SUVA_{204}$	0.9825	0.0156	7.929	0.009[**]
$SUVA_{254}/Color_{436}$	1.0422	0.0246	0.440	0.731
COD_{Mn}	0.9336	0.0363	4.281	0.044[*]
Alkalinity	0.6635	0.1236	63.480	6.4E−06[***]
Conductivity	2.0094	0.5306	75.678	3.3E−06[***]

***$p < 0.001$; **$p < 0.01$; *$p < 0.05$.

Table 4
Descriptive statistics and summary of analysis of variance (ANOVA) for heat treatment of Pittaway pond water

Normalized characteristics	Mean	SD	F-value	p-value
$SUVA_{254}$	0.9974	0.0109	0.204	0.891
$SUVA_{260}$	0.9904	0.0282	0.009	0.999
$SUVA_{280}$	0.9770	0.0321	0.507	0.688
E_2/E_3	1.0034	0.0544	0.004	1.000
$SUVA_{254}/SUVA_{204}$	0.9984	0.0039	0.153	0.925
$SUVA_{254}/Color_{436}$	1.0073	0.0028	2.819	0.107
COD_{Mn}	0.9972	0.0221	0.024	0.994
Alkalinity	0.9944	0.0687	0.003	1.000
Conductivity	1.0042	0.0147	0.030	0.993

of Pittaway pond water, while the changes in the remaining three characteristics namely $SUVA_{254}$, $SUVA_{260}$ and $SUVA_{254}/SUVA_{436}$ were not significant. Table 4 shows that the temperature rise from 2 to 11°C during ultrasound treatments has a negligible effect on the characteristics of the treated water. Similar findings were reported by Destaillats et al. [54], who found that the increase in the bulk temperature of the treated water by ultrasound from 2 to 12°C led only to a marginal change in the concentration of dichloromethane by less than 2–4% of the initial concentration. Hence, it can be concluded that the significant change in the properties of the treated water is solely attributed to ultrasound effects. The concomitant thermal effect of ultrasound treatment and the insignificant changes of $SUVA_{254}$, $SUVA_{260}$ and $SUVA_{254}/SUVA_{436}$ will not be discussed in terms of their implications on the surface water treatment train.

3.2. Comparison between pulsed and continuous ultrasound treatments

Table 5 shows the analysis of LSD post-hoc test for the significantly changed water characteristics of

Pittaway pond water. The significance level considered in this table is $p < 0.05$. It can be seen from Table 5 that in all the significantly changed characteristics except $SUVA_{254}/SUVA_{204}$, there is at least one pulsed ultrasound treatment that is not significantly different in its effect to the continuous treatment. In fact, for some characteristics such as alkalinity, the change caused by pulsed ultrasound R 3:1 exceeded that of continuous ultrasound. This means that applying pulsed ultrasound treatment in this study resulted in a comparable or in some cases better effect as compared to continuous ultrasound treatment. This finding is in agreement with the observations reported in Refs. [55,56] as Xiao et al. [55] reported a higher reduction of carbamazepine with pulsed ultrasound by 6% as compared to the reduction with continuous ultrasound. Similarly, Yang et al. [56] observed that the degradation rate constant of sodium 4-octylbenzene sulphonate under pulsed ultrasound was nearly twice the degradation rate of continuous ultrasound. The high efficiency of pulsed ultrasound as opposed to continuous ultrasound in terms of water characteristics alteration is attributed to the occurrence of shielding effects more pronouncedly in continuous ultrasound than in pulsed ultrasound [20].

Table 5
Descriptive statistics and summary of analysis of variance (ANOVA) for ultrasound treatment of Pittaway pond water; comparison between treatment levels

Treatment levels	R 1:1		R 2:1		R 3:1		Continuous	
Normalized characteristics	Mean	SD	Mean	SD	Mean	SD	Mean	SD
$SUVA_{280}$	0.9390a	0.0438	0.9015ab	0.0144	0.8843b	0.0188	0.8605b	0.0130
E_2/E_3	1.0373a	0.0180	1.0889b	0.0124	1.1003b	0.0268	1.1179b	0.0078
$SUVA_{254}/SUVA_{204}$	0.9955a	0.0063	0.9879a	0.0019	0.9857a	0.0057	0.9610b	0.0162
COD_{Mn}	0.9451a	0.0125	0.9629a	0.0152	0.8891b	0.0272	0.9373ab	0.0408
Alkalinity	0.8472a	0.0443	0.6318b	0.0253	0.5262c	0.0102	0.6488b	0.0261
Conductivity	1.1450a	0.0144	2.2990b	0.2283	2.2750b	0.0187	2.3188b	0.0062

Note: Means in the same row that do not share the same letter are significantly different ($p < 0.05$) by LSD post-hoc test.

It can also be noticed from Table 5 that the change in $SUVA_{254}/SUVA_{204}$ was the only case where pulsed ultrasound R1:1 was not significantly different from the other pulsed treatments. The low efficiency of pulsed ultrasound R 1:1 could be due to the long off-period in this treatment as opposed to the other pulsed treatments which could result in the disappearance of ultrasonic effects. This in turn leads to a subsequent pulse with fewer cavitation sites in the case of R 1:1 as compared to the other treatments.

3.3. Spectroscopic properties analysis

3.3.1. $SUVA_{280}$

The change in $SUVA_{280}$ is related to the change in the bulk aromaticity of the water samples as explained in Table 2. Fig. 4 demonstrates the effect of pulsed and continuous ultrasound treatments on the bulk aromaticity of Pittaway pond water. The normalized UV absorbance in Fig. 4 and other water characteristics in the following figures of this study are expressed by the mean of the measurements, and the error bars represent the standard error of the mean. The results obtained from the UV analysis for Pittaway pond water at 280 nm (Fig. 4) demonstrate that ultrasound treatments in its different levels destroyed the aromatic structure of the organic compounds presented in Pittaway pond water. Fig. 4 shows that as the pulse length increases, the reduction of aromaticity increases. However, the difference between continuous treatment and pulsed treatments (R 2:1 and R 3:1) is not statistically significant (Table 5). These results are in agreements with earlier work conducted by Naffrechoux et al. [57] that illustrated the capacity of ultrasound on destructing phenol as model for aromatic compounds. Equally, some other studies presented the ultrasonic degradation of other aromatic compounds such as polycyclic aromatic compounds [58]. The ultrasonic decaying of bulk aromaticity is attributed to two possible mechanisms, the cleavage of the aromatic rings [58,59] or the destruction of the aromatic side chain of the organic compounds [60].

Aromaticity is an important property of the aquatic organic matter that can be utilized to estimate the behaviour of water contaminants with the treatment processes. It was noted that the amenability of the organic matter to the removal by coagulation increases with increasing the aromatic moieties of the organic matter [61,62]. The other important aspect in water treatment is the blockage of filtration media on account of organic materials accumulation on filters. Fan et al. [63] examined the effect of the NOM properties of three Australian surface waters on fouling

tendency of MF membrane and observed that water with high aromaticity caused a greater permeate flux decline as compared to other waters. In another investigation for the mechanisms of humic acid fouling to UF membrane, Yuan and Zydney [64] noticed that Suwannee River humic acid solution that was less aromatic than Aldrich humic acid solution caused less flux decline than its comparative Aldrich humic acid solution. The increase in flux declines as the aromaticity of the foulants' increases is attributed to the strong ring structure of the aromatic compounds that increase the hydraulic resistance of the fouling layer. The aromaticity indicated by $SUVA_{280}$ has also been frequently correlated to the formation of DBPs [65–67]. $SUVA_{280}$ has been also applied to predict the reaction sites of NOM with chlorine [68].

Since ultrasound decreased the $SUVA_{280}$ of Pittaway pond water, it can be deduced that this water has become less aromatic under the effect of ultrasound. Less aromaticity means that the NOM of Pittaway pond water has less amenability to coagulation removal, membrane fouling and DBPs formation.

3.3.2. E_2/E_3 ($SUVA_{250}/SUVA_{365}$)

The modification occurs in the E_2/E_3 of water samples implies change in the molecular size distribution of the NOM presented in the samples. Fig. 5 shows that ultrasound treatments increased E_2/E_3 of Pittaway pond water. The increment in E_2/E_3 is directly proportional with the pulse length. Nevertheless, the differences between continuous and pulsed ultrasound treatments, R 2:1 and R 3:1, were found to be insignificant as presented in Table 5. The molecular size of NOM is directly correlated to the aromaticity ($SUVA_{280}$) [42,43,46,47], so when the aromaticity decreases, E_2/E_3 increases. Such relationship has been observed in this study as it is illustrated in Fig. 6 ($R^2 = 0.967$).

The molecular size distribution of the NOM has a significant effect on the sequential treatment processes of surface water (Fig. 1). Starting from coagulation/flocculation processes, several researches have elaborated that NOM with intermediate to large molecular size are the most susceptible compounds to the removal by coagulation [69]. A study conducted by Nissinen et al. [70] on various Finnish waterworks confirmed that coagulation using common coagulants successfully removed the largest molecular size humic fraction from the tested waters.

Filtration fouling by NOM is largely affected by its molecular size distribution. The effect of the molecular size of NOM on the membrane fouling and rejection

to these contaminants emanates from the fact that the membrane capacity in separating pollutants from water relies on two mechanisms, sieving effects and physiochemical interaction (i.e. repulsion) [5,71]. The general consensus in the literature indicates that NOM with hydrophobic characteristic and high molecular weight are regarded as the major contributors to membrane fouling [72,73]. More specifically, organic materials with high molecular size are mostly associated with the cake layer fouling of the membrane [74,75], whereas the low molecular weight NOM causes pore plugging fouling [76]. However, the molecular size of NOM is governed by the solution chemistry characteristics such as pH, ionic strength and the presence of mono- and multi-valence species [73].

The reactivity of NOM with disinfectants does not have a conclusive correlation with the molecular size distribution. For example, Kitis et al. [77] reported that out of two surface waters that were investigated for their potential to form Trihalomethanes (THMs) and Haloaceticacid (HAAs), the results of one of the water resources showed that DPBs increased with increasing the molecular size, whilst the results of the other water resource showed the opposite. Zhao et al. [78] explored the generation of THMs from the reaction of different DOC-sized fractionates with chlorine and chlorine dioxide. Their findings showed that generally the smaller the size of the DOC fractionate, the higher the THMs formed. Nevertheless, the formed THMs with chlorine dioxide did not show clear trend and it was independent of the DOC molecular size. Amy et al. [79] pointed to the decrement of the reactivity of organic matter with chlorine when converted to a lower molecular weight compounds. Similarly, Amy et al. [80] observed that the destruction of organic materials of ground water into smaller fractions by ozone did not increase THM formation potential (THMFP) of the water.

The results obtained from the quotient E_2/E_3 in this study suggest that ultrasound treatments for 4 min were sufficient to bring about a small change in the molecular size of the NOM for Pittaway pond water. The increase of E_2/E_3 ratio of Pittaway pond water may negatively affect the amenability of NOM to the removal by coagulation. It also indicates that the treated water would more likely cause pore blocking than cake layer fouling. The effect of the molecular size distribution of NOM on the DBPs formation was not decisive from the knowledge available in the literature. Therefore, the interpretation regarding the effect of NOM molecular size change due to ultrasound on the potential of waters to form DBPs has not been discussed herein.

3.3.3. $SUVA_{254}/SUVA_{204}$ (A_{ET}/A_{Bz})

The change of $SUVA_{254}/SUVA_{204}$ reflects a change in the concentration of aromatic compounds with oxygen-containing functional groups [30] as explained in Table 1. The impacts of ultrasound treatments on the $SUVA_{254}/SUVA_{204}$ of Pittaway pond water is shown in Fig. 7. The general trend of Fig. 7 is in mutual agreement with that of Fig. 4 as both reveal a reduction in the aromatic compounds of Pittaway pond water. It can be noted from Figs. 4 and 7 that the extent of ultrasound effect on $SUVA_{254}/SUVA_{204}$ (maximum decrease of 4%) is less than its effect on $SUVA_{280}$ (maximum decrease of 14%). This means that small portion of the destructed aromatic compounds by ultrasound was activated aromatic rings of oxygen-containing functional groups. These results are comparable with the results obtained by Chen et al. [81], as the latter showed that the acidity of organic matter was slightly reduced when treated with low frequency ultrasound. Since the acidity of natural organic matter is attributed to the presence of carboxylic and phenolic groups [82], the slight deterioration in the acidity of organic matter in Chen et al. [81] study can be accounted for the degradation of ultrasound to the phenolic and carboxylic groups which agrees with findings of this study.

$SUVA_{254}/SUVA_{204}$ can be used as an indication for the tendency of NOM to involve in adsorption and complexation reactions [30]. The absorption intensity of $SUVA_{254}/SUVA_{204}$ ratio is related to the presence of aromatic rings substituted with oxygen-containing functional groups [30]. These functional groups play a significant role in the NOM adsorption to coagulants and its potential to form DBPs [83–85]. Korshin et al. [30]
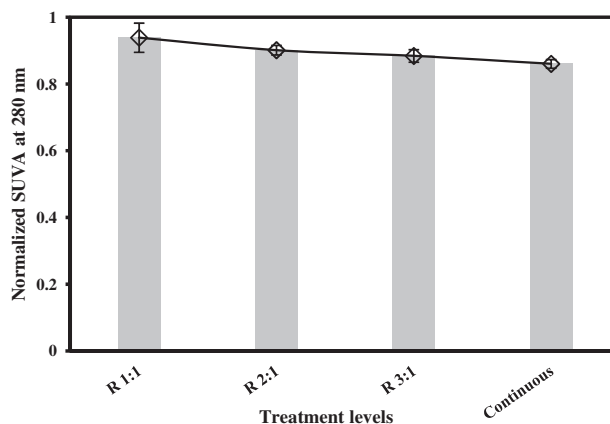

Fig. 4. Normalized $SUVA_{280}$ of Pittaway pond water after exposure to ultrasound (21.5 W/cm^2) for effective treatment time of 4 min.

observed that coagulation with alum selectively removes aromatic compounds substituted with oxygen-containing functional groups. This can be interpreted as water with high $SUVA_{254}/SUVA_{204}$ exhibits high NOM removal by coagulation with metallic salts. On the other hand, recent reports on the correlation between $SUVA_{254}/SUVA_{204}$ and DBPs formation potential [16,42,86] asserted the existence of direct correlation between DBPs formation and $SUVA_{254}/SUVA_{204}$, the higher the $SUVA_{254}/SUVA_{204}$ of the water, the more DBPs form in the disinfected water by chlorine. The adsorption tendency of NOM could also be adapted as an index for its fouling potential to filtration medium. Sotto et al. [87] showed that some of the aromatic compounds with substituted hydroxyl groups (e.g. 2-nitrophenol and 2-chlorophenol) have the potential to adsorb onto RO and NF membranes, causing a decline in the permeate flux.

Taking lead from the findings of the reviewed literature above, one can deduce that ultrasound has slightly decreased the aromatic compounds with oxygen-containing groups in Pittaway pond water, which in turn can reduce the risk associated with these compounds in terms of membrane fouling and DBPs formation. However, such decrease in the oxygen-containing groups may adversely affect the coagulability of Pittaway pond water by metallic salts.

3.4. Effect of ultrasound treatments on COD_{Mn}

The change in COD_{Mn} implies alteration in the oxidabizality and/or reactivity of the water pollutants. Since the COD_{Mn} of the samples depends on the amount of carbon in the samples [88], the COD_{Mn} of the treated water samples was standardized by the DOC of the samples and referred to as specific COD_{Mn}, expressed as mg O_2/mg C.

Fig. 8 depicts the effect of ultrasound treatments on the oxidant demands of Pittaway pond water. Fig. 8 shows that the specific COD_{Mn} of the Pittaway pond water decreased after ultrasound treatments. It can be noticed that the decrease in COD_{Mn} in Fig. 8 did not follow a regular pattern, and this is attributed to the superiority of pulsed ultrasound effect (R 3:1) on COD_{Mn} as compared to other treatments. The results of this study are consistent with those obtained by Naffrechoux et al. [57], who reported 50% reduction of COD of wastewater after ultrasound and UV treatments.

It was reported that potassium permanganate reacts preferentially with the aromatic ring-structured organic compounds of large molecular weight [52]. This means that the COD_{Mn} is related to aromaticity and E_2/E_3 ratio. It can be noticed from the general
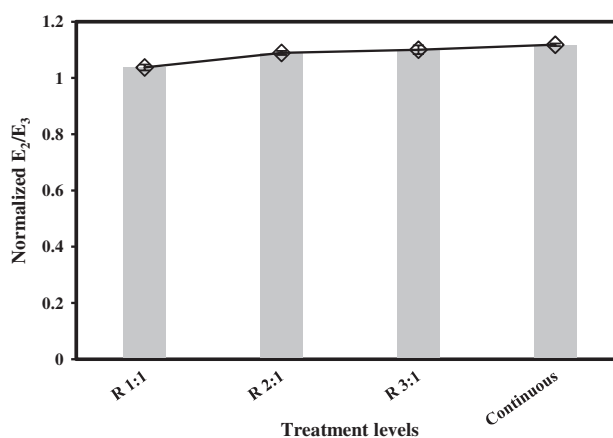
Fig. 5. Normalized E_2/E_3 of Pittaway pond water after exposure to ultrasound (21.5 W/cm^2) for effective treatment time of 4 min.
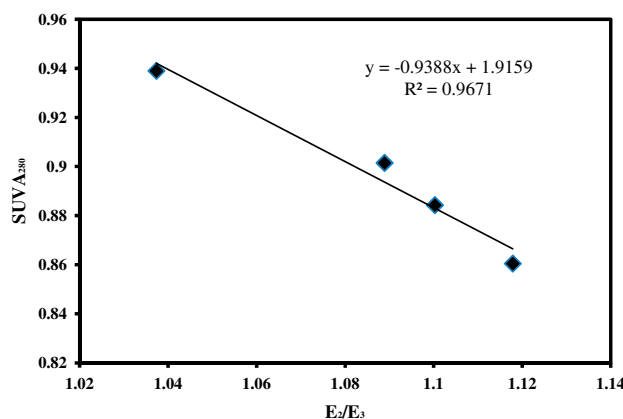
Fig. 6. Relationship between E_2/E_3 with $SUVA_{280}$ for the treated Pittaway pond water.
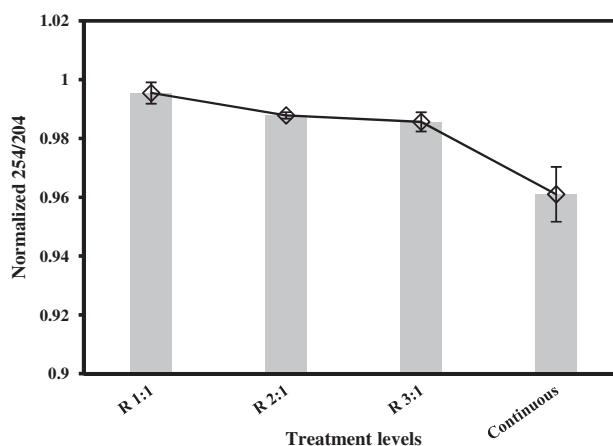
Fig. 7. Normalized $SUVA_{254}/SUVA_{204}$ of Pittaway pond after exposure to ultrasound (21.5 W/cm^2) for effective treatment time of 4 min.
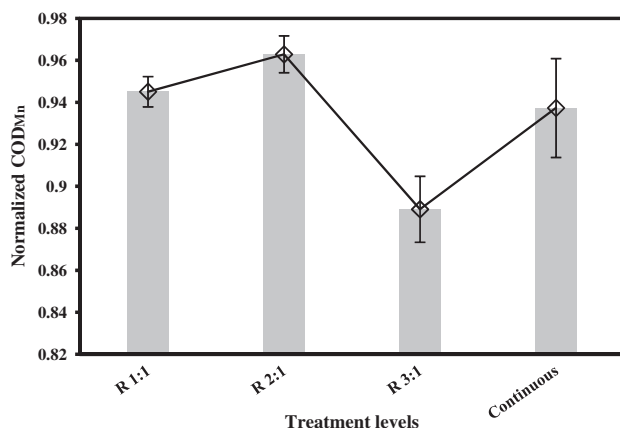
Fig. 8. Normalized COD_{Mn} of Pittaway pond water after exposure to ultrasound ($21.5 \ W/cm^2$) for 4 min.
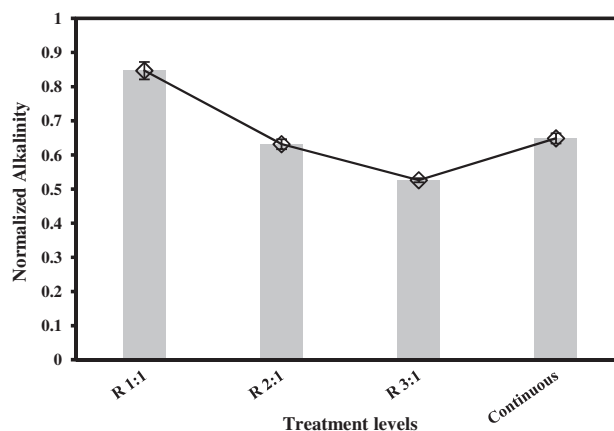

Fig. 9. Normalized alkalinity of Pittaway pond water after exposure to ultrasound ($21.5 \ W/cm^2$) for 4 min.

trend of Figs. (4, 5 and 8) (regardless of the variation in the results) that COD_{Mn} exhibited a direct correlation with $SUVA_{280}$ and inverse correlation with E_2/E_3, which agrees with Pittaway and Ancker statement [52]. The results obtained in this work are also in agreement with the findings of Mrkva [89] that underlined a direct relation between $SUVA_{254}$ and COD_{Mn} (both exhibit reduction, Table 3).

With regard to the effect of COD_{Mn} change on the performance of coagulation process, it appears from the literature that there is no obvious relationship between COD_{Mn} and coagulability of NOM. For instance, the results of Ma and Liu [90] showed that the turbidity removal with metallic coagulants did not exhibit a consistent trend with the initial COD_{Mn} of the treated water. Hence, the prediction of coagulability of the treated water depending on the COD_{Mn} results is not discussed in this study. The COD_{Mn} was found to have fair direct correlation ($R = 0.587$) with THMs [91]. This means that ultrasound reduced the potential of Pittaway pond water to form THMs. With regard to filtration performance, to the knowledge of the authors no linkages have been established between the performance of filtration and COD_{Mn} of water.

3.5. Effect of ultrasound treatments on alkalinity

The normalized alkalinity of the treated Pittaway pond water by ultrasound is presented in Fig. 9. It appears from Fig. 9 that ultrasound treatments dropped the alkalinity of the treated water. These results are in agreements with the findings of Suresh et al. [92] who also observed a reduction in water alkalinity under the effect of ultrasound. Pulsed ultrasound *R* 3:1 showed more effective alteration of

alkalinity than the other treatments (also supported by Table 5).

The decrement in the treated water alkalinity in this study is a result of destruction of the alkalinity-forming agents (bicarbonates (HCO_3), carbonates (CO_3) or hydroxyl anions (OH^-)). Since the pH of Pittaway pond was below 10 (Table 2), the alkalinity of this water is mainly caused by carbonates and bicarbonates [93], and thus it can be appropriately said that ultrasound has destroyed the carbonate and bicarbonate species in the treated water. The mechanism via which ultrasound causes destruction to water forming alkalinity agents is the production of highly reactive radicals (i.e. $OH^\bullet$) that are able to oxidize the carbonate and bicarbonate producing H_2O and CO_2.

Alkalinity has a strong influence on water treatment process through its buffering effects. In coagulation process, alkalinity can alter the charge of the NOM by changing the pH of the bulk water. When the pH of the water exceeds or becomes lower than the isoelectric point of the NOM molecules, the molecules' charge alters to negative or positive [5]. Similarly, the change in pH has an influence upon the hydrolysis of the metal salts and their charge production [61,94]. For instance, Edzwald and Tobiason [95] reported that the charge of aluminium hydrolysis species reduces from +1.5 $Al(OH)_{1.5}$ to +0.5 $Al(OH)_{2.5}^{+0.5}$ when the pH rises from 5.5 to 6.5. So, decreasing the alkalinity to some extent as a result of ultrasound treatment should have a positive impact on coagulation, especially when the water is very alkaline (the case of this study, Table 1) [61,96].

Similar to coagulation process, the separation of contaminants from water via filtration is affected by the charge of the contaminants [5]. In addition to the effect of alkalinity on pH and subsequently on the

charge of contaminants, the carbonate alkalinity may interact with cations presented in water such as Ca^{+2} and forms $CaCO_3$. Such interaction could have a positive effect on water purification if it takes place at the stage of coagulation, as $CaCO_3$ may improve the retention of sludge produced by coagulation [97]. However, the production of calcium carbonate in the filtration feed water can impose risk of filters' scaling [98]. The other concern of high alkalinity is the promotion of membrane filters fouling with silica [99]. It has been suggested by number of studies that decreasing alkalinity can be applied to alleviate the problems of scaling in filtration processes [100,101].

There is also a possibility of alkalinity being a trigger to the formation of DBPs [102]. Adedapo [103] observed an increase in the formation of some classes of DBPs such as dichloroacetonitrile and chloroform when the alkalinity of the water increased. Amy et al. [104] pinpointed a positive direct correlation between alkalinity and bromate formation. Additionally, since alkalinity affects the hydrolysis of coagulants [105] and the charge of substances in water, it is a crucial factor that determines the ability of treatment processes that proceed the disinfection step in removing DBPs precursors. In conclusion, decreasing the alkalinity by ultrasound treatments in this study suggests that ultrasound can be used to alleviate the scaling problems caused by cations, promote the removal of contaminants in coagulation process and hinder the formation of some DBPs classes.

3.6. Effect of ultrasound treatments on conductivity

The change that occurred in the conductivity of Pittaway pond water on account of ultrasound treatments can be seen in Fig. 10. Fig. 10 illustrates that ultrasound noticeably increased the conductivity of Pittaway pond water. Continuous and pulsed ultrasound *R* 2:1 and *R* 3:1 treatment had the same effect on the conductivity. The increase in the conductivity of water due to ultrasound can be explained as the extreme conditions inside the bubble and in its vicinity promote the concurrent decomposition and binding of dissolved gasses and subsequently, produce acids that makes the water more conductive [106,107]. The observed conductivity increase in this study is in agreement with data reported in Naddeo et al. [25], as the latter showed an increase in the conductivity of humic acid solution as a model for aquatic NOM after ultrasound treatment.

The conductivity of water gives an indication to the tendency of contaminants to adsorb to surfaces such as coagulants and filters. It is important to
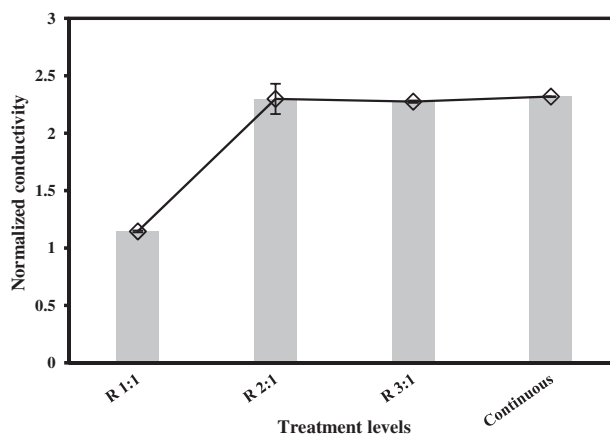

Fig. 10. Normalized conductivity of Pittaway pond water after exposure to ultrasound (21.5 W/cm^2) for 4 min.

elaborate here the link between conductivity and adsorption of pollutants to surfaces. Conductivity is directly related to the ion strength [108], and increasing the ionic strength of water reduces the thickness of electrical double layer leading to a reduction in the magnitude of electrical double layer interaction [109,110]. Electrical double layer interaction is one of three physiochemical interactions that govern the stability of the particles in the solution. These interactions include Lifshitz–van der Waals, Electrical double layer and Lewis acid–base [111–113]. When the total free energy (ΔG) of the combined three interactions is negative, the adsorption of molecules or living organisms to surfaces is favourable, otherwise the adsorption is unlikely to occur when ΔG is positive [109,112]. So, the increase in the conductivity of Pittaway pond water under the effect of ultrasound reduces the thickness of electrical double layer between the suspended contaminants and surfaces. This in turn can improve contaminants removal by coagulation through adsorption and enmeshment mechanisms. Kobya et al. [114] and Bazrafshan et al. [115] noticed an enhancement in the removal of organic compounds from water by electrocoagulation when water conductivity increased.

The change of ionic strength of water also has an influence on membrane filtration performance [6]. Increasing ionic strength increases the thickness and compactness of the fouling layer, and thereby increases the hydraulic resistance of fouling layer [73]. Decreasing the electrical double interaction increases the adsorption of the NOM and micro-organisms to the membranes which in turn increases the thickness of the fouling layer [109,116]. Similarly, the increase of ionic strength causes a conformational change in the

structure of organic materials. With increasing the ionic strength, the humic and fulvic acid molecules behave like rigid spherocolloids, while decreasing ionic strength makes these molecules behave like flexible linear colloids [117]. The spherical shape of the NOM molecules makes the fouling layer more compact. In addition to the membrane fouling, the increase of ionic strength decreases the rejection of salts and DBPs due to the increase in the osmotic pressure [118]. The enhancement of fouling as a result of increasing the conductivity of water has been confirmed by several researchers [119,120]. So, increasing the conductivity of the treated Pittaway pond water can exacerbate the fouling problem and decrease the rejection rate of DBPs.

In relation to the effect of ionic strength on the formation of DBPs, some studies observed that ionic strength is inversely correlated to DBPs formation. For example, Siddiqui and Amy [121] reported a decrease in the $CHBr_3$ from 43 to 36 μg/L when the ionic strength increased from 0.006 to 0.075 M. However, technically it is hard to establish links between the formation of DBPs and ionic strength, as the latter reflects the ionic content of water with no specific information on the concentration of particular ions. In addition, the ionic strength affect equally the physio-chemical interactions of NOM with disinfectants and the dissociation of disinfectants [122,123], which makes evaluating the effect of ionic strength on DBPs formation hard to perform through a literature survey. In summary, it can be said that the relationship between ionic strength and DBPs formation is dependent on treatment conditions and the physico-chemical properties of water and can be established experimentally.

4. Overall evaluation for ultrasound application in surface water

The effects of ultrasound on the characteristics of an Australian surface water with fresh organic materials have been investigated along with their implications on the performance of conventional treatment processes. In this section, an assessment table (Table 6) has been developed to help choosing the most suitable location of ultrasound in surface water treatment systems depending on UV–vis absorbance, COD_{Mn}, alkalinity and conductivity. Only the significantly changed characteristics have been considered in the

Table 6
Assessment scheme for ultrasound treatment in surface water system

Treatment process	Measured characteristics		Maximum change (%)	Effect of change	Net effect	Suitability
Coagulation/flocculation	Specific UV absorbance (SUVA), $L\,mg^{-1}\,cm^{-1}$	280	14^D	−	+	✔
		250/365	11.7^I	−		
		254/204	4^D	−		
	Specific permanganate index (mg O_2/mg DOC)		11^D	*		
	Alkalinity (meq/L)		47.3^D	+		
	Conductivity, 25°C		131^I	+		
Filtration	Specific UV absorbance (SUVA), $L\,mg^{-1}\,cm^{-1}$	280	14^D	+	−	×
		250/365	11.7^I	#		
		254/204	4^D	+		
	Specific permanganate index (mg O_2/mg DOC)		11^D	*		
	Alkalinity (meq/L)		47.3^D	+		
	Conductivity, 25°C		131^I	−		
Disinfection	Specific UV absorbance (SUVA), $L\,mg^{-1}\,cm^{-1}$	280	14^D	+	+	✔
		250/365	11.7^I	*		
		254/204	4^D	+		
	Specific permanganate index (mg O_2/mg DOC)		11^D	−		
	Alkalinity (meq/L)		47.3^D	+		
	Conductivity, 25°C		131^I	*		

Notes: (−) Negative effect; (+) Positive effect; (*) inconclusive effect; (#) neutral effect; (I) increment; (D) decrement.

assessment. The assessment criteria are based on the effect of the water characteristics change on the performance of coagulation, filtration and disinfection.

The symbols that have been used in the assessment table to indicate the effects of the change on a certain treatment process are; (−) possible adverse effect, (+) possible positive effect, (*) inconclusive effect and (#) indefinite effect. It should be mentioned here that although the decrease of $SUVA_{280}$ of Pittaway pond water is marked as possible negative change for coagulation process, ultrasound has a positive effect represented by the decrease of DOC concentration (Table 7). The effect is marked as inconclusive (*) when there is no scientific explanation available in the literature. The hash symbol was used to describe situations where the change in the characteristic cannot be regarded positive or negative (i.e. indefinite). For example, the effect of E_2/E_3 alteration on filtration performance is indefinite, as both small and large molecules have the potential to foul the membrane.

To establish an acceptable assessment strategy using the measured characteristics, we assumed that all characteristics have the same weight in terms of their effect on the treatment processes. The net effect of the change was determined by combining the maximum percentage of the change occurred in the characteristics with their signs excluding the inconclusive and the indefinite effects. If the net effect of the changes on a particular treatment process is positive, the use of ultrasound as pre-treatment for this process is suitable (✔), otherwise the application of ultrasound is not suitable, indicated by a cross sign. It is clear from Table 6 that ultrasound is suitable pre-treatment for coagulation/flocculation and disinfection processes for Pittaway pond water. Contrarily, ultrasound is not suitable as a pre-treatment for filtration process when organic fouling is concerned. However, it is worth mentioning that when bio-fouling and inorganic fouling are considered, ultrasound is an effective pre-treatment technique due to its disinfection and oxidizing effects [18,19,124].

Implementing ultrasound as pre-treatment for coagulation process is the best arrangement for ultrasound application in surface water treatment as ultrasound has no residual effect [5] and its application prior to disinfection can be ineffective practice. In addition to the positive effect of ultrasound in enhancing the amenability of organic contaminants towards removal by coagulation, ultrasound destruction of micro-organisms and oxidizing of inorganic species can improve the coagulation and subsequent treatment processes. For instance, the disintegration of micro-organisms and the release of intracellular products may enhance the coagulation as cell products may act as non-ionic polyelectrolytes that aid the removal of organic compounds by coagulation [125]. Moreover, the oxidation of inorganic species such as iron and manganese by ultrasound can be harnessed as a replacement for the pre-chlorination prior coagulation that is normally adapted for oxidizing metals [124,126]. This in turn reduces the formation of DBPs by reducing the amount of added chlorine to water.

5. Conclusions and recommendations

In this work, the effect of ultrasound treatment (pulsed and continuous) on UV–vis absorbance, COD_{Mn}, alkalinity and conductivity of an Australian surface water with fresh NOM mainly driven from vegetation was investigated. The bulk temperature rise of the water that accompanied ultrasound treatments was recorded and subsequently used to perform thermal treatments that had the same temperature rise pattern as ultrasound treatments. ANOVA of the obtained results revealed that thermal treatments had no significant effect on the properties of the treated water and the changes occurred were mainly attributed to ultrasonic effects.

LSD post-hoc analysis showed that pulsed ultrasound treatments (R 2:1 and R 3:1) had similar or in some cases stronger influence on the properties of the treated water as compared to continuous treatment. However, pulsed ultrasound with equal pulse and interval periods was significantly less effective than the continuous ultrasound in terms of the treatment effect on water properties. This confirms that pulsed ultrasound can conveniently be used as a replacement for continuous ultrasound in water treatment with less requirement for cooling process (Fig. 2).

An assessment based on experimental observation backed by extensive literature survey was carried out to identify the best location of ultrasound in surface water treatment schemes. The outcomes of the assessment

Table 7
DOC concentration of Pittaway pond water (initial concentration of 6.5 ± 0.15) after ultrasound treatments

Treatments	DOC concentration of Pittaway pond water (mg/L)
R 1:1	5.76 ± 0.08
R 2:1	5.31 ± 0.12
R 3:1	5.3 ± 0.11
Continuous	5.25 ± 0.06

indicated that implementing ultrasound before coagulation/flocculation (Fig. 1) is the most beneficial location for ultrasound in surface water treatment system. The effect of ultrasound as pre-treatment on coagulation performance with various coagulants at various operating conditions is recommended to be experimentally investigated in the future. It is also important for the future work to explore the down-stream effects of ultrasound as pre-treatment for coagulation on the efficiency of filtration and disinfection processes in terms of fouling and DBPs formation.

Acknowledgements

References

[1] J. Fawell, M.J. Nieuwenhuijsen, Contaminants in drinking water: Environmental pollution and health, Br. Med. Bull. 68 (2003) 199–208.

[2] P.S. Murdoch, J.S. Baron, T.L. Miller, Potential effects of climate change on surface-water quality in North America, J. Am. Water Resour. Assoc. 36 (2000) 347–366.

[3] D.W. Kicklighter, D.J. Hayes, J. McClelland, B.J. Peterson, A.D. McGuire, J.M. Melillo, Insights and issues with simulating terrestrial DOC loading of arctic river networks, Ecol. Appl., 23 (2013) 1817–1836.

[4] D. Tetzlaff, S. Carey, C. Soulsby, Catchments in the future North: Interdisciplinary science for sustainable management in the 21st Century, Hydrol. Process. 27 (2013) 635–639.

[5] R.A. Al-Juboori, T. Yusaf, Biofouling in RO system: Mechanisms, monitoring and controlling, Desalination 302 (2012) 1–23.

[6] A.W. Zularisam, A.F. Ismail, R. Salim, Behaviours of natural organic matter in membrane filtration for surface water treatment—A review, Desalination 194 (2006) 211–231.

[7] C. Driscoll, R. Letterman, Chemistry and fate of Al (III) in treated drinking water, J. Environ. Eng. 114 (1988) 21–37.

[8] C.J. Gabelich, T.I. Yun, B.M. Coffey, I.H.M. Suffet, Effects of aluminum sulfate and ferric chloride coagulant residuals on polyamide membrane performance, Desalination 150 (2002) 15–30.

[9] J.J. Costello, Post precipitation in distribution systems, J. Am. Water Works Assoc. 76 (1984) 46–49.

[10] H.C. Flemming, Reverse osmosis membrane biofouling, Exp. Therm. Fluid Sci. 14 (1997) 382–391.

[11] H.C. Flemming, Biofouling in water systems—Cases, causes and countermeasures, Appl. Microbiol. Biotechnol. 59 (2002) 629–640.

[12] P.K. Abdul Azis, I. Al-Tisan, N. Sasikumar, Biofouling potential and environmental factors of seawater at a desalination plant intake, Desalination 135 (2001) 69–82.

[13] J. Kim, Y. Chung, D. Shin, M. Kim, Y. Lee, Y. Lim, D. Lee, Chlorination by-products in surface water treatment process, Desalination 151 (2003) 1–9.

[14] S.D. Richardson, Disinfection by-products and other emerging contaminants in drinking water TrAC, Trends Anal. Chem. 22 (2003) 666–684.

[15] S.D. Richardson, J.E. Simmons, G. Rice, Peer reviewed: Disinfection byproducts: The next generation, Environ. Sci. Technol. 36 (2002) 198A–205A.

[16] H.C. Kim, M.-J. Yu, Characterization of natural organic matter in conventional water treatment processes for selection of treatment processes focused on DBPs control, Water Res. 39 (2005) 4779–4789.

[17] P.A. Neale, A. Antony, M.E. Bartkow, M.J. Farré, A. Heitz, I. Kristiana, J.Y.M. Tang, B.I. Escher, Bioanalytical assessment of the formation of disinfection byproducts in a drinking water treatment plant, Environ. Sci. Technol. 46 (2012) 10317–10325.

[18] R.A. Al-Juboori, T. Yusaf, V. Aravinthan, Investigating the efficiency of thermosonication for controlling biofouling in batch membrane systems, Desalination 286 (2012) 349–357.

[19] L. Stępniak, U. Kępa, E. Stańczyk-Mazanek, The research on the possibility of ultrasound field application in iron removal of water, Desalination 223 (2008) 180–186.

[20] D. Chen, S.K. Sharma, A. Mudhoo (Eds.), Handbook on Applications of Ultrasound: Sonochemistry for Sustainability, CRC Press, London, 2011.

[21] M. Furuta, M. Yamaguchi, T. Tsukamoto, B. Yim, C.E. Stavarache, K. Hasiba, Y. Maeda, Inactivation of Escherichia coli by ultrasonic irradiation, Ultrason. Sonochem. 11 (2004) 57–60.

[22] P.R. Gogate, A.M. Kabadi, A review of applications of cavitation in biochemical engineering/biotechnology, Biochem. Eng. J. 44 (2009) 60–72.

[23] F.R. Young, Cavitation, Imperial College Press, London, 1999.

[24] R.A. Roy, Cavitation sonophysics, Nato. Adv. Sci. I C-Mat 524 (1999) 25–38.

[25] V. Naddeo, V. Belgiorno, R. Napoli, Behaviour of natural organic mater during ultrasonic irradiation, Desalination 210 (2007) 175–182.

[26] F. Chemat, P. Teunissen, S. Chemat, P. Bartels, Sono-oxidation treatment of humic substances in drinking water, Ultrason. Sonochem. 8 (2001) 247–250.

[27] V. Naddeo, M. Landi, V. Belgiorno, R. Napoli, Wastewater disinfection by combination of ultrasound and ultraviolet irradiation, J. Hazard. Mater. 168 (2009) 925–929.

[28] D. Sarkar, A. Haldar, Physical and Chemical methods in Soil Analysis: Fundamental Concepts of Analytical Chemistry and Instrumental Techniques. New Age International, New Delhi, 2005.

[29] L.S. Clesceri, E.W. Rice, A.E. Greenberg, A.D. Eaton (Eds.), Standard methods for examination of water and wastewater: centennial edition, twenty-first ed.,

American Public Health Association, Washington, DC, 2005.

[30] G.V. Korshin, C.-W. Li, M.M. Benjamin, Monitoring the properties of natural organic matter through UV spectroscopy: A consistent theory, Water Res. 31 (1997) 1787–1795.

[31] J. Dilling, K. Kaiser, Estimation of the hydrophobic fraction of dissolved organic matter in water samples using UV photometry, Water Res. 36 (2002) 5037–5044.

[32] J.L. Weishaar, G.R. Aiken, B.A. Bergamaschi, M.S. Fram, R. Fujii, K. Mopper, Evaluation of specific ultraviolet absorbance as an indicator of the chemical composition and reactivity of dissolved organic carbon, Environ. Sci. Technol. 37 (2003) 4702–4708.

[33] G. Amy, Fundamental understanding of organic matter fouling of membranes, Desalination 231 (2008) 44–51.

[34] R.M. Silverstein, T.C. Morrill, G.C. Bassler, Spectrometric identification of organic compounds, third ed., Wiley, New York, NY, 1974.

[35] P. Westerhoff, G. Aiken, G. Amy, J. Debroux, Relationships between the structure of natural organic matter and its reactivity towards molecular ozone and hydroxyl radicals, Water Res. 33 (1999) 2265–2276.

[36] M. Müller, C. Alewell, F. Hagedorn, Effective retention of litter-derived dissolved organic carbon in organic layers, Soil Biol. Biochem. 41 (2009) 1066–1074.

[37] B. Eikebrokk, T. Juhna, S.W. Østerhus, Water treatment by enhanced coagulation—Operational status and optimization issues, TECHNEAU for a project funded by the European Commission, Document No. D 5.3.1, 2006.

[38] R.L. Wershaw, Evaluation of conceptual models of natural organic matter (humus) from a consideration of the chemical and biochemical processes of humification, US Department of the Interior, US Geological Survey, Virginia, 2004.

[39] Y.-P. Chin, G. Aiken, E. O'Loughlin, Molecular weight, polydispersity, and spectroscopic properties of aquatic humic substances, Environ. Sci. Technol. 28 (1994) 1853–1858.

[40] C.S. Uyguner, M. Bekbolet, Evaluation of humic acid photocatalytic degradation by UV–vis and fluorescence spectroscopy, Catal. Today 101 (2005) 267–274.

[41] M.U. Kumke, C.H. Specht, T. Brinkmann, F.H. Frimmel, Alkaline hydrolysis of humic substances—Spectroscopic and chromatographic investigations, Chemosphere 45 (2001) 1023–1031.

[42] S. Valencia, J.M. Marín, G. Restrepo, F.H. Frimmel, Application of excitation–emission fluorescence matrices and UV/Vis absorption to monitoring the photocatalytic degradation of commercial humic acid, Sci. Total Environ. 442 (2013) 207–214.

[43] J. Peuravuori, K. Pihlaja, Molecular size distribution and spectroscopic properties of aquatic humic substances, Anal. Chem. Acta 337 (1997) 133–149.

[44] J. Peuravuori, K. Pihlaja, Preliminary study of lake dissolved organic matter in light of nanoscale supramolecular assembly, Environ. Sci. Technol. 38 (2004) 5958–5967.

[45] A. Matilainen, E.T. Gjessing, T. Lahtinen, L. Hed, A. Bhatnagar, M. Sillanpää, An overview of the methods used in the characterisation of natural organic matter (NOM) in relation to drinking water treatment, Chemosphere 83 (2011) 1431–1442.

[46] K. Hautala, J. Peuravuori, K. Pihlaja, Measurement of aquatic humus content by spectroscopic analyses, Water Res. 34 (2000) 246–258.

[47] C.S. Uyguner, M. Bekbolet, Implementation of spectroscopic parameters for practical monitoring of natural organic matter, Desalination 176 (2005) 47–55.

[48] X. He, B. Xi, Z. Wei, X. Guo, M. Li, D. An, H. Liu, Spectroscopic characterization of water extractable organic matter during composting of municipal solid waste, Chemosphere 82 (2011) 541–548.

[49] Drinking Water Guidelines for Australia, National Health and Medical Research Council, Commonwealth of Australia, Canberra, 2011.

[50] O. Thomas, C. Burgess, UV–visible Spectrophotometry of Water and Wastewater, vol. 27, Elsevier Science, Amsterdam, 2007.

[51] H.H. Rump and H. Krist, Laboratory manual for the examination of water, waste water and soil, VCH Verlagsgesellschaft mbh, Weinheim, 1988.

[52] P. Pittaway, T. van den Ancker, Properties of natural microlayers on Australian freshwater storages and their potential to interact with artificial monolayers, Mar. Freshwater Res. 61 (2010) 1083–1091.

[53] M. Gutierrez, A. Henglein, Chemical action of pulsed ultrasound: Observation of an unprecedented intensity effect, J. Phys. Chem. 94 (1990) 3625–3628.

[54] H. Destaillats, T.M. Lesko, M. Knowlton, H. Wallace, M.R. Hoffmann, Scale-up of sonochemical reactors for water treatment, Ind. Eng. Chem. Res. 40 (2001) 3855–3860.

[55] R. Xiao, D. Diaz-Rivera, Z. He, L.K. Weavers, Using pulsed wave ultrasound to evaluate the suitability of hydroxyl radical scavengers in sonochemical systems, Ultrason. Sonochem. 20 (2013) 990–996.

[56] L. Yang, J.F. Rathman, L.K. Weavers, Degradation of alkylbenzene sulfonate surfactants by pulsed ultrasound, J. Phys. Chem. B 109 (2005) 16203–16209.

[57] E. Naffrechoux, S. Chanoux, C. Petrier, J. Suptil, Sonochemical and photochemical oxidation of organic matter, Ultrason. Sonochem. 7 (2000) 255–259.

[58] A.P. D'silva, S.K. Laughlin, S.J. Weeks, W.H. Buttermore, Destruction of polycyclic aromatic hydrocarbons with ultrasound, Polycyclic Aromat. Compd. 1 (1990) 125–135.

[59] Y. Nagata, K. Hirai, H. Bandow, Y. Maeda, Decomposition of hydroxybenzoic and humic acids in water by ultrasonic irradiation, Environ. Sci. Technol. 30 (1996) 1133–1138.

[60] A. Weissler, Biochemical effects of ultrasound: Destruction of tryptophan, J. Acoust. Soc. Am. 32 (1960) 1499–1500.

[61] A.D. Archer, P.C. Singer, An evaluation of the relationship between SUVA and NOM coagulation using the ICR database, J. Am. Water Works Assoc. 98 (2006) 110–123.

[62] J. Edzwald, Coagulation in drinking water treatment: Particles, organics and coagulants, Water Sci. Technol. 27 (1993) 21–35.

[63] L. Fan, J.L. Harris, F.A. Roddick, N.A. Booker, Influence of the characteristics of natural organic matter on the fouling of microfiltration membranes, Water Res. 35 (2001) 4455–4463.

[64] W. Yuan, A.L. Zydney, Humic acid fouling during ultrafiltration, Environ. Sci. Technol. 34 (2000) 5043–5050.

[65] J.K. Edzwald, W.C. Becker, K.L. Wattier, Surrogate parameters for monitoring organic matter and THM precursors, J. Am. Water Works Assoc. (1985) 122–132.

[66] S.W. Krasner, M.J. McGuire, J.G. Jacangelo, N.L. Patania, K.M. Reagan, E.M. Aieta, The occurrence of disinfection by-products in US drinking water, J. Am. Water Works Assoc. 81 (1989) 41–53.

[67] M. Kitis, T. Karanfil, J.E. Kilduff, The reactivity of dissolved organic matter for disinfection by-product formation, Turk. J. Eng. Environ. Sci. 28 (2004) 167–180.

[68] B.I. Harman, H. Koseoglu, N.O. Yigit, E. Sayilgan, M. Beyhan, M. Kitis, The removal of disinfection by-product precursors from water with ceramic membranes, Water Sci. Technol. 62 (2010) 547–555.

[69] D.M. Owen, G.L. Amy, Z.K. Chowdhury, R. Paode, G. McCoy, K. Viscosil, NOM: characterization and treatability: Natural organic matter, J. Am. Water Works Assoc. 87 (1995) 46–63.

[70] T.K. Nissinen, I.T. Miettinen, P.J. Martikainen, T. Vartiainen, Molecular size distribution of natural organic matter in raw and drinking waters, Chemosphere 45 (2001) 865–873.

[71] A. Matilainen, R. Liikanen, M. Nyström, N. Llndqvist, T. Tuhkanen, Enhancement of the natural organic matter removal from drinking water by nanofiltration, Environ. Technol. 25 (2004) 283–291.

[72] M.A. Schlautman, J.J. Morgan, Adsorption of aquatic humic substances on colloidal-size aluminum oxide particles: Influence of solution chemistry, Geochim. Cosmochim. Acta 58 (1994) 4293–4303.

[73] S. Hong, M. Elimelech, Chemical and physical aspects of natural organic matter (NOM) fouling of nanofiltration membranes, J. Membr. Sci. 132 (1997) 159–181.

[74] J. Mallevialle, C. Anselme, O. Marsigny, Effects of humic substances on membrane processes, in: I.H. Suffet, P. MacCarthy, Aquatic Humic Substances, American Chemical Society, Washington, DC, 1988, pp. 749–767.

[75] J.A. Nilson, F.A. DiGiano, Influence of NOM composition on nanofiltration, J. Am. Water Works Assoc. 88 (1996) 53–66.

[76] A.L. Lim, R. Bai, Membrane fouling and cleaning in microfiltration of activated sludge wastewater, J. Membr. Sci 216 (2003) 279–290.

[77] M. Kitis, T. Karanfil, A. Wigton, J.E. Kilduff, Probing reactivity of dissolved organic matter for disinfection by-product formation using XAD-8 resin adsorption and ultrafiltration fractionation, Water Res. 36 (2002) 3834–3848.

[78] Z.-Y. Zhao, J.-D. Gu, X.-J. Fan, H.-B. Li, Molecular size distribution of dissolved organic matter in water of the Pearl River and trihalomethane formation characteristics with chlorine and chlorine dioxide treatments, J. Hazard. Mater. 134 (2006) 60–66.

[79] G.L. Amy, L. Tan, M.K. Davis, The effects of ozonation and activated carbon adsorption on trihalomethane speciation, Water Res. 25 (1991) 191–202.

[80] G.L. Amy, R.A. Sierka, J. Bedessem, D. Price, L. Tan, Molecular size distributions of dissolved organic matter, J. Am. Water Works Assoc. (1992) 67–75.

[81] D. Chen, Z. He, L.K. Weavers, Y.-P. Chin, H.W. Walker, P.G. Hatcher, Sonochemical reactions of dissolved organic matter, Res. Chem. Intermed. 30 (2004) 735–753.

[82] E.C. Bowles, R.C. Antweiler, and P. MacCarthy, Acid-Base titration and hydrolysis of fulvic acid from the Suwannee river, in: R. Averett, J.A. Leenheer, D.M. McKnighc, K.A. Thorn, Humic substances in the Suwannee River, Georgia: Interactions, properties, and proposed structures, Department of the Interior, US Geological Survey, Denver, CO, 1990.

[83] B. Gu, J. Schmitt, Z. Chen, L. Liang, J.F. McCarthy, Adsorption and desorption of natural organic matter on iron oxide: Mechanisms and models, Environ. Sci. Technol. 28 (1994) 38–46.

[84] R. Sinsabaugh, R. Hoehn, W. Knocke, A. Linkins, Precursor size and organic halide formation rates in raw and coagulated surface waters, J. Environ. Eng. 112 (1986) 139–153.

[85] D.L. Norwood, R.F. Christman, P.G. Hatcher, Structural characterization of aquatic humic material. 2. Phenolic content and its relationship to chlorination mechanism in an isolated aquatic fulvic acid, Environ. Sci. Technol. 21 (1987) 791–798.

[86] H.-C. Kim, M.-J. Yu, Characterization of aquatic humic substances to DBPs formation in advanced treatment processes for conventionally treated water, J. Hazard. Mater. 143 (2007) 486–493.

[87] A. Sotto, J.M. Arsuaga, B. Van der Bruggen, Sorption of phenolic compounds on NF/RO membrane surfaces: Influence on membrane performance, Desalination 309 (2013) 64–73.

[88] A. Tirol-Padre, J.K. Ladha, Assessing the reliability of permanganate-oxidizable carbon as an index of soil labile carbon, Soil. Sci. Soc. Am. J. 68 (2004) 969–978.

[89] M. Mrkva, Evaluation of correlations between absorbance at 254 nm and COD of river waters, Water Res. 17 (1983) 231–235.

[90] J. Ma, W. Liu, Effectiveness of ferrate (VI) preoxidation in enhancing the coagulation of surface waters, Water Res. 36 (2002) 4959–4962.

[91] M.A. El-Shafy, A. Grünwald, THM formation in water supply in South Bohemia, Czech Republic, Water Res. 34 (2000) 3453–3459.

[92] R. Suresh, L. Hiremath, G.V. Kumar, Application of ultrasound and microbial treatment for biomass effluent, J. Appl. Sci. Environ. Sanit. 6 63–68.

[93] AWWA, Staff, Water Quality (Fourth ed.), American Water Works Association, Denver, CO, 2010.

[94] S.W. Krasner, G. Amy, Jar-test evaluations of enhanced coagulation, J. Am. Water Works Assoc. 87 (1995) 93–107.

[95] J.K. Edzwald, J.E. Tobiason, Enhanced coagulation: US requirements and a broader view, Water Sci. Technol. 40 (1999) 63–70.

[96] C. Volk, K. Bell, E. Ibrahim, D. Verges, G. Amy, M. LeChevallier, Impact of enhanced and optimized coagulation on removal of organic matter and its biodegradable fraction in drinking water, Water Res. 34 (2000) 3247–3257.

[97] S. Arabi, G. Nakhla, Impact of calcium on the membrane fouling in membrane bioreactors, J Membr. Sci 314 (2008) 134–142.

[98] S. Judd, A review of fouling of membrane bioreactors in sewage treatment, Water Sci. Technol. 49 (2004) 229–235.

[99] R. Sheikholeslami, I. Al-Mutaz, T. Koo, A. Young, Pretreatment and the effect of cations and anions on prevention of silica fouling, Desalination 139 (2001) 83–95.

[100] A. Antony, J.H. Low, S. Gray, A.E. Childress, P. Le-Clech, G. Leslie, Scale formation and control in high pressure membrane water treatment systems: A review, J. Membr. Sci. 383 (2011) 1–16.

[101] A.M. Al-Rehaili, Comparative chemical clarification for silica removal from RO groundwater feed, Desalination 159 (2003) 21–31.

[102] J.M. Symons, Factors Affecting Disinfection By-product Formation during Chloramination, American Water Works Association, Denver, 1998.

[103] R.Y. Adedapo, Disinfection By-Product Formation in Drinking Water Treated with Chlorine Following UV Photolysis & UV/H_2O_2, in Civil Engineering, University of Waterloo, Ontario, ON, 2005.

[104] G. Amy, R. Bull, G.F. Craun, R. Pegram, M. Siddiqui, Environmental health criteria 216: Disinfectants and disinfectant by-products, World Health Organization, Geneva, 2000.

[105] J.C. Wei, B.Y. Gao, Q.Y. Yue, Y. Wang, L. Lu, Performance and mechanism of polyferric-quaternary ammonium salt composite flocculants in treating high organic matter and high alkalinity surface water, J. Hazard. Mater. 165 (2009) 789–795.

[106] R. Feng, Y. Zhao, C. Zhu, T.J. Mason, Enhancement of ultrasonic cavitation yield by multi-frequency sonication, Ultrason. Sonochem. 9 (2002) 231–236.

[107] J. Huang, R. Feng, C. Zhu, Z. Chen, Low-MHz frequency effect on a sonochemical reaction determined by an electrical method, Ultrason. Sonochem. 2 (1995) S93–S97.

[108] U.S. Environmental Protection Agency, Ways to Measure Ionic Strength, 2012 [cited Mrach 2013]; Available from: http://www.epa.gov/caddis/ssr_ion_wtm.html.

[109] H.J. Busscher, W. Norde, P.K. Sharma, H.C. van der Mei, Interfacial re-arrangement in initial microbial adhesion to surfaces, Curr. Opin. Colloid. Interface Sci. 15 (2010) 510–517.

[110] M. Hocking, K. Klimchuk, S. Lowen, Polymeric flocculants and flocculation, J. Macromol. Sci. C. 39(2) (1999) 177–203.

[111] H.J. Busscher, A.H. Weerkamp, Specific and non-specific interactions in bacterial adhesion to solid substrata, FEMS Microbiol. Lett. 46 (1987) 165–173.

[112] J.A. Brant, A.E. Childress, Assessing short-range membrane-colloid interactions using surface energetics, J. Membr. Sci 203 (2002) 257–273.

[113] C.J. van Oss, Acid-base interfacial interactions in aqueous media, Colloids Surf., A 78 (1993) 1–49.

[114] M. Kobya, O.T. Can, M. Bayramoglu, Treatment of textile wastewaters by electrocoagulation using iron and aluminum electrodes, J. Hazard. Mater. 100 (2003) 163–178.

[115] E. Bazrafshan, H. Biglari, A.H. Mahvi, Humic acid removal from aqueous environments by electrocoagulation process using iron electrodes, J. Chem. 9 (2012) 2453–2461.

[116] K. Hori, S. Matsumoto, Bacterial adhesion: From mechanism to control, Biochem. Eng. J. 48 (2010) 424–434.

[117] k. Ghosh and m. Schnitzer, Macromolecular Structures of Humic Substances, Soil Sci. 129 (1980) 266–276.

[118] I. Sentana, R.D. Puche, E. Sentana, D. Prats, Reduction of chlorination byproducts in surface water using ceramic nanofiltration membranes, Desalination 277 (2011) 147–155.

[119] C. Jarusutthirak, S. Mattaraj, R. Jiraratananon, Factors affecting nanofiltration performances in natural organic matter rejection and flux decline, Sep. Purif. Technol. 58 (2007) 68–75.

[120] Á. de la Rubia, M. Rodríguez, D. Prats, pH, Ionic strength and flow velocity effects on the NOM filtration with TiO_2/ZrO_2 membranes, Sep. Purif. Technol. 52 (2006) 325–331.

[121] M.S. Siddiqui, G.L. Amy, Factors affecting DBP formation during ozone-bromide reactions, J. Am. Water Works Assoc. 85 (1993) 63–72.

[122] S. Batterman, L. Zhang, S. Wang, Quenching of chlorination disinfection by-product formation in drinking water by hydrogen peroxide, Water Res. 34 (2000) 1652–1658.

[123] P.J. Vikesland, K. Ozekin, R.L. Valentine, Monochloramine decay in model and distribution system waters, Water Res. 35 (2001) 1766–1776.

[124] A. Anderson, R. Reimers, P. DeKernion, A brief review of the current status of alternatives of chlorine disinfection of water, Am. J. Public Health 72 (1982) 1290–1293.

[125] M. Ma, R. Liu, H. Liu, J. Qu, W. Jefferson, Effects and mechanisms of pre-chlorination on Microcystis aeruginosa removal by alum coagulation: Significance of the released intracellular organic matter, Sep. Purif. Technol. 86 (2012) 19–25.

[126] K.H. Choo, H. Lee, S.-J. Choi, Iron and manganese removal and membrane fouling during UF in conjunction with prechlorination for drinking water treatment, J. Membr. Sci. 267 (2005) 18–26.

Paper IV

Effect of ultrasound treatment on characteristics of terrestrial aquatic carbon: comparison between continuous and pulsed treatments

Raed A. Al-Juboori[a*], Talal Yusaf[b], Vasantha Aravinthan[a], Pamela A. Pittaway[c], Leslie Bowtell[b]

a) School of Civil Engineering and Surveying, Faculty of Health, Engineering and Sciences, University of Southern Queensland, Toowoomba, 4350 QLD Australia
b) School of Mechanical and Electrical Engineering, Faculty of Health, Engineering and Sciences, University of Southern Queensland, Toowoomba, 4350 QLD Australia
c) Cooperative Research Centre for Irrigation Futures, National Centre for Engineering in Agriculture, University of Southern Queensland, Toowoomba, 4350 QLD Australia

*corresponding author: Raed A. Al-Juboori, contact details: Tel. +61 413424126, +61 7 4631 1366; emails: RaedAhmed.mahmood@gmail.com, RaedAhmed.Mahmood@usq.edu.au

Abstract

The use of chemical-free techniques such as ultrasound technology in water treatment has gained great popularity in recent years owing to the benign environmental effects this technology. The performance evaluation of this technology for water treatment techniques has mostly been conducted using synthetic water samples. This study however, evaluates ultrasound technology in improving the quality of natural water with organic carbon predominantly derived from terrestrial sources. Ultrasound treatments were applied in continuous and pulsed modes with a range of On:Off ratios (R) at power intensity of 21.5 W/cm² for 4 minutes. Surrogate physio-chemical and spectroscopic properties were measured to determine the effect of ultrasound treatments on the quantity and quality of dissolved organic carbon (DOC) in the treated water. Post-hoc statistical analysis at a significance level of 0.05 showed that the performance of pulsed ultrasound treatments at least at one of pulse settings was better than that of a continuous treatment. Overall, it was found that ultrasound treatments decreased DOC in the treated water and altered its nature to become more amenable to coagulation, but also increased its potential to form fouling and disinfection by-products (DBPs). Hence, ultrasound is recommended to be applied as a pre-treatment for the coagulation process.

Keywords: Pulsed ultrasound, DOC, physio-chemical properties**,** Spectroscopic properties**,** LSD post-hoc analysis

1. Introduction

The nature of DOC in water governs its behaviour towards the treatment processes. The structural characteristics of the aquatic organic matter depends on source materials, geology and topography of the catchment (Matilainen et al. 2011). There are three main categories of DOC that are of concern to water treatment; allochthonous, autochthonous and anthropogenic (Knapik et al. 2015). Allochthonous DOC is originated from the vegetative decomposition and terrestrial sources. Autochthonous DOC is derived mostly from algal and microbial activities. The source of anthropogenic DOC is human activities and the microbial products that result from the biological treatment of waste water. The water resources that are utilized for drinking water production mostly contain allochthonous and autochthonous carbon (Park et al. 2009). However, the occurrence of autochthonous DOC in water resources depends on the hydraulic residence time of water in the reservoirs, and this would naturally reduce its contribution to carbon budget of the water. Thus, focusing on the enhancement of allochthonous DOC removal would be of more importance to drinking water treatment practices as compared to the other DOC types.

Generally, DOC can be removed from drinking water through sequential processes of coagulation/flocculation and filtration. However, some DOC can still reach the disinfection step. The presence of DOC in the disinfection step causes detrimental problems to the treatment as it reacts with the disinfectants leading to an inefficient microbial inactivation and the formation of pernicious DBPs (Al-Juboori and Yusaf 2012). The common classes of DBPs are trihalomethanes (THMs) and haloacetic acids (HAAs). DBPs are potential carcinogenic and mutagenic complexes that can cause serious health issues (Al-Juboori and Yusaf 2012). Since chemical treatments produce harmful by-products, the use of chemical-free techniques such as ultrasound is encouraged in the recent water treatment research investigations.

Ultrasound technology is an attractive method for DOC removal owing to its benign environmental effects and its simple implementation (Al-Juboori et al. 2015a). However, a number of studies reported that ultrasound requires high energy levels for achieving low decomposition rate of DOC (Naffrechoux et al. 2000). To promote the use of chemical-free technologies such as ultrasound, ways of reducing energy requirement in these technologies should be explored. One of the energy-saving ways for running ultrasound is the pulsed mode operation. Pulsed ultrasound refers to the intermittent wave irradiation where there are On periods followed by Off periods. In sonochemistry, the ratio of On:Off is denoted as R. Pulsed ultrasound operation saves the wasted energy in the continuous operation that occurs due to the formation of a cloud of bubbles near the irradiating surface that scatters the waves in different directions (shielding effects). This phenomenon decreases significantly in the pulsed operation as such bubbles dissolve into smaller sized bubbles during the quiescent period serving as cavitation nuclei in the next pulse. However, the improvement in energy recovery in pulsed ultrasound depends largely on choosing the suitable pulses and quiescent periods.

In this work, the effect of pulsed ultrasound at three different pulse settings of R = 0.5:0.5, 0.6:0.2 and 0.6:0.3 s on the quality and quantity of DOC in natural water samples was investigated and compared to the standard continuous operation. It is important to use natural water samples in evaluating the efficiency of ultrasound, as the use of synthetic samples may lead to performance mis-assessment of the technology. Also, the effectiveness of ultrasound is usually measured based on the quantity of DOC removed while the structural change of DOC is not taken into

consideration. The structural change of DOC due to ultrasound treatments was also evaluated using surrogate measurements such as conductivity, alkalinity, COD, single wavelength UV absorbance and UV ratios. The use of surrogate measurements is a common practice for evaluating the performance of water treatment units (Hendricks 2006). Single wavelength measurements included absorbance at 254 and 280 nm as indicators for humic and aromatic fractions of DOC (Al-Juboori et al. 2015a). Single wavelength measurements were normalized by DOC concentration (SUVA) to detect the structural change of DOC rather than the change in DOC concentration. UV absorbance ratios of A_{250}/A_{365} (E_2/E_3), A_{254}/A_{204} (A_{ET}/A_{Bz}) and A_{254}/A_{436} were applied as indicators for molecular size, abundance of aromatic compounds with functional groups and the ratio of UV absorbance to colour forming DOC moieties, respectively (Al-Juboori et al. 2015a). Statistical analyses were applied to determine the significance of the change in DOC concentration and structure, and also to compare between the treatments.

2. Materials and methods

2.1. Water sample

Logan water was selected in this study as a model for South East Queensland (SEQ) water bodies. Logan water is an agricultural storage with NOM mainly driven from soil and grass degradation. The characteristics of Logan water are shown in Table 1.

Table 1: Characteristics of Logan water

Water properties		Measured values
pH, 25˚C		9.10 ± 0.30
DOC (mg/L)		8.57 ± 0.17
Specific COD_{Mn} (mg O_2/mg DOC)		1.17 ± 0.13
Total suspended solids (TSS) (mg/L)		44.00 ± 1.20
SUVA (L/mg.cm)	254	0.046 ± 0.005
	280	0.033 ± 0.004
	250/365	5.36 ± 0.55
	254/204	0.33 ± 0.02
	254/436	17.9 ± 1.2
Alkalinity (meq/L)		3.00 ± 0.26
Conductivity (mS/cm), 25 ˚C		0.3 ± 0.04
Iron (mg/L)		0.060 ± 0.008
Nitrate (mg/L)		1.02 ± 0.1
Chloride (mg/L)		44.0 ± 2.7
Sulphate (mg/L)		0.94 ± 0.07
Phosphate (mg/L)		$<0.1^*$
Bromide (mg/L)		$<0.1^*$

* Below the detection limit of the standard method 4110 B using ICS-2000 ion chromatography

2.2. Ultrasound treatment

Fig. 1 shows a schematic representation for the experimental set-up. A low frequency 20 kHz ultrasonic horn device equipped with a titanium probe of 19 mm diameter (digital Branson sonifier 450 W) was used for treating water samples. In a typical experimental run, 200 ml of water sample in a Pyrex beaker was treated ultrasonically with an immersed horn for a depth of 1 cm. An ice bath was used for maintaining water temperature at approximately 20°C. The temperature of the water sample being treated by ultrasound was measured using a calibrated thermometer.

Ultrasound treatments for both modes continuous and pulsed were conducted at power intensity of 21.5 W/cm^2 for 4 minutes. Ultrasonic power was measured calorimetrically applying the techniques reported in (Al-Juboori et al. 2015c). The pulsed mode was performed at three R ratios of 0.5:0.5, 0.6:0.3 and 0.6:0.2 s. In order to apply the same amount of ultrasonic energy in the pulsed mode as that of the continuous mode, ultrasonic system was operated for a longer time in the case of pulsed mode. The treatment time required for applied pulse mode settings was calculated based on the treatment time of continuous mode as well as the set R ratio using equation 1 (Al-Juboori et al. 2015a).

$$t_p = t_o(1 + 1/R)$$
(1)

where t_p is the treatment time of pulsed treatments and t_o is the treatment time of continuous ultrasound. The treatment time of the pulsed treatments of 0.5:0.5, 0.6:0.3 and 0.6:0.2 s was found to be 480, 360 and 320 s, respectively. It is worth mentioning that ultrasound treatments were conducted in triplicates.
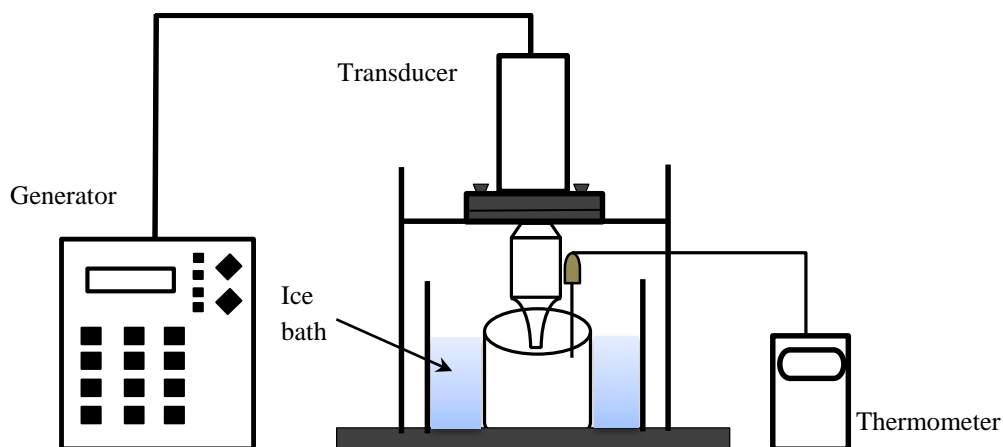
Fig. 1 Schematic of the experimental set-up

2.3. Analytical methods

A range of the physio-chemical and spectroscopic properties of water samples were measured before and after ultrasound treatments applying the following analytical techniques. These techniques were applied to evaluate the effect of ultrasound treatments on DOC concentration and structure. It is important to note here that all the measurements were conducted in triplicate for each water sample.

2.3.1. Dissolved organic carbon

The DOC of water samples was measured applying the standard high temperature combustion method. Water samples were filtered through 0.45 µm prior to DOC measurements. A total Carbon Analyser (TOC-V$_{CSH}$, SHIMADZU, Australia) equipped with an auto-sampler (ASI-V) was utilised for DOC measurements. Three replicate injections were made that resulted in coefficient of variance of < 0.02.

2.3.2. UV-vis absorbance

The spectrophotometric absorbance of water samples was measured using JENWAY UV/Vis spectrophotometer, model 6705. Quartz cuvette of 1 cm path length was used to carry the filtered water samples through 0.45 µm. Water samples were scanned for a wavelength range of 200-500 nm with distilled water being used as base line. Absorbance of water samples at selected wavelengths of 204, 250, 254, 280, 365 and 436 nm was recorded.

The effect of the interfering ions on UV measurements was ignored in this study due to the fact that either the concentration of the ions was below the effective limit or their peak absorbance falls outside the studied range (see Table 1). For instance, the maximum effective ranges of iron and nitrate are 0.5 mg/L and 5 mg/L respectively (Al-Juboori et al. 2015a), which are higher than the concentrations of these species in Logan water. Chloride and sulphate only have a tangible absorbance at wavelength < 200 nm (Crompton 2003). Bromide and phosphate were found to be very small to affect UV-vis absorbance (<0.1 mg/L).

2.3.3. Permanganate chemical oxygen demand (COD$_{Mn}$)

COD$_{Mn}$ was measured following the procedure detailed in (Rump and Krist 1988). Briefly, 5 mL of sulphuric acid (1.27 g/mL) was added to a 100 mL of filtered water samples (0.45 µm). To avoid violent boiling and spillage, anti-bumping granules were added to the mixture. The samples were heated to boiling and then 15 mL of 0.002 M potassium permanganate was added to the boiled mixture. The samples were left to boil for exactly 10 minutes. Therewith, 15 mL of 0.05 M oxalic acid was added to the samples. After the addition of the oxalic acid to the water sample, the sample becomes colourless. Finally, the resultant solution was titrated with potassium permanganate until the colour of the solution turns to feint pink. The consumed volume of potassium permanganate was recorded and used for calculating COD$_{Mn}$.

2.3.4. Alkalinity and conductivity

The alkalinity and conductivity of water samples was measured using titration workstation TitraLab, TIM 845 and ion analyser, MeterLab model ION 450 (Radiometer-Analytical, Australia).

2.4. Statistical analyses

To evaluate the significance of the change occurs in the treated water sample characteristics, analysis of variance (one way ANOVA) was carried out for the measured characteristics at $P<0.05$ using SPSS 19 statistics software. Only when there is an overall significant change observed in the measured characteristic, the least Significant Difference (LSD) Post Hoc test was performed to compare the differences in the water characteristics for continuous and pulsed treatments.

3. Results and discussions

3.1. Overall effect of the treatments

Table 2 presents the overall effect of ultrasound treatments on the measured characteristics of the treated water. The values in Table 2 represent the mean of the characteristics of triplicate treatments normalized by their counterparts of the untreated water. The significance level applied in this study was 0.05, so the normalized change of a characteristic with a P-value of less 0.05 is considered significant and higher than that is considered insignificant. Applying this criteria, one can clearly see that ultrasound treatments had insignificant effect on normalized $SUVA_{254}$ and $SUVA_{280}$, whereas the other characteristics were significantly altered by ultrasound treatments. The slight increment in $SUVA_{254}$ and $SUVA_{280}$ is in agreement with the results reported by Naddeo et al. (2007). Such agreement is attributed to the resembling in the structure between the carbon source of Logan water (i.e. terrestrial) and that used in (Naddeo et al. 2007) (i.e. Aldrich humic acid) as both known to be highly aromatic (Bob and Walker 2001). The slight increments in $SUVA_{254}$ and $SUVA_{280}$ can be explained in two possible scenarios; sonication extraction of humic acids from suspended soil particles (Ramunni and Palmieri 1985) or alteration of UV absorbing moieties under the effect of ultrasound (Naddeo et al. 2007). Both scenarios are equally valid, however the presence of high TSS level in Logan water (44 ppm) as compared to the usual TSS levels in natural waters (i.e. 10-20 ppm) (Gregory 2005) supports the second scenario. This high level of TSS can increase the chances of humic substances released from soil particles under the effect of sonication. Since the changes in $SUVA_{254}$ and $SUVA_{280}$ were found to be statistically insignificant, so it will not be discussed further in this study and the attention will rather be focused on the significantly changed characteristics.

Table 2: Analysis of variance (ANOVA) and descriptive statistics for overall effect

of ultrasound treatments

Normalized characteristics	Mean	SD	*F-value*	*P-value*
DOC	0.953	0.0245	99.611	0.000
$SUVA_{254}$	1.113	0.0167	3.285	0.140
$SUVA_{280}$	1.107	0.0222	3.346	0.137
E_2/E_3	1.110	0.0757	7.914	0.037
A_{254} / A_{204}	1.125	0.0259	16.572	0.010
$A_{254} /Color_{436}$	0.873	0.1180	17.741	0.009
I_{Mn}	1.024	0.0240	8.421	0.033
Conductivity	1.043	0.0143	8.980	0.030
Alkalinity	0.888	0.0661	11.597	0.019
pH	0.890	0.0183	8.997	0.030

3.2. Comparison between the treatments

The significance of the difference between the treatments' effects on water characteristics was evaluated applying LSD post-hoc analysis at a significance level of 0.05 as shown in Table 3. The mean and standard deviation values in Table 3 were calculated from averaging the normalized change of the treated water characteristics for three replicates of each treatment.

It can be seen from Table 3 that the effect of pulsed treatment with *R* ratio of 0.5:0.5 s on the treated water characteristics was not significantly different than that of continuous ultrasound except for E_2/E_3 and conductivity. This is could be due to the long quiescent period of 0.5:0.5 treatment as compared to the other treatments. For instance, Orzechowska and Poziomek (1994) found that continuous ultrasound caused significantly higher increment in conductivity of different solutions as compared to pulsed ultrasound with 60% duration (i.e. 0.6:0.4 s). However, increasing the pulse duration to 80% made the difference between the effects of two treatments on conductivity marginal as it is the case in this study.

The effect of pulsed treatment of 0.6:0.2 s on water characteristics was also not significantly different from that of continuous treatment for most of the characteristics except for DOC, E_2/E_3 and $A_{254} /Color_{436}$. This indicates that shortening the resting period of pulsed ultrasound with having a relatively high pulse period brings the effect of the pulsed treatment closer to that of continuous treatment.

The effect of pulsed treatment of 0.6:0.3 s on most of the treated water characteristics was significantly different from those of the other treatments. This highlights that this treatment falls in the pulsed cavitation peak range for the applied power level in this study. The pulse cavitation peak was described to be the pulsed cavitation conditions during which the maximum cavitation activity is generated (Wang et al. 1996). The higher effect of pulsed cavitation peak conditions as compared to other treatment conditions is believed to be due to the clarification effect of pulsed ultrasound (i.e. reduction of shielding effects). During the quiescent period of pulsed ultrasound, the density of the bubbles in the irradiating liquid decreases and this reduces the coalescence between bubbles leaving the bubbles in their spherical shape (Wang et al. 1996). These bubbles would then act as source for the transient

cavitational bubbles in the subsequent pulse. The collapse of the spherical bubbles generates physical and chemical effects with higher energy than the effects of bubbles collapse with deformed shape. There are other mechanisms that can explain the superiority of pulsed ultrasound effects as compared to continuous ultrasound such as time availability for species diffusion into the collapsing bubbles during the quiescent period, effect of residual pressure on driving cavitation activities during the quiescent period and spatial enlargement of the active zone (Al-Juboori et al. 2015b). However, it should be noted that the roles of these mechanisms would only come to play when the suitable pulse and quiescent periods are selected. Otherwise, pulsed ultrasound would result in similar or less effect than continuous ultrasound.

Table 3: Descriptive statistics and LSD post-hoc comparison between ultrasound treatments

Treatment levels	0.5:0.5		0.6:0.3		0.6:0.2		Continuous	
Normalized characteristics	Mean	SD	Mean	SD	Mean	SD	Mean	SD
DOC	0.978^a	0.0053	0.923^b	0.0017	0.938^c	0.0035	0.971^a	0.0035
E_2/E_3	1.040^a	0.0297	1.100^a	0.0287	1.084^a	0.0316	1.217^b	0.0555
A_{254}/A_{204}	1.136^a	0.0183	1.089^b	0.0006	1.124^a	0.0011	1.152^{ac}	0.0039
$A_{254}/Color_{436}$	0.934^a	0.0437	0.784^b	0.0411	0.757^b	0.0411	1.015^a	0.0389
COD_{Mn}	1.010^{ac}	0.0006	0.998^c	0.0043	1.047^b	0.0027	1.042^{ab}	0.0229
Conductivity	1.022^a	0.0047	1.052^b	0.0047	1.044^b	0.0117	1.054^b	0.0023
Alkalinity	0.949^a	0.0466	0.796^b	0.0094	0.882^a	0.0287	0.927^a	0.0078
pH	0.913^a	0.0008	0.871^b	0.0047	0.879^{bc}	0.0155	0.897^{ac}	0.0062

*Means in the same row that do not share the same letter are significantly different ($p < 0.05$) by LSD post-hoc test

3.3. Ultrasonic effect on physio-chemical properties and its interpretation

3.3.1. DOC

The average normalized DOC of Logan water treated with different ultrasound treatments is shown in Fig. 2. It can be seen from Fig. 2 that DOC removal of the applied ultrasound treatments was in the order of 0.6:0.3 s > 0.6:0.2 s > continuous > 0.5:0.5 s. DOC removal levels obtained in this study were consistent with the ones reported in previous studies. For instance, Stepniak et al. (2009) reported a DOC removal of <10% in natural water treated with continuous ultrasound. Two of the pulsed treatments had a better DOC removal than continuous treatment, while the other pulsed treatment had lower DOC removal as compared to continuous treatment. Such variation in pulsed ultrasound performance is likely to be due to the selection of pulse settings as explained in earlier sections.

DOC removal with ultrasound treatment takes place through chemical and mechanical effects of ultrasound. The prominent chemical mechanism of ultrasonic is the cleavage of the aromatic rings under the effect of oxidative radicals (Nagata et al. 1996). The mechanical degradation of DOC with sonication occurs due to the powerful shear forces produced from cavitation and streaming effects (Price et al. 2002). The

shear degradation is focused in the regions with high agitation. Such regions form in the adjacent area of the bubbles, as bubbles' oscillation and collapse cause high velocity movements of the liquid layers resulting in energetic turbulences and shock waves. In general, decreasing the concentration of DOC using ultrasound should have a positive impact on the treatment processes, as DOC concentration is linked to the common treatment problem such as fouling and the formation of DBPs.
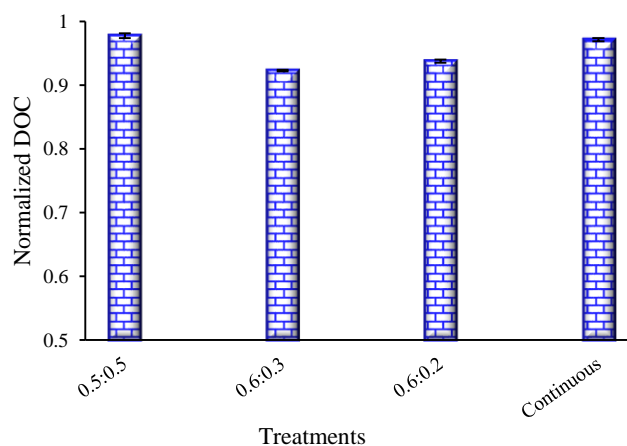

Fig. 2 Normalized DOC of ultrasound treatments

3.3.2. COD_{Mn}

Fig. 3 illustrates the change in COD_{Mn} of Logan water with various ultrasound treatments. Fig. 3 presents an interesting trend as COD_{Mn} of the treated water increased with most of ultrasound treatments except for 0.6:0.3 s where there was a slight decrease in COD_{Mn}. The change of COD under the effect of sonication did not follow a certain pattern in the literature. For instance, Naffrechoux et al. (2000) obtained a 50 % reduction in COD of water samples treated with a combination of ultrasound and UV radiation, whereas another study observed COD increment with ultrasound (Suresh et al. 2011). The variation of COD_{Mn} with ultrasound treatments could be attributed to the preferential reaction of permanganate with large molecular weight compounds (Tirol-Padre and Ladha 2004). Different ultrasound treatments may have different effects on the molecular size of the treated compounds through the concurrent extraction and destruction of the organic compounds presented in the heterogeneous mixture of particle aggregates and surface water.
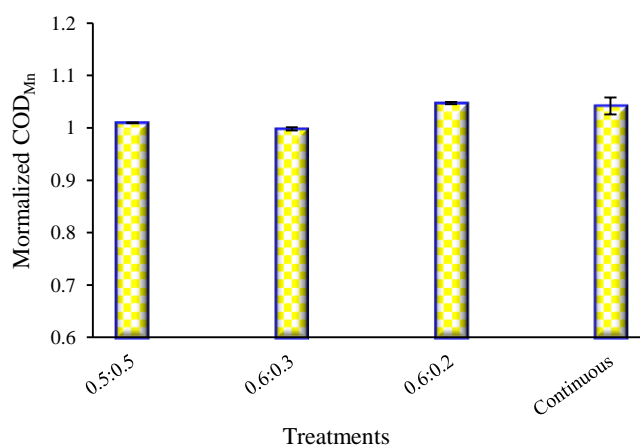

Fig. 3 Normalized permanganate index of ultrasound treatments

The alteration of Logan water COD_{Mn} under the effect of ultrasound treatments can give an indication to the tendency of contaminants towards the involvement in oxidation reactions. El-Shafy and Grünwald (2000) reported that there is a weak correlation between the formation of THMs and COD_{Mn} of the water ($R^2 = 0.587$). This means that the alteration of Logan water COD_{Mn} after sonication treatments might not cause any change in the tendency of the treated water to form DBPs.

3.3.3. Alkalinity

The alteration of Logan water alkalinity under the effect of ultrasound treatments is presented in Fig. 4. The alkalinity of Logan water decreased after the exposure to ultrasound treatments. It can be seen from Fig. 4 that pulsed ultrasound of 0.6:0.3 s resulted in the highest reduction of alkalinity ~ 20% followed by 0.6:0.2 s, continuous and 0.5:0.5 s at approximate reduction percentages of 12%, 7% and 5%, respectively. Alkalinity reduction of treated water is attributed to the reaction of bicarbonates with the hydroxyl radicals produced from the collapsing bubbles as illustrated in the equation below (Suri et al. 2010):
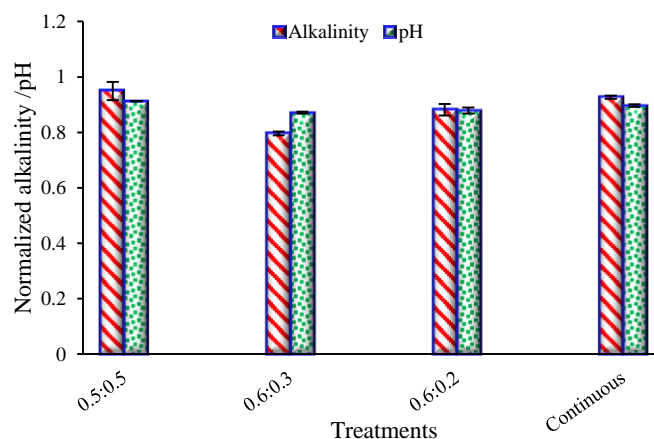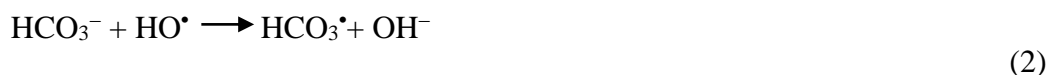
$$HCO_3^- + HO^\bullet \longrightarrow HCO_3^\bullet + OH^-$$

(2)

Fig.4 Normalized alkalinity and pH of ultrasound treatments

Alkalinity plays a crucial role in most of water treatment processes, however its effect is usually studied in conjunction with pH. Hence, the effect of ultrasound treatment on the pH of the treated water was also measured and the results are presented in Fig. 4. The pH reduction trend is similar to that of alkalinity. However, the reduction of pH was more pronounced than the reduction of alkalinity for all treatments except for 0.6:0.3 s.

Alkalinity consumes hydrogen ions in the solution affecting pH and the redox reactions occurring in the water. The pH of a solution controls the surface charge of chemical and biological species in the water. If the pH of a solution exceeds the isoelectric point (IES) of the existing contaminants, the charge of these contaminants becomes negative, and if it drops below IES, the charge of the contaminants becomes positive (Al-Juboori and Yusaf 2012). The pH of the solution can also influence the solubility of the metals and organic matter in water.

Ultrasound reduction of Logan water pH could positively affect its coagulability as it brings the pH level closer to the optimum level for DOC removal (6.5-5.5 (USEPA 1999)) with zero addition of chemicals. Also, reducing water alkalinity due to ultrasound treatment can be useful particularly for water with high alkalinity. In this case, the addition of coagulant would be sufficient to bring the pH to the optimum level for DOC removal, and the addition of pH reducing agents becomes unnecessary. The reduction of pH and alkalinity of treated water could also affect the filtration process owing to the dependence of filtration on surface charge of contaminants (Al-Juboori and Yusaf 2012). Decreasing the alkalinity could also help in alleviating inorganic fouling in filtration (Al-Juboori et al. 2015a). Alkalinity was found to have a direct correlation with the formation of DBPs (Adedapo 2005), hence reducing it with ultrasound treatment could potentially reduce the risk of DBPs formation in the treated Logan water.

3.3.4. Conductivity

The normalized conductivity of the treated Logan water with different ultrasound treatments is shown in Fig. 5. Generally, the conductivity of Logan water increased after ultrasound treatments. The increment of water conductivity upon ultrasound treatment can be attributed to the gaseous reactions occur in the thermolytic centre of transient bubbles producing acid in the adjacent areas to the collapsing bubbles (Al-Juboori et al. 2015a). The observed conductivity increase with ultrasound treatments is consistent with the results reported by Naddeo et al. (2007) who found that the conductivity of humic acid solution increased when treating it with ultrasound. The variation in conductivity of the treated water with pulsed and continuous ultrasound treatments was found be insignificant except for 0.5:0.5 s treatment as compared to other treatments (section 3.2).

Conductivity plays a crucial role in the electrochemistry interactions between contaminants and the treatment processes. For instance, the adherence of contaminants to filtration medias or metal complexes (coagulants) is affected by the electrical double layer interaction (Hocking et al. 1999). Increasing the conductivity of Logan water indicates either an increase in the concentration of the charged contaminants or an increase in their charge density. In either way, the thickness of the electrical double layer decreases and the affinity between contaminants and filters or coagulants complexes increases (Hocking et al. 1999). Based on the conductivity results presented here, ultrasound treatment can promote the coagulability of Logan water, but at the same time can increase its fouling potential. Effect of conductivity on DBPs formation is complex as such characteristic can not only affect the electrochemistry interaction between disinfectants and DOC, but also affects dissociation and recombination reactions of the disinfectants (Vikesland et al. 2001).
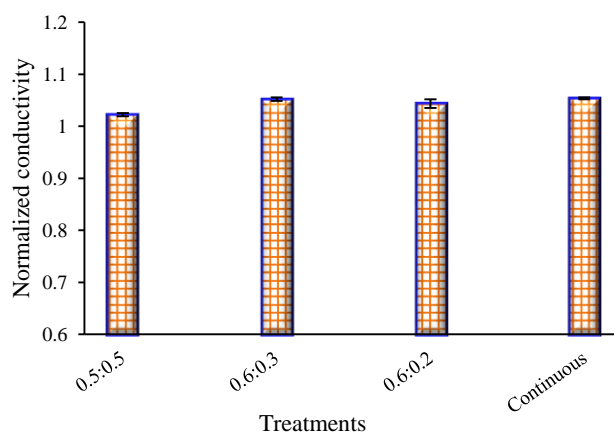
Fig. 5 Normalized conductivity of ultrasound treatments

3.4. Ultrasonic effect on spectroscopic properties and its interpretation

The impact of ultrasound treatments on UV ratios of Logan water is presented in Fig. 6. It can be noticed from this figure that ultrasound treatments increased the proportion of small sized molecules to large sized molecules, and these results are in agreement with previous studies that were conducted on synthetic organic solutions and wastewater samples (Chen et al. 2004). It is clear that continuous treatment have higher effect on molecular size of DOC as compared to pulsed treatments. Among pulse treatments, 0.6:0.2 s resulted in the highest A_{250}/A_{365} increment. The large increment of A_{250}/A_{365} in continuous treatment as opposed to the pulsed treatments suggests that molecular size degradation under the effect of ultrasound depends on the mechanical effects more than the chemical effects of ultrasound. This statement is supported by the findings of Henglein and Gutierrez (1990), as the latter reported that the size destruction of polymers was favoured at bubbles coalesce conditions which occur mostly in continuous operation. The unremitting agitation in the continuous treatment could also play a role in the observed A_{250}/A_{365} results, as such agitation produces high level of shear stresses capable of breaking down the molecules into smaller sized ones. Fig. 6 also shows that ultrasound treatments increased the ratio A_{254}/A_{204} of Logan water. Increasing A_{254}/A_{204} reflects an increase in the bulk aromaticity of the treated water and this is consistent with the results presented in Table 2. The increase of aromatic compounds with oxygen containing functional groups is believed to be due to the extraction effects of ultrasound that led to the release of aromatic compounds from the soil aggregates in Logan water. The released aromatic compounds might have undergone hydroxyl radicals attack in later stages of the treatment (Al-Juboori et al. 2015c). Fig. 6 reveals that pulsed ultrasound treatment of 0.6:0.2 s had the least effect on A_{254}/A_{204}, and continuous treatment had the highest effect, while the other two treatments had effects fall in between these two ranges.

Interestingly, continuous ultrasound treatment increased A_{254}/A_{436}, while pulsed ultrasound treatments decreased this ratio as shown in Fig. 6. This trend suggests that pulsed ultrasound was more effective in removing UV absorbing portion of DOC than removing colour forming moieties of DOC. This could be ascribed to the nature of DOC moieties, as the moieties that absorb UV light are likely to be of a hydrophobic nature, while the colour forming moieties are mostly of autochthonous origin that possesses a hydrophilic nature (Battin 1998). In general, ultrasound favourably destructs DOC of hydrophobic nature, however this destruction can be more pronounced with pulsed treatments as opposed to continuous treatment due to the time

given to these compounds to diffuse into the collapsing bubbles or their vicinity in the pulsed treatments. The decrease in the A_{254}/A_{436} of Logan water could also be ascribed to the release of coloured organic matter from soil aggregates (Bossio et al. 2008).
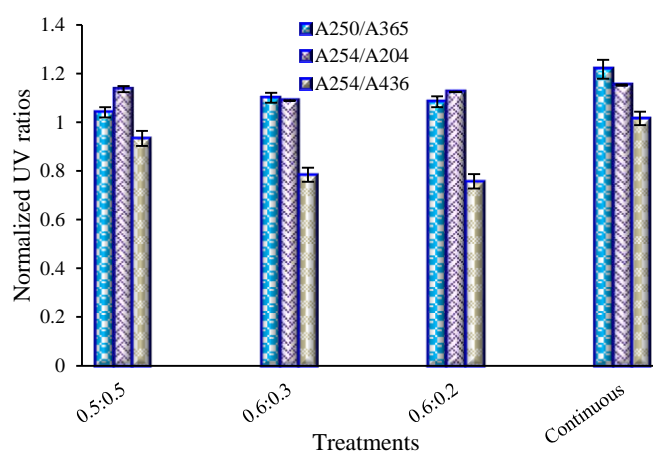

Fig. 6 Normalized UV ratios of ultrasound treatments

The size spectrum of DOC has an important effect on its removal via the common treatment processes. Some studies showed that the larger the size of DOC molecules, the higher the removal of DOC can be achieved with coagulation process (Nissinen et al. 2001). Although that ultrasound treatment of Logan water decreased the size of DOC molecules, the number of the broken molecules and aggregates increased which would increase the chance of these molecules and aggregates to get in contact with the coagulants and ultimately increases their removal (Pizzi 2011). The abundance of oxygen containing functional groups in DOC promotes adsorption and complexation reactions (Korshin et al. 1997). This implies that the increase of A_{254}/A_{204} after sonication can potentially increase the amenability of DOC towards coagulation. However, the residual DOC after coagulation might become more ready to foul filters or to form DBPs. The preferential removal of colour forming moieties with continuous ultrasound or UV absorbing moieties in pulsed ultrasound would not affect the performance of any of the treatment processes as both portions can form fouling and DBPs (Fabris et al. 2007; Valencia et al. 2012). However, knowing the portion of coloured DOC might help in choosing the right coagulant, as coloured DOC is more effectively scavenged by polymer based than metallic salt coagulants (Smith et al. 1991).

4. Conclusions

The effect of pulsed and continuous ultrasound treatments on concentration and structure of natural DOC originated mainly from terrestrial sources was investigated in this study. All the changes occurred in water properties were statistically significant except for SUVA at 254 and 280 nm. Pulsed treatments of 0.6:0.2 s and 0.5:0.5 s were statistically similar to continuous treatment in their effects on the treated water properties. Pulsed treatment of 0.6:0.3 s was significantly different than the other ultrasound treatments in terms of its effect on DOC concentration and properties.

The alteration of Logan water properties due to ultrasound treatments indicates that the treatment improves the coagulability of the water through reducing DOC concentration and alkalinity and increasing conductivity and aromatic compounds with

oxygen containing functional groups. However, some of these changes such as increment of conductivity and aromaticity might increase the potential of fouling and DBPs formation of the water. Hence, based on the results obtained in this study, it can be concluded that the best fit of ultrasound treatment in water treatment train would be prior to coagulation.

5.   Acknowledgements

6. References

Adedapo RY (2005) Disinfection By-Product Formation in Drinking Water Treated with Chlorine Following UV Photolysis & UV/H₂O₂. University of Waterloo, Ontario, Canada

Al-Juboori RA, Yusaf T (2012) Biofouling in RO system: Mechanisms, monitoring and controlling Desalination 302:1-23 doi:10.1016/j.desal.2012.06.016

Al-Juboori RA, Yusaf T, Aravinthan V, Pittaway PA, Bowtell L (2015a) Investigating the feasibility and the optimal location of pulsed ultrasound in surface water treatment schemes Desalin Water Treat:1-19 doi:10.1080/19443994.2014.996771

Al-Juboori RA, Yusaf T, Bowtell L (2015b) Energy Conversion Efficiency of Pulsed Ultrasound. Paper presented at the The 7th International Conference on Applied Energy – ICAE2015, Abu Dhabi, UAE, 2015 March 28-31

Al-Juboori RA, Yusaf T, Bowtell L, Aravinthan V (2015c) Energy characterisation of ultrasonic systems for industrial processes Ultrasonics 57:18-30

Battin TJ (1998) Dissolved organic matter and its optical properties in a blackwater tributary of the upper Orinoco river, Venezuela Org Geochem 28:561-569 doi:http://dx.doi.org/10.1016/S0146-6380(98)00028-X

Bob MM, Walker HW (2001) Effect of natural organic coatings on the polymer-induced coagulation of colloidal particles Colloids and Surfaces A: Physicochemical and Engineering Aspects 177:215-222 doi:http://dx.doi.org/10.1016/S0927-7757(00)00679-8

Bossio JP, Harry J, Kinney CA (2008) Application of ultrasonic assisted extraction of chemically diverse organic compounds from soils and sediments Chemosphere 70:858-864

Chen D, He Z, Weavers LK, Chin Y-P, Walker HW, Hatcher PG (2004) Sonochemical reactions of dissolved organic matter Res Chem Intermed 30:735-753 doi:10.1163/1568567041856954

Crompton TR (2003) Chromatography of natural, treated and waste waters. CRC Press,

El-Shafy MA, Grünwald A (2000) THM formation in water supply in South Bohemia, Czech republic Water Res 34:3453-3459 doi:http://dx.doi.org/10.1016/S0043-1354(00)00078-6

Fabris R, Lee EK, Chow CWK, Chen V, Drikas M (2007) Pre-treatments to reduce fouling of low pressure micro-filtration (MF) membranes J Membrane Sci 289:231-240 doi:http://dx.doi.org/10.1016/j.memsci.2006.12.003

Gregory J (2005) Particles in Water: Properties and Processes. CRC Press,

Hendricks DW (2006) Water Treatment Unit Processes: Physical and Chemical. Taylor & Francis,

Henglein A, Gutierrez M (1990) Chemical effects of continuous and pulsed ultrasound: a comparative study of polymer degradation and iodide oxidation J Phys Chem 94:5169-5172

Hocking M, Klimchuk K, Lowen S (1999) Polymeric flocculants and flocculation

Knapik H, Fernandes CS, de Azevedo J, dos Santos M, Dall'Agnol P, Fontane D (2015) Biodegradability of anthropogenic organic matter in polluted rivers using fluorescence, UV, and BDOC measurements Environ Monit Assess 187:1-15 doi:10.1007/s10661-015-4266-3

Korshin GV, Li C-W, Benjamin MM (1997) Monitoring the properties of natural organic matter through UV spectroscopy: a consistent theory Water Res 31:1787-1795

Matilainen A, Gjessing ET, Lahtinen T, Hed L, Bhatnagar A, Sillanpää M (2011) An overview of the methods used in the characterisation of natural organic matter (NOM) in relation to drinking water treatment Chemosphere 83:1431-1442 doi:http://dx.doi.org/10.1016/j.chemosphere.2011.01.018

Naddeo V, Belgiorno V, Napoli R (2007) Behaviour of natural organic mater during ultrasonic irradiation Desalination 210:175-182

Naffrechoux E, Chanoux S, Petrier C, Suptil J (2000) Sonochemical and photochemical oxidation of organic matter Ultrason Sonochem 7:255-259 doi:http://dx.doi.org/10.1016/S1350-4177(00)00054-7

Nagata Y, Hirai K, Bandow H, Maeda Y (1996) Decomposition of hydroxybenzoic and humic acids in water by ultrasonic irradiation Environ Sci Technol 30:1133-1138

Nissinen TK, Miettinen IT, Martikainen PJ, Vartiainen T (2001) Molecular size distribution of natural organic matter in raw and drinking waters Chemosphere 45:865-873 doi:http://dx.doi.org/10.1016/S0045-6535(01)00103-5

Orzechowska GE, Poziomek EJ (1994) Potential use of ultrasound in chemical monitoring. Environmental Monitoring Systems Laboratory-Las Vegas, Office of Research and Development, U.S. Environmental Protection Agency, Las Vegas, Nevada

Park HK, Byeon MS, Shin YN, Jung DI (2009) Sources and spatial and temporal characteristics of organic carbon in two large reservoirs with contrasting hydrologic characteristics Water Resour Res 45

Pizzi NG (2011) Water Treatment: Principles and practices of water supply operations series American Water Works Association, Denver

Price GJ, Lenz EJ, Ansell CWG (2002) The effect of high-intensity ultrasound on the ring-opening polymerisation of cyclic lactones Eur Polym J 38:1753-1760 doi:http://dx.doi.org/10.1016/S0014-3057(02)00056-3

Ramunni AU, Palmieri F (1985) Use of ultrasonic treatment for extraction of humic acid with inorganic reagents from soil Org Geochem 8:241-246 doi:http://dx.doi.org/10.1016/0146-6380(85)90002-6

Rump HH, Krist H (1988) Laboratory manual for the examination of water, waste water and soil. VCH Verlagsgesellschaft mbh,

Smith JE, Renner RC, Hegg BA, Bender JH (1991) Upgrading existing or designing new drinking water treatment facilities. US Environmental Protection Agency, Noyes Data Corporation, Park Ridge, NJ.

Stepniak L, Kepa U, Stanczyk-Mazanek E (2009) Influence of a high-intensity ultrasonic field on the removal of natural organic compounds from water Desalin Water Treat 5:29-33 doi:10.5004/dwt.2009.560

Suresh R, Hiremath L, Kumar GV (2011) Application of ultrasound and microbial treatment for biomass effluent J Appl Sci Environ Sanit 6:63-68

Suri RPS, Singh TS, Abburi S (2010) Influence of Alkalinity and Salinity on the Sonochemical Degradation of Estrogen Hormones in Aqueous Solution Environ Sci Technol 44:1373-1379 doi:10.1021/es9024595

Tirol-Padre A, Ladha JK (2004) Assessing the Reliability of Permanganate-Oxidizable Carbon as an Index of Soil Labile Carbon Soil Sci Soc Am J 68:969-978 doi:10.2136/sssaj2004.9690

USEPA (1999) Enhanced coagulation and enhanced precipitative softening guidance manual (815-R-99-012). USEPA, Office of Water,

Valencia S, Marín J, Velásquez J, Restrepo G, Frimmel FH (2012) Study of pH effects on the evolution of properties of brown-water natural organic matter as revealed by size-exclusion chromatography during photocatalytic degradation Water Res 46:1198-1206

Vikesland PJ, Ozekin K, Valentine RL (2001) Monochloramine decay in model and distribution system waters Water Res 35:1766-1776

Wang S, Feng R, Mo X (1996) Study on 'pulse cavitation peak' in an ultrasound reverberating field Ultrason Sonochem 3:65-68 doi:http://dx.doi.org/10.1016/1350-4177(95)00030-5

Summary-Objective 2

To conduct a systematic evaluation for the application of ultrasound in drinking water treatment, it is important to identify the optimum location of ultrasound within the treatment scheme and objective 2 was designed to satisfy this step. Objective 2 was accomplished in *papers III* and *IV*. The optimum location of ultrasound technology in the drinking water treatment system was estimated using natural water samples with DOC of vegetative (*paper III*) and terrestrial (*paper IV*) origins. Surrogate measurements such as DOC, UV indices and COD were applied to evaluate the effect of ultrasound treatments on concentration and structure of organic contaminants. Continuous and pulsed modes were applied in *papers III* and *IV*. Although the bulk characteristics of the two water samples behaved differently to ultrasound treatments, the overall evaluation of surrogate measurements showed that the best fit of ultrasound technology in drinking water treatment system is prior to coagulation/flocculation processes. Therefore, application of ultrasound in this location will be evaluated in further stages of this study.

Al-Juboori, R. A., Aravinthan, V. & Yusaf, T., Impact of pulsed ultrasound on bacteria reduction of natural waters, *Ultrasonics Sonochemistry*, (2015), 27, 137-147.

Impact of pulsed ultrasound on bacteria reduction of natural waters

Raed A. Al-Juboori [a,*], Vasantha Aravinthan [a], Talal Yusaf [b]

[a] School of Civil Engineering and Surveying, Faculty of Health Engineering and Sciences, University of Southern Queensland, Toowoomba 4350, QLD, Australia
[b] School of Mechanical and Electrical Engineering, Faculty of Health Engineering and Sciences, University of Southern Queensland, Toowoomba 4350, QLD, Australia

ARTICLE INFO

ABSTRACT

There is a limited work on the use of pulsed ultrasound for water disinfection particularly the case of natural water. Hence, pulsed ultrasound disinfection of natural water was thoroughly investigated in this study along with continuous ultrasound as a standard for comparison. Total coliform measurements were applied to evaluate treatment efficiency. Factorial design of 2^3 for the tested experimental factors such as power, treatment time and operational mode was applied. Two levels of power with 40% and 70% amplitudes, treatment time of 5 and 15 min and operational modes of continuous and pulsed with *On* to *Off* ratio (R) of 0.1:0.6 s were investigated. Results showed that increasing power and treatment time or both increases total coliform reduction, whereas switching from continuous to pulsed mode in combination with power and treatment time has negative effect on total coliform reduction. A regression model for predicting total coliform reduction under different operating conditions was developed and validated. Energy and cost analyses applying electrical and calorimetric powers were conducted to serve as selection guidelines for the choosing optimum parameters of ultrasound disinfection. The outcome of these analyses indicated that low power level, short treatment time, and high R ratios are the most effective operating parameters.

© 2015 Elsevier B.V. All rights reserved.

1. Introduction

Water disinfection is an important treatment step that maintains the water free from waterborne microbes [1]. Disinfecting water for human consumption has become a challenging task due to stringent health standards and the increasing contamination of water resources [2–4]. The most commonly used disinfection techniques are the conventional chemical methods with chlorination being the most popular one among all. The use of chlorine and its compounds (e.g. chlorine dioxide) has been repeatedly linked to several problems such as the formation of hazardous disinfection by products (DBPs) [5,6], production of unpleasant flavour and poor disinfection of endospores [7,8]. Hence, alternative disinfection techniques were sought such as ozonation and Ultraviolet (UV) light [9]. However, ozonation and UV light are also hindered by their adverse health effects [8]. Ozonation was found to produce carcinogenic and mutagenic compounds such as bromate and iodate [10,11]. The UV treated microbes were reported to be capable of self-repair which may lead to the production of treatment-resistant generation of microbes [8].

The health concerns related to common disinfection techniques have spurred researchers to explore techniques with benign effects such as ultrasound. Ultrasound technology refers to the use of longitudinal sound waves with frequency range higher than the audible level of human (>16 kHz) [12]. The propagation of ultrasound waves through water produces cavitation and range of physical effects that, in turn, generate mechanical and chemical germicidal effects. Normally, power ultrasound with low frequency ranging between 20 and 100 kHz is applied for disinfection purposes [13].

Ultrasound technology has the advantage of being simple to implement and upgrade besides being efficient in deactivating wide range of microbes and viruses [12,14]. However, ultrasound has some disadvantages such as high energy requirement and rapid temperature rise that are undesirable for water treatment application [8]. To alleviate these problems, pulsed ultrasound can be used as an effective operational mode [5]. In pulsed ultrasound, the liquid being treated is exposed to ultrasound energy intermittently with repeated *On* and *Off* periods. The *On:Off* ratio is denoted as *R*. The energy wasted due to shielding and scattering effects in continuous mode can be recovered in the pulsed mode [15]. The large bubbles that cause scattering of ultrasound waves in the continuous mode would dissolve or float to the surface during the *Off* period of pulsed ultrasound operation reducing shieling and scattering. Operating ultrasound on pulsed mode can also reduce the undesirable temperature rise [16].
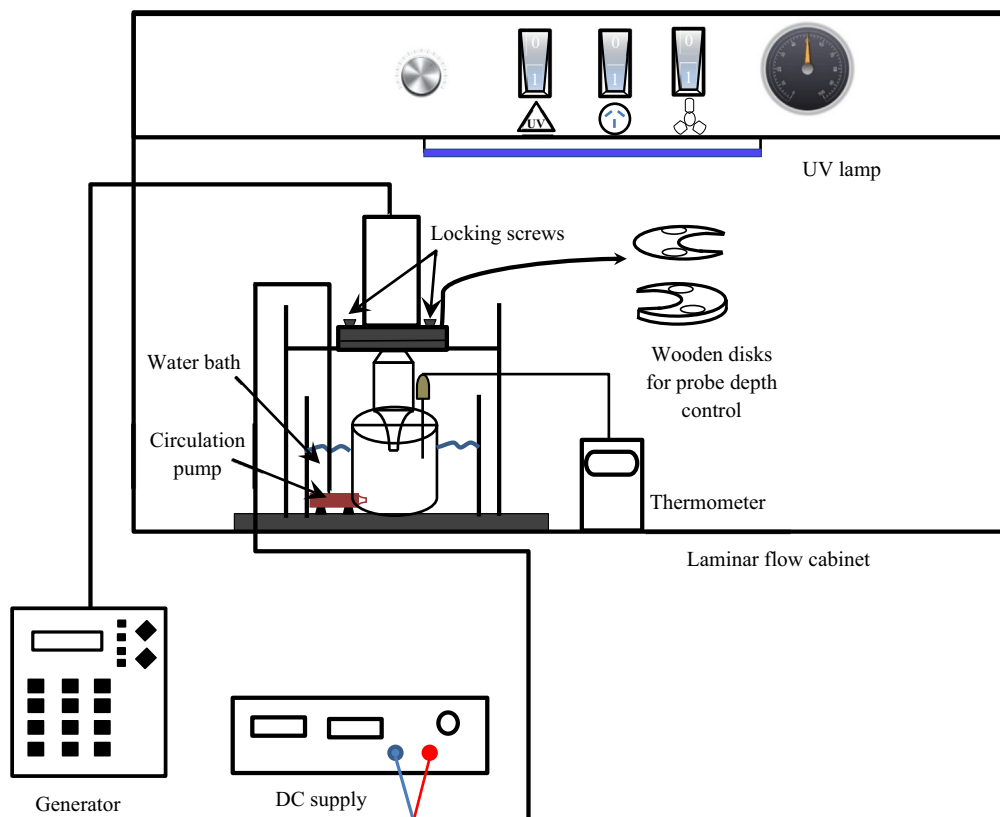
Fig. 1. Configuration of the experimental setup.

Despite the high efficiency of pulsed ultrasound in driving chemical reactions [15], pulsed ultrasound disinfection of water has been only investigated by limited number of studies [17–19]. Nevertheless, pure strain of microorganisms were mostly used in these studies [7]. The use of pure strains of microbes does not represent the real case of water treatment where the microbes are more recalcitrant and have more chance to be naturally protected from the treatment [20–22]. In addition, none of the studies conducted on pulsed ultrasound disinfection has dealt with natural water samples. Hence, this study was designed to investigate the capability of pulsed ultrasound in disinfecting natural water samples as compared to the common continuous mode of operation.

Natural water samples were treated with two amplitude percentages of 40% and 70% for treatment time of 5 and 15 min applying two operational modes; continuous and pulsed with R of 0.1:0.6 s. Total coliform was measured for the untreated and treated samples to determine the disinfection efficiency. Statistical analyses was applied to gain insights into the effect the operating parameters and their interactions on the disinfection efficiency. Pulsed ultrasound experiments with R = 0.2:0.1 s were also performed to validate the predictability of the statistical model that fits the measured total coliform data. Energy and cost analyses of ultrasonic disinfection were also addressed.

2. Materials and methods

2.1. Water sample

Narda lagoon is located at the Southeast Queensland (SEQ), Australia was selected as sampling site in this study. The samples were collected in pre-cleaned 5 L plastic containers during July–September 2014. The total coliform concentration in Narda lagoon water was approximately 250 CFU/100 mL.

2.2. Ultrasound experiments

2.2.1. Experimental setup

The experimental setup used in this study is illustrated in Fig. 1. The setup consists of ultrasonic system and cooling system. Branson digital sonifier model 450 with a maximum power of 400 W and fixed frequency of 20 kHz was used for sonicating water samples. The digital sonifier was equipped with 3/4″ titanium horn. The cooling system encompasses of water bath and a small centrifugal submersible pump powered by DC supply. Ultrasound treatments were conducted in a laminar flow cabinet to avoid air contamination. The depth of the horn in water samples was maintained at 2 cm using wooden spacers fixed to an in-house made stand by locking screws as illustrated in Fig. 1.

2.2.2. Experimental procedure

Laminar flow cabinet was sterilised with UV light and 75% ethanol prior to the experimental work. A 500 mL Pyrex beaker was filled with water sample and placed in the water bath. Ultrasonic horn was immersed in the sample at the desired depth. Two power levels were investigated in this study; 40% and 70% amplitudes which corresponds to electrical power of 93 W and 145 W and approximate calorimetric power of 48 W and 84 W respectively. The calorimetric power measurements were conducted using the techniques described in [23]. The ultrasonic system was operated for two sets of sonication treatment time of 5 and 15 min on continuous and pulsed modes. Two operational modes pulsed of R = 0.1:0.6 s and continuous were applied. Total coliform reduction of pulsed ultrasound with R = 0.2:0.1 s was determined to confirm the validity of the statistical model for predicting total coliform reduction under the applied experimental factors. It is worth mentioning that the power levels and pulse settings applied in this study were chosen based on chemical measurements conducted

in our previous works [23,24]. Amplitude percentages of 40% and 70% and pulse settings of $R = 0.1:0.6$ s and 0.2:0.1 s were found to have the highest sonochemical efficiencies as compared to the other tested operating parameters. Sonochemical efficiency was determined based on hydroxyl and hydrogen peroxide yields. The sonication treatment time levels of 5 and 15 min were applied in this study owing to the fact that these levels are commonly applied in studying the biological effects of ultrasound. Besides, some studies reported that ultrasound inactivation of microbes at high power level for a treatment time up to 15 min can be an uneconomic operation [25]. This indicates that the 15 min of ultrasound operation can be the cut-off limit for an effective application of ultrasound for microbes' inactivation.

Once the selected parameters for a certain run are set, the transducer was turned on. The temperature of the sample being sonicated was measured using calibrated digital thermometer equipped with platinum probe PT 1000 (Hanna instruments, Australia). The temperature of the sample was maintained at ∼20 °C with the aid of a water bath supplemented by ice when needed. It should be noted here that the horn and the platinum temperature probe were decontaminated between the consecutive runs using 75% ethanol followed by successive washes with deionised water.

2.3. Biological assays

Total coliform concentration expressed as colony forming units (CFU)/100 mL of the samples was measured following the standard membrane filtration method 9222 B [26]. Total coliform measurements were conducted before and after each run and the percentage change was taken as a measure for ultrasonic disinfection effects. M-ColiBlue24® media (Millipore, Australia) was used as a cultural media in this study due to its quick and accurate results in detecting total coliform species [27,28]. *Escherichia coli* (*E. coli*) forms blue coloured colonies on this media, while the colonies of other coliforms appear red. Total coliform concentration of untreated and treated water samples was measured by culturing aliquots of the treated samples on m-ColiBlue24® media applying the following procedure;

1. m-ColiBlue24® broth was mixed well and poured evenly onto a sterile absorbent pad situated in a petri dish (Millipore, Australia).
2. Aliquot of 10 mL of the water sample was mixed with 90 mL of dilution water and filtered through a gridded sterile mixed cellulose esters filter using an autoclaved vacuum filtration system. Dilution water was prepared based on the recipe provided in [26].
3. The gridded filter was then transferred from the filtration assembly to the petri dish using sterile forceps. The filter was placed on the absorbent pad in a rolling motion to avoid air entrapment between the pad and the filter.
4. Finally, the petri dish was incubated at 35 ± 0.5 °C for 24 h after which the colonies were counted using SUNTEX colony counter model 570 and the total coliform concentration was calculated using the equation below:

Total coliform (CFU/100 mL)
$$= (\text{Colonies counted/sample volume (mL)}) \times 100 \qquad (1)$$

Sample volume in Eq(1) refers to the actual sample volume not the final volume of the diluted sample.

2.4. Statistical analyses

Statistical analyses were conducted in three stages; sample size calculation, design of experiments and data analyses.

Table 1
Ultrasonic pulse settings and their corresponding *R* values.

R value	Ultrasonic pulse settings (numeric values)
Continuous	1
0.2:0.1	1.5
0.1:0.6	7

Table 2
Coded and uncoded values of 2^3 design.

Factors	Levels	Uncoded values	Coded values
Power (W)	Low	48	−1
	High	84	+1
Treatment time (min)	Low	5	−1
	High	15	+1
Pulse	Low	1	−1
	High	7	+1

GPower software (version 3.1.7) was used for estimating the sample size applying priori analyses. For two power levels, two treatment time levels and three levels of the operational modes of continuous, 0.2:0.1 s and 0.1:0.6 s with 95% confidence level, sample size was calculated to be 72. This means that each experimental run will be repeated six times. Design of experiments and data analyses were executed using MINITAB 17 software. The order of the experiments was randomized to obtain an unbiased distribution of the experimental errors.

The two factors power and treatment time were of numeric category, whereas the operating mode factor was of text category. For easer statistical analyses, the category of the factors were unified by converting the operating mode factor to numeric value using the time correlation between pulsed and continuous mode as follows [29];

$$t_p = t_o(1 + 1/R) \qquad (2)$$

where t_p is the treatment time for pulsed mode and to is the treatment time for continuous mode. The ratio of t_p to t_o was used to convert the operational mode levels to numeric values as it is shown in Table 1. In continuous ultrasound, $R = \infty$ which produces a ratio of t_p/t_o equal to 1. *R* ratios of 0.2:0.1 s and 0.1:0.6 s result in t_p/t_o ratios of 1.5 and 7, respectively.

It is important to note here that Eq(2) was also used to calculate the treatment time levels of pulsed ultrasound treatments. For instance, the equivalent sonication treatment time of 5 min continuous operation for pulsed treatments of $R = 0.2:0.1$ s and 0.1:0.6 s were found to be 7.5 and 35 min, respectively.

Factorial design of 2^3 was performed for continuous vs. 0.1:0.6 s and the factors and their levels in coded and uncoded format are presented in Table 2. The experimental observations of 0.2:0.1 s was used to examine the validity of the prediction model of continuous vs. 0.1:0.6 s.

3. Results and discussions

3.1. Normality and residual analyses

One of the important assumptions for the statistical analyses of experimental data is that the observed data are normally distributed [30,31]. The normality of the measured total coliform is presented in the normal probability plot of the residuals shown in Fig. 2A. It is clear from this figure that the total coliform reduction data are normally distributed demonstrated by the closeness of the points to the fitted regression line [32].
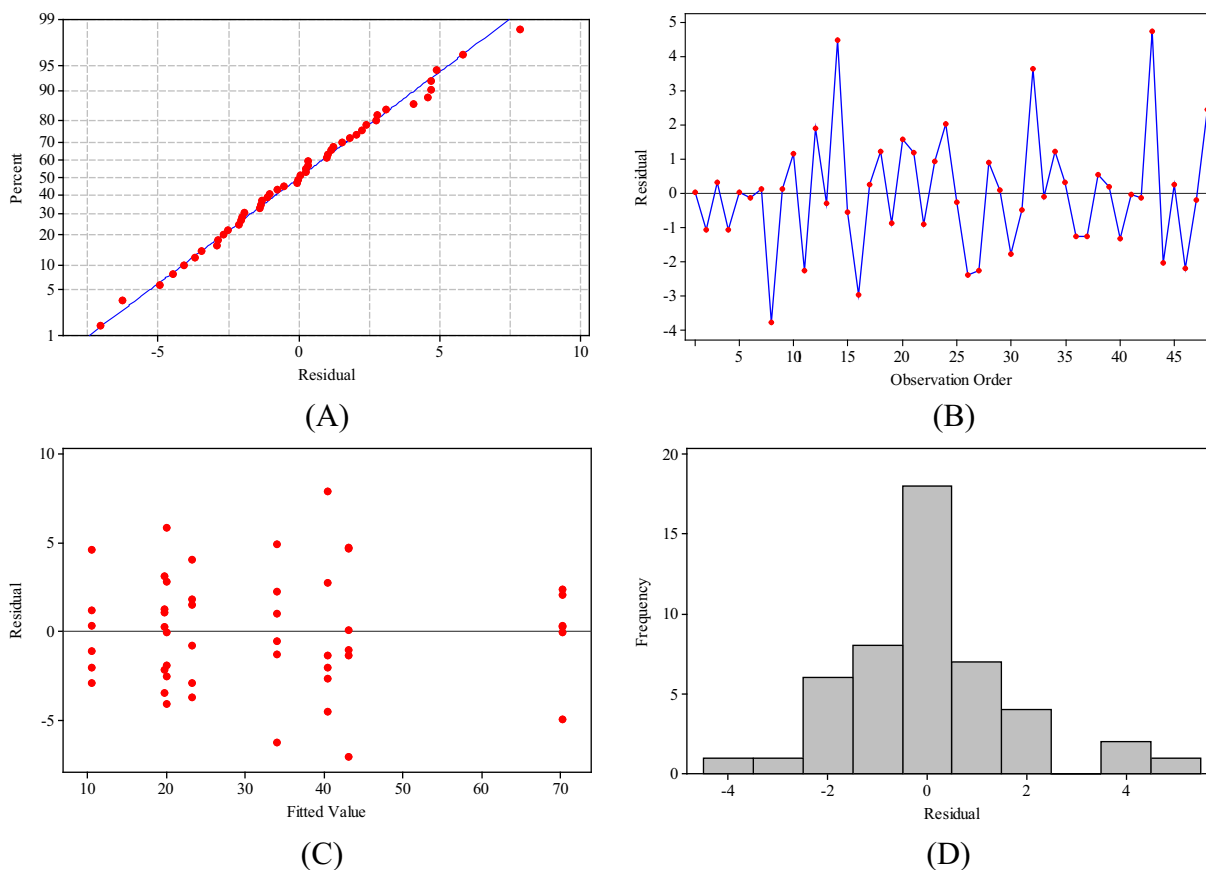
Fig. 2. Statistical diagnostic tests of total coliforms reduction for continuous vs. 0.1:0.6; normal probability plot of residuals (A), residuals vs. observation order (B), residuals vs. fitted values (C) and residual vs. frequency (D).

The variation of residuals with the order of experiments was also explored and the results are illustrated in Fig. 2B. It can be seen that total coliform data did not follow a certain pattern which ascertain its random distribution throughout the experiments [33]. Further evidence for the random distribution of the data are presented in Fig. 2C and D. The fact that the residuals of the total coliform reduction showed no obvious pattern with fitted values indicates that the obtained data have constant variance and they are randomly distributed around zero [34]. Also, the symmetrical bell-like shape of the histogram of the residuals in Fig. 2D points out the normal distribution of the residuals around mean value of zero [35].

3.2. Effects and interactions of experimental factors

The average total coliform reduction percentage under various ultrasonic parameters (uncoded) is shown in Table 3 along with the standard deviation (stdev) of 6 replicates. Although complete removal of total coliform was not achieved with the applied treatment conditions, such removal level can be attained by increasing, power, treatment time or both. It should be noted here that the focus of this work is to investigate the effect of pulsed ultrasound treatment on microbial reduction rather than complete microbial removal from natural water samples. However, an estimation of energy and cost requirements for complete microbial removal will be addressed in later sections of this article based on the obtained removal levels in this work. The estimated parameters of the fitted model for total coliform reduction of continuous vs. 0.1:0.6 s are presented in Tables 4 and 5. The model coefficients are the product of dividing the net effects of the factors by the number of levels.

Table 3
Experimental results of total coliform reduction with various experimental factors and levels (uncoded).

Power (W)	Treatment time (min)	Pulse	Average total coliform reduction (%)	Stdev
48	5	0.1/0.6	11.52	0.8008
48	15	0.1/0.6	23.87	0.5532
48	5	Continuous	20.24	1.1646
48	15	Continuous	40.71	2.5908
84	5	0.1/0.6	20.39	2.4141
84	15	0.1/0.6	43.45	3.0850
84	5	Continuous	30.49	1.5676
84	15	Continuous	70.83	1.6589

Table 4
Estimated effects and coefficients for total coliform reduction (coded) (%).

Term	Net effect	Coef. (coded)	Standardised effect (T)	P
Constant		33.084	122.21	0.000
Power (A)	17.987	8.993	33.22	0.000
Treatment time (B)	23.255	11.628	42.95	0.000
Pulse (C)	−16.560	−8.280	−30.59	0.000
Power × treatment time	6.852	3.426	12.66	0.000
Power × pulse	−3.775	−1.888	−6.97	0.000
Treatment time × pulse	−5.558	−2.779	−10.27	0.000
Power × treatment time × pulse	−1.502	−0.751	−2.77	0.008

Standardised effects are determined by dividing the model coefficients by the standard error coefficient [30] which was found to be 0.2707 for the results observed in this study.

Table 5
Analysis of variance for total coliform reduction (%) (coded units).

| Source	DF	Seq SS	Adj SS	Adj MS	F	P
Main effects	3	13662.7	13662.7	4554.22	1294.68	0.000
Power (A)	1	3882.2	3882.2	3882.19	1103.63	0.000
Treatment time (B)	1	6489.6	6489.6	6489.55	1844.86	0.000
Pulse (C)	1	3290.9	3290.9	3290.93	935.55	0.000
2-Way interactions	3	1105.2	1105.2	368.38	104.72	0.000
Power × treatment time	1	563.4	563.4	563.38	160.16	0.000
Power × pulse	1	171.1	171.1	171.05	48.63	0.000
Treatment time × pulse	1	370.7	370.7	370.72	105.39	0.000
3-Way Interactions	1	27.1	27.1	27.07	7.69	0.008
Power × treatment time × pulse	1	27.1	27.1	27.07	7.69	0.008
Residual error	40	140.7	140.7	3.52		
Pure error	40	140.7	140.7	3.52		
Total	47	14935.6				
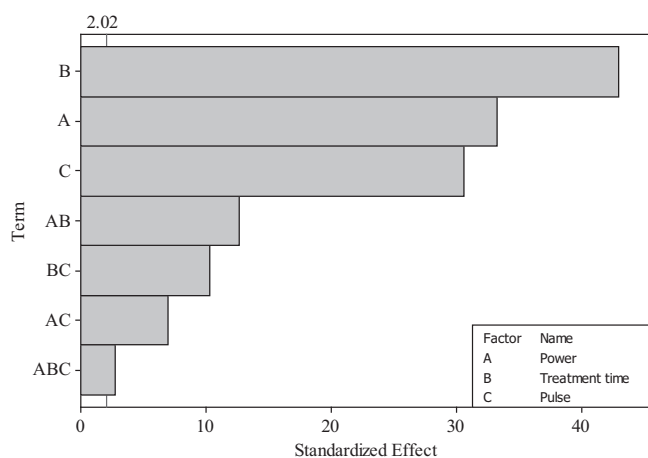
Fig. 3. Pareto chart of the standardised effects for total coliform reduction.

The chosen limit of P-value in this study is 0.05, so changes with P-value $\leqslant 0.05$ are regarded significant. Hence the model parameters presented in Table 3 illustrates that all the factors and their interactions have a significant effect on total coliform reduction (P-value = 0.000) with three ways interaction being the least effective among all (P-value = 0.008).

Pareto chart and normal probability plot for standardised effects were plotted as shown in Figs. 3 and 4 to gain some insights into the extent of factors and interactions effects. Pareto chart shows graphically the absolute values of the effects of factors and interactions represented by horizontal bars. The vertical line in the Pareto chart symbolises the minimum statistically significant effect beyond which every effect is regarded significant [31,36].

The normal probability plot in Fig. 4 depicts the distribution of standardised effects of factors and their interactions around the conceptual probability line [37]. Normally, the effects that lie on or close to the probability line are within the randomness of the responses and considered insignificant, while the effects that lie reasonably away from the probability line are regarded significant [38]. The negative side of the normal probability plot features the factors and interactions that have negative effects on total coliform reduction, whilst the positive side indicates factors and interactions that positively affect total coliform reduction [39]. Among the main three factors, treatment time has the highest effect on total coliform reduction followed by power and then pulse. The positive effect of power and treatment means higher power for longer treatment time result in higher total coliform reduction. The negative effect of pulse means that increasing the numeric value of pulse or in another word increasing the *off* period of ultrasound leads to a lower total coliform reduction.

Fig. 4 reveals that the interaction effect of power × treatment on total coliform reduction is positive and more significant than the interaction effects of power × pulse and treatment time × pulse that are negative. These findings can be further supported through the visual representation of the interaction plot shown in Fig. 5. If the lines representing the factors are parallel, there is no interactions between the factors. If they are diverted or crossed, there is an interaction between the factors [40]. Fig. 5 also shows that increasing power and treatment time increases total coliform reduction (lines pointing up). On the contrary, increasing the *Off* period of ultrasound with power or treatment time decreases total coliform reduction (lines pointing down).

Three levels interaction of power × treatment time × pulse has the lowest effect on total coliform reduction. The negative sign of the three levels interaction effects suggests that the pulse has the dominant effect when combining the three factors.

3.3. Development and validation of prediction model

A regression model of the total coliform reduction was developed for the applied experimental factors (coded) based on the
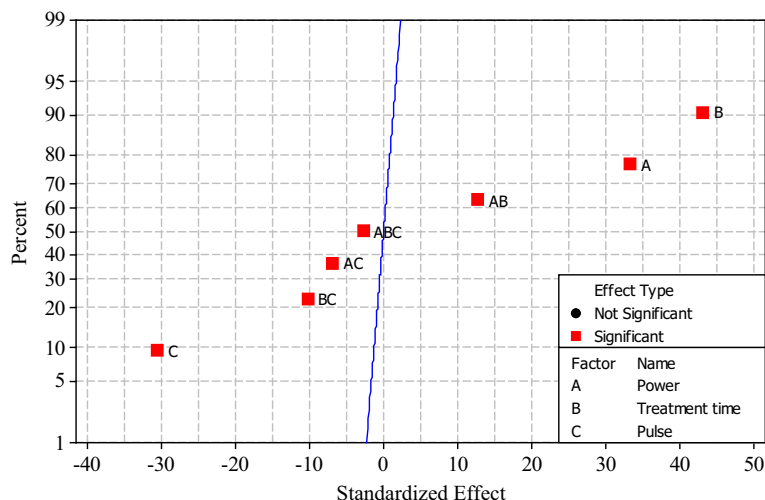

Fig. 4. Normal probability plot of the standardised effects for total coliform reduction.
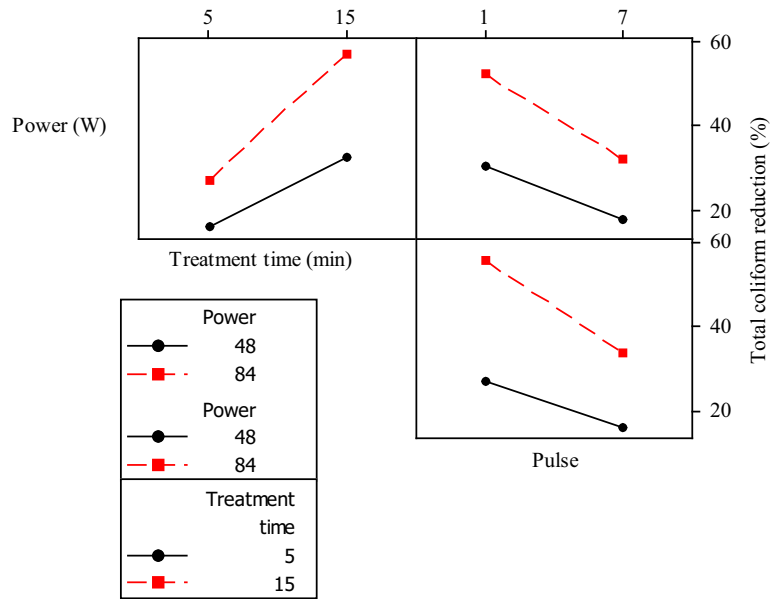
Fig. 5. Interaction effects plot for total coliform reduction.

Table 6
Predicted and experimental values of total coliform reduction for testing the regression model.

Experimental factors			Predicted total coliform reduction (%)	Experimental total coliform reduction (%)
Pulse	Power (W)	Treatment time (min)		
−1	−1	−1	20.25	20.24
−1	−1	+1	40.71	40.71
−1	+1	−1	33.66	30.49
−1	+1	+1	70.83	70.83
+1	−1	−1	11.52	11.52
+1	−1	+1	23.87	23.87
+1	+1	−1	20.38	20.39
+1	+1	+1	43.43	43.45

Table 7
Predicted and experimental values of total coliform reduction for validating the regression model.

Experimental factors			Predicted total coliform reduction (%)	Experimental total coliform reduction (%)
−0.833	−1	−1	19.525	20.370
−0.833	−1	+1	39.307	33.600
−0.833	+1	−1	32.552	30.494
−0.833	+1	+1	68.541	62.158

determined coefficients of factors and their interactions presented in Table 4. The model is formulated in Eq. (3) with R^2 = 99.06;

$$Y = 33.084 + 8.993A + 11.628B - 8.28C + 3.426AB$$
$$- 1.888AC - 2.779BC - 0.751ABC \quad (3)$$

where, Y is the total coliform reduction (%), A is power (W), B is treatment time (min) and C is pulse. Positive sign of the coefficient in Eq. (5) indicates synergistic effects of factor or interaction and negative sign indicated antagonistic effects [41]. It can be noticed from Eq (3) that the coefficient of the three levels interaction is small as compared to the coefficients of other factors and interactions. However, the three levels interaction term cannot be ignored owning to two reasons; (i) it was classified significant based on all the applied significance criteria (e.g. P-value = 0.008) and
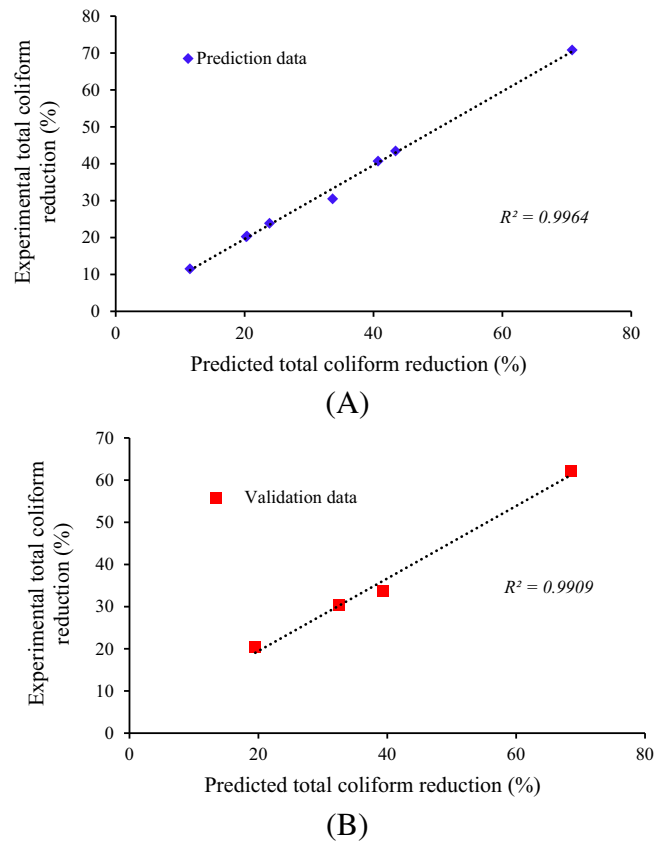

Fig. 6. Parity plot of total coliform reduction for various factors at different levels for (A) prediction and (B) validation.

(ii) ignoring it can introduce a considerable error when predicting total coliform reduction using Eq. (3), especially for the lower levels of the applied factors. For example, in the pulse treatment case of R = 0.1:0.6 s with power of 48 W for 5 min, the total coliform reduction was ~11.5%, and the amount of total coliform reduction represented by the three levels interaction is 0.751 which makes up a percentage of 6.5% of the aforementioned removal percentage.

To test the functionality of the model presented in Eq. (3), the predicted values of total coliform reduction from the model were compared to the obtained experimental values for the same operating conditions as shown in Table 6. The experimental data of 0.2:0.1 s were used to validate the model and the results are presented in Table 7. The coded value of 0.2:0.1 s in Table 7 (−0.833) was calculated from the coded values of continuous and 0.1:0.6 s through interpolation. The adequacy of the model in representing total coliform reduction was tested via parity plot for experimental versus predicted values as demonstrated in Fig. 6. It is clear from this figure that the regression model presented in this study can sufficiently predict total coliform reduction within the tested levels of the factors ($R^2 = 0.9964$ for prediction and $R^2 = 0.9906$ for validation).

3.4. Analysis of surface and contour plots

In order to reach a decision on the optimum levels of parameters that result in a desirable response (highest reduction of total coliform), scrutinising the behaviour of the response under the selected levels of the factors is required [42]. The behaviour of total coliform reduction under various levels of power, treatment time and pulse settings was explored through 3D surface and 2D contour plots as shown in Figs. 7–9.

Fig. 7 shows the effect of power and treatment time on total coliform reduction for two operating modes continuous (A) and pulsed 0.1:0.6 s (B). Generally, the pattern of the surface plot for continuous and pulsed modes is similar, but the minima and the maxima of total coliform reduction for pulsed is lower than that of continuous mode. The contour plot shows that the minima and maxima of total coliform reduction for continuous ultrasound are <30% and >70% respectively as opposed to <15% and >40% for 0.1:0.6 s. The distribution of the contour lines of continuous treatment differs from that of 0.1:0.6 s treatment which reflects the difference in behaviour of total coliform reduction under different modes. Previous studies on pulsed and continuous ultrasound disinfection also pointed out the difference in the behaviour of microbes under continuous and pulsed modes at the same levels of power and treatment time [17,18,43]. The microbial reduction increases more sharply at the first few minutes (∼5 min) with continuous sonication as compared to pulse sonication, and then the reduction increment becomes gradual for both modes at longer treatment time with the reduction of continuous being higher than that of pulsed [43].

Fig. 8 reveals the surface and contour plots of total coliform reduction of power vs. pulse for 5 and 15 min. Interestingly, the patterns in the surface and contour plots for both treatment times are almost identical expect for their minima and maxima values. This suggests that the combined effects of power and pulse on total coliform reduction is less effective than that of power and treatment time which agrees with the results presented in Fig. 4 and Table 4. However, the combined effects of treatment time and pulse presented in Fig. 9 appears to be more pronounced than the combined effect of pulse and power. This is evident through the difference in the configuration of the contour lines for 48 W and 84 W.
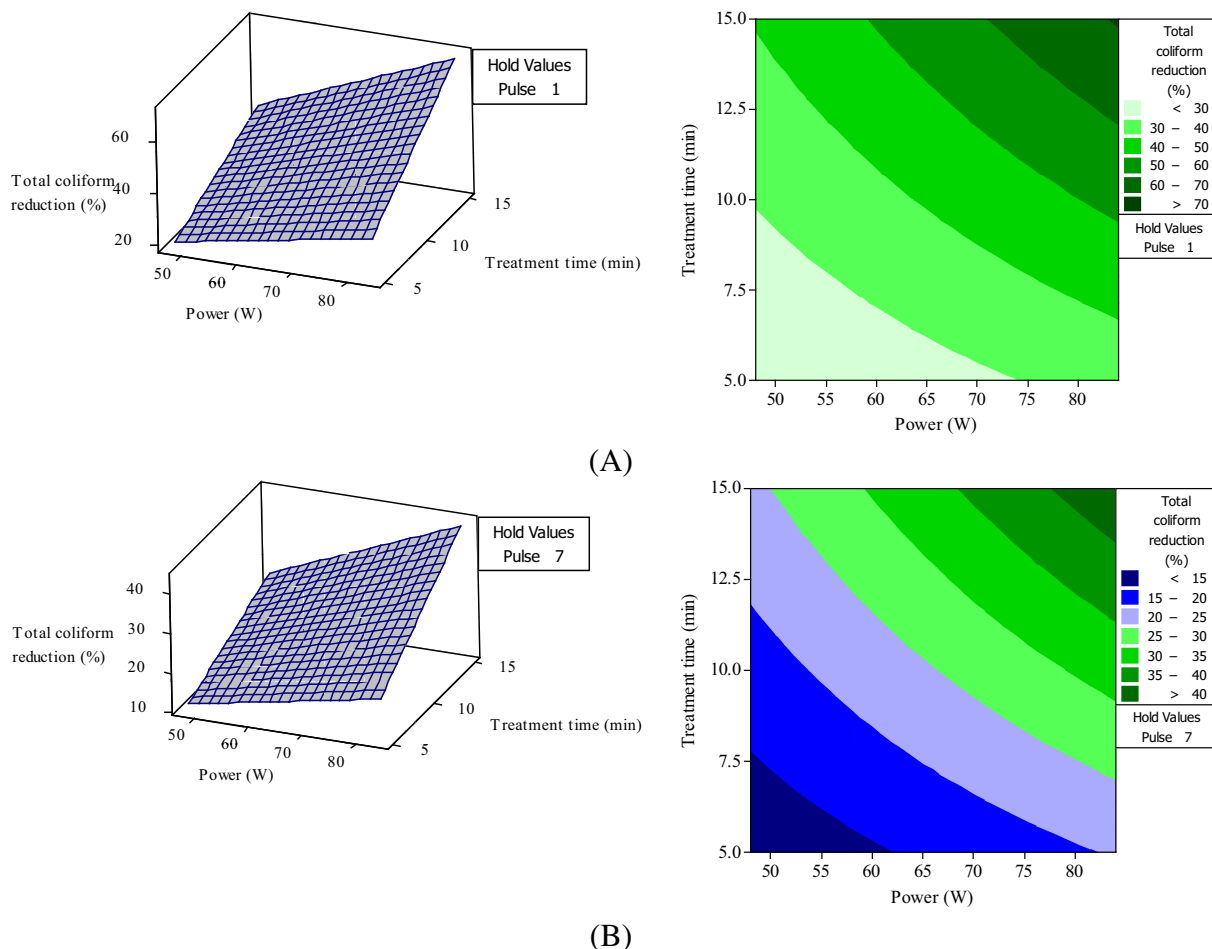

(A)

(B)

Fig. 7. Surface and contour plots for the effect of power and treatment time on total coliform reduction for (A) continuous and (B) 0.1:0.6 s.
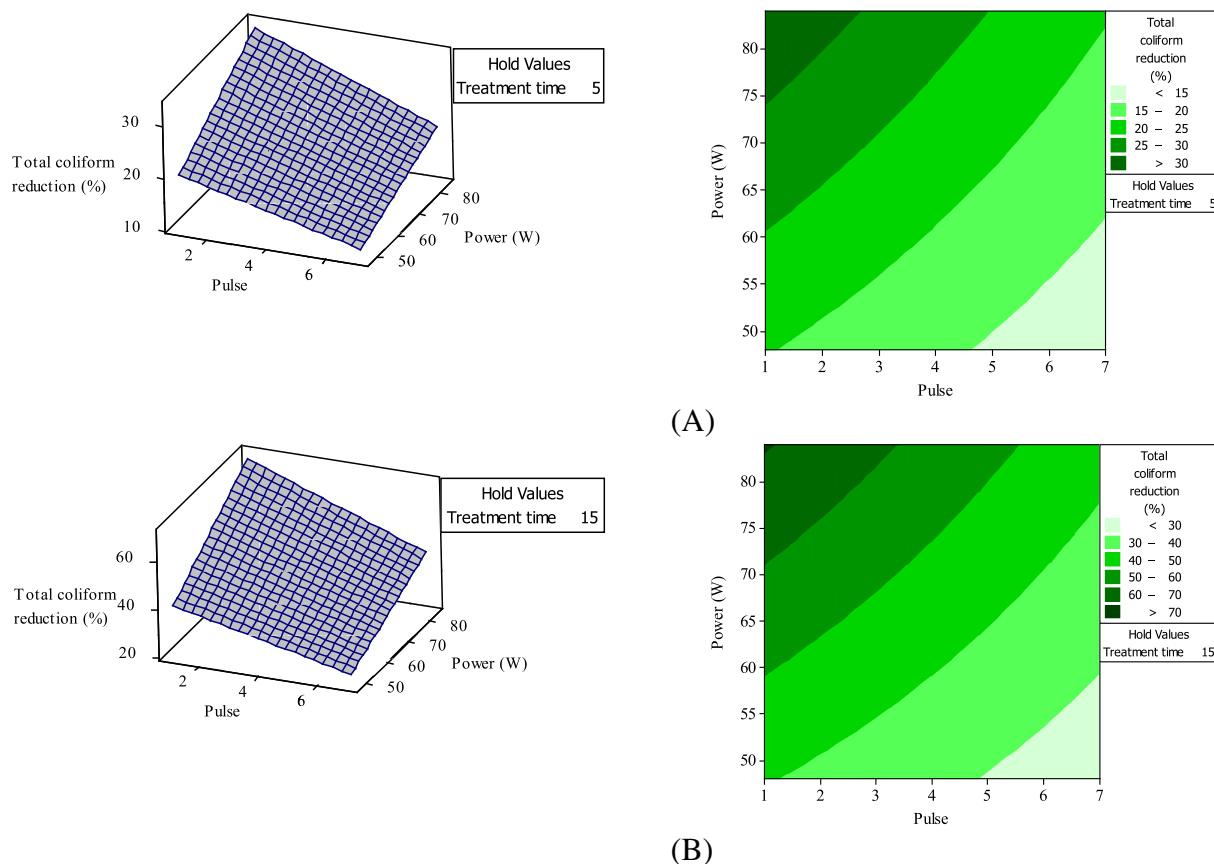
(A)

(B)

Fig. 8. Surface and contour plots for the effect of power and pulse on total coliform reduction for (A) 5 min and (B) 15 min.

3.5. Optimisation of operating conditions (energy and cost perspectives)

Energy consumption is a determinant factor for the application of ultrasound in water treatment. In sonochemistry, the chemical yield of ultrasound is usually normalised by the calorimetric power to calculate sonochemical efficiency [44]. In this study, the germicidal efficiency of ultrasound was determined in a similar manner using the following equation:

$$\text{Germicidal efficiency} = \text{total coliform reduction}(\%)/P \times t \qquad (4)$$

where, P is the calorimetric power (W) and t is the sonication treatment time (s)

The developed regression model in Eq. (3) was applied to predict total coliform reduction for various ranges of power, treatment time and ultrasound pulse settings within the investigated levels for the aforementioned factors. The produced values of total coliform reduction was then substituted in Eq. (4) to determine the germicidal efficiency of different operating parameters. Fig. 10 shows a contour plot of germicidal efficiency of ultrasound at various ultrasonic parameters. The values of ultrasonic pulse settings in Fig. 10 were determined from R ratios based on the calculations explained in Section 2.4.

It can be noticed from Fig. 10 that the germicidal efficiency of ultrasound peaks at low ultrasonic energy and high R ratios. So the closer the R ratio to continuous, the better the disinfection of pulsed ultrasound. Similar trend was observed with pulsed ultrasound disinfection of *Escherichia coli* and *Enterococcus faecalis*, as increasing the number of pulses per second was found to increase microbial removal [45]. From energy perspective, R ratios between 1:1 and continuous is the optimum range for pulsed ultrasound

disinfection of natural waters. However, this is valid for conditions similar to those investigated in this study. Different microbes or different media could expand or narrow down the effective range of R in pulsed ultrasound disinfection. For example, R ratio of 0.1:0.9 s was found to be enough to result in a similar reduction of *Cryptosporidium oocysts* to that of continuous ultrasound [19]. Bermúdez-Aguirre and Barbosa-Cánovas [43] found that pulsed ultrasound with R ratio of 0.5:0.5 s was more effective than continuous ultrasound in deactivating *Saccharomyces cerevisiae* in Cranberry juice, whilst the case was the opposed when different medias such as pineapple and grape juices were tested under the same operating conditions.

The operating cost of treatment is the primary selection criteria when determining economic viability of water treatment techniques. Taking lead from this concept, the treatment cost of ultrasound disinfection has been calculated for the experimental total coliform reduction obtained with each set of parameters based on electrical and calorimetric power consumption. The average price of 1 kWh was taken as 25 cents based on the electricity prices in Queensland Australia [46]. The ultrasonic treatment cost for 1 L of surface water is calculated using Eq(5).

$$\text{Cost of the treatment} = (\text{ultrasonic energy density} \times \text{cost of 1 kWh}) \qquad (5)$$

Ultrasonic energy density (electrical or calorimetric) (J/L) was first converted to kWh/L and then multiplied by the price of 1 kWh ($). The cost of 100% removal of total coliform was also calculated from the cost of the obtained reduction percentages. The cost of 100% removal of total coliform is important as such removal is required for the water to be used for human consumption [47].
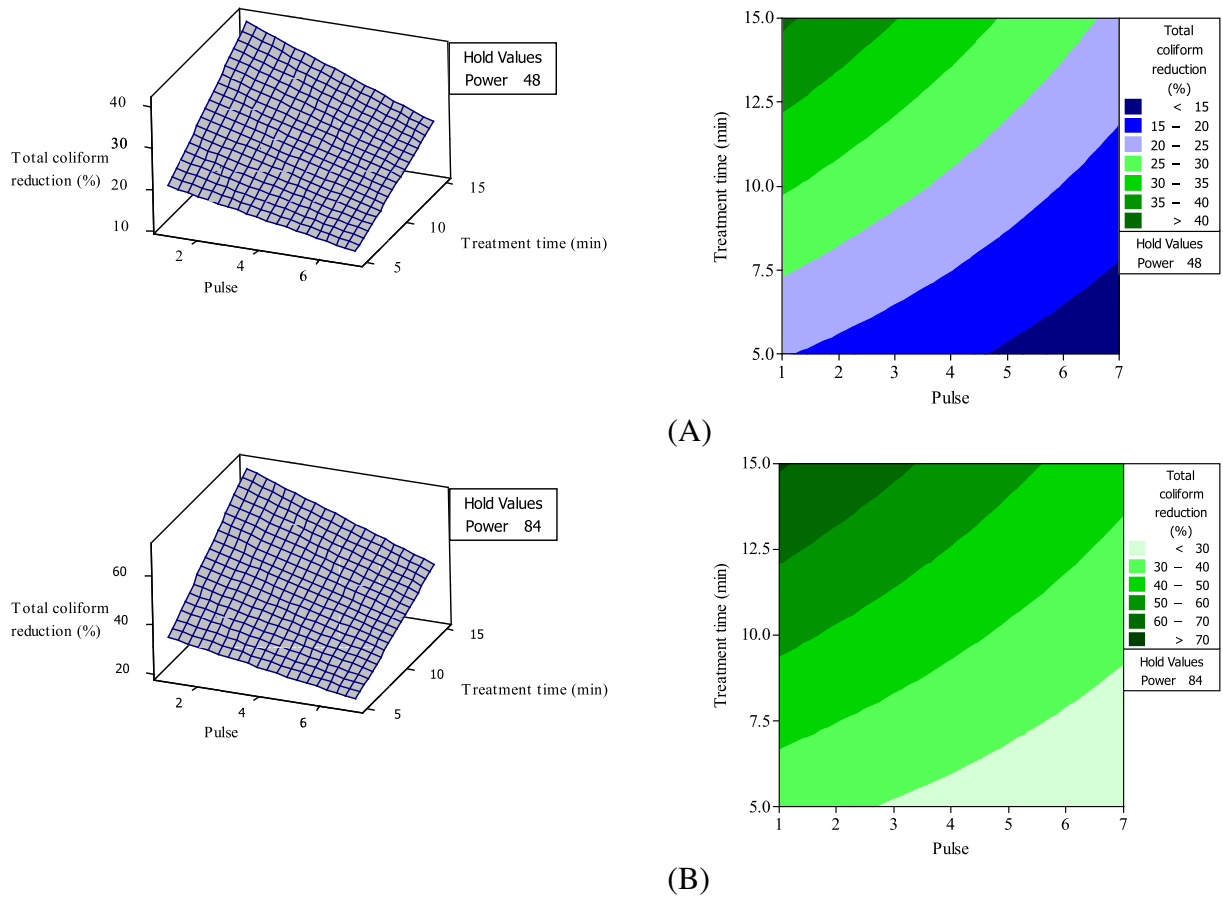
Fig. 9. Surface and contour plots for the effect of treatment time and pulse on total coliform reduction for (A) 5 48 W and (B) 84 W.
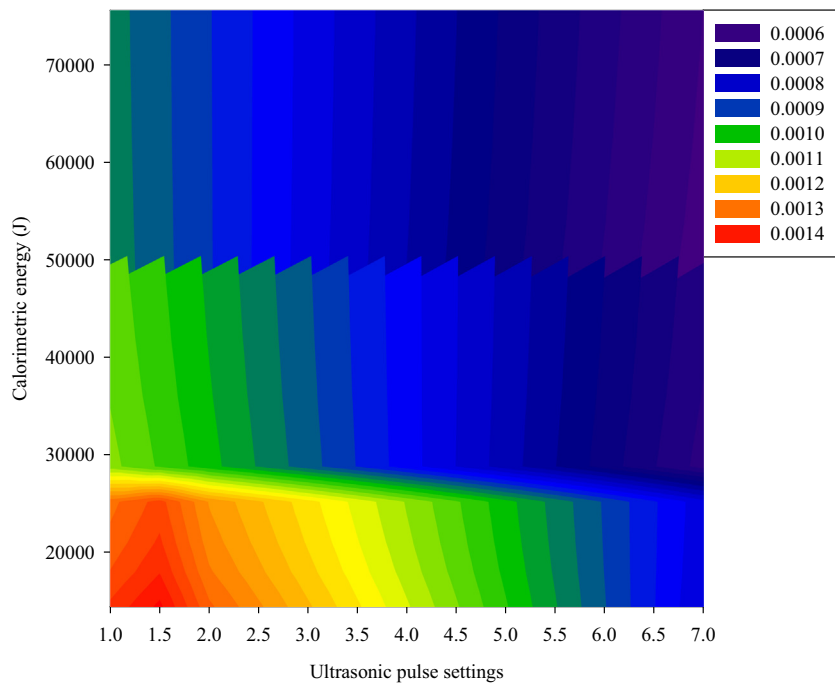
Fig. 10. Germicidal efficiency of ultrasound treatment at various ultrasonic pulse settings.

Table 8 shows the cost of ultrasound disinfection with various operating parameters along with the cost of 100% total coliform reduction for the same parameters. The cost figures of ultrasound

disinfection of total coliform presented in this study are within the ranges reported in [48,49]. The results presented in Table 8 suggests that low power levels short treatment time and high *R*

Table 8
Cost of ultrasonic disinfection of surface water.

Electrical power (W)	Calorimetric power (W)	Treatment time (s)	Mode	Average total coliform reduction (%)	Cost electrical power ($/L)	Cost calorimetric power ($/L)	Cost of 100% removal electrical power ($/L)	Cost of 100% removal calorimetric power ($/L)
93	48	300	0.1:0.6 s	11.52	0.003875	0.002	0.0336	0.0174
93	48	900	0.1:0.6 s	23.87	0.011625	0.006	0.0487	0.0251
93	*48*	*300*	*0.2:0.1 s*	*20.38*	*0.003875*	*0.002*	*0.0190*	*0.0098*
93	48	900	0.2:0.1 s	33.60	0.011625	0.006	0.0346	0.0178
93	48	300	Continuous	20.24	0.003875	0.002	0.0191	0.0099
93	48	900	Continuous	40.71	0.011625	0.006	0.0285	0.0147
145	84	300	0.1:0.6 s	20.39	0.006042	0.0035	0.0296	0.0172
145	84	900	0.1:0.6 s	43.45	0.018125	0.0105	0.0417	0.0242
145	84	300	0.2:0.1 s	30.49	0.006042	0.0035	0.0198	0.0115
145	84	900	0.2:0.1 s	62.16	0.018125	0.0105	0.0291	0.0170
145	84	300	Continuous	30.49	0.006042	0.0035	0.0198	0.0115
145	84	900	Continuous	70.83	0.018125	0.0105	0.0256	0.0148

ratio are the most cost effective operating condition for total coliform removal. The most cost effective ultrasonic parameters and their cost figures were put in bold and italic font to differentiate them from the other parameters. It should be noted here that the cost of ultrasound disinfection provided here only concerns the treatment cost and can constructively be used in combination with the analysis of the capital and maintenance cost to reach a rational decision with regards to the application of ultrasonic disinfection in water treatment practices.

4. Conclusions

Ultrasonic disinfection of natural water samples under various operating conditions and modes was thoroughly investigated applying robust experimental and statistical procedures. Total coliform removal was used as a measure for disinfection efficiency. Statistical analysis of the experimental data illustrated that power, treatment time and operational mode and their interaction had significant effects on total coliform reduction. Power and treatment time and their interaction had a positive effect on total coliform reduction, while the operational mode and the other interactions had a negative effect. Further analysis using surface and contour plots showed that the response of total coliform to power and treatment time in pulsed mode differs from that of continuous mode.

A regression model for predicting total coliform reduction under different operating parameters was developed and its validity was verified against the experimental data of 0.2:0.1 s. Energy and cost analyses for ultrasonic disinfection were also conducted to evaluate the germicidal efficiency of ultrasound at different operating conditions. The results of the analyses revealed that lower levels of power and treatment time for continuous and high R ratio modes are the most energy and cost efficient parameters for ultrasound disinfection.

Disinfection is an important water treatment step, but it is not the only step to be considered in evaluating ultrasound application in water treatment. Thus, further research work is needed for evaluating the concomitant effects of ultrasound disinfection on other contaminants such as aquatic carbon.

Acknowledgement

References

[1] S. Vajnhandl, T. Željko, A. Majcen Le Marechal, J.V. Valh, Feasibility study of ultrasound as water disinfection technology, Desalin. Water Treat. (2014) 1–7.
[2] N.H. Ince, R. Belen, Aqueous phase disinfection with power ultrasound: process kinetics and effect of solid catalysts, Environ. Sci. Technol. 35 (2001) 1885–1888.
[3] D. Tetzlaff, S. Carey, C. Soulsby, Catchments in the future north: interdisciplinary science for sustainable management in the 21st century, Hydrol. Processes 27 (2013) 635–639.
[4] D.W. Kicklighter, D.J. Hayes, J. McClelland, B.J. Peterson, A.D. McGuire, J.M. Melillo, Insights and issues with simulating terrestrial DOC loading of arctic river networks, Ecol. Appl. 23 (2013) 1817–1836.
[5] R.A. Al-Juboori, T. Yusaf, V. Aravinthan, P.A. Pittaway, L. Bowtell, Investigating the feasibility and the optimal location of pulsed ultrasound in surface water treatment schemes, Desalin. Water Treat. (2015) 1–19.
[6] X. Zhang, W. Li, E.R. Blatchley Iii, X. Wang, P. Ren, UV/chlorine process for ammonia removal and disinfection by-product reduction: comparison with chlorination, Water Res. 68 (2015) 804–811.
[7] S. Gao, Y. Hemar, M. Ashokkumar, S. Paturel, G.D. Lewis, Inactivation of bacteria and yeast using high-frequency ultrasound treatment, Water Res. 60 (2014) 93–104.
[8] R.A. Al-Juboori, T. Yusaf, Biofouling in RO system: mechanisms, monitoring and controlling, Desalination 302 (2012) 1–23.
[9] M. Dore, Threats to human health: use of chlorine, an obsolete treatment technology, in: Global Drinking Water Management and Conservation, Springer International Publishing, 2015, pp. 197–212.
[10] S.D. Richardson, Disinfection by-products and other emerging contaminants in drinking water, TrAC, Trends Anal. Chem. 22 (2003) 666–684.
[11] U. Von Gunten, Ozonation of drinking water: part I. Oxidation kinetics and product formation, Water Res. 37 (2003) 1443–1467.
[12] T. Yusaf, R.A. Al-Juboori, Alternative methods of microorganism disruption for agricultural applications, Appl. Energy 114 (2014) 909–923.
[13] P. Declerck, L. Vanysacker, A. Hulsmans, N. Lambert, S. Liers, F. Ollevier, Evaluation of power ultrasound for disinfection of both *Legionella pneumophila* and its environmental host *Acanthamoeba castellanii*, Water Res. 44 (2010) 703–710.
[14] V. Naddeo, D. Mantzavinos, D. Fatta-kassinos, V. Belgiorno, Water and wastewater disinfection by ultrasound irradiation – a critical review, Global NEST J. 16 (2014) 561–577.
[15] D. Chen, S.K. Sharma, A. Mudhoo, Handbook on Applications of Ultrasound: Sonochemistry for Sustainability, CRC Press, 2011.
[16] T.J. Mason, D. Peters, Practical Sonochemistry: Power Ultrasound Uses and Applications, Woodhead Publishing, 2002.
[17] V.F. Evora, G.J. Kavarnos, Ultrasonic Disinfection of Water Suspensions of *Escherichia Coli* and *Legionella Pneumophila*, Naval Undersea Warfare Center Division, Newport Rhode, Island, 1999, pp. 1–13.
[18] A. Antoniadis, I. Poulios, E. Nikolakaki, D. Mantzavinos, Sonochemical disinfection of municipal wastewater, J. Hazard. Mater. 146 (2007) 492–495.
[19] M. Ashokkumar, T. Vu, F. Grieser, A. Weerawardena, N. Anderson, N. Pilkington, D.R. Dixon, Ultrasonic treatment of *Cryptosporidium oocysts*, Health Related Water Microbiol. 47 (2003) 173–177.
[20] S. Drakopoulou, S. Terzakis, M.S. Fountoulakis, D. Mantzavinos, T. Manios, Ultrasound-induced inactivation of gram-negative and gram-positive bacteria in secondary treated municipal wastewater, Ultrason. Sonochem. 16 (2009) 629–634.
[21] E. Joyce, S.S. Phull, J.P. Lorimer, T.J. Mason, The development and evaluation of ultrasound for the treatment of bacterial suspensions. A study of frequency, power and sonication time on cultured *Bacillus species*, Ultrason. Sonochem. 10 (2003) 315–318.
[22] E.J. Stewart, Growing Unculturable bacteria, J. Bacteriol. 194 (2012) 4151–4160.

[23] R.A. Al-Juboori, T. Yusaf, L. Bowtell, V. Aravinthan, Energy characterisation of ultrasonic systems for industrial processes, Ultrasonics 57 (2015) 18–30.

[24] R.A. Al-Juboori, T. Yusaf, L. Bowtell, Energy conversion efficiency of pulsed ultrasound, in: The 7th International Conference on Applied Energy – ICAE2015, Elsevier, Abu Dhabi, UAE, 2015.

[25] S.S. Phull, A.P. Newman, J.P. Lorimer, B. Pollet, T.J. Mason, The development and evaluation of ultrasound in the biocidal treatment of water, Ultrason. Sonochem. 4 (1997) 157–164.

[26] L.S. Clesceri, E.W. Rice, A.E. Greenberg, A.D. Eaton, Standard Methods for Examination of Water and Wastewater: Centennial Edition, American Public Health Association, 2005.

[27] W.P. Hamilton, M. Kim, E.L. Thackston, Comparison of commercially available Escherichia coli enumeration tests: implications for attaining water quality standards, Water Res. 39 (2005) 4869–4878.

[28] M. Grant, A new membrane filtration medium for simultaneous detection and enumeration of *Escherichia coli* and total coliforms, Appl. Environ. Microbiol. 63 (1997) 3526–3530.

[29] M. Gutierrez, A. Henglein, Chemical action of pulsed ultrasound: observation of an unprecedented intensity effect, J. Phys. Chem. 94 (1990) 3625–3628.

[30] A. Srinivasan, T. Viraraghavan, Oil removal from water by fungal biomass: a factorial design analysis, J. Hazard. Mater. 175 (2010) 695–702.

[31] D. Pokhrel, T. Viraraghavan, Arsenic removal from aqueous solution by iron oxide-coated fungal biomass: a factorial design analysis, Water Air Soil Pollut. 173 (2006) 195–208.

[32] J. Antony, Design of Experiments for Engineers and Scientists, Elsevier, 2014.

[33] T.T. Khanh, Application of response surface method as an experimental design to optimize coagulation tests, Environ. Eng. Res. 15 (2010) 63–70.

[34] B. Ryan, B. Joiner, J. Cryer, MINITAB Handbook: Update for Release, Cengage Learning, 2012.

[35] D. Ranjan, P. Srivastava, M. Talat, S.H. Hasan, Biosorption of Cr(VI) from water using biomass of aeromonas hydrophila: central composite design for optimization of process variables, Appl. Biochem. Biotechnol. 158 (2009) 524–539.

[36] D. Bingöl, D. Saraydin, D.Ş. Özbay, Full factorial design approach to Hg (II) adsorption onto hydrogels, Arab. J. Sci. Eng. 40 (2015) 109–116.

[37] Á. Anglada, A. Urtiaga, I. Ortiz, D. Mantzavinos, E. Diamadopoulos, Boron-doped diamond anodic treatment of landfill leachate: evaluation of operating variables and formation of oxidation by-products, Water Res. 45 (2011) 828–838.

[38] S. Saadat, A. Karimi-Jashni, Optimization of Pb(II) adsorption onto modified walnut shells using factorial design and simplex methodologies, Chem. Eng. J. 173 (2011) 743–749.

[39] A. Hegazy, N. Abdel-Ghani, G. El-Chaghaby, Adsorption of phenol onto activated carbon from *Rhazya stricta*: determination of the optimal experimental parameters using factorial design, Appl. Water Sci. 4 (2014) 273–281.

[40] P.O. Boamah, Y. Huang, M. Hua, Q. Zhang, Y. Liu, J. Onumah, W. Wang, Y. Song, Removal of cadmium from aqueous solution using low molecular weight chitosan derivative, Carbohydr. Polym. 122 (2015) 255–264.

[41] S. Sadri Moghaddam, M.R. Alavi Moghaddam, M. Arami, Coagulation/flocculation process for dye removal using sludge from water treatment plant: optimization through response surface methodology, J. Hazard. Mater. 175 (2010) 651–657.

[42] A. Boubakri, N. Helali, M. Tlili, M.B. Amor, Fluoride removal from diluted solutions by Donnan dialysis using full factorial design, Korean J. Chem. Eng. 31 (2014) 461–466.

[43] D. Bermúdez-Aguirre, G.V. Barbosa-Cánovas, Inactivation of *Saccharomyces cerevisiae* in pineapple, grape and cranberry juices under pulsed and continuous thermo-sonication treatments, J. Food Eng. 108 (2012) 383–392.

[44] S. Koda, T. Kimura, T. Kondo, H. Mitome, A standard method to calibrate sonochemical efficiency of an individual reaction system, Ultrason. Sonochem. 10 (2003) 149–156.

[45] M. Gholami, R. Mirzaei, R. Mohammadi, Z. Zarghampour, A. Afshari, Destruction of Escherichia coli and *Enterococcus faecalis* using low frequency ultrasound technology: a response surface methodology, Health Scope 3 (2014) 1–9.

[46] Origin-Australia, Business energy price fact sheets, viewed in 2015, 2015. <http://www.originenergy.com.au/976/Energy-price-fact-sheets>.

[47] NHMRC, Review of Coliforms as Microbial Indicators of Drinking Water Quality, National Health and Medical Research Council, Canberra, Australia, 2003.

[48] K.K. Jyoti, A.B. Pandit, Effect of cavitation on chemical disinfection efficiency, Water Res. 38 (2004) 2249–2258.

[49] K.K. Jyoti, A.B. Pandit, Ozone and cavitation for water disinfection, Biochem. Eng. J. 18 (2004) 9–19.

Paper VI

Al-Juboori, R. A., Yusaf, T., Aravinthan, V. & Bowtell, L., Investigating natural organic carbon removal and structural alteration induced by pulsed ultrasound, *Science of the Total Environment*, (2016), 541, 1019-1030.

Investigating natural organic carbon removal and structural alteration induced by pulsed ultrasound

Raed A. Al-Juboori [a,*], Talal Yusaf [b], Vasantha Aravinthan [a], Leslie Bowtell [b]

[a] School of Civil Engineering and Surveying, Faculty of Health, Engineering and Sciences, University of Southern Queensland, Toowoomba, 4350 QLD, Australia
[b] School of Mechanical and Electrical Engineering, Faculty of Health, Engineering and Sciences, University of Southern Queensland, Toowoomba, 4350 QLD, Australia

HIGHLIGHTS

- Natural carbon removal under the effect of pulsed ultrasound was investigated.
- Overall pulsed ultrasound treatment resulted in carbon removal of 7–15%.
- High microbial concentration interfered with DOC removal.
- Sonication decreased hydrophobic fraction and increased the hydrophilic fraction.
- Pulse mode at low power and treatment time is the most energy effective treatment.

GRAPHICAL ABSTRACT
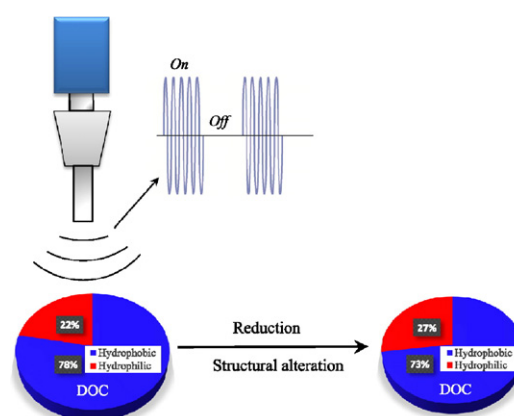
ARTICLE INFO

ABSTRACT

The application of pulsed ultrasound for DOC removal from natural water samples has been thoroughly investigated in this work. Natural water samples were treated with ultrasound at power levels of 48 and 84 W with treatment times of 5 and 15 min. Chemical fractionation was conducted for both untreated and treated samples to clearly identify the change in DOC structure caused by ultrasonic treatments. Statistical analyses applying 2^3 factorial design were performed to study the behaviour of the response (i.e. DOC removal) under different operating conditions. Overall, ultrasonic treatments resulted in DOC removal of 7–15% depending on the applied operating conditions. The treated water had high microbial loading that interfered with DOC removal due primarily to the release of microbial products when exposed to ultrasound. Pulse ultrasound was found to be more effective than the continuous mode for DOC removal at the same effective power level. A regression model was developed and tested for DOC removal prediction. The model was adequate in predicting DOC removal with a maximum deviation from the experimental data of <11%. Pulsed ultrasound at low power levels and short treatment times was found to be the most energy efficient treatment for DOC removal.

© 2015 Elsevier B.V. All rights reserved.

* Corresponding author.
E-mail addresses: RaedAhmed.mahmood@usq.edu.au, Raedahmed.mahmood@gmail.com (R.A. Al-Juboori).

1. Introduction

DOC is a major contaminant in natural water resources and it has a significant impact on the characteristics of the water such as colour and taste. DOC is an important target contaminant for water treatment practices owing to its contribution to common water treatment problems. For instance, organic fouling caused by the adsorption of DOC onto filtration media is one of the main fouling types that occur in the water treatment processes (Al-Juboori and Yusaf, 2012a; Chun et al., 2015). In addition, DOC has the capacity to react with heavy metals and form soluble complexes (Liu et al., 2008). DOC that escapes the final water treatment stages can also promote growth of bio-film in the water distribution systems (Soh et al., 2008). More importantly, DOC can react with the disinfectants used in water treatment practices producing carcinogenic and mutagenic compounds known as disinfection by-products (DBPs) (Narotsky et al., 2013).

The removal of DOC from water at the early stages of treatments has become the focus of recent research activities for engineers and scientists involved in water treatment field. Coagulation/flocculation proceeded by sedimentation is conventionally used for removing DOC from water. However, these conventional techniques suffer from the production of high amounts of sludge that in turn needs additional treatment and proper disposal (Chemat et al., 2001). Moreover, depending on the characteristics of the DOC, some DOC structures require high dosage levels of coagulants (e.g. Al or Fe) that could result in both aesthetic and health problems (Gabelich et al., 2002). Augmenting coagulation with chemical oxidation initially emerged as a method to improve the removal of DOC, but even with the chemical oxidation process DPBs were produced and having inherent mass transfer limitations causing performance to be crippled (Chemat et al., 2001; Richardson, 2003). Thus, it is still necessary to find effective chemical-free techniques for improving DOC removal.

One of the known chemical-free techniques for DOC removal is ultrasound. Ultrasound has a unique way for DOC degradation utilizing both physical and chemical effects. The chemical effects of ultrasound rely on the production of short-lived oxidants such as hydroxyl radicals, hence there is no formation of DBPs (Naddeo et al., 2007). The physical effects of ultrasound such as shock waves and shear stresses produced from bubbles oscillation and collapse are also capable of degrading DOC (Henglein and Gutierrez, 1990; Pasupuleti and Madras, 2010). The simplicity of installing and maintaining ultrasound equipment is another merit of this technology (Patist and Bates, 2008).

Most of the studies concerning ultrasound technology have dealt with synthetic water samples which might not allow performing a realistic assessment for DOC removal with ultrasound (Naddeo et al., 2007). Synthetic water studies were based on removing single or known mixtures with a limited number of pollutants. The majority of these pollutants are refractory pollutants existing in wastewater (Zhou et al., 2015). It is also worth noting that studies on ultrasound application in water treatment usually tackle either microbial contamination or organic contamination separately, while in reality these two categories of contaminants occur concurrently in the complex mixture of natural water. This highlights the need for thorough investigations into ultrasound performance in removing contaminants from natural water.

The high operational energy of ultrasound is a commonly cited main hindrance for the application of this technology in water treatment industry (Hulsmans et al., 2010). There are several ways to reduce energy demand for ultrasound operation such as reactor design modification, combination with other techniques, optimizing the operating conditions and running the technology on pulsed mode (Al-Juboori et al., 2015b; Yusaf and Al-Juboori, 2014). Operating ultrasound on a pulsed mode is usually referred to as pulsed ultrasound. In pulsed ultrasound, the ultrasonic equipment is run in repetitive cycles. The *On:Off* ratio is denoted as *R*, which represents an important operating parameter in pulsed ultrasound operation. The main mechanism through which the pulsed mode reduces energy demand of ultrasound technology is by

reducing energy wasted due to wave scattering caused by the cloud of bubbles that form close to the irradiating surface (hence reducing shielding effects) (Wang et al., 1996). Also, pulsed ultrasound was found to be more chemically reactive than the continuous ultrasound for the same level of ultrasonic energy (Al-Juboori et al., 2015c). However, DOC removal using pulsed mode has been rarely explored.

The aim of this work was to investigate the effect of pulsed ultrasound treatment on DOC concentration and structure in natural water and compare it with the continuous treatment. The water sample that was chosen in this study contains a high concentration of microbes (approximately 250 CFU/100 mL of total coliform), thus allowing the effect of microbial contamination on DOC removal to be inspected. The change in the structure of DOC was tracked using the rapid chemical fractionation technique (Chow et al., 2004). Tracking the change in DOC further improves the understanding of DOC degradation under the effects of ultrasound and allows better planning for the treatment design. Statistical analyses applying factorial design were employed to identify the operating conditions with significant effects on DOC removal. A regression model for DOC removal prediction was developed and tested, and later used for determining energy consumption requirement for DOC removal under various operating condition.

2. Materials and methods

2.1. Water sample

The natural water samples used in this study were collected from Narda lagoon located in southeast Queensland, Australia. Pre-cleaned plastic containers with a capacity of 5 L were used for sample collection. The samples were collected during July–September 2014. To remove large particles and insects, the samples were passed through 0.5 mm sieve that simulates the required screening for natural water samples in treatment practices (Van Nieuwenhuijzen and Van der Graaf, 2011). DOC concentration and structure components of Narda water are presented in Table 1.

2.2. Experimental system

The ultrasonic system used in this work is illustrated in Fig. 1. The system comprises an ultrasonic horn apparatus and cooling bath. Experimental work was carried out with a digital Branson sonifier model 450 with low frequency of 20 kHz and maximum electrical power of 400 W (Branson, USA). The titanium horn ($\varnothing = 19$ mm) was used for irradiating water samples of 500 mL accommodated in a Pyrex beaker. The sample vessel was continuously cooled during the experiments using a cooling bath. The bath consisted of a plastic container with dimensions of $335 \times 275 \times 140$ cm ($l \times w \times h$) and centrifugal submersible circulation pump operated by a DC supply with a maximum power and voltage of 2.5 A and 24 V, respectively. The transducer was placed on a custom made stand, and the depth of the horn in the water sample was fixed at 2 cm using wooden spacers and screws as shown in Fig. 1.

2.3. Experimental procedure

Prior to the commencement of natural water samples treatment, the calorimetric power and chemical throughput of the ultrasonic system

Table 1
Characteristics of Narda water.

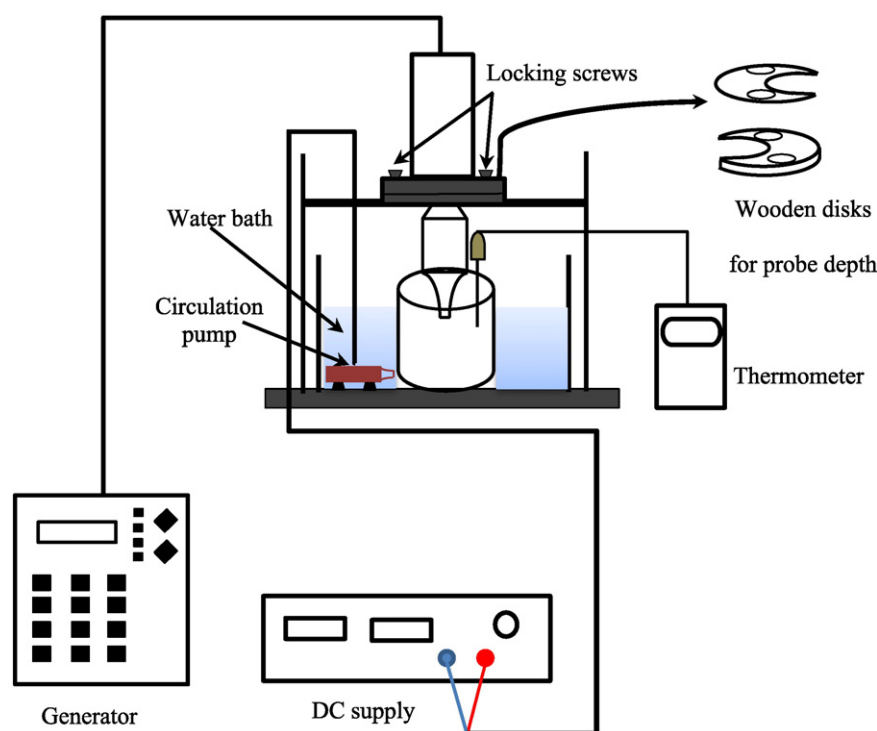| Characteristics		Levels
DOC (mg/L)		9.8
DOC fractions (%)	VHA	65
	SHA	13
	CHA	12
	NEU	10

Fig. 1. Schematic of the experimental system.

were determined at the applied operating conditions. Details of the calorimetric power and chemical throughput measurements can be found in our previous works (Al-Juboori et al., 2015c; Al-Juboori et al., 2015d).

The water samples were treated at two ultrasonic amplitudes of 40% and 70% consuming electrical powers of 93 and 145 W and producing calorimetric powers of 48 and 84 W, respectively. The ultrasonic system was operated at two modes; the standard continuous mode and the pulsed mode. Two pulse settings applied in this study were $R = 0.1{:}0.6$ s and $R = 0.2{:}0.1$ s. The latter pulse setting was not included in the statistical analyses and was only used for testing the validity of the statistical model in predicting DOC removal within the applied range of the operating parameters. The samples were treated for two treatment times of 5 and 15 min (based on effective continuous operation). To apply the same amounts of ultrasonic energy for the two modes of operation used, the treatment time of pulsed mode needed to be higher than that of the continuous mode. The required treatment time of pulsed treatments was calculated based on the R ratio and the corresponding treatment time for the continuous treatment using the following formula (Gutierrez and Henglein, 1990):

$$t_p = t_o \, (1 + 1/R) \qquad (1)$$

where t_p is the treatment time for pulsed mode and t_o is the treatment time for continuous mode. Based on Eq. (1), the equivalent treatment times of 5 and 15 min of continuous treatment are 7.5 min and 22.5 min for $R = 0.2{:}0.1$ s and 35 min and 105 min for $R = 0.1{:}0.6$ s, respectively.

It is important to note here that the applied operating conditions in this study were selected based on the observations of our previous works and the recommendations available in cited literature. The applied power and ultrasonic pulse settings found to produce the highest chemical throughput compared to a range of settings were explored in our earlier works (Al-Juboori et al., 2015c; Al-Juboori et al., 2015d). Ultrasonic treatment time of more than 15 min at high power densities similar to the ones applied in this study was reported to be economically unviable (Phull et al., 1997). Hence, the maximum treatment time applied in this study was limited to 15 min.

In a typical experimental run, the beaker was filled with water sample and placed underneath the transducer with the horn immersed in the sample at the desired depth. The selected ultrasonic amplitudes and pulse levels were set from the generator control panel. The temperature of the water samples was monitored during ultrasonic treatments using a calibrated digital thermometer equipped with platinum probe PT 1000 (Hanna instruments, Australia). The temperature of the water sample was maintained at approximately 20 °C using the cooling water bath. Aliquot of water sample was withdrawn after each treatment and the change in water characteristics was evaluated using a range of analytical methods.

2.4. Analytical measurements

2.4.1. Dissolved organic carbon

DOC of the water samples was measured following the standard high-temperature combustion method (5310 B) detailed in Clesceri et al. (2005). A total carbon analyser (TOC-V$_{CSH}$, SHIMADZU, Australia) with an auto-sampler (ASI-V) was used for DOC measurements. Triplicate injections were made that resulted in coefficient of variance of <0.02. Water samples were filtered through 0.45 μm filter before loading them into the carbon analyser.

2.4.2. Chemical fractionation

The rapid fractionation method proposed by Chow et al. (2004) was applied in this study to explore the change in DOC structure induced by ultrasound treatments. The rapid fractionation technique was developed from full-scale fractionation procedures introduced by Croue et al. (1993) and Bolto et al. (1999). The DOC in this technique is fractionated into four fractions based on their adsorption onto ionic and nonionic resins. The DOC fractions that result from the rapid fractionation techniques are very hydrophobic acids (VHA), slightly hydrophobic acids (SHA), charged hydrophilic acids (CHA), and hydrophilic neutral (NEU).

Three polymer based resins namely Supelite™ DAX-8, Amberlite® XAD-4 and Amberlite® IRA-958 supplied by Sigma-Aldrich, Australia were used in this work. Virgin resins were cleaned in 500 mL glass

beakers by successive washing with HPLC grade methanol and deionised water for 1 h. Each washing cycle involves gentle stirring for a minute followed by settling for 15 min for methanol and 8 min for deionised water. After the last cycle of washing, the resin slurry was packed into three chromatography columns with 20 cm (length) and 1 cm (inner diameter) (Sigma-Aldrich, Australia). The columns were pre-cleaned by 0.1 N NaOH and deionised water prior to their use. The effectiveness of the columns and resin cleaning processes were tested by passing deionised water through the columns of the virgin resins and measuring the DOC of their eluents. The columns were connected in series using three peristaltic pumps and tubing (Cole-Parmer, Australia).

Chemical fractionation procedure is demonstrated in Fig. 2. Water samples of 250 mL were filtered through 0.45 μm cellulose nitrate membranes and acidified to pH 2 using concentrated HCl acid. The acidified filtered sample was then passed through the DAX-8 column at a rate of 1.6 mL/min (0.2 bed volume/min as recommended in Chow et al. (2004) using a peristaltic pump. The first two bed volumes (16 mL) were discarded and a sample of 25 mL of the eluent was collected for DOC measurements. The same procedure was repeated for the other two columns except that the eluent of XAD-4 was adjusted to pH 8 using 1 M NaOH before pumping it through IRA-958 column. The chemicals used such as sodium hydroxide and hydrochloric acid for pH adjustment were all AR grade chemicals supplied by chem-supply, Australia.

The fractions of DOC were calculated using the calculations below:

$$VHA = DOC_{raw} - DOC_{DAX-8\ effluent} \qquad (2)$$

$$SHA = DOC_{DAX-8\ effluent} - DOC_{XAD-4\ effluent} \qquad (3)$$

$$CHA = DOC_{XAD-4\ effluent} - DOC_{IRA-958\ effluent} \qquad (4)$$

$$NEU = DOC_{IRA-958\ effluent} \qquad (5)$$

2.4.3. Microbial measurements

Total coliform concentration in the untreated and treated water samples was quantified as a measure for the effect of ultrasound treatment on microbial contamination. The standard membrane filtration method 9222 B was used for measuring total coliform (standard methods for the examination of water and wastewater (Clesceri et al.,

2005)). M-ColiBlue24® media supplied by Millipore, Australia was utilised for total coliform measurements. Detailed information regarding total coliform measurements can be found in our earlier work (Al-Juboori et al., 2015a).

2.5. Statistical analyses

Factorial design of 2^3 was applied to analyse the obtained experimental results. MINITAB 17 software was used for performing the statistical analyses. The experimental factors investigated in this work are shown in Table 2 along with their levels and coded and uncoded values. DOC removal with pulse treatment of $R = 0.2:0.1$ was not included in the statistical analyses, however its observations were used to validate the predictability of the regression model in estimating DOC removal within the applied range of pulse setting (e.g.1–7) as it falls within this range with a numeric pulse value of 1.5.

The levels of pulse setting were of text category (i.e. 0.1:0.6), and they were converted to numeric category to be consistent with the levels of power and treatment time. The conversion of the pulse setting levels from text to numeric was conducted using Eq. (1) by calculating the ratio of t_p/t_o. For example, the ratio of t_p/t_o for continuous treatment is equal to 1 ($R = \infty$), while the same ratio of $R = 0.1:0.6$ s is equal to 7 as illustrated in Table 2. The number of replicates was estimated with a priori sample size calculations based on a 95% confidence level using GPower software (version 3.1.7). Based on these calculations, it was found that each experimental run should be repeated six times to adequately detect subtle changes in water characteristics caused by ultrasound treatments. It is important to mention that the experimental runs were randomly conducted to ensure fair distribution of the experimental errors throughout all the experiments.

3. Results and discussions

3.1. Normality tests of the experimental data

It is important to test the normality of the experimental error distribution prior to commencing any statistical analysis on the experimental data as such test would ensure the repeatability of the observations (Minis, 2010). In this work, the normality of the experimental errors for DOC removal data was checked through the normal probability plot and residual vs. frequency plot as illustrated in Fig. 3. The adjacency of the residual points to the regression line in Fig. 2a ascertains the
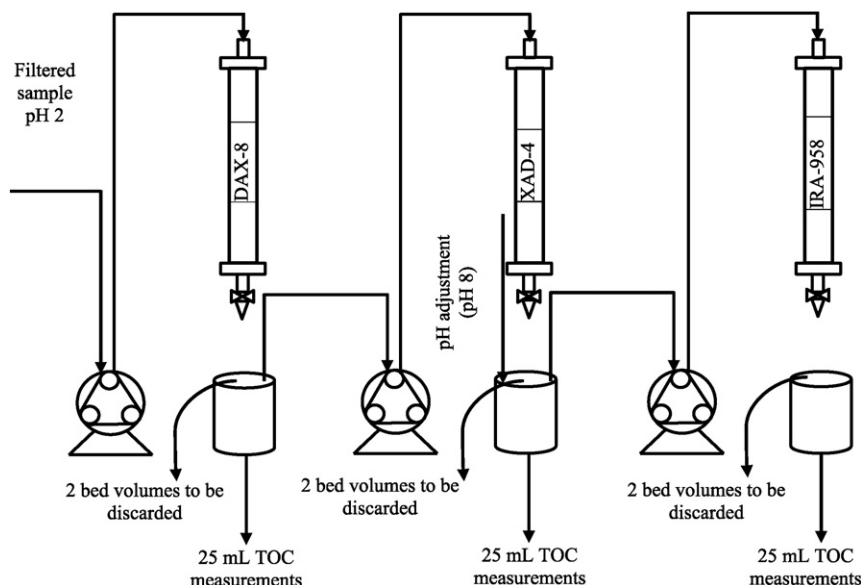

Fig. 2. Illustration of fractionation process.

Table 2
Elements of 2^3 factorial design.

Factors	Levels	Uncoded values	Coded values
Power (W)	Low	48	−1
	High	84	+1
Treatment time (min)	Low	5	−1
	High	15	+1
Pulse setting	Low	1	−1
	High	7	+1

normal distribution of the experimental errors (Antony, 2014). The occurrence frequency of the residuals being in bell-like shape in Fig. 3b provides another evidence for the normal distribution of the experimental errors (Ranjan et al., 2009). Based on the outcomes of the normality tests, it can conveniently be said that the errors are normally distributed and further statistical analysis can be conducted on the experimental data with no additional treatment required for the data (Montgomery, 2010).

3.2. Residual analysis of the experimental data

Further diagnostic statistical tests were conducted on the residuals of DOC removal data to explore time-related effects on error distribution and verify the random distribution of the errors throughout the experiments. The outcomes of the diagnostic tests are presented in Fig. 4. It is clear that the order in which the experiments were conducted had no effect on the distribution of errors as it is illustrated in the random variation of the residuals around zero in Fig. 4a (Khanh, 2010). The random distribution of the residuals vs. fitted values on both sides of zero suggests that the error was randomly distributed throughout the experiments (Venkatesan et al., 2015). This means that the external effects such as experimenter performance and conditions of the experimental environment had no effect on the experiments and measurements.

3.3. Main effects and interaction of the operating parameters

The significance of the operating parameter effects and their interactions on DOC removal is illustrated in the analysis of variance (ANOVA) in Table 3. The significance criterion (P-value) was set as 0.05. Any change in DOC percentage removal of ≤0.05 is regarded significant, otherwise the change is insignificant. It can be noticed from Table 3 that all the operating parameters and their interactions had a significant effect on DOC removal percentage. All the parameters and the 2-way interactions of power × treatment time and power × pulse had very significant effects (P-value = 0.000), while the 2-way interaction of treatment time × pulse and the 3-way interaction of power × Treatment time × pulse were less significant at P-value of 0.001 and 0.024,

respectively. These results suggest that the power has the dominating effect among the investigated operating parameters.

Although the ANOVA table provides insights into the significance of the operating parameters effects on the measured response, it does not show the influence of the effects on the response as being positive or negative. To do so, the normal probability plot for the standardized effects was drawn as shown in Fig. 5. The standardized effect is the product of normalizing the regression model coefficient of a particular factor or interaction by standard error coefficient (0.0898 in the case of this study) (Srinivasan and Viraraghavan, 2010). The parameters of the regression models including coefficients and standardized effects are presented in Table 4. The regression model will be discussed in details in the following section. The probability plot of the standardized effects is divided into negative and positive sides. The effects and interactions that lie on the negative side have effects that diminish DOC removal, whilst the ones on the positive side have beneficial effects on DOC removal. The probability plot can also show the significance of the effects on DOC removal percentages based on how far the respective points of the effects are from the conceptual line of the plot. The closer the points are to the line, the less significant their effects are.

From Fig. 5, one can see that all the factors and interactions had negative effects on the DOC removal except for pulse and the associated interaction of pulse × power. This implies that operating the ultrasound system on pulsed mode is more effective than the continuous mode in removing organic carbon from water. Also, with increasing power levels of pulsed ultrasound the DOC removal increased. The higher DOC removal for pulsed ultrasound as compared to continuous ultrasound can be attributed to many mechanisms:

1. Clarification effects or reduction of shielding effects (Wang et al., 1996).
2. The collapsing bubbles maintain a spherical shape in the advanced stages of bubbles collapse resulting in higher energy implosion (Francescutto et al., 1999).
3. Improving the diffusion of the polar natured compounds (e.g. hydrophobic compounds) into the vicinity of the collapsing bubbles during the *Off* period of pulsed ultrasound, resulting in better chemical decomposition (Yang et al., 2005).
4. Better utilization of the applied acoustic energy as the residual bubbles and pressure in the *Off* period can still produce chemical effects (Dekerckheer et al., 1998).
5. Spatial enlargement of chemically active zones in the liquid being irradiated (Tuziuti et al., 2008).

The improvement of the above-mentioned mechanisms with regards to the chemical effects of pulsed ultrasound was investigated and discussed in our previous work for a wide range of operating parameters including the ones applied in this study (Al-Juboori et al., 2015c). Since DOC degradation with ultrasound occurs due to a
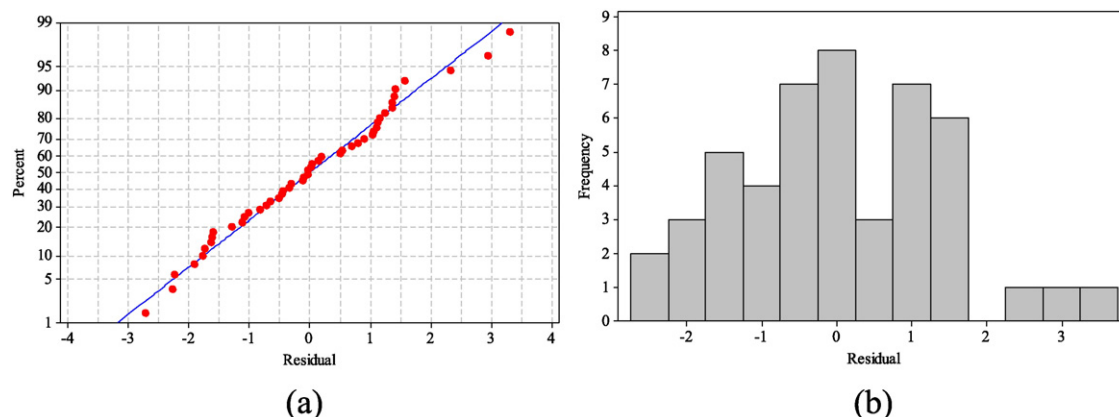

Fig. 3. Normality test figures; (a) normal probability plot and (b) residual vs. frequency plot.
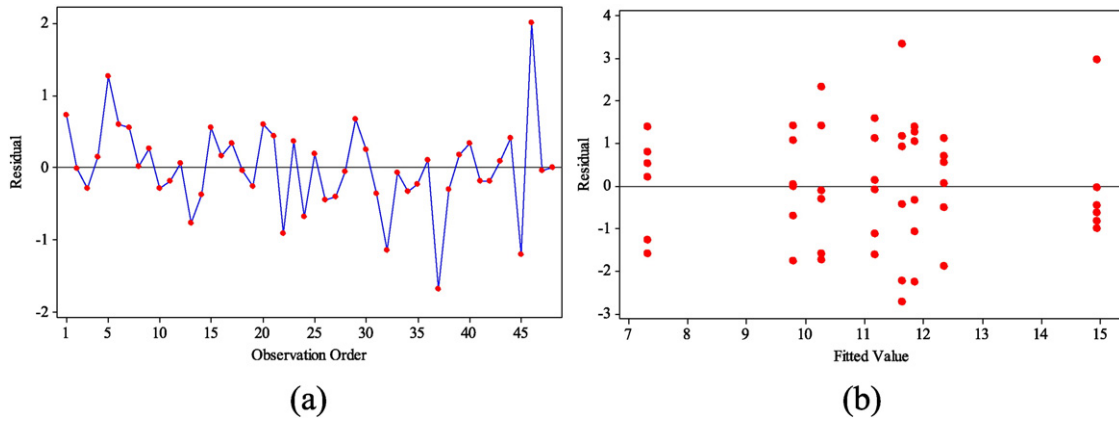
Fig. 4. Residual distribution vs. (a) observation order and (b) fitted values.

combination of physical effects (e.g. shear and thermal degradation) and chemical effects (e.g. hydroxyl and oxidative species degradation) (Eren and Ince, 2010; Henglein and Gutierrez, 1990), the enhancement of the chemical effects would naturally improve DOC removal and that ties well with the results of this study.

Fig. 5 reveals that the power and treatment time or their combination had negative effects on DOC removal. It is known that increasing power and treatment time increases DOC removal in pure synthetic DOC solution (Tran et al., 2015; Zúñiga-Benítez et al., 2015), however, in this study the opposite was observed. The only logical explanation to this observation is that there is a source of DOC that increases in its yield as the power and/or treatment time increases. Since we are dealing with natural water with a relatively high microbial load (total coliform concentration of ca. 250 CFU/100 mL), the possible release of intercellular products due to cell rupture under the mechanical effects of sonication (Al-Juboori and Yusaf, 2012b) can be the reason behind the observed DOC removal trend. Tiehm et al. (2001) found that increasing ultrasound power and treatment time increases the release of intracellular products into the treated water. This in turn was found to cause an increased DOC concentration in the treated water (Savun et al., 2012). To investigate this postulation, the total coliform of the treated water samples was measured and the correlation between DOC and microbes reduction for continuous and $R = 0.1:0.6$ s was investigated as illustrated in Fig. 6.

Fig. 6 confirms that there is a fairly negative correlation between DOC and microbial removal ($R^2 = 0.61$), i.e. as the microbial removal increases, DOC removal decreases. However, through testing the significance of the correlation based on *P-value* of 0.05, the correlation between DOC removal and microbial removal was found to be

significant with an approximate *P-value* of 0.022. This means that there are two concurrent processes occurring simultaneously when ultrasonically treating natural water with a high microbial load; DOC destruction and intercellular products being released. This observation cannot be realised when treating synthetic water with single contaminants (DOC or microbial load). Even the process of contaminant removal in synthetic water solutions differs from that of natural water for both DOC (Xu et al., 2015) and microbes (Al-Juboori et al., 2015a), which highlights the importance of using natural water samples in the treatment regime assessment studies.

3.4. Development and validation of the regression model

A regression model was developed, based on the parameters and interactions in Table 4 that describe DOC removal under the effects of the applied ultrasound treatments. The regression model for DOC removal of the coded operating parameters is shown in Eq. (6).

$$DOC\ removal\ (\%) = 10.8077 - 0.5533A - 0.8281B + 0.974C - 0.6387AB + 1.0304\ AC - 0.3134\ BC - 0.2115ABC \quad (6)$$

where A is ultrasonic calorimetric power (W), B is treatment time (min) and C is pulse setting (ranging from 1 to 7). Eq. (6) helps in predicting DOC removal levels for different values of power, treatment time and pulse settings within the applied ranges in this study. However, to confidently use the model for predicting DOC removal two diagnostic tests needed to be performed;

1. Validation of the model by testing it against real experimental data for identical operating conditions, and

Table 3
Analysis of variance (ANOVA) DOC removal (%) (coded factors).

Source	DF	Seq SS	Adj SS	Adj MS	F	P
Main effects	3	93.152	93.152	31.0506	80.19	0.000
Power (A)	1	14.695	14.695	14.6945	37.95	0.000
Treatment time (B)	1	32.918	32.918	32.9178	85.01	0.000
Pulse (C)	1	45.539	45.539	45.5394	117.60	0.000
2-Way interactions	3	75.255	75.255	25.0848	64.78	0.000
Power∗Treatment time	1	19.581	19.581	19.5813	50.57	0.000
Power∗Pulse	1	50.959	50.959	50.9593	131.60	0.000
Treatment time∗Pulse	1	4.714	4.714	4.7140	12.17	0.001
3-Way interactions	1	2.148	2.148	2.1476	5.55	0.024
Power∗Treatment time∗Pulse	1	2.148	2.148	2.1476	5.55	0.024
Residual error	40	15.489	15.489	0.3872		
Pure error	40	15.489	15.489	0.3872		
Total	47	186.043				

DF = Degree of freedom, Seq SS = Sequential sums of squares, Adj SS = Adjusted sums of squares, Adj MS = Adjusted mean squares, F = F-statistics, P = significance (*P-value*).
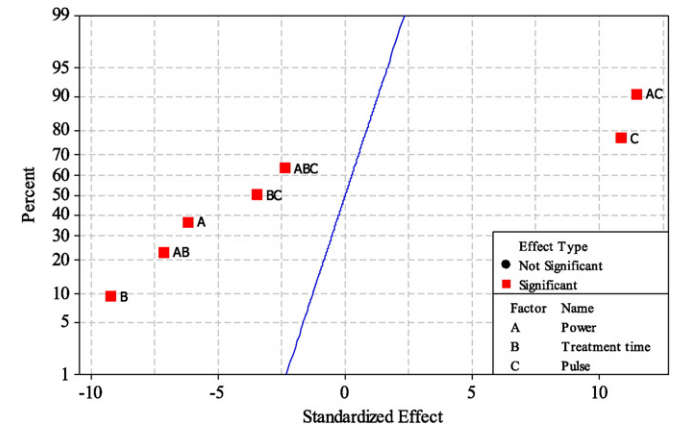

Fig. 5. Normal probability plot for the standardized effects of DOC removal percentage.

Table 4
Regression model parameters of DOC removal (%) (coded factors).

Term	Net effect	Coef. (coded)	Standardized effect (T)	P
Constant		10.8077	120.33	0.000
Power (A)	−1.1066	−0.5533	−6.16	0.000
Treatment time (B)	−1.6562	−0.8281	−9.22	0.000
Pulse (C)	1.9481	0.9740	10.84	0.000
Power∗Treatment time	−1.2774	−0.6387	−7.11	0.000
Power∗Pulse	2.0607	1.0304	11.47	0.000
Treatment time∗Pulse	−0.6268	−0.3134	−3.49	0.001
Power∗Treatment time∗Pulse	−0.4230	−0.2115	−2.35	0.024

2. Examining the accuracy of the model in estimating DOC removal by comparing the predicted values of $R = 0.2{:}0.1$ s treatment with their experimental counterparts.

Table 5 shows the experimental and the predicted values of DOC removal percentage for continuous and pulsed treatments of $R = 0.1{:}0.6$ s for the same power and treatment time levels. It is important to note that the experimental values of DOC removal are the mean values of six replicates. The deviation percentage of the predicted values from the real experimental values was calculated applying the formula below:

$$\text{Deviation} (\%) = \left| \frac{\text{Experimental} - \text{predicted}}{\text{Experimental}} \times 100 \right| \qquad (7)$$

The deviation of the predicted values from experimental ones was very small <5% which indicates a good model predictability for continuous and pulsed treatments for $R = 0.1{:}0.6$ s. The validity of the model in estimating DOC removal with pulse settings different to those applied in the development of the model such as $R = 0.2{:}0.1$ s was also tested and summary of the results is shown in Table 6. The coded value of pulse setting of $R = 0.2{:}0.1$ s in Table 6 (−0.833) was calculated from the coded values of continuous and $R = 0.1{:}0.6$ s via interpolation. Table 6 demonstrates the validity of the model in predicting DOC removal for the applied range of pulse settings with a maximum deviation of less than 11%.

The increase in the deviation of the predicted DOC removal from the experimental data in the case of $R = 0.2{:}0.1$ s treatment suggests that increasing the pulse setting or in other words increasing the Off period would not always lead to an increase in DOC removal, and this can be noticed in some of the cases presented in Tables 5 and 6. For instance, experimental DOC removal of $R = 0.2{:}0.1$ s treatment was 12.88%, while the experimental DOC removal for the treatment $R = 0.1{:}0.6$ s at the same power and treatment time was 12.02%. However, at high
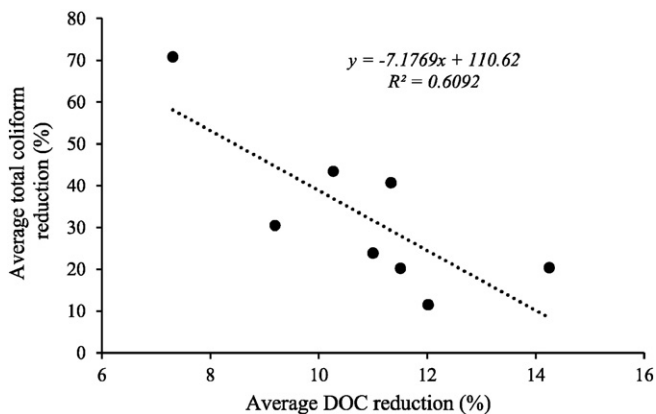

Fig. 6. Relationship between average DOC and total coliform reductions for continuous and R = 0.1:0.6 s treatments.

Table 5
Experimental vs. predicted values of DOC removal (%) for continuous and $R = 0.1{:}0.6$ treatments.

Experimental factors			Experimental DOC removal (%)	Predicted DOC removal (%)	Deviation (%)
Pulse	Power (W)	Treatment time (min)			
−1	−1	−1	11.50	11.50	0.00
−1	−1	+1	11.33	11.32	0.10
−1	+1	−1	9.20	9.19	0.10
−1	+1	+1	7.30	7.30	0.00
+1	−1	−1	12.02	11.60	3.50
+1	−1	+1	10.99	11.01	0.18
+1	+1	−1	14.25	14.25	0.00
+1	+1	+1	10.27	10.27	0.00

power and long treatment time the long Off period $(+1, +1, +1)$ resulted in higher DOC removal percentage as compared to shorter Off period $(−0.833, +1, +1)$, 10.27 vs. 8.35%. The difference in DOC removal percentages between the two pulse settings was marginal in some instances as it is the case with low power and long treatment time $((−0.833, −1, +1)$ vs. $(+1, −1, +1))$.

The variation in DOC removal with different pulse settings is ascribed to the release of intercellular products as explained earlier as well as variation in the nature of pulse cavitation peak with the change in the operating parameters such as power (Wang et al., 1996). Pulse cavitation peak refers to pulse settings that have the highest chemical and physical effects at a given power level. As the power changes, the effective ranges of On and Off periods shift. The pulse cavitation phenomenon is explained as the cavitation bubbles generated in the pulse cavitation peak conditions reach bigger sizes as compared to other cavitation conditions, and hence their collapse is more energetic (Flynn and Church, 1984). The pulse cavitation peak appears more pronounced with a short Off period and low power or long Off period and high power as shown in Tables 5 and 6 for DOC removal of $R = 0.2{:}0.1$ s and $R = 0.1{:}0.6$ s.

3.5. Surface and contour plot interpretations

Surface and contour plots depict the behaviour of the response (i.e. DOC removal) for the developed regression model (Mosbah et al., 2015). These plots were drawn by varying two factors and fixing the third factor. Surface and contour plots provide a valuable tool not only for visual inspection of the response behaviour, but also for quick identification of the optimum parameters for the treatment (Boubakri et al., 2014). Surface and contour plots of DOC removal for various pairs of experimental parameters are illustrated in Figs. 7–9.

Fig. 7 illustrates the response of DOC removal to the change of power and treatment time for two treatments; continuous (a) and $R = 0.1{:}0.6$ s (b). It is clear that the behaviour of DOC removal with pulsed ultrasound differs from that of the continuous ultrasound. The contour plots show clearly that the DOC removal levels for pulsed exceeded those of continuous as the minimum and maximum DOC removal of continuous were <8% and >11%, respectively, while these levels were <11% and >14% for $R = 0.1{:}0.6$ s. These observations are consistent with the findings reported on pulsed ultrasound performance on

Table 6
Experimental vs. predicted values of DOC removal (%) for pulsed treatment of $R = 0.2{:}0.1$.

Experimental factors			Experimental DOC removal (%)	Predicted DOC removal (%)	Deviation (%)
Pulse	Power (W)	Treatment time (min)			
−0.833	−1	−1	12.88	11.51	10.63
−0.833	−1	+1	11.03	11.30	2.44
−0.833	+1	−1	10.50	9.61	8.50
−0.833	+1	+1	8.35	7.55	9.60

removing different types of organic carbon. It was shown that pulsed ultrasound treatment resulted in 6% higher degradation of carbamazepine than the continuous ultrasound (Xiao et al., 2013). Moreover, Yang et al. (2005) found that the degradation rate of sodium 4-octylbenzene sulfonate with pulsed ultrasound was approximately double that of continuous ultrasound. It can also be seen that increasing the treatment time had negative effect on DOC removal for both continuous and pulsed treatments especially at high power levels which was explained by the release of cellular products due to ultrasound treatments.

Fig. 8 shows the pattern of DOC removal for different treatment time and pulse settings while fixing the power level at (a) 48 W and (b) 84 W. The variation in DOC removal with pulse setting and treatment time of low ultrasonic power was small, of the order of 1% as presented in Fig. 8a. The case is different at high power levels as the negative effect of increasing the treatment time on DOC removal is more prevalent due to the increase in the released cellular materials with time. In general, it can be seen that the effect of treatment time on DOC removal with pulsed ultrasound was more noticeable than with continuous ultrasound application (Fig. 8b). This difference in treatment time effect on DOC removal can be ascribed to DOC degradation mechanisms occurring in these modes. The prevailing degradation mechanisms in pulsed ultrasound are radicals attack and thermal decomposition in or around the collapsing bubbles. In continuous ultrasound, the aforementioned mechanisms also occur but to a lesser extent, whereas the continuous mechanical agitation exceeds that of pulsed ultrasound. Since the concentration of intracellular products increases with increasing treatment time and that these products are hydrophilic in nature and have a polymer-like structure (e.g. polysaccharides) (Liu et al., 2008; Walker and Rapley, 2000), the removal of such products is better dealt with using continuous mode ultrasound where the mechanical agitation is higher (Henglein and Gutierrez, 1990).

The effects of power and pulse settings on DOC removal for two sets of treatment time of (a) 5 min and (b) 15 min are depicted in Fig. 9. It can be seen in Fig. 9 that the pattern of surface plot for the two treatment time is similar except that the descending trend at high power is more clear for the case of high treatment time. This was explained earlier by the increase in the release of cellular products at high power and long treatment time. The difference between the minima and maxima of DOC removal for short treatment time was higher than that of long treatment time as shown in the contour plots.

Overall, the surface and contour plots show that:

1. Ultrasonic power had negative effect on DOC removal with continuous treatment regardless of the applied treatment time, while for pulsed treatment the power had almost no effect on DOC removal at long treatment time and noticeable positive effect at short treatment time.

2. Treatment time had insignificant impact on DOC removal of continuous and pulsed treatments at low power (variation of DOC reduction ≤1%). at high ultrasonic power, increasing treatment time negatively affected DOC removal of continuous and pulsed treatments.

3.6. DOC structure alteration

To gain a more in-depth understanding of the ultrasonic mechanisms of DOC degradation in a complex mixture of microbes and organic carbon present in natural water, the chemical fractions of DOC for different ultrasound treatments were quantified and the results are illustrated in Fig. 10. The columns in Fig. 10 represent the mean values of the change in DOC fractions produced from 6 replicates for each treatment, and the error bars symbolize the standard errors of the replicates. The negative change in DOC fractions implies a decrease in the factions, whereas the positive change means an increase in the fractions. The treatment descriptions on the x-axis were expressed as acronyms, and the definitions of these are given in Table 7.

The percentage change of DOC fractions varied from one treatment to another. Pulse treatment at high power and long treatment time caused the highest reduction in VHA fraction. The same treatment but for a short treatment time of 5 min resulted in the second highest VHA reduction. The trends of SHA change were different as the highest
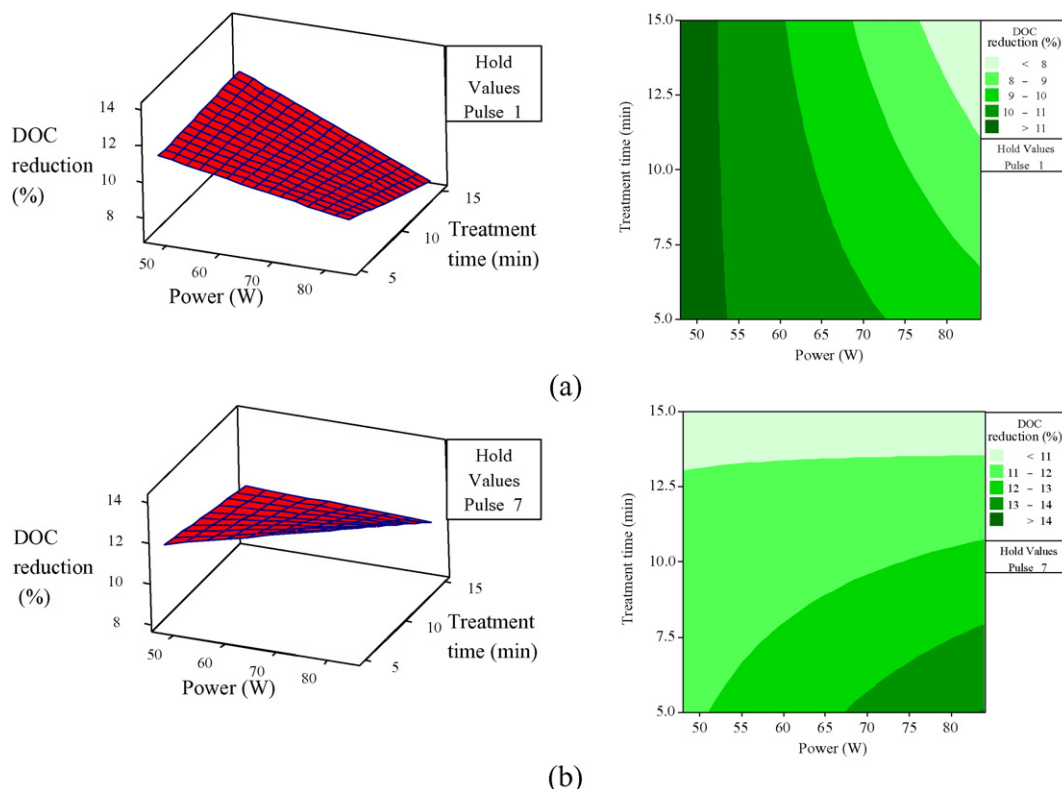

(a)

(b)

Fig. 7. Surface and contour plots of DOC removal (%) at different power and treatment time for (a) continuous treatment and (b) $R = 0.1:0.6$ s treatment.
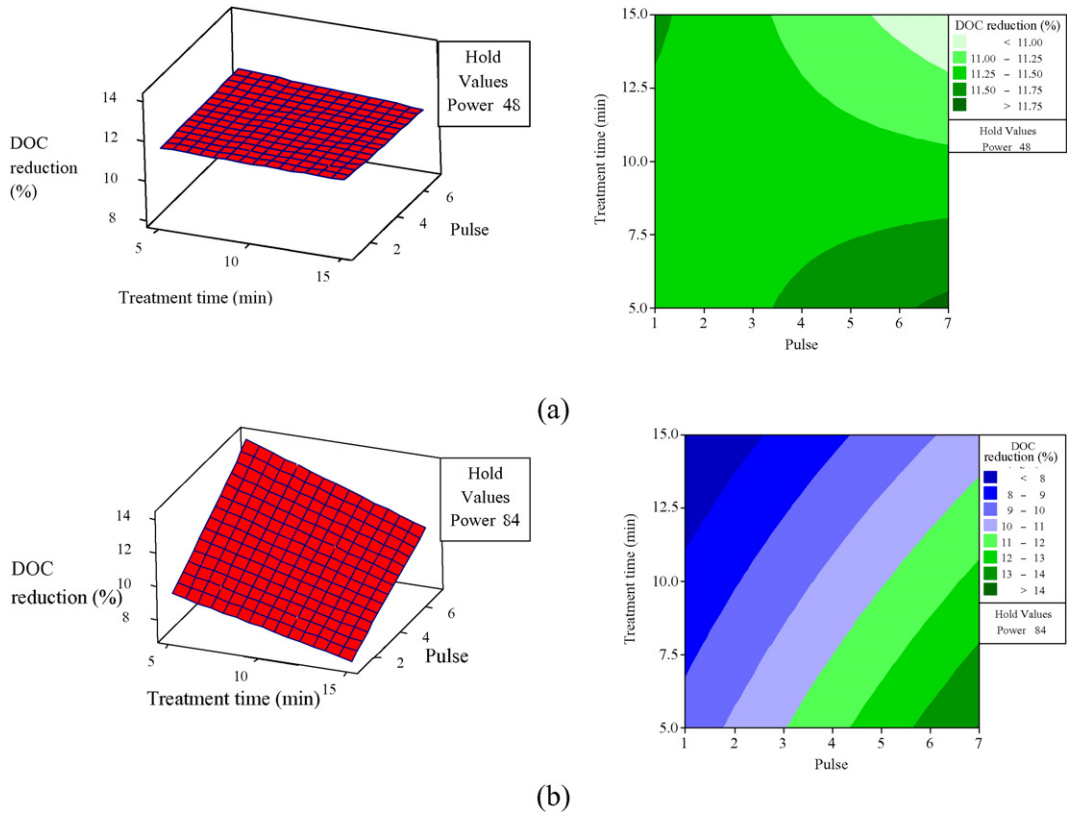
Fig. 8. Surface and contour plots of DOC removal (%) at different pulse setting and treatment time for (a) 48 W and (b) 84 W.
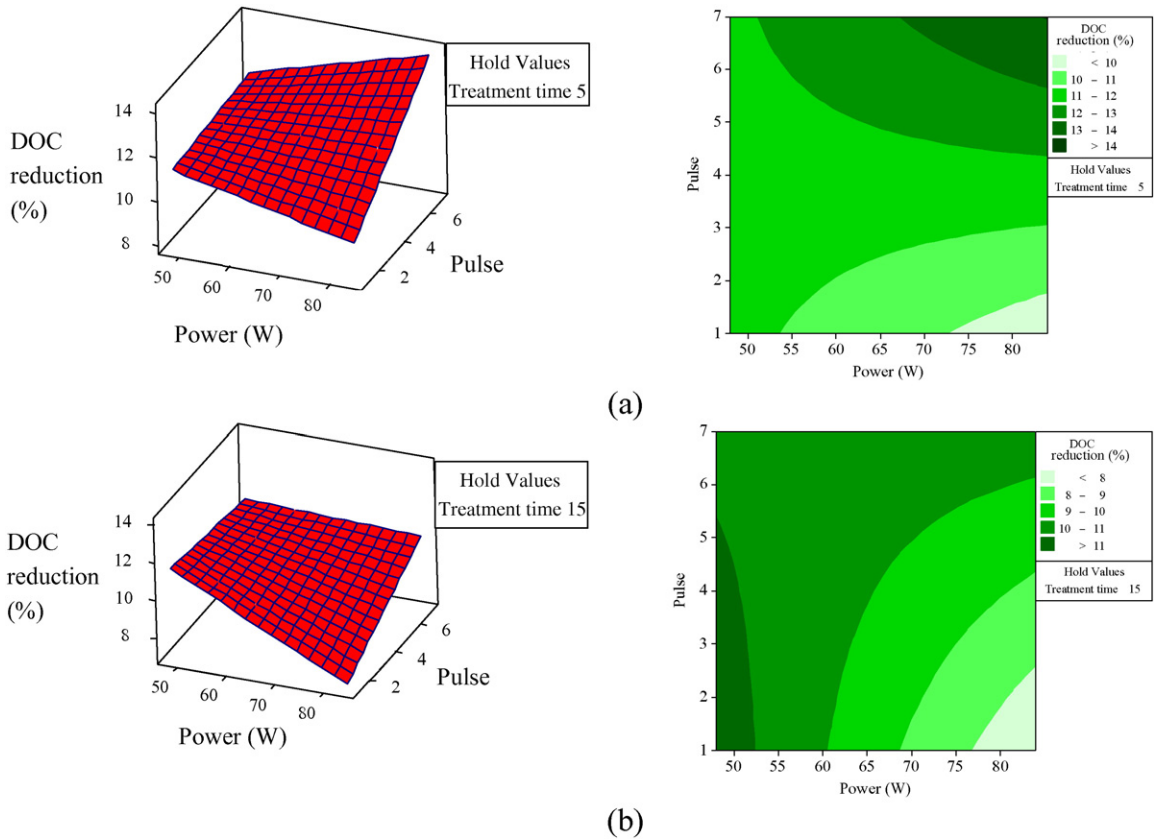

Fig. 9. Surface and contour plots of DOC removal (%) at different power and pulse setting for treatment time of (a) 5 min and (b) 15 min.

reduction was achieved with continuous treatment at high power and low treatment time followed by pulse treatment at low power for short treatment time. The lowest reduction of VHA was observed with pulse treatment at low power and short treatment time followed by continuous treatment at high power and short treatment time. The lowest two levels of SHA reduction were obtained with pulse treatment at high power for both treatment levels. The highest increment of CHA and NEU was attained at continuous treatments for long treatment time with low and high power levels, respectively. Pulse treatment at high power and short treatment time recorded the lowest increase in CHA and NEU.

Overall, the reduction in the hydrophobic fraction (VHA + SHA) was higher than the increase in the hydrophilic fraction (CHA + NEU). The CHA fraction experienced the least change among all DOC fractions. These results are similar to the results obtained with DOC degradation using UV techniques (Buchanan et al., 2005; Liu et al., 2008). The common factor between UV and ultrasound is that in both techniques hydroxyl attack is a dominant mechanism for DOC degradation (Al-Juboori et al., 2015c; Thomson et al., 2002). The difference between the results of our study and those reported in Buchanan et al. (2005) is that in our study CHA witnessed the least change due to ultrasound treatments, while in the other study SHA experienced the least change due to UV treatments. This suggests that ultrasound differs from UV treatment in its mechanisms of DOC degradation, likely to be due to the fact that the hydrophobic nature of DOC does not only promote reactivity with radicals (Galindo et al., 2000; Xu et al., 2015) (occurs in UV and ultrasound), but also promote the attraction of DOC to the collapsing bubbles sites (mechanical degradation occurs in ultrasound only).

The increment in the hydrophilic fraction after ultrasound treatment is attributed to two factors. Firstly, the conversion of the hydrophobic fractions to hydrophilic intermediates under the effect of ultrasound (Ghernaout, 2014; Liu et al., 2008); secondly, the release of the intracellular products due to ultrasound deactivation of microbes, as these compounds are mostly of a hydrophilic nature and the slow degradation of

Table 7
Definition of the acronyms in Fig. 9.

Acronyms	Description
L	Low level of the parameter
H	Low level of the parameter
P	Pulse treatment
C	Continuous
Subscript t.t	Treatment time
Subscript P	power

the hydrophilic DOC fraction can support the cumulative increase of this fraction.

The alteration of DOC structure can have some implications on water treatment processes. For instance, the hydrophobic fraction of DOC has been frequently reported to be a major contributor to the common water treatment problems such as fouling and formation of DBPs (Al-Juboori et al., 2015b; Soh et al., 2008). Hence, degrading this fraction by ultrasound would have a positive effect on water treatment processes. Although ultrasound treatment led to an increase in the hydrophilic fraction, such a fraction can effectively be removed through coagulation processes by applying polymer based coagulants (Liu et al., 2004) or through using hydrophilic membrane filtration (Raspati et al., 2011). The changes in DOC structure discussed herein suggest that integrating ultrasound into conventional water treatment systems can have multiple benefits: reducing microbial and DOC contamination; and altering the structure of the remaining DOC to become less problematic.

3.7. DOC removal in energy perspective

For ultrasound technology to be successfully applied on an industrial scale, two important criteria should be satisfied; technical feasibility and economic viability (Mahamuni and Adewuyi, 2010). Ultrasound has proven to be technically feasible due to its attractive traits such as ease of installation and retrofitting, the compact size of its equipment
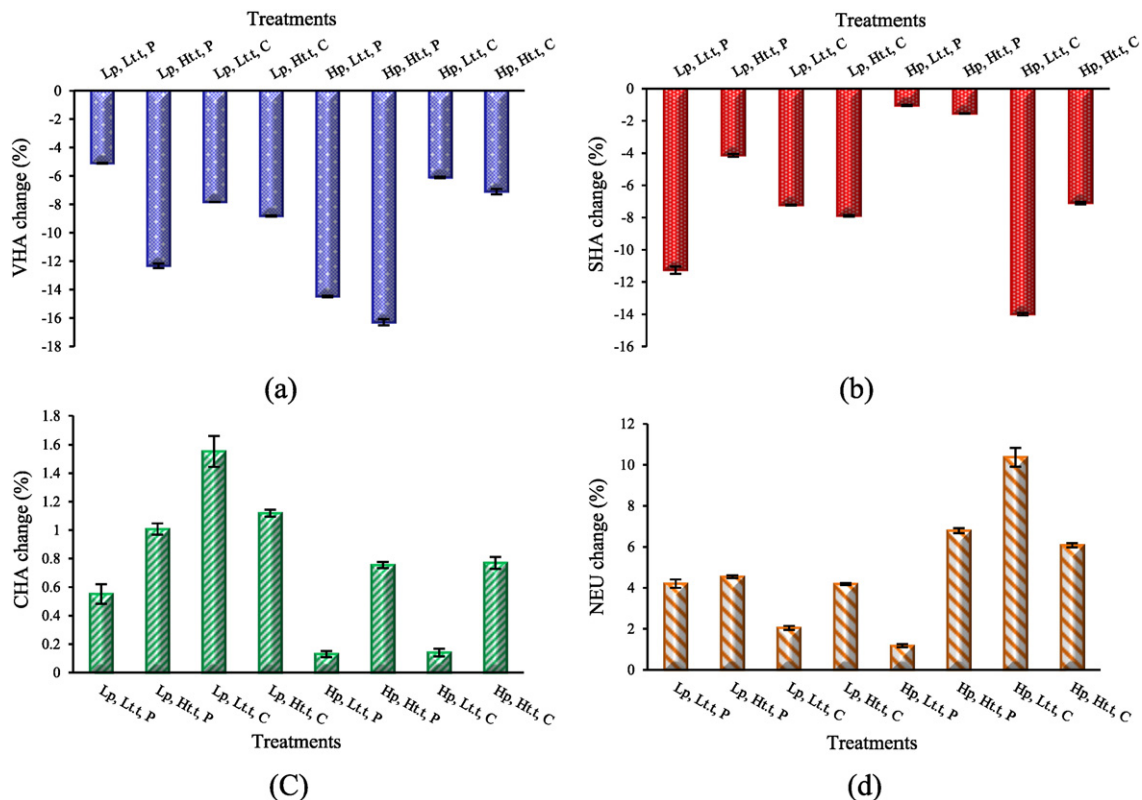

Fig. 10. Percentage changes of DOC fractions with ultrasound treatment at various operating conditions: (a) VHA, (b) SHA, (c) CHA and (d) NEU.

and the simplicity in automating the technology (Khanal et al., 2007; Patist and Bates, 2008). The economic viability is normally evaluated based mainly on the energy figures related to operation and maintenance. The technical feasibility of ultrasound implies that the maintenance of ultrasound units is easy, and hence the energy required is low. However, the operational energy of ultrasound relies heavily on the type of the treatment. In this study, the energy required for DOC removal from natural water was calculated for various operating conditions. To get a meaningful representation of energy requirements for DOC removal, the removal percentage at certain operating conditions was normalized by using the respective calorimetric energy. A contour plot of the normalized DOC removal was drawn for various pulse settings at different calorimetric power levels as demonstrated in Fig. 11. It is important to note that the pulse setting values that appear on the x-axis of Fig. 11 were calculated by applying the conversion of *R* ratios to numerical values as explained in Section 2.5. The DOC removal for the various pulse settings was determined using the regression model in Eq. (6).

It can be seen from Fig. 11 that generally the normalized DOC removal was the highest at low calorimetric energy levels for continuous and pulsed ultrasound. It should be noted that although the pulsed ultrasound had a higher DOC removal compared to continuous ultrasound as presented in Tables 5 and 6, when normalizing the removal with calorimetric energy applied, the differences between the two treatments become almost indiscernible. However, as the calorimetric energy increases the high DOC removal with pulsed ultrasound compared to continuous ultrasound becomes more noticeable as it is shown in the colour coded contours in Fig. 11. At calorimetric energy level of 20 kJ, the normalized DOC removal of continuous treatment (pulse setting = 1) is around 5×10^{-4} (% removal/J), while the normalized DOC removal of pulsed treatment $R = 0.1{:}0.6$ is approximately 7×10^{-4} (% removal/J). This means that from an applied energy perspective applying pulse treatment at low power and short treatment time can be a viable option for ultrasonic removal of DOC from natural waters.

4. Conclusions

DOC removal and structural alteration with low frequency continuous and pulsed ultrasound treatments at a range of different power and treatment time levels were scrutinized in this study. Factorial design was applied to identify the parameters that have significant effects on DOC removal and to help understand the behaviour of DOC removal response for various operating parameters. Rapid chemical fractionation was utilized to track the change in DOC fractions for different treatment settings.

The statistical analysis showed that all operating parameters and their interactions had significant effects on DOC reduction. Power and treatment time were found to have negative effects on DOC removal for some ultrasonic treatments due to the release of microbial products that coincides with DOC destruction during the treatments of natural water. The release of microbial products was confirmed through microbial measurements and DOC structural change analyses. Microbial reduction showed a significant negative correlation with DOC removal with *P-value* of approximately 0.022. The chemical fractionation of DOC exhibited an increase in the hydrophilic fraction and a decrease in the hydrophobic fraction after ultrasound treatment that indicated an abundance of microbial products in the treated water. Pulse width and its interaction with power were found to have a positive effect on DOC removal which proved the benefits return of operating pulsed mode ultrasound for water treatment purposes.

A regression model that describes DOC removal under the effect of various operating conditions was developed for pulse settings varying from 1 (i.e. continuous) to 7 (i.e. $R = 0.1{:}0.6$ s). The functionality of the model was tested through measuring the deviation of the predicted DOC removal for $R = 0.2{:}0.1$ s against the real experimental data of the same pulse setting. The predictability of the model was fairly good with a maximum deviation of <11%. The developed model was then utilized for DOC removal prediction at various pulse settings and ultrasonic energy levels, identifying the operating parameters for the highest normalized DOC removal for ultrasonic energy consumed. It was found that from an energy perspective, low power and short treatment time at pulse mode are the most viable ultrasonic parameters for DOC removal. Investigating the implications of ultrasound effects such as DOC removal and structural alteration on the water treatment process as whole would be a valuable goal for future work.

Fig. 11. Sonochemical efficiency of DOC removal at various calorimetric energy levels and pulse settings.

References

Al-Juboori, R.A., Yusaf, T., 2012a. Biofouling in RO system: mechanisms, monitoring and controlling. Desalination 302, 1–23.

Al-Juboori, R.A., Yusaf, T., 2012b. Identifying the optimum process parameters for ultrasonic cellular disruption of *E. coli*. Int. J. Chem. React. Eng. 10, 1–32.

Al-Juboori, R.A., Yusaf, T., Bowtell, L., 2015c. Energy conversion efficiency of pulsed ultrasound. Energy Procedia 75, 1560–1568.

Al-Juboori, R.A., Yusaf, T., Aravinthan, V., Pittaway, P.A., Bowtell, L., 2015b. Investigating the feasibility and the optimal location of pulsed ultrasound in surface water treatment schemes. Desalin. Water Treat. 1–19.

Al-Juboori, R.A., Yusaf, T., Bowtell, L., Aravinthan, V., 2015d. Energy characterisation of ultrasonic systems for industrial processes. Ultrasonics 57, 18–30.

Al-Juboori, R.A., Aravinthan, V., Yusaf, T., 2015a. Impact of pulsed ultrasound on bacteria reduction of natural waters. Ultrason. Sonochem. 27, 137–147.

Antony, J., 2014. Design of experiments for engineers and scientists: elsevier.

Bolto, B., Abbt-Braun, G., Dixon, D., Eldridge, R., Frimmel, F., Hesse, S., et al., 1999. Experimental evaluation of cationic polyelectrolytes for removing natural organic matter from water. Water Sci. Technol. 40, 71–79.

Boubakri, A., Helali, N., Tlili, M., Amor, M.B., 2014. Fluoride removal from diluted solutions by Donnan dialysis using full factorial design. Korean J. Chem. Eng. 31, 461–466.

Buchanan, W., Roddick, F., Porter, N., Drikas, M., 2005. Fractionation of UV and VUV pretreated natural organic matter from drinking water. Environ. Sci. Technol. 39, 4647–4654.

Chemat, F., Teunissen, P., Chemat, S., Bartels, P., 2001. Sono-oxidation treatment of humic substances in drinking water. Ultrason. Sonochem. 8, 247–250.

Chow, C., Fabris, R., Drikas, M., 2004. A rapid fractionation technique to characterise natural organic matter for the optimisation of water treatment processes. Aqua 53, 85–92.
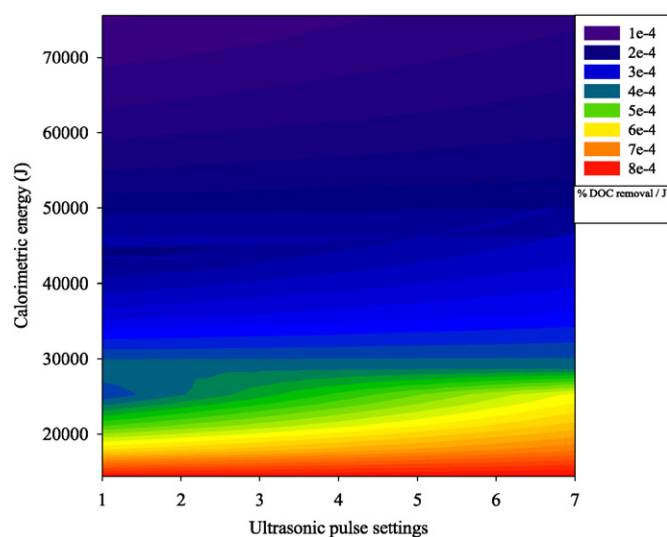
Chun, Y., Zaviska, F., Cornelissen, E., Zou, L., 2015. A case study of fouling development and flux reversibility of treating actual lake water by forward osmosis process. Desalination 357, 55–64.

Clesceri, L.S., Rice, E.W., Greenberg, A.E., Eaton, A.D., 2005. Standard Methods for Examination of Water and Wastewater: Centennial Edition. American Public Health Association, Washington, D.C.

Croue, J.P., Martin, B., Deguin, A., Legube, B., 1993. Isolation and characterization of dissolved hydrophobic and hydrophilic organic substances of a reservoir water. Natural Organic Matter in Drinking Water Workshop, Chamoix, France, pp. 73–81.

Dekerckheer, C., Bartik, K., Lecomte, J.-P., Reisse, J., 1998. Pulsed sonochemistry. J. Phys. Chem. A 102, 9177–9182.

Eren, Z., Ince, N.H., 2010. Sonolytic and sonocatalytic degradation of azo dyes by low and high frequency ultrasound. J. Hazard. Mater. 177, 1019–1024.

Flynn, H.G., Church, C.C., 1984. A mechanism for the generation of cavitation maxima by pulsed ultrasound. J. Acoust. Soc. Am. 76, 505–512.

Francescutto, A., Ciuti, P., Iernetti, G., Dezhkunov, N., 1999. Clarification of the cavitation zone by pulse modulation of the ultrasound field. Europhys. Lett. 47, 49.

Gabelich, C.J., Yun, T.I., Coffey, B.M., Suffet, I.H.M., 2002. Effects of aluminum sulfate and ferric chloride coagulant residuals on polyamide membrane performance. Desalination 150, 15–30.

Galindo, C., Jacques, P., Kalt, A., 2000. Photodegradation of the aminoazobenzene acid orange 52 by three advanced oxidation processes: UV/H2O2, UV/TiO2 and VIS/TiO2: comparative mechanistic and kinetic investigations. J. Photochem. Photobiol. A Chem. 130, 35–47.

Ghernaout, D., 2014. The hydrophilic/hydrophobic ratio vs. dissolved organics removal by coagulation — a review. J. King Saud Univ. Sci. 26, 169–180.

Gutierrez, M., Henglein, A., 1990. Chemical action of pulsed ultrasound: observation of an unprecedented intensity effect. J. Phys. Chem. 94, 3625–3628.

Henglein, A., Gutierrez, M., 1990. Chemical effects of continuous and pulsed ultrasound: a comparative study of polymer degradation and iodide oxidation. J. Phys. Chem. 94, 5169–5172.

Hulsmans, A., Joris, K., Lambert, N., Rediers, H., Declerck, P., Delaedt, Y., et al., 2010. Evaluation of process parameters of ultrasonic treatment of bacterial suspensions in a pilot scale water disinfection system. Ultrason. Sonochem. 17, 1004–1009.

Khanal, S.K., Grewell, D., Sung, S., Van Leeuwen, J., 2007. Ultrasound applications in wastewater sludge pretreatment: a review. Crit. Rev. Environ. Sci. Technol. 37, 277–313.

Khanh, T.T., 2010. Application of response surface method as an experimental design to optimize coagulation tests. Environ. Eng. Res. 15, 63–70.

Liu, S., Lim, M., Fabris, R., Chow, C., Chiang, K., Drikas, M., et al., 2008. Removal of humic acid using TiO2 photocatalytic process — fractionation and molecular weight characterisation studies. Chemosphere 72, 263–271.

Liu, H., Wang, D., Xia, Z., Tang, H., Zhang, J., 2004. Removal of natural organic matter in a typical south-China source water during enhanced coagulation with IPF-PACl. J. Environ. Sci. (China) 17, 1014–1017.

Mahamuni, N.N., Adewuyi, Y.G., 2010. Advanced oxidation processes (AOPs) involving ultrasound for waste water treatment: a review with emphasis on cost estimation. Ultrason. Sonochem. 17, 990–1003.

Minis, I., 2010. Supply Chain Optimization, Design, and Management: Advances and Intelligent Methods: Advances and Intelligent Methods: Business Science Reference.

Montgomery, D.C., 2010. Design and Analysis of Experiments. John Wiley & Sons, Minitab Manual.

Mosbah, H., Aissa, I., Hassad, N., Farh, D., Bakhrouf, A., Achour, S., 2015. Improvement of biomass production and glucoamylase activity by Candida famata using factorial design. Biotechnol. Appl. Biochem. http://dx.doi.org/10.1002/bab.1389.

Naddeo, V., Belgiorno, V., Napoli, R., 2007. Behaviour of natural organic mater during ultrasonic irradiation. Desalination 210, 175–182.

Narotsky, M.G., Klinefelter, G.R., Goldman, J.M., Best, D.S., McDonald, A., Strader, L.F., et al., 2013. Comprehensive assessment of a chlorinated drinking water concentrate in a rat multigenerational reproductive toxicity study. Environ. Sci. Technol. 47, 10653–10659.

Pasupuleti, S., Madras, G., 2010. Ultrasonic degradation of poly (styrene-co-alkyl methacrylate) copolymers. Ultrason. Sonochem. 17, 819–826.

Patist, A., Bates, D., 2008. Ultrasonic innovations in the food industry: from the laboratory to commercial production. Innovative Food Sci. Emerg. Technol. 9, 147–154.

Phull, S.S., Newman, A.P., Lorimer, J.P., Pollet, B., Mason, T.J., 1997. The development and evaluation of ultrasound in the biocidal treatment of water. Ultrason. Sonochem. 4, 157–164.

Ranjan, D., Srivastava, P., Talat, M., Hasan, S.H., 2009. Biosorption of Cr(VI) from water using biomass of Aeromonas hydrophila: central composite design for optimization of process variables. Appl. Biochem. Biotechnol. 158, 524–539.

Raspati, G.S., Høvik, H.N., Leiknes, T., 2011. Preferential fouling of natural organic matter (NOM) fractions in submerged low-pressure membrane filtration. Desalin. Water Treat. 34, 416–422.

Richardson, S.D., 2003. Disinfection by-products and other emerging contaminants in drinking water. TrAC Trends Anal. Chem. 22, 666–684.

Savun, B., Neis, U., Ince, N.H., Yenigün, O., 2012. Pretreatment of sewage sludge by low-frequency ultrasound. J. Adv. Oxid. Technol. 15, 374–379.

Soh, Y.C., Roddick, F., van Leeuwen, J., 2008. The impact of alum coagulation on the character, biodegradability and disinfection by-product formation potential of reservoir natural organic matter (NOM) fractions. Water Sci. Technol. 58, 1173–1179.

Srinivasan, A., Viraraghavan, T., 2010. Oil removal from water by fungal biomass: a factorial design analysis. J. Hazard. Mater. 175, 695–702.

Thomson, J., Roddick, F., Drikas, M., 2002. Natural organic matter removal by enhanced photo-oxidation using low pressure mercury vapour lamps. Water Supply 2, 435–443.

Tiehm, A., Nickel, K., Zellhorn, M., Neis, U., 2001. Ultrasonic waste activated sludge disintegration for improving anaerobic stabilization. Water Res. 35, 2003–2009.

Tran, N., Drogui, P., Brar, S.K., 2015. Sonochemical techniques to degrade pharmaceutical organic pollutants. Environ. Chem. Lett. 13, 251–268.

Tuziuti, T., Yasui, K., Lee, J., Kozuka, T., Towata, A., Iida, Y., 2008. Mechanism of enhancement of sonochemical-reaction efficiency by pulsed ultrasound. J. Phys.Chem. A 112, 4875–4878.

Van Nieuwenhuijzen, A., Van der Graaf, J., 2011. Handbook on Particle Separation Processes. IWA Publishing, London.

Venkatesan, G., Kulasekharan, N., Muthukumar, V., Iniyan, S., 2015. Regression analysis of a curved vane demister with Taguchi based optimization. Desalination 370, 33–43.

Walker, J.M., Rapley, R., 2000. Molecular Biology and Biotechnology. Royal Society of Chemistry, Cambridge.

Wang, S., Feng, R., Mo, X., 1996. Study on 'pulse cavitation peak' in an ultrasound reverberating field. Ultrason. Sonochem. 3, 65–68.

Xiao, R., Diaz-Rivera, D., He, Z., Weavers, L.K., 2013. Using pulsed wave ultrasound to evaluate the suitability of hydroxyl radical scavengers in sonochemical systems. Ultrason. Sonochem. 20, 990–996.

Xu, L., Chu, W., Graham, N., 2015. Sonophotolytic degradation of phthalate acid esters in water and wastewater: influence of compound properties and degradation mechanisms. J. Hazard. Mater. 288, 43–50.

Yang, L., Rathman, J.F., Weavers, L.K., 2005. Degradation of alkylbenzene sulfonate surfactants by pulsed ultrasound. J. Phys. Chem. B 109, 16203–16209.

Yusaf, T., Al-Juboori, R.A., 2014. Alternative methods of microorganism disruption for agricultural applications. Appl. Energy 114, 909–923.

Zhou, Z., Yang, Y., Li, X., Zhang, Y., Guo, X., 2015. Characterization of drinking water treatment sludge after ultrasound treatment. Ultrason. Sonochem. 24, 19–26.

Zúñiga-Benítez, H., Soltan, J., Peñuela, G.A., 2015. Application of ultrasound for degradation of benzophenone-3 in aqueous solutions. Int. J. Environ. Sci. Technol. 1-10.

Paper VII

Al-Juboori, R. A., Yusaf, T., Aravinthan, V. & Bowtell, L., Tracking ultrasonically structural changes of natural organic carbon: chemical fractionation and spectroscopic approaches, *Chemosphere*, (2016), 145, 231-248.

CrossMark

Tracking ultrasonically structural changes of natural aquatic organic carbon: Chemical fractionation and spectroscopic approaches

Raed A. Al-Juboori [a, *], Talal Yusaf [b], Vasantha Aravinthan [a], Leslie Bowtell [b]

[a] School of Civil Engineering and Surveying, Faculty of Health, Engineering and Sciences, University of Southern Queensland, Toowoomba, 4350, QLD, Australia
[b] School of Mechanical and Electrical Engineering, Faculty of Health, Engineering and Sciences, University of Southern Queensland, Toowoomba, 4350, QLD, Australia

HIGHLIGHTS

- Natural surface water samples were treated with pulsed and continuous ultrasound.
- DOC structural alteration was monitored using chemical fractionation and UV−vis.
- Hydrophobic DOC decreased while hydrophilic DOC somewhat increased.
- Pulsed ultrasound degraded aromatic humic-like DOC.
- Most of UV−vis indices showed strong correlations with DOC fractions.

ARTICLE INFO

ABSTRACT

In this study, the structural alteration to DOC for a range of ultrasound treatments was investigated with chemical fractionation and UV−vis spectroscopic measurement. Ultrasound treatments were applied in continuous and pulsed modes at power levels of 48 and 84 W for effective treatment times of 5 and 15 min. Overall results show that the ultrasound treatments tended to degrade the hydrophobic aromatic fraction, while increasing the hydrophilic fraction to a lesser extent. The highest recorded reduction of hydrophobic DOC (17.8%) was achieved with pulse treatment of 84 W for 15 min, while the highest increase in the hydrophilic DOC (10.5%) was obtained with continuous treatment at 84 W and 5 min. The optimal ultrasound treatment conditions were found to be pulse mode at high power and short treatment time, causing a minimal increase in the hydrophilic fraction of 1.3% with moderate removal of the hydrophobic fraction of 15.52%. The same treatment conditions, with longer treatment time, resulted in the highest removal of SUVA$_{254}$ and SUVA$_{280}$ of 17.09% and 16.93, respectively. These results indicate the potential for ultrasound treatments in DOC structural alteration.

The hydrophobic fraction showed strong and significant correlations with UV absorbance at 254 and 280 nm. A_{254}/A_{204} also exhibited strong and significant correlations with the hydrophobic/hydrophilic ratio. The other UV ratios (A_{250}/A_{365} (E_2/E_3) and A_{254}/A_{436}) had weak and insignificant correlations with the hydrophobic/hydrophilic ratio. This confirms the applicability of UV indices as a suitable surrogate method for estimating the hydrophobic/hydrophilic structure.

1. Introduction

The presence of DOC in surface water resources is a major concern for the drinking water production industry due to its involvement in many technical, aesthetic and health related problems (Xing et al., 2012). DOC can adsorb onto the filtration media causing one of the major fouling problems known as organic fouling (Al-Juboori and Yusaf, 2012a). It can also block the pores of the adsorption media that are designed to remove specific synthetic pollutants (Xing et al., 2012). DOC has the capability to bind to heavy metals and micro-pollutants forming complexes that are difficult to be remove by standard water treatment processes (Kim

et al., 2015). If DOC is not completely removed during the final stages of water treatment, it can also promote the formation of biofouling in the distribution systems (Soh et al., 2008). In addition, the occurrence of DOC in water can cause odour colour and taste issues (Audenaert et al., 2015). The most concerning issue from a community health perspective is the reaction of DOC with disinfectants to produce hazardous disinfection by-products (DBPs) (Zhang et al., 2005; Richardson et al., 2007; Richardson and Postigo, 2012; Pan and Zhang, 2013; Al-Juboori et al., 2015b). The extent of detrimental effects on drinking water quality by DOC in water treatment systems is largely dependent on the concentration and nature of DOC present.

A fair proportion of DOC can be conventionally removed from surface water by applying a standard coagulation/flocculation process followed by filtration (typically multi-media gravity filtration). However, downstream problems (e.g. DBPs) are still common with these conventional methods of DOC removal (Lavonen, 2015). To solve this problem chemical oxidation prior to coagulation has been proposed, however, the pre-oxidation process was found to have some drawbacks such as formation of DBPs and mass transfer limitations (Chemat et al., 2001). Hence, chemical-free techniques for removing DOC such as ultrasound are being investigated. Zero chemical DOC degradation is not the only positive trait of ultrasound technology, it also has the advantage of simple installation/retrofitting and ease of maintenance (Patist and Bates, 2008). To date, the work on this technology for DOC removal from natural surface water tends to focus on DOC removal levels with little published on DOC structural changes due to ultrasound treatment. In addition, while operating ultrasound in pulsed mode has been shown to be more energy efficient than continuous ultrasound for removing water contaminants (Al-Juboori et al., 2015a, 2015c, 2016). The effect of pulsed ultrasound on the structure of natural DOC has yet to be examined. Hence, this work is devoted to investigating and comparing the effects of ultrasound in pulsed and continuous modes on the DOC structure prevalent in natural surface water samples.

An in-depth understanding of the transformation of DOC structure caused by a particular treatment technique is critical for the design of an efficient treatment scheme. The change of DOC structure induced by ultrasound treatments was analysed by applying rapid chemical fractionation and UV–vis spectroscopic measurements. The rapid chemical fractionation technique, introduced by Chow et al. (2004) was based on full fractionation processes proposed by Croue et al. (1993) and Bolto et al. (1999). In this fractionation procedure, the DOC is divided into four fractions: very hydrophobic acids (VHA) which adsorbs to DAX-8 resin at pH 2, slightly hydrophobic acids (SHA) which adsorbs to XAD-4 resin at pH 2, hydrophilic charged (CHA) which adsorbs to IRA-958 resin at pH 8 and hydrophilic neutral (NEU) that does not adsorb to any of the aforementioned resins. This fractionation process serves as a valuable tool for studying the response of different DOC fractions in different treatment processes (Chow et al., 2004; Liu et al., 2008). In addition to looking at the change in DOC polarity through chemical fractionation, the change in DOC chemical structure such as alteration of aromatic contents or molecular weight was inspected using a range of UV–vis indices. Absorbance at 254 and 280 nm was applied for evaluating the change in humic-like aromatic DOC. UV absorbance at 254 nm is used to study the electronic structure of DOC as it specifically detects the conjugated structure of DOC which is prevalent in humic DOC (Silverstein, 1974). The electron delocalization in the pi orbital of the conjugated structure of some of the aromatic compounds such as phenolic arenes, benzoic acids and polycyclic aromatic hydrocarbons falls within the UV absorbance range of 270–280 nm (Uyguner and Bekbolet, 2005a), therefore absorbance at 280 nm is used as a measure for DOC bulk

aromaticity. Absorbance ratios of 254/204 and 250/365 (E_2/E_3) nm were utilized to determine the respective changes in aromatic DOC with oxygen containing functional groups and DOC molecular weight, while 254/436 nm was used to measure the ratio of UV absorbing to colour forming DOC (Al-Juboori et al., 2015b). The correlation between the applied UV–vis indices and chemical fractions was also investigated to explore the possibility of using UV–vis indices for detecting change in DOC polarity.

2. Materials and methods

2.1. Water sample

Natural water samples were collected from Narda lagoon located in Southeast Queensland, Australia. The samples were collected during July–September 2014 using 5 L pre-cleaned plastic containers. Prior to the application of ultrasound, the samples were screened through a 0.5 mm sieve to simulate standard water treatment practices (Food Safety and Regulatory Activities Victorian, 2009; Van Nieuwenhuijzen and Van der Graaf, 2011). The DOC concentration and chemical fractionations of Narda water along with other characteristics are presented in Table 1.

2.2. Sonication treatments

The description of the system used for performing ultrasonic treatments is provided in our previous work (Al-Juboori et al., 2015a). Briefly, the system consists of a digital Branson sonifier model 450 operating at 20 kHz with rated electrical power of 400 W (Branson, USA). Ultrasonic energy was delivered sample through a titanium horn ($\varnothing = 19$ mm) into a 500 mL Pyrex beaker filled with the screened water sample. The temperature of water samples was maintained at approximately 20 °C using a cooling bath with dimensions of $335 \times 275 \times 140$ mm (l × w × h) and centrifugal submersible pump. The temperature was monitored using a calibrated digital thermometer (Hanna instruments, Australia).

The operating parameters for the experimental work were selected depending on both the economic viability of the treatment and our prior knowledge of the effective ranges (Phull et al., 1997; Al-Juboori et al., 2015c, 2015d). The water samples were treated with two ultrasonic modes i.e. continuous mode and pulsed mode. Two pulse settings were tested; On:Off ratio (R) of 0.1:0.6 s and 0.2:0.1 s. Only the results of the first pulse setting will be presented in this work, while the latter results will be used for validation of the statistical analysis. The effects of continuous and pulsed treatments of $R = 0.1$:0.6 s on DOC fractions and spectroscopic properties were used to construct a statistical model for predicting the change in DOC structure and properties under different experimental factors. The validity of the model was confirmed by testing the predicted changes of DOC structure and spectroscopic properties for pulsed treatment of $R = 0.2$:0.1 s against the experimental data with the same treatment conditions.

Two levels of ultrasonic calorimetric power and treatment time of 48 and 84 W, and 5 and 15 min (based on effective continuous operation), were applied. The details of calorimetric power measurements are detailed in our previous work (Al-Juboori et al., 2015d). It is important to note here that the applied power levels of 48 and 84 W correspond to power intensities and densities of 16.93 and 29.63 W/cm^2 and 96 and 168 W/L, respectively. The treatment time of pulsed treatments was determined based on the applied R ratios and the corresponding treatment time for the continuous treatments (referred to as effective treatment time) as follows (Gutierrez and Henglein, 1990):

Table 1
Characteristics of Narda water.

Characteristics		Levels
DOC (mg/L)		9.80
pH		6.90
Total coliform (CFU/100 mL)		250
Fractions (%)	VHA	65.00
	SHA	13.00
	CHA	12.00
	NEU	10.00
Spectroscopic properties	$SUVA_{254}$ (L mg^{-1} cm^{-1})	0.036
	$SUVA_{280}$ (L mg^{-1} cm^{-1})	0.025
	A_{254}/A_{204}	0.467
	A_{250}/A_{365}	5.130
	A_{254}/A_{436}	12.320
Inorganic species (mg/L)	Chloride	39.00
	Nitrate	n.a[a]
	Iron	0.37

[a] n.a indicates that the concentration of the ion is below the detection limit of measurement method.

$$t_p = t_o(1 + 1/R) \tag{1}$$

where t_p is the treatment time for pulsed mode and t_o is the treatment time for continuous mode. The equivalent treatment times of 5 and 15 min of continuous treatment were 7.5 min and 22.5 min for $R = 0.2{:}0.1$ s and 35 min and 105 min for $R = 0.1{:}0.6$ s, respectively.

2.3. Analytical methods

2.3.1. DOC measurements

The water samples were filtered through 0.45 μm filter prior to DOC measurements. The standard high-temperature combustion method was applied for DOC measurements (Clesceri et al., 2005). The measurements were conducted using total carbon analyser model TOC-V$_{CSH}$ (SHIMADZU, Australia). The measurements were performed in triple injections that resulted in coefficient of variance of <0.02.

2.3.2. Resin fractionation

Three polymer based resins namely Supelite™ DAX-8, Amberlite® XAD-4 and Amberlite® IRA-958 were utilized for performing DOC fractionation of water samples. Virgin resins were cleaned through successive washing with HPLC grade methanol and deionised water for 1 h. Thereafter, the slurries of washed resins were packed into three pre-cleaned chromatography columns with 0.1 N NaOH and deionised water. The columns were 20 cm long and 1 cm inner diameter supplied by Sigma–Aldrich, Australia. The water samples and column eluents were pumped to the columns using three peristaltic pumps (Cole–Parmer, Australia).

A 250 mL water sample was filtered through 0.45 μm cellulose nitrate membrane, acidified to pH 2 using concentrated HCl acid, and then fed to DAX-8 column at a rate of 1.6 mL/min (0.2 bed volume/min as recommended in Chow et al. (2004)). Aliquot of 16 mL of DAX-8 eluent (two bed volumes) was discarded and a sample of 25 mL of the eluent was collected for DOC and spectroscopic measurements. The rest of DAX-8 eluent was then fed into the XAD-4 column. This procedure was repeated for XAD-4 and IRA-958columns except for the feed of the IRA-958 column being adjusted to pH 8 using 1 M NaOH.

The DOC fractions produced from this fractionation procedure were calculated as follows:

$$VHA = DOC_{raw} - DOC_{DAX-8 \text{ effluent}} \tag{2}$$

$$SHA = DOC_{DAX-8 \text{ effluent}} - DOC_{XAD-4 \text{ effluent}} \tag{3}$$

$$CHA = DOC_{XAD-4 \text{ effluent}} - DOC_{IRA-958 \text{ effluent}} \tag{4}$$

$$NEU = DOC_{IRA-958 \text{ effluent}} \tag{5}$$

2.3.3. Spectroscopic measurements

The spectroscopic measurements of water samples were carried out using a single cell holder JENWAY UV/Vis spectrophotometer model 6705. The samples were filtered through a 0.45 μm filter and scanned in the 200–500 nm wavelength range. The absorbance for untreated and treated samples at the selected wavelengths were recorded for untreated and treated samples. The concentrations of the interfering anions (e.g. nitrate and iron) were measured using an ion chromatography system ICS-2000 and Atomic Absorption Spectrophotometer AA-7000 (SHIMADZU, Australia). The concentration of such anions were found to be below the effective interfering ranges (<0.5 mg/L for iron (Weishaar et al., 2003) and <5 mg/L for nitrate (Thomas and Burgess, 2007), see Table 1). Since UV absorbance is affected by DOC concentration, single wave measurements (254 and 280 nm) were normalized by DOC concentration (SUVA) to better detect the effect of ultrasound treatments on the structure of aquatic DOC.

2.4. Statistical analysis

MINITAB 17 software was used for carrying out the statistical analyses applying 2^3 factorial design. To unify the category of the input experimental factors, the text nature of the pulsed mode settings factor (i.e. 0.1:0.6 s) was transformed into numeric factors (similar to power and time factors) using the correlation between pulse and treatment time settings (equation (1)). The ratio format of pulse setting was converted to a numeric format of t_p/t_o ratio. For instance, when applying $R = 0.1{:}0.6$ s in equation (1), it results in t_p/t_o ratio of 7. The numeric values of pulse settings, uncoded and coded values of the experimental factors and their corresponding levels are presented in Table 2. The coded value of the validation pulse in Table 2 was calculated through interpolation using the high and low values of uncoded and coded pulse settings. Sample size calculations for the applied experimental design were conducted at confidence level of 95% using GPower software (version 3.1.7). The results of sample size calculation showed that each experimental run should be repeated six times to obtain an adequate detection of the changes in the measured responses. The experimental runs were randomly executed to equally distribute the experimental errors throughout all the experiments.

3. Results and discussions

3.1. Overall ultrasonic effects on DOC fractions and spectroscopic properties

Tables 3 and 4 present the overall effects of ultrasound treatments on DOC and its chemical fractions and illustrate the selected spectroscopic properties of the treated water. It should be noted here that the change of spectroscopic properties for DOC fractions was outside the scope of this study and was only measured for few experiments to confirm the correlations between DOC fractions and spectroscopic properties as explained later in section 3.7. The changes in respective DOC fractions and spectroscopic properties in

Table 2
Uncoded and coded values of the experimental factors and levels.

Factors	Levels	Uncoded values	Coded values
Power (W)	Low	48	−1
	High	84	+1
Treatment time (min)	Low	5	−1
	High	15	+1
Pulse setting	Low (continuous)	1	−1
	Validation pulse ($R = 0.2{:}0.1$ s)	1.5	−0.833
	High (0.1:0.6 s)	7	+1

Tables 3 and 4 are expressed as mean values of the 6 trials performed for each treatment, with accompanying standard deviations.

Generally speaking, Table 3 shows that the hydrophobic fraction (VHA + SHA) decreased, as indicated by a negative sign under the effect of ultrasound treatments, while the hydrophilic fraction increased and therefore was assigned with a positive sign. These results corroborate the reported observations in previous studies (Jiang et al., 2011) where the hydrophobic fraction of DOC underwent more degradation than the hydrophilic fraction when treated with ultrasound. Our results were also in agreement with trends achieved with the UV decomposition of DOC fractions (Buchanan et al., 2005; Liu et al., 2008), given that both treatments have a common decomposition mechanism referred to as 'radicals attack'. It can be observed in Table 3 that the overall change of the hydrophobic fraction exceeded that of the hydrophilic fraction. Changes in the resulting DOC fractions were clearly seen when different ultrasonic treatment parameters were used. The highest reduction of VHA was achieved with pulsed ultrasound treatment of $R = 0.1{:}0.6$ s at a power level of 84 W and effective treatment time of 15 min. The lowest reduction of VHA was obtained at the same pulse setting but at a lower power level (48 W) and shorter effective treatment time (5 min). The reduction of SHA peaked under the effect of continuous treatment with power level of 84 W and treatment time of 5 min, whereas the least effective reduction of this fraction was observed with pulsed treatment of $R = 0.1{:}0.6$ s at a power level of 84 W for a treatment time of 15 min. Continuous ultrasound treatments for the same treatment time of 5 min, but at different power levels of 48 and 84 W resulted in the highest increase in the hydrophilic fractions of CHA and NEU, respectively. The smallest percentage increase of these two fractions was obtained at ultrasonic treatment parameters of $R = 0.1{:}0.6$ s, power = 84 W and treatment time = 5 min.

The reduction of the hydrophobic fraction under the effect of ultrasound treatments is attributed mainly to the polar nature of the hydrophobic fraction that drives it close to the collapsing bubbles (Yao et al., 2010), and this explains the highest reduction of VHA at pulsed treatment where such phenomena are further enhanced (Yang et al., 2005). By contrast, the hydrophilic fraction as

the name suggests is more soluble in water and has a lesser tendency to interact with collapsing bubbles. Hence, an increase due to ultrasound treatments was recorded. The increase in the hydrophilic fraction is likely to be due to the transformation of the hydrophobic DOC into hydrophilic DOC as suggested in Liu et al. (2008); Jiang et al. (2011) and Ghernaout (2014). It is also plausible to ascribe the hydrophilic fraction increase to the release of microbial products induced by the bactericidal effects of ultrasound (Jiang et al., 2011; Wang et al., 2014) since we are dealing with natural water samples that have high microbial load (250 CFU/100 mL). The conversion of particulate organic carbon (POC) to DOC under the effect of ultrasound treatments can also affect the distribution of DOC fractions in the treated water samples (only screened).

Table 4 shows that ultrasound treatments with different operating parameters led to a decrease in all of the measured spectroscopic properties of Narda water. The highest decreases were achieved with SUVA$_{254}$ and SUVA$_{280}$, whereas the lowest occurred in E_2/E_3 and A_{254}/A_{204}. The absorbing DOC moieties at 254 and 280 nm were most degraded with pulsed ultrasonic treatment at high power. The decrease in SUVA$_{254}$, SUVA$_{280}$ in this study is consistent with the findings of previous studies (Chen et al., 2004; Naddeo et al., 2007). The reduction in these two spectroscopic indices is translated into a reduction in the content of humic-like aromatic materials in the treated water.

Ultrasound treatment is known to decease the size of the molecules in the treated solution (Hakata et al., 2011), nevertheless such a trend is usually observed with synthetic samples (Chen et al., 2004). The case is different in this study as the surrogate measurement for molecular size spectrum (i.e. E_2/E_3) decreased upon the exposure to ultrasound treatments suggesting a higher decomposition rate of the small sized DOC molecules compared to the large sized molecules. The release of the microbial products by ultrasonic cell rupture may provide justification for the observed decrease in A_{250}/A_{365}, as these products have been found to contribute to the large molecules pool of DOC (Santos et al., 2014).

The higher reduction of SUVA$_{280}$ compared to that of A_{254}/A_{204} illustrates the low efficiency of ultrasound treatments in removing aromatic DOC with oxygen containing functional groups. However,

Table 3
Experimental data of average ultrasonic effect on DOC and its chemical fractions.

Power (W)	Effective treatment time (min)	Pulse settings	Average DOC change (%)	Std dev	Average VHA change (%)	Std dev	Average SHA change (%)	Std dev	Average CHA change (%)	Std dev	Average NEU change (%)	Std dev
48	5	0.1:0.6	−12.02	1.72	−5.10	0.03	−11.26	0.23	0.55	0.07	4.20	0.20
48	15	0.1:0.6	−10.99	0.39	−12.32	0.16	−4.14	0.09	1.00	0.04	4.54	0.07
48	5	Continuous	−11.50	0.32	−7.83	0.0	−7.23	0.03	1.55	0.11	2.05	0.09
48	15	Continuous	−11.33	0.16	−8.8	0.05	−7.89	0.04	1.12	0.02	4.20	0.05
84	5	0.1:0.6	−14.25	1.02	−14.47	0.05	−1.05	0.03	0.13	0.02	1.17	0.07
84	15	0.1:0.6	−10.27	0.57	−16.30	0.22	−1.54	0.02	0.76	0.02	6.78	0.12
84	5	Continuous	−9.20	0.17	−6.10	0.05	−14.00	0.08	0.14	0.03	10.37	0.46
84	15	Continuous	−7.30	0.24	−7.10	0.19	−7.10	0.07	0.77	0.04	6.07	0.10

Table 4
Experimental data of average ultrasonic effect on spectroscopic properties.

Power (W)	Effective treatment time (min)	Pulse settings	$SUVA_{254}$ reduction (%)	Std dev	$SUVA_{280}$ reduction (%)	Std dev	E_2/E_3 reduction (%)	Std dev	A_{254}/A_{204} reduction (%)	Std dev	A_{254}/A_{436} reduction (%)	Std dev
48	5	0.1:0.6	10.6	0.02	10.41	0.09	4.06	0.02	3.062	0.04	10.04	0.02
48	15	0.1:0.6	12.2	0.05	12.15	0.03	2.05	0.03	3.2	0.01	3.05	0.03
48	5	Cont.	12.43	0.04	12.14	0.01	2.6	0.02	3.23	0.01	3.51	0.01
48	15	Cont.	12.02	0.05	10.88	0.03	1.21	0.01	3.11	0.01	10.53	0.02
84	5	0.1:0.6	16.2	0.10	16.45	0.03	3.22	0.02	3.3	0.01	7.51	0.01
84	15	0.1:0.6	17.09	0.04	16.93	0.02	2.7	0.01	4.75	0.02	5.51	0.01
84	5	Cont.	11.4	0.03	11.04	0.02	1.9	0.01	2.51	0.01	7.81	0.01
84	15	Cont.	12.02	0.02	12	0.01	1.02	0.00	3.41	0.01	11.83	0.01

pulsed ultrasound at a high power level was still the most effective treatment in removing this portion of the aromatic compounds. The reduction of A_{254}/A_{436} was relatively high compared to the other absorbance ratios. The reduction of A_{254}/A_{436} was lower than that of $SUVA_{254}$ which implies that ultrasound has lower capability in the removal of colour forming DOC as opposed to UV absorbing DOC.

3.2. Validation of diagnostic statistical tests

A range of diagnostic statistical tests were run on the obtained experimental data to verify the assumptions of normal distribution, consistency and independence of residuals. Residuals are defined as the difference between the experimental values and the predicted values of the statistical model that fits the experimental data (Simarani et al., 2015). Satisfying these assumptions assures the reproducibility of the experimental work and allows accurate analysis of the experimental factors effects (Minis, 2010). The normal distribution assumption was tested by analysing normality plots and subsequent residuals frequency occurrence with histograms of measured responses as illustrated in Figs. 1 and 2 respectively. It is clear from these figures that the residuals of DOC fractions and spectroscopic properties were normally distributed as they fall close to the percentage line in the normality plot and the histograms of the residuals form a bell-like shape (Antony, 2014; Simarani et al., 2015). The consistency of residuals was checked by plotting the residuals of responses against the fitted values of responses in Fig. 3. The residuals independence was examined by plotting the residuals of the responses versus the order of the experiments as shown in Fig. 4. Both Figs. 3 and 4 show no pattern, confirming the independence and the consistency of residuals throughout all of the experimental observations (Tezcan Un et al., 2015).

3.3. Main and interaction effects of factors

The effects of individual experimental factors and the combined effects of the interacting factors on DOC fractions and spectroscopic properties were tested against significance criteria of P-value = 0.05 and the results are illustrated in summarised ANOVA Tables 5 and 6, respectively. It can be seen from Table 5 that all the experimental factors and their interactions had a highly significant effects on all DOC fractions change (P-value = 0.000) except for the effect of power × treatment time interaction on SHA fraction change that was insignificant (P-value = 0.686). Also, the effect of treatment time × pulse interaction on SHA was less significant than the other effects presented in Table 5 (P-value = 0.001). The inclusion of the pulse setting in the least significant interactions highlights the possible negative effect of pulsed mode on the degradation of the SHA fraction. Table 6 shows that the all the tested factors and their interactions had a significant effect on the measured spectroscopic

properties at P-value = 0.000.

Despite that ANOVA tables reveal the significance level of the main and interaction effects, these tables do not show the direction of the effect on the response whether it is positive or negative. This can be done through inspecting the distribution of the standardized effects around the conceptual probability line in the effects plot (Anglada et al., 2011). The effects plots of DOC fractions and spectroscopic characteristics are shown in Fig. 5. The experimental factors are symbolized with letters, power is expressed as A, treatment time as B and pulse setting as C. In the effects plots, the effects or interactions that lie close to the probability line are insignificant as it is the case with power × treatment time interaction effect on SHA (depicted as a black dot), while the factors and interactions that lie far from the line are significant (Saadat and Karimi-Jashni, 2011). The other feature of the effects plot is that the probability line divides the plot into two areas positive and negative. The effects that fall on the negative side are antagonistic, whereas the effects that fall on the positive side are synergistic.

It can be noted that all the experimental factors had positive effects on VHA change with the pulse setting having the dominant effect. The 2-way interactions of pulse setting with power and treatment time also had positive effects on VHA change, while the 3-way interaction of pulse setting, power and treatment time resulted in an overall negative effect on VHA change. This is clearly attributed to the negative effect of the interaction of power and treatment time that overrode the positive effect of pulse setting. The response of the SHA fraction to the factors and their interactions was almost the opposite to that of VHA. Most of the experimental factors had negative effects on SHA change. The effect of power × treatment time interaction was insignificant, and the only positive effect was that of 3-way interaction of power, treatment time and pulse setting. Power and pulse setting had a positive effect on CHA change, whereas treatment time had a negative effect on the change of this fraction. The change of CHA was negatively impacted by all the interactions except for the 3-way interaction of power, treatment time and pulse setting. The case is different for the NEU fraction as the only main factor that had positive effect on the change of this fraction was pulse setting. The combination of power with pulse setting or treatment time positively influenced the change of NEU fraction, while the other interactions had a negative impact on the change of this fraction.

Based on the results presented in Fig. 5, one can deduce that operating ultrasound on a pulsed mode is effective for removing VHA, but it has no effect in removing the other DOC fractions represented by the negative effect on SHA removal and positive effect on the increment of CHA and NEU fractions. The effective removal of the VHA fraction with pulsed mode is attributed to the enhancement of polar DOC transfer (e.g. VHA) to the collapsing bubbles sites (Yang et al., 2005). The increase of the other DOC fractions under the effect of pulsed ultrasound is likely to be due to the high degradation of VHA fraction into intermediates of
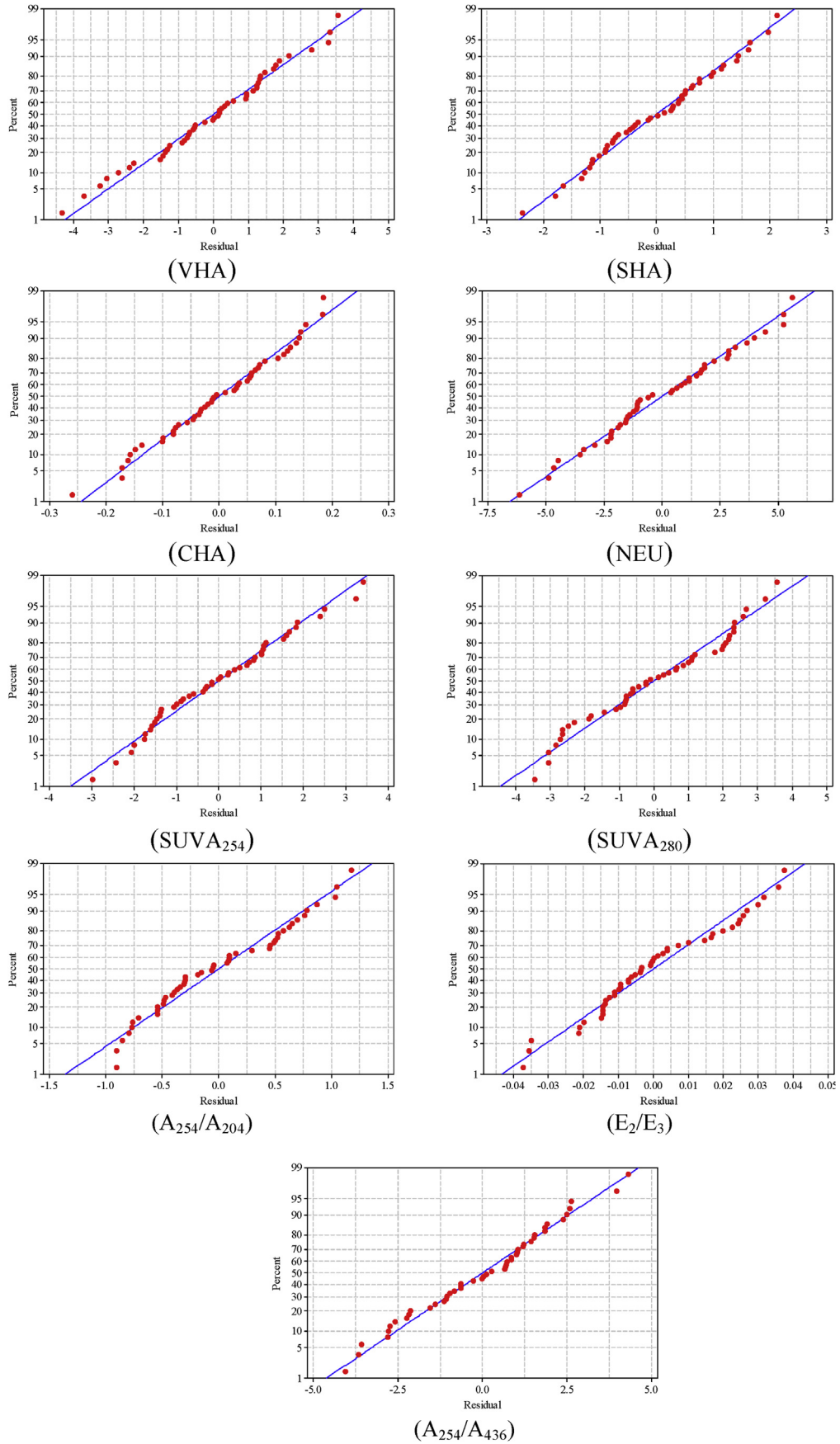
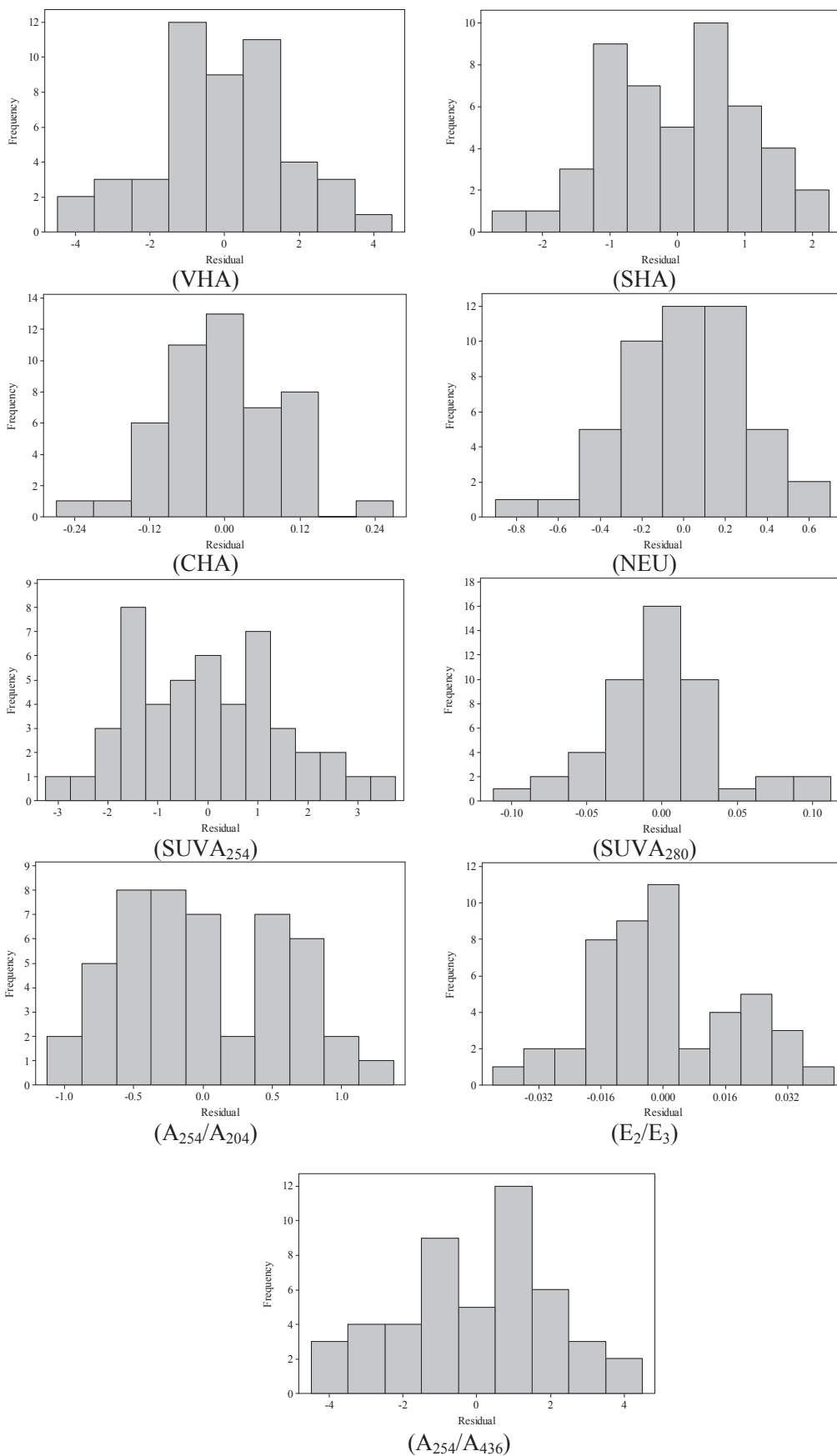**Fig. 1.** Normal distribution plot for measured responses.

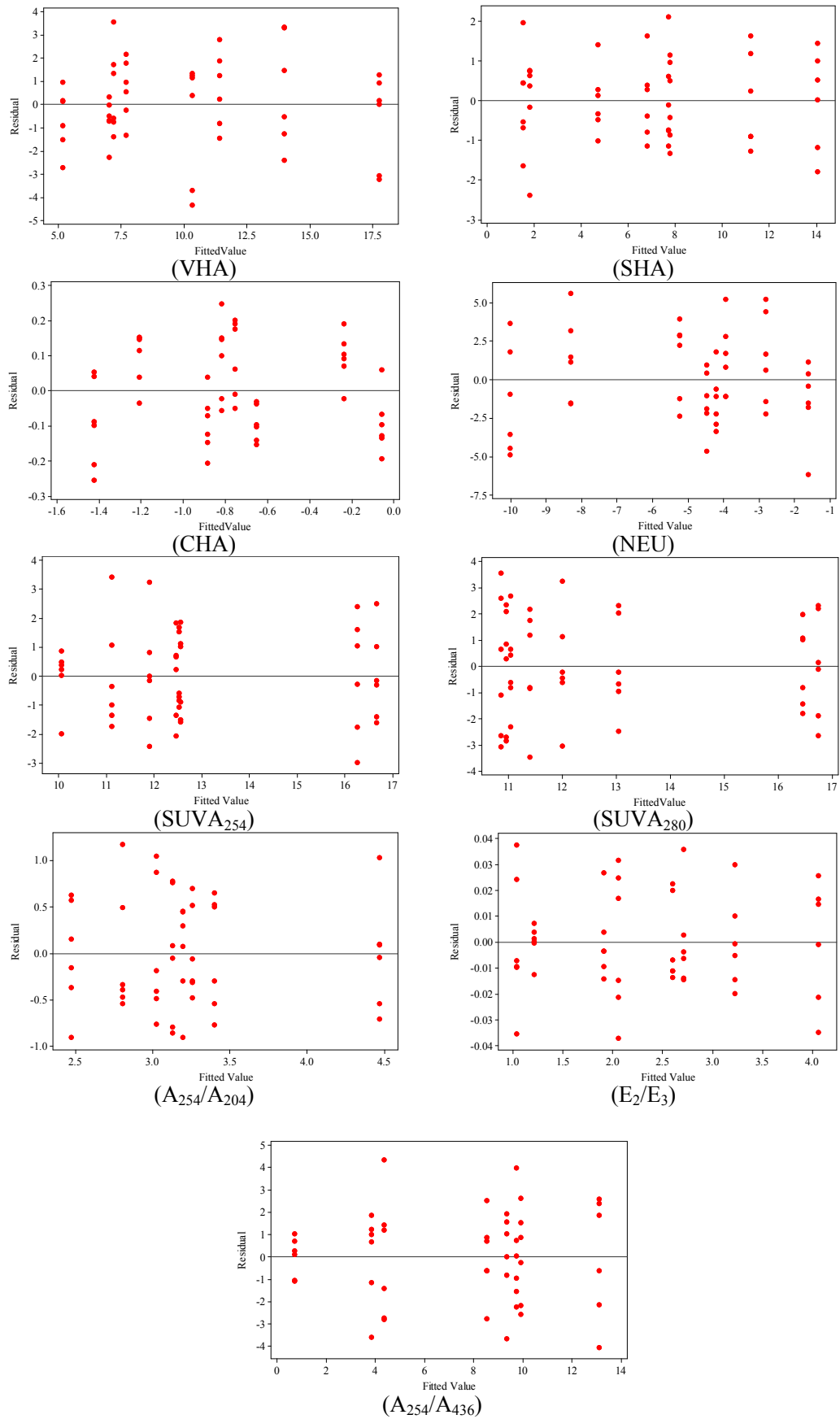**Fig. 2.** Histograms of residual frequency for measured responses.

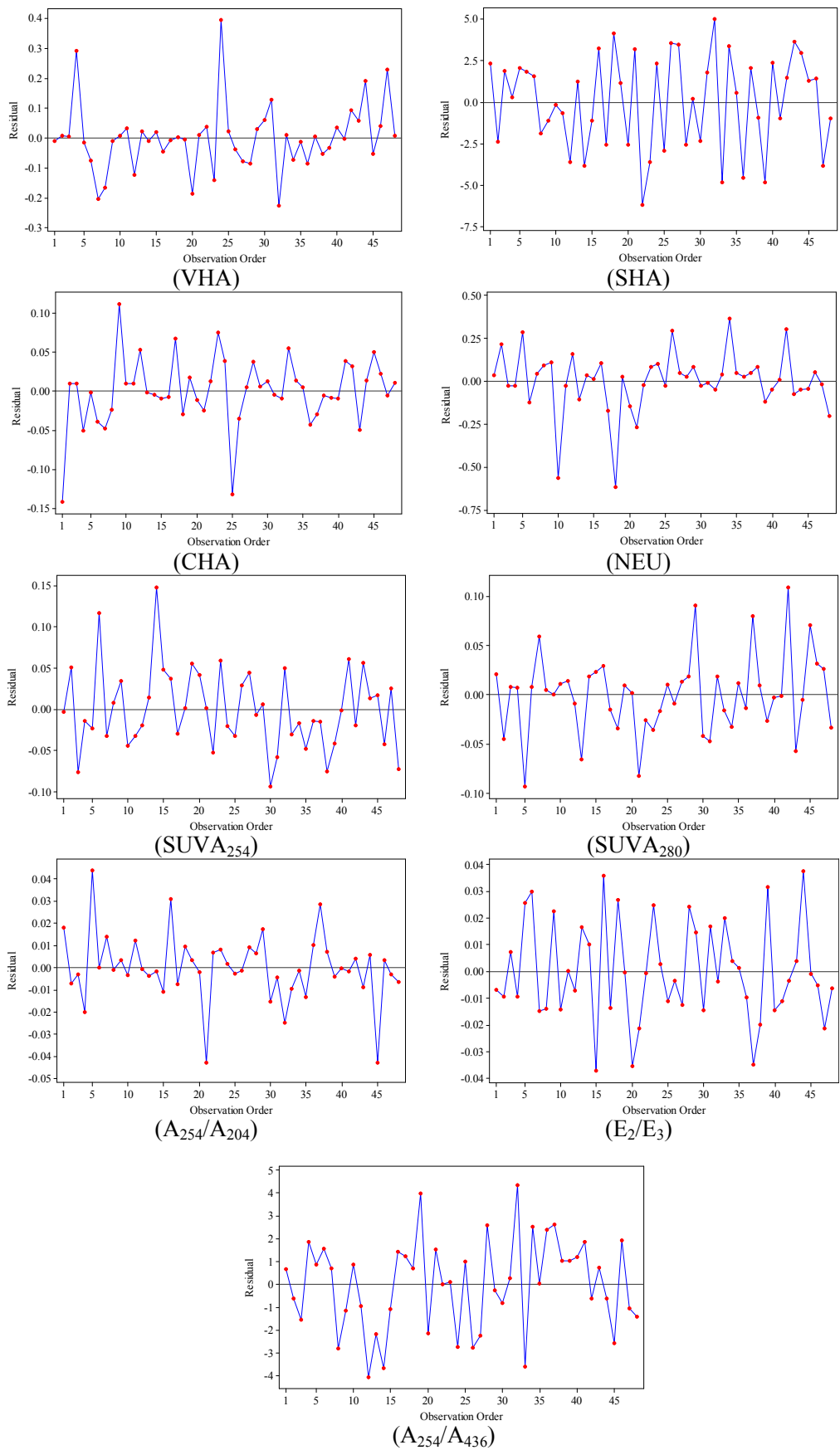**Fig. 3.** Residuals vs. fitted values of measured responses.

Fig. 4. Residuals vs. experiments order of measured responses.

Table 5
Summary of analysis of variance (ANOVA) for DOC fractions.

Source	DF	VHA		SHA		CHA		NEU	
		F-value	P-value	F-value	P-value	F-value	P-value	F-value	P-value
Main effects	3	9213.11	0.000	14737.44	0.000	966.31	0.000	949.07	0.000
Power (A)	1	4868.99	0.000	3791.91	0.000	2094.83	0.000	1815.37	0.000
Treatment time (B)	1	6020.45	0.000	13442.58	0.000	452.62	0.000	296.17	0.000
Pulse (C)	1	16749.88	0.000	26977.84	0.000	351.49	0.000	735.68	0.000
2-Way interactions	3	5974.73	0.000	9559.88	0.000	366.47	0.000	1278.87	0.000
Power × Treatment time	1	1434.27	0.000	0.17	0.686	579.20	0.000	28.28	0.000
Power × Pulse	1	14003.80	0.000	28667.38	0.000	319.31	0.000	2463.58	0.000
Treatment time × Pulse	1	2486.13	0.000	18706.40	0.001	200.89	0.000	1344.77	0.000
3-Way interactions	1	1454.13	0.000	18706.40	0.000	205.94	0.000	2802.06	0.000
Power × Treatment time × Pulse	1	1454.13	0.000	14737.44	0.000	205.94	0.000	2802.06	0.000
Residual error	40								
Pure error	40								
Total	47								

Table 6
Summary of analysis of variance (ANOVA) for Spectroscopic properties.

Source	DF	$SUVA_{254}$		$SUVA_{280}$		A_{254}/A_{204}		E_2/E_3		A_{254}/A_{436}	
		F-value	P-value	F-value	P-value	F-value	P-value	F-value	P-value	F-value	P-value
Main effects	3	14542.44	0.000	28474.10	0.000	10749.41	0.000	31834.62	0.000	20818.26	0.000
Power (A)	1	23734.75	0.000	46554.52	0.000	5287.12	0.000	2035.46	0.000	20764.44	0.000
Treatment time (B)	1	1927.03	0.000	1536.98	0.000	15313.70	0.000	42053.04	0.000	2735.22	0.000
Pulse (C)	1	17965.55	0.000	37330.80	0.000	11647.40	0.000	51415.34	0.000	38955.11	0.000
2-Way interactions	3	12360.91	0.000	15574.49	0.000	10184.51	0.000	2818.80	0.000	100159.63	0.000
Power × Treatment time	1	31.22	0.000	441.25	0.000	14949.92	0.000	7471.43	0.000	2776.14	0.000
Power × Pulse	1	35706.46	0.000	43936.39	0.000	13693.77	0.000	868.05	0.000	22352.81	0.000
Treatment time × Pulse	1	1345.05	0.000	2345.83	0.000	1909.84	0.000	116.92	0.000	275349.93	0.000
3-Way interactions	1	813.85	0.000	4969.93	0.000	199.80	0.000	1759.96	0.000	43991.60	0.000
Power × Treatment time × Pulse	1	813.85	0.000	4969.93	0.000	199.80	0.000	1759.96	0.000	43991.60	0.000
Residual error	40										
Pure error	40										
Total	47										

other DOC fractions (Liu et al., 2008). Ultrasonic power has similar effect to that of pulse setting on all of DOC fractions except for NEU fraction. Increasing the power decreased the fractions of VHA and NEU, but increased CHA. It is known that increasing ultrasonic power increases the violence of bubble collapse and hence better physical and chemical effects are produced (Al-Juboori and Yusaf, 2012b). This in turn improves VHA removal. The increase of CHA could be related to the release of cellular products (mostly of hydrophilic nature (Walker and Rapley, 2000)) as a result of microbial inactivation under the effect of ultrasound as mentioned earlier. However, the decrease of NEU fraction with increasing ultrasonic power accentuates the refractory nature of CHA to ultrasonic power increment. Increasing ultrasonic power increases microbial rupture leading to an increase in CHA and NEU fractions, nevertheless, the produced NEU is degraded with increasing ultrasonic power while the produced CHA remained unaffected, and it rather accumulated with increasing ultrasonic power.

The effects plots of the spectroscopic properties show that the main effects of the factors on the reduction of $SUVA_{254}$, $SUVA_{280}$ and A_{254}/A_{204} were positive, while the effects of some of these factors on E_2/E_3 and A_{254}/A_{436} reduction were negative. For instance, power and treatment time had negative effects on E_2/E_3 reduction. Also, applying pulsed treatment negatively affected the reduction of A_{254}/A_{436}. The reduction of A_{254}/A_{204} was positively affected by all the main and interactions effects. All the interactions except the 3-way interaction of power, treatment time and pulse setting had positive effects on the reduction of $SUVA_{254}$ and $SUVA_{280}$. The collective effects of pulse setting and treatment time on the reduction of E_2/E_3 was negative. Similarly, combining pulse setting with power or treatment time affected negatively on the reduction of A_{254}/A_{436}.

Increasing power, treatment time, pulse setting or the combination of any pair of these factors can increase the removal of humic-like DOC with aromatic nature. These results are in agreement with $SUVA_{254}$ removal trends reported in previous works (Naddeo et al., 2007; Stepniak et al., 2009). However, increasing all of the aforementioned factors at the same time can have a negative effect on removing aromatic DOC. Contrarily, increasing this combination of factors can improve the removal of aromatic DOC with oxygen containing functional groups. The destruction of high molecular weight DOC fractions (decrease in E_3) into smaller molecular weight fractions (increase in E_2) is favoured with continuous ultrasound treatment where the mechanical effects reach their climax due to the continuous agitation (Henglein and Gutierrez, 1990). This explains the positive effect of pulse setting on E_2/E_3 reduction. Increasing ultrasonic power, treatment time or both are the only possible scenarios where E_2/E_3 ratio increased. These scenarios were also found in the literature to decrease the molecular size of DOC (Zhang et al., 2011; Jambrak et al., 2014). Operating ultrasound on pulsed mode and increasing power or treatment in this mode had negative effects on A_{254}/A_{436} reduction.

3.4. Regression models

The regression models for the measured responses were formulated based on the coefficients of the coded factors and their interactions with incorporating the nature of the effects (positive or negative) as shown in Table 7. The effects that are insignificant were not included in the regression models as it is the case for the effect of power × treatment (AB) interaction on SHA reduction.
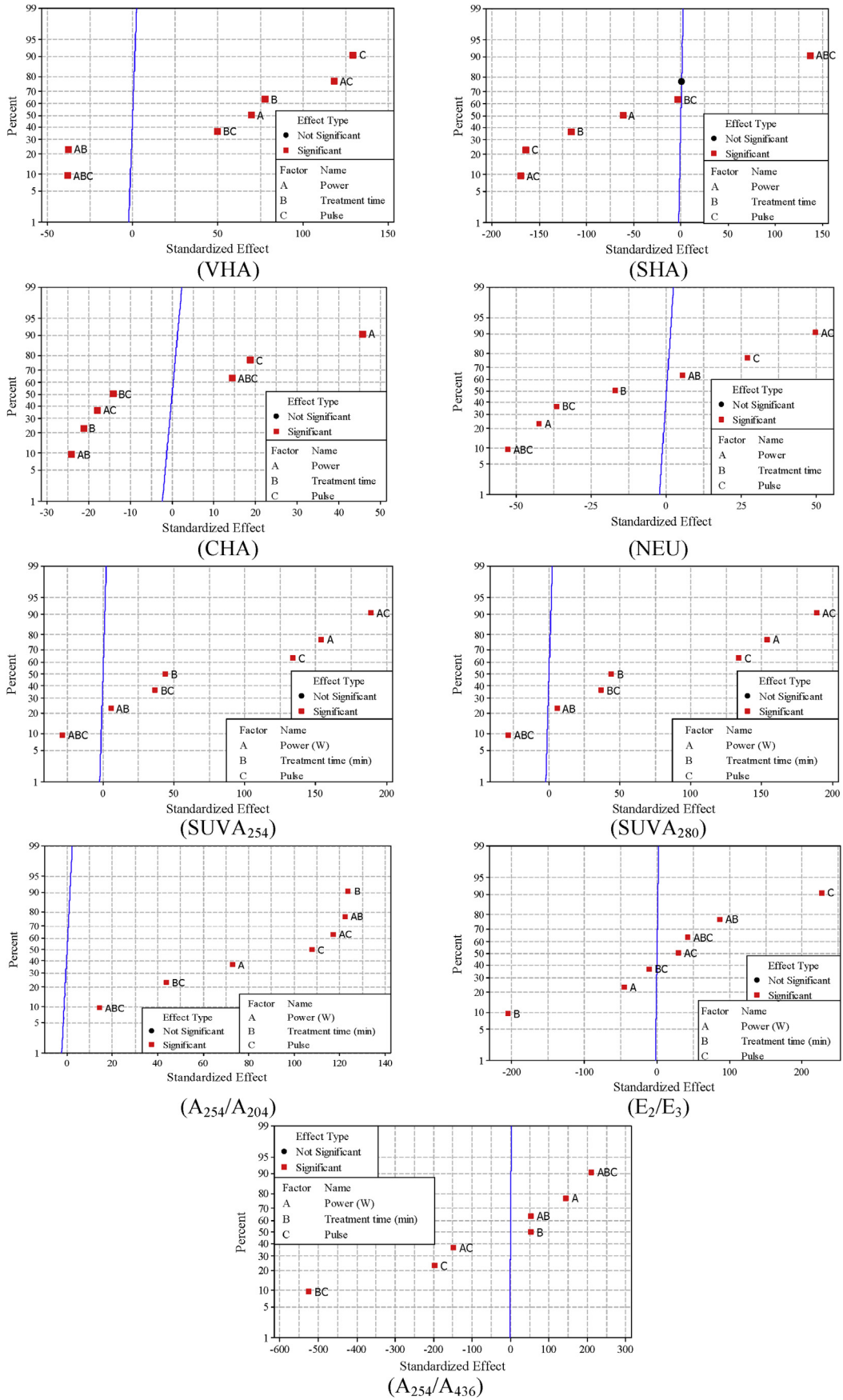
Fig. 5. Effects plots of measured responses.

The adequacy of the regression models in predicting the values of the responses was checked against the experimental values of the responses at various operating conditions. The deviation of the predicted values from the experimental values was calculated for both groups of responses; DOC fractions and spectroscopic properties applying equation (6). The outcomes of deviation calculations for DOC fractions and spectroscopic properties are presented in Tables 8 and 9 respectively. The deviation of the predicted values of the responses from their analogous experimental values for continuous (−1) and $R = 0.1:0.6$ s (+1) (applied conditions for developing the regression models) was used to determine the sufficiency of the models in predicting responses values. The percentage values of these deviations were presented in normal font in Tables 8 and 9. To verify the capability of the models in forecasting the values of the responses at operating conditions differ from the ones applied in developing the regression models, the deviation of the models in predicting the responses values for the pulsed treatments of $R = 0.2:0.1$ s was calculated and the results presented in bold italic font in Tables 8 and 9.

$$Deviation\ (\%) = \left| \left(\frac{(Experimental - Predicted)}{Experimental} \right) \times 100 \right| \quad (6)$$

It is clear form Table 8 that the regression models that represent the change of DOC fractions under the effect of different ultrasound treatments were reasonably good for predicting the change in DOC fractions with a maximum deviation of <20%. Interestingly, the models of all DOC fractions had a higher deviation for $R = 0.2:0.1$ s treatments as compared to other treatments except for CHA where the deviation of continuous treatments exceeded those of $R = 0.2:0.1$ s. This means that the change of CHA is better predicted with different pulsed treatments at various conditions than with continuous treatments at the same conditions.

Generally, it can be noticed that models predictability for changes of DOC fractions is better than those of spectroscopic properties change marked by the high values of deviation up to approximately 78%. The lowest deviation values in Table 9 were those calculated for SUVA$_{254}$, SUVA$_{280}$ and A$_{254}$/A$_{204}$. The deviation values of SUVA$_{254}$, SUVA$_{280}$ and A$_{254}$/A$_{204}$ for the treatments $R = 0.2:0.1$ s were higher than those of the other treatments highlighting the better predictability of the models at the operating conditions they were developed for. The model of A$_{254}$/A$_{436}$ exhibited similar trends to those of SUVA$_{254}$, SUVA$_{280}$ and A$_{254}$/A$_{204}$, but the deviation values of $R = 0.2:0.1$ s treatments at 15 min were noticeably high (maximum of 68.5%) suggesting that the model cannot be used appropriately for predicting A$_{254}$/A$_{436}$ change for pulsed mode at long treatment time. The deviation percentages of the model for predicting E$_2$/E$_3$ were the highest among all other responses, and they were consistently high for all the treatments. This means that the current regression model of E$_2$/E$_3$ failed to predict the change in this spectroscopic characteristic of DOC.

3.5. DOC fractions change expressed by surface plots

The behaviour of DOC fractions under the effects of various operation factors within the defined boundary conditions of the factors was studied through constructing the 3D surface plots for the absolute change of DOC fractions as demonstrated in Fig. 6. The 3D surface plots presented in this section and the following sections were drawn based on the regression models for the responses in Table 7. The way the 3D plots are laid out is by changing two factors and maintaining the other factor constant. In the case of this study, the 3D plots of the responses were set out by changing power and treatment time while fixing the pulse setting. The 3D surface plots facilitate the identification of the optimum levels of factors or interactions efficiently (Boubakri et al., 2014).

Fig. 6 illustrates the surface plots of DOC fractions percentage change with various operating factors. It can be seen from Fig. 6 a that increasing the power of continuous treatment within a short treatment time had insignificant effect on the reduction of VHA. In contrast, applying higher levels of power for the same treatment but at a long treatment time had a significant negative effect on VHA reduction. This trend can be attributed to bactericidal effects of ultrasound as the cell debris and cellular products increase in the water with increasing power and treatment time (More and Ghangrekar, 2010). These cellular materials along with the existing particles (e.g. POC) can then compete with the VHA for the reaction sites of the collapsing bubbles (heterogeneous cavitation (Al-Juboori and Yusaf, 2012c)). Fig. 6 a also shows that increasing the power of pulsed ultrasound treatment increased VHA reduction at both treatment time levels 5 and 15 min at almost the same rate. Upon inspecting the corner points of the surface plots in Fig. 6 a, one can notice that increasing the pulse setting from 1 to 7 at low power and short treatment time negatively impacted the decrement of VHA, while the case is opposite for high power and long treatment time. This trend suggests that the conditions of low power and short treatment time (low ultrasonic energy) are not suitable for degrading VHA fraction with pulsed treatment.

The change of the SHA reduction under different power and treatment levels at fixed pulse settings is depicted in Fig. 6 b. Increasing the treatment from 5 to 15 min did not seem to have much effect on SHA reduction with continuous treatment at low power level. Increasing the treatment time for the continuous treatment at high power level adversely affected SHA reduction. Rising the treatment time from 5 to 15 min for pulsed treatment resulted exactly in an opposite trend to that observed in continuous treatment. This implies that the favourable conditions for removing SHA fraction are short treatment time and high power for continuous operation or low power for pulsed operation.

Fig. 6 c demonstrates the surface plot of the change in CHA increment with different ultrasonic conditions. The surface plot for CHA increment of continuous treatment exhibits almost the same patterns as that of the pulsed treatment except for the direction of the change when increasing the treatment time at lower power.

Table 7
Regression models for measured responses.

Response	Respective regression model in coded factors
VHA	$Y = 9.75 + 1.237A + 1.376B + 2.295C - 0.671AB + 2.098AC + 0.884BC - 0.68ABC$
SHA	$Y = 6.778 - 0.854A - 1.61B - 2.28C - 2.35AC - 0.048BC + 1.9ABC$
CHA	$Y = -0.766 + 0.317A - 0.147B + 0.13C - 0.167AB - 0.124AC - 0.098BC + 0.199ABC$
NEU	$Y = -4.92 - 1.18A - 0.476B + 0.75C + 0.147AB + 1.373AC - 1.014BC - 1.464ABC$
SUVA$_{254}$	$Y = 13 + 1.18A + 0.335B + 1.025C + 0.043AB + 1.445AC + 0.28BC - 0.22ABC$
SUVA$_{280}$	$Y = 12.77 + 1.367A + 0.249B + 1.224C + 0.133AB + 1.33AC + 0.307BC - 0.447ABC$
A$_{254}$/A$_{204}$	$Y = 3.322 + 0.173A + 0.294B + 0.257C + 0.291AB + 0.278AC + 0.104BC + 0.033ABC$
E$_2$/E$_3$	$Y = 2.351 - 0.131A - 0.598B + 0.661C + 0.252AB + 0.86AC - 0.031BC + 0.122ABC$
A$_{254}$/A$_{436}$	$Y = 7.48 + 0.688A + 0.25B - 0.943C + 0.252AB - 0.714AC - 2.51BC + 1.002ABC$

Table 8
Deviation of the predicted values of DOC fractions from their experimental counterparts.

Experimental settings (coded)			VHA deviation (%)	SHA deviation (%)	CHA deviation (%)	NEU deviation (%)
Power	Treatment time	Pulse				
−1	−1	1	0.066	0.006	0.026	0.417
−1	1	1	0.035	0.012	9.800	0.003
−1	**−1**	**−0.833**	**17.950**	**16.230**	**12.814**	**11.643**
−1	**1**	**−0.833**	**6.665**	**0.882**	**2.890**	**4.014**
−1	−1	−1	0.045	0.093	6.520	0.033
−1	1	−1	0.103	0.082	8.872	0.202
1	−1	1	0.023	0.093	12.456	0.304
1	1	1	0.018	0.616	13.182	0.081
1	**−1**	**−0.833**	**3.716**	**7.790**	**10.014**	**17.470**
1	**1**	**−0.833**	**16.570**	**18.240**	**11.040**	**18.984**
1	−1	−1	0.088	0.111	18.652	0.055
1	1	−1	0.0575	0.106	12.955	0.053

Bold font represents the deviation of the predicted responses from their experimental values at operating conditions differ from the ones applied in developing the regression models.

Table 9
Deviation of the predicted values of spectroscopic properties from their experimental counterparts.

Experimental settings (coded)			$SUVA_{254}$ deviation (%)	$SUVA_{280}$ deviation (%)	A_{254}/A_{204} deviation (%)	E_2/E_3 deviation (%)	A_{254}/A_{436} deviation (%)
Power	Treatment time	Pulse					
−1	−1	1	0.016	0.080	0.278	19.103	0.320
−1	1	1	0.008	0.114	0.009	37.693	0.127
−1	**−1**	**−0.833**	**5.543**	**7.000**	**12.078**	**45.296**	**15.158**
−1	**1**	**−0.833**	**1.636**	**4.681**	**34.850**	**27.503**	**64.543**
−1	−1	−1	0.106	0.012	0.0100	29.626	0.075
−1	1	−1	0.116	0.107	0.250	63.929	0.042
1	−1	1	0.030	0.018	0.006	24.026	0.0208
1	1	1	0.004	0.015	0.048	28.891	0.069
1	**−1**	**−0.833**	**21.600**	**22.492**	**11.840**	**45.111**	**15.605**
1	**1**	**−0.833**	**5.880**	**2.910**	**0.189**	**77.906**	**68.500**
1	−1	−1	0.080	0.125	0.015	40.502	0.001
1	1	−1	0.035	0.035	0.003	74.488	0.016

Bold font represents the deviation of the predicted responses from their experimental values at operating conditions differ from the ones applied in developing the regression models.

Increasing the treatment time for continuous treatment at lower power caused a decrease in CHA change, whereas such change increased CHA change for pulsed treatment. The 3D presentation of CHA change elucidates that the production of CHA fraction peaks at low power for both treatment modes continuous and pulsed. However, the highest increase in CHA fraction coincided with low treatment time for continuous treatment and high treatment time for pulsed treatment. The lowest production of CHA fraction was obtained at high power and short treatment time for continuous and pulsed treatments.

The response of NEU fraction increment to a range of ultrasonic operating conditions is demonstrated in Fig. 6 d. The pattern for NEU fraction increase in continuous ultrasound is almost the opposite to that of the pulsed ultrasound except for their common incremental trend when increasing the treatment time at low po-wer. The increase in NEU reaches its apex at high power but different treatment time for continuous (short treatment time) and pulsed (long treatment time) treatments. It is noteworthy that the least production of NEU fraction occurred at the same operating conditions for the least production of CHA for the pulsed treatment. The same conditions resulted in moderate to high reduction of VHA, therefore these conditions are very important for DOC structural alteration using pulsed ultrasound. CHA and NEU fractions were found to be recalcitrant to water treatment processes such as coagulation and because of their biodegradability, they may promote biofouling in the distribution system (Liu et al., 2008; Soh et al., 2008). The same conditions for the lowest NEU production of

the pulsed treatment resulted in the highest NEU production for the continuous treatment. The highest degradation percentage of VHA with continuous ultrasound did not coincide with lowest increment of CHA and NEU fractions which makes it challenging to choose the optimum conditions for DOC removal in continuous ultrasound treatment.

3.6. Spectroscopic properties change expressed by surface plots

Fig. 7 shows the surface plots for the five measured spectroscopic indices. This figure gives more insights into the change in the structure of DOC as the operation conditions changed. Fig. 7 a shows that the humic-like DOC is best removed at low power and short treatment time for continuous treatment and high power and long treatment time for pulsed treatment. The conditions for the highest removal of $SUVA_{254}$ in continuous treatment do not match the commonly reported conditions of high power and long treatment time for the highest removal of this parameter from synthetic humic solution (Stepniak et al., 2009). The anomaly behaviour of $SUVA_{254}$ reduction trend with the continuous treat-ment is most likely related to the interference of the microbial products released with high power and long treatment time. This highlights that the structural alteration of DOC due to ultrasound treatments of natural water samples differs from that of synthetic water samples. The minimum removal of $SUVA_{254}$ was observed at short treatment time and high power for continuous treatment and low power for pulsed treatment. Increasing the power had a
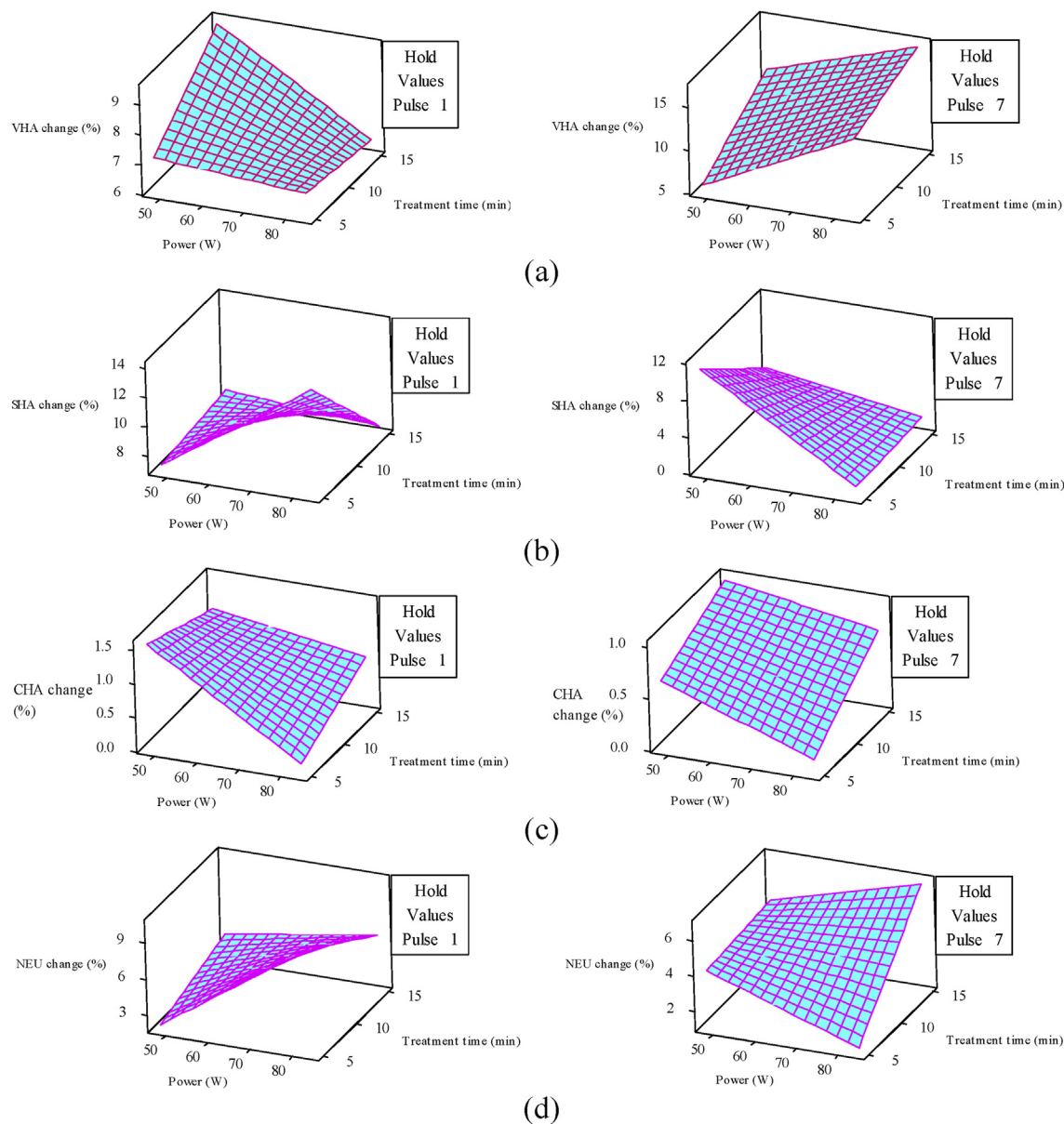
Fig. 6. Surface plots of DOC fractions change (a) VHA, (b) SHA, (c) CHA and (d) NEU under the effect of various ultrasonic power treatment time levels at fixed pulse settings.

positive effect on SUVA$_{254}$ reduction for all the treatment scenarios except for continuous treatment at short treatment time. Similar patterns can be seen in the surface plots of SUVA$_{280}$ and A$_{254}$/A$_{204}$ with a difference that increasing the treatment time had more pronounced effect on SUVA$_{280}$ and A$_{254}$/A$_{204}$ removal for continuous treatment at low power. The similarities between surface plots of SUVA$_{254}$, SUVA$_{280}$ and A$_{254}$/A$_{204}$ are logical observations as the correlation between aromaticity and humification expressed by these UV indices has been repeatedly reported in the literature (Chin et al., 1994; Korshin et al., 1997; Huang et al., 2008). However, Fig. 6 reveals that removing SUVA$_{254}$, SUVA$_{280}$ and A$_{254}$/A$_{204}$ requires operating conditions for the continuous mode that totally differ from those of the pulsed mode.

The shape of the surface plot for E$_2$/E$_3$ reduction is different from the shape of the surface plots of SUVA$_{254}$, SUVA$_{280}$ and A$_{254}$/A$_{204}$. In fact the trends of E$_2$/E$_3$ surface plots are opposite to the ones appear on the surface plots of SUVA$_{254}$, SUVA$_{280}$ and A$_{254}$/A$_{204}$. This remark is consistent with the reported inverse correlation between

SUVA$_{280}$ and E$_2$/E$_3$ by other studies (Peuravuori and Pihlaja, 1997; Uyguner and Bekbolet, 2005b). It is also clear from Fig. 7 d that unlike the surface plots of SUVA$_{254}$, SUVA$_{280}$ and A$_{254}$/A$_{204}$, the plot of E$_2$/E$_3$ does not have a sudden drop or increase that reflects almost a pure liner response of E$_2$/E$_3$ to the change in ultrasonic factors. This could explain the poor predictability of E$_2$/E$_3$ model. To test that, the second order multiplication terms (interactions) were removed from the model and the predictability was retested. Again, the deviation was calculated for the predicted value of the reformulated E$_2$/E$_3$ regression model and the results are presented in Table 10. By comparing Tables 10–9, it can be clearly seen that removing the interaction terms significantly improved the predictability of E$_2$/E$_3$ model and brought the deviation percentages to reasonable limits except for $R = 0.2{:}0.1$ s at high power and long treatment time.

The surface plot of A$_{254}$/A$_{436}$ removal for continuous treatment elucidates that increasing either the power or treatment time while fixing the other increased the removal of A$_{254}$/A$_{436}$, but the trend of
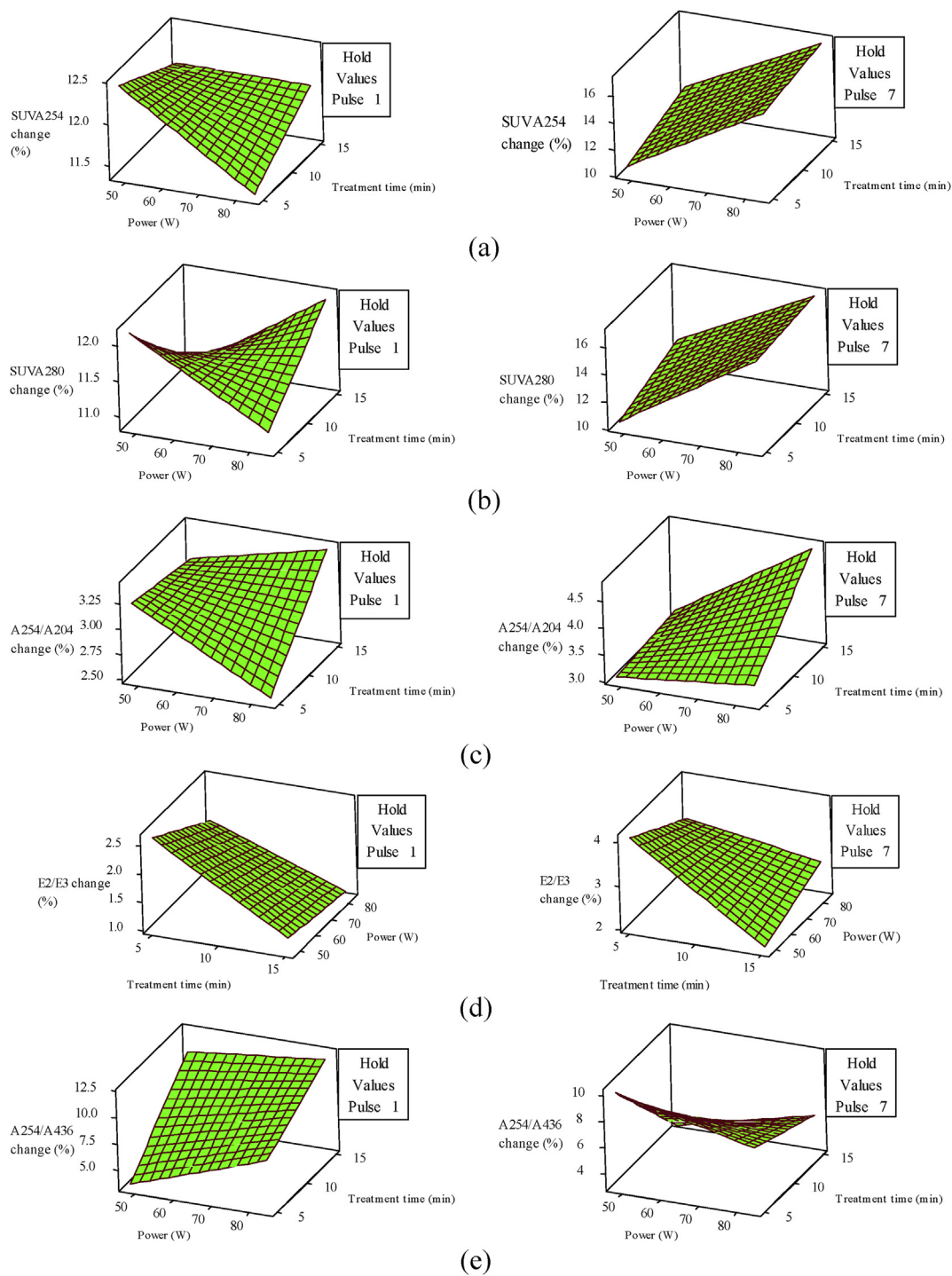
Fig. 7. Surface plots of spectroscopic properties change (a) SUVA$_{254}$, (b) SUVA$_{280}$, (c) A$_{254}$/A$_{204}$, (d) E$_2$/E$_3$ and (e) A$_{254}$/A$_{436}$ under the effect of various ultrasonic power treatment time levels at fixed pulse settings.

the removal with increasing treatment time was sharper than that of increasing the power. The surface plot of A$_{254}$/A$_{436}$ removal with pulsed ultrasound exhibited a saddle-like shape where increasing the treatment time had almost no effect on high power treatments, while such increase negatively impacted the removal of low power treatments. The highest removals of A$_{254}$/A$_{436}$ were achieved with high levels of power and treatment time for continuous mode, and low levels of the same conditions for pulsed treatment. These results help in determining the appropriate operating conditions for

the proportionate ultrasonic removal of coloured and humic DOC based on the desirable criteria of the treatments.

3.7. Correlations between spectroscopic properties and chemical fractionation

The first step in exploring the correlations between DOC fractions and spectroscopic absorbance and ratios was by taking UV–vis scan for treated water samples and eluents of the resins for

Table 10
Predictability deviation of reformulated E_2/E_3 regression model ($Y = 2.351 - 0.131A - 0.598B + 0.661C$).

Experimental settings (coded)			E_2/E_3 deviation (%)
Power	Treatment time	Pulse setting	
−1	−1	1	7.900
−1	1	1	23.884
−1	**−1**	**−0.833**	**9.043**
−1	**1**	**−0.833**	**11.692**
−1	−1	−1	7.174
−1	1	−1	1.051
1	−1	1	7.980
1	1	1	15.588
1	**−1**	**−0.833**	**9.476**
1	**1**	**−0.833**	**55.439**
1	−1	−1	12.972
1	1	−1	6.424

Bold font represents the deviation of the predicted responses from their experimental values at operating conditions differ from the ones applied in developing the regression models.

the range where most of UV—vis indices fall in (i.e. 200—500 nm) as shown in Fig. 8. The UV—vis scans in this figure were deliberately taken for the same water sample collected in different days and treated with different ultrasound treatments to ensure the consistency of the trends observed. It can be seen from Fig. 8 that the eluents of all the resins had an absorbance close to zero at 254 nm except for DAX-8 eluent that had a slight absorbance at this wavelength. The reason that DAX-8 eluent has a slight absorbance at 254 nm is because of the presence of fulvic acids in the eluent (Liu et al., 2008) that can still have an absorbance at this wavelength (Grimvall and de Leer, 2012). This suggests that the hydrophobic fraction (VHA + SHA) have a good correlation with UV absorbance at 254 nm. This correlation was confirmed via plotting the hydrophobic fraction of all water samples treated with ultrasound against their absorbance values at 254 nm as illustrated in Fig. 9. This Figure confirms that the hydrophobic fraction has a strong correlation with A_{254}. The significance of this correlation was tested via regression analysis and it turned out to be highly significant with *P-value* of <0.000. Since A_{254} is strongly correlated with A_{280}, it is expected that A_{280} would also have a strong correlation with the hydrophobic fraction and that is what our results in Fig. 9 confirmed.

The UV region 200—240 nm is known as benzenoid (Bz) region and it has a maximum absorbance at 204 nm (Korshin et al., 1997). The region with an absorbance more than 240 nm is known as electron-transfer (ET) region which has a maximum absorbance at 254 nm. We and other studies (Her et al., 2004; Valencia et al., 2013) have utilized the ratio of these two regions (A_{254}/A_{204}) as

an important index for monitoring the change in the aromatic structure of DOC. Based on our results here, it seems that this ratio is also related to the ratio of hydrophobic/hydrophilic structure as the eluents of DAX-8 and XAD-4 have the highest absorption at the UV region 200—240 nm and absorbance of approximately zero at 254 nm. The correlation between A_{254}/A_{204} and hydrophobic/hydrophilic for the treated water samples was checked and the results are presented in Fig. 9. It appears that A_{254}/A_{204} has a correlation with hydrophobic/hydrophilic ratio that is even stronger than the correlations of the hydrophobic fraction with A_{254} and A_{280}. The other UV ratios such as E_2/E_3 and A_{254}/A_{436} might also have correlations with hydrophobic/hydrophilic ratio, as the numerator of these ratios (i.e. 254 nm) showed a strong correlation with the hydrophobic fraction. The correlations between the hydrophobic/hydrophilic ratio and E_2/E_3 and A_{254}/A_{436} were tested and they were found to be weak and insignificant as illustrated in Fig. 9. In addition to the extensive use of A_{254}, A_{280} and A_{254}/A_{204} as indicators for bulk aromaticity and humification of DOC, our study has confirmed that these UV indices can further be used as quick effective techniques for monitoring the hydrophobic/hydrophilic proportion in DOC.

4. Conclusions

The change of DOC structure in natural water samples treated with ultrasound at different operating conditions was investigated in this work by applying rapid chemical fractionation techniques and UV—vis spectroscopic measurements. Generally, ultrasound treatments decreased the hydrophobic DOC and increased the hydrophilic DOC, with the decrease in the hydrophobic fraction higher than the hydrophilic fraction increase. Pulsed ultrasound treatments, especially those at higher power levels were more effective than the continuous treatments in removing the hydrophobic DOC. The highest increase in the hydrophilic fraction was observed with continuous ultrasound treatment at high power levels. All the spectroscopic indices SUVA$_{254}$, SUVA$_{280}$, A_{254}/A_{204}, E_2/E_3 and A_{254}/A_{436} decreased after ultrasound treatments.

2^3 factorial design was applied to statistically analyse the effect of ultrasonic operating conditions and their interactions on DOC nature. Most of the operating conditions and interactions had significant impacts on chemical fractions distribution of DOC and its spectroscopic properties. Regression models were developed for predicting the response of DOC fractions and spectroscopic properties at various operating conditions. The predictability of the models were reasonably good except for E_2/E_3 and A_{254}/A_{204}. Upon inspection of surface plots of DOC fractions and spectroscopic properties, it was found that the optimum ultrasound treatment that resulted in the lowest increase in the hydrophilic fraction and
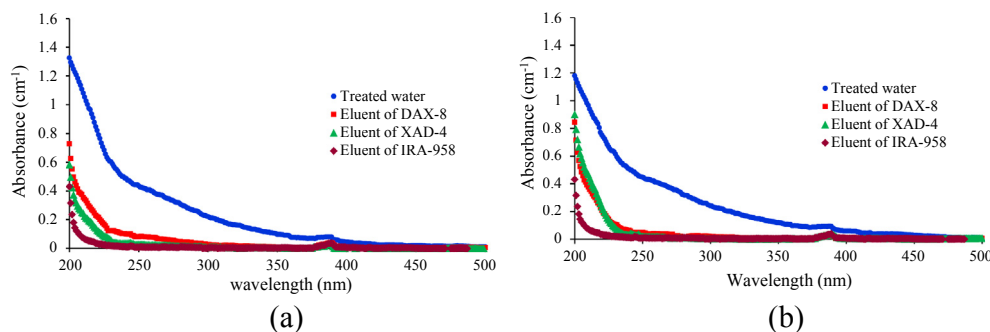

Fig. 8. UV—vis spectrum Narda water and eluents of DAX-8 and XAD-4 after treatment with different ultrasound treatments: (a) power = 84 W, effective treatment time = 15 min and R = 0.1:0.6 and (b) power = 48 W, effective treatment time = 5 min and R = 0.1:0.6.
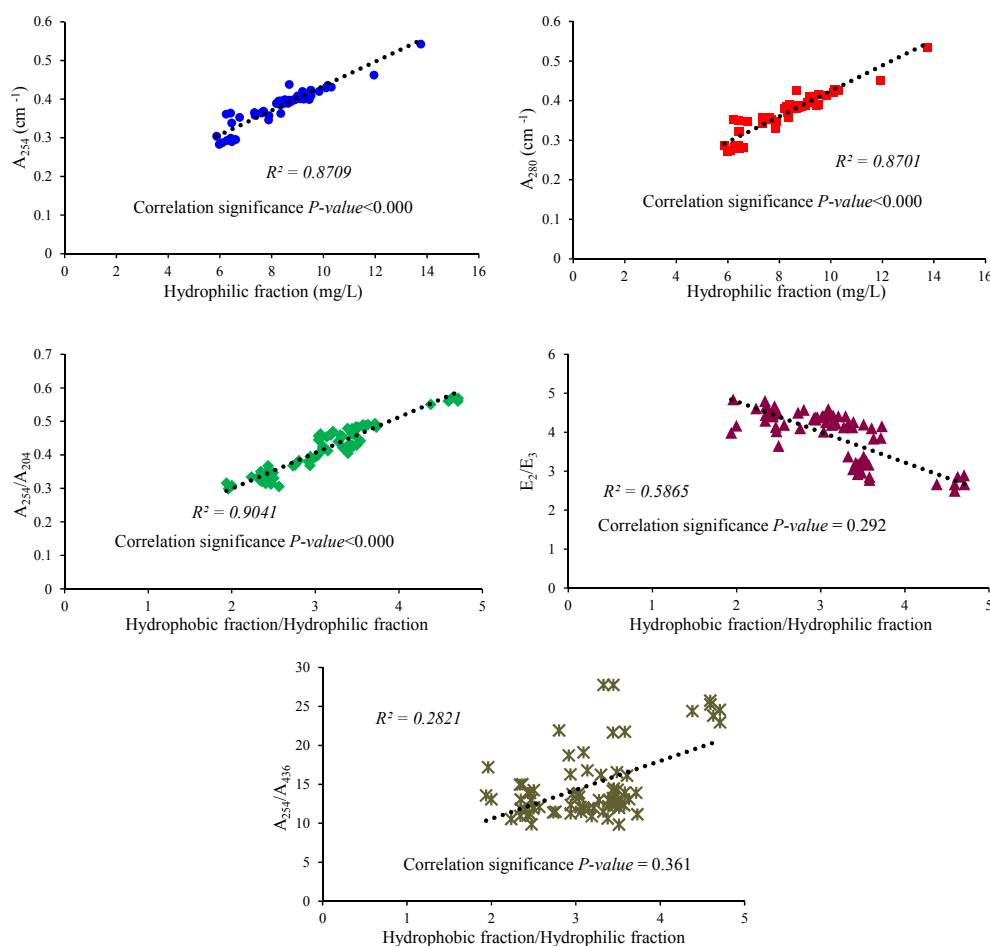
Fig. 9. Correlation of spectroscopic properties vs. DOC fractions of all experiments.

moderate to high degradation of hydrophobic fraction was pulsed treatment at high power and low treatment time. Similar treatment conditions but with longer treatment times resulted in the highest removal of humic-like aromatic DOC. These optimum conditions can be utilized for ultrasound application for natural water treatment purposes.

Correlations between DOC fractions and spectroscopic properties were also explored. The correlation between A_{254}/A_{204} and hydrophobic/hydrophilic ratio was the strongest and most significant among all other correlations. A_{254} and A_{280} also exhibited strong and significant correlations with the hydrophobic fraction. The correlations between E_2/E_3 and A_{254}/A_{204} and hydrophobic/hydrophilic ration were weak and insignificant. The correlations obtained in this study confirm that UV measurements can further be harnessed for monitoring the change in DOC polarity.

Acknowledgement

References

Al-Juboori, R., Yusaf, T., Aravinthan, V., Bowtell, L., 2016. Investigating natural organic carbon removal and structural alteration induced by pulsed ultrasound. Sci. Total Environ. 541, 1019–1030.

Al-Juboori, R.A., Aravinthan, V., Yusaf, T., 2015a. Impact of pulsed ultrasound on bacteria reduction of natural waters. Ultrason. Sonochem. 27, 137–147.

Al-Juboori, R.A., Yusaf, T., 2012a. Biofouling in RO system: mechanisms, monitoring and controlling. Desalination 302, 1–23.

Al-Juboori, R.A., Yusaf, T., 2012b. Identifying the optimum process parameters for ultrasonic cellular disruption of E. coli. Int. J. Chem. React. Eng. 10, 1–32.

Al-Juboori, R.A., Yusaf, T., Aravinthan, V., Pittaway, P.A., Bowtell, L., 2015b. Investigating the feasibility and the optimal location of pulsed ultrasound in surface water treatment schemes. Desalin. Water Treat. 1–19.

Al-Juboori, R.A., Yusaf, T., Bowtell, L., 2015c. Energy conversion efficiency of pulsed ultrasound. Energy Proc. 75, 1560–1568.

Al-Juboori, R.A., Yusaf, T., Bowtell, L., Aravinthan, V., 2015d. Energy characterisation of ultrasonic systems for industrial processes. Ultrasonics 57, 18–30.

Al-Juboori, R.A., Yusaf, T.F., 2012c. Improving the performance of ultrasonic horn reactor for deactivating microorganisms in water. IOP Conf. Ser. Mater. Sci. Eng. 36, 1–13.

Anglada, Á., Urtiaga, A., Ortiz, I., Mantzavinos, D., Diamadopoulos, E., 2011. Boron-doped diamond anodic treatment of landfill leachate: evaluation of operating variables and formation of oxidation by-products. Water Res. 45, 828–838.

Antony, J., 2014. Design of Experiments for Engineers and Scientists. Elsevier.

Audenaert, W.T.M., Van Beneden, L., Van Hulle, S.W.H., 2015. Removal of natural organic matter (NOM) by ion exchange from surface water for drinking water production: a pilot-scale study. Desalin. Water Treat. 1–12.

Bolto, B., Abbt-Braun, G., Dixon, D., Eldridge, R., Frimmel, F., Hesse, S., King, S., Toifl, M., 1999. Experimental evaluation of cationic polyelectrolytes for removing natural organic matter from water. Water Sci. Technol. 40, 71–79.

Boubakri, A., Helali, N., Tlili, M., Amor, M.B., 2014. Fluoride removal from diluted solutions by Donnan dialysis using full factorial design. Korean J. Chem. Eng. 31, 461–466.

Buchanan, W., Roddick, F., Porter, N., Drikas, M., 2005. Fractionation of UV and VUV pretreated natural organic matter from drinking water. Environ. Sci. Technol. 39, 4647–4654.

Chemat, F., Teunissen, P., Chemat, S., Bartels, P., 2001. Sono-oxidation treatment of

humic substances in drinking water. Ultrason. Sonochem. 8, 247–250.

Chen, D., He, Z., Weavers, L.K., Chin, Y.-P., Walker, H.W., Hatcher, P.G., 2004. Sono-chemical reactions of dissolved organic matter. Res. Chem. Intermed. 30, 735–753.

Chin, Y.-P., Aiken, G., O'Loughlin, E., 1994. Molecular weight, polydispersity, and spectroscopic properties of aquatic humic substances. Environ. Sci. Technol. 28, 1853–1858.

Chow, C., Fabris, R., Drikas, M., 2004. A rapid fractionation technique to characterise natural organic matter for the optimisation of water treatment processes. Aqua 53, 85–92.

Clesceri, L.S., Rice, E.W., Greenberg, A.E., Eaton, A.D. (Eds.), 2005. Standard Methods for Examination of Water and Wastewater, centennial edition. American Public Health Association, Washington, D.C.

Croue, J.P., Martin, B., Deguin, A., Legube, B., 1993. Isolation and characterization of dissolved hydrophobic and hydrophilic organic substances of a reservoir water. In: Natural Organic Matter in Drinking Water Workshop, Chamoix, France, pp. 73–81.

Food Safety and Regulatory Activities Victorian, 2009. Guidelines for Private Drinking Water Supplies at Commercial and Community Facilities. Government Department of Health, Melbourne, Victoria, Melbourne.

Ghernaout, D., 2014. The hydrophilic/hydrophobic ratio vs. dissolved organics removal by coagulation – a review. J. King Saud. Univ. Sci. 26, 169–180.

Grimvall, A., de Leer, E.W.B., 2012. Naturally-produced Organohalogens. Springer Netherlands, Dordrecht Netherlands.

Gutierrez, M., Henglein, A., 1990. Chemical action of pulsed ultrasound: observation of an unprecedented intensity effect. J. Phys. Chem. 94, 3625–3628.

Hakata, Y., Roddick, F., Fan, L., 2011. Impact of ultrasonic pre-treatment on the microfiltration of a biologically treated municipal effluent. Desalination 283, 75–79.

Henglein, A., Gutierrez, M., 1990. Chemical effects of continuous and pulsed ultra-sound: a comparative study of polymer degradation and iodide oxidation. J. Phys. Chem. 94, 5169–5172.

Her, N., Amy, G., Park, H.-R., Song, M., 2004. Characterizing algogenic organic matter (AOM) and evaluating associated NF membrane fouling. Water Res. 38, 1427–1438.

Huang, X., Leal, M., Li, Q., 2008. Degradation of natural organic matter by TiO_2 photocatalytic oxidation and its effect on fouling of low-pressure membranes. Water Res. 42, 1142–1150.

Jambrak, A.R., Mason, T.J., Lelas, V., Paniwnyk, L., Herceg, Z., 2014. Effect of ultra-sound treatment on particle size and molecular weight of whey proteins. J. Food Eng 121, 15–23.

Jiang, J., Zhao, Q., Wei, L., Wang, K., Lee, D.-J., 2011. Degradation and characteristic changes of organic matter in sewage sludge using microbial fuel cell with ul-trasound pretreatment. Bioresour. Technol. 102, 272–277.

Kim, E., Hwang, B.-R., Baek, K., 2015. Effects of natural organic matter on the coprecipitation of arsenic with iron. Environ. Geochem. Health 1–11.

Korshin, G.V., Li, C.-W., Benjamin, M.M., 1997. Monitoring the properties of natural organic matter through UV spectroscopy: a consistent theory. Water Res. 31, 1787–1795.

Lavonen, E., 2015. Tracking Changes in Dissolved Natural Organic Matter Compo-sition. Department of Aquatic Sciences and Assessment. Swedish University of Agricultural Sciences, Uppsala.

Liu, S., Lim, M., Fabris, R., Chow, C., Chiang, K., Drikas, M., Amal, R., 2008. Removal of humic acid using TiO_2 photocatalytic process – fractionation and molecular weight characterisation studies. Chemosphere 72, 263–271.

Minis, I., 2010. Supply Chain Optimization, Design, and Management: Advances and Intelligent Methods: Advances and Intelligent Methods. Business Science Reference.

More, T.T., Ghangrekar, M.M., 2010. Improving performance of microbial fuel cell with ultrasonication pre-treatment of mixed anaerobic inoculum sludge. Bio-resour. Technol. 101, 562–567.

Naddeo, V., Belgiorno, V., Napoli, R., 2007. Behaviour of natural organic mater during ultrasonic irradiation. Desalination 210, 175–182.

Pan, Y., Zhang, X., 2013. Four groups of new aromatic halogenated disinfection byproducts: effect of bromide concentration on their formation and speciation in chlorinated drinking water. Environ. Sci. Technol. 47, 1265–1273.

Patist, A., Bates, D., 2008. Ultrasonic innovations in the food industry: from the laboratory to commercial production. Innov. Food Sci. Emerg. Technol. 9, 147–154.

Peuravuori, J., Pihlaja, K., 1997. Molecular size distribution and spectroscopic properties of aquatic humic substances. Anal. Chim. Acta 337, 133–149.

Phull, S.S., Newman, A.P., Lorimer, J.P., Pollet, B., Mason, T.J., 1997. The development and evaluation of ultrasound in the biocidal treatment of water. Ultrason. Sonochem. 4, 157–164.

Richardson, S., Postigo, C., 2012. Drinking water disinfection by-products. In: Barceló, D. (Ed.), Emerging Organic Contaminants and Human Health. Springer, Berlin Heidelberg, pp. 93–137.

Richardson, S.D., Plewa, M.J., Wagner, E.D., Schoeny, R., DeMarini, D.M., 2007. Occurrence, genotoxicity, and carcinogenicity of regulated and emerging disinfection by-products in drinking water: a review and roadmap for research. Mutat. Res./Rev. Mutat. Res. 636, 178–242.

Saadat, S., Karimi-Jashni, A., 2011. Optimization of Pb(II) adsorption onto modified walnut shells using factorial design and simplex methodologies. Chem. Eng. J. 173, 743–749.

Santos, L., Santos, E.B.H., Dias, J.M., Cunha, A., Almeida, A., 2014. Photochemical and microbial alterations of DOM spectroscopic properties in the estuarine system Ria de Aveiro. Photochem. Photobiol. Sci. 13, 1146–1159.

Silverstein, R.M., 1974. Spectrometric Identification of Organic Compounds, third edition. Wiley, New York.

Simarani, K., Saat, M.N., Mohamad Annuar, M.S., 2015. Efficient removal of azo dye by grated copra biomass. Desalin. Water Treat. 1–8.

Soh, Y.C., Roddick, F., van Leeuwen, J., 2008. The impact of alum coagulation on the character, biodegradability and disinfection by-product formation potential of reservoir natural organic matter (NOM) fractions. Water Sci. Technol. 58, 1173–1179.

Stepniak, L., Kepa, U., Stanczyk-Mazanek, E., 2009. Influence of a high-intensity ultrasonic field on the removal of natural organic compounds from water. Desalin. Water Treat. 5, 29–33.

Tezcan Un, U., Ates, F., Erginel, N., Ozcan, O., Oduncu, E., 2015. Adsorption of Disperse Orange 30 dye onto activated carbon derived from Holm Oak (Quercus Ilex) acorns: a 3k factorial design and analysis. J. Environ. Manage 155, 89–96.

Thomas, O., Burgess, C., 2007. UV-visible Spectrophotometry of Water and Waste-water. Elsevier Science.

Uyguner, C.S., Bekbolet, M., 2005a. Evaluation of humic acid photocatalytic degra-dation by UV–vis and fluorescence spectroscopy. Catal. Today 101, 267–274.

Uyguner, C.S., Bekbolet, M., 2005b. Implementation of spectroscopic parameters for practical monitoring of natural organic matter. Desalination 176, 47–55.

Valencia, S., Marín, J.M., Restrepo, G., Frimmel, F.H., 2013. Application of excita-tion–emission fluorescence matrices and UV/Vis absorption to monitoring the photocatalytic degradation of commercial humic acid. Sci. Total Environ. 442, 207–214.

Van Nieuwenhuijzen, A., Van der Graaf, J., 2011. Handbook on Particle Separation Processes. IWA Publishing, London.

Walker, J.M., Rapley, R. (Eds.), 2000. Molecular Biology and Biotechnology. Royal Society of Chemistry, Cambridge.

Wang, B.-B., Chang, Q., Peng, D.-C., Hou, Y.-P., Li, H.-J., Pei, L.-Y., 2014. A new clas-sification paradigm of extracellular polymeric substances (EPS) in activated sludge: separation and characterization of exopolymers between floc level and microcolony level. Water Res. 64, 53–60.

Weishaar, J.L., Aiken, G.R., Bergamaschi, B.A., Fram, M.S., Fujii, R., Mopper, K., 2003. Evaluation of specific ultraviolet absorbance as an indicator of the chemical composition and reactivity of dissolved organic carbon. Environ. Sci. Technol. 37, 4702–4708.

Xing, L., Murshed, M.F., Lo, T., Fabris, R., Chow, C.W.K., van Leeuwen, J., Drikas, M., Wang, D., 2012. Characterization of organic matter in alum treated drinking water using high performance liquid chromatography and resin fractionation. Chem. Eng. J. 192, 186–191.

Yang, L., Rathman, J.F., Weavers, L.K., 2005. Degradation of alkylbenzene sulfonate surfactants by pulsed ultrasound. J. Phys. Chem. B 109, 16203–16209.

Yao, J.-J., Gao, N.-Y., Deng, Y., Ma, Y., Li, H.-J., Xu, B., Li, L., 2010. Sonolytic degradation of parathion and the formation of byproducts. Ultrason. Sonochem. 17, 802–809.

Zhang, H., Claver, I.P., Zhu, K.-X., Zhou, H., 2011. The effect of ultrasound on the functional properties of wheat gluten. Molecules 16, 4231.

Zhang, X., Minear, R.A., Barrett, S.E., 2005. Characterization of high molecular weight disinfection byproducts from chlorination of humic substances with/without coagulation pretreatment using UF–SEC–ESI-MS/MS. Environ. Sci. Technol. 39, 963–972.
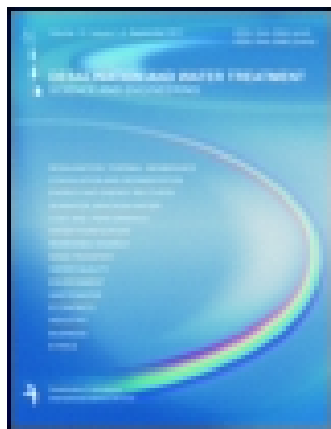
Paper VIII

Al-Juboori, R. A., Yusaf, T. & Pittaway, P. A., Exploring the correlations between common UV measurements and chemical fractionation for natural waters, *Desalination and Water Treatment*, (2015), 1-12.

Desalination and Water Treatment

Exploring the correlations between common UV measurements and chemical fractionation for natural waters

Raed A. Al-Juboori[a], Talal Yusaf[b] & Pamela A. Pittaway[c]

[a] Faculty of Health, Engineering and Sciences, School of Civil Engineering and Surveying, University of Southern Queensland, Toowoomba 4350, QLD, Australia, Tel. +61 413424126, +61 7 4631 1366

[b] Faculty of Health, Engineering and Sciences, School of Mechanical and Electrical Engineering, University of Southern Queensland, Toowoomba 4350, QLD, Australia, Tel. +61 7 4631 2691

[c] Cooperative Research Centre for Irrigation Futures, National Centre for Engineering in Agriculture, University of Southern Queensland, Toowoomba 4350, QLD, Australia, Tel. +61 7 4631 2144

Published online: 18 Aug 2015.

PLEASE SCROLL DOWN FOR ARTICLE

Exploring the correlations between common UV measurements and chemical fractionation for natural waters

Raed A. Al-Juboori[a,*], Talal Yusaf[b], Pamela A. Pittaway[c]

[a]Faculty of Health, Engineering and Sciences, School of Civil Engineering and Surveying, University of Southern Queensland, Toowoomba 4350, QLD, Australia, Tel. +61 413424126; +61 7 4631 1366; emails: RaedAhmed.mahmood@gmail.com, RaedAhmed.Mahmood@usq.edu.au (R.A. Al-Juboori)
[b]Faculty of Health, Engineering and Sciences, School of Mechanical and Electrical Engineering, University of Southern Queensland, Toowoomba 4350, QLD, Australia, Tel. +61 7 4631 2691; email: talal.yusaf@usq.edu.au
[c]Cooperative Research Centre for Irrigation Futures, National Centre for Engineering in Agriculture, University of Southern Queensland, Toowoomba 4350, QLD, Australia, Tel. +61 7 4631 2144; email: pam.pittaway@usq.edu.au

ABSTRACT

Chemical fractionation is a powerful tool for unravelling the reasons behind water treatment problems such as the formation of disinfection by-products (DBPs). This technique can however be costly and time-consuming. Hence, exploring quick affordable surrogate measurements to this technique is of great importance for water treatment operators. In this study, the correlations between aquatic carbon fractions and single wavelength and UV ratios of A_{254}, A_{280}, A_{254}/A_{204}, A_{250}/A_{365} and A_{254}/A_{436} were examined for seven water bodies located in South-east Queensland, Australia. It was observed that A_{254}/A_{204} has a strong and significant correlation with hydrophobic/hydrophilic ratio ($R^2 = 0.984$). A_{250}/A_{365} exhibited a weak but significant correlation with the same fraction ratio ($R^2 = 0.687$) suggesting that the chemical fractions cannot be assumed of a certain molecular size. A_{254}/A_{436} had a weak and insignificant correlation with carbon fractions ($R^2 = 0.0506$). The hydrophobic fraction of the seven water bodies showed a strong and significant correlation with A_{254} ($R^2 = 0.968$) and A_{280} ($R = 0.958$). The diverse carbon source of the tested water bodies confirms the reliability of the observed correlations. The results of this study highlight the potential use of UV absorbance as a real-time technique for monitoring the structural change of aquatic carbon.

Keywords: DOC; Chemical fractionation; Hydrophobicity; Hydrophilicity; Single wavelength UV and UV ratio

1. Introduction

Natural organic matter (NOM) is a ubiquitous heterogeneous mixture present in terrestrial and aquatic systems. NOM is derived from either vegetative debris and terrestrial sources (allochthonous) or microbial activities (autochthonous) [1]. The source of NOM has a pivotal role in natural and man-made systems. In aquatic ecosystems, NOM represents the source of carbon for living organisms and it can bind to inorganic pollutants controlling their transport and fate [2]. Also, the presence of NOM in water treatment

systems causes detrimental problems such as production of unpleasant odours and tastes [3], fouling [4] and the formation of carcinogenic DBPs [5]. Hence, understanding the structure of NOM has become imperative for the environmental scientist and the operators of water treatment industries, particularly drinking water production [6,7].

NOM can be broadly classified into dissolved organic carbon (DOC) and particulate organic carbon (POC) [8]. These two categories are operationally defined. DOC is the carbon fraction that passes through a filter with porosity of 0.45 μm, while POC is the fraction retained by such a filter. POC represents a small fraction of the TOC in water (below 10%) [8]. Removal of POC from water is easier than DOC, which makes the latter the main concern from water treatment perspective.

DOC can further be classified into subgroups depending on the molecular size and physiochemical properties. DOC is commonly segregated into size-based groups using size exclusion chromatography and serial filtration with selected pore size filters [9,10]. The size of molecules can only govern their filterability through membrane/multimedia filters via sieving mechanisms [11]. In addition, the aforementioned segregation techniques have the disadvantages of introducing artefacts to the treated samples [12,13]. Hence, obtaining knowledge of DOC molecular structure can be more beneficial, especially when designing an efficient treatment scheme. The complex structure of DOC can be unravelled based on elemental composition, functional groups or compounds classification. Elemental and functional group analyses such as the use of nuclear magnetic resonance spectroscopy and gas and liquid chromatography are expensive and require extensive sample manipulation [10,14]. Such analyses are hard to adapt for industrial routine measurements. Less complicated DOC structural analysis that can easily be integrated into industrial measurement protocols is the use of resin fractionation [15].

The resin fractionation technique classifies DOC into three main groups hydrophobic, hydrophilic and transphilic based on their affinity to a series of ionic and non-ionic resins. This technique dates back to the 1960s when the product of Rohm and Haas Company (XAD-1) was tested for separating organic materials from sea water [16]. Since then, resin fractionation has been undergoing various developments and amendments [17–20]. Recently, Chow et al. [15] proposed the use of a rapid fractionating technique that was based on previous fractionation schemes [19,20]. In this rapid fractionation method, DOC is fractionated into four fractions: VHA (adsorbed by DAX-8); SHA (adsorbed by XAD-4); CHA (adsorbed by IRA-958) and NEU which was not adsorbed by any of the used resins. The chemical classes of these fractions are presented in Table 1.

Fractionation techniques have been applied to gain insight into the most commonly encountered problems in drinking water treatment such as fouling and DBPs formation. Raspati et al. [21] reported that the VHA fraction was the major foulant in micro- and ultra-membrane filtration, particularly with hydrophobic membranes, whereas NEU seemed to be the dominant foulant for hydrophilic membranes. VHA was also found to be the main contributor to DBPs formation which is believed to be due to the fact that this fraction is rich in reactive sites (activated aromatic rings) [2–4]. Chemical fractionation has also been applied for identifying DOC fractions that are amenable to coagulation. It was observed that the removal of the hydrophobic fraction (VHA + SHA) increased by increasing the coagulant (alum) dosage up to the optimum level, while the removal of CHA fraction peaked at low and high dosages [15]. The same study also showed that NEU was the least amenable to alum coagulation. It was suggested that the removal of the hydrophobic fraction in coagulation takes place through two distinct mechanisms: charge neutralization under acidic conditions and adsorption (sweep flocculation) under alkaline conditions [7].

Despite the useful implementation of the fractionation technique for understanding water treatment challenges, this technique has disadvantages of altering DOC structure (esters hydrolysis [13]) and having a long turnaround time [15]. So, finding a method to

Table 1
Proposed structure of natural organic matter (NOM) fractions [4,22]

Fractions		Class of organic compounds
Hydrophobic fraction	VHA SHA	Humic acids, fulvic acids, C5–C9 aliphatic carboxylic acids, 1- and 2-ring phenols, proteinaceous compounds, 1- and 2-ring aromatic except pyridine and amines
Hydrophilic fraction	CHA NEU	>C5 aliphatic carboxylic acids, short-chain aliphatic amines, polysaccharides, amino acids, carbohydrates aldehydes, ketones, alcohols, proteins, <C9 aliphatic amines and <C5 aliphatic amides

allow quick surrogate measurements for the fractionation technique would clearly be beneficial to water treatment operators. This study was designed to investigate the possibility of applying UV absorbance measurements as a potential alternative to the fractionation technique. UV absorbance measurements that were examined in this study included common single wavelength analysis of A_{254} and A_{280} and UV ratios of A_{254}/A_{204}, A_{250}/A_{365} and A_{254}/A_{436}. The correlations between UV ratio components and their counterparts of DOC fractions were also investigated to further understand the correlations between the ratios. These UV measurements were chosen in this study due to their common use in characterizing aquatic organic carbon in terms of humification, aromaticity, functional groups, molecular size and colour [5]. The relationships between DOC fractions and UV measurements for seven Australian water bodies were studied and correlations were obtained. The DOC of the selected water bodies varies between being allochthonous, autochthonous or a mixture of both. Such variation is helpful for measuring the consistency of the obtained correlations.

2. Materials and methods

2.1. Water samples

It is known that the structural characteristics of aquatic DOC depend strongly on source materials, geology and topography of catchment [10]. Hence, in this study, water samples were collected from seven
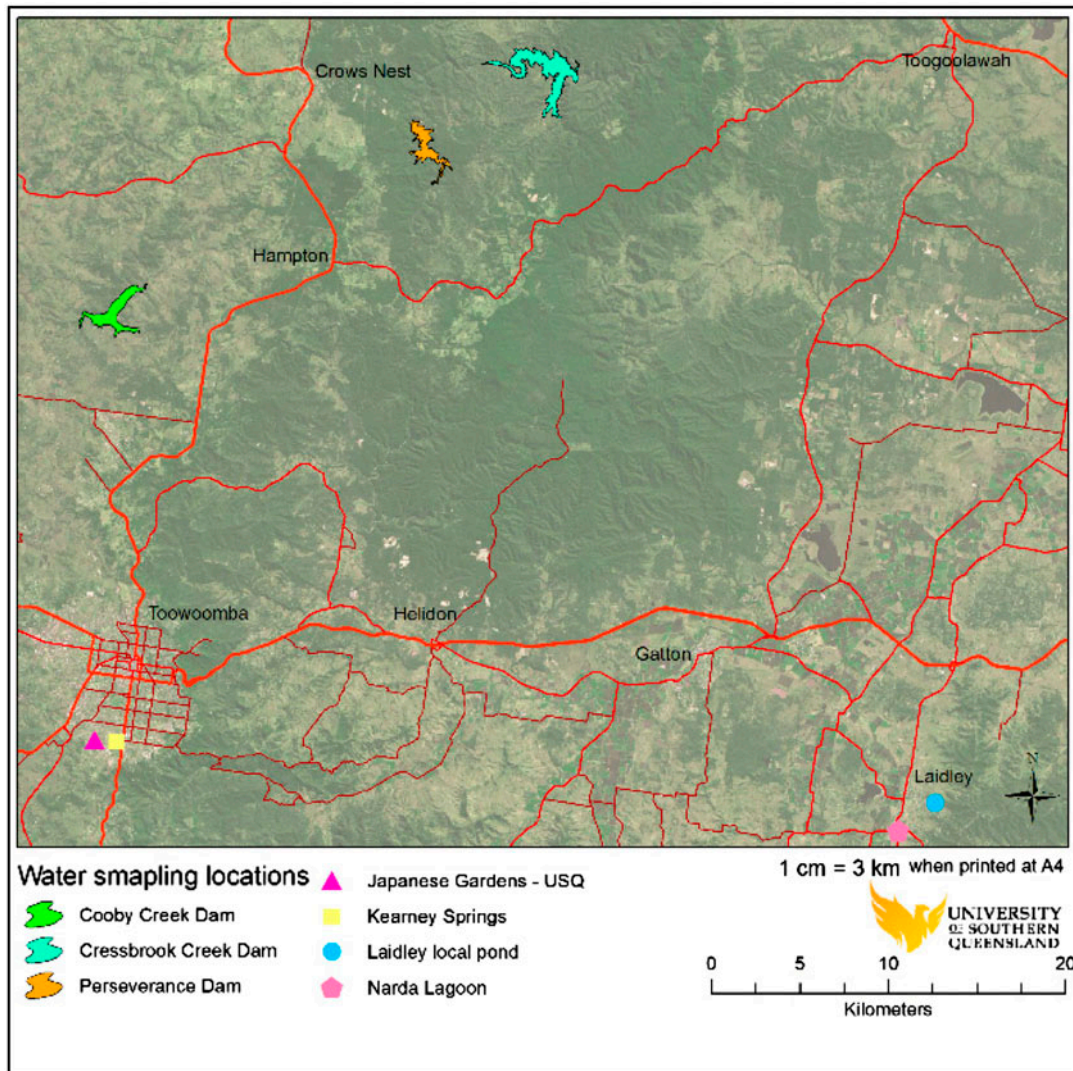

Fig. 1. Sampling sites.

Table 2
DOC and interfering ions concentrations of water samples

Water body	pH	DOC (mg/L)	Iron (mg/L)	Nitrate (mg/L)	Chloride (mg/L)
Narda lagoon	6.90	9.81	0.37	n.a	39
Cressbrook lake	7.90	6.05	0.13	0.39	40.4
Perseverance lake	7.88	2.93	0.09	n.a	31
Cooby dam	9.10	8.15	0.10	n.a	131
Kearnys spring	9.43	9.14	1.63	0.37	107
Japanese garden	7.57	3.30	0.40	n.a	88.4
Laidley local pond	6.45	32	4.73	0.38	32

Note: n.a indicates that the concentration of the ion is below the detection limit of measurement method.

locations at South-east Queensland (SEQ) to investigate the effect of such variety in DOC sources on the correlation between the spectroscopic properties and chemical structure of DOC. The geographical location of the water bodies is illustrated in Fig. 1. DOC concentration of water bodies and their content of UV interfering ions are shown in Table 2.

Lake Cressbrook, Lake Perserverance and Lake Cooby are major water storages for drinking water production in Toowoomba, Australia. The carbon sources in these storages are mostly generated from eucalypt woodland and soil. Kearney Springs and the Japanese Garden are recreational water ponds in which the main sources of carbon are grassland and bird manure. All of the aforementioned water bodies are lightly coloured. Narda lagoon and Laidley local pond are dark brown water. The carbon in Narda lagoon is originated from acacia and eucalyptus trees, grass and sawdust produced from sawmill located in its proximity [23]. The carbon sources of Laidley pond are originated from spotted gum bark, leaf litter and animal manure.

2.2. Analytical methods

2.2.1. DOC measurements

The DOC of water samples was measured by high-temperature combustion method using total carbon analyser (TOC-VCSH, SHIMADZU, Australia). The DOC of each sample was measured in duplicate. At least three injections of each measured sample were made, which resulted in coefficient of variance lower than 0.02. Water samples were filtered through 0.45-μm glass fibre filters using syringe filter holder prior to the DOC measurements.

2.2.2. UV–vis spectroscopy analysis

JENWAY UV–vis spectrophotometer model 6,705 equipped with a single cell holder was used for measuring the absorbance of water samples. Quartz cuvette with path length of 1 cm was used for measuring UV–vis measurements of filtered water samples (0.45 μm). The samples' filtrate was scanned in wavelength range of 200–500 nm.

The pH of water samples was adjusted to 6–7 using 0.1 N HCl or NaOH. The concentrations of interfering species (e.g. nitrate and iron) were measured using ion chromatography system ICS-2000 and atomic absorption spectrophotometer AA-7000 (SHIMADZU, Australia).

The interfering effects of nitrate and chloride in the water samples were insignificant due to their low concentration (Table 2) [5]. It is worth mentioning that the concentrations of the other interfering ions such as bromide sulphate and phosphate were very small under the detection limit of ICS-2000, and hence their interfering effect can be ignored. The concentration of iron in the water samples was below the effective interference limit for most of the water samples <0.5 mg/L [24] except for Laidley local pond and Kearnys Spring samples which were on average of 4.73 and 1.63 mg/L as shown in Table 2. The possible interference of iron was dealt with by subtracting spectrum of iron(III) solution from that of the water sample containing high levels of iron [24]. Iron in the form of ferrous ion has a very little effect on UV absorbance [25], thus its interference is neglected in this study. Iron(III) solution was prepared from AR grade ferric chloride anhydrous (Sigma-Aldrich, Australia).

2.3. Fractionation process

The fractionation procedure performed in this study was based on the rapid fractionation technique proposed by Chow et al. [15]. Fig. 2 shows graphical representation of the fractionation process. Deionized water produced by Millipore system was used to carry out washing of chromatography columns and adsorbent resins. Three polymer-based resins, namely
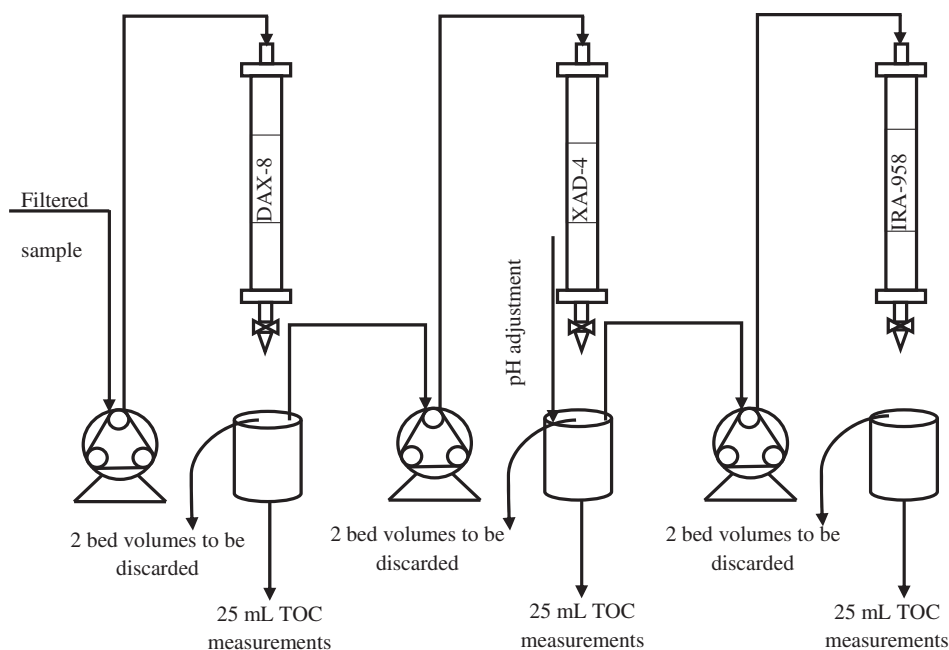
Fig. 2. Illustration of fractionation process.

Supelite™ DAX-8, Amberlite® XAD-4 and Amberlite® IRA-958 were used for fractionating the DOC of water samples. Three chromatography columns with 20 cm length and 1 cm inner diameter were used to accommodate the resins. The columns were set with a series of three peristaltic pumps (Cole-Parmer, Australia).

Virgin resins were wetted and cleaned in 500-ml glass beakers by successive washing with HPLC grade methanol and deionised water for 1 h. Each washing cycle involved gentle stirring for a minute followed by settling for 15 min for methanol and 8 min for deionized water. After the last cycle of washing, the resin slurry was decanted into a pre-cleaned column by 0.1 N NaOH and deionised water. The performance of the cleaning process was tested by running deionized water through the columns of the virgin resins and an aliquot of the eluent of each column was collected for DOC and UV measurements.

In a typical fractionation run, water sample of 250 mL is filtered through 0.45-μm cellulose nitrate membrane and acidified to pH 2 using concentrated HCl acid. The filtered acidified sample is passed through DAX-8 column at a rate of 1.6 mL/min (0.2 bed volume/min as recommended in [15]). The first two bed volumes of 16 mL were discarded from DAX-8 eluent. A sample of 25 mL of the eluent was collected for DOC and UV measurements, and the remaining DAX-8 eluent was pumped through XAD-4

column at the same flow rate as DAX-8 column. Two bed volumes were discarded from XAD-4 eluent and 25 mL of the sample was collected for DOC and UV analyses. The remaining of XAD-4 eluent was then adjusted to pH 8 using 1 M NaOH and pumped through IRA-958 column. Two bed volume of the IRA-958 eluent was discarded and the remaining was used for UV and DOC analyses. The chemicals used such as sodium hydroxide and hydrochloric acid for pH adjustment were all AR grade chemicals supplied by Chem-Supply, Australia.

The fractions of DOC were calculated using the calculations below:

$$VHA = DOC_{raw} - DOC_{DAX-8\ effluent}$$
$$SHA = DOC_{DAX-8\ effluent} - DOC_{XAD-4\ effluent}$$
$$CHA = DOC_{XAD-4\ effluent} - DOC_{IRA-958\ effluent}$$
$$NEU = DOC_{IRA-958\ effluent}$$

3. Results and discussions

3.1. DOC fractions of water bodies

The percentage of each DOC fraction presents in the tested water bodies is shown in Fig. 3. It can be seen from this figure that Laidley pond and Narda lagoon are the most hydrophobic water bodies followed by Cooby dam. Kearnys spring and Cressbrook dam have a close percentage of VHA fraction,
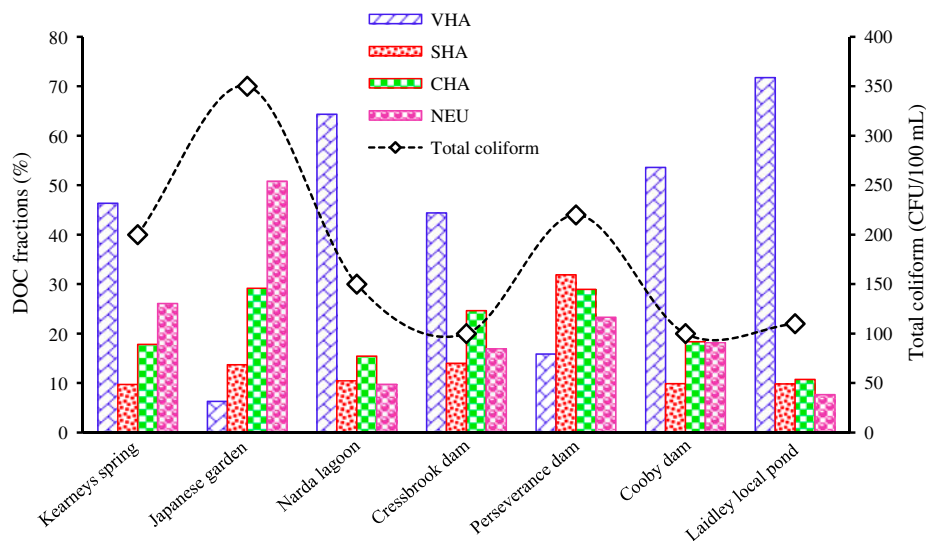
Fig. 3. DOC fractions and total coliform for the seven water bodies.

approximately 46 and 44%, respectively. Perseverance dam and Japanese garden have the lowest VHA fractions of all the water bodies, in fact their VHA fractions are the least among their other DOC fractions. Perseverance dam has the highest SHA fraction of approximately 32% as opposed to the other six water bodies that have the percentage of this fraction in the range of 9–14%.

Laidley pond has the lowest CHA fraction, while the rest of the water bodies are divided into two groups according to their CHA content. The group that contains Japanese garden, Perseverance and Cressbrook dams have a comparable percentage of CHA in the range of 20–30%. The second group that consists of Kearneys spring, Cooby dam and Narda lagoon possesses CHA range of 15–18%. Japanese garden has the highest NEU fraction among all the tested waters. The rest of the water bodies can be divided into three groups according to the percentage of NEU fractions; Keraney springs and Perseverance dam (23–26%), Cooby and Cressbrook dams (16–18%) and Narda lagoon and Laidley pond (7–10%).

From Table 1 and Fig. 3, one can deduce the chemical classes of the organic carbon in the tested watersheds. The high percentage of the hydrophobic fraction in Laidley pond and Narda lagoon indicates abundance of humic acid in these water bodies [4]. The abundance of humic acid implies that the carbon of the water is mostly allochthonous originated mainly from terrestrial runoff and vegetative debris [1,26], and this is consistent with the description of Narda lagoon in [23]. The highest percentage of SHA in Perseverance dam implies that this water source has higher fulvic acid content than the other water sources [4].

The water bodies that have high hydrophilic fraction such as Japanese garden and Perseverance dam are rich in polysaccharides, proteins, carbohydrates and alcohols (Table 1). These chemical classes are associated with microbial activities and the presence of bird's manure [27,28], so the carbon in these waters is predominantly autochthonous. These remarks are confirmed by the total coliform data of the tested water depicted in Fig. 3 as diamond markers and dashed curve. The total coliform data of Cooby, Perseverance and Cressbrook dams were provided by the laboratory services of Mt Kynoch water treatment plant in Toowoomba,Australia, while the total coliform of the rest water bodies was measured in the lab applying membrane filtration standard method (method 9222 B in [29]) using m-ColiBlue24 Broth [30,31].

3.2. Relationships between UV absorbance and DOC fractions

The UV–vis spectra of the seven water bodies and their fractions are shown in Fig. 4. The eluent of virgin resins had a UV reading of approximately zero for the whole tested wavelength range (Fig. 4(h)), which highlights the efficiency of the cleaning procedure and eliminates the possibility of resins contribution to UV absorbance of water samples.

It can be seen from Fig. 4 that the UV spectrum of DAX-8 and XAD-4 eluents for all the tested bodies drops close to zero at a wavelength ca. 230–240 nm.
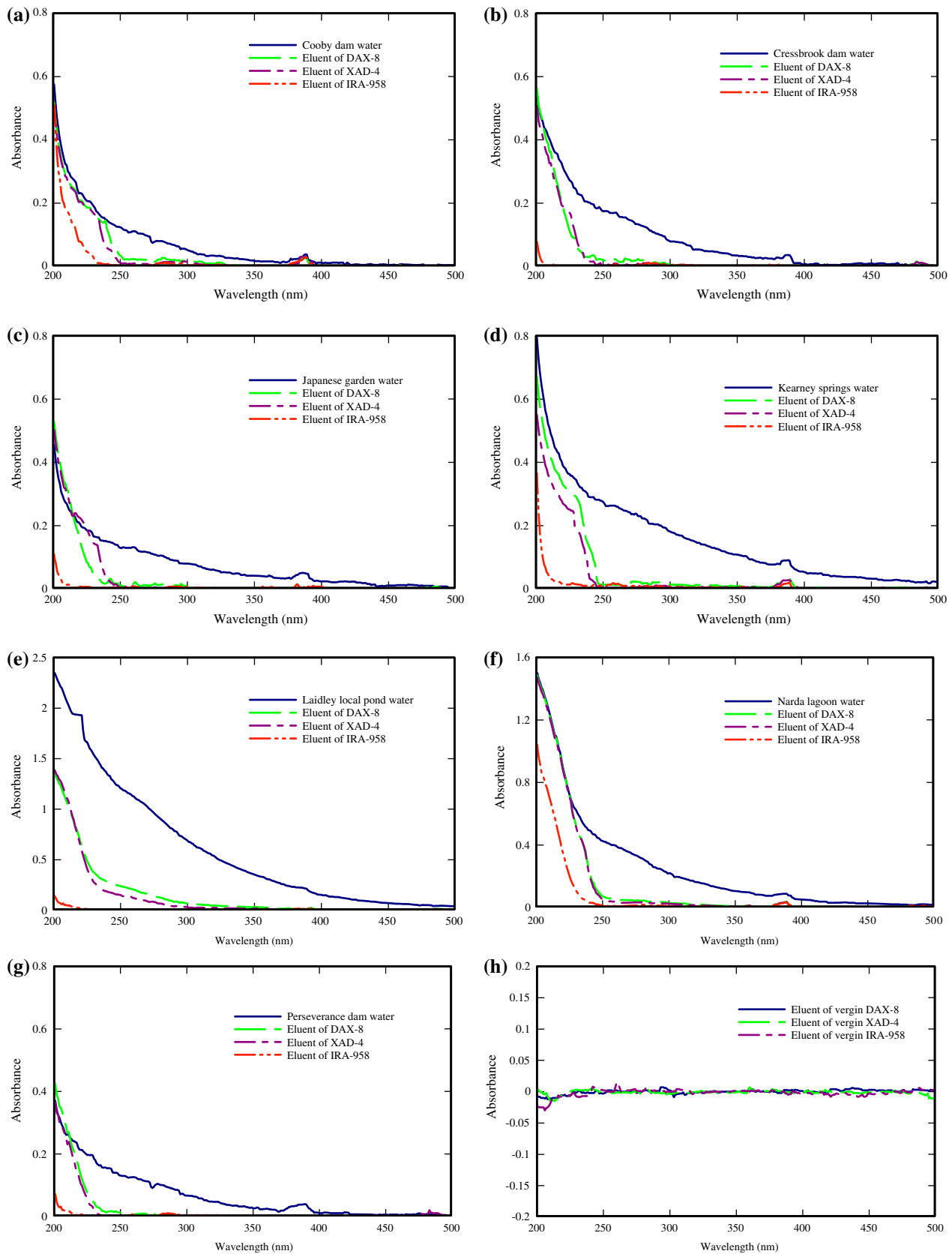
Fig. 4. UV–vis spectrum of (a) Cooby dam, (b) Cressbrook dam, (c) Japanese garden water, (d) Kearneys spring, (e) Laidley local pond, (f) Narda lagoon, (g) Perseverance dam and (h) eluent of virgin resins.

Whilst UV absorbance of IRA-958 eluent is close to zero over most of the measured UV range for all the water bodies except for Cooby dam and Narda lagoon. UV absorbance of IRA-958 eluent for Cooby dam and Narda lagoon dropped to zero at ca. 230 nm. These results are consistent with the trends reported in the literature. Some studies showed a very low UV absorbance of SHA, CHA and NEU fractions at 254 (<0.05) [22,32].

The fall of UV spectra for DAX-8 and XAD-4 eluents close to zero at approximately 240 nm demonstrates that SHA and CHA fractions only have UV absorption at the range of 200–240 nm. Korshin et al. [33] categorized UV absorbance of DOC in the range of 190–400 nm into three regions; local excitation region with absorbance of $<\sim 190$ nm, beneznoid (Bz) region with absorbance range of 190–240 nm and electron-transfer (ET) region with absorbance of >240 nm. The absorbance of Bz region is centred at 204 nm, whereas the absorbance of ET region is centred at 254 nm. Based on these categories, one can deduce that there is a relationship between DOC fractions and UV absorbance at Bz and ET regions. Korshin et al. [33] found that the ratio of the absorbance at the centre of ET region (254 nm) to that of Bz region (204) of natural water samples gives a good indication to the tendency of DOC to involve in adsorption and complexation reactions. These reactions determine the amenability of DOC to coagulation process and its potential to form DBPs. The relationship between absorbance ratio of ET to Bz regions (A_{254}/A_{204}) and the ratio of hydrophobic/hydrophilic of the seven water bodies was investigated and the outcome is illustrated in Fig. 5.

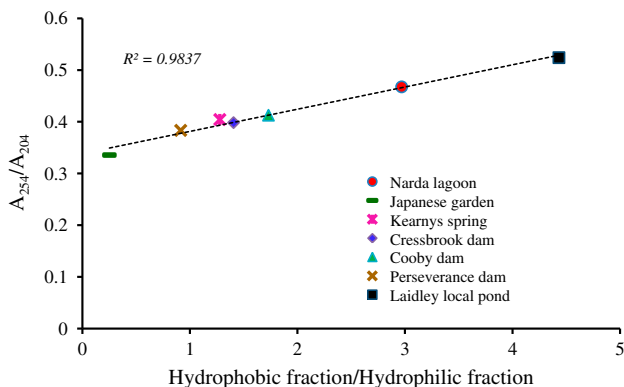Hydrophobic/hydrophilic appears to have a strong correlation with A_{254}/A_{204}, $R^2 = 0.9837$. The significance of this correlation was also investigated at a significance level of 0.05 (i.e. p-value = 0.05), and the results showed that the correlation was statistically significant with a p-value of 1.16×10^{-5}. It was reported that the amino groups in NOM absorb higher UV at 210 nm (in the proximity of 204) than at 254 nm [34]. This could explain the strong correlation between A_{254}/A_{204} and hydrophobic/hydrophilic ratio as the amino groups are prevalent in the hydrophilic fraction (Table 1). Based on the structural analysis for DOC fractions in Table 1, non-aromatic structure is dominant in the hydrophilic fraction as opposed to the hydrophobic fraction where the aromatic structure is prevailing. The strong correlation between A_{254}/A_{204} and hydrophobic/hydrophilic ratio indicates that this ratio can also be used as an indicator for distinguishing bulk properties of water samples such as aromaticity and hydrophobicity.

To further explore the relationship between DOC fractions and UV absorbance at Bz and ET regions, the correlation between the component of the ratios was inspected. The correlations between the hydrophobic fraction and A_{254} and the hydrophilic fraction and A_{204} were examined and the results are demonstrated in Figs. 6 and 7. In general, A_{254} showed stronger correlation with the hydrophobic fraction ($R^2 = 0.9682$) as compared to the correlation between the hydrophilic fraction and A_{204} ($R^2 = 0.8465$). However, when testing the significance of the two correlations, they were both found to be statistically significant with p-values of 6.21×10^{-5} and 0.034 for A_{254} vs. hydrophobic fraction and A_{204} vs. hydrophilic fraction, respectively. This confirms the versatile use of A_{254} not only for predicting DOC concentration [29] and humification [5], but also for predicting the bulk hydrophobicity of the water samples.

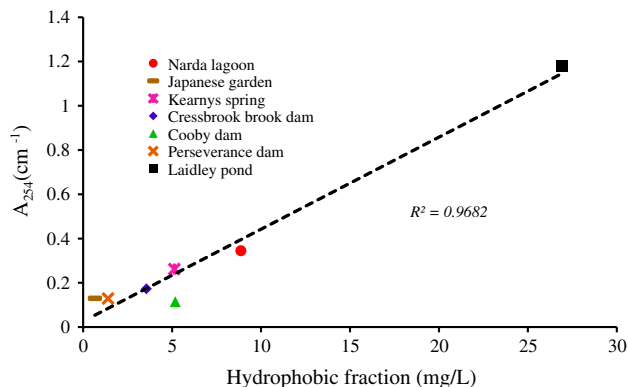The relationship between DOC fractions and other common UV measurements, namely A_{280} and the

Fig. 5 A_{254}/A_{204} vs. Hydrophobic/hydrophilic for the tested water bodies.

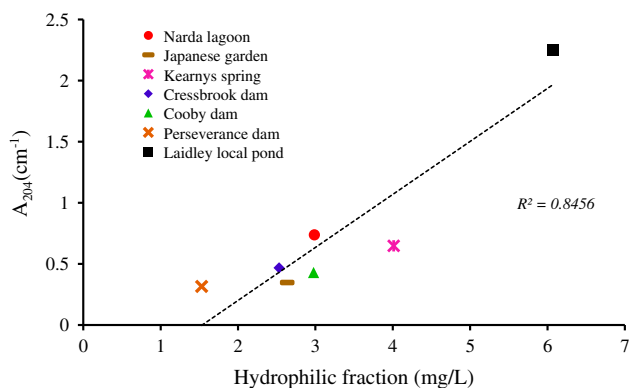Fig. 6. A_{254} vs. hydrophobic fraction for the tested water bodies.

Fig. 7. A_{204} vs. hydrophilic fraction for the tested water bodies.

ratios A_{250}/A_{365}, A_{254}/A_{436} and their components were also investigated. A_{254} and A_{280} have been used extensively in the literature as an indicator for humification and aromaticity [1,12,24,35]. Aromaticity and A_{254} were also reported to be correlated [12,36]. Hence, the correlation between A_{280} and the hydrophobic ratio was studied and the results are depicted in Fig. 8. The results in Fig. 8 demonstrate a good correlation between the hydrophobic fraction of all the water bodies and A_{280}. However, the hydrophobicity correlation with A_{254} is stronger than that with A_{280} ($R^2 = 0.9682$ for A_{254} vs. hydrophobic fraction and $R^2 = 0.9578$ for A_{280} vs. hydrophobic fraction). It should be noted though that the correlation between A_{280} and the hydrophobic fraction was found to be significant with a p-value of 1.26×10^{-4}. Such trend was also indicated in previous studies where the hydrophobic fraction was found to have the highest aromaticity among the other DOC fractions [37]. In fact, Schafer [38] reported that the aromaticity of DOC fractions follows the order of humic acids > fulvic acid > hydrophilic acids, which is consistent with the findings of this study (Fig. 8).
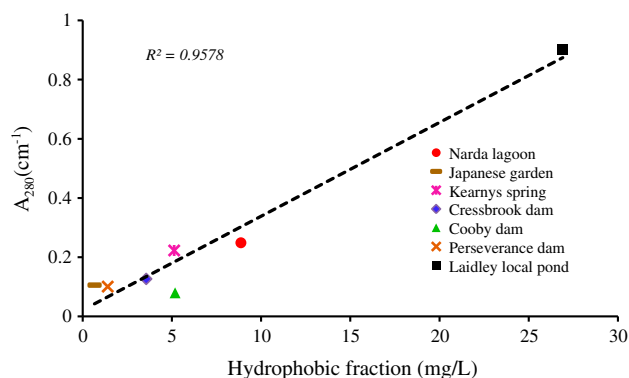
The lower correlation between hydrophobic fraction and A_{280} as opposed to A_{254} could be attributed to the fact that some of the aromatic DOC can be of hydrophilic nature (e.g. aromatic amines) [39].

A_{250}/A_{365} is commonly known as E_2/E_3 ratio, and it is used as an indicative for the proportion of low to high molecular weight organic materials in water [10,35,40,41]. Since hydrophobic fraction is believed to contain high molecular weight molecules and the hydrophilic fraction consists of smaller molecules [22], then hydrophobic/hydrophilic ratio would have inverse correlation with E_2/E_3. This inverse correlation between the hydrophobic/hydrophilic and A_{250}/A_{365} was tested, and found to be relatively a weak correlation as compared to the aforementioned correlations ($R^2 = 0.6873$) as shown in Fig. 9. Nevertheless, when evaluating the significance of this correlation, it was found to be significant with a p-value of 0.021. The weak correlation between hydrophobic/hydrophilic and A_{250}/A_{365} is attributed to the fact that UV absorbance is dependent on the presence of chromophores in the organic molecules rather than the molecular weight of the molecules [42]. In addition, A_{254} which is in the vicinity of the absorbance at 250 nm was found to have a significant correlation with the hydrophobic fraction, which suggests that A_{250} would have an insignificant correlation with the hydrophilic fraction. Such possibility was checked and confirmed that it is true that A_{250} has statistically insignificant correlation with the hydrophilic fraction with a p-value of 0.054. Buchanan et al. [22] found that the VHA fraction has some conjugated low molecular weight moieties highlighting that the hydrophobic fraction does not contain only high molecular weight molecules. It was observed by another study that aquatic humic acid consists mainly of molecules with small to moderate molecular weight [43].
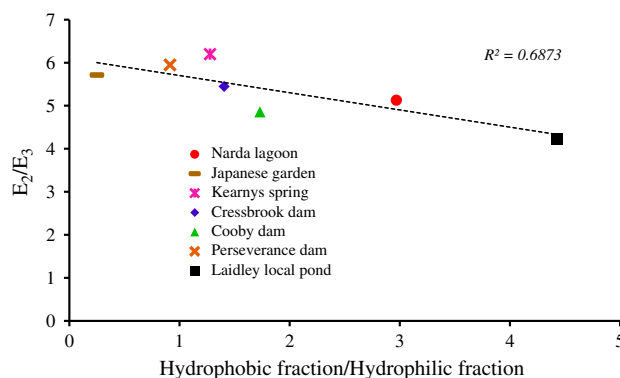

Fig. 8 A_{280} vs. hydrophobic fraction for the tested water bodies.

Fig. 9. E_2/E_3 vs. Hydrophobic fraction/hydrophilic fraction for the tested water bodies.
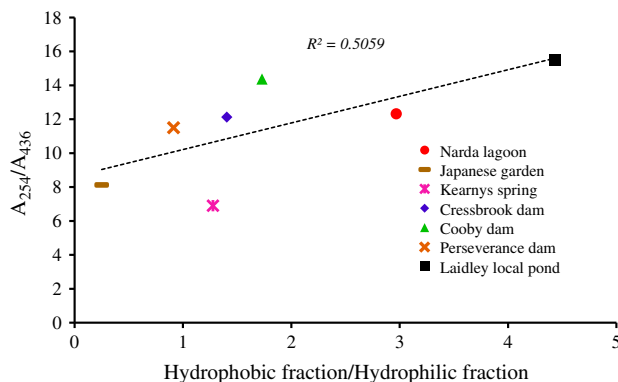
Fig. 10. A_{254}/A_{436} vs. Hydrophobic fraction/hydrophilic fraction for the tested water bodies.

A_{254}/A_{436} has been utilized in the literature to estimate the ratio of the UV absorbing groups of DOC to the colour-forming groups [44]. It was reported in some studies that the UV-absorbing moieties of DOC are of hydrophobic nature, while some of the colour-forming moieties are of hydrophilic nature [45]. To test these claims, the correlation between hydrophobic/hydrophilic and A_{254}/A_{436} was examined, and the results are depicted in Fig. 10. It appears that the correlation between DOC fractions and this absorbance ratio is weak. Even testing the significance of this correlation at p-value of 0.05 revealed that this correlation is insignificant (p-value = 0.073).

The relationships presented in this study ascertain that UV absorbance can be a good surrogate for the chemical fractionation analyses, particularly A_{254}, A_{280} and A_{254}/A_{204}. The fact that the UV absorbance was used in this study rather than specific absorbance (i.e. SUVA) highlights the feasibility of using A_{254}, A_{280} and A_{254}/A_{204} as in situ monitoring techniques for tracking the change in the structure of NOM in natural water resources. However, special attention needs to be given to the pH and the levels of the interfering inorganic species of the water.

4. Conclusion

Chemical fractionation and UV measurements were performed on seven water bodies situated in SEQ, Australia. The correlations between the DOC fractions and selected common UV measurements, namely A_{254}, A_{280}, A_{254}/A_{204}, A_{250}/A_{365} and A_{254}/A_{436} were investigated. A_{254}/A_{204} vs. hydrophobic/hydrophilic ratio showed a strong and significant correlation. The correlations of A_{250}/A_{365} and A_{254}/A_{436} vs. hydrophobic/hydrophilic were both weak, however, the former correlation was found to be statistically significant,

while the latter correlation was statistically insignificant. Both A_{254} and A_{280} showed good correlations with the hydrophobic fraction. The observed correlations in this study can effectively be harnessed by environmental or water treatment professionals as cost- and time-effective surrogate measurements for monitoring the structural changes in NOM. However, evaluating the correlation between UV measurements and DOC fractions for natural water undergoing specific treatment steps is a valuable goal for future work.

References

[1] G. Amy, Fundamental understanding of organic matter fouling of membranes, Desalination 231 (2008) 44–51.
[2] Y.C. Soh, F. Roddick, J. Van Leeuwen, The impact of alum coagulation on the character, biodegradability and disinfection by-product formation potential of reservoir natural organic matter (NOM) fractions, Water Sci. Technol. 58 (2008) 1173–1179.
[3] W. Buchanan, F. Roddick, N. Porter, Formation of hazardous by-products resulting from the irradiation of natural organic matter: Comparison between UV and VUV irradiation, Chemosphere 63 (2006) 1130–1141.
[4] S. Liu, M. Lim, R. Fabris, C. Chow, K. Chiang, M. Drikas, R. Amal, Removal of humic acid using TiO_2 photocatalytic process—Fractionation and molecular weight characterisation studies, Chemosphere 72 (2008) 263–271.
[5] R.A. Al-Juboori, T. Yusaf, V. Aravinthan, P.A. Pittaway, L. Bowtell, Investigating the feasibility and the optimal location of pulsed ultrasound in surface water treatment schemes, Desalin. Water Treat. (2015) 1–19.
[6] I. Ivančev-Tumbas, The fate and importance of organics in drinking water treatment: A review, Environ. Sci. Pollut. Res. 21 (2014) 11794–11810.
[7] D. Ghernaout, The hydrophilic/hydrophobic ratio vs. Dissolved organics removal by coagulation—A review, J. King Saud Univ Sci. 26 (2014) 169–180.
[8] J.A. Leenheer, J.-P. Croué, Peer reviewed: Characterizing aquatic dissolved organic matter, Environ. Sci. Technol. 37 (2003) 18A–26A.
[9] F.C. Kent, K.R. Montreuil, A.K. Stoddart, V.A. Reed, G.A. Gagnon, Combined use of resin fractionation and high performance size exclusion chromatography for characterization of natural organic matter, J. Environ. Sci. Health., Part A 49 (2014) 1615–1622.

[10] A. Matilainen, E.T. Gjessing, T. Lahtinen, L. Hed, A. Bhatnagar, M. Sillanpää, An overview of the methods used in the characterisation of natural organic matter (NOM) in relation to drinking water treatment, Chemosphere 83 (2011) 1431–1442.

[11] R.A. Al-Juboori, T. Yusaf, Biofouling in RO system: Mechanisms, monitoring and controlling, Desalination 302 (2012) 1–23.

[12] Y.-P. Chin, G. Aiken, E. O'loughlin, Molecular weight, polydispersity, and spectroscopic properties of aquatic humic substances, Environ. Sci. Technol. 28 (1994) 1853–1858.

[13] G. Abbt-Braun, U. Lankes, F. Frimmel, Structural characterization of aquatic humic substances—The need for a multiple method approach, Aquat. Sci.—Res. Across Boundaries 66 (2004) 151–170.

[14] J. Hur, M.A. Williams, M.A. Schlautman, Evaluating spectroscopic and chromatographic techniques to resolve dissolved organic matter via end member mixing analysis, Chemosphere 63 (2006) 387–402.

[15] C. Chow, R. Fabris, M. Drikas, A rapid fractionation technique to characterise natural organic matter for the optimisation of water treatment processes, Aqua 53 (2004) 85–92.

[16] J.P. Riley, D. Taylor, The analytical concentration of traces of dissolved organic materials from sea water with Amberlite XAD-1 resin, Anal. Chim. Acta. 46 (1969) 307–309.

[17] E.M. Thurman, R.L. Malcolm, Preparative isolation of aquatic humic substances, Environ. Sci. Technol. 15 (1981) 463–466.

[18] J.A. Leenheer, Comprehensive approach to preparative isolation and fractionation of dissolved organic carbon from natural waters and wastewaters, Environ. Sci. Technol. 15 (1981) 578–587.

[19] J.P. Croue, B. Martin, A. Deguin, B. Legube, Isolation and characterization of dissolved hydrophobic and hydrophilic organic substances of a reservoir water, in: Natural Organic Matter in Drinking Water Workshop, Chamoix, France, American Water Works Association Research Foundation (AwwaRF), 1993, pp. 19–22.

[20] B. Bolto, G. Abbtbraun, D. Dixon, R. Eldridge, F. Frimmel, S. Hesse, S. King, M. Toifl, Experimental evaluation of cationic polyelectrolytes for removing natural organic matter from water, Water Sci. Technol. 40 (1999) 71–79.

[21] G.S. Raspati, H.N. Høvik, T. Leiknes, Preferential fouling of natural organic matter (NOM) fractions in submerged low-pressure membrane filtration, Desalin. Water Treat. 34 (2011) 416–422.

[22] W. Buchanan, F. Roddick, N. Porter, M. Drikas, Fractionation of UV and VUV pretreated natural organic matter from drinking water, Environ. Sci. Technol. 39 (2005) 4647–4654.

[23] P.A. Pittaway, T.R. van den Ancker, Properties of natural microlayers on Australian freshwater storages and their potential to interact with artificial monolayers, Mar. Freshwater Res. 61 (2010) 1083–1091.

[24] J.L. Weishaar, G.R. Aiken, B.A. Bergamaschi, M.S. Fram, R. Fujii, K. Mopper, Evaluation of specific ultraviolet absorbance as an indicator of the chemical composition and reactivity of dissolved organic carbon, Environ. Sci. Technol. 37 (2003) 4702–4708.

[25] T.A. Doane, W.R. Horwáth, Eliminating interference from iron(III) for ultraviolet absorbance measurements of dissolved organic matter, Chemosphere 78 (2010) 1409–1415.

[26] D.M. McKnight, E.W. Boyer, P.K. Westerhoff, P.T. Doran, T. Kulbe, D.T. Andersen, Spectrofluorometric characterization of dissolved organic matter for indication of precursor organic material and aromaticity, Limnol. Oceanogr. 46 (2001) 38–48.

[27] D. Waltner-Toews, The origin of feces: What excrement tells us about evolution, Ecology, and a Sustainable Society, ECW Press, Ontario, 2013.

[28] J.M. Walker, R. Rapley (Eds.), Molecular Biology and Biotechnology, fifth ed., Royal Society of Chemistry, Cambridge, 2000.

[29] L.S. Clesceri, E.W. Rice, A.E. Greenberg, A.D. Eaton (Eds.), Standard Methods for Examination of Water and Wastewater: Centennial edition, twenty-first ed., American Public Health Association, Washington, DC, 2005.

[30] M. Grant, A new membrane filtration medium for simultaneous detection and enumeration of Escherichia coli and total coliforms, Appl. Environ. Microbiol. 63 (1997) 3526–3530.

[31] W.P. Hamilton, M. Kim, E.L. Thackston, Comparison of commercially available Escherichia coli enumeration tests: Implications for attaining water quality standards, Water Res. 39 (2005) 4869–4878.

[32] W. Sun, H. Chu, B. Dong, D. Cao, S. Zheng, The degradation of natural organic matter in surface water by a nano-TiO$_2$/diatomite photocatalytic reactor, Clean Soil Air Water 42 (2014) 1190–1198.

[33] G.V. Korshin, C.-W. Li, M.M. Benjamin, Monitoring the properties of natural organic matter through UV spectroscopy: A consistent theory, Water Res. 31 (1997) 1787–1795.

[34] N. Her, G. Amy, H.-R. Park, M. Song, Characterizing algogenic organic matter (AOM) and evaluating associated NF membrane fouling, Water Res. 38 (2004) 1427–1438.

[35] C.S. Uyguner, M. Bekbolet, Evaluation of humic acid photocatalytic degradation by UV–vis and fluorescence spectroscopy, Catal. Today 101 (2005) 267–274.

[36] X. Huang, M. Leal, Q. Li, Degradation of natural organic matter by TiO$_2$ photocatalytic oxidation and its effect on fouling of low-pressure membranes, Water Res. 42 (2008) 1142–1150.

[37] C.J. Hwang, S. Krasner, M. Sclimenti, Polar NOM: Characterization DBPs, Treatment, American Water Works Association, Denver, CO, 2001.

[38] A. Schafer, Natural Organics Removal using Membranes: Principles, Performance, and Cost, Technomic publication, Pennsylvania, 2001.

[39] J. Leenheer, T. Noyes, Effects of organic wastes on water quality from processing of oil shale from the Green River Formation, Colorado, Utah, and Wyoming, US Geol. Surv. Prof. Pap. 1338. 75 (1986) 1–56.

[40] J. Peuravuori, K. Pihlaja, Molecular size distribution and spectroscopic properties of aquatic humic substances, Anal. Chim. Acta. 337 (1997) 133–149.

[41] J. Peuravuori, K. Pihlaja, Preliminary study of lake dissolved organic matter in light of nanoscale supramolecular assembly, Environ. Sci. Technol. 38 (2004) 5958–5967.

[42] A.I. Scott, Interpretation of the Ultraviolet Spectra of Natural Products, Pergamon Press distributed by Macmillan, Oxford, 1964.

[43] Q. Wei, R. Fabris, C.W. Chow, C. Yan, D. Wang, M. Drikas, Characterization of dissolved organic matter from Australian and Chinese source waters by combined fractionation techniques, Water Sci. Technol. 64 (2011) 171–177.

[44] S. Valencia, J.M. Marín, G. Restrepo, F.H. Frimmel, Application of excitation–emission fluorescence matrices and UV/Vis absorption to monitoring the photocatalytic degradation of commercial humic acid, Sci. Total Environ. 442 (2013) 207–214.

[45] T.J. Battin, Dissolved organic matter and its optical properties in a blackwater tributary of the upper Orinoco river, Venezuela, Org. Geochem. 28 (1998) 561–569.

Summary-Objective 3

After identifying the effective operating parameters (***papers I*** and ***II***) and the optimum location of ultrasound in the drinking water treatment scheme (***papers III and IV***), the next step is to carefully investigate the effect of the operating parameters on the quantity and quality of natural contaminants (Objective 3). Objective 3 was achieved in ***papers V*** through ***VIII***. The effective operating parameters identified in objective 1 (amplitude of 40% and 70% and $R = 0.2:0.1$ and $0.1:0.6$ s) along with treatment time levels of 5 and 15 mins were applied in these papers. Statistical analyses were also employed to detect the trends of contaminants behaviour under the effect of ultrasound treatments and pinpoint the most energy efficient treatment scenario. ***Papers V*** and ***XII*** (Appendix B) were devoted to explore the effects of ultrasound treatment on deactivating natural water microbes. The effect of ultrasound treatment on the concentration and structure of aquatic organic carbon was investigated in ***papers VI*** and ***VII***. The results of objective 3 showed that ultrasound treatments were capable of deactivating 10-70% of microbes and removing 7-15% of DOC. It was also found that ultrasound treatment with amplitude of 40%, $R = 0.2:0.1$ s and 5 mins was the most energy efficient treatment scenario. With regards to DOC structure, ultrasound treatments were found to decrease the hydrophobic DOC fraction and slightly increase the hydrophilic DOC fraction. The correlations between DOC fractions and UV measurements were evaluated in paper ***VII*** and ***VIII***. DOC fractions showed strong and significant correlations with most of UV measurements. These correlations will be utilized as quick measurements for DOC structural change in further stages of this study.

Paper IX

Al-Juboori, R. A., Aravinthan, V., Yusaf, T. & Bowtell, L., Assessing the application and downstream effects of pulsed ultrasound as a pre-treatment for Alum coagulation, *Ultrasonics Sonochemistry*, (2016), 31, 719.

Assessing the application and downstream effects of pulsed mode ultrasound as a pre-treatment for alum coagulation

Raed A. Al-Juboori [a,*], Vasantha Aravinthan [a], Talal Yusaf [b], Leslie Bowtell [b]

[a] School of Civil Engineering and Surveying, Faculty of Health, Engineering and Sciences, University of Southern Queensland, Toowoomba, 4350 QLD, Australia
[b] School of Mechanical and Electrical Engineering, Faculty of Health, Engineering and Sciences, University of Southern Queensland, Toowoomba, 4350 QLD, Australia

ARTICLE INFO

ABSTRACT

The application of pulsed mode ultrasound (PMU) as a pre-treatment for alum coagulation was investigated at various alum dosages and pH levels. The effects of the treatments on turbidity and dissolved organic carbon (DOC) removal and residual Al were evaluated. Response surface methodology (RSM) was utilized to optimize the operating conditions of the applied treatments. The results showed that PMU pre-treatment increased turbidity and DOC removal percentages from maximum of 96.6% and 43% to 98.8% and 52%, respectively. It also helped decrease the minimum residual Al from 0.100 to 0.094 ppm. The multiple response optimization was carried out using the desirability function. A desirability value of >0.97 estimated respective turbidity removal, DOC removal and Al residual of 89.24%, 45.66% and ~0.1 ppm for coagulation (control) and 90.61%, >55% and ~0 for coagulation preceded by PMU. These figures were validated via confirmatory experiments. PMU pre-treatment increased total coliform removal from 80% to >98% and decreased trihalomethane formation potential (THMFP) from 250 to 200 ppb CH_3Cl. Additionally, PMU application prior to coagulation improved the settleability of sludge due to the degassing effects. The results of this study confirms that PMU pre-treatment can significantly improve coagulation performance.

© 2015 Elsevier B.V. All rights reserved.

1. Introduction

Coagulation is an important process in surface water treatment. It is normally applied for removing turbidity, color, microbes and DOC [1]. Recently, much attention is given for improving coagulation performance particularly for DOC removal owing to the involvement of DOC in causing technical and health problems such as filtration fouling and formation of disinfection by-products (DBPs) [2]. Increasing DOC removal with coagulation requires in-depth understanding of coagulation mechanisms. There are four main mechanisms through which coagulants can scavenge DOC from water: charge neutralisation, adsorption, enmeshment and complexation of DOC with coagulants [3]. In reality, these mechanisms occur concurrently, however, there is always a dominant mechanism depending on the properties of the water and the quantity of the applied coagulant [4]. Based on this principle, the term enhanced coagulation came into existence where the amount of coagulants and pH are adjusted to achieve maximum DOC removal. As mentioned earlier the role of coagulation is not con-

fined to DOC removal only, other forms of contaminations are targeted too (e.g., turbidity). Unfortunately, the optimum conditions for DOC removal do not always align with the removal of other forms of contaminants, making it harder to achieve the desired highest level of DOC removal [3]. Therefore, the application of pre-treatment techniques prior to coagulation is essential to maximize DOC removal.

Oxidation pre-treatment techniques are generally utilized for partial removal of DOC prior to coagulation [5]. Chlorine or chlorine derivatives were traditionally used for pre-oxidation [6], but the risk of DBPs formation led to their replacement with other oxidants such as ozone. However, ozone has also been found to form toxic materials such as aldehydes [7]. Recently, the application of advanced oxidation techniques (AOP) such UV light has emerged as a safe pre-oxidation method for removing DOC prior to coagulation. As the water prior to coagulation can be turbid, the penetration of UV light through it would be weak, resulting in low DOC removal levels. Therefore, the application of another AOP namely ultrasound for improving coagulation performance was proposed in this study.

Applying ultrasound for such a purpose has not been investigated thoroughly in previous works. A very limited number of publications touched on this topic such as the work conducted by

* Corresponding author.
E-mail addresses: RaedAhmed.mahmood@usq.edu.au, Raedahmed.mahmood@gmail.com (R.A. Al-Juboori).

Ziylan and Ince [8], and these research efforts only went as far as measuring DOC removal when combining ultrasound with coagulation. In this work, the application of ultrasound as a suitable pre-treatment for the most commonly used coagulant (alum) was carefully evaluated. Pulsed mode ultrasound (PMU) was selected for this study due to the high efficiency of this mode in removing water contaminants when compared to standard continuous mode [9,10]. Two treatment types: coagulation alone (control) and coagulation with PMU pre-treatment were applied at various alum dosage and pH levels. In addition to DOC removal, other important treatment criteria such as turbidity removal and residual dissolved Al were measured to assess the overall improvement that ultrasound pre-treatment can introduce to coagulation performance. The dissolved form of Al is of concern to water treatment practices due to its toxicity, involvement in neurological diseases and removal difficulty as compared to other Al species [11,12]. Most countries around the world have set a maximum limit for dissolved Al in their finished drinking water. For example, the maximum limit set for dissolved Al in Australia is 0.2 mg/L [13].

The optimization of the experimental factors applied in the control and PMU with coagulation treatments was performed using centre composite design (CCD) of RSM in Design-Expert software. RSM is an effective optimization tool that facilitates identifying the effective levels of experimental factors with minimal number of experiments [14]. Multiple response optimization was conducted using the desirability function where the optimization criteria were set as both maximum turbidity and DOC removal along with minimum residual dissolved Al concentration. The desirability function of the Design-Expert software has the capacity for simultaneous determination of the optimum levels of experimental factors for several responses [15]. The levels of total coliform and THMFP in the treated water with optimum control and coagulation preceded by PMU treatments were measured and compared to gauge the downstream effects of PMU as a pre-treatment technique.

2. Materials and methods

2.1. Water sample

Narda lagoon, situated in the South-East Queensland, Australia was chosen as the sampling site for this study. The samples were collected using 5 L plastic containers. The water samples were sieved through 0.5 mm to simulate the screening required for natural water samples in water treatment practices [16,17]. Detailed information regarding the levels and nature of contaminants in Narda water is shown in Table 1. Table 1 shows that Narda water can be categorized as alkaline hydrophobic water with high microbial load.

Table 1
Water sample properties.

Properties	Levels
pH	7.6
Alkalinity (mg CaCO$_3$/L)	254
Turbidity (NTU)	20
Conductivity (mS/cm), 25 °C	0.26
Total coliform (CFU/100 mL)	250
DOC (mg/L)	9.8
Hydrophobic fraction (%)	78
Hydrophilic fraction (%)	22
SUVA$_{254}$ (L mg^{-1} cm^{-1})	0.036
SUVA$_{280}$ (L mg^{-1} cm^{-1})	0.025

2.2. Pulsed ultrasound treatments

Ultrasound was used in this study as a pre-treatment for the coagulation process. Ultrasonic treatments were carried out using a digital Branson sonifier model 450 with operating low frequency of 20 kHz and a maximum electrical power of 400 W (Branson, USA). The sonifier is equipped with a titanium horn ($\varnothing$ = 19 mm). The treatments were conducted in batches using 500 mL Pyrex beaker. The temperature of water samples was maintained at approximately 20 °C using a water bath. Power characterization of the ultrasonic system was studied and discussed in our previous work [18]. The water samples were treated by applying pulse ratio (On:Off) of 0.2:0.1 s at a calorimetric power of 48 W for an effective treatment time of 5 min. The aforementioned treatment parameters were selected in this study due to their efficient removal of contaminants such as microbes [10].

2.3. Coagulation/flocculation treatments

Coagulation/flocculation treatments were performed using VLEP-Scientifica jar tester (Model JLT 6). The mixing time and speed of coagulation and flocculation processes were set through an electronic register. Six 1 L Pyrex beakers were used for carrying water samples. Alum coagulant prepared from Al$_2$(SO$_4$)$_3$ salt and used for water treatment. The important factors for coagulation/flocculation processes are coagulant dosage, pH and the operating parameters of the processes viz. mixing speeds and times. The effective range of coagulant dosage and pH for the tested water were determined through preliminary experiments. The pH of water samples was controlled using 0.1 N HCl and 0.05 N NaOH solutions. The operating parameters for the jar test were selected based on the reported conditions in the literature for the use of alum in surface water coagulation as summarized in Table 2. Water samples were coagulated at 150 rpm for 1 min followed by flocculation at 30 rpm for 15 min and finally were left for 30 min to settle. After settlement, samples of the supernatant were withdrawn at 2 cm depth from the water surface and used for measuring the targeted characteristics such as turbidity, DOC and residual dissolved Al. The downstream effects of ultrasound pre-treatment were evaluated by measuring total coliform and THMFP of the supernatant with and without ultrasound pre-treatment. Prior to total coliform and THMFP measurements, the supernatant samples were filtered through 11 μm filter paper (Whatman, grade 1) to simulate a sand filtration process that is commonly used in water treatment practices [19,20].

2.4. Analytical methods

DOC of water samples was measured by applying the standard high-temperature combustion method as described in [21]. Total carbon analyzer model TOC-V$_{CSH}$ supplied with an auto-sampler (ASI-V) (SHIMADZU, Australia) was utilized for DOC measurements. Three injections were made for each sample resulting in coefficient of variance of less than 0.02.

Residual dissolved Al in the treated samples was measured applying the standard direct nitrous oxide–acetylene flame

Table 2
Ranges of jar test operating parameters reported in relevant literature.

Operating parameters	Range	Refs.
Coagulation speed (rpm)	100–300	[21–27]
Duration of coagulation (min)	1–1.5	[21–27]
Flocculation speed (rpm)	20–40	[21–27]
Duration of flocculation (min)	15	[21,22,24–26]
Settling time (min)	30	[21–23,25,26]

method [21]. An atomic Absorption Spectrophotometer model AA-7000 (SHIMADZU, Australia) was employed for Al measurements. Water samples were filtered through 0.45 μm cellulose ester membrane prior to DOC and Al measurements. The samples were further acidified to pH 2 using concentrated HNO_3 for Al measurements.

Alkalinity and turbidity were measured according to nephelometric and titration methods, respectively [21]. Turbidity measurements were done using Lovibond turbidity meter (model TB 210 IR). Alkalinity of water samples was measured through titration to pH end-point of 4.3 with 0.1 N HCl using pH Eutech meter (model PC 2700).

Total coliform concentration in untreated and treated water samples was quantified using membrane filtration method [10]. Briefly, after filtering the water sample through 0.45 μm gridded sterile mixed cellulose ester, the filter was then placed on a saturated pad with M-ColiBlue24® media in a Petri dish and incubated at 35 ± 0.5 °C for 24 h.

THMFP measurements were performed based on the standard method 5710 detailed in [21]. The chlorination conditions in this methods are pH 7 ± 0.2 at temperature of 25 ± 2 °C for 7 days with free residual chlorine of 3–5 mg/L. Chlorine dosing solution was prepared from stock NaOCl solution 10–15% chlorine supplied by Sigma–Aldrich, Australia. The pH of the water sample was controlled using a phosphate buffer solution. Chlorine demand for treated, filtered and buffered water sample was determined using the calculations explained in the standard method. Free chlorine concentration in the spiked water samples was measured using N,N-dimethyl-p-phenylenediamine DPD colorimetric (method 10102, Hach Co.). After 7 days of incubation, the total trihalomethanes (TTHMs) of chlorinated water samples expressed as ppb CH_3Cl was measured applying THM Plus™ method (method 10132, Hach Co.). Hach spectrophotometer model DR2700 was utilized for free chlorine and TTHMs measurements.

Some other analytical measurements were applied in this study to help in understanding the effects of ultrasound pre-treatment on the mechanisms of contaminants removal. These measurements were chemical fractionation using polymeric resins and conductivity. Detailed information on the aforementioned measurements can be found in our previous studies [22,23].

2.5. Statistical analysis

The statistical analysis were conducted using Design-Expert Software version 9.0 (Stat-Ease, Inc.). The statistical design of the experimental work was based on RSM applying CCD. This design was selected in this work due to its efficiency in developing and testing the responses prediction models with minimal experimental runs [24]. The effects of two independent variables ($k = 2$) namely alum dosage (X_1) and pH (X_2) on three response; turbidity removal (Y_1), DOC removal (Y_2) and residual dissolved Al (Y_3) were inspected for both sonicated coagulated and only coagulated water samples. To construct a CCD design, 2^K cube experimental points, 2^K axial experimental points and 3–5 replicate points at the center of the design are required as illustrated in Fig. 1 [25]. The correlations between the coded values of CCD design in Fig. 1 and their equivalent actual values of the experimental points are shown in Table 3. To ensure the rotation of CCD design, α value is set as $[2^K]^{1/4}$. The coded and uncoded values of the experimental factors of each run are shown in Table 4. The overall experimental points were 13, however each point was repeated twice to increase the accuracy of the model.

The behavior of measured responses was expressed in the following second-order polynomial equation [26,27]:

$$Y = \beta_0 + \sum_{i=1}^{k} \beta_i X_i + \sum_{i=1}^{k} \sum_{j=i+1}^{k} \beta_{ij} X_i X_j + \sum_{i=1}^{k} \beta_{ii} X_i^2 \qquad (1)$$

where, Y is the predicted response (removal of turbidity and DOC and residual dissolved Al); k the number of experimental factors, X is the experimental factor (alum dosage and pH), β_0 is the model constant, and β_i, β_{ij} and β_{ii} are linear, interaction and quadratic coefficients, respectively. The optimal combination of the factors was determined using desirability function for maximum turbidity and DOC removal and minimum residual dissolved Al. Confirmatory experiments of the optimum factors combination were conducted in triplicate for coagulated and sonicated coagulated water samples, and the percentage error was calculated.

3. Results and discussions

3.1. Analysis of residuals

Studying the nature of residuals (differences between experimental and predicated values of responses [28]) is an essential prerequisite for the statistical analyses of any experimental work. The nature of residuals of the measured responses in this study was scrutinized through a range of diagnostic tests. The distribution of residuals was evaluated by plotting the normal probability percentage against the studentized residuals of the measured responses [29]. The assumption of normal distribution of residuals is valid if the residual points of the measured responses fall close to the probability line [30]. Checks for residuals consistency and independency form order of experimental runs were performed through plotting studentized residuals vs. predicted values of responses and experimental runs' order, respectively. If the residual points are randomly scattered around zero in studentized residuals vs. predicted and studentized vs. run number plots this implies that there is no effect of predicted values of experiments order on residuals [31,32].

The diagnostic plots of turbidity removal, DOC removal and residual dissolved Al for control and PMU with coagulation treatments are shown in Figs. 2–4. It can be seen from these figures that the experimental errors in this study are normally distributed and independent from responses values and measurements order.

3.2. Analysis of variance (ANOVA) of responses

The significance of linear, quadratic and interaction effects of alum dosage and pH on turbidity removal, DOC removal and residual dissolved Al of control and PMU with coagulation treatments were evaluated for confidence level of 95% (*P-value* = 0.05) as illustrated in Tables 5–7 respectively. The effects with *P-value* < 0.05 are regarded significant and will further be investigated in this study, otherwise the effects are insignificant and will be ignored.

It is clear from Tables 5–7 that first order, second order and interaction effects for all responses were significant. Residual dissolved Al was equally influenced by all effects regardless of the effect source (first order, second order or interaction) with a high significance level *P-value* = 0.000. The response of residual dissolved Al to the change of experimental factors was independent of the treatment type as it showed a similar significance level for both control and PMU with coagulated water samples. Interestingly, the other two responses turbidity and DOC removals were both less affected by the interaction of alum dosage and pH when compared to other effects. It can be seen from Tables 5 and 6 that ultrasound treatment had noticeably improved the significance of the interaction effect on turbidity removal (*P-value* decreased from 0.042 to 0.012). This improvement can be attributed to the effect of
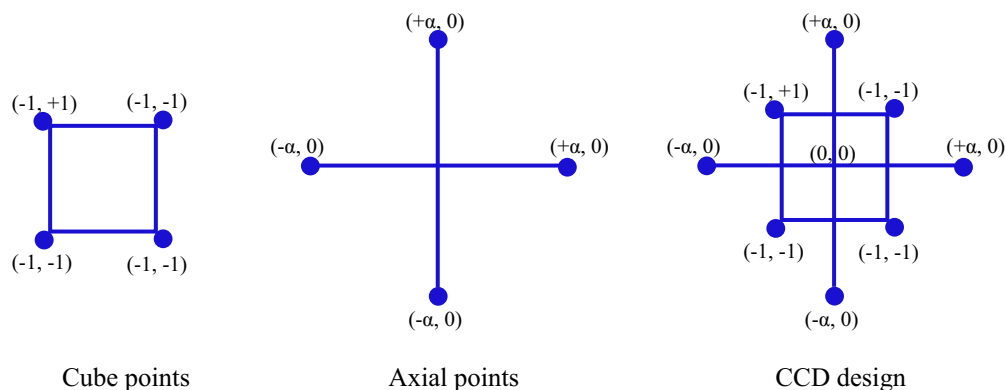
Cube points   Axial points   CCD design

Fig. 1. Components of CCD design.

Table 3
Correlations between codded and actual experimental points.

Coded values	Actual values as a function of coded values
$-\alpha$	X_{min}
-1	$\frac{(\alpha-1)X_{max}+(\alpha+1)X_{min}}{2\alpha}$
0	$\frac{X_{max}+X_{min}}{2}$
$+1$	$\frac{(\alpha-1)X_{min}+(\alpha+1)X_{max}}{2\alpha}$
$+\alpha$	X_{max}

Table 4
Actual values of the coded factors for each experimental run.

Order of experimental runs	Alum dosage (mg/L)		pH	
	Uncoded value	Coded value	Uncoded value	Coded value
1	55	0	6.5	0
2	10	−1.414	6.5	0
3	55	0	6.5	0
4	86.8	+1	4.73	−1
5	86.8	+1	8.27	+1
6	55	0	4	−1.414
7	23.2	−1	4.73	−1
8	100	+1.414	6.5	0
9	23.2	−1	8.27	+1
10	55	0	9	+1.414
11	55	0	6.5	0
12	55	0	6.5	0
13	55	0	6.5	0

ultrasound pre-treatment on water properties and consequently on coagulants–contaminants interaction [33].

3.3. Empirical models

The quadratic regression models developed that represent the respective behavior of turbidity removal, DOC removal and residual dissolved Al for coagulated and sonicated coagulated water samples are presented in Tables 8–10. The models were formulated based on the coefficients of linear, quadratic and interaction effects of factors (coded). The positive sign of the models terms implies a synergistic effect of the term, whereas a negative sign suggests an antagonistic effect of the term [34].

The adequacy of the models in representing the change in responses as a function of the changes in factors was tested with a number of diagnostic measures. The significance of the models was examined at a confidence level of 95%, the models with *P-value* < 0.05 are significant, which means that the models can sufficiently predict the change of responses as the factors change [35]. The goodness of fit of the models was tested through calculat-

ing the lack of fit (LOF) of the models. If the significance value of LOF for the models is more than 0.05, this indicates that the deviation of the models from the trends of the actual experimental data is insignificant [36]. The other measures for the goodness of fit for the models are the coefficient of determination R^2 and adj.R^2. The closer these coefficients are to 1 the better the goodness of fit [37]. The precision of the models was checked by inspecting the adequate precision (AP) values of the models. Adequate precision is a measure for signal/noise ration of the models, and normally the model is said to be precise if it has AP value of >4 [36]. The reproducibility of the models was evaluated through calculating the coefficient of variance in percentage (CV%) of the models. The coefficient of variance is defined as the ratio of the standard error of estimate to the mean value of the observed response [27]. Models with CV% of <10% are regarded as reproducible.

On the basis of the aforementioned diagnostic checks, one can deduce that all the response models presented in Tables 8–10 are significant and can be used to precisely predict the behavior of the response under selected experimental factors. The predicted values of turbidity removal, DOC removal, and residual dissolved Al were calculated and presented along with their corresponding actual values in Tables 11–13, respectively. The percentage deviation of the predicted values from the actual values for all the responses at different operating conditions was also determined as shown in Tables 11–13. In general, turbidity removal models produced the least deviation percentage from the actual values when compared to the other prediction models (maximum deviation of 4.17%). DOC removal models had the highest deviation percentages among all models (maximum deviation of 17.27%). It can be noticed in Tables 11–13 that ultrasound treatment increased the deviation in the prediction models of all responses. This is likely to be due to the effects of ultrasound on the quantity and nature of contaminants in the treated water such as DOC degradation (<10%), turbidity increase (ca. 15%), alkalinity decrease (from 254 to 244 mg CaCO$_3$/L, ca. 4%), conductivity increase (from 0.26 to 0.27 mS, ca. 4%) and possible changes in hydrophobic/hydrophilic structure.

3.4. Responses optimization

The behavior of the measured responses under various pH and alum dosages for two treatments control (a) and PMU with coagulation (b) is depicted in a form of 3D surface plots in Figs. 5–7. These figures help in quickly identifying the optimum levels of the applied experimental factors that results in the desirable responses [38].

It can be seen from Fig. 5, that for both treatments control and PMU with coagulation the turbidity removal increases with
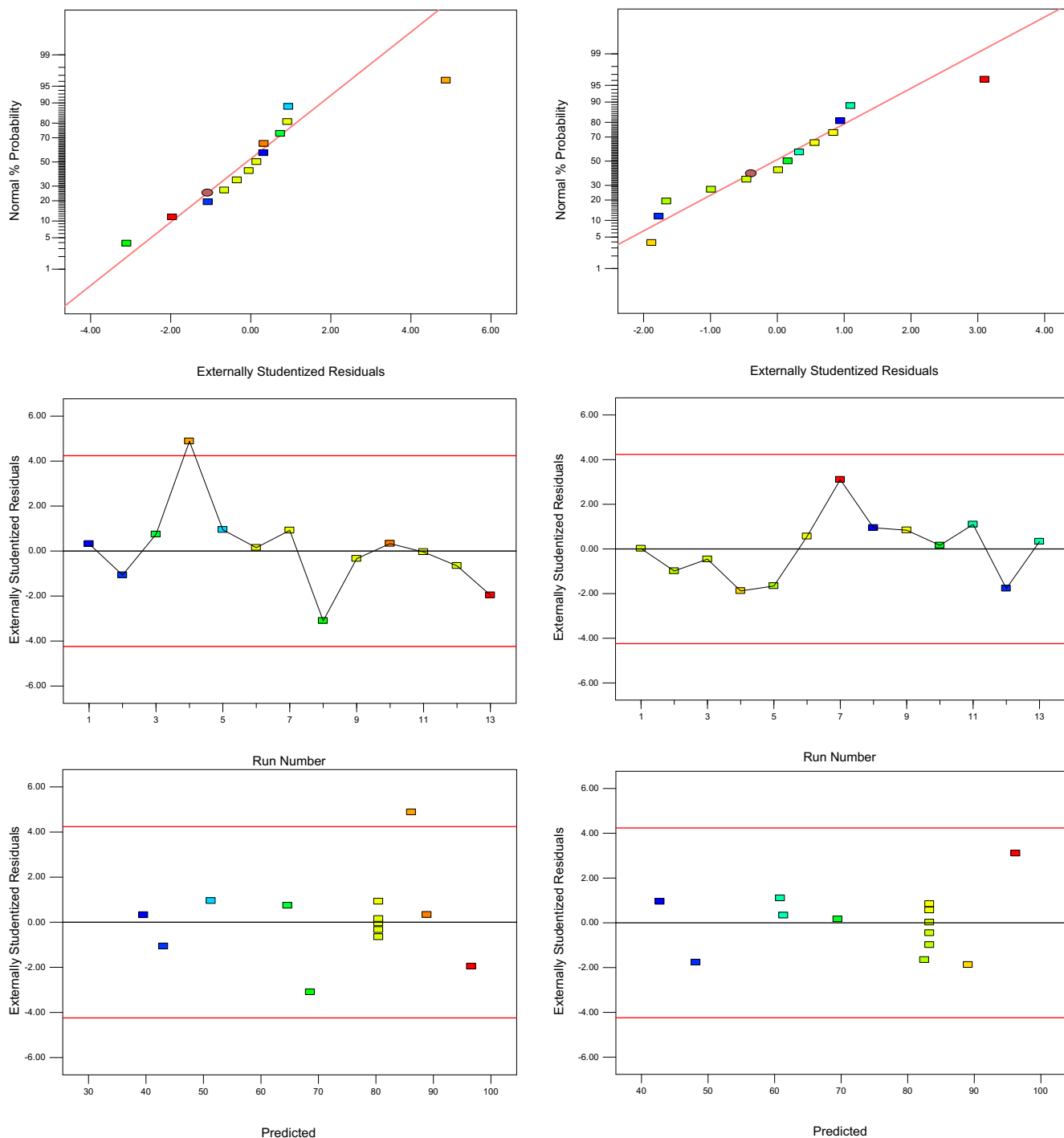
Fig. 2. Diagnostic plots for turbidity removal of coagulated water (left) and sonicated coagulated water (right).

increasing alum dosage. pH had different effect on turbidity removal depending on the dosage range. At low alum dosage levels, turbidity removal went through a maxima around 6.5 pH and dropped at the acidic and alkaline ends. At high alum dosage levels, the behavior of turbidity removal can be described as an exponential increment. These two trends suggest that turbidity removal mechanisms of the surface water used in this study are mostly charge neutralization at high coagulant dosage and a combination of charge neutralization and adsorption at low coagulant dosage. Destabilisation mechanisms of suspended particles in water depends on the chemistry of the coagulant used. Generally, for the case of alum the hydrolysis of this coagulant in water

results in products such as Al^{+3}, $Al(OH)^{+2}$ and $Al(OH)_4^-$ in equilibrium with amorphous $Al(OH)_{3(am)}$ [39]. The availability of these products in water depends on pH, with acidic pH conditions (4–5.5) the positively charged species are prevalent [35], at a pH range of neutral to alkaline, the dominant product is $Al(OH)_4^-$ [40]. Other highly positively charged Al species (e.g., $Al_3(OH)_4^{+5}$ and $Al_2(OH)_2^{+4}$) can also occur in acidic pH of less than 5 [40]. This means that the contaminant removals with alum at acidic pH occurs mainly due to charge neutralization (abundance of positively charges species), while at neutral to alkaline pH, contaminants removal happens through adsorption to the negatively charged precipitating Al hydroxides.
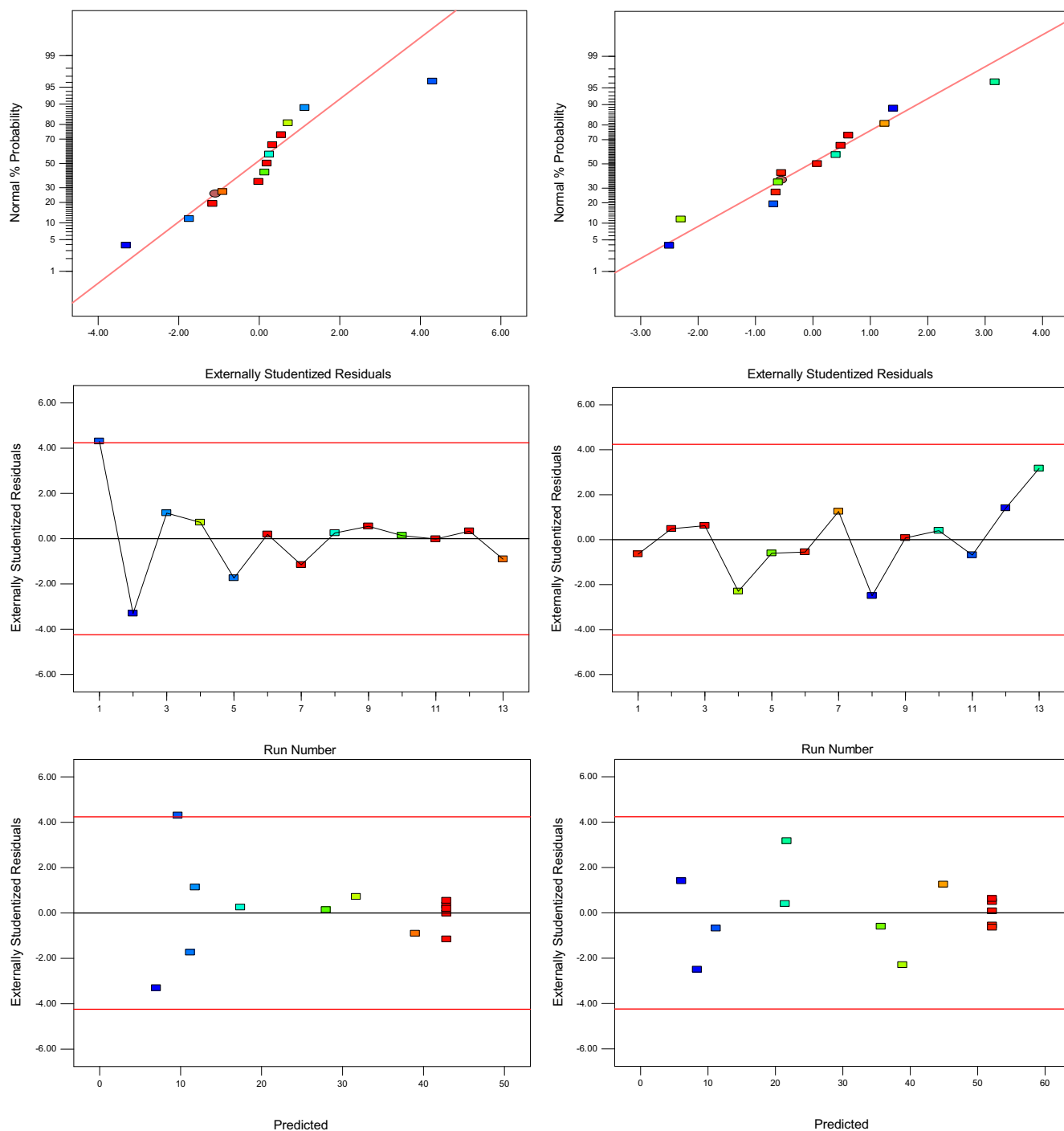
Fig. 3. Diagnostic plots for DOC removal of coagulated water (left) and sonicated coagulated water (right).

Overall, the response surface plot in Fig. 5 illustrates that the maximum turbidity removal for both treatment at acidic to neutral pH and high alum dosage. PMU pre-treatment improved turbidity removal in most of treatment scenarios (Table 11). The maximum turbidity removal achieved with control treatment was 96.6%. Pre-treating water with PMU increased the maximum turbidity removal to 98.8%. This observation is likely to be attributed to the properties alteration of pre-treated water with PMU. Increasing initial turbidity increases turbidity removal [41] and similarly decreasing alkalinity positively affects turbidity removal [42]. Increasing the conductivity of ultrasonically pre-treated water

can also increase turbidity removal through compressing the electrical double layer giving a rise to adsorption mechanisms [23].

DOC removal for control and PMU with coagulation treatments under different alum dosage and pH conditions is demonstrated in Fig. 6. It can be noticed that pre-treating water samples with PMU increased DOC removal at all the applied treatment conditions. Maximum DOC removal of ca. 43% with control treatment increased to a maximum of ca. 52% when applying PMU with coagulation. It appears that the favorite DOC removal conditions lie in alum dosage limit of >50 ppm and approximate pH ranges of 4.7–6.5 for unsonicated water and alum dosage of >40 ppm and
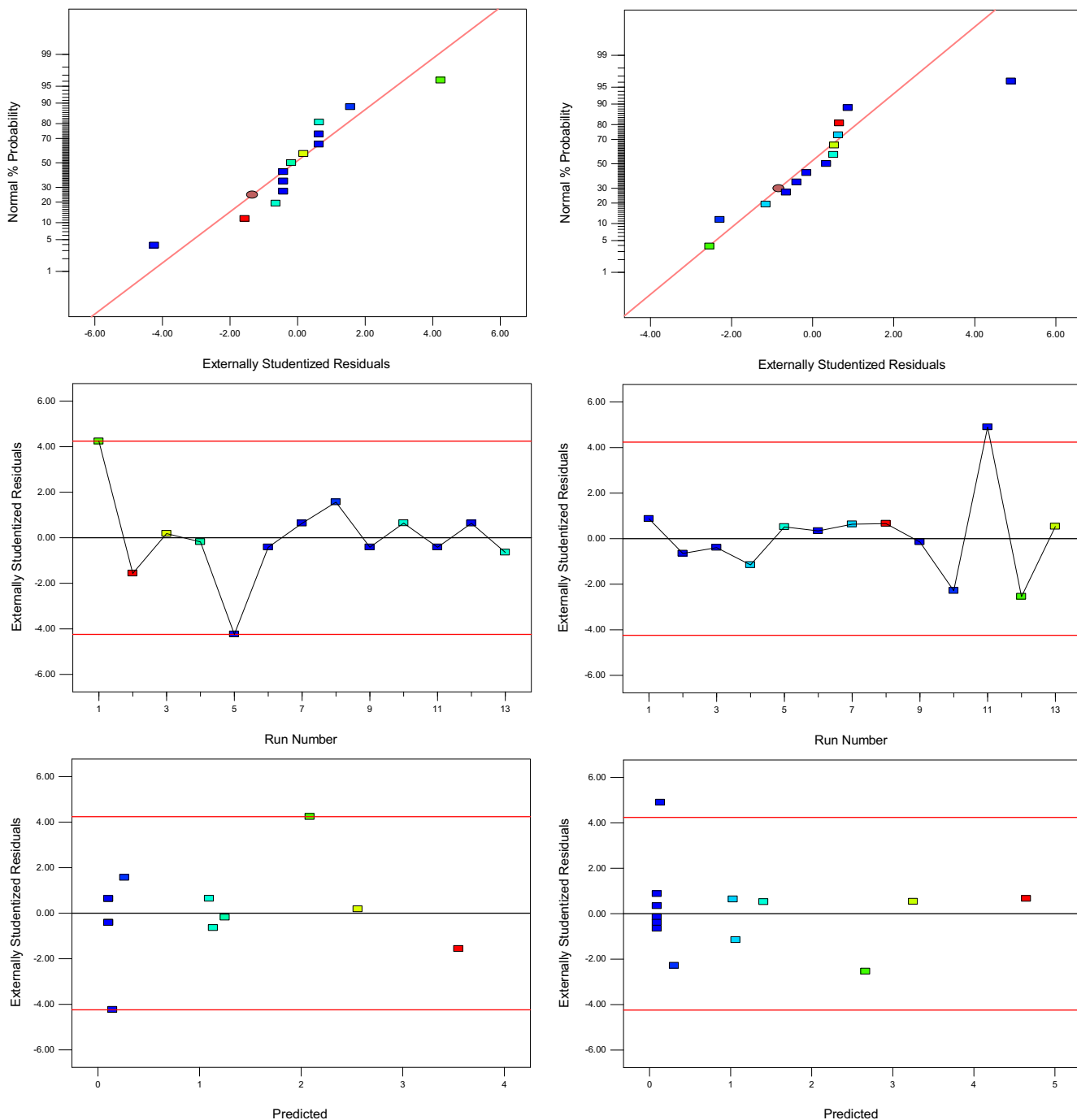
Fig. 4. Diagnostic plots for residual dissolved Al of coagulated water (left) and sonicated coagulated water (right).

Table 5
Summary of ANOVA results for turbidity removal.

Source	df	Control				PMU with coagulation			
		Sum of squares	Mean square	F-value	P-value	Sum of squares	Mean square	F-value	P-value
Alum dosage (X_1)	1	1409.87	1409.87	3970.32	0.000	796.40	643.73	195.28	0.000
pH (X_2)	1	1857.77	1857.77	5231.63	0.000	1580.29	796.40	387.48	0.000
X_1X_2	1	2.18	2.18	6.13	0.042	45.83	1580.29	11.24	0.012
X_1^2	1	186.94	186.94	526.44	0.000	120.23	45.83	29.48	0.001
X_2^2	1	437.34	437.34	1231.57	0.000	740.15	120.23	181.48	0.000
Residual	7	2.49	0.36			28.55	740.15		
Pure error	4	0.42	0.11			7.53	1.88		
Cor total	12	3831.50				3247.18			

Table 6
Summary of ANOVA results for DOC removal.

Source	df	Control				PMU with coagulation			
		Sum of squares	Mean square	F-value	P-value	Sum of squares	Mean square	F-value	P-value
Alum dosage (X_1)	1	281.06	281.06	12380.96	0.000	764.30	764.30	675.40	0.000
pH (X_2)	1	609.86	609.86	26864.36	0.000	743.73	743.73	657.23	0.000
X_1X_2	1	94.58	94.58	4166.09	0.000	15.41	15.41	13.61	0.008
X_1^2	1	941.59	941.59	41477.11	0.000	1282.31	1282.31	1133.16	0.000
X_2^2	1	961.11	961.11	42337.16	0.000	1581.30	1581.30	1397.38	0.000
Residual	7	0.16	0.023			7.92	1.13		
Pure error	4	0.032	0.008			1.34	0.34		
Cor total	12	2668.82				4066.63			

Table 7
Summary of ANOVA results of residual dissolved Al.

Source	df	Control				PMU with coagulation			
		Sum of squares	Mean square	F-value	P-value	Sum of squares	Mean square	F-value	P-value
Alum dosage (X_1)	1	0.91	0.91	8895.05	0.000	0.86	0.86	287,400	0.000
pH (X_2)	1	5.28	5.28	51844.14	0.000	10.50	10.50	47042.7	0.000
X_1X_2	1	0.040	0.040	392.84	0.000	0.0048	0.00483	57,190	0.000
X_1^2	1	0.46	0.46	4547.66	0.000	0.44	0.44	263.19	0.000
X_2^2	1	9.17	9.17	90039.43	0.000	14.98	14.98	24145.4	0.000
Residual	7	0.00071	0.0001			0.00013	0.00018		
Pure error	4	0.00012	0.00003			0.00023	0.00058		
Cor total	12	15.48				26.37			

Table 8
Statistics of turbidity removal models (coded).

Water type	Model	P	LOF	R^2	Adj.R^2	AP	CV%
Coagulated	$Y_1 = 80.5 + 13.3X_1 - 15.2X_2 - 0.74X_1X_2 - 5.2X_1^2 - 7.9X_2^2$	0.000	0.052	0.999	0.998	140.87	0.82
US+ coagulated	$Y_1 = 83.3 + 10X_1 - 14X_2 - 3.4X_1X_2 - 4.2X_1^2 - 10.3X_2^2$	0.000	0.118	0.991	0.985	38.96	2.70

Table 9
Statistics of DOC removal models (coded).

Water type	Model	P	LOF	R^2	Adj.R^2	AP	CV%
Coagulated	$Y_2 = 42.8 + 5.9X_1 - 8.7X_2 - 4.9X_1X_2 - 11.6X_1^2 - 11.7X_2^2$	0.000	0.072	0.999	0.999	350.29	0.53
US+ coagulated	$Y_2 = 52.2 + 9.8X_1 - 9.6X_2 - 2X_1X_2 - 13.6X_1^2 - 15.1X_2^2$	0.000	0.051	0.998	0.997	63.80	3.08

Table 10
Statistics of residual dissolved Al (coded).

Water type	Model	P	LOF	R^2	Adj.R^2	AP	CV%
Coagulated	$Y_3 = 0.1 + 0.3X_1 + 0.8X_2 - 0.1X_1X_2 + 0.311.6X_1^2 + 1.2X_2^2$	0.000	0.051	0.999	0.999	50.2	0.53
US+ coagulated	$Y_3 = 0.09 + 0.3X_1 + 1.2X_2 - 0.03X_1X_2 + 0.25X_1^2 + 1.5X_2^2$	0.000	0.057	0.999	0.999	156.5	0.37

approximate pH levels of 4.7–7.0 for sonicated water. The favorite pH ranges of DOC removal for both treatments fall within the effective range for alum [43]. The conditions of DOC removal for unsonicated water are consistent with the reported conditions in the literature for removal of hydrophobic DOC using alum [44], which is the case in this study (hydrophobic DOC = 78%, Table 1).

Broadening of the effective pH range of DOC removal due to PMU pre-treatment is attributed to ultrasound effects on water properties such as conductivity increase and alkalinity decrease. Such alteration promotes the dominant DOC removal mechanism at pH > 6 (i.e., adsorption [44]) and increases the availability of coagulants (less consumption due to alkalinity). The improvement in DOC removal with PMU pre-treatment can also be explained by ultrasonic degradation of DOC. Similar findings were reported by

Ziylan and Ince [8] who found that combining ultrasound with coagulation can improve DOC removal.

The behavior of residual dissolved Al for coagulated and sonicated coagulated water samples as a function of alum dosage and pH changes is shown in Fig. 7. The surface plots of the applied treatments are almost identical except that ultrasound resulted in higher Al residual in the alkaline range. Al residual levels in the neutral and acidic pH ranges were in most cases lower for PMU along with coagulation as compared to the control treatment (Fig. 7 and Table 13). The minimum residual dissolved Al for control treatment and PMU with coagulation were about 0.100 and 0.094 ppm, respectively. The concave shape of Al residual surfaces can be explained by the high consumption of Al at pH range of 5.0–6.5 (best performance of alum and high charge neutralization)

Table 11
Experimental and predicted turbidity removal levels.

Experimental runs	Alum dosage (mg/L)	pH	Control			PMU with coagulation		
			Turbidity removal experimental	Turbidity removal predicted	Deviation coded (%)	Turbidity removal experimental	Turbidity removal predicted	Deviation coded (%)
1	−1	1	39.7	39.57	0.33	46.25	48.18	4.17
2	0	1.414	42.67	43.06	0.90	43.96	42.81	2.62
3	1	1	64.93	64.65	0.43	61.79	61.36	0.70
4	0	−1.414	87.02	86.15	0.99	80.70	82.54	2.30
5	−1.414	0	51.67	51.33	0.67	62.20	60.86	2.15
6	0	0	80.55	80.46	0.11	83.32	83.29	0.04
7	0	0	80.96	80.46	0.62	81.50	83.29	2.20
8	−1	−1	67.82	68.57	1.10	69.72	69.50	0.31
9	0	0	80.27	80.46	0.24	82.41	83.29	1.07
10	1.414	0	89.00	88.88	0.13	87.09	89.08	2.30
11	0	0	80.44	80.46	0.02	84.36	83.29	1.27
12	0	0	80.10	80.46	0.45	84.84	83.29	1.83
13	1	−1	96.00	96.61	0.63	98.80	96.24	2.60

Table 12
Experimental and predicted DOC removal levels.

Experimental runs	Alum dosage (mg/L)	pH	Control			PMU with coagulation		
			DOC removal experimental	DOC removal predicted	Deviation coded (%)	DOC removal experimental	DOC removal predicted	Deviation coded (%)
1	−1	1	9.88	9.67	2.12	6.94	6.08	12.40
2	0	1.414	6.80	7.01	3.13	7.17	8.40	17.27
3	1	1	11.90	11.81	0.76	23.07	21.70	5.94
4	0	−1.414	31.76	31.70	0.18	35.26	35.70	1.16
5	−1.414	0	11.06	11.21	1.40	10.75	11.22	4.40
6	0	0	42.88	42.85	0.07	51.55	52.19	1.24
7	0	0	42.70	42.85	0.35	52.68	52.19	0.93
8	−1	−1	17.43	17.41	0.11	21.72	21.44	1.30
9	0	0	42.93	42.85	0.19	52.81	52.19	1.17
10	1.414	0	27.98	27.98	0.01	37.68	38.85	3.11
11	0	0	42.85	42.85	0.00	51.64	52.19	1.07
12	0	0	42.90	42.85	0.12	52.27	52.19	0.15
13	1	−1	38.90	38.99	0.23	45.70	44.90	1.75

Table 13
Experimental and predicted residual dissolved Al.

Experimental runs	Alum dosage (mg/L)	pH	Control			PMU with coagulation		
			Residual Al experimental	Residual Al predicted	Deviation coded (%)	Residual Al experimental	Residual Al predicted	Deviation coded (%)
1	−1	1	2.1	2.08	0.95	2.66	2.669	0.34
2	0	1.414	3.54	3.54	0.13	4.65	4.66	0.2
3	1	1	2.56	2.56	0.01	3.254	3.259	0.15
4	0	−1.414	1.25	1.25	0.31	1.41	1.4	0.21
5	−1.414	0	0.13	0.14	6.98	0.14	0.13	9.12
6	0	0	0.1	0.1	0	0.097	0.094	3.1
7	0	0	0.11	0.1	9.10	0.091	0.094	3.3
8	−1	−1	0.27	0.26	3.70	0.3	0.299	0.34
9	0	0	0.1	0.1	0	0.092	0.094	2.17
10	1.414	0	1.1	1.10	0.05	1.06	1.06	0.04
11	0	0	0.1	0.1	0	0.095	0.094	1.05
12	0	0	0.11	0.1	9.1	0.093	0.094	1.07
13	1	−1	1.13	1.14	0.88	1.033	1.029	0.38

and also the low solubility of alum around this pH range [39]. It appears that the only treatment scenario with dissolved Al residuals that complies with the recommended limit in the Australian drinking water guidelines (i.e., ~0.2) is coagulation at neutral pH range and moderate coagulation dosage.

Figs. 5–7 illustrate that each individual response has favorite operating conditions of alum dosage and pH level through which the desirable outcomes can be achieved. The desirable outcomes in this study are maximum turbidity and DOC removal and minimum residual dissolved Al. To achieve these outcomes, the desirability function was utilized to determine the optimum levels of alum dosage and pH for both treatments; control and PMU with coagulation as shown in Fig. 8a and b, respectively. It should be noted that the units of responses in Fig. 8 are % for turbidity and DOC removal and ppm for residual dissolved Al. The high desirability value of >0.97 for both treatments implies that the maximum turbidity and DOC removal and minimum Al residual achieved in individual optimizations are almost met in multiple response optimization. It can be seen from Fig. 8 that to achieve turbidity removal of 89.24%, DOC removal of 45.66% and residual dissolved
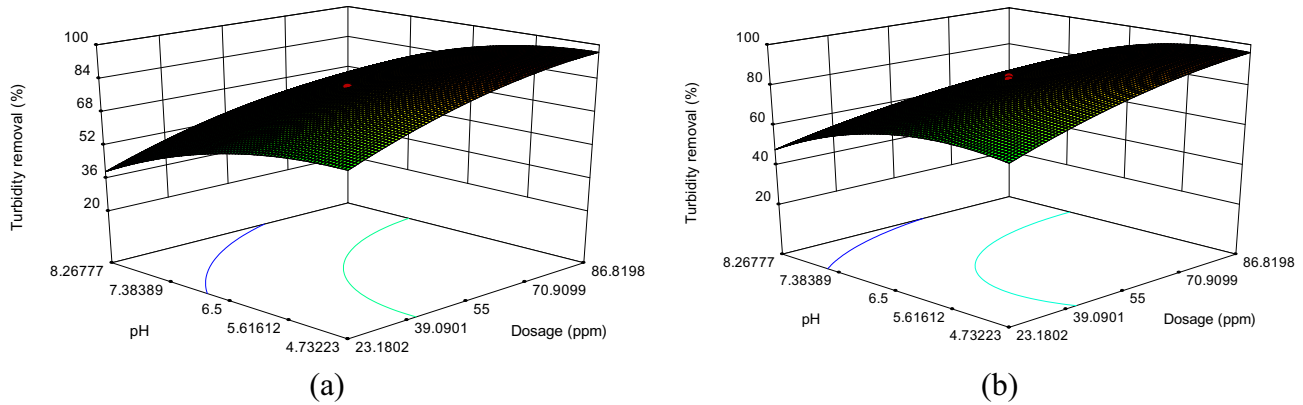
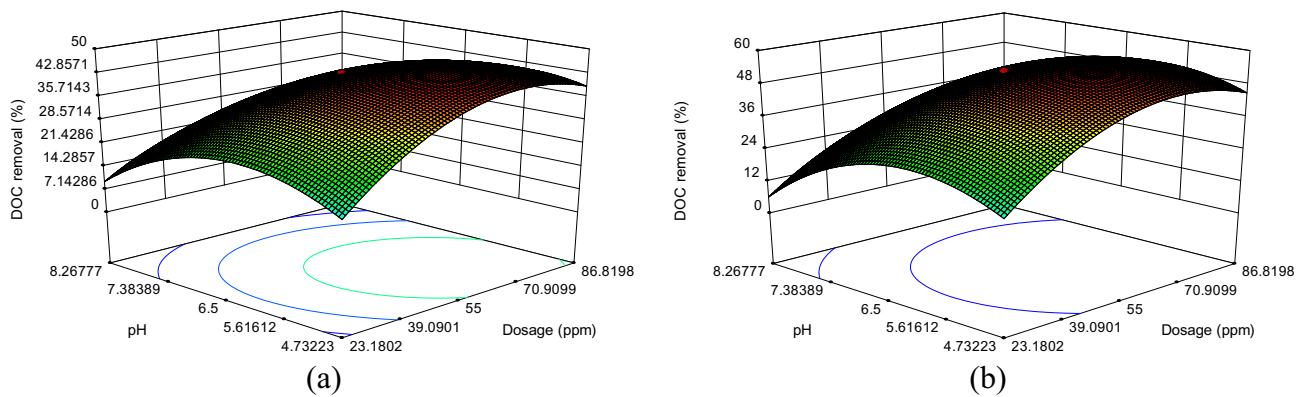**Fig. 5.** Response surface plots of turbidity removal for (a) coagulated and (b) sonicated and coagulated water sample.

Fig. 6. Response surface plots of DOC removal for (a) coagulated and (b) sonicated and coagulated water sample.
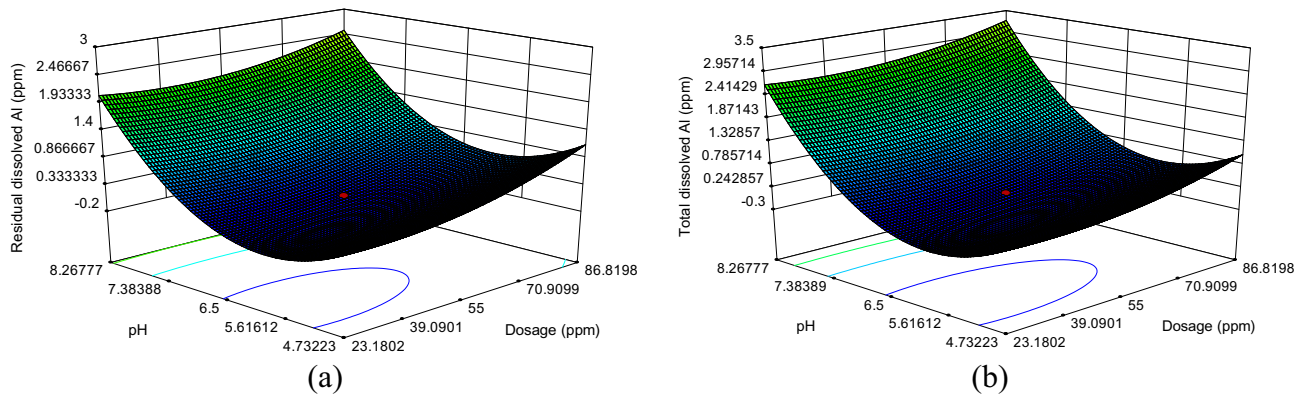

Fig. 7. Response surface plots of residual dissolved Al for (a) coagulated and (b) sonicated and coagulated water sample.

Al of ∼0.1 ppm, alum dosage of ∼63.20 mg/L at pH of 5.62 are required to be applied for unsonicated water. Although pre-treating the water with PMU slightly increased the required alum dosage and pH levels as shown in Fig. 8, it leads to benefits including a slight increase in turbidity removal (90.61%), significant improvement in the DOC removal (>55%) and an appreciable drop in residual dissolved Al (approximately 0).

The obtained levels of alum dosage and pH from desirability analysis were applied in confirmatory experiments and the obtained response levels are presented in Table 14 along with the predicted response levels by the desirability function. Table 14 illustrates that the experimental and expected responses were in good agreement.

3.5. Downstream effects examination

It was demonstrated in the previous sections that PMU pre-treatment improved the performance of coagulation/flocculation process. However, the implications of ultrasound application on the quality of the finished water is yet to be explored. Hence, microbes and DBPs levels in water samples treated with control and PMU with coagulation were measured and compared in this section as shown in Fig. 9. It can be noticed that combining PMU with alum coagulation resulted in almost complete removal of total coliform (>98%), whereas control treatment only removed approximately 80% of total coliform. This means that PMU with coagulation requires very little amount of chlorine addition to
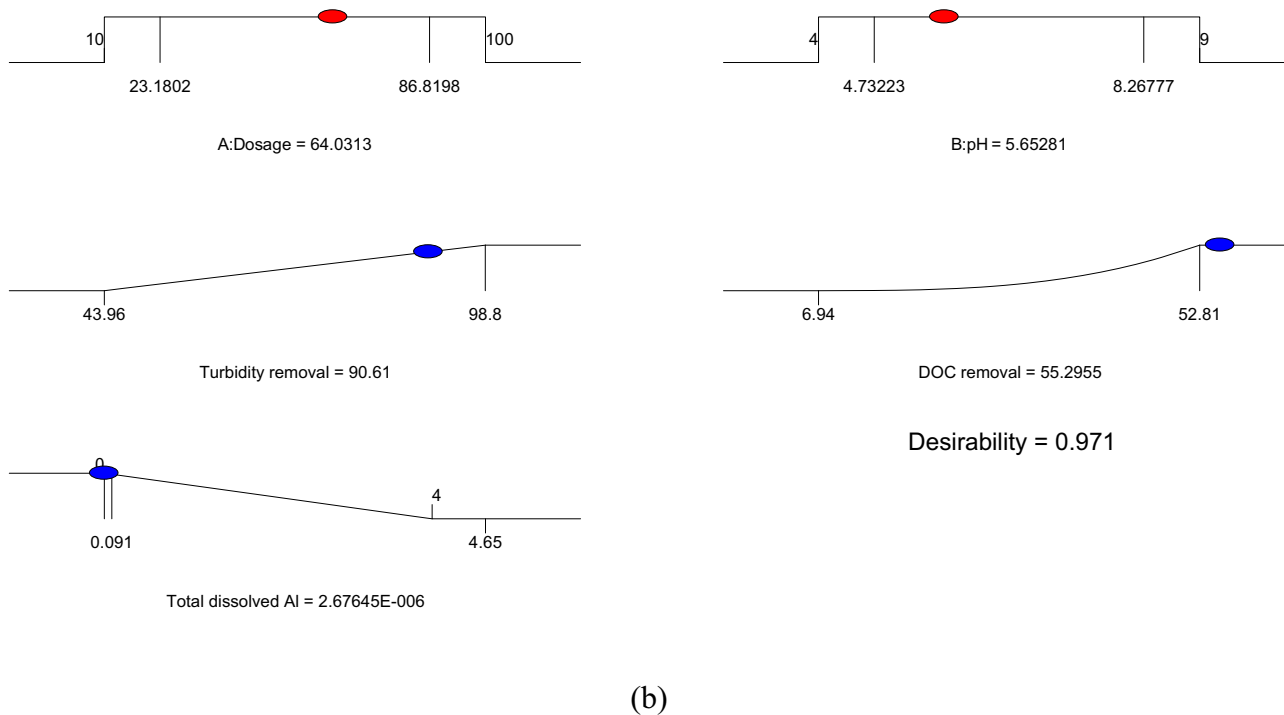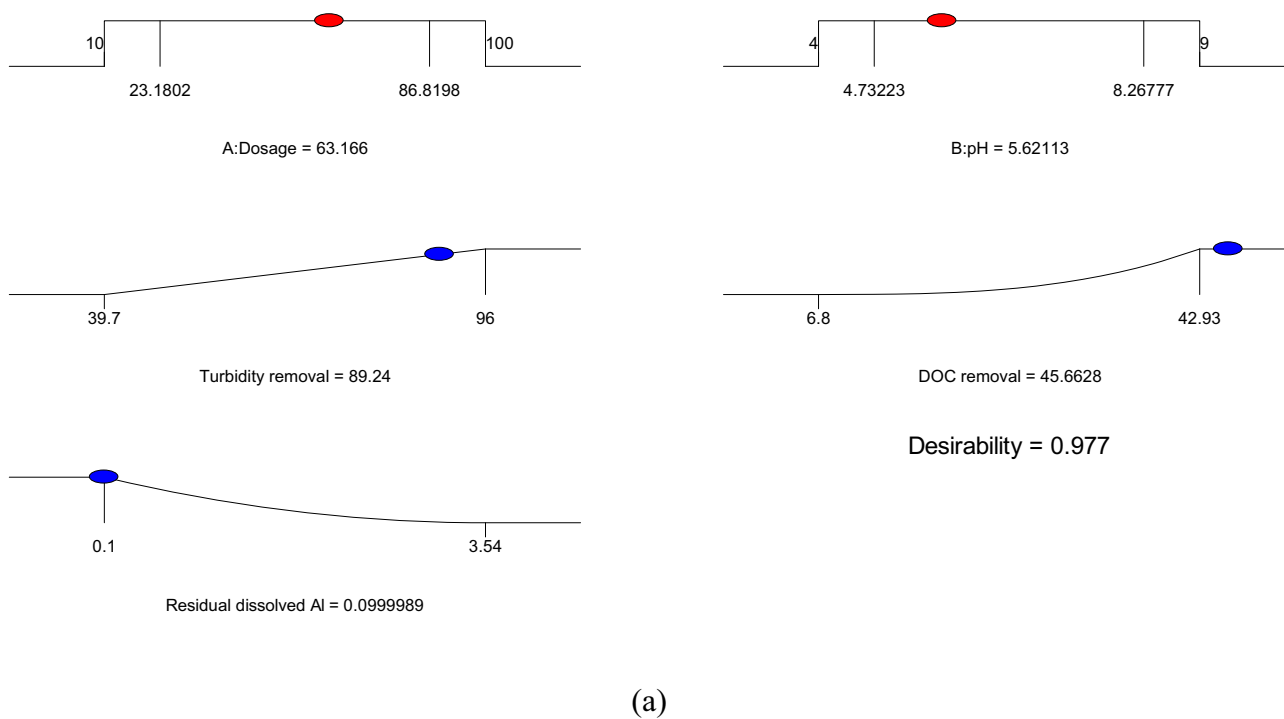
Fig. 8. Desirability plots for optimum levels of experimental factors of (a) control and (b) PMU with coagulation.

make the finished water safe for consumption from microbial contamination perspective.

Fig. 9b shows that the untreated water produced THMFP expressed as ppb of chloroform of ∼250 which is at the maximum contamination level accepted in Australian drinking water [13], while PMU pre-treatment decreased THMFP to ∼200. The reduction of THMFP with PMU pre-treatment is attributed to the reduction of chlorine demand due to DOC and microbial reduction and

degradation of DBPs precursors. PMU pre-treatment decreased the percentage of hydrophobic DOC from 78% to 73% (data not shown) which would reduce THMFP as this DOC fraction has been repeatedly found as a major contributor to DBPs formation [45].

In addition to the positive effects of PMU pre-treatment on the quality of the finished water, it also had a technical advantage by improving sludge sedimentation after flocculation. Fig. 10 shows photographs of treated water by control and PMU with coagulation

Table 14
Results of validation experiments.

Responses	Control		PMU with coagulation	
	Expected value	Experimental value	Expected value	Experimental value
Turbidity removal (%)	89.24	88.61	90.61	90.84
DOC removal (%)	45.67	44.06	55.3	54.55
Residual dissolved Al (ppm)	0.1	0.09	2.7×10^{-6}	0
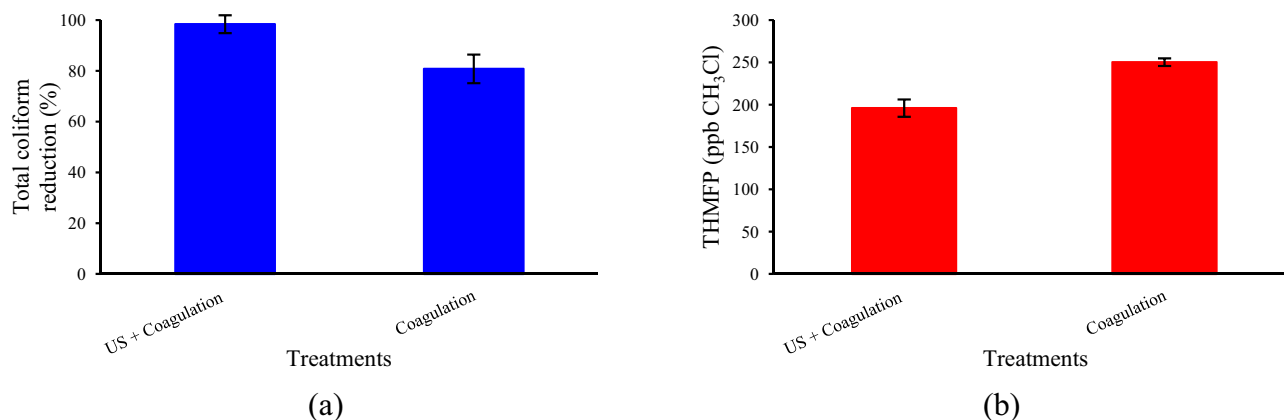
Fig. 9. THMFP (a) and total coliform reduction (b) for water samples treated with control and PMU with coagulation.
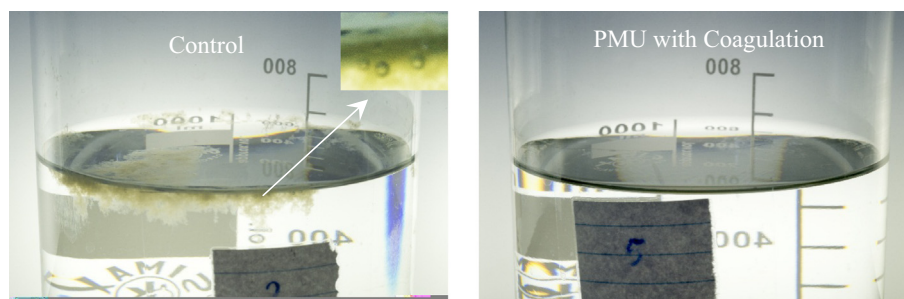
Fig. 10. Effect of ultrasound treatment on sludge separation in coagulation process.

treatments. It can be seen from this figure that water sample treated with control treatment had a floating layer of flocs on the surface, while the surface of water sample pre-treated with PMU was almost clear. Typically, the vigorous mixing of coagulation forces some atmospheric air into the mixed water sample and this excess of air forms bubbles that entrap into the formed flocs making them float. The case is different for the pre-treated sample with PMU as the introduced air into the water sample due to coagulation barely makes up for the lost air during PMU pre-treatment (degassing effect). The presence of floating sludge can be a costly problem particularly for treatment practices that apply sedimentation after coagulation/flocculation as an extra removal technique needs to be put in place to tackle such a problem. This demonstrates that ultrasound application does not only improve the quality of the produced water, it can also reduce treatment cost.

4. Conclusions

The use of PMU as a pre-treatment for alum coagulation at various pH and alum dosage conditions was thoroughly investigated in this study. RSM with CCD design was applied to optimize the effects of alum dosage and pH on turbidity removal, DOC removal and residual dissolved Al of two treatments; control and PMU with

coagulation. First order, second order and interaction effects of alum dosage and pH on measured responses were all found to be significant. Prediction models of the measured responses were developed and tested. The models passed all the adequacy tests and produced predicted values of the responses that were close to their corresponding actual values.

The optimization of the individual responses was carried out using response surface plots. Generally, the untreated and pre-treated water samples with PUS had similar surface plots for all the response reflecting almost identical behavior. In most cases, water samples pre-treated with PUS had higher DOC and turbidity removal and lower Al residuals than the untreated samples. Maximum removal levels of turbidity and DOC were 98.8% and 52% for PMU with coagulation and 96.6% and 43% for control treatment. The minimum residual dissolved Al for PMU with coagulation was lower than that of control treatment (0.094 ppm vs. 0.100 ppm). The multiple response optimization was conducted using desirability function and the results were validated through confirmatory experiments. Desirability value of >0.97 reflects a good agreement between individual and multiple response optimization. Downstream effects of PMU application were evaluated by measuring THMFP and total coliforms of the treated water with PMU with coagulation and compared with that of the untreated

water. It was shown that PMU pre-treatment of alum coagulation increased total coliform removal from 80% to >98% and decreased THMFP from 250 to 200 ppb CH$_3$Cl. PMU pre-treatment application also improved the separation of sludge produced after coagulation/flocculation. These positive outcomes of ultrasound pre-treatment highlight the potential application of this technology in water treatment and encourage large-scale application of this technique.

References

[1] D. Ghernaout, The hydrophilic/hydrophobic ratio vs. dissolved organics removal by coagulation – a review, J. King Saud Univ. Sci. 26 (2014) 169–180.
[2] L. Xing, M.F. Murshed, T. Lo, R. Fabris, C.W.K. Chow, J. van Leeuwen, M. Drikas, D. Wang, Characterization of organic matter in alum treated drinking water using high performance liquid chromatography and resin fractionation, Chem. Eng. J. 192 (2012) 186–191.
[3] A. Matilainen, M. Sillanpää, Removal of natural organic matter from drinking water by advanced oxidation processes, Chemosphere 80 (2010) 351–365.
[4] C.W.K. Chow, J.A. van Leeuwen, R. Fabris, M. Drikas, Optimised coagulation using aluminium sulfate for the removal of dissolved organic carbon, Desalination 245 (2009) 120–134.
[5] R.A. Minear, G. Amy, Disinfection By-Products in Water Treatment. The Chemistry of Their Formation and Control, Taylor & Francis, Boca Raton, Florida, 1995.
[6] W. Yang, J. Chen, X. Li, H. Liang, W.-J. He, G.-B. Li, Using chloramine as a coagulant aid in enhancing coagulation of Yellow River water in China, J. Zhejiang Univ. – Sci. A 8 (2007) 1475–1481.
[7] G. Silvestre, B. Ruiz, M. Fiter, C. Ferrer, J.G. Berlanga, S. Alonso, A. Canut, Ozonation as a pre-treatment for anaerobic digestion of waste-activated sludge: effect of the ozone doses, Ozone: Sci. Eng. 37 (2014) 316–322.
[8] A. Ziylan, N.H. Ince, Ozonation-based advanced oxidation for pre-treatment of water with residuals of anti-inflammatory medication, Chem. Eng. J. 220 (2013) 151–160.
[9] R.A. Al-Juboori, T. Yusaf, L. Bowtell, Energy conversion efficiency of pulsed ultrasound, Energy Proc. 75 (2015) 1560–1568.
[10] R.A. Al-Juboori, V. Aravinthan, T. Yusaf, Impact of pulsed ultrasound on bacteria reduction of natural waters, Ultrason. Sonochem. 27 (2015) 137–147.
[11] C. Driscoll, R. Letterman, Chemistry and fate of Al(III) in treated drinking water, J. Environ. Eng. 114 (1988) 21–37.
[12] Z.L. Yang, B.Y. Gao, Q.Y. Yue, Y. Wang, Effect of pH on the coagulation performance of Al-based coagulants and residual aluminum speciation during the treatment of humic acid–kaolin synthetic water, J. Hazard. Mater. 178 (2010) 596–603.
[13] Australian National Health and Medical Research Council, in: Australian Drinking Water Guidelines 6, 2011.
[14] Y. Wang, K. Chen, L. Mo, J. Li, J. Xu, Optimization of coagulation–flocculation process for papermaking-reconstituted tobacco slice wastewater treatment using response surface methodology, J. Ind. Eng. Chem. 20 (2014) 391–396.
[15] M. Mourabet, A. El Rhilassi, H. El Boujaady, M. Bennani-Ziatni, R. El Hamri, A. Taitai, Removal of fluoride from aqueous solution by adsorption on Apatitic tricalcium phosphate using Box–Behnken design and desirability function, Appl. Surf. Sci. 258 (2012) 4402–4410.
[16] A. Van Nieuwenhuijzen, J. Van der Graaf, Handbook on Particle Separation Processes, IWA Publishing, London, 2011.
[17] Food-Safety-and-Regulatory-Activities-Victorian, in: Guidelines for Private Drinking Water Supplies at Commercial and Community Facilities, Government Department of Health, Melbourne, Victoria, Melbourne, 2009.
[18] R.A. Al-Juboori, T. Yusaf, L. Bowtell, V. Aravinthan, Energy characterisation of ultrasonic systems for industrial processes, Ultrasonics 57 (2015) 18–30.
[19] R. Fabris, C.W. Chow, M. Drikas, Comparison of coagulant type on natural organic matter removal using equimolar concentrations, J. Water Supply: Res. Technol. – AQUA 61 (2012) 210–219.
[20] M.J. Farré, H. King, J. Keller, W. Gernjak, N. Knight, K. Watson, G. Shaw, F. Luesch, R. Sadler, M. Bartkow, P. Burrell, Disinfection by-products in South East Queensland: assessing potential effects of transforming disinfectants in the SEQ water grid, in: D.K. Begbie, S.L. Wakem (Eds.), Urban Water Security Research Alliance Science Forum and Stakeholder Engagement, Building Linkages, Collaboration and Science Quality, CSIRO Publishing, Brisbane, Australia, 2011, pp. 94–101.
[21] L.S. Clesceri, E.W. Rice, A.E. Greenberg, A.D. Eaton, in: Standard Methods for Examination of Water and Wastewater: Centennial Edition, American Public Health Association, Washington, D.C., 2005.
[22] R.A. Al-Juboori, T. Yusaf, P.A. Pittaway, Exploring the correlations between common UV measurements and chemical fractionation for natural waters, Desalin. Water Treat. 1–12 (2015).
[23] R.A. Al-Juboori, T. Yusaf, V. Aravinthan, P.A. Pittaway, L. Bowtell, Investigating the feasibility and the optimal location of pulsed ultrasound in surface water treatment schemes, Desalin. Water Treat. 1–19 (2015).
[24] W. Subramonian, T.Y. Wu, S.-P. Chai, An application of response surface methodology for optimizing coagulation process of raw industrial effluent using Cassia obtusifolia seed gum together with alum, Ind. Crops Prod. 70 (2015) 107–115.
[25] T.K. Trinh, L.-S. Kang, Application of response surface method as an experimental design to optimize coagulation tests, Environ. Eng. Res. 15 (2010) 63–70.
[26] J.-P. Wang, Y.-Z. Chen, X.-W. Ge, H.-Q. Yu, Optimization of coagulation–flocculation process for a paper-recycling wastewater treatment using response surface methodology, Colloids Surf. A: Physicochem. Eng. Aspects 302 (2007) 204–210.
[27] S. Ghafari, H.A. Aziz, M.H. Isa, A.A. Zinatizadeh, Application of response surface methodology (RSM) to optimize coagulation–flocculation treatment of leachate using poly-aluminum chloride (PAC) and alum, J. Hazard. Mater. 163 (2009) 650–656.
[28] K. Simarani, M.N. Saat, M.S. Mohamad Annuar, Efficient removal of azo dye by grated copra biomass, Desalin. Water Treat. 1–8 (2015).
[29] T.P. Ryan, Modern Experimental Design, Wiley, New Jersey, 2006.
[30] A. Aggarwal, H. Singh, P. Kumar, M. Singh, Optimizing power consumption for CNC turned parts using response surface methodology and Taguchi's technique—a comparative analysis, J. Mater. Process. Technol. 200 (2008) 373–384.
[31] M. Li, Y. Yu, Y. Feng, J. Tan, Optimization and modeling of preparation conditions of poly-Si-Fe-Zn (PSFZ) coagulant from industrial wastes using response surface methodology, Desalin. Water Treat. 1–10 (2015).
[32] M. Ghasemlou, F. Khodaiyan, S. Gharibzahedi, Enhanced production of Iranian Kefir grain biomass by optimization and empirical modeling of fermentation conditions using response surface methodology, Food Bioprocess Technol. 5 (2012) 3230–3235.
[33] N.G. Pizzi, Water Treatment: Principles and Practices of Water Supply Operations Series, American Water Works Association, Denver, 2011.
[34] S.F.A. Halim, A.H. Kamaruddin, W.J.N. Fernando, Continuous biosynthesis of biodiesel from waste cooking palm oil in a packed bed reactor: optimization using response surface methodology (RSM) and mass transfer studies, Bioresour. Technol. 100 (2009) 710–716.
[35] A.L. Ahmad, S. Ismail, S. Bhatia, Optimization of coagulation–flocculation process for palm oil mill effluent using response surface methodology, Environ. Sci. Technol. 39 (2005) 2828–2834.
[36] M.S. Bhatti, A.S. Reddy, R.K. Kalia, A.K. Thukral, Modeling and optimization of voltage and treatment time for electrocoagulation removal of hexavalent chromium, Desalination 269 (2011) 157–162.
[37] C. Hong, H. Hao, W. Haiyun, Process optimization for PHA production by activated sludge using response surface methodology, Biomass Bioenergy 33 (2009) 721–727.
[38] A. Boubakri, N. Helali, M. Tlili, M.B. Amor, Fluoride removal from diluted solutions by Donnan dialysis using full factorial design, Korean J. Chem. Eng. 31 (2014) 461–466.
[39] D.J. Pernitsky, Coagulation 101, in: Alberta Water and Wastewater Operators Association (AWWOA) Annual Seminar, Alberta, Canada, 2004.
[40] F. Xiao, B. Zhang, C. Lee, Effects of low temperature on aluminum(III) hydrolysis: theoretical and experimental studies, J. Environ. Sci. 20 (2008) 907–914.
[41] P. Senthil Kumar, V.M. Centhil, R. Kameshwari, M. Palaniyappan, V.D. Kalaivani, K.G. Pavithra, Experimental study on parameter estimation and mechanism for the removal of turbidity from groundwater and synthetic water using Moringa oleifera seed powder, Desalin. Water Treat. (2015) 1–10.
[42] A. Diaz, N. Rincon, A. Escorihuela, N. Fernandez, E. Chacin, C.F. Forster, A preliminary evaluation of turbidity removal by natural coagulants indigenous to Venezuela, Process Biochem. 35 (1999) 391–395.
[43] W. Subramonian, T.Y. Wu, S.-P. Chai, A comprehensive study on coagulant performance and floc characterization of natural Cassia obtusifolia seed gum in treatment of raw pulp and paper mill effluent, Ind. Crops Prod. 61 (2014) 317–324.
[44] W. Xu, B. Gao, Q. Yue, Y. Wang, Effect of shear force and solution pH on flocs breakage and re-growth formed by nano-Al13 polymer, Water Res. 44 (2010) 1893–1899.
[45] Y.C. Soh, F. Roddick, J. van Leeuwen, The impact of alum coagulation on the character, biodegradability and disinfection by-product formation potential of reservoir natural organic matter (NOM) fractions, Water Sci. Technol. 58 (2008) 1173–1179.

Summary-Objective 4

The questions pertaining to the optimum location and most energy efficient operating parameters of ultrasound were carefully addressed in the previous objectives. The performance of ultrasound at the optimum operating parameters in the nominated location was tested in objective 4 (*paper IX*). Coagulation treatments were conducted using alum. Surface response methodology was applied to identify alum dosage and pH range that results in the highest removal of microbes and DOC, and minimal Al residuals. THMFP was measured for untreated and ultrasonically pre-treated water samples to gauge the downstream effects of ultrasound as a pre-treatment for coagulation. It was found that ultrasound significantly increased DOC and microbes' removal and slightly decreased Al residuals. Ultrasound pre-treatment also reduced the formation of DBPs (measured as THMFP) and improved the settling of coagulation sludge. These promising results formed a motive for scaling up ultrasound technology for water treatment purposes, which will be thoroughly addressed in the next paper.

Paper X

Al-Juboori, R. A., Bowtell, L. A., Yusaf, T. & Aravinthan, V., Insights into the scalability of magnetostrictive ultrasound technology for water treatment applications, *Ultrasonics Sonochemistry*, (2016), 28, 357-366.

Insights into the scalability of magnetostrictive ultrasound technology for water treatment applications

CrossMark

Raed A. Al-Juboori [a,*], Leslie A. Bowtell [b], Talal Yusaf [b], Vasantha Aravinthan [a]

[a] School of Civil Engineering and Surveying, Faculty of Health, Engineering and Sciences, University of Southern Queensland, Toowoomba, 4350 QLD, Australia
[b] School of Mechanical and Electrical Engineering, Faculty of Health, Engineering and Sciences, University of Southern Queensland, Toowoomba, 4350 QLD, Australia

ARTICLE INFO

ABSTRACT

To date, the successful application of large scale ultrasound in water treatment has been a challenge. Magnetostrictive ultrasound technologies for constructing a large-scale water treatment system are proposed in this study. Comprehensive energy evaluation of the proposed system was conducted. The effects of chosen waveform, scalability and reactor design on the performance of the system were explored using chemical dosimetry. Of the fundamental waveforms tested; sine, triangle and square, the highest chemical yield resulted from the square wave source. Scaling up from the 0.5 L bench-scale system to the 15 L large-scale unit resulted in a gain of approximately 50% in sonochemical efficiency (SE) for the system. The use of a reactor tank with 45° inclined sides further increased SE of the system by 70%. The ability of the large scale system in removing contaminants from natural water samples was also investigated. The results revealed that the large-scale unit was capable of achieving a maximum removal of microbes and dissolved organic carbon (DOC) of 35% and 5.7% respectively at a power density approximately 3.9 W/L. The results of this study suggest that magnetostrictive ultrasound technology excited with square wave has the potential to be competitive in the water treatment industry.

© 2015 Elsevier B.V. All rights reserved.

1. Introduction

Ultrasound technology has gained popularity in both research and industrial investigations owing to its versatile applications. It has been extensively used in a wide range of applications such as cleaning, chemical synthesis, food processing, fuel preparation and environmental remediation [1–3]. The reason behind such a wide use of ultrasound is the attractive merits of this technology [4–6] such as;

(1) Compact size of the ultrasonic equipment
(2) Ease of installation and/or retrofitting the existing systems using ultrasound equipment
(3) Low maintenance cost
(4) Readiness of ultrasound technology to be automated
(5) Chemical-free technology

The only drawback of ultrasound technology is the relatively high energy requirements for operation, however, this is valid only for some applications where the conventional treatments require

low energy compared to ultrasound. For instance, in food processing industries, ultrasound has competitive energy requirements as compared to the conventional homogenization or thermal treatments [4]. Therefore, ultrasound application in food processing has flourished in recent years with successful large-scale implementations. In some other applications such as water treatment, the conventional treatment methods (e.g. chemical disinfection) require lower operational energy than ultrasound. Hence, the application of ultrasound in water treatment practices did not receive much attention in the past few decades. Recently, the public awareness of the harmful effects of the by-products of chemical treatments on human health and the environment (e.g. production of disinfection by-products (DBPs)) have rekindled the interest in the application of ultrasound in water treatment [7]. However, the perceived high operational energy is still a major hindrance for applying ultrasound on a large-scale as a chemical-free water treatment method.

The potentially high energy demand of ultrasound application for water treatment can be reduced through optimizing ultrasonic reactor design and the operating parameters for ultrasonic processes [8]. There are plethora of design configurations proposed in the literature for improving ultrasonic performance in specific applications such as water treatment. Details regarding these designs can be found in [9]. The reactor designs suggested in the

literature focused on improving important aspects for large-scale applications such as the uniformity of ultrasonic effects via using multiple transducers [10], capability to operate in a flow regime using Sonitube [11] and maximizing the utilization of ultrasonic energy through adapting the reflection feature in the reactors [12,13].

The effect of some of the operating parameters such as power, frequency and treatment time on the performance of ultrasound in removing water contaminants were extensively studied and the outcomes can be summarized as follows;

(i) Increasing power increases contaminants removal to a certain level after which increasing the power would have minimal or no effect on contaminants removal. This phenomenon is mainly attributed to the formation of bubbles cloud near to the irradiation source at high power levels causing scattering to ultrasound energy with shielding effects. This can be alleviated through operating ultrasound on a pulse mode [14].

(ii) Applying low frequency allows the collapsing bubbles to grow larger leading to a sever collapse with a very energetic physical effects (high pressure and temperature) [15]. Such bubble collapse conditions suit application that mainly rely on the physical effects of ultrasound such as microbial inactivation [16]. On the contrary, applying high frequency ultrasound results in gentler bubbles collapse, however, the number of collapsing bubbles is higher. Hence, the amount of chemical species produced (e.g. OH· and H_2O_2) is higher resulting in better chemical activities [17]. Ultrasound with high chemical activities is best utilized for removing contaminants such as DOC from water. Nevertheless, DOC removal with ultrasound requires higher power and longer treatment time [18] and its removal levels are much lower than those of microbes with the same power level. Thus, it would be wise to apply frequency ranges that suit the microbial removal for water treatment application. Moreover, low frequency ultrasound is known to be more efficient in distributing the acoustic energy in large-scale reactors than high frequency ultrasound [19].

(iii) Increasing treatment time increases contaminants removal with ultrasound. However, microbes' removal with ultrasound is likely to follow an exponential trend and increasing the treatment time after a certain limit would have a little effect on the removal levels.

The less explored ultrasonic operating parameter is the effect of the waveform used for exciting ultrasonic transducers on the performance of ultrasound. Only limited studies have investigated this aspect [20].

When considering the scale-up of ultrasound technology, the way through which ultrasound waves are generated becomes important. There are three types of transducers based on the mechanisms of generating ultrasound waves; liquid-driven, magnetostrictive and piezoelectric transducers [21]. The last two types are the most common ones. The vibration generated in magnetostrictive transducers is due to the contraction and expansion of the ferromagnetic core material caused by the change in the magnetic field around it (induced by electric current). The vibration of the piezoelectric transducers emanates from the change in the dimensions of the crystalline material when exciting it with electrical current. Table 1 shows a comparison between the characteristics of the magnetostrictive and piezoelectric transducers.

Despite the clear advantages of magnetostrictive transducers (Table 1), there have been hardly any thorough investigations conducted on the use of this type of transducers for water treatment applications on a large-scale. In this work, we attempted to provide

Table 1
Characteristics of piezoelectric and magnetostrictive transducers (information adapted from [22–24].

Piezoelectric transducers	Magnetostrictive transducers
1. Relatively inexpensive	1. Higher capital outlay than piezoelectric transducers
2. Small and light	2. Heavy and bulky
3. Cannot withstand high temperature >150 °C	3. Tolerant of high temperatures >250 °C
4. Susceptible to mechanical impact	4. Extremely resistant to mechanical impacts
5. Age quickly	5. Have a prolonged working life >∼20 years
6. Have relatively lower strain in static conditions as compared to Terfenol-D	6. New alloy core (e.g. Terfenol-D) has large field-induced strain in static conditions
7. Good coupling coefficient (slightly lower than Terfenol-D)	7. Superior coupling coefficient
8. Good dynamic strain (lower than that of Terfenol-D at resonance)	8. Dynamic strain of Terfenol-D is higher than the piezoelectric transducers at resonance

some insights into the application of magnetostrictive ultrasonication for water treatment focusing on the effects of waveform, scalability and reactor design on the performance of ultrasound. New design for ultrasonic reactor that adopted the notions of multi-transducers and reflection feature was proposed and tested in this study. Energy and chemical characterisations of the designed ultrasonic system were conducted. The potency of the system in removing contaminants from natural water was also examined. The targeted contaminants were total coliform and DOC. The change in DOC structure was studied through single wavelength and UV ratios analysis at 254 and 280 nm and ratios of 254/204, 250/365 and 254/436. Absorbance at 254 and 280 nm was applied to detect change in humification and aromaticity, respectively. UV ratios of 254/204, 250/365 and 254/436 were measured to track changes in oxygen containing aromatic functional groups, molecules size and the ratio of UV absorbance to color forming moieties of DOC [7]. Absorbance at 250 nm represents small sized molecules of DOC, whereas absorbance at 365 nm represents large sized molecules.

2. Materials and methods

2.1. Ultrasonic system

The experimental setup used in this work is illustrated in Fig. 1a. The setup is comprised of three parts; ultrasonic system, power amplifier and associated signal source and the cooling system. The ultrasonic system consists of two Terfenol-D ultrasonic magnetostrictive transducers (CU18A, Etrema Products, Inc.) each connected to a titanium horn ($\varnothing$ = 19 mm). The frequency range of the transducers used is 0–20 kHz. The transducers were mounted on a detachable acrylic top cover of a custom made metal tank. The features and dimensions of the tank are shown in details in Fig. 1b. The maximum capacity of the tank is 17 L, however the applied working volume in this work was 15 L. The tank was designed with base inclines of 45° to reflect the waves emitting from the horns to the center of the tank, thus obtaining a good distribution of ultrasonic events in the liquid. The tank was designed with two acrylic windows on the longitudinal sides of the tank. The two purposes of the acrylic windows were to precisely locate the depth of the sampling point in the irradiating liquid and to observe the sonication events during operation. The acrylic top cover has three openings. The two openings close to the edges ($\varnothing$ = 32 mm) were used as an access for the ultrasonic horns and
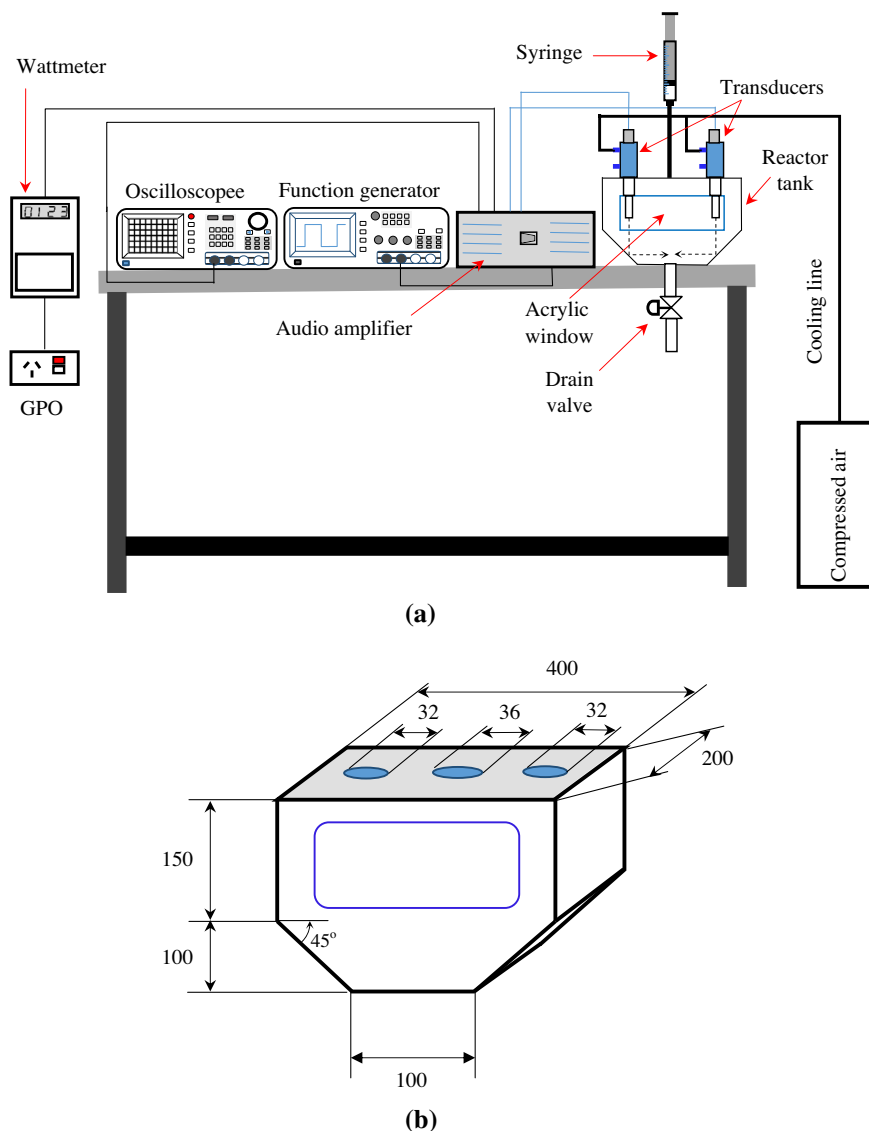
Fig. 1. (a) Schematic diagrams of (a) the experimental setup and (b) reactor tank (measurements shown on the figure are in mm).

the middle one ($\varnothing$ = 36 mm) was used for sampling using a syringe and PTFE tubing as shown in Fig. 1a.

The transducers were driven using a two channel audio power amplifier (IP-8.5C Peavey, USA), the maximum power with the channels bridged is 1100 W into a 2 Ω load. This amplifier allowed for the running of the transducers on different waveforms (e.g. sine, square or triangle) using a function generator (Tektronix, AFG 3022B) as the precise signal source. The electrical power drawn by the amplifier from the general purpose outlet (GPO) was measured using a high precision wattmeter (EDMI MK7C Single Phase Smart Meter). The electrical power consumed by the transducers was measured using an oscilloscope (Tektronix, TPS2014) equipped with a current probe (Tektronix, TCP 202). The power measurement equipment and ultrasonic system were placed on a stainless steel test bench. The transducers were constantly cooled during operation using compressed air as shown in Fig. 1a. Although at the power levels used, it should be noted that the cooling requirement was very low.

2.2. Experimental procedure

The experimental work was conducted in three phases; energy characterisation of system, chemical yield measurements and system performance investigation using natural water samples. Prior to the commencement of the experimental work, a frequency sweep was performed in the range 0–20 kHz with the aim of finding the resonant frequency of the transducers for the applied waveforms. The resonance frequency was found to be approximately 17.8 kHz with small variations for different waveforms. Thereafter, the resonance frequency was applied and thorough electrical and calorimetric power measurements were conducted.

Following the power measurements, the chemical throughput of the ultrasonic system for each different waveform was determined by measuring the productivity of OH· and H_2O_2 in 0.5 L using a single transducer at the respective calorimetric power of each waveform. The calorimetric power was measured following the procedure detailed in [25]. The calorimetric power of a single transducer excited with square, sine and triangle waves were found to be 9.5, 9 and 9.3 W, respectively. The optimum waveform was identified based on the chemical measurements. Later on, the optimum waveform was applied in a larger volume of 15 L (large-scale) using two transducers to test the effect of scaling up on the system performance. It is worth mentioning that single transducer was used at calorimetric power of 9.5 W for 0.5 L experiments, while two transducers at calorimetric power of 19 W were used for 15 L experiments. For fair comparison between the two scales,

SE was used where the effects of power and reaction volume were taken into account (see Section 2.4). To gauge the effect of the inclination feature of the tank on the performance of the system, a rectangular tank with the same working volume was used and chemical measurements were applied at the optimum waveform for the two configurations. It is important to note that only H_2O_2 measurements were conducted with the experiments that involved the use of large volumes.

The performance of the large-scale ultrasonic system in removing contaminants from natural water samples was also tested. The contaminants that were targeted in this work were DOC and total coliform. Two sets of calorimetric power were applied in natural water treatment experiments; 19 and 58 W. The system was operated for 15 min during which samples were taken after each 5 min. All the treatments were conducted in triplicate.

2.3. Sonochemical efficiency measurements

Exposing liquid medium such as water to ultrasound waves creates two types of effects; physical and chemical effects. The physical effects of sonication represented by the energetic turbulences, shock waves and high temperature and pressure, while the chemical effects are due to highly oxidative agents such as OH· and H_2O_2 produced from bubbles collapse [8]. The physical effects of ultrasound are ultimately converted into thermal energy causing temperature rise in the irradiated liquid measured as calorimetric power [26]. In the field of sonochemistry, the amount of the oxidative species produced in moles is normalized by the calorimetric energy in joules to produce the so-called sonochemical efficiency [27]. SE is an important indicator for measuring the performance of ultrasonic systems under certain operating conditions.

In this study, SE of ultrasound system at different operating conditions was measured based on the production of OH· and H_2O_2 as the former is important for the reactions occurring in the thermolytic center and the vicinity of collapsing bubbles [28] while the latter plays an important role in the bulk reactions. OH· and H_2O_2 were measured using potassium iodide (KI) dosimetry [27] and iodometric method [29], respectively. OH· and H_2O_2 oxidize iodine ions into tri-iodide ions through a series of reactions [25]. The amount of the produced tri-iodide can be measured spectrophotometrically at a wavelength of 355 nm and molar absorptivity $(\varepsilon) = 26,303$ L/mol cm.

KI solution was prepared by dissolving 0.1 mol of KI salt in 1 L of deionised water. Prior to ultrasound treatments, KI solution was air saturated by introducing filtered air bubbles into the solution for 30 min [27]. H_2O_2 was produced by ultrasonically irradiating deionised water, and measured using iodometric method [29]. In this method, aliquot of the ultrasonically treated deionised water was mixed with equal amounts of solutions A and B. Solution A was prepared by dissolving 33 g of KI, 1 g of NaOH and 0.1 g of $(NH_4)_6Mo_7O_{24}·4H_2O$ in 500 mL of deionised water. Solution B was made of 10 g of KHP in 500 mL of deionised water. The final mixture of A, B and treated water was left for 5 min in the dark prior to UV measurements [30].

The spectrophotometric measurements were conducted using JENWAY UV/Vis spectrophotometer, model 6705 with a single cell holder. Quartz cuvette with path length of 1 cm was used for carrying samples in the spectrophotometric analysis. Deionised water was used as baseline. The effect of the inadvertent oxidation of iodine due to exposure to light during treatments and measurements periods was deduced from the effect of ultrasound treatment by subtracting the absorbance of KI and the mixture of A and B solutions from that of the treated solution for each run. All the chemicals used in these measurements were of analytical grade quality.

2.4. Natural water samples

Water samples were collected from Narda lagoon which is located in Southeast Queensland (SEQ), Australia. The samples were collected using pre-cleaned 5 L plastic containers. Some of the measured characteristics of Narda water are presented in Table 2.

2.5. Water treatment measurements

The concentrations of contaminants in Narda water were measured before and after ultrasound treatments to evaluate the performance of the designed ultrasonic system in water treatment applications. The change in DOC concentration was measured applying the standard high temperature combustion method 5310 B using total carbon analyser (TOC-V$_{CSH}$, SHIMADZU, Australia) equipped with an auto-sampler (ASI-V) [31]. Triplicate injections were made which resulted in coefficient of variance of <0.02.

The change in the structure of DOC due to ultrasound treatments was tracked using surrogate UV measurements. Single wavelength analyses at 254 and 280 nm and UV ratio analyses of 254/204, 250/365 and 254/436 were conducted. The single wave measurements at 254 and 280 nm were normalized by the DOC concentration to produce the specific UV measurements denoted as SUVA. Measuring SUVA allows detecting the change in DOC structure rather than DOC concentration [7]. It can be seen from Table 2 that the levels of the interfering anions in Narda water are too low to cause any change in UV absorbance [7]. The anions such as nitrate, chloride, phosphate and sulfate were measured applying the standard method 4110 B using Ion Chromatography system ICS-2000. The concentration of iron in Narda water was quantified using atomic absorption spectrophotometer model AA-7000 (SHIMADZU, Australia) following the direct air–acetylene flame method [31]. UV measurements were performed using the spectrophotometer described in Section 2.4. Water samples were filtered through 0.45 μm prior to DOC, anions and UV measurements. Total coliform concentration was measured applying the standard membrane filtration method 9222 B using M-ColiBlue24® media (Millipore, Australia) [32].

3. Power analysis

For a practical ultrasonic system to be viable at an industrial scale, it must have a reasonable system electrical efficiency. It is also an important feature of a practical system to allow power to be easily adjusted and have that level easily confirmed by surrogate measurements. A further consideration was the waveform shape. Amplification of a complicated waveform such as a sine wave required a linear amplifier as per Fig. 2, whereas a simple square waveform is readily produced by a basic H-Bridge topology

Table 2
Properties of Narda water.

Properties	Levels
pH	6.90
Total coliform (CFU/100 mL)	250
DOC (mg/L)	9.81
Iron (mg/L)	0.37
Nitrate (mg/L)	n.a[*]
Chloride (mg/L)	39
Phosphate (mg/L)	0.21
Sulfate (mg/L)	n.a[*]

[*] n.a indicates that the concentration of the ion is below the detection limit of measurement method.

as shown in Fig. 3. Therefore our testing was done using a linear amplifier.

In order to conduct a fair comparison of the system with a range of different waveforms, the approach chosen was to supply the transducers with a consistent voltage of 60 V rms. The resulting current waveforms produced then converted this electrical energy into changes in electrical field causing mechanical displacement energy at the transducers probe tip.

The linear amplifier system described in Fig. 2 is a high quality class A/B audio amplifier. It consists mainly of a filtered power supply, push–pull transistor amplifier stage and final filter stage to minimise distortion. This effectively allows any shape waveform with frequency components of 20 kHz or less to be amplified. In typical audio applications the output drive is optimized for a 4 Ω or 8 Ω loads. For a small output power as is the case in our setup of 20 W at 20 kHz this would typically mean a fairly small voltage requirement of less than 15 V rms to drive an 8 Ω load in an audio application. Unfortunately the magnetostrictive transducers we used are of the order of 60 Ω and mainly inductive by nature. In order to drive this higher impedance, highly inductive load of 60 V rms was required. Consequently for an off the shelf audio amplifier a relatively high power unit was required in order to deliver the desired wattage into a high impedance load. In fact an 1100 W rated unit was the one chosen as suitable in our case. This enabled easy experimentation on a range of waveforms with a standard design, although amplifier efficiency at the power level used was hardly ideal. As the square wave is simple to generate, a simple digital amplifier class D (Fig. 3) would be used in future, designed such that the high impedance transducers would have a lesser impact than it did on the standard amplifier class A/B design.

The respective efficiency curves for both class A/B and class D amplifier types are shown in Fig. 4. It is worth noting for both cases that either linear or digital amplifiers are capable of driving transducer loads in the order of several kilowatts, however at such levels the class D or digital H-bridge is both far more simple to control and offers much higher efficiency than it's linear counterpart.

The digital H-bridge efficiency characteristic is dominated by the switching losses that can be represented by the following formulae [34]:

$$E_{on} = 1/2\ Vc \cdot I \cdot t_{on} \tag{1}$$

$$E_{off} = 1/2\ V_c \cdot I \cdot t_{off} \tag{2}$$

where, Vc is DC bus voltage, I is on-state current, t_{on} is the insulated gate bipolar transistor (IGBT) turn on time and t_{off} is the IGBT turn off time.

Other elements of the system such as the base waveform generation and gate drive systems consume relatively small amounts of 1 W and 3 W respectively and these losses are independent of the output power delivered.
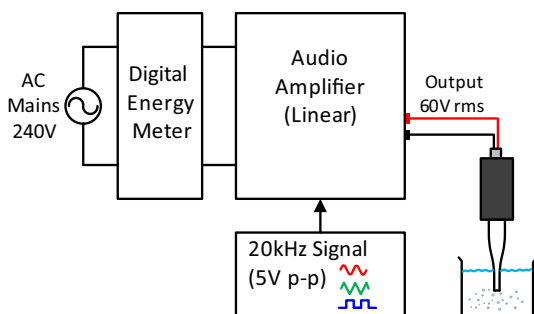

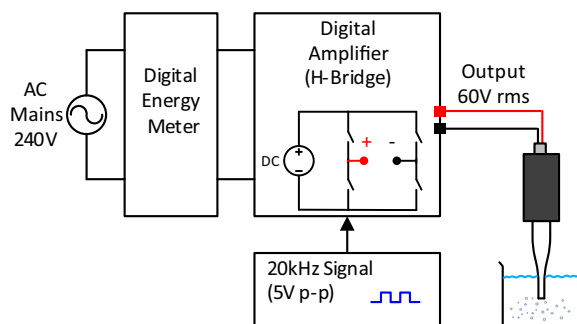**Fig. 2.** Block diagram of linear analog ultrasonic system.

Fig. 3. Block diagram of digital ultrasonic system.

For a digital amplifier system capable of 5–10 kW, full-load efficiencies >90% are achievable at load factors above 40% and easily verified with the above loss assumptions. At lower power levels, circa 20 W efficiencies of the same large digital amplifier systems is closer to 60% increasing to approximately 70% at the 100 W level. By comparison, the linear amplifiers would have efficiency of around 10% for respective light load (20 W) [35].

4. Results and discussions

4.1. Effect of waveform on chemical yield

The produced amounts of tri-iodide with different waveforms for treatment times of 5, 10 and 15 min are shown in Fig. 5. The values presented in Fig. 5 and the other figures onward are the mean values of three measurements and error bars represent the standard error of the measurements. It is clear from this figure that square wave had the highest production of OH· followed by sine and triangle waves. The fitting lines reveal that square and sine waves had the same production rates of OH·, 0.0019 µmol/s, whereas triangle wave resulted in a smaller production rate of 0.0015 µmol/s. The difference between OH· production for square and sine waves is almost constant throughout all the applied treatment times. OH· production for sine and triangle waves is very close for treatment time of 5 min, but it started diverging away as the treatment time increased and it became very noticeable at a treatment of 15 min (difference of ~0.2 µmol). To gain better understanding of the effect of waveform on the chemical yield of the ultrasonic system, sonochemical efficiency of iodine oxidation at 5 min treatment was plotted for different waveform in Fig. 6. This figure also shows that operating the system on a square wave resulted in the best chemical throughput of the system.

Hydrogen peroxide production with different waveforms was also explored and the results are presented in Fig. 7. The production trends of H_2O_2 were similar to that of OH· except that the amounts produced are lower. The difference between the production of H_2O_2 with square wave as opposed to sine wave was higher than the difference in the production levels of OH· for the two waveforms. This difference can be seen even clearer in the SE of H_2O_2 measurements as revealed in Fig. 8. This difference suggests that the waveform has an effect on the recombination reactions of the hydroxyl radicals.

The trends obtained in the chemical measurements are in agreement with the observations reported in the literature. In a comparison study between the performances of ultrasonic system with different waveforms in producing stable emulsion of biodiesel [36], it was found that the square wave results in the best product as compared to sine, cosine and saw-tooth waves. Emulsions preparation requires efficient physical and chemical activities of ultrasound and that is what the square wave demonstrated in this
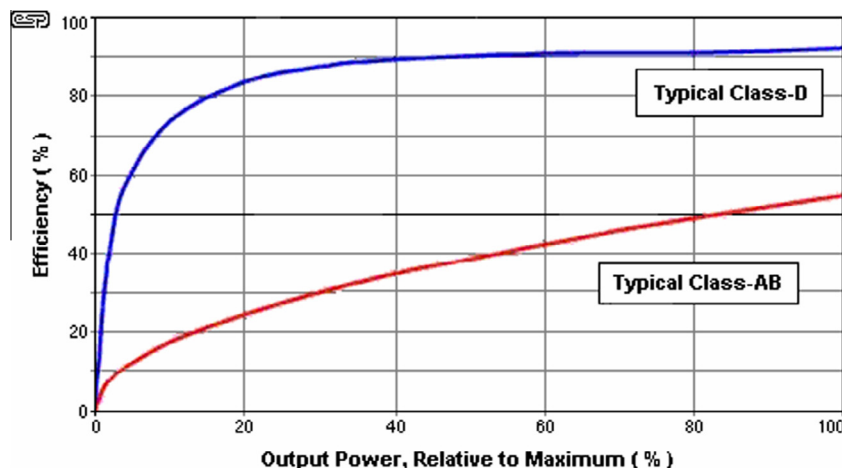
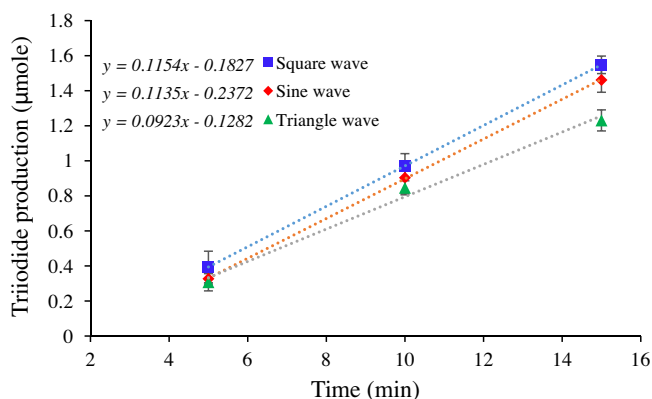**Fig. 4.** Efficiency curve vs. relative output power for linear (class-AB) and digital (class-D) amplifiers [33].

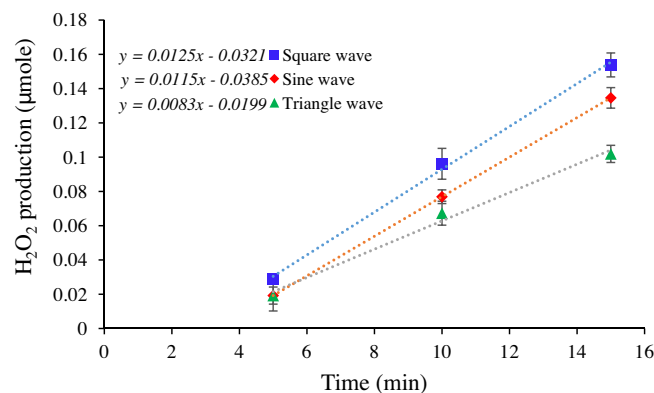**Fig. 5.** Tri-iodide production with different waveforms.

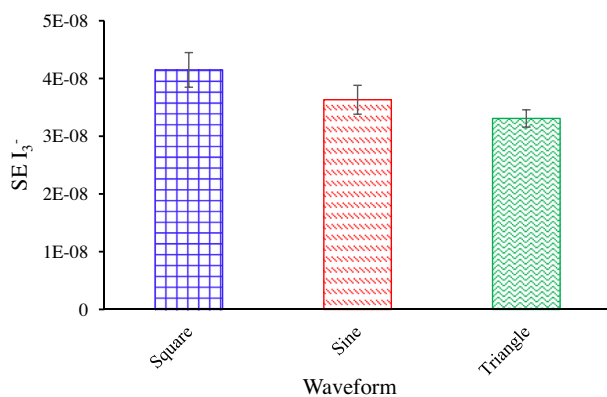**Fig. 7.** Hydrogen peroxide production at different waveform.

Fig. 6. Sonochemical efficiency based on tri-iodide production for different waveforms.

study as it produced the highest calorimetric power and chemical yields. Another study investigated the effect of the same waveform settings on the efficiency of ultrasound in micro-feeding of powder into solid substrates also confirmed that ultrasound systems perform better with square wave as compared to the other waveforms [37].

The high performance of ultrasound with the square wave as opposed to the other waveforms is attributed to the better displacement of the transducers when excited with square wave. This is evident through the wave analysis of the input current to the transducers for different waveforms at a fixed peak-to-peak voltage of 60 V rms as illustrated in Fig. 9a. At a fixed voltage, the vibration of the transducers are directly related to the change in the current. As shown in Fig. 9a, the square wave has the highest peak-to-peak current change (1.94 A) followed by triangle (1.56) and sine (1.48 A). Suomi, Cleveland and Edwards [38] reported a similar finding, as they found that the sine amplitude modulation had a lower peak-to-peak displacement as compared to the square amplitude modulation at frequency of 3.3 MHz. In addition, square wave offers wider frequency tolerance window as compared to triangle and sine waves, and this is clear from the transducers response in a form of current to the change in frequency as demonstrated in Fig. 9b. Small changes in the irradiating media due to degassing effects or temperature rise can shift the resonance frequency of the transducer. Therefore, having a very narrow tolerance window for frequency change as it is the case in the sine wave can potentially reduce the performance of ultrasound. This problem can be tackled by implementing tracking and control systems in the generator which makes it expensive to manufacture. Hence, square wave would be a practical and economic option for designing large-scale ultrasonic systems for water treatment. Based on that, square wave will be the only waveform applied in the upcoming investigations of this work.

4.2. Effect of scaling-up on chemical yield

Chemical measurements were also applied to investigate the effect of scalability and the reactor tank configuration on the
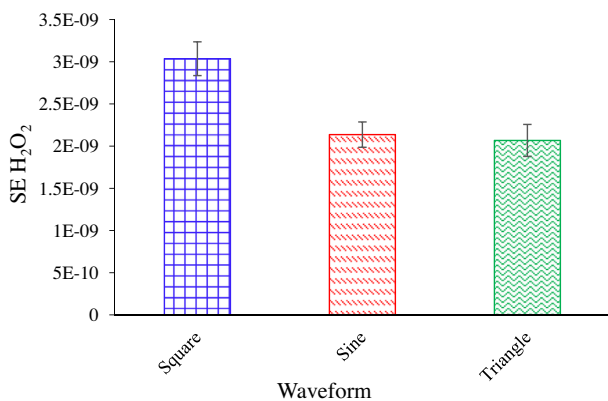
Fig. 8. Sonochemical efficiency based on hydrogen peroxide production for different waveforms.

chemical yield of ultrasonic system. Hydrogen peroxide production levels for three different reactor configurations irradiated with square wave ultrasound at different power levels for treatment time of 5–15 min is shown in Fig. 10. The 0.5 L scale was treated at 9.5 W, while the 15 L scale was treated with 19 W.

It seems that scaling up the reaction volume from beaker scale of 0.5 L to 15 L had a positive effect on the chemical throughput of

ultrasonic system. It can be seen from Fig. 10 that H_2O_2 yield in the large-scale was higher than that of the small-scale. The difference in H_2O_2 yield between the two scales increased as the treatment time increased to reach a maximum of approximately >7-fold higher yield. Although the power level was doubled for the large-scale as opposed to the small-scale, the volume of the large scale was 30 times bigger than the small-scale. So to rule out the effects of power and solution volume on chemical productivity of the system, SE of H_2O_2 for small and large scales was determined and the results are presented in Fig. 11. The results of Fig. 11 confirm that scaling-up increased the chemical productivity of the system (increase of ~50% in SE H_2O_2).

The positive effect of scalability could be attributed to the fact that irradiating a confined volume may lead to undesirable reflections of the waves (e.g. reflection back to the irradiating horn) that causes disturbance in the ultrasonic energy transformation. It is also possible that running ultrasound in a small vessel can only induce the near field effects (e.g. cavitation), while the far field effects (recombination of radicals, bubbles growth under residual pressure at the far field) may be absent. These views are in accordance with the recent opinions on the small scale assessments of ultrasound feasibility in water treatment applications [39]. Destaillats, Lesko, Knowlton, Wallace and Hoffmann [40] reported a similar findings to ours, as they observed an improvement in the degradation of different pollutants when moving from small-scale ultrasonic reactor (max. 0.65 L) to a large-scale reactor
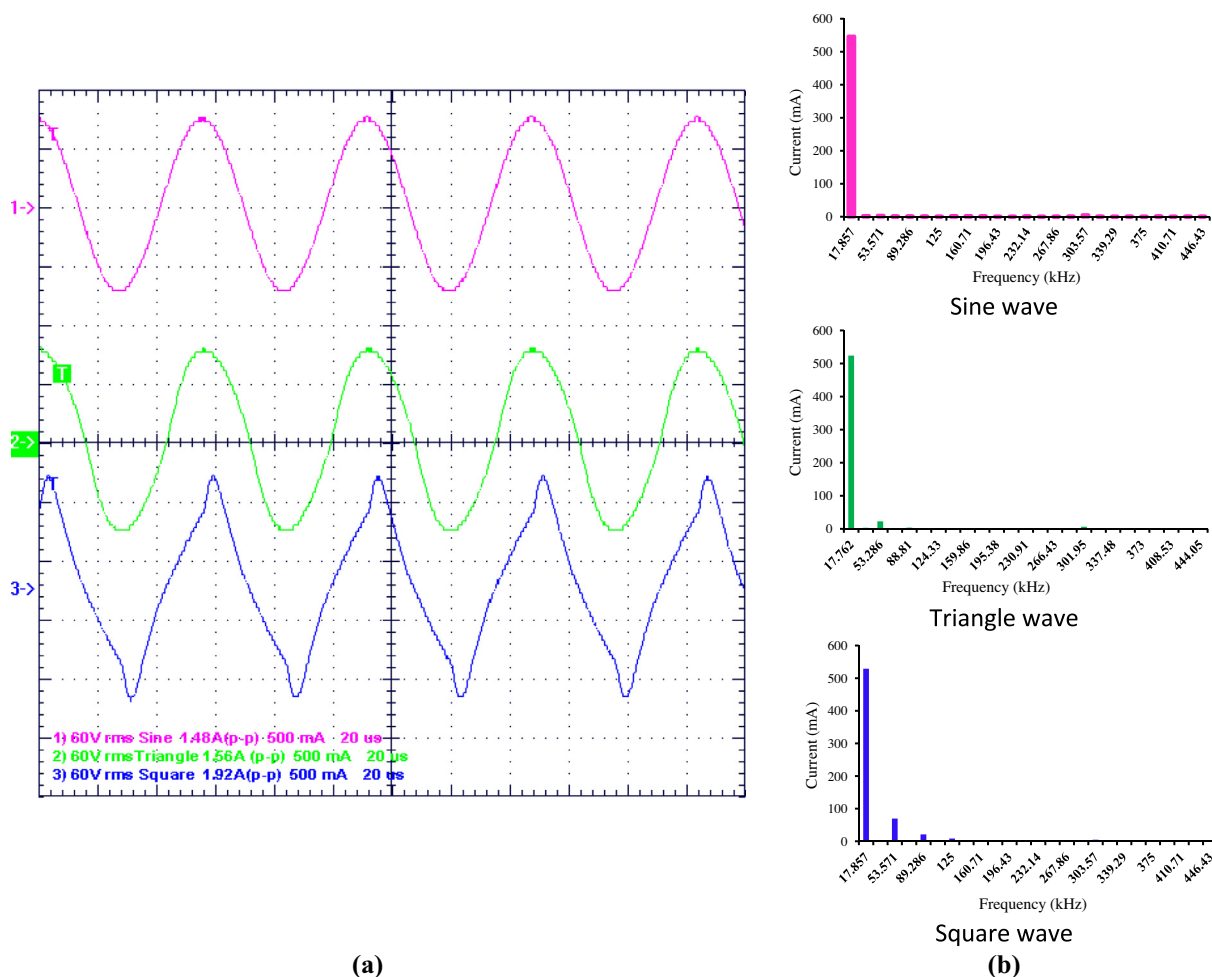

(a)　　　　　**(b)**

Fig. 9. Current input to transducers for different waveforms at a fixed RMS peak-to-peak voltage of 60 V_{p-p} (a) and transducers response to different waveform at different frequencies (b).
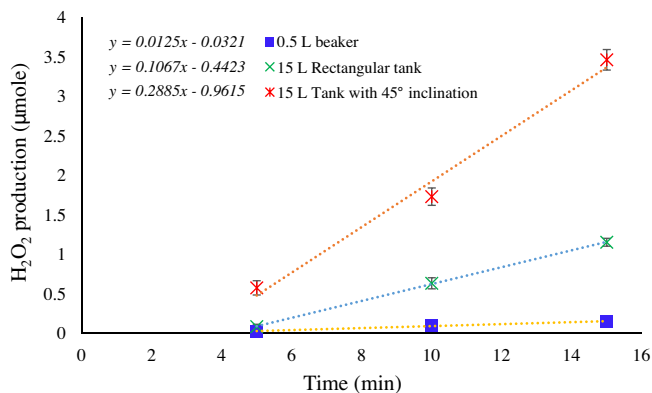
Fig. 10. Hydrogen peroxide production for different reaction tank configurations.

(max. 45 L). The improvement in the degradation rates varied between 3 and 7-fold depending on the targeted pollutant.

Fig. 10 also shows that using the reaction tank designed with a reflection of 45° on the sides enhanced the chemical throughput of the system significantly. It seems that the enhancement of H_2O_2 production due to the reflection feature increased with time until it reached as high as ∼3-fold increase at 15 min. Fig. 11 reveals that the inclination feature further improved the SE H_2O_2 of the large-scale system by approximately 70%. The increment of H_2O_2 production with time is attributed to the accumulation of the chemical effects of ultrasound in the middle area of the tank making a focus zone [12]. The 15 L reactor tank with 45° inclination resulted in the highest chemical throughput as compared to 15 L rectangular tank and 0.5 L beaker glass, thus this tank will be used in the following natural water treatment experiments.

4.3. Preliminary results of natural water samples

4.3.1. Total coliform reduction

Fig. 12 shows the survival ratio of total coliform in the ultrasonically treated Narda water (15 L) with two power levels of 19 and 58 w using square waveform and reactor tank configuration with 45° inclination over treatment time range of 0–15 min. The maximum total coliform reduction with lower power treatment for 15 min was about 10%, while at the high power for the same treatment time, the reduction was approximately 35%. It is clear that increasing the treatment time and the power decreased the survival ratio. In can also be noticed that the difference between the survival curves for the two different power levels increased with
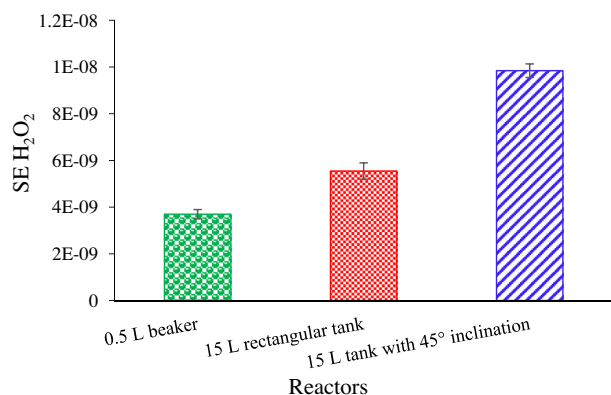

Fig. 11. Comparison of SE H_2O_2 for lab scale and pilot scale systems with two different reaction tank configurations.
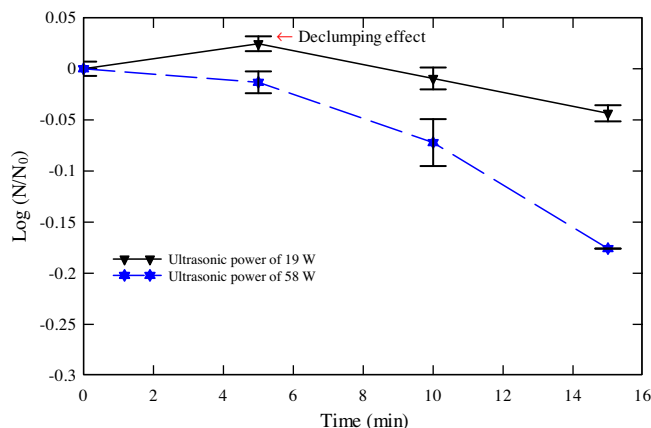

Fig. 12. Effect of ultrasound treatments on total coliform count for two sets of power.

increasing the treatment time. This trend is ascribed to the accumulation of the chemically active species with time as explained earlier and also the declumping act of the physical effects as illustrated in Fig. 12. The declumping effects of ultrasound are expected to appear at lower energy level (relatively low power and short treatment time) [41]. These results are in agreement with the outcomes of the previous studies on germicidal effects of ultrasound [16], as both point to the importance of the collective role of mechanical and chemical effects of ultrasound in deactivating microbes.

4.3.2. DOC

The effect of ultrasound treatment on DOC of Narda water at two power levels is presented in Fig. 13. It can be seen from Fig. 13 that the DOC removal with ultrasound increased with increasing the treatment time. The high power of ultrasound had a high DOC removal than the lower power at all the tested treatment time levels. However, the improvement in DOC removal with power increase in the case of short treatment time of 5 min was slightly lower than that of high treatment time (e.g. 10 and 15 min). The maximum DOC reduction for high power ultrasound achieved at long treatment time of 15 min was approximately 5.7%. The DOC reduction percentage at lower power for the same treatment time was around 2.7%.

The results presented in Fig. 13 shows that the obtained ultrasonic DOC removal levels are higher than the reported levels in previous studies. For instance, Stepniak, Kepa and Stanczyk-Mazanek [42] observed an approximate DOC removal of 40% in natural water samples treated with high power ultrasound of
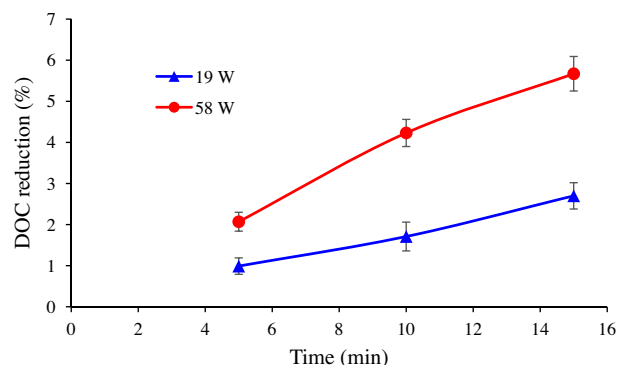

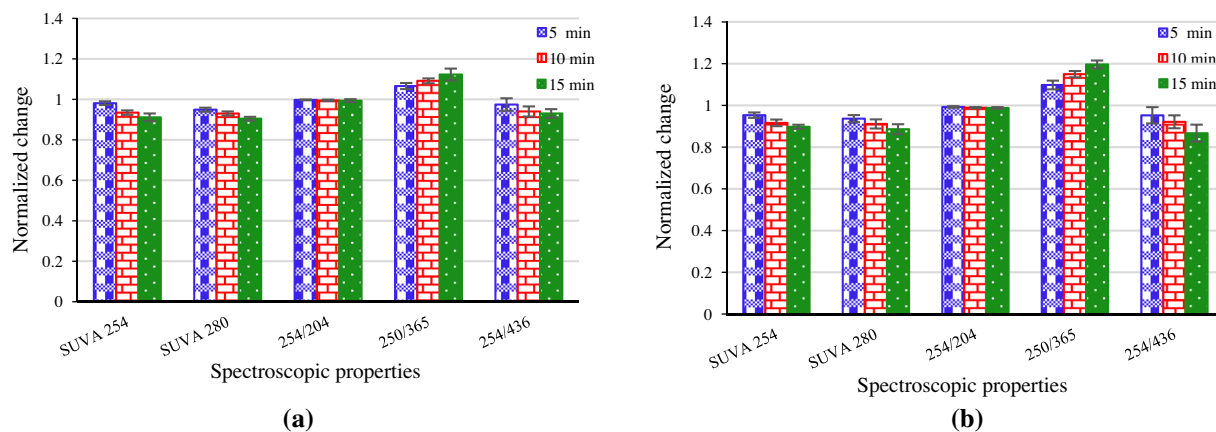**Fig. 13.** Effect of ultrasound treatments of DOC of Narda water.

Fig. 14. Effect of ultrasound treatments (a) 19 W and (b) 58 W on the spectroscopic properties of Narda water.

$60\,W/cm^2$ for short treatment of 5 min. In the case of this study, DOC removal at 58 W ($\sim$2.6 W/cm^2) for 5 min was about 2.1%. If a linear correlation assumed between power intensity and DOC removal, then the removal level of DOC for $60\,W/cm^2$ would be approximately 48%. From scalability perspective, comparing power density figures would give better idea on the system performance in removing DOC. For low frequency ultrasound, the reported power densities for DOC removal of $\leqslant$10% range between tens to hundreds W/L [43], while in this study, the power density for a maximum removal of 5.7% was approximately 3.9 W/L. The high DOC removal levels achieved in this study as opposed to the reported levels in the literature could be attributed to number of factors such as the high performance of magnetostrictive Terfonl-D transducers with square wave, the positive effects of scalability and the hydrophobic nature of Narda water [44].

4.3.3. Spectroscopic properties

The alteration of DOC structure due to ultrasound treatments represented by the change in the spectroscopic measurements is illustrated in Fig. 14. It is clear that increasing ultrasound power from 19 W to 58 W increased the change in DOC structure as shown in Fig. 14a and b. It can also be noticed that increasing the treatment time resulted in further alteration in DOC structure. In general, all the spectroscopic properties underwent a noticeable change under the effect of ultrasound except the ratio 254/204. This could be attributed to the simultaneous process of humic-like DOC destruction (reduction in $SUVA_{254}$) and the release of the intercellular materials (e.g. amino acids) caused by cell rupture under the effect of ultrasound. Amino acid compounds were found to absorb higher UV light at the proximity of 204 nm than at 254 nm [45].

The reduction of $SUVA_{254}$ and $SUVA_{280}$ with ultrasound treatments reflect a destruction in the humic and aromatic moieties of DOC. Such destruction is a very useful effect of ultrasound treatment considering that such DOC moieties have been involved in most of water treatment problems such as fouling and DBPs formation [7]. The destruction of these moieties with ultrasound treatment is attributed to the hydrophobic nature of such moieties that brings them close to the collapsing bubbles.

The increment of the absorbance ratio of 250/365 suggests that ultrasound broke down large sized molecules into smaller sized ones. The size reduction of DOC due to ultrasound treatments is mainly caused by the mechanical effects of ultrasound such as high pressure shock waves, strong shear forces and turbulences in the vicinity of the collapsing bubbles.

The reduction levels of UV ratio of 254/436 were almost the same as those of $SUVA_{254}$. This indicates that ultrasound treatment is more effective in disintegrating UV absorbing DOC fractions as compared to color forming DOC fractions. This observation is likely to be due to the hydrophilic nature of color forming DOC fractions [46] that drives these moieties away from reactive sites of the collapsing bubbles.

In addition to the germicidal and DOC mineralization effects of ultrasound treatment, this treatment could also alter the structure of DOC to make it less problematic to water treatment processes. Hence, all these positive effects of ultrasound technology should be taken into account when assessing the viability of this technology as a chemical-free water treatment technique.

5. Conclusions and recommendations

Large-scale application of magnetostrictive ultra-sonication in water treatment was carefully assessed in this study. Power analyses were conducted to evaluate the efficiency of the system in converting the electrical power into acoustical effects. Liner amplifier was used to study the performance of the system at different waveforms. The linear amplifier had a very low efficiency around 10% at the low power level applied. Hence, the use of digital amplifier for driving the magnetostrictive ultrasound system was recommended.

The effects of waveform, scalability and reactor configuration on chemical productivity of ultrasound system was investigated. Square wave was found to be the most efficient waveform in producing physical and chemical effects of ultrasound. Scaling up from bench-scale to a large-scale had positive effects on the chemical throughput of the ultrasonic systems, as it increased SE of H_2O_2 by $\sim$50%. Designing the reactor with an inclination feature further improved H_2O_2 production of large-scale system by $\sim$70%.

The large-scale ultrasonic system was capable of removing a maximum of 35% total coliform and 5.7% DOC at power density of approximately 3.9 W/L. Ultrasound treatment also altered the structure of DOC to make it less harmful to treatment processes and public health. Based on the results obtained from this study, the use of magnetostrictive ultrasound transducers excited by a square wave is the most efficient way for large-scale ultrasound in water treatment application. Modifying the reactor design in a way that maximizes the utilization of ultrasonic energy would make magnetostrictive ultrasound technology economically attractive technique for water treatment. Further work is required to optimize the proposed system to be used in a continuous regime.

References

[1] R.A. Al-Juboori, T. Yusaf, V. Aravinthan, Investigating the efficiency of thermosonication for controlling biofouling in batch membrane systems, Desalination 286 (2012) 349–357.

[2] S.H. Al-lwayzy, T. Yusaf, R.A. Al-Juboori, Biofuels from the fresh water microalgae Chlorella vulgaris (FWM-CV) for diesel engines, Energies 7 (2014) 1829–1851.

[3] W. Wang, X. Ma, Y. Xu, Y. Cao, Z. Jiang, T. Ding, X. Ye, D. Liu, Ultrasound-assisted heating extraction of pectin from grapefruit peel: optimization and comparison with the conventional method, Food Chem. 178 (2015) 106–114.

[4] A. Patist, D. Bates, Ultrasonic innovations in the food industry: from the laboratory to commercial production, Innovative Food Sci. Emerg. Technol. 9 (2008) 147–154.

[5] S.K. Khanal, D. Grewell, S. Sung, J. Van Leeuwen, Ultrasound applications in wastewater sludge pretreatment: a review, Crit. Rev. Environ. Sci. Technol. 37 (2007) 277–313.

[6] R.A. Al-Juboori, T. Yusaf, Biofouling in RO system: mechanisms, monitoring and controlling, Desalination 302 (2012) 1–23.

[7] R.A. Al-Juboori, T. Yusaf, V. Aravinthan, P.A. Pittaway, L. Bowtell, Investigating the feasibility and the optimal location of pulsed ultrasound in surface water treatment schemes, Desalin. Water Treat. (2015) 1–19.

[8] T. Yusaf, R.A. Al-Juboori, Alternative methods of microorganism disruption for agricultural applications, Appl. Energy 114 (2014) 909–923.

[9] J.A. Gallego-Juárez, K.F. Graff, Power Ultrasonics: Applications of High-Intensity Ultrasound, Elsevier Science, 2014.

[10] P.R. Gogate, S. Mujumdar, A.B. Pandit, Large-scale sonochemical reactors for process intensification: design and experimental validation, J. Chem. Technol. Biotechnol. 78 (2003) 685–693.

[11] F. Faïd, F. Contamine, A.M. Wilhelm, H. Delmas, Comparison of ultrasound effects in different reactors at 20 kHz, Ultrason. Sonochem. 5 (1998) 119–124.

[12] J.D. Seymour, H.C. Wallace, R.B. Gupta, Sonochemical reactions at 640 kHz using an efficient reactor. Oxidation of potassium iodide, Ultrason. Sonochem. 4 (1997) 289–293.

[13] Y.G. Adewuyi, B.A. Oyenekan, Optimization of a sonochemical process using a novel reactor and Taguchi statistical experimental design methodology, Ind. Eng. Chem. Res. 46 (2007) 411–420.

[14] R.A. Al-Juboori, T. Yusaf, L. Bowtell, Energy Conversion Efficiency of Pulsed Ultrasound, in: The 7th International Conference on Applied Energy – ICAE2015, Abu Dhabi, UAE, 2015.

[15] R.A. Al-Juboori, T. Yusaf, Identifying the optimum process parameters for ultrasonic cellular disruption of E. coli, Int. J. Chem. Reactor Eng. 10 (2012) 1–32.

[16] A. Hulsmans, K. Joris, N. Lambert, H. Rediers, P. Declerck, Y. Delaedt, F. Ollevier, S. Liers, Evaluation of process parameters of ultrasonic treatment of bacterial suspensions in a pilot scale water disinfection system, Ultrason. Sonochem. 17 (2010) 1004–1009.

[17] L.A. Crum, Comments on the evolving field of sonochemistry by a cavitation physicist, Ultrason. Sonochem. 2 (1995) S147–S152.

[18] E. Naffrechoux, S. Chanoux, C. Petrier, J. Suptil, Sonochemical and photochemical oxidation of organic matter, Ultrason. Sonochem. 7 (2000) 255–259.

[19] S.K. Sharma, R. Sanghi, Advances in Water Treatment and Pollution Prevention, Springer, Netherlands, 2012.

[20] D.J. Casadonte Jr, M. Flores, C. Petrier, Enhancing sonochemical activity in aqueous media using power-modulated pulsed ultrasound: an initial study, Ultrason. Sonochem. 12 (2005) 147–152.

[21] J.W. Povey, T.J. Mason, Ultrasound in Food Processing, Springer, 1998.

[22] F. Claeyssen, D. Colombani, A. Tessereau, B. Ducros, Giant dynamic magnetostrain in rare earth-iron magnetostrictive materials, IEEE Trans. Magn. 27 (1991) 5343–5345.

[23] L.H. Thompson, L.K. Doraiswamy, Sonochemistry: science and engineering, Ind. Eng. Chem. Res. 38 (1999) 1215–1249.

[24] F. Claeyssen, N. Lhermet, T. Maillard, Magnetostrictive actuators compared to piezoelectric actuators, in: European Workshop on Smart Structures in Engineering and Technology, SPIE, Giens, France, 2003, pp. 194–200.

[25] R.A. Al-Juboori, T. Yusaf, L. Bowtell, V. Aravinthan, Energy characterisation of ultrasonic systems for industrial processes, Ultrasonics 57 (2015) 18–30.

[26] M. Toma, S. Fukutomi, Y. Asakura, S. Koda, A calorimetric study of energy conversion efficiency of a sonochemical reactor at 500 kHz for organic solvents, Ultrason. Sonochem. 18 (2011) 197–208.

[27] S. Koda, T. Kimura, T. Kondo, H. Mitome, A standard method to calibrate sonochemical efficiency of an individual reaction system, Ultrason. Sonochem. 10 (2003) 149–156.

[28] D. Chen, S.K. Sharma, A. Mudhoo, Handbook on Applications of Ultrasound: Sonochemistry for Sustainability, CRC Press, 2011.

[29] N.V. Klassen, D. Marchington, H.C.E. McGowan, H_2O_2 determination by the I3-method and by KMnO4 titration, Anal. Chem. 66 (1994) 2921–2925.

[30] S. Merouani, O. Hamdaoui, F. Saoudi, M. Chiha, Influence of experimental parameters on sonochemistry dosimetries: KI oxidation, Fricke reaction and H_2O_2 production, J. Hazard. Mater. 178 (2010) 1007–1014.

[31] L.S. Clesceri, E.W. Rice, A.E. Greenberg, A.D. Eaton, Standard Methods for Examination of Water and Wastewater, centennial edition., American Public Health Association, 2005.

[32] R.A. Al-Juboori, V. Aravinthan, T. Yusaf, Impact of pulsed ultrasound on bacteria reduction of natural waters, Ultrason. Sonochem. 27 (2015) 137–147.

[33] Elliott-Sound-Products, Class D Audio Amplifiers – Theory and Design, in: Sergio Sánchez Moreno, 2005.

[34] F. Sargos, IGBT Power Electronics Teaching System Principle for sizing power converters, Application note, Semikron, Nuremberg, 2008.

[35] Semikron-international, Semikron Data Book part number 11 23 21 70 DM10, Semikron international Dr. Fritz Martin GmbH & Co. KG Nürnberg, Germany, 1999.

[36] X.-L. Wei, S.-Y. Wang, Study on the optimal ultrasonic emulsification system of bio-diesel fuel based on dds, J. Theor. Appl. Inf. Technol. 48 (2013).

[37] X. Lu, S. Yang, J.R. Evans, Studies on ultrasonic microfeeding of fine powders, J. Phys. D Appl. Phys. 39 (2006) 2444.

[38] V. Suomi, R. Cleveland, D. Edwards, Measuring and modelling of harmonic acoustic radiation force induced deformations, in: 15th International Symposium on Therapeutic Ultrasound, International Society for Therapeutic Ultrasound (ISTU), Utrecht, Netherlands, 2015, p. 45.

[39] B. Thokchom, A.B. Pandit, P. Qiu, B. Park, J. Choi, J. Khim, A review on sonoelectrochemical technology as an upcoming alternative for pollutant degradation, Ultrason. Sonochem. (2015).

[40] H. Destaillats, T.M. Lesko, M. Knowlton, H. Wallace, M.R. Hoffmann, Scale-up of sonochemical reactors for water treatment, Ind. Eng. Chem. Res. 40 (2001) 3855–3860.

[41] X. Wu, E.M. Joyce, T.J. Mason, Evaluation of the mechanisms of the effect of ultrasound on Microcystis aeruginosa at different ultrasonic frequencies, Water Res. 46 (2012) 2851–2858.

[42] L. Stepniak, U. Kepa, E. Stanczyk-Mazanek, Influence of a high-intensity ultrasonic field on the removal of natural organic compounds from water, Desalin. Water Treat. 5 (2009) 29–33.

[43] V. Naddeo, V. Belgiorno, R. Napoli, Behaviour of natural organic mater during ultrasonic irradiation, Desalination 210 (2007) 175–182.

[44] P.A. Pittaway, T.R. van den Ancker, Properties of natural microlayers on Australian freshwater storages and their potential to interact with artificial monolayers, Mar. Freshwater Res. 61 (2010) 1083–1091.

[45] N. Her, G. Amy, H.-R. Park, M. Song, Characterizing algogenic organic matter (AOM) and evaluating associated NF membrane fouling, Water Res. 38 (2004) 1427–1438.

[46] T.J. Battin, Dissolved organic matter and its optical properties in a blackwater tributary of the upper Orinoco river, Venezuela, Org. Geochem. 28 (1998) 561–569.

Summary-Objective 5

After confirming the capacity of ultrasound technology on improving the performance of drinking water treatment system, a large-scale reactor was designed and tested in objective 5 (*paper X*). The effects of two design aspects namely reactor tank configuration and the form of the excitation waves on the performance of ultrasound in removing natural water contaminants were investigates in this objective. Overall, scaling up ultrasonic reactor from 0.5 L to 15 L resulted in better contaminants removal. The use of large-scale reactor tank with 45° inclination on the sides further improve the performance of ultrasound. Operating ultrasound reactor on a square wave resulted in the highest electro-mechanical efficiency. The use of ultrasound system with reactor tank of 45° inclination on the sides and square waveform resulted in microbes and DOC removal of 35% and 8.7%, respectively with a small power density of 3.9 W/L.

Conclusions

Publication outcomes summary and future recommendations

The application of pulsed ultrasound for enhancing the performance of conventional surface water treatment systems was carefully scrutinized in this study. Natural water samples were used to provide industry relevant experimental results that can be conveniently used as guidelines for ultrasound applications in surface water treatment processes. The study was conducted in five phases:

1. Development of an accurate practical energy characterisation method for a proper evaluation of energy conversion efficiency of the ultrasonic system used in this study.
2. Finding the most beneficial location of ultrasound technology in the surface water treatment process.
3. Optimizing the operating parameters of pulsed ultrasound to achieve the desired removal/alteration of microbes and DOC.
4. Investigating the downstream effects of pulsed ultrasound at the optimal location and operating conditions.
5. Designing and testing large-scale magnetostrictive ultrasonic rector.

Energy characterisation of an ultrasonic horn system at different power levels was performed by applying empirical heat transfer correlations and accurate electrical measurements *(paper 1)*. Two horn sizes $\varnothing = 1/2''$ and $\varnothing = 3/4''$ were tested in this step. The electrical measurements were utilized to determine energy conversion efficiencies of ultrasonic system components. The results obtained from heat transfer calculations were verified using convection heat transfer correlations based on flow information inside the reaction chamber. The results obtained from both sets of calculations were in good agreement.

The conversion of acoustical power into chemical yield was gauged using inorganic (e.g. KI and Fricke solution) and organic (e.g. 4-nirophenol) dosimeters. The yields of inorganic and organic dosimeters showed similar behaviour with ultrasonic amplitude in continuous mode. The chemical yield peaked around an amplitude range of 70-80% and showed a significant decline at higher amplitudes (due to shielding effects). This suggests the suitability of using one dosimeter type (inorganic or organic) for predicting the behaviour of the other. Sonochemical efficiency (SE) of $^{\bullet}$OH was calculated for the system at various power levels. The obtained SE values

were in the range of 10^{-10} mol/J. The ultrasonic horn with the larger diameter resulted in slightly higher SE compared to the small diameter horn, and hence the larger diameter horn was used in the further study.

In *paper II*, the energy characterisation was repeated for the same ultrasonic horn system, but with two modes of operation: continuous and pulsed at various *On*:*Off* ratios (*R*). Three groups of pulse settings viz. *R* with long *On* period, *R* with long *Off* period, and *R* with *On* = *Off* were tested in *paper II*. It was found that operating the ultrasonic system with pulsed mode did not affect the conversion of electrical power to calorimetric power. Furthermore the chemical yield of the ultrasound system measured as $^{\bullet}OH$ and H_2O_2 was lower for the continuous mode as opposed to the pulsed mode in most of the applied pulse settings. *R* ratios of 0.2:0.1 and 0.1:0.6 s produced the highest yield of $^{\bullet}OH$ and H_2O_2. Interestingly, the highest H_2O_2 yield of $R = 0.2$:0.1 and 0.1:0.6 s was achieved at the relatively low amplitude of 40%. The outcomes of *papers I* and *II* highlighted the importance of operating parameters such as amplitude of 40 % and 70% (corresponding to calorimetric power of 48 and 84 W respectively) and pulse settings of $R = 0.2$:0.1 and 0.1:0.6 s where the system achieved the highest chemical yield.

The effects of ultrasound treatment on the bulk characteristics of treated water were studied in *papers III* and *IV*. These effects were crucial factors used in determining the appropriate location of ultrasound in the surface water treatment process. Two types of natural water samples: water with vegetative carbon (Pittaway pond) and water with terrestrial carbon (Logan storage) were used in this step. The effects of ultrasound on bulk characteristics of treated water samples were evaluated using surrogate measurements such as UV-vis absorbance, conductivity, alkalinity and chemical oxygen demand. The two types of water samples showed different behaviours in response to ultrasound treatments. The properties of the Logan storage that were significantly affected by ultrasound treatment (e.g. $SUVA_{254}/Color_{436}$) showed only minor effects for the case of Pittaway pond water. Overall evaluation of surrogate measurements indicated that the best location of ultrasound technology is prior to coagulation/flocculation stages in the treatment process.

papers V, *VI* and *VII* investigated the relative effects on total coliform removal, DOC removal and DOC structural alteration for ultrasonic power levels of 48 and 84 W for continuous and pulsed treatments with effective treatment times of 5 and 15 mins. Statistical analysis of 2^3 factorial design were adapted to study the individual and interaction effects of power, pulse setting and treatment time on removal and alteration of contaminants. It was observed that increasing power and/or treatment time of any pulse setting increased microbial and DOC removal levels. To decide whether such increases in power and treatment time was viable from an energy perspective, the removal percentages of all treatment scenarios were normalized by the consumed ultrasonic energy (%/J) and contour plots were constructed for analysis.

Ultrasound treatments resulted in total coliform reduction between 10-70% depending on the applied operating parameters (*papers V and XII*). It was also found that increasing the *Off* period in pulsed ultrasound treatment negatively affected total coliform removal regardless of power and treatment time levels. Energy consumption analysis for total coliform removal revealed that continuous and pulsed treatments with high *R* ratio at low power and treatment time are the most energy efficient treatment parameters for total coliform removal.

Paper VI showed that generally ultrasound treatments resulted in DOC removal of 7-15%. It was postulated that the high microbes' concentration in the treated water (approximately 250 CFU/100 mL) affected negatively on DOC removal as increasing

power and treatment time did not result in an increase in DOC removal. This postulation was confirmed through two measures: 1) testing the correlation between total coliform and DOC removal and DOC structural analysis via chemical fractionation. DOC removal showed a significant inverse correlation with total coliform removal suggesting release of microbial products that negatively affected DOC removal. The release of such products was further confirmed through the fractionation results of the treated DOC that witnessed an increase in the hydrophilic DOC fraction where these products are prevalent. Similar to microbial removal, low power for short treatment time was found to be the most efficient treatment option for DOC removal from an energy consumption point of view. However, energy analyses further showed that pulsed treatments were slightly better that continuous treatments.

The structural change of DOC induced by ultrasound treatments was thoroughly investigated in *paper VII* using chemical fractionation and UV-vis indices. Overall, ultrasound treatment decreased the hydrophobic fraction and to a lesser extent increased the hydrophilic fraction. The highest degradation of the hydrophobic fraction was achieved with pulsed treatments, while the highest production of the hydrophilic fraction was observed with continuous treatments. Pulsed treatments at high power and short treatment times resulted in the lowest increase in the hydrophilic fraction and a moderate to high decrease in the hydrophobic fraction. The same power levels but with long treatment times caused the highest removal of humic-like aromatic DOC measured as a decrease in SUVA at 254 and 280 nm.

The correlations between DOC fractions and UV-vis measurements of the treated water were also examined in *paper VII*. The strongest and most significant correlation was observed between A_{254}/A_{204} and hydrophobic/hydrophilic ratios. SUVA at 254 and 280 nm also showed strong and significant correlations with the hydrophobic DOC fraction. E_2/E_3 and A_{254}/A_{436} ratios showed weak and insignificant correlations with hydrophobic/hydrophilic ratio. To verify the appropriateness of using UV-vis indices as quick indicators for the distribution of DOC fractions, the observed DOC fractions-UV-vis correlations were examined for different water sources located in the same geographical location of the sampling site in *paper VIII*. The results were consistent with the observed trends in *paper VII*.

Based on the optimization conducted in *papers V* through *VII*, it was found that pulsed ultrasound treatment with high *R* ratio at low power and short treatment time was the most energy efficient treatment option. Hence, pulsed ultrasound treatment of $R = 0.2:0.1$ s at 48 W and effective treatment time of 5 min was chosen to be used as a pre-treatment for alum coagulation in *paper IX*. Coagulation with and without (control) pulsed ultrasound treatments were performed with various pH and alum dosage conditions. The measured responses in this step were turbidity removal, DOC removal and residual dissolved aluminium. Individual response optimization was conducted using centre composite design of response surface methodology to find the optimum pH and alum dosage that result in the highest DOC and turbidity removal and lowest residual dissolved aluminium. Multi-responses optimization was performed using a desirability function. The multi-response optimisation showed that the optimum alum dosage and pH were 63.2 mg/L and 5.62 for control treatment and 64 mg/L and 5.62 for coagulation preceded by pulsed ultrasound (desirability>0.97). The applicability of these conditions was verified with confirmatory experiments and the results were in good agreement. The respective obtained turbidity removal, DOC removal and residual dissolved aluminium were 98.8%, 52% and 0.094 ppm for coagulation with pulsed ultrasound pre-treatment and 96.6%, 43% and 0.1 ppm for the control treatment.

Total coliform and THMFP of coagulated water with and without pulsed ultrasound treatment were measured to evaluate the downstream effects of pulsed ultrasound applications in surface water treatment. It was observed that pulsed ultrasound pre-treatment improved total coliform removal from approximately 80% to >98%. Pulsed ultrasound pre-treatment also decreased THMFP from approximately 250 to just above 200 ppb of chloroform. Pulsed ultrasound pre-treatment showed another impressive technical advantage by improving the ability of sludge to effectively settle.

To conduct constructive and fair evaluation for the application of ultrasound technology in surface water treatment, testing the performance of the technology on a large-scale is important especially after observing the positive effects of the treatment on treated water quality. In *paper X*, a magnetostrictive ultrasonic reactor was designed and tested using standard dosimeters and the same natural water sample used in the previous steps. Three waveforms namely sine, triangle and square were tested. The performance of the ultrasound system with three reactor tank configurations was evaluated: 0.5 L beaker, 15 L rectangular tank and 15 L tank with a 45° inclined base. The system was found to perform best with square wave excitation with reliable performance and good electro-mechanical efficiency. Scaling up of the system from 0.5 L to 15 L increased SE_{H2O2} by 50%. The use of an inclined base in the large-scale tank improved SE_{H2O2} by 70%. These improvements have resulted in a decent total coliform and DOC removal of 35% and 5.7%, respectively with a small power density of 3.9 W/L.

The results obtained in this study showed that pulsed ultrasound is a promising technology that can significantly improve the performance of surface water treatment systems. However, continuing to find ways to further improve this application is important. The following aspects are recommended to be further investigated in future work:

1. Performance of ultrasound with coagulants other than Alum.
2. Measurements of additional forms of DBPs especially the newly emerging ones.
3. Economic viability of large scale reactor.
4. Performance of large scale reactor in continuous systems.

Appendix A

Paper XI

Yusaf, T. & **Al-Juboori, R. A.**, Alternative methods of microorganism disruption for agricultural applications, *Applied Energy*, (2014), 114, 909-923.

Alternative methods of microorganism disruption for agricultural applications

CrossMark
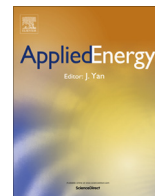
Talal Yusaf [a,*], Raed A. Al-Juboori [b,c]

[a] School of Mechanical and Electrical Engineering, Faculty of Health, Engineering and Sciences, University of Southern Queensland, Toowoomba, 4350 QLD, Australia
[b] School of Civil Engineering and Surveying, Faculty of Health, Engineering and Sciences, University of Southern Queensland, Toowoomba, 4350 QLD, Australia
[c] University of Kirkuk, Kirkuk, Iraq

HIGHLIGHTS

- Microorganism disruption in agriculture is the key point of this research.
- Thermal and chemical treatments are suggested to be replaced.
- Mechanical methods for microorganism disruption are potential alternative.
- Advantages and disadvantages of using mechanical methods were addressed.

ARTICLE INFO

ABSTRACT

This paper reviews various non-conventional techniques for microorganism disruption. Microorganism disruption plays a pivotal role in various agricultural applications such as disinfection of irrigation water, processing of crops and livestock products and the newly emerging area of bioenergy production for agricultural uses. Methods of treatment to destroy microorganisms for the purposes of disinfection or extraction of bio-products can be generally categorized as either thermal treatment methods or non-thermal treatment methods. The thermal methods for microbial disruption are not favorable in many applications such as food processing and water treatment due to its negative impact on product quality and process performance. The discussion of thermal methods for microorganism disruption will not be included in this review. Non-thermal treatments are divided into two groups; chemical and physical treatments. Owing to the concerns of the health organisations with regards to the use of chemical methods for microorganism disruption, the recent research efforts have been directed towards exploring alternative physical methods for rupturing microorganisms. The common alternative physical methods for microorganism disruption include mechanical and non-mechanical treatments. This paper discusses in details the use of the common mechanical treatments for cell disintegration. Such methods include ultrasound, shock wave, High Pressure Homogenization (HPH), Hydrodynamic Cavitation (HC), shear stress, bead milling and micro-fluidizer. The application of the non-mechanical methods for microbial disruption such as electrical treatment, non-thermal plasma, Ultra-Violet (UV), non-conventional chemical methods and some other treatments are also briefly addressed in this paper. Due to the importance of the mechanical methods in the current cell disruption research, more attention is directed to these methods in this work.

© 2013 Elsevier Ltd. All rights reserved.

1. Introduction

Managing the presence of microorganisms in the agricultural environments and products is an important aspect in modern agriculture. Some microorganisms' species are useful in the conversion processes for the supply chain of crops and livestock products, while others are harmful for human, animals and plants.

Microorganisms have a great impact on various areas in agriculture sector. In irrigation, several factors such the increasing demand in crop yields to cope with the increasing population [1], the effect of vagaries of climate on water resources [2] and the ever-increasing competition between water consumers (i.e. human, natural animal habitats, industry, agriculture, etc.) has spurred the use of alternative water resources such as municipal and food processing waste-waters for irrigation purposes [3]. Despite the benefits of using wastewater for irrigation from sustainability and water security point of views, the use of such waters is associated with some risks

among which the presence of harmful microorganisms (e.g. human microbial pathogens) represents one of the potential risks. Several countries have established guidelines for the quality of irrigation water that set maximum levels of microbial contamination in irrigation water which depends on the types of crops and microbes. For example, the Australian and New Zealand Guidelines for Fresh and Marine Water Quality has set the level of thermo-tolerant coliform to be less than 10 Colony Forming Unit (CFU)/100 mL for the raw human food crops [4].

In principle, the use of adequate pre-treatment for the recycled wastewater in irrigation can eliminate completely or reasonably the risk arises from microbial contamination of irrigation water [1]. A study conducted by Peasey et al. [5] on the use of wastewater for irrigation in Mexico showed that the farm worker and their children had a high prevalence of *Ascaris* infection, which was decreased when the waste water was partially pre-treated. The traditional disinfection treatments are thermal and chemical techniques.

Temperatures in the range of 160–280 °C are commonly used in thermal disruption of microorganisms [6]. Thermal treatments can be used to kill the complex microorganisms in wastewater through exposure to 300 °C for a short treatment time, 1.75 min [7]. Such high levels of temperature require high energy consumption and can negatively affect the integrity of the construction materials of the treatment unit. The implementation of the thermal techniques for the purpose of disinfection in water treatment applications can have a negative effect on the performance of the treatment units. Al-Ahmad et al. [8] reported that increasing the water temperature might exacerbate the problem of bio-fouling in the treatment units, which in turn can negatively affect the cost of the operation and its performance.

The chemical methods were thought to be an efficient replacement for the thermal treatment for microbial disruption. Using chemical treatments as a tool for killing microbes started after Pasteur and Koch presented the germ theory of diseases. Koch coined the bactericidal properties of chlorination in 1881 [9]. With this finding, the use of chemical disinfection started in developed nations in the early 1900s [10]. The chemical methods for microbial disruption encompass the use of oxidizing agents such as chlorine and ozone [11]. The chemical methods for microorganisms deactivation are regarded as an economic technique for microbial disruption from operation point of view. However, the residual of disinfectants (i.e. chlorine) and the by-products that result from the reaction of disinfectants and organic materials is of great concern due to its negative effects on crops and the health of the crops' consumers [2]. The negative effect of chemical techniques on human health and environment [10,12] can render these techniques uneconomic option for microbial destruction, especially if the cost associated with the research that is devoted to diagnose and cure the distributions that these techniques can introduce to the environment and the body of consumers is taken into account. Hence, the possibility of using alternative chemical-free techniques for disinfecting irrigation water should be investigated.

The other agricultural areas where microorganism disruption plays a crucial role, is in the supply chain of agricultural products and the production of bioenergy. Processing raw crops and livestock products usually requires a sufficient control of microorganisms. Thermal methods are traditionally used in food and dairy products industries. The exposure time to destruct microorganisms varies from 2.5 to 30 min depending on the nature of the microorganisms [13]. Pasteurization is one of the most important steps in processing milk. Ultra Heat Treatment (UHT) is another form of thermal sterilisation which is widely used to destroy the microorganisms in milk [14]. However, these processes may alter the nutritional quality and flavor of the milk, rendering it a less desirable product [15]. In the case of using membrane filtration for separation in food industry [16], the temperature rise of the treated liquid can negatively affect the separation process, as temperature rise alters the physical and chemical properties of liquid and membrane filters (e.g. pore dilation and viscosity). Hence, the industrial need for replacement of thermal disinfection techniques has driven the research efforts towards finding alterative techniques for microbial disruption.

The chemical methods for microbial control are other widely used conventional methods for treating the water used in various food processing areas such as the fresh-cut industry. Nevertheless, the application of chemical disinfectants in food processing is always concomitant with health and technical problems. Chlorine as one of the widely used disinfectant in food processing has been identified as an inefficient preventive of food-borne pathogen contamination and a precursor for production of health hazard by-products [17]. In fact Ölmez and Kretzschmar [17] reported that the use of chlorine for disinfection in food industry has been forbidden in some European countries. The use of alternative chemicals for microbial control in food industry is also accompanied by many limitations. For instance, peroxyacetic acid and hydrogen peroxide have insufficient germicidal effects when used for restraining contamination in fresh-cut industry [18,19]. So, there is a need in the current research to replace or enhance the conventional sanitization techniques in food processing field [20]. This need can be satisfied by integrating the physical methods for microorganism disruption into food processing industry. There are some attempts that have been already made in merging physical and chemical techniques or solely using physical methods for microbial control in food processing [21,22].

In addition to the importance of physical methods for microorganism disruption in food processing and water irrigation disinfection, physical methods have also a crucial role in bioenergy production. For example ultrasound and bead mill have been successfully applied in enhancing the extraction of oil from microalgae [23], which can be used as alternative fuel for agricultural machineries [24]. However, the implementation of physical methods for microorganism disruption in agricultural applications requires deep understanding to the mechanisms of these methods and careful analysis to the benefits and shortcomings of the methods.

This work has been prepared as an attempt to contribute to the understanding of the physical microbial disruption methods with special focus on the mechanical techniques via reviewing and discussing the available information pertaining to the mechanisms, energy consumption, advantages and disadvantages of these methods.

2. Common mechanical methods

Mechanical methods aim to disrupt microorganisms without adding substances or changing the internal structure of the suspension containing the microorganisms. For the optimization of mechanical methods, a good understanding of the cell wall's mechanical properties and the cytoplasm is required, this is how the likely mechanical loads and disruption probability can be identified.

Mechanical disinfection methods involve a number of techniques that use pressure pulse, shock wave and shear stress for rupturing microorganisms. Mechanical methods are recommended to treat microorganisms that required high energy (power) for disruption because these methods can generate sufficient energy and shear to rupture those microorganisms [25]. For instance in alternative fuel researches, mechanical methods are used as pre-treatments for the process of oil extraction from microalgae [26]. The mechanisms through which these methods deactivated the cell of microorganisms are different for each method. The common

reported mechanical methods for cell disruption include ultrasound, shock wave, High Pressure Homogenization (HPH), Hydrodynamic Cavitation (HC), shear stress, bead milling and micro-fluidizer.

2.1. Ultrasonic methods

The term ultrasound waves refers to the application of sound waves with a frequency range higher than the upper limit of human hearing (more than 16 kHz) [27]. The typical limit for the frequency that is usually used in ultrasound applications ranges between 20 kHz and 500 MHz [28]. When ultrasound is applied with sufficient intensity and time, it has the potential to cause the death of a microorganism [29]. Scherba et al. [29] reported that when sonar was investigated and used for anti-submarine warfare, the source waves were killing fishes [30]. This eventually motivated the researchers to explore ultrasound technology as a method of destroying or inactivating cells [31]. In the 1960s, research concentrated on understanding the mechanism of ultrasound interaction with microbial cells [30]. By 1975, it had been shown that brief exposure to ultrasound caused thinning of cell walls. This led to separation of the membrane from the cell [32]. Table 1 provides a summary of the historical pathways of ultrasound technology.

The effectiveness of ultrasound in disintegrating microorganisms lies in the concurrent events of acoustic cavitation. Acoustic cavitation is defined as the process of generation, growing and subsequent collapse of the bubbles as a response to the introduction of ultrasound waves to a liquid body [45,46]. The propagation of ultrasound waves and bubble oscillation and subsequent collapse of bubbles generate three effects: mechanical, thermal and chemical effects [46]. Mechanical effects are represented by the generation of high pressure shock (collapse pressure), shear stresses and turbulences that level up as a result of liquid movements during the mechanical events of acoustic cavitation [47]. Fig. 1 shows a graphical representation of the mechanical events of acoustic cavitation which include acoustic streaming, micro-streaming, micro-jets and shock waves. Acoustic streaming can be defined as the convective liquid motion due to the passage of ultrasound waves. Micro-streaming is the liquid motion in the adjacent area to a bubble as a result of bubble oscillation. Micro-jetting is the resultant liquid motion from bubble collapse symmetrically close to solid/liquid interface [48].

It was confirmed that there are two types of bubbles occurring in the liquid as a result of ultrasound irradiation: bubbles with gentle collapse (stable cavitation) and bubbles with violent collapse (transient cavitation) [49]. The latter exists normally for one cycle of the sound pressure in which bubbles expand to at least double their size and collapse severely, often disintegrating into small bubbles. In comparison, stable bubbles can oscillate for more than one cycle of sound pressure and grow due to mass diffusion through the bubble skin [49]. Thermal effects are evident through the generation of localized high temperature spots, whereas the chemical effects appear as the pyrolysis of water producing free radicals [47].

2.2. High power ultrasound for sterilization

High power ultrasound can generate localized high pressures and temperatures when cavitation bubbles collapse. It has been repeatedly reported that the mechanical effects of ultrasound are more responsible for the microbial disruption than thermal and chemical effects [50]. Gogate [46] reported that the micro-streaming generated from the oscillation of stable bubbles produce shear stresses sufficient to rupture the membrane of a microbial cell. Micro-streaming causes large localized forces to shear the cell wall surfaces resulting in physical damage to the cells [51]. Doulah et al. [52] and then Doulah [51] described the theory of shear stress as a main cause of a microorganism rupture. Doulah [51] has also reported that when small gas bubbles oscillate during the compression and rarefaction phases of the sound wave, strong eddies are developed in the area surrounding the bubbles which ultimately spread into the liquid. According to Doulah [51], this effect leads to a significant localized shear force that rubs the cell wall surfaces of surrounding organisms and causes the cell wall to rupture. Yusaf [6] has found through his systematic investigation on the mechanical effects of acoustic cavitation that among the mechanical effects of cavitation, the shock waves resulting from bubble collapse are the main effect responsible for the disruption of yeast cell. Scherba et al. [29] also ascribed cell disruption in ultrasound treatment to the high pressures generated from ultrasound. Other researchers pointed that the combination of pressure and temperature generated by high power ultrasound contribute to the death of the microorganisms [53].

During the 1980s, researchers continued to study the effect of ultrasound in combination with other treatments for use in the food industry [54–56]. Furthermore, the effects of low frequency ultrasound combined with increased temperature on the disruption of microorganism suspended in water has been investigated [57]. The tests were conducted at different treatment temperatures

Table 1
Summary of the important events in the history of ultrasound technology from the early observation until recently [33].

| Date	Events
1895	The first observation of cavitational effects by Thornycroft and Barnaby [34], who noted pitting and erosion in the propeller of the submarine
1917	Lord Rayleigh published the first theoretical model to describe the collapse of spherical bubble in a body of incompressible fluid [35]
1927	The first documented survey of the chemical effects of ultrasound conducted by Richards and Loomis [36]. In the same year, Wood and Loomis [37] investigated, for the first time, the physical and biological effect of ultrasound
1937	Brohult [38] discovered the potential of ultrasound in degrading the biological polymers
1944	Harvey et al. [39] proposed the earliest model for heterogeneous bubble formation on cracks and crevices of solid surfaces
1949	Plesset [40] published the first study on the dynamics of cavitating bubble, which was integrated into Rayleigh's work [35] on bubble collapse resulting in the well-known Rayleigh-Plesset equation that describes bubble dynamics in liquid irradiated by ultrasound
1950	Noltingk and Neppiras [41] conducted the first computer calculations to model a cavitating bubble
1964	The first emergence of the terms transient cavitation and stable cavitation, introduced by Flynn [42]. In the same year Neppiras and Hughes [43] investigated the effect of hydrostatic pressure on the rupture of yeast cell using ultrasound, which was the first exploration for the use of the combination of ultrasound and pressure or so-called Manosonication
1972	Burgos et al. [44] investigated the effect of ultrasound treatment on the heat-sensitivity of Bacillus cereus and Bacillus licheniformis, which opened the door to the use of Thermsonication treatment (ultrasound combined with thermal treatment)
In late 1980s–the early 1990s	The commercial era of ultrasound technology began, as the manufacturers started designing and marketing ultrasonic devices to be used for sonochemical researches [28]
Last decade until currently	Researchers have been trying to extend the use of ultrasound technology to cover various chemical and biological applications
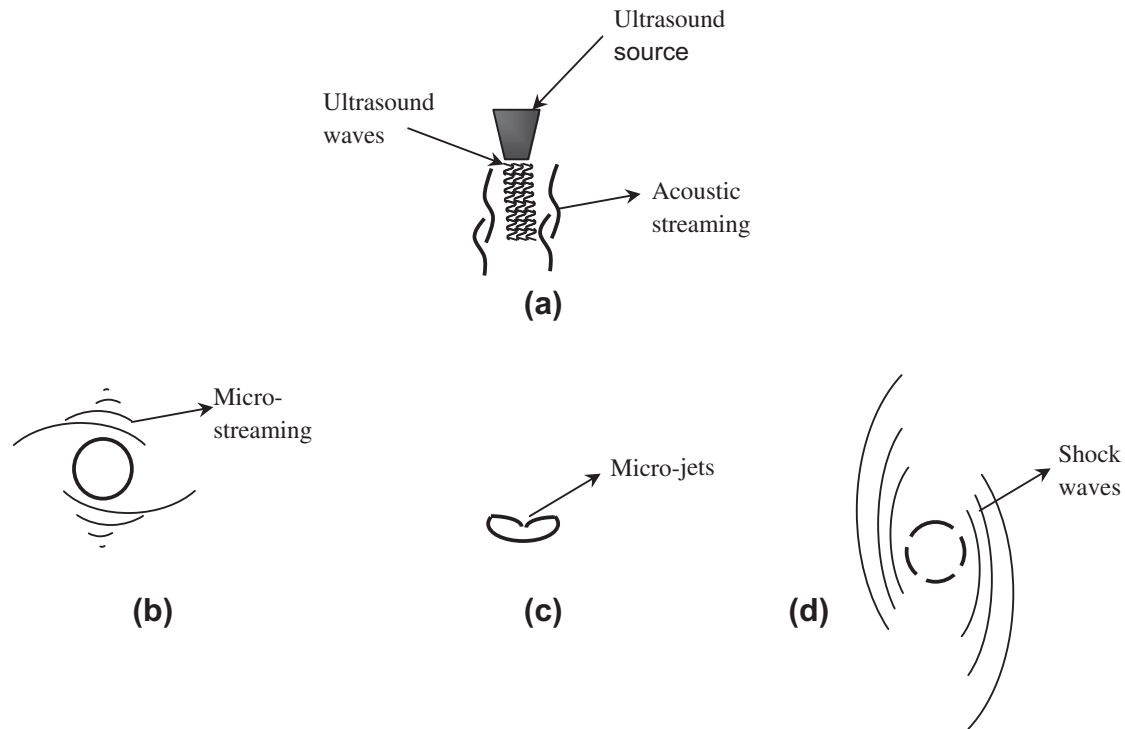
Fig. 1. Mechanical events of acoustic cavitation: (a) acoustic streaming, (b) micro-streaming, (c) micro-jets and (d) shock wave.

of 45 °C, 50 °C and 55 °C and ultrasonic powers of 50 W, 100 W and 180 W. Koda et al. [58] used an ultrasound power of 12.8 W and frequency of 20 kHz to treat 50 cm³ on water contaminated with *Streptococcus mutans* for 15 min and reported a percentage reduction of about 97%. The results of Koda and co-workers indicate that ultrasonic waves do not completely destroy the cells, but damaged some of them by increasing the cells sensitivity to heat. The optimum ultrasonic power for a maximum deactivating effect was found to be around 100 W. Despite the effectiveness and the benign environmental effect of ultrasound, high energy demand in this technology still concerns the industries operators when the application of ultrasound technology in an industrial scale is considered. There are various ways to improve energy conversion and/or consumption in ultrasound treatments for the purpose of microbial disruption, such ways will discussed in the following subsections.

2.3. Solutions to overcome high energy consumption in ultrasound technology

The high operation cost of ultrasonic microbial disruption is standing in the way of applying the ultrasonic technology on an industrial scale. This can be alleviated through several methods including the optimization of operating conditions for particular purposes, choosing the right ultrasonic reactor design and combining ultrasound with other technologies.

2.3.1. Optimizing operating conditions of ultrasound application
Applying suitable operating conditions is one of the key solutions to solve the problem of high energy consumption in ultrasound treatments. Some studies have emphasized the necessity for optimizing the operating conditions of ultrasound treatments prior to any application [47,59,60]. In our previous study [61] on ultrasonic inactivation of *Escherichia coli* (*E. coli*), we observed that increasing the power level of ultrasound does not always result in an increase in the disinfection rate, as the power has an optimum

limit after which any increase in the power would not cause an increase in the ultrasonic disruption of *E. coli*. This observation is supported by many studies such as Thompson and Doraiswamy [28] and Sivakumar and Pandit [60]. The logical interpretation for this observation is that at high power levels, the bubble shielding effect occurs. This is where a cloud of bubbles near the irradiating surface scatters the ultrasonic waves and minimizes the ultrasonic energy transformation to the other parts of the irradiated liquid. The same applies to the other operating conditions such as frequency, treatment time, pressure and temperature. Applying the optimum operating conditions can save energy and as a consequence can extend the operating life of an ultrasonic device. For example, operating the horn reactor at the highest power causes high displacement in the transducer which in turn might result in a stress failure in the construction material of the horn [47]. Alternatively, operating ultrasonic horn at the optimum level which mostly falls between the intermediate and the high power levels would have a milder effect as compared to that of the high power level on the material of the horn. In a similar way, choosing the appropriate frequency for a specific application can also help in extending the working life of the horn. Santos et al. [62] pinpointed that applying high frequency ultrasound waves increases the cavitation threshold, hence more ultrasound power is required to rupture the liquid and create cavities. Fig. 2 shows the relationship between the threshold frequencies and their corresponding power levels.

2.3.2. Modifying ultrasonic reactor design
2.3.2.1. Ultrasonic horn reactor. This reactor design is the most commonly used design in ultrasonic applications especially in laboratory investigations and small scale applications. The typical configuration of this design is shown in Fig. 3. Cavitation region of high energy usually appears near the irradiating surface (the immersed horn) and decreases exponentially away from the horn in both directions, axial and radial [47]. Since ultrasound energy is directly deposited into the liquids, the area beneath the horn is
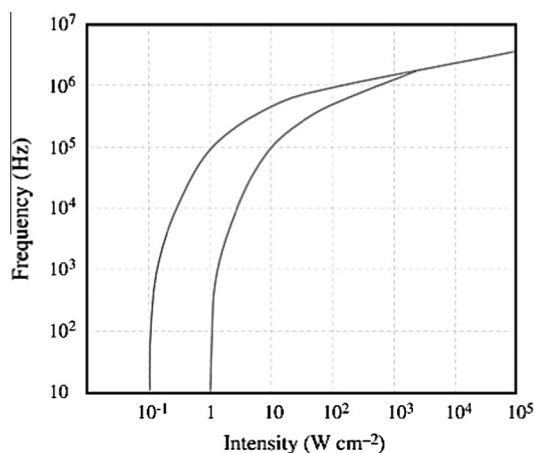
Fig. 2. Relationship between threshold frequency and ultrasound power, the figure is originally quoted from [63] by [62].
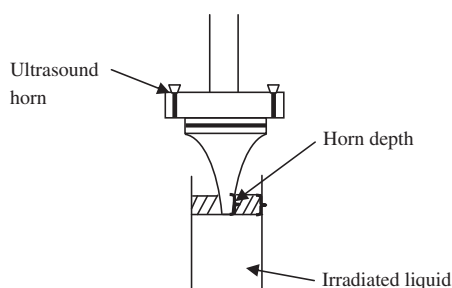

Fig. 3. Ultrasonic horn reactor design.

exposed to high levels of energy that are sufficient to rupture microorganisms in small scale.

2.3.2.2. Ultrasonic bath reactor. This reactor design consists of a generator and reaction vessel that is irradiated from its bottom by one or multiple transducers as shown in Fig. 4. Unlike the horn type design, this design is known by its wide cavitation region. Owing to the large irradiating surface in this design, the cavitation intensity is weak compared to the horn design. The cavitation intensity is more pronounced in the area above the transducers as opposed to the other areas of the reactor [46]. Since the cavitation intensity is weak in the ultrasonic bath reactor, in most cases this design is not suitable for rupturing microorganisms. However, ultrasonic bath design can be a valuable tool in sonochemical applications and applications in which the microorganisms' growth is promoted [64].

The problems associated with common ultrasonic reactor designs that are suitable for microbial disruption (i.e. horn design) are represented by the limited cavitation region that makes it hard to treat large volume liquids, high energy consumption and the
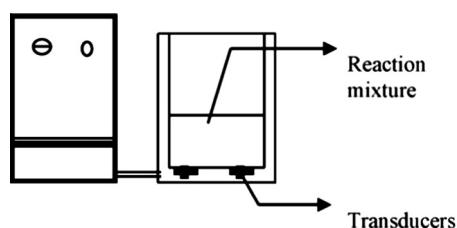

Fig. 4. Ultrasonic bath [47].

erosion that occurs in the irradiating surface at high ultrasonic power. Gogate and Kabadi [47] listed reasonable explanations for the pitting and erosion phenomenon of the horn design and these are high energy intensity to small irradiating area, acoustic decoupling, and deterioration of the horn construction material when applying high ultrasonic amplitudes.

The inherited problems in the ultrasonic reactors are related, as applying high level of amplitudes is normally put into action to compensate for the limited cavitation region in ultrasonic reactors. Similarly, decoupling problems are mostly experienced when one tries to keep the distance between the irradiating surface and the bottom of the reactor within the effective axial range of the reactor. So in a concise expression, one can attribute the problems that are usually experienced in ultrasound reactors to its limited active area. These problems can be alleviated in a way that makes the ultrasound technology more energy efficient by optimizing the operating condition and modifying reactor design.

2.3.2.3. Energy efficient ultrasonic reactor designs. Modifying the ultrasonic reactor can reduce the ultrasonic energy required to achieve desirable outcomes which can mitigate the concomitant problems to the conventional design. Adjusting the reactor design involves changing the shape of the reactor chamber (the carrying vessel for the treated liquid) and/or introducing new elements to the reactor. Capelo et al. [65] and Priego-Capote and de Castro [66] have marked the ultrasonic reactors chambers with conical or round bottom as effective configurations in terms of transformation and distribution of ultrasonic energy. The reason behind this positive trait of the aforementioned cavitation chamber shapes is that the ultrasonic waves get reflected in different directions back to the treated liquid body when impinging the conical or the round bottom of the reactor. So, simply designing reactors with conical or round ends could help in utilizing some of the lost ultrasonic power in the traditional reactors.

Seymour et al. [67] and Adewuyi and Oyenekan [68] have tested the use of novel ultrasonic reactors that utilize the reflection of ultrasonic waves for the aim of increasing the benefit of deposited ultrasonic energy into liquids. The reactors used in [67] are shown in Fig. 5. Reactor A is made of glass with a concaved end that reflects the ultrasound incident back to the treated solution. This distinctive feature of reactor A helps in utilizing most of ultrasonic power. Reactor B is made of aluminum which provides good heat transfer with the coolant liquid in the surrounding bath or jacket. The same perspective as that adopted in reactor A, reactor B was also designed to employ the reflection of the round structure of the reactor for the purpose of getting the maximum benefit of the delivered ultrasonic power to the liquid. The irradiated surfaces of reactors A and B are isolated from the reaction liquid by gab and the ultrasonic power is transferred through a polymer window. This feature reduces the temperature rise during treatment and at the same time eliminates the possibility of the treated liquid contamination with eroded materials of the irradiating surface. The performance of these reactors was tested for sonochemical reactions such as the oxidation of potassium iodide [67] and the results obtained with 640 kHz showed a significant improvement in the production of iodine as compared to the reported results in the literature. The improved chemical throughput of ultrasound can potentially increase microbial disruption through chemical effects. Destaillats et al. [69] has used a prototype ultrasound flow reactor, shown in Fig. 6. Similar to reactors A and B in Fig. 5, this reactor has the ultrasonic window isolation feature that separates the reaction liquid from the irradiating source. This feature has the advantage of minimizing the heat rise in the reaction liquid during ultrasound treatments that might bring about undesirable side effects in food processing applications Destaillats et al. [69] conducted methodical analyses for the
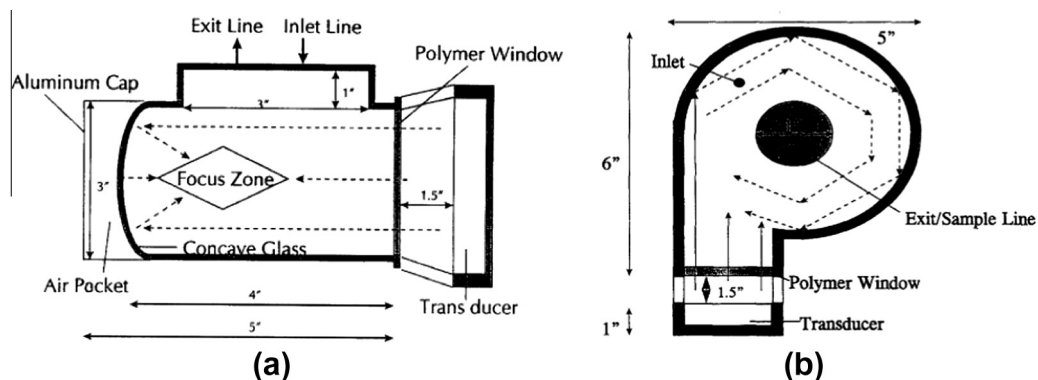
Fig. 5. Ultrasonic reactors that use the reflection techniques to achieve maximum utilization of ultrasonic power, (A) glass reactor with concave end and (B) aluminium reactor with round structure [67]
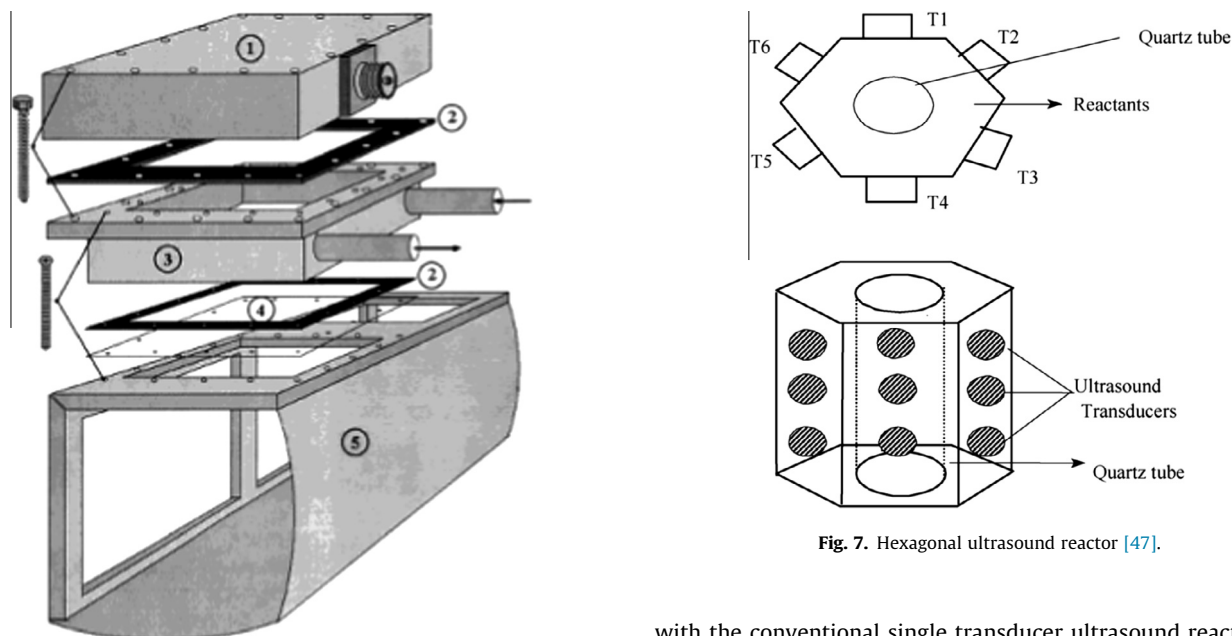

Fig. 6. Ultrasonic reactor with minimal heat dissipation into the treated liquids, 1, transducer housing (17.5 cm × 17.5 cm); 2, gasket; 3, transducer cooling water jacket; 4, PTFE acoustic window (11.5 cm × 11.5 cm); 5, reactor vessel body. Vessel is shown with one of four transducers and with end-closures removed [69].

Fig. 7. Hexagonal ultrasound reactor [47].

electrical power fate in the ultrasound reactor they used in their study (Fig. 6). They found that about one third of the electrical power consumed by their ultrasonic reactor was utilized in cavitation and sonochemical reactions of degrading chlorinated volatile contaminants. There are some other energy efficient ultrasonic reactor designs such as the one proposed by Gonze et al. [70] that consists of a tubular ultrasonic reactor that has one end with a transducer and the other end with a reflector. From the energy utilization feature in above-mentioned reactors, one can deduce that these reactors can be effectively used for cell disruption.

Integrating multi transducer into ultrasonic reactor can be another design aspect that provides a solution to the problem of high energy consumption and limited reaction area in the single transducer ultrasound reactors. Kumar et al. [71] suggested the use of hexagonal ultrasound reactors with multi transducers to overcome the drawbacks in single transducer reactors. The hexagonal ultrasound reactor proposed by Kumar et al. [71] is shown in Fig. 7. Kumar and co-workers used hydrophone and a cavitation activity indicator to evaluate the intensity and distribution of the cavitational energy in their reactor design and eventually compared it

with the conventional single transducer ultrasound reactor. Their observations indicated that operating the hexagonal ultrasound reactor with a multi transducer at various frequencies, 20, 30 and 50 kHz resulted in higher cavitational activity as compared to the single transducer design. Mapping of the ultrasound reactors with the means of hydrophone and cavitation activity indicator also showed that the axial and radial variation in the cavitational intensity in the hexagonal design is much lower than that of the horn design. The variation of the cavitational intensity in the axial and radial directions of the hexagonal design was about 10–30%, while the horn design was around 100–300% [71].

Integrating enhancement elements into ultrasonic reactors such as micro-bubble injection, solid particle seeding or using corrugated surfaces is another approach that could have a positive impact on the energy consumption in ultrasound treatments. Mahulkar et al. [72] have tested the effect of micro-bubble injection (diameter of 750 μm) into ultrasonic reactors on the reactor throughput measured by iodine liberation from potassium iodide. They found that introducing the steam bubbles to ultrasonic reactors improved the energy efficiency of the reactor by 4–16 times. Likewise, Tuziuti et al. [73] showed that the injection of micro-meter sized air bubbles into ultrasound reactors improved the chemical effects of ultrasound represented by the iodine liberation and intensity of sonochemiluminescence. Broekman et al. [74] have also examined the combination of low power ultrasound and micro-bubble injection in controlling bacteria and algae growth in industrial water. They explained that the introduction

of micro-bubbles into irradiating water with low ultrasound power lifted the number of the collapsing sites. They ascribed this phenomenon to the reduction of cavitation threshold in the presence of external micro-bubbles.

Similar efforts were also made to improve the efficiency of ultrasound reactor in the destruction of E. coli in water by seeding the water with solid particles such as activated carbon, ceramic and metallic zinc particles [75]. Ince and Belen [75] found that among the three types of particles seeded in the water, activated carbon had the most pronounced effect on E. coli destruction. They asserted through the microbiological numeration tests that the main mechanism behind the improvement in ultrasonic disruption of E. coli in the presence of activated carbon granular is the surface heterogeneity of the granular that helps in increasing the cavitational events. Dadjour et al. [76] showed that the deactivation of E. coli in water using ultrasound reactors can be improved by seeding the suspension with pellets of titanium dioxide with a diameter of 2 mm. Dadjour's research group attributed the enhancement of ultrasonic microbial disinfection to the catalytic effect of titanium dioxide and the surface irregularities of the pellets that induced heterogeneous cavitation activities.

In our previous study [77], we investigated the effect of covering the cavitation chamber bottom with corrugated surface as a source of heterogeneous cavities on ultrasonic E. coli disruption measured by log of Colony Forming Unit (CFU). Fig. 8 depicts a schematic of the steps for the procedure of the corrugated surface study. First, the cavitation chamber was covered with the corrugated surface and filled with deionised water. Next, the deionised water was treated with ultrasound, and the treated water was filtered to separate the eroded particles from the corrugated surface. Finally, two treatments were conducted; suspension seeded with the eroded particles and treated in a cavitation chamber with no corrugated surface, and suspension treated in chamber with no eroded particles and corrugated surface. In this way, the effect of the eroded particles on the death of E. coli was identified (steps 1–4 in the Fig. 8) prior treating E. coli suspension in the ultrasonic reactor with corrugated surface. We found that covering the cavitation chamber with a corrugated surface has improved the disruption of E. coli especially for low ultrasonic power experiments, and the improvement in the disruption was mainly attributed to the corrugated surface and not the particles eroded.

2.3.3. Combination of ultrasound with other treatments

2.3.3.1. Combination of ultrasound with heat. Microorganisms become more sensitive to heat treatment if they have undergone an ultrasonic treatment and vice versa [54,55]. The combination of heat treatment with ultrasonic treatment is called "thermo-sonication" TS [78]. There are two contradictory effects of increasing the temperature of the liquid being treated by ultrasound with respect to the physics of bubble dynamics. The positive effect of temperature rise is facilitating the formation and growth of the bubbles, as temperature increases, viscosity and surface tension

of the liquid drop [61] and as a consequence cavitation threshold decreases [28]. The negative effect of the temperature increase of the liquid is the cushioning effect especially when the irradiated liquid is water which represents the reaction media in most of ultrasound applications (e.g. disinfection and food processing). The temperature increase leads to an increase in the vapor pressure and as a result the vapor content of the bubbles increases which in turn leads to less violent collapse of the bubbles [28].

There are number of studies that applied thermo-sonication in microorganism disruption. Ordoñez et al. [79] studied the effect of thermo-sonication on the survival of a strain of Staphylococcus aureus in a phosphate buffer. Garcia et al. [55] found that treating Bacillus subtilis spores with thermo-sonication (5 W/mL) was not significantly effective in killing the spores in water at temperatures close to boiling point (100 °C). The low effectiveness was attributed to the decrease in the violence of bubble collapse due to the higher vapor pressure acting like a cushion to the collapse [32,55].

Sequential or simultaneous application of ultrasonic and heat treatments result in the destruction of bacteria at much lower temperatures than would be required for heat treatment alone. Earnshaw et al. [78] demonstrated that the elimination of bacteria can be improved by subjecting them to a combination of ultrasonic and heat treatments compared to bacteria that are only subjected to ultrasonic treatment. Garcia et al. [55] reported a 43% reduction in the heat resistance of Bacillus subtilis (B. subtilis) when it was subjected to ultrasonication in hot water at temperatures ranging from 70 °C to 95 °C. Al-Juboori and Yusaf [61] have investigated the effect of sub-lethal temperatures of 45, 50, 55 and 60 °C in thermo-sonication treatment to water-based E. coli suspension on the intensity of collapse pressure and the viability of microorganisms. They found that rise in the temperature of the suspension within the tested range has a slight positive effect on bubble collapse, and the improvement in E. coli disinfection was mainly attributed to the thermal effect on the structure of E. coli. The results of Al-Juboori and Yusaf [61] showed also that combining low sub-lethal temperatures of microorganisms with ultrasound can be the best arrangement for thermo-sonication as at higher temperatures the deactivation effect of the combined treatments is mainly ascribed to thermal effect and applying ultrasound would be a waste of energy. Numerous number of studies have emphasized that the application of ultrasound and heat treatments is more energy efficient compared to either treatment individually [80,81].

2.3.3.2. Combination of ultrasound with pressure. The synergistic combination of ultrasound with pressure or so called Mano-Sonication (MS) was developed to improve ultrasonic microbial deactivation and decrease the energy requirements to deactivate the most resistant microorganisms and spores [82]. It is worth mentioning that combining ultrasound with external pressure can enhance the overall rupture of microorganisms to a certain limit after which the increase in the pressure would have no
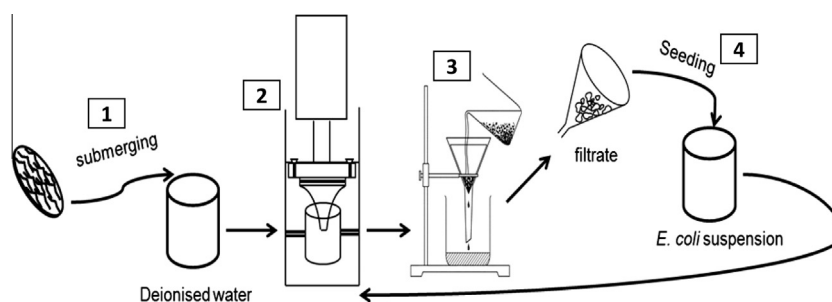

Fig. 8. Schematic reveals the procedure of corrugated surface investigation in Al-Juboori and Yusaf [77].

further effect. In our previous study [61], we observed that increasing the pressure beyond 2 bars had a slight effect on the deactivation of *E. coli ATCC 25922*. Lee et al. [83] found that the upper limit of the pressure in MS treatment of *E. coli K12* was 3 bars. Raso et al. [82] reported that the upper pressure limit in MS treatment for *Yersinia enterocolitica* was 4 bars and increasing the pressure to 6 bars did not result in a pronounced increase in the inactivation rate. The possible explanation for these observations can be the negative effect of the treated liquid pressure on bubble growth [61]. The variation in the reported upper limit of the MS pressure in the literature could be ascribed to the difference in the sensitivity of microorganisms' stains and species to the treatments [84].

2.3.3.3. Combination of ultrasonic with temperature and pressure. When the temperature of a liquid exceeds the boiling point, a loss in the cavitation effect takes place due to the high vapor pressure [55]. In order to overcome this problem, pressure is often applied to thermo-sonication. This kind of combination treatment is known as Mano–Thermo-Sonication (MTS). In the MTS technique, the negative effect of medium temperature on cavitation collapse intensity can be offset by increasing in the pressure of the irradiated medium [78].

2.3.3.4. Other possible combinations involving ultrasound. Apart from TS, MS and MTS treatments, there are other combinations that have proven to be effective against microorganisms.

Combination with pH control: Microorganisms have been observed to vary in their response to ultrasonic treatment when subjected to treatment at different pH [85]. It was found that a lower pH value reduces the resistance of microorganisms during ultrasonic treatments [85] which lead to a better destruction result.

Combination with Ultra-Violet (UV) light: One of the shortcomings of the UV disinfection is the fouling on the UV lamp. Therefore, combining UV light with ultrasound has been suggested by some researchers [27,86,87] to overcome the lamp fouling problems and at the same time enhance the disinfection capacity of ultrasound. The microbial destruction by UV light is medium dependent [88], so if there are large sized entities (i.e. particles) present in the medium, these entities would protect the microorganisms from UV light and render the UV disinfection ineffective. While, when merging ultrasound with UV, this problem can be overcome. Ultrasound has the advantage of cleaning the particles' surfaces [89], so under the effect of ultrasound the particles are disintegrated to smaller sizes, which means the transfer of UV light through the medium becomes easier and the adhered microorganisms to the particles get detached and exposed to UV and ultrasound treatments.

Combination with chemical control: Lillard [90] demonstrated that the effectiveness of ultrasound treatment can be enhanced through the use of a chemical such as chlorine. In this research, the focus is on mechanical methods. Therefore, other reported possible combinations related to chemical control are not explained further.

2.4. Shock wave treatment

Shock waves can be generated by methods such as shock tubes or electrical discharge shock wave generators [91]. It has been reported that a static pressure of about 100 MPa is required to destroy bacteria [92], a pressure at which the proteins structure would not be changed.

Oshima et al. [93] used a shock tube to generate a transient positive pressure of about 0.1 MPa with pulse duration of approximately 900 μs. However, *E. coli* was found to be difficult to destroy. Tamagawa and Akamastsu [94] used the same diaphragm-less shock tube as Oshima et al. [93] for their experiment on recombinant cells of *E. coli*. The pressure pulses generated with

their device had duration of about 20 μs and amplitude of up to 14 MPa. They noticed that cell rupture occurred after 100 shock waves at 14 MPa. This suggests that using higher pressures will lead to a higher level of damage to the microorganism, for repeated shock wave loads.

The research of Kerfoot et al. [95] aimed to isolate the effects of shock waves on *Pseudomonas aerugmiosa*, *Streptococcus faecalis*, *Staphylococcus aureus* and *E. coli* as well as to determine whether bactericidal activity exists. For this purpose, an electrohydraulic lithotripter of 20 kV was used together with a shock wave rate of 100 shocks per minute [55]. The result of the study was discouraging as no bactericidal activity was noticed. Loske et al. [92] studied the effects of an experimental electrohydraulic shock wave generation on *E. coli* suspension. The frequency of the device used was 0.4 kHz with a capacitance of 80 nF and voltage of 20 kV. The duration of the experiment was 24 min while the pressure pulse amplitude and pulse duration were 44 MPa and 4 μs respectively. The cells were suspended in tap water, which had a conductivity of about 960 μs and a temperature of 27 °C. The treatment resulted in a log reduction of 0.9 (from 10^6 to 10^5 CFU/mL). Lado and Yousef [96] found that to inactivate the entire cell population, 6 *D*-value or about 143 min would be required. *D*-value is the decimal reduction time and defined as the time required to kill 90% of microorganisms at a certain temperature. The results of this study differ from those of Kerfoot et al. [95] who used the same 20 kV electrohydraulic lithotripter.

Loske et al. [92] concluded that the effectiveness of shock wave microbial inactivation depends on the maximum pressure amplitude (peak compression and rarefaction), the rise time, duration of the pulse and the repetition rate. The authors also noted that the importance of the suspension container (test tubes in the case of Loske et al. [92]) and the environment around the test tubes would influence the transmission of shock waves to the cells.

2.5. High Pressure Homogenization (HPH)

A homogenizer is a device that is mostly used in the dairy industry to break-up fat globules into smaller particles [97]. The first emergence of the homogenization technique was in 1900, when Auguste Gaulin invented the first homogenizer and presented it at the World Fair in Paris [98]. However, the earliest attempt to use HPH for microorganisms disruption dates back to 1932 [99]. After this time, many studies investigated the use of HPH technique for extracting enzymes and intracellular products from various species of microorganisms such as *yeast* [100], *E. coli* [101], *Bacillus* [102], Microalgae [103] and filamentous fungi *Aspergillus niger* [104].
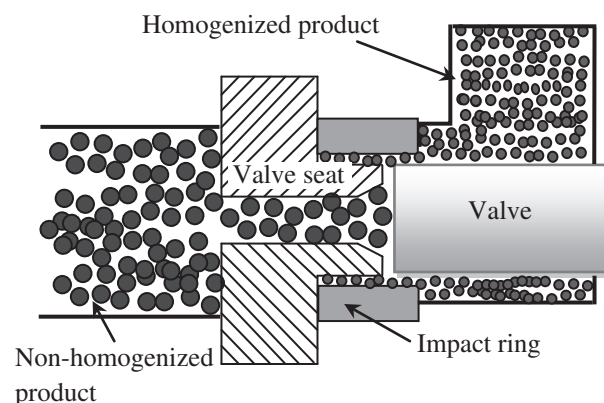

Fig. 9. Schematic diagram for standard homogenizer [98].

A standard homogenizer consists mainly of a positive displacement pump, valve seat, homogenizer valve and impact ring as shown in Fig. 9 [98,99].

The pump is used to force the fluid through a small orifice between the valve and the valve seat. When the fluid leaves the aperture between the seat and the valve, it strikes the impact ring and after that the homogenized fluid arrives at the discharge side. The pressure of the homogenizer can be regulated by changing the force applied to the valve [99].

The seat valve used for cell disruption can be found in different configurations, as illustrated in Fig. 10. The homogenization process is normally accompanied with a cooling procedure to control the friction temperature rise that is generated because of high fluid velocity [98]. It was found that the increase the in the pressure load on the valve can cause an increase in the temperature of the homogenized product in the order of 2–2.5 °C per 10 MPa [105].

The main mechanisms through which the HPH can disrupt the microbial cell has been a controversial issue [98]. However, the most acceptable reported scenarios in the literature are presented herein

(1) Rupture of microorganisms under the effect of the generated eddies in the turbulent flow [52].

Doulah et al. [52] postulated that most of the applied compression energy onto the homogenizer valve converts to kinetic energy dissipated in the liquid. The dissipated kinetic energy in the fluid can contribute to the generation of turbulences in the liquid body. The turbulences in turn can lead to the formation of eddies with different scales and intensities. The larger eddies can only cause cell movement, while the smaller ones are the main cause for the cell rupture. Small eddies have the potential to impart the dissipated kinetic energy in the fluid on the microorganism and thus cause the rupture. The condition for the cell disruption can be met when the kinetic energy of the small eddies exceeds the strength of the cell wall.

(2) Rupture of microorganism under the effect of impingement [106].

It was postulated that the microbial disruption in HPH can happen when the high velocity jets of the suspensions strikes the stationary surfaces in the homogenizer. The impact area of the stationary surfaces can have an influence on the efficiency of the microbial disruption and this influence varies from one species of microorganism to another. Middelberg [99] reported that increas-
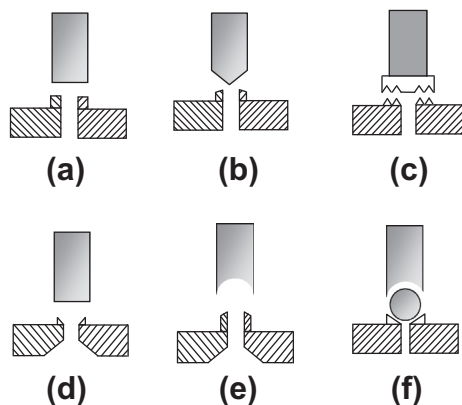
ing the impact distance in HPH can decrease the disruption of *Saccharomyces cerevisiae* and *E. coli*. However, the decrease in the microbial disruption was more pronounced with *E. coli* than *S. cerevisiae*.

(3) Rupture of microorganism under the effect of cavitation [107,108].

The microbial cell disruption in this scenario is attributed to the effect of hydrodynamic cavitation on the microorganism. Hydrodynamic cavitation phenomenon can occur throughout particular parts in the homogenizer such as the orifice and the gap between the valve and the valve seat where the pressure of the fluid drops below the saturated vapor pressure. However, the formation of hydrodynamic cavitation in throttling flow geometries such as the orifice and venturi and its mechanisms in rupturing microorganisms is explained in detail in the next section.

2.6. Hydrodynamic Cavitation (HC)

Hydrodynamic cavitation can be defined as the process of generating, growing and the subsequent collapse of bubbles resulting from a pressure fall of the liquid under the saturated vapor pressure as it flows through throttling geometries at a certain temperature. As the velocity of the liquid increases in the discharge side of the cavitation chamber, the pressure decreases. The common design of the HC chamber includes venturi and orifice configurations as illustrated in Fig. 11(a) and (b).

The most important parameters in HC microbial disruption include pressure parameters and time scale parameters. The pressure parameters include inlet pressure, minimum pressure and the recovered pressure. The time scale parameters of HC include three time scales, time for pressure decrease, rarefaction time and time for pressure recovery [109].

The inlet pressure is the most studied parameter among the other pressure parameters; this is because of the simplicity in controlling this parameter. However, the effect of the inlet pressure on the cavitational yield of HC is not completely understood [109].

The second pressure parameter in HC is the minimum pressure. This parameter is considered to be one of the most important pressure parameters in HC due to its critical effect on bubble growth and the number of the bubbles that grow explosively during the process of HC [109]. The minimum pressure in HC is a function of the flow rate of the liquid and the design of the cavitation chamber. The last pressure parameter in HC is the recovered pressure. This parameter also plays a crucial role in the HC process, as increasing this parameter can increase the intensity of bubble collapse and control the generation of excessive bubble cloud. The generation of the bubble cloud in the discharge side of the cavitation chamber can reduce the efficiency of the HC process. The recovered pressure can be controlled using some techniques such as the use stagnation plate after the cavitation chamber [109].

Time scales in HC can be evaluated from the residence time of the solution inside cavitation chamber which can be found from the volume of the chamber and the flow rate of the solution. The time for pressure decrease in HC does not have a significant role in the process, as none of the important events such as bubble
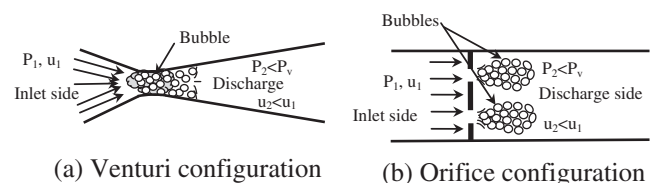
Fig. 10. Configurations of the valves that are used for cell disruption; (A) standard valve, (B) cell rupture valve, (C) grooved valve, (D) knife edge valve, (E) conical valve, and (F) ball cell disruption valve [98].

(a) Venturi configuration   (b) Orifice configuration

Fig. 11. Standard configurations for the hydrodynamic cavitation chamber [33].

growth or bubble collapse take place during this interval [109]. On the contrary, rarefaction and pressure recovery intervals can determine the efficacy of bubble growth and the intensity of bubble collapse respectively. An increase in the rarefaction period can generate bubbles with a large size and lower cavitation threshold. Nonetheless longer rarefaction periods can result in a production of bubble clouds. The effect of the rarefaction period on the bubble growth appears more conspicuously with large bubbles than small ones. The growth of large bubbles requires a long time due to their low natural frequency.

The effect of pressure recovery time on the efficacy of HC is just as crucial as that of the rarefaction period as pressure recovery time has an effect on bubble wall velocity and energy loss during collapse. Arrojo and Benito [109] expressed the loss of the energy during bubble collapse in HC by a non-dimensional parameter called the non-dimensional energy loss parameter. This parameter correlates the energy dissipated through the bubble wall throughout the collapse to the thermal energy that is stored in the bubble body at its maximum temperature. The non-dimensional energy loss parameter decreases with fast collapse which can be achieved with short pressure recovery time. It was observed that decreasing the pressure recovery time can lead to an increase in the degradation of p-nitrophenol by two folds in magnitude [109]. The effect of the pressure and time scales parameter on the physical and chemical yield of HC is summarized in Table 2.

The disruption of microorganisms with the HC technique can happen through chemical and mechanical effects. Chemical effects are represented by the liberation of free radicals such as OH^-, which is an unstable radical, and this radical can react with its counterparts producing H_2O_2. OH^- and H_2O_2 are strong oxidant agents that have the potential to rupture microorganisms. The oxidants H_2O_2 and OH^- can attack and penetrate the cell wall of the microorganisms causing disorder in the cell physiology thus resulting in cell death. Paleologou et al. [110] reported that OH^- can attack the polyunsaturated phospholipids components of the membranes' lipid causing disorder in the membrane integrity.

The reported mechanical effects of the hydrodynamic cavitation include impingement of microorganisms onto the solid surfaces, turbulences produced by high-velocity liquid jets, shear rates generated in the adjacent area to the jets and shock waves generated by bubbles' explosion [111]. The latter one is considered to be a dominant effect among the other mechanical effects of HC.

Sawant et al. [111] tested the feasibility of hydrodynamic cavitation as a disinfection technique to deactivate zooplankton in seawater. The configuration of the cavitation chamber that was used for this purpose was an orifice design. They suggested that the opened area of the orifice could have an effect on the viability of microorganisms, as the achieved deactivating percentage of the zooplankton with an opened area of the orifice of 25%, 50% and 75% was around 79%, 78%, and 82% respectively. Another study of using HC for microbial disruption was carried out by Arrojo et al. [9] to deactivate E. coli in wastewater. They used two types of

cavitation chamber designs; orifice with various number of holes and venture with different cross-sectional areas. The outcomes of Arrojo et al. [9] showed that the venturi configuration is more effective than orifice configuration. Among the different venturi configurations; the venturi with the smallest cross sectional area was the best in terms of E. coli deactivation.

2.7. Bead mill

This technique was first used for wet-grinding of pigments in the paint industry [112] and grinding of ceramic and limestone [113]. The standard design for the bead mill device consists of a jacketed chamber that has a rotating shaft located in the center of the chamber. The shaft has agitators that are attached to it in different configurations and designs as shown in Fig. 12 [99].

The function of the agitators is to transfer the energy that results from the rotation of the shaft to the solution body in order to induce the beads–microorganisms collision in the treated suspension. Part of the energy generated due to the rotation of the shaft converts to thermal energy. Therefore, the chamber of the bead mill is usually surrounded by a cooling jacket. The beads detain in the chamber by using sieve with mesh openings smaller than that of the beads [114].

Middelberg [99] reported that the mechanism of cell disruption in the bead mill could be due to shearing or compaction actions [113,115] and the effect of the transferred energy from beads to the microorganisms [114]. The effectiveness of the cell disruption in the bead mill is influenced by many factors including; bead size, agitator peripheral velocity, flow rate, concentration of microorganisms, volume fraction of beads in the chamber and temperature.

The effect of bead size on the efficacy of cell disruption was investigated by many studies and the outcomes of these studies were different. Currie et al. [116] showed that cell disruption with small beads is better than that with larger beads especially with low concentrations of microorganisms. However, small beads tend to float in a suspension with a high concentration of microorganisms. Garrido et al. [117] pointed to another advantage of using small beads, as beads with small size can be fluidized easier compared to large beads which results in a higher bead–bead collision and hence higher rate of cell disruption. On the contrary, Deters et al. [118] found that loading the mill with small beads can reduce the number of the ruptured cells.

The effectiveness of cell disruption in the bead mill technique is directly proportional to the agitation speed [119], volume fraction of the beads [120] and the concentration of microorganisms in the treated suspension [121]. Nevertheless, in some studies the concentration of microorganisms showed no influence on the cell disruption in the bead mill process [122]. Effect of temperature on the cell disruption in the bead mill is similar to that of other disinfection techniques, as increasing the temperature of the suspension can weaken the resistance of microorganisms against treatment [123].

Table 2
key parameters that affect the efficiency of hydrodynamic cavitation versus the designs of cavitation chamber [109].

	Rarefaction period		Compression period		Discharge pressure	
	Long	Short	Long	Short	Large	Small
Positive effects	Large bubbles, lower cavitation threshold	Avoids excessive bubble cloud density	None	More violent collapse, higher diffusion of OH^- radicals	Avoids excessive bubble growth, more violent collapses	More energy efficient
Negative effects	Excessive bubble cloud density	Higher cavitation threshold, smaller bubbles	Less violent collapse, lower diffusion of OH^- radicals	None	Energy un efficient, if excessive it might prevent bubble growth	Excessive bubble cloud density
Possible designs	Venturi with long throat	Orifice and multi-orifice plates	Single orifice plate or Venturi tube	Stagnation plates and/or multi-orifice plates	Stagnation plates or throttling device	Atmospheric or depressurized tank

(a) Agitator with eccentrically impellers attached to the shaft.

(b) Agitator with double disc stirrer.
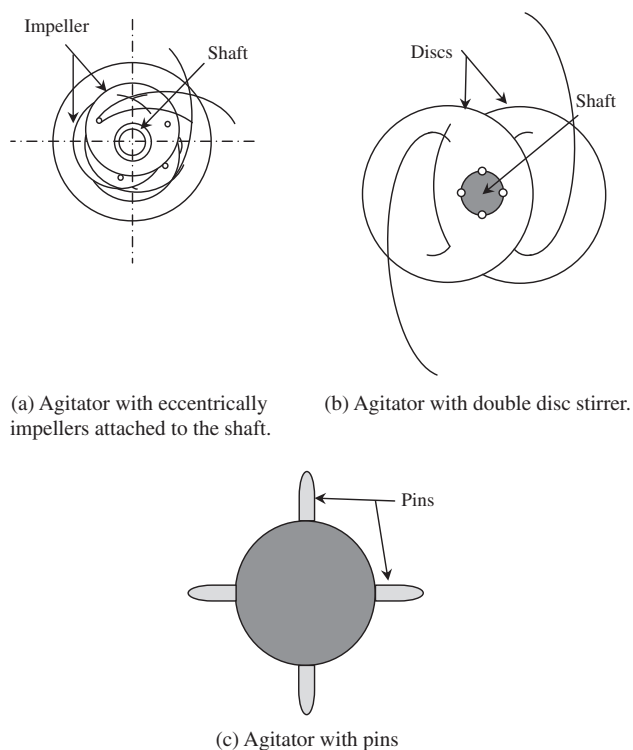
(c) Agitator with pins

Fig. 12. The common agitator designs of bead mill [99].

2.8. Micro-fluidizer

Micro-fluidizer is another form of the mechanical technique of microorganism disruption. In this technique, two streams of microorganisms suspensions are impacted at high velocity on a stationary surface, where the disruption takes place at the impact point [124]. The disruption chamber of the micro-fluidizer has the highest temperature compared to other parts of the fluidizer, and therefore it requires a cooling process. The efficiency of cell disruption is affected by the concentration of microorganisms in the treated suspension, the strain and the growth rate of the microorganisms [99,124]. The fragments of the disintegrated cells increase with increasing pressure and the number of passes through the chamber. Increasing the fragments of microorganisms in the product can deteriorate the efficiency of the subsequent centrifugal separation [124].

3. Other mechanical methods

There are some other mechanical methods that are less common than those reviewed in the previous sub-sections such as Rotor–Stator Homogenizer, French Press and Parr Cell Disruption Bomb [125–127]. Various designs of Rotor–Stator homogenizers have been reported in the literature as a useful tool for microorganism disruption such as toothed disks dispersing homogenizer [126] and cylindrical rotor–stator homogenizer [125]. The design of toothed disks dispersing homogenizer comprises of two or more coaxial interlocking rows of teeth [126]. The internal rotor is driven by electrical motor at a certain speed depending on the size of the sample and the type of the microorganism. The disruption mechanisms of the toothed disks dispersing homogenizer are represented by the impingement and cutting action in the narrow gaps between the openings of the rotor and stator disks and the stretching action that results from the rotational movements in the annulus between the rotor and stator. The gap between the rotor and the

stator in the toothed disks dispersing homogenizer ranges between 300 and 500 μm. The design of cylindrical rotor–stator homogenizer consists of rotational solid stainless steel cylinder (a rotor) situated inside a fixed core-shelled stainless steel cylinder with slightly bigger diameter (the stator). The mechanism of cell disruption in cylindrical rotor–stator homogenizer is the shear forces that rub the entrapped cells in the narrow annulus (400 μm) between the stationary and rotating surfaces.

French Press apparatus consists of a cylindrical vessel (pressure chamber) constructed from material that withstands moderate to high pressure (e.g. steel) with a piston at one end and exit valve at the other end [126]. The pressure chamber is normally loaded with a certain volume of microorganism suspension with the exit valve closed. The piston is pressed hydraulically to build up a pressure inside the pressure chamber. Once the desirable pressure is achieved, the exist valve is opened to allow the suspension to be discharged at low flow rate. Owing to the difference between the atmospheric pressure (low) and the pressure of the discharged suspension (high), the outflow of cell contents is induced causing cell wall rupture.

The Parr cell disruption bomb consists of pressure vessel with two openings at the top; one is used to fit dip tube (gas access) and the other one is to fit a pressure release valve. The pressure vessel is loaded by microorganism suspension while the pressure relief valve and gas access locked. Then an inert gas such as nitrogen is pumped through the dip tube with pressure relief valve is shut. The inert gas dissolves in the suspension. When the pressure released, the rarefication in the headspace above the suspension drives the dissolved nitrogen to escape the suspension in a form of large bubbles. The escape of the nitrogen as large bubbles causes the cells in the adjacent areas to the bubbles to stretch and consequently rapture. It is worth mentioning here that the rotor–stator homogenizers are suitable for rupturing microorganisms with tough cell wall, while French Press and Parr cell are suitable for microorganisms with soft cell wall. All of the reviewed techniques in this section have been mostly applied in bench scale studies which indicate their suitability in small scale applications such as gene transformation or extraction of proteins and *Deoxyribonucleic acid* (*DNA*) [128] that have a potential application in researching the possibility of enhancing the characteristics of new generations of crops and animals.

There are some advantages and disadvantages associated with using mechanical methods for cell disruption as summarized in Table 3.

4. Non-mechanical methods

4.1. Pulse electrical field (PEF)

Pulsed electric fields (PEF), oscillating magnetic fields (OMF) and light pulses (LP) are attractive and popular methods used in the food industry and research laboratories for sterilization purposes [131]. These methods offer good alternatives to conventional thermal processes where nutritive aspects and costs are a concern. These methods avoid the use of chemical preservatives that may cause a change in the nutritional value of the food. To adopt this technology on a larger scale, a good understanding of the electrochemistry is required [91,132].

The PEF method is strongly affected by the required electric power and the time to apply the power. PEF was used to kill *S. cerevisiae* in a medium of water and glycerol and the power applied was low-intensity electric fields and with long-duration pulses [131]. The destruction was attributed to the direct effect of the electromechanical phenomena and the indirect effect of the membrane polarization phenomena. Hence, it was suggested that the

Table 3
Advantages and disadvantages of the mechanical methods for cell disruption.

Mechanical techniques	Advantages	Disadvantages
High Pressure Homogenization (HPH)	(1) Chemical free (2) Possibility of scale-up [124]	(1) Low performance with filamentous microorganisms [129] (2) Causing mechanical erosion to the equipment [47] (3) Low efficiency [47] (4) No residual effect
Hydrodynamic cavitation	(1) Chemical free (2) Possibility of scale-up [111]	(1) Difficulty in controlling the key parameters that influence the chemical and physical yield of cavitation in HC chambers [109] (2) Causing mechanical erosion to the equipment [47] (3) No residual effect (4) Requires long treatment time
Bead mill	(1) Chemical free (2) Possibility of scale-up [124]	(1) Effect of some of the process parameters on the cell disruption is not clear such as bead size [116,118] (2) Low efficiency [47] (3) No residual effect
Micro-fluidizer	(1) Chemical free (2) Possibility of scale-up [124]	(1) Low efficiency [47] (2) No residual effect
Ultrasound	(1) Chemical free (2) New generation of ultrasound transducers has energy conversion efficiency as high as 70%, which reflects potential possibility to scale up [72] (3) Ultrasound reactors with reflection feature utilize about third of the electrical power [69] (4) Simplicity to implement in water treatment process [130]	(1) High energy demand (2) No residual effects
Other mechanical methods (e.g. rotor–stator homogenizers, French press and Parr cell)	(1) Chemical free (2) Easy fabrication	(1) High cost (2) Difficult to control temperature in some of the techniques such as cylindrical rotor–stator homogenizer (3) Hard to have a complete cell reduction (4) Hard to scale up

suitable technique used is high intensity electric field with short duration pulses [131].

The application of electrical fields in biological cells medium such as contaminated suspension can cause a build-up of electrical charges at the membrane of the cell as reported by Schoenbach et al. [133]. Membrane disruption takes place when the critical value of the cellular system exceeds the induced membrane potential of approximately 1 V (e.g. corresponds to an external electric field of about 10 kV/cm for *E. coli*) [134]. Many PFE theories have been suggested to explain microbial disruption [11]. The common studies focused on electrical breakdown and electroporation or disruption of cell membranes [134–136].

Dunn et al. [137] studied with homogenized milk contaminated with *Salmonella dublin* (*S. dublin*), and then treated using 36.7 kV/cm and 40 pulses for 25 min. It was found that there was no *S. dublin* after the PEF treatment. The concentration of the bacteria in the untreated milk was 10^7 CFU/mL, while the treated milk presented about 4×10^2 CFU/mL (i.e. log reduction of 5). Furthermore, Dunn et al. [137] showed that there are no changes in the flavor of milk, chemical and/or physical quality related to subsequent cheese making. A log reduction 3 was achieved when *E. coli* was used.

4.2. Non-thermal plasma

Plasma is a neutral ionized gas; it includes photons, electrons, positive and negative ions, free radicals and excited and non-excited molecules [138]. Plasma can be either thermal or non-thermal depending on the conditions of its creation. Non-thermal plasma is created with low pressure and low power, such as the plasma which is generated by an electric discharge with low pressure gas [138]. Factors that affect the activity of plasma in terms of destroying microorganisms are: the electric charge that causes the interaction between the microorganism and the plasma, the diffusion constant of the microorganism and the acidity (pH) of the medium. The general microbial disruption mechanism of this method is that the surface of the cell wall absorbs components from the plasma to form volatile components that are then removed from the cell causing its destruction [139].

4.3. Ultra-Violet (UV) light method

UV light is an electromagnetic radiation that occurs for example in sunlight and can also be emitted by electric arcs. UV light has been used for microorganism disruption in number of agricultural applications such as disinfection of wastewater for irrigation purposes [140] and food processing [141]. However, the use of UV light alone is not as effective as the other microorganism disruption methods that have been mentioned previously [142]. Since UV light is propagated by electrical fields, the parameters which affect its effectiveness are the level of electric power and the time. Other factors that impact this method of sterilisation include the medium which contains the microorganism and the type of microorganism which will be treated by the UV light. The unique element of this method is that UV light could attack the *DNA* as well as the cell wall of the microorganism. UV light combined with laser light has been used to inactivate *Bacillus cereus* [143]. Laser application alone was not enough to disrupt the microorganism effectively and UV light was effective for an exposure duration of more than 6 min [142]. While a combined treatment of laser and UV light can be an optimum method to kill bacteria such as *B. cereus*. According to these cited references [142,143], the combination of UV with other methods can produce better microorganism disruption. The UV method requires high security equipment which makes it expensive.

5. Chemical treatment methods

Some chemical methods rely on the addition of chemical substances to weaken the structure of the microorganism. Some examples are identified below:

a. *Biofilm removal caused by chemical treatments*: Biofilm is a heterogeneous matrix of microorganisms and their products in which cells are adhered to each other and to a surface [144]. Biofilm can be problematic in food processing industry as it is thought to be the cause behind the inefficient sanitation in this industry [20].

b. *Using supercritical carbon dioxide and hydrogen peroxide to kill Bacillus anthracis: Bacillus anthracis* is a Gram-positive spore-forming, rod-shaped bacterium with a width of $1–1.2\ \mu m$ and a length of $3–5\ \mu m$. These bacteria can be found in the blood of sheep suffering from anthrax, which is a fatal disease [124]. An example of chemical treatment is *Inhalation spores of B. anthraces'* can be chemically killed by a mixture of supercritical carbon dioxide ($SCCO_2$) and hydrogen peroxide (H_2O_2). The percentage of peroxide is 30% and the purity of carbon dioxide is 99.8%. This method uses medium temperature and high pressure to effectively kill *B. anthracis* [124].

c. *Chemical process*: Another way to chemically treat the bacteria is via a chemical processes such as hydrogenations and oxidations. An example of this method is the *oxidative killing of microorganism by neutrophils. Neutrophils* are the most abundant type of white blood cells in mammals and form an essential part of the immune system [145]. This method has wide applications in medicine.

6. Other methods

There are several other methods of treating microorganisms which are beyond the scope of this study. They include enzymatic, ionizing and osmotic methods.

Enzymatic methods involve attacking the enzyme of the cell without destroying the integrity of the cell. *Ionizing radiation* is another method which is designed to produce safe healthy food, while maintaining the nutrition values and sensory qualities [96]. *Osmotic shock or osmotic stress* is a method where a sudden change in the solute concentration around a cell leads to a fast change in the water movement across the membrane [146].

7. Conclusions and recommendations

Controlling microorganisms in one of the important aspects in agriculture due to its involvement in many agricultural areas such as irrigation and processing of crops and livestock products. The traditional measures for controlling microorganisms such as thermal and chemical methods suffer from many shortcomings including negative effect on quality of the products, deterioration of the construction materials of the treatment units (i.e. thermal stress and corrosion) and imposing threats to the consumers and environment. Much research has been conducted in the past decades in an effort to replace conventional thermal and chemical methods of microbe treatment with alternative environmentally friendly technologies. The alternative methods suggested in the literature involve the use of alternative chemicals with less by-product formation, mechanical methods, and non-mechanical physical methods.

The application of alternative methods for microorganism disruption in agricultural field requires thorough understanding to the mechanisms of these methods and careful scrutinizing to the benefits of integrating such methods to agricultural applications.

This manuscript has been dedicated to meet such requirements as the microorganism disruption mechanisms along with advantages and disadvantages of the alternative techniques have been discussed. Unfortunately, most of the alternative microorganism disruption methods have been categorized as high energy consumption methods. It should be mentioned that most of the judgments on the energy status of the alternative methods have been made based on bench scale application. Furthermore, the energy consumption is usually determined depending on the electrical power consumed and the prices of the instruments and the materials with no consideration to the repercussions of environmental damage and health risks that could result from the continual usage of traditional techniques. Moreover, the use of bioenergy for operating the alternative techniques for microorganism disruption can reduce the burden of high energy consumption of these techniques.

In this review, an insight to the microbial disruption mechanisms of the alternative techniques has been provided for the aim of developing strategies to reduce the high energy demand of these techniques. Many technical solutions to the high energy demand of some mechanical methods such as ultrasound and HC has been highlighted in this review. The use of combined methods for microorganism disruption is recommended in this study. The priority of the future research work should be given to physical–physical combination rather than physical–chemical combination when chemical residual effect is not important in order to promote the use of environmentally safe techniques.

References

[1] Toze S. Reuse of effluent water—benefits and risks. Agric Water Manage 2006;80:147–59.
[2] Bouwer H. Integrated water management for the 21st century: problems and solutions. J Irrig Drain Eng 2002;128:193–202.
[3] Tanji K. Irrigation with marginal quality waters: issues. J Irrig Drain Eng 1997;123:165–9.
[4] Anzecc A. Australian and New Zealand guidelines for fresh and marine water quality. National water quality management strategy paper; 2000. p. 4.
[5] Peasey A, Blumenthal U, Mara D, Ruiz-Palacios G. A review of policy and standards for wastewater reuse in agriculture: a Latin American perspective. WELL study, Task; 2000.
[6] Yusaf TF. Mechanical treatment of microorganisms using ultrasound, shock and shear technology. Toowoomba: University of Southern Queensland; 2011 [PhD thesis].
[7] Tan TC, Lim EWC. Thermally killed cells of complex microbial culture for biosensor measurement of BOD of wastewater. Sens Actuat B: Chem 2005;107:546–51.
[8] Al-Ahmad M, Abdul Aleem F, Mutiri A, Ubaisy A. Biofouling in RO membrane systems Part 1: fundamentals and control. Desalination 2000;132:173–9.
[9] Arrojo S, Benito Y, Martínez Tarifa A. A parametrical study of disinfection with hydrodynamic cavitation. Ultrason Sonochem 2008;15:903–8.
[10] Richardson SD. Disinfection by-products and other emerging contaminants in drinking water. TrAC Trends Anal Chem 2003;22:666–84.
[11] Al-Juboori RA, Yusaf T. Biofouling in RO system: mechanisms, monitoring and controlling. Desalination 2012.
[12] Richardson SD, Simmons JE, Rice G. Peer reviewed: disinfection byproducts: the next generation. Environ Sci Technol 2002;36:198A–205A.
[13] Tan TC, Qain Z. BOD measurement in the presence of heavy metal ion using a thermally-killed-bacillus subtilise. Biosensor Water Res 1999;33:2923–8.
[14] Prakash S, Huppertz T, Karvchuk O, Deeth H. Ultra-high-temperature processing of chocolate flavoured milk. J Food Eng 2010;96:179–84.
[15] Aslihan D, Taner B. The use of ultrasound and combined technologies in food preservation. Food Rev Int 2009;25:1–11.
[16] Zydney AL. Protein separations using membrane filtration: new opportunities for whey fractionation. Int Dairy J 1998;8:243–50.
[17] Ölmez H, Kretzschmar U. Potential alternative disinfection methods for organic fresh-cut industry for minimizing water consumption and environmental impact. LWT – Food Sci Technol 2009;42:686–93.
[18] Hellstrom S, Kervinen R, Lyly M, Ahvenainen-Rantala R, Korkeala H. Efficacy of disinfectants to reduce *Listeria monocytogenes* on precut iceberg lettuce. J Food Prot 2006;69:1565–70.
[19] Park C, Beuchat L. Evaluation of sanitizers for killing *Escherichia coli* O157: H7, Salmonella, and naturally occurring microorganisms on cantaloupes, honeydew melons, and asparagus. Dairy Food Environ Sanit 1999;19:842–7.
[20] Gil MI, Selma MV, López-Gálvez F, Allende A. Fresh-cut product sanitation and wash water disinfection: problems and solutions. Int J Food Microbiol 2009;134:37–45.

[21] Huang TS, Xu C, Walker K, West P, Zhang S, Weese J. Decontamination efficacy of combined chlorine dioxide with ultrasonication on apples and lettuce. J Food Sci 2006;71:M134–9.

[22] Gera N, Doores S. Kinetics and mechanism of bacterial inactivation by ultrasound waves and sonoprotective effect of milk components. J Food Sci 2011;76:M111–9.

[23] Mercer P, Armenta RE. Developments in oil extraction from microalgae. Eur J Lipid Sci Technol 2011;113:539–47.

[24] Al-lwayzy S, Yusaf T. Chlorella protothecoides microalgae as an alternative fuel for tractor diesel engines. Energies 2013;6:766–83.

[25] Joyce E, Phull SS, Lorimer JP, Mason TJ. The development and evaluation of ultrasound for the treatment of bacterial suspensions. A study of frequency, power and sonication time on cultured Bacillus species. Ultrason Sonochem 2003;10:315–8.

[26] Rawat I, Ranjith Kumar R, Mutanda T, Bux F. Dual role of microalgae: phycoremediation of domestic wastewater and biomass production for sustainable biofuels production. Appl Energy 2011;88:3411–24.

[27] Gibson JH, Nien Yong DH, Farnood RR, Seto P. A literature review of ultrasound technology and its application in wastewater disinfection. Water Qual Res J Can 2008;43:23–35.

[28] Thompson LH, Doraiswamy LK. Sonochemistry: science and engineering. Ind Eng Chem Res 1999;38:1215–49.

[29] Scherba G, Weigel RM, O'Brien WD. Quantitative assessment of the germicidal efficacy of ultrasonic energy. Appl Environ Microbiol 1991;57:2079–84.

[30] Hughes DE, Nyborg WL. Cell disruption by ultrasound. Science 1962;138:108–14.

[31] Mousavi SAAA, Feizi H, Madoliat R. Investigations on the effects of ultrasonic vibrations in the extrusion process. J Mater Process Technol 2007;187–188:657–61.

[32] Alliger H. New methods in ultrasonic processing. Am Lab 1978;10:81–7.

[33] Al-juboori RA. Ultrasound technology as a pre-treatment for biofouling control in reverse osmosis (RO) system. University of Southern Queensland; 2012 [Research Masters thesis].

[34] Thornycroft JI, Barnaby SW. Torpedo boat destroyers. J Am Soc Naval Eng 1895;7:711–36.

[35] Rayleigh L. VIII. On the pressure developed in a liquid during the collapse of a spherical cavity. Philos Mag Ser 6 1917;34:94–8.

[36] Richards WT, Loomis AL. The chemical effects of high frequency sound waves: a preliminary survey. J Am Chem Soc 1927;49:3086–100.

[37] Wood EW, Loomis AL. XXXVIII. The physical and biological effects of high-frequency sound-waves of great intensity. Philos Mag Ser 7 1927;4:417–36.

[38] Brohult S. Splitting of the haemocyanin molecule by ultrasonic waves. Nature 1937;140:805.

[39] Harvey EN, Whiteley AH, McElroy WD, Pease DC, Barnes DK. Bubble formation in animals. II. Gas nuclei and their distribution in blood and tissues. J Cell Compar Physiol 1944;24:23–34.

[40] Plesset M. The dynamics of cavitation bubbles. J Appl Mech 1949;16:277.

[41] Noltingk BE, Neppiras EA. Cavitation produced by ultrasonics. Proc Phys Soc 1950;63B:674–85.

[42] Flynn HG. Physics of acoustic cavitation in liquids. In: Mason WP, editor. Physical acoustics. New York: Acad. Press; 1964.

[43] Neppiras EA, Hughes DE. Some experiments on the disintegration of yeast by high intensity ultrasound. Biotechnol Bioeng 1964;6:247–70.

[44] Burgos J, Ordonez JA, Sala F. Effect of ultrasonic waves on the heat resistance of Bacillus cereus and Bacillus licheniformis spores. Appl Environ Microbiol 1972;24:497–8.

[45] Vichare NP, Senthilkumar P, Moholkar VS, Gogate PR, Pandit AB. Energy analysis in acoustic cavitation. Ind Eng Chem Res 2000;39:1480–6.

[46] Gogate PR. Application of cavitational reactors for water disinfection: current status and path forward. J Environ Manage 2007;85:801–15.

[47] Gogate PR, Kabadi AM. A review of applications of cavitation in biochemical engineering/biotechnology. Biochem Eng J 2009;44:60–72.

[48] Birkin PR, Silva-Martinez S. A study of the effect of ultrasound on mass transport to a microelectrode. J Electroanal Chem 1996;416:127–38.

[49] Young FR. Cavitation. London: Imperial College Press; 1999.

[50] Hulsmans A, Joris K, Lambert N, Rediers H, Declerck P, Delaedt Y, et al. Evaluation of process parameters of ultrasonic treatment of bacterial suspensions in a pilot scale water disinfection system. Ultrason Sonochem 2010;17:1004–9.

[51] Doulah MS. Mechanism of disintegration of biological cells in ultrasonic cavitation. Biotechnol Bioeng 1977;19:649–60.

[52] Doulah MS, Hammond TH, Brookman JSG. A hydrodynamic mechanism for the disintegration of Saccharomyces cerevisiae in an industrial homogenizer. Biotechnol Bioeng 1975;17:845–58.

[53] Balachandran S, Kentish SE, Mawson R, Ashokkumar M. Ultrasonic enhancement of the supercritical extraction from ginger. Ultrason Sonochem 2006;13:471–9.

[54] Ordoñez JA, Sanz B, Hernandez PE, Lopez-Lorenzo P. A note on the effect of combined ultrasonic and heat treatments on the survival of thermoduric streptococci. J Appl Microbiol 1984;56:175–7.

[55] Garcia ML, Burgos J, Sanz B, Ordonez JA. Effect of heat and ultrasonic waves on the survival of two strains of Bacillus subtilis. J Appl Bacteriol 1989;67:619–28.

[56] Wrigley DM, Liorca NG. Decrease in Salmonella typhimurium in skim milk and egg by heat and ultrasonic wave treatment. J Food Prot 1992;55:678–80.

[57] Ciccolini L, Taillandier P, Wilhem AM, Delmas H, Strehaiano P. Low frequency thermoultrasonication of Saccharomyces cerevisiae suspensions: effect of temperature and of ultrasonic power. Chem Eng J 1997;65:145–9.

[58] Koda S, Miyamoto M, Toma M, Matsuoka T, Maebayashi M. Inactivation of Escherichia coli and Streptococcus mutans by ultrasound at 500 kHz. Ultrason Sonochem 2009;16:655–9.

[59] Naffrechoux E, Chanoux S, Petrier C, Suptil J. Sonochemical and photochemical oxidation of organic matter. Ultrason Sonochem 2000;7:255–9.

[60] Sivakumar M, Pandit AB. Ultrasound enhanced degradation of Rhodamine B: optimization with power density. Ultrason Sonochem 2001;8:233–40.

[61] Al-Juboori RA, Yusaf T. Identifying the optimum process parameters for ultrasonic cellular disruption of E. coli. Int J Chem Reactor Eng 2012;10:1–32.

[62] Santos HM, Lodeiro C, Capelo-Martínez J-L. The power of ultrasound. Ultrasound in chemistry. Wiley-VCH Verlag GmbH & Co. KGaA; 2009. p. 1–16.

[63] Mason TJ, Lorimer JP. Sonochemistry: theory, applications and uses of ultrasound in chemistry. Ellis Horwood; 1988.

[64] Xie B, Wang L, Liu H. Using low intensity ultrasound to improve the efficiency of biological phosphorus removal. Ultrason Sonochem 2008;15:775–81.

[65] Capelo JL, Galesio MM, Felisberto GM, Vaz C, Pessoa JC. Micro-focused ultrasonic solid–liquid extraction (µFUSLE) combined with HPLC and fluorescence detection for PAHs determination in sediments: optimization and linking with the analytical minimalism concept. Talanta 2005;66:1272–80.

[66] Priego-Capote F, de Castro L. Ultrasound-assisted digestion: a useful alternative in sample preparation. J Biochem Biophys Methods 2007;70:299–310.

[67] Seymour JD, Wallace HC, Gupta RB. Sonochemical reactions at 640 kHz using an efficient reactor. Oxidation of potassium iodide. Ultrason Sonochem 1997;4:289–93.

[68] Adewuyi YG, Oyenekan BA. Optimization of a sonochemical process using a novel reactor and Taguchi statistical experimental design methodology. Ind Eng Chem Res 2007;46:411–20.

[69] Destaillats H, Lesko TM, Knowlton M, Wallace H, Hoffmann MR. Scale-up of sonochemical reactors for water treatment. Ind Eng Chem Res 2001;40:3855–60.

[70] Gonze E, Gonthier Y, Boldo P, Bernis A. Standing waves in a high frequency sonoreactor: visualization and effects. Chem Eng Sci 1998;53:523–32.

[71] Kumar A, Gogate PR, Pandit AB. Mapping the efficacy of new designs for large scale sonochemical reactors. Ultrason Sonochem 2007;14:538–44.

[72] Mahulkar AV, Bapat PS, Pandit AB, Lewis FM. Steam bubble cavitation. AIChE J 2008;54:1711–24.

[73] Tuziuti T, Yasui K, Kozuka T, Towata A, Iida Y. Enhancement of sonochemical reaction rate by addition of micrometer-sized air bubbles. J Phys Chem A 2006;110:10720–4.

[74] Broekman S, Pohlmann O, Beardwood ES, de Meulenaer EC. Ultrasonic treatment for microbiological control of water systems. Ultrason Sonochem 2010;17:1041–8.

[75] Ince NH, Belen R. Aqueous phase disinfection with power ultrasound: process kinetics and effect of solid catalysts. Environ Sci Technol 2001;35:1885–8.

[76] Dadjour MF, Ogino C, Matsumura S, Shimizu N. Kinetics of disinfection of Escherichia coli by catalytic ultrasonic irradiation with TiO_2. Biochem Eng J 2005;25:243–8.

[77] Al-Juboori RA, Yusaf TF. Improving the performance of ultrasonic horn reactor for deactivating microorganisms in water. IOP Conf Ser: Mater Sci Eng 2012;36:1–13.

[78] Earnshaw RG, Appleyard J, Hurst RM. Understanding physical inactivation processes: combined preservation opportunities using heat, ultrasound and pressure. Int J Food Microbiol 1995;28:197–219.

[79] Ordoñez JA, Aguilera MA, Garcia ML, Sanz B. Effect of combined ultrasonic and heat treatment (thermoultrasonication) on the survival of a strain of Staphylococcus aureus. J Dairy Res 1987;54:61–7.

[80] Piyasena P, Mohareb E, McKellar RC. Inactivation of microbes using ultrasound: a review. Int J Food Microbiol 2003;87:207–16.

[81] Knorr D, Ade-Omowaye BIO, Heinz V. Nutritional improvement of plant foods by non-thermal processing. Proc Nutr Soc 2002;61:311–8.

[82] Raso J, Pagan R, Condon S, Sala FJ. Influence of temperature and pressure on the lethality of ultrasound. Appl Environ Microbiol 1998;64:465–71.

[83] Lee H, Zhou B, Liang W, Feng H, Martin SE. Inactivation of Escherichia coli cells with sonication, manosonication, thermosonication, and manothermosonication: microbial responses and kinetics modeling. J Food Eng 2009;93:354–64.

[84] Baumann AR, Martin SE, Feng H. Power ultrasound treatment of Listeria monocytogenes in apple cider. J Food Prot 2005;68:2333–40.

[85] Kinsloe H, Ackerman E, Reid JJ. Exposure of microorganisms to measured sound fields. J Bacteriol 1954;68:373–80.

[86] Naddeo V, Landi M, Belgiorno V, Napoli RMA. Wastewater disinfection by combination of ultrasound and ultraviolet irradiation. J Hazard Mater 2009;168:925–9.

[87] Joyce EM, Mason TJ, Lorimer JP. Application of UV radiation or electrochemistry in conjunction with power ultrasound for the disinfection of water. Int J Environ Pollut 2006;27:222–30.

[88] Char C, Mitilinaki E, Guerrero S, Alzamora S. Use of high-intensity ultrasound and UV-C light to inactivate some microorganisms in fruit juices. Food Bioprocess Technol 2010;3:797–803.

[89] Chen D, Sharma SK. Handbook on applications of ultrasound: sonochemistry for sustainability. CRC Press; 2011.

[90] Lillard HS. Bactericidal effect of chlorine on attached salmonellae with and without sonication. J Food Prot 1993;56:716–7.

[91] Yu LJ, Ngadi M, Raghavan GSV. Effect of temperature and pulsed electric field treatment on rennet coagulation properties of milk. J Food Eng 2009;95:115–8.

[92] Loske AM, Prieto FE, Zavala ML, Santana AD, Armenta E. Repeated application of shock waves as a possible method for food preservation. Shock Waves 1999;9:49–55.

[93] Oshima Y, Sakamoto T, Sonoda K-h, Yoshida H, Ishibashi T, Inomata H. Effect of electric pulses and antiproliferative drugs on cultured bovine retinal pigment epithelial cells. Curr Eye Res 1997;16:64–70.

[94] Tamagawa M, Akamastsu. Mechanism of damage two living cells by plan shock waves in water (mathematical model of two cells). In: The 21st international symposium on shock wave. Great Keppel Island Australia; 1997.

[95] Kerfoot WW, Beshai AZ, Carson CC. The effect of isolated high-energy shock wave treatments on subsequent bacterial growth. Urol Res 1992;20:183–6.

[96] Lado BH, Yousef AE. Alternative food-preservation technologies: efficacy and mechanisms. Microbes Infect 2002;4:433–40.

[97] Kleinig AR, Middelberg APJ. On the mechanism of microbial cell disruption in high-pressure homogenisation. Chem Eng Sci 1998;53:891–8.

[98] Diels AMJ, Michiels CW. High-pressure homogenization as a non-thermal technique for the inactivation of microorganisms. Crit Rev Microbiol 2006;32:201–16.

[99] Middelberg APJ. Process-scale disruption of microorganisms. Biotechnol Adv 1995;13:491–551.

[100] Follows M, Hetherington PJ, Dunnill P, Lilly MD. Release of enzymes from bakers' yeast by disruption in an industrial homogenizer. Biotechnol Bioeng 1971;13:549–60.

[101] Higgins JJ, Lewis DJ, Daly WH, Mosqueira FG, Dunnill P, Lilly MD. Investigation of the unit operations involved in the continuous flow isolation of β-galactosidase from Escherichia coli. Biotechnol Bioeng 1978;20:159–82.

[102] Augenstein DC, Thrasher K, Sinskey AJ, Wang DIC. Optimization in the recovery of a labile intracellular enzyme. Biotechnol Bioeng 1974;16:1433–47.

[103] Halim R, Harun R, Danquah MK, Webley PA. Microalgal cell disruption for biofuel development. Appl Energy 2012;91:116–21.

[104] Zetelaki K. Disruption of mycelia for enzymes. Process Biochem 1969;4:19–22.

[105] Popper L, Knorr D. Applications of high-pressure homogenization for food preservation. Food Technol 1990;44:84–9.

[106] Engler CR, Robinson CW. Disruption of Candida utilis cells in high pressure flow devices. Biotechnol Bioeng 1981;23:765–80.

[107] Save SS, Pandit AB, Joshi JB. Microbial cell disruption: role of cavitation. Chem Eng J Biochem Eng J 1994;55:B67–72.

[108] Donsì F, Ferrari G, Maresca P. High-pressure homogenization for food sanitization. In: Gustavo B-C, Alan M, David L, Walter S, Ken B, Paul C, editors. Global issues in food science and technology. San Diego: Academic Press; 2009. p. 309–52.

[109] Arrojo S, Benito Y. A theoretical study of hydrodynamic cavitation. Ultrason Sonochem 2008;15:203–11.

[110] Paleologou A, Marakas H, Xekoukoulotakis NP, Moya A, Vergara Y, Kalogerakis N, et al. Disinfection of water and wastewater by TiO2 photocatalysis, sonolysis and UV-C irradiation. Catal Today 2007;129:136–42.

[111] Sawant SS, Anil AC, Krishnamurthy V, Gaonkar C, Kolwalkar J, Khandeparker L, et al. Effect of hydrodynamic cavitation on zooplankton: a tool for disinfection. Biochem Eng J 2008;42:320–8.

[112] Kula M-R, Schütte H. Purification of proteins and the disruption of microbial cells. Biotechnol Prog 1987;3:31–42.

[113] Bunge F, Pietzsch M, Müller R, Syldatk C. Mechanical disruption of Arthrobacter sp. DSM 3747 in stirred ball mills for the release of hydantoin-cleaving enzymes. Chem Eng Sci 1992;47:225–32.

[114] MacNeill C, Sneeringer JR, Szatmary A. Optimization of cell disruption with bead mill. Pharmaceut Eng 1985;5:34–8.

[115] Melendres AV, Unno H, Shiragami N, Honda H. A concept of critical velocity for cell disruption by bead mill. Tokyo, Japan: Society of Chemical Engineers; 1992.

[116] Currie JA, Dunnill P, Lilly MD. Release of protein from Bakers' yeast (Saccharomyces cerevisiae) by disruption in an industrial agitator mill. Biotechnol Bioeng 1972;14:725–36.

[117] Garrido F, Banerjee UC, Chisti Y, Moo-Young M. Disruption of a recombinant yeast for the release of B-galactosidase. Bioseparation 1994;4:319–28.

[118] Deters D, Müller U, Homberger H. Breakage of yeast cells: large scale isolation of yeast mitochondria with a continuous-flow disintegrator. Anal Biochem 1976;70:263–7.

[119] Schütte H, Kroner KH, Hustedt H, Kula MR. Experiences with a 20 litre industrial bead mill for the disruption of microorganisms. Enzyme Microb Technol 1983;5:143–8.

[120] Tamer IM, Moo-Young M, Chisti Y. Disruption of Alcaligenes latus for recovery of poly(β-hydroxybutyric acid): comparison of high-pressure homogenization, bead milling, and chemically induced lysis. Ind Eng Chem Res 1998;37:1807–14.

[121] Ricci-Silva ME, Vitolo M, Abrahão-Neto J. Protein and glucose 6-phosphate dehydrogenase releasing from Baker's yeast cells disrupted by a vertical bead mill. Process Biochem 2000;35:831–5.

[122] Mogren H, Lindblom M, Hedenskog G. Mechanical disintegration of microorganisms in an industrial homogenizer. Biotechnol Bioeng 1974;16:261–74.

[123] Condón S, Raso J, Pagán R. Microbial inactivation by ultrasound. In: Barbosa-Cánovas VG, Tapia MS, Cano MP, editors. Novel food processing technologies. Boca Raton, Florida: CRC Press LLC; 2005. p. 423–42.

[124] Geciova J, Bury D, Jelen P. Methods for disruption of microbial cells for potential use in the dairy industry – a review. Int Dairy J 2002;12:541–53.

[125] Yusaf T. Experimental study of microorganism disruption using shear stress. Biochem Eng J 2013;79:7–14.

[126] Goldberg S. Mechanical/physical methods of cell disruption and tissue homogenization. 2D PAGE: sample preparation and fractionation. Springer; 2008. p. 3–22.

[127] Garrett PE, Tao F, Lawrence N, Ji J, Schumacher RT, Manak MM. Tired of the same old grind in the new genomics and proteomics era? TARGETS 2002;1:156–62.

[128] Tan SC, Yiap BC. DNA, RNA, and protein extraction: the past and the present. J Biomed Biotechnol 2009;2009.

[129] Keshavarz E, Bonnerjea J, Hoare M, Dunnill P. Disruption of a fungal organism, Rhizopus nigricans, in a high-pressure homogenizer. Enzyme Microb Technol 1990;12:494–8.

[130] Furuta M, Yamaguchi M, Tsukamoto T, Yim B, Stavarache CE, Hasiba K, et al. Inactivation of Escherichia coli by ultrasonic irradiation. Ultrason Sonochem 2004;11:57–60.

[131] Guyot S, Ferret E, Boehm J-B, Gervais P. Yeast cell inactivation related to local heating induced by low-intensity electric fields with long-duration pulses. Int J Food Microbiol 2007;113:180–8.

[132] Mosqueda-Melgar J, Raybaudi-Massilia RM, Martín-Belloso O. Combination of high-intensity pulsed electric fields with natural antimicrobials to inactivate pathogenic microorganisms and extend the shelf-life of melon and watermelon juices. Food Microbiol 2008;25:479–91.

[133] Schoenbach KH, Peterkin FE, Alden III RW, Beebe SJ. The effect of pulsed electric fields on biological cells: experiments and applications. IEEE Trans Plasma Sci 1997;25:284–92.

[134] Castro AJ, Barbosa-CÁNovas GV, Swanson BG. Microbial inactivation of foods by pulsed electric fields. J Food Process Preserv 1993;17:47–73.

[135] Zimmermann U. Electrical breakdown, electropermeabilization and electrofusion. Rev Physiol Biochem Pharmacol 1986;105:176–256.

[136] Vega-Mercado H, MartÍN-Belloso O, Chang F-J, Barbosa-CcAnovas GV, Swanson BG. Inactivation of Escherichia coli and Bacillus subtilis suspended in pea soup using pulsed electric fields. J Food Process Preserv 1996;20:501–10.

[137] Dunn JE, LaCosta R, Pearlman JS, Diego S. Methods and apparatus for extending the shelf life of fluid food products, U.S.A.; 1987.

[138] Moreau M, Orange N, Feuilloley MGJ. Non-thermal plasma technologies: new tools for bio-decontamination. Biotechnol Adv 2008;26:610–7.

[139] Lerouge S, Wertheimer MR, Marchand R, Tabrizian M, Yahia LH. Effect of gas composition on spore mortality and etching during low-pressure plasma sterilization. J Biomed Mater Res 2000;51:128–35.

[140] Lubello C, Gori R, Nicese FP, Ferrini F. Municipal-treated wastewater reuse for plant nurseries irrigation. Water Res 2004;38:2939–47.

[141] Guerrero-Beltr J, Barbosa-C G. Advantages and limitations on processing foods by UV light. Food Sci Technol Int 2004;10:137–47.

[142] Ward GD, Watson IA, Stewart-Tull DES, Wardlaw AC, Wang RK, Nutley MA, et al. Bactericidal action of high-power Nd:YAG laser light on Escherichia coli in saline suspension. J Appl Microbiol 2000;89:517–25.

[143] Armstrong GN, Watson IA, Stewart-Tull DE. Inactivation of B. cereus spores on agar, stainless steel or in water with a combination of Nd:YAG laser and UV irradiation. Innov Food Sci Emerg Technol 2006;7:94–9.

[144] Chen X, Stewart PS. Biofilm removal caused by chemical treatments. Water Res 2000;34:4229–33.

[145] Roos D, van Bruggen R, Meischl C. Oxidative killing of microbes by neutrophils. Microbes Infect 2003;5:1307–15.

[146] Flores HE, Galston AW. Polyamines and plant stress: activation of putrescine biosynthesis by osmotic shock. Science 1982;217:1259–61.

Appendix B

Paper XII

Al-Juboori, R. A., Yusaf, T. & Aravinthan, V., Evaluating the impact of operating parameters on biocidal effects of pulsed ultrasound in natural water disinfection, *Journal of Biotechnology*, (2015), 208, Supplement, S17-S18.

anti-OTA immobilization, blank QCM's performance is tested with BSA conjugated OTA (0.5–250 ng/ml). For the ES-QCM, CA fibers are prepared from 15% w/w CA solution in acetone/DMAC (3:1). The average diameters of the CA fibers are about 250 nm. The aldehyde groups are produced by $NaIO_4$ oxidation of CA. The antigens immobilized on ES-QCM are OTA (0.5–100 ng/ml) or BSA conjugated OTA (0.5–250 ng/ml). The amount of adsorbed OTA is determined by calculating the frequency shift due to binding of a toxin on the surface. The calibration curves of the blank QCM and ES-QCM are obtained and these curves are compared with in terms of response time, linearity and detection limit. Selectivity of the immunosensor is tested with citrinin (100–250 ng/ml).

Molecular cloning, characterization and phylogenetic analysis of pirarucu (*Arapaima gigas*) FSH and LH β-subunits

Paolo Bartolini [1,*], Roberto Feitosa Carvalho [1], Thais Cristina Dos Anjos Sevilhano [1], João Ezequiel Oliveira [1], Riviane Garcez [2]

[1] *Biotechnology, IPEN-CNEN/SP, Cidade Universitária, São Paulo, 05508-000, Brazil*
[2] *Genetic Ichthyology, Bioscience Institute, University of São Paulo, 05508-090, Brazil*

E-mail address: pabartoli@hotmail.com (P. Bartolini).

Pirarucu (*Arapaima gigas*) is a giant, fresh water fish, native to the Amazon River basin, reaching 3 meters in length and weighing up to 250 kg. Its common gonadotropin α-subunit has been previously isolated by our research group from *A.gigas* pituitaries; in the present work the cDNA sequences encoding FSHβ- and LHβ-subunits have also been isolated from the same pituitaries. The FSHβ-subunit was found of 126 amino acids with an 18 amino acid signal peptide and a 108 amino acid mature peptide, while the LHβ-subunit of 141 amino acids with a 24 amino acid signal peptide and a 117 amino acid mature peptide. The highest identity, based on amino acid sequences, was with the order of Anguilliformes (61%) for FSHβ and of Cypriniformes (76%) for LHβ. Interestingly, the identity with the corresponding human amino acid sequences was still remarkable: 45.1% for FSHβ and 51.4% for LHβ. The phylogenetic tree, based on concatenated DNA sequences of FSHβ and LHβ from 41 fish species, placed *A. gigas* (Osteoglossomorpha) as the sister group of Clupeocephala, while Anguilliformes (Elopomorpha) appears as the earliest branching lineage among teleosts. This will allow the synthesis of *A. gigas* gonadotropins, useful for physiology and fertility studies of this extremely important source of food for the region.

Comparative study on antimicrobial activity of *Sambucus* spp. plant extracts

Steliana Rodino [1,*], Marian Butu [2], Constanta Negoescu [3], Reta Condei [4], Ioana Niculae [4], Alina Butu [2], Calina Petruta Cornea [4]

[1] *UASVM, Bucharest, Romania; NIRDBS, Bucharest, Romania*
[2] *NIRDBS, Bucharest, Romania*
[3] *Banat's UASVM "Regele Mihai I al României" from Timişoara, Romania*
[4] *University of Agronomical Sciences and Veterinary Medicine of Bucharest, Romania*

E-mail address: steliana.rodino@yahoo.com (S. Rodino).

Researchers from various fields such as chemistry, microbiology, pharmacology, agriculture and horticulture are investigating natural sources to find active chemical substances that might be used as agents for drug synthesis, in the design of novel antimicrobial products. The present paper studies the antimicrobial activity of plant extracts aiming to draw attention on the role of plant natural compounds as a primary source of antimicrobials. Three *Sambucus* species extracts were evaluated for their potential as antimicrobial agents. The vegetal material used for obtaining ethanolic extracts was obtained from healthy dried plants collected from natural populations existing on non-polluted lands. Agar diffusion method was applied in testing the inhibitory effect of the plant extracts against several plant phytopathogens. The experiments pointed that medicinal plants show strong antimicrobial activity being effective in inhibition of microbial growth. The results highlight the potentiality of further development of pathogen control schemes based on natural antimicrobials.

Evaluating the impact of operating parameters on biocidal effects of pulsed ultrasound in natural water disinfection

Raed A. Al Juboori [1,*], Talal Yusaf [2], Vasantha Aravinthan [1]

[1] *School of Civil Engineering and Surveying, Faculty of Health, Engineering and Sciences, University of Southern Queensland, Toowoomba, 4350 QLD, Australia*
[2] *School of Mechanical and Electrical Engineering, Faculty of Health, Engineering and Sciences, University of Southern Queensland, Toowoomba, 4350 QLD, Australia*

E-mail address: RaedAhmed.Mahmood@usq.edu.au (R.A. Al Juboori).

The knowledge available in the literature regarding the use of pulsed ultrasound for water disinfection is limited. Hence, this study was designed to provide a thorough investigation for the application of pulsed ultrasound disinfection in water treatment. High power low frequency pulsed ultrasound was used to disinfect natural water samples. Two levels of power, treatment time and On/Off ratio (R) of 40% and 70% amplitudes, 5 and 15 min and 0.2:0.1 and 0.1:0.6, respectively were tested. To scrutinize the effect of the operating parameters on pulsed ultrasound disinfection efficiency,

rigorous statistical analyses were performed applying factorial design of 23. Total coliform Quantification was applied as a measure for disinfection efficiency. It was found that increasing power, treatment time or both had a positive effect on total coliform reduction, whereas increasing the off period of pulsed ultrasound resulted in lower total coliform reduction. The disinfection effects of 2-way interaction of power * R and 3-way interaction of power * treatment time * R were statistically insignificant ($P > 0.05$). Linear regression model was developed for predicting total coliform reduction under pulsed ultrasound effect. Cost analyses of the treatments were also conducted.

PROTOFILWW: Two year-sampling of protozoa, little metazoa and filamentous bacteria in 37 Portuguese wastewater treatment plants

Ana Nicolau*, Marta Neto, Liliana Santos, Vânia Fernandes, Manuel Mota

Centre of Biological Engineering, University of Minho, Braga, Portugal

E-mail address: protozoa@deb.uminho.pt (A. Nicolau).

Activated-sludge represents a component of the largest biotechnology in the world: wastewater treatment. Yet it differs substantially from the large-scale production of economically important metabolites or biomass: for decades, the aerating tanks of the wastewater treatment plants (WWTP) have remained "black boxes", its complexity discouraging most microbiologists.

Moreover, studies integrating both the prokaryotic and the eukaryotic populations in activated-sludge are, even presently, rare. Particularly, there is an assumed difficulty in establishing how the interactions between the bacterial and the protozoa populations can affect the performance of the activated sludge system.

On the other hand, excessive growth of filamentous bacteria is considered the main concern of WWTP managers. It is said that every WWTP in the world went, go or will go through the well-known phenomena of filamentous bulking or foaming. It is also said that the basis for understanding and fighting these problems depends on the proper identification of the causing microorganisms: by acting upon the factor favoring the problematic species, one can expect to control its overgrowth.

In the 80s and 90s of the last century, some surveys suddenly revealed the extent and severity of filamentous overgrowth. In Portugal, a detailed investigation has been carried out recently through the PROTOFILWW Project: protozoa, little metazoa and filamentous bacteria populations of 37 WWTP were extensively studied during two years. The prevalence and the correlations among the prokaryotic and eukaryotic components and between them and the operational and performance parameters will be presented.

Salt tolerant tomatoes local landraces from Romania – Preserving the genetic resources for future sustainable agriculture

Radu Liviu Sumalan[1,*], Ioana Popescu[2], Brigitta Schmidt[1], Ranata Maria Sumalan[1], Cristina Popescu[3], Sorin Gaspar[2]

[1] *Banat's University of Agricultural Sciences and Veterinary Medicine "King Michael Ist of Romania" From Timişoara, Romania*
[2] *Centre for Consultancy and Euro-Regional Rural Cooperation, Romania*
[3] *"Vasile Goldiş" Western University of Arad, Romania*

E-mail address: sumalanagro@yahoo.com (R.L. Sumalan).

Continuous climate changes and intensive anthropic activities affect larger and larger areas, causing desertification, soil salinization, and environmental pollution. One way to assure a sustainable agriculture for future generations is preserving and utilization of genetic resources with tolerance to stress factors.

Fifteen populations of tomatoes (*Solanum lycopersicum* L.) were collected from Romanian rural areas for salt tolerance and tested at 150 mM and 300 mM NaCl for 2 months. Proline, catalase and chlorophyll content were assessed before and after 1 and 2 months of stress.

Of all populations Sânmartinul Sârbesc 180b which was also one with the greatest tomato yield had the highest values for all three characters at a long-term application of high concentrations of NaCl. Livezile 498 cultivar had also high values for proline and catalase concentrations at 300 mM saline solution.

Results demonstrate the huge potential of local landraces of tomatoes collected from saline areas of Romania.

Diagnosis of activated sludge in the biological treatment of gas emissions

Anna Mazurina[1,*], Vlada Zabolotskikh[1], Andrey Vasilyev[2]

[1] *Department of Chemistry and Environmental Engineering, Togliatti State University, Togliatti, Russia*
[2] *Department of Chemical Engineering, Samara State Technical University, Samara, Russia*

E-mail address: annamazurina90@gmail.com (A. Mazurina).

The basis of biological treatment processes of gas emissions is biochemical oxidation of organic contaminants by microorganisms of the activated sludge under aerobic or anaerobic conditions.

In the cells of microorganisms of activated sludge, which is the main agent of the biological treatment process many reactions are simultaneously catalyzed by different enzymes that are closely related to each other and form a complex poly enzymatic systems. A feature of biological fermentative systems in the cells is their ability to self-regulation. With data about their self-control can greatly simplify the complex relationship chains of biochemical reactions.

It is known that the regulation of metabolism in living cells (anaerobically) has three key points are: oxygen uptake, the use of the substrates and reaction pathways branching points.
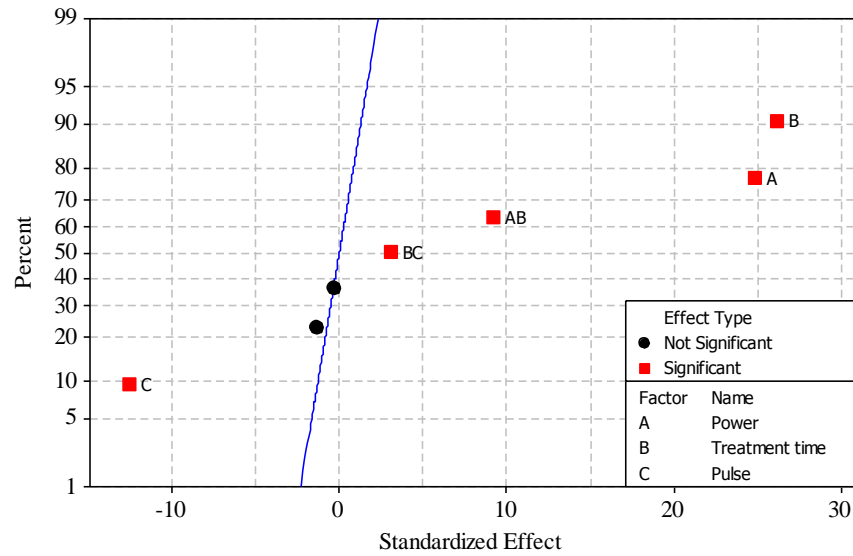
Results presented in paper XII

1. Diagnostic statistical tests
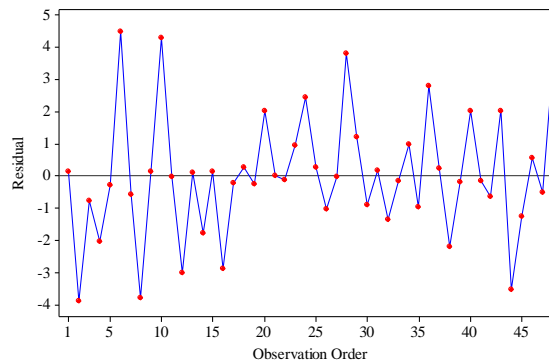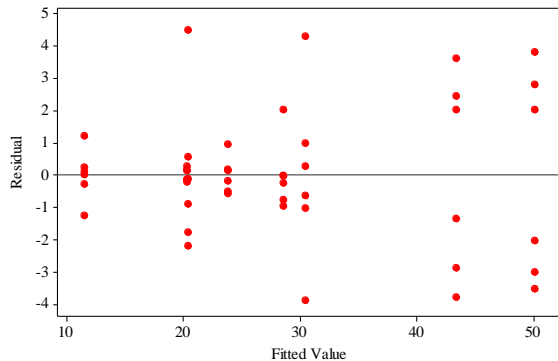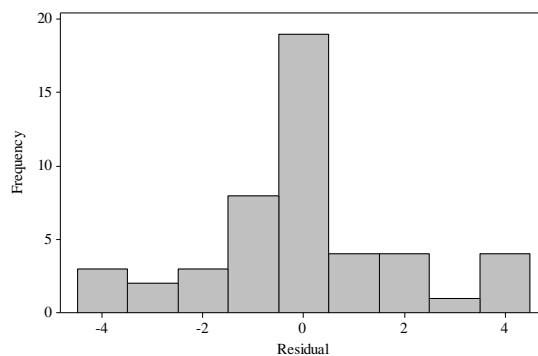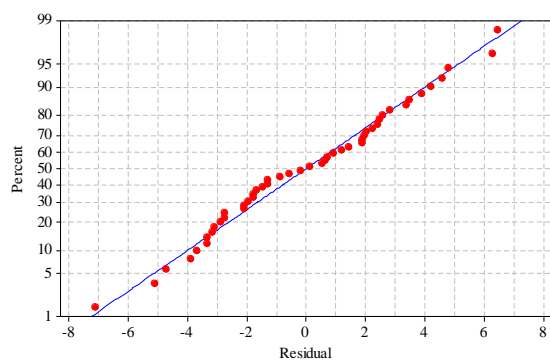
2. Uncoded and coded values of experimental factors

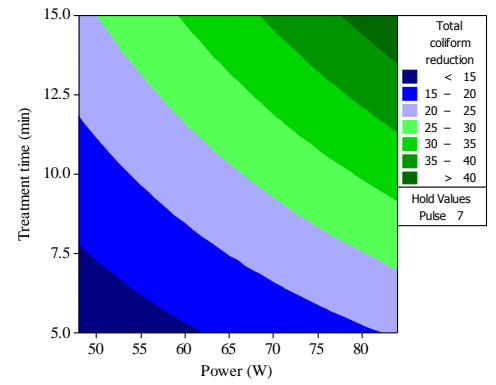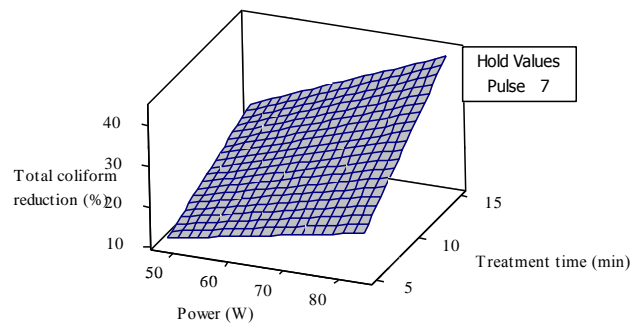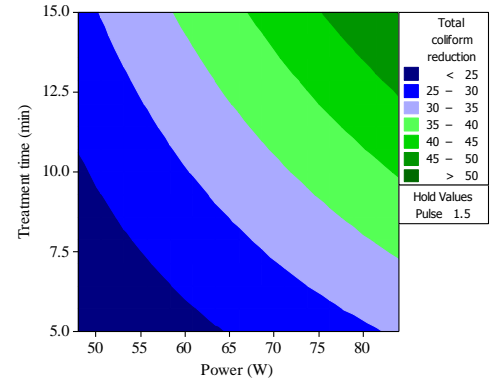| Factors	Uncoded values		Coded values	
	low	high	low	high
Power (W)	48	84	-1	1
Treatment time (min)	5	15	-1	1
Pulse setting (s)	0.1:0.2	0.1:0.6	-1	1

## 3. Significance of factors interactions

4. Analysis of variance (ANOVA) for coded factors

Source	DF	Seq SS	Adj SS	Adj MS	F	P
Main Effects	3	6407.70	6407.70	2135.90	487.75	0.000
Power	1	2710.08	2710.08	2710.08	618.87	0.000
Treatment time	1	3004.62	3004.62	3004.62	686.13	0.000
Pulse	1	693.00	693.00	693.00	158.25	0.000
2-Way Interactions	3	418.59	418.59	139.53	31.86	0.000
Power*Treatment time	1	368.25	368.25	368.25	84.09	0.000
Power*Pulse	1	7.85	7.85	7.85	1.79	0.188
Treatment time*Pulse	1	42.49	42.49	42.49	9.70	0.003
3-Way Interactions	1	0.39	0.39	0.39	0.09	0.766
Power*Treatment time*Pulse	1	0.39	0.39	0.39	0.09	0.766
Residual Error	40	175.16	175.16	4.38		
Pure Error	40	175.16	175.16	4.38		
Total	70	7001.85				

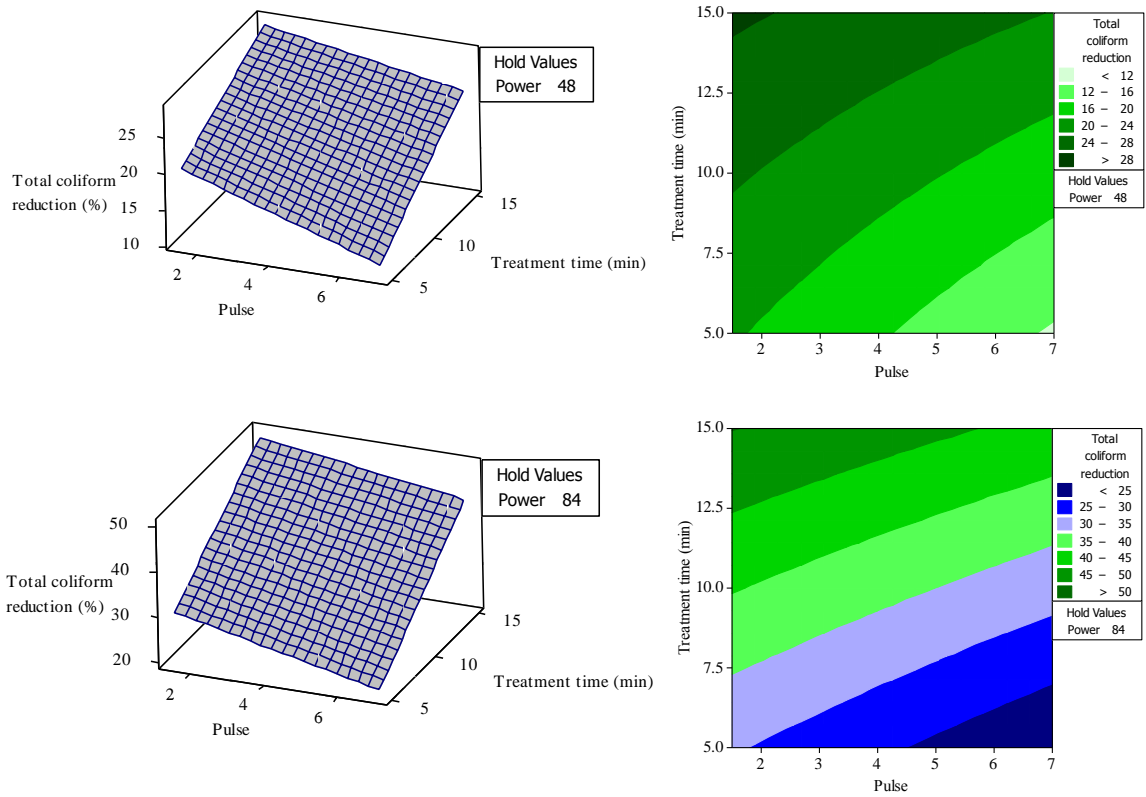# 5. Surface and contour plots

5.1. Effects of treatment time and power
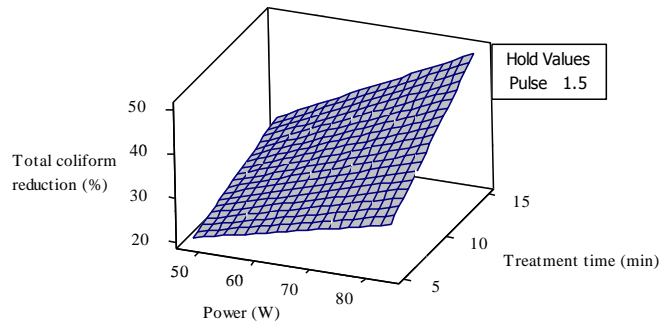
5.2. Effects of power and pulse settings
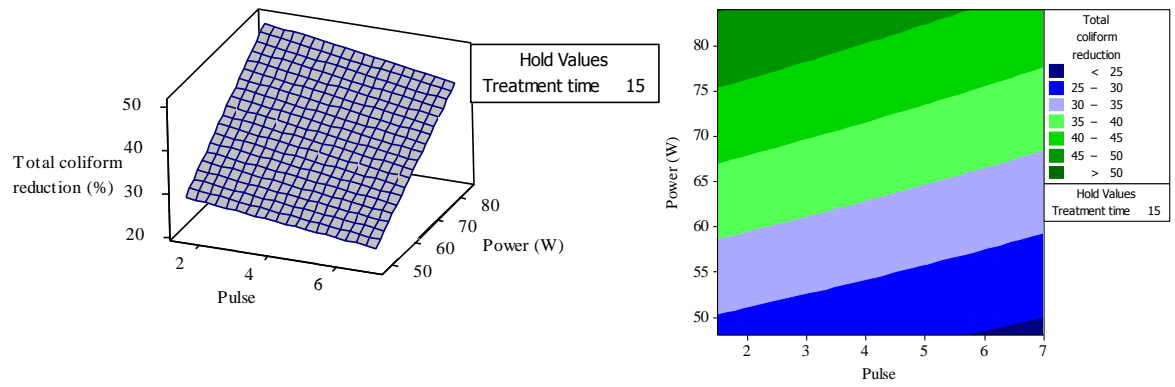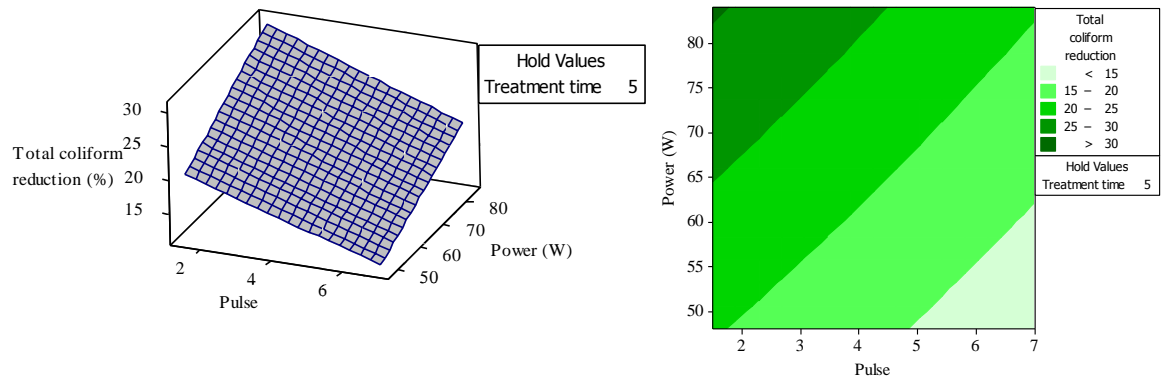
5.3. Effects treatment time and pulse settings

6. Regression models for coded factors

$$Y = 28.61 + 7.51A + 7.91B - 3.80C + 2.77AB - 0.40AC + 0.94BC - 0.09ABC$$

Y = Total coliform reduction (%)
A = Coded value of power
B = Coded value of treatment time
C = Coded value of pulse settings